frontiers | Research Topics

# Advances in the imaging and treatment of valvular heart disease

**Edited by**
Marko Banovic and Ronak Rajani

**Published in**
Frontiers in Cardiovascular Medicine

ISSN 1664-8714
ISBN 978-2-8325-3532-5
DOI 10.3389/978-2-8325-3532-5

## About Frontiers

Frontiers is more than just an open access publisher of scholarly articles: it is a pioneering approach to the world of academia, radically improving the way scholarly research is managed. The grand vision of Frontiers is a world where all people have an equal opportunity to seek, share and generate knowledge. Frontiers provides immediate and permanent online open access to all its publications, but this alone is not enough to realize our grand goals.

## Frontiers journal series

The Frontiers journal series is a multi-tier and interdisciplinary set of open-access, online journals, promising a paradigm shift from the current review, selection and dissemination processes in academic publishing. All Frontiers journals are driven by researchers for researchers; therefore, they constitute a service to the scholarly community. At the same time, the *Frontiers journal series* operates on a revolutionary invention, the tiered publishing system, initially addressing specific communities of scholars, and gradually climbing up to broader public understanding, thus serving the interests of the lay society, too.

## Dedication to quality

Each Frontiers article is a landmark of the highest quality, thanks to genuinely collaborative interactions between authors and review editors, who include some of the world's best academicians. Research must be certified by peers before entering a stream of knowledge that may eventually reach the public - and shape society; therefore, Frontiers only applies the most rigorous and unbiased reviews. Frontiers revolutionizes research publishing by freely delivering the most outstanding research, evaluated with no bias from both the academic and social point of view. By applying the most advanced information technologies, Frontiers is catapulting scholarly publishing into a new generation.

## What are Frontiers Research Topics?

Frontiers Research Topics are very popular trademarks of the *Frontiers journals series*: they are collections of at least ten articles, all centered on a particular subject. With their unique mix of varied contributions from Original Research to Review Articles, Frontiers Research Topics unify the most influential researchers, the latest key findings and historical advances in a hot research area.

Find out more on how to host your own Frontiers Research Topic or contribute to one as an author by contacting the Frontiers editorial office: frontiersin.org/about/contact

# Advances in the imaging and treatment of valvular heart disease

**Topic editors**

Marko Banovic — University of Belgrade, Serbia

Ronak Rajani — Guy's and St Thomas' NHS Foundation Trust, United Kingdom

**Citation**

Banovic, M., Rajani, R., eds. (2023). *Advances in the imaging and treatment of valvular heart disease*. Lausanne: Frontiers Media SA. doi: 10.3389/978-2-8325-3532-5

# Table of contents

frontiers | Frontiers in Cardiovascular Medicine

TYPE Editorial
PUBLISHED 07 September 2023
DOI 10.3389/fcvm.2023.1276202



OPEN ACCESS

EDITED AND REVIEWED BY
Elena Aikawa,
Harvard Medical School, United States

*CORRESPONDENCE
Marko Banovic
markobanovic71@gmail.com

RECEIVED 11 August 2023
ACCEPTED 30 August 2023
PUBLISHED 07 September 2023

CITATION
Banovic M and Rajani R (2023) Editorial: Advances in the imaging and treatment of valvular heart disease: "rising to the challenge". Front. Cardiovasc. Med. 10:1276202. doi: 10.3389/fcvm.2023.1276202



# Editorial: Advances in the imaging and treatment of valvular heart disease: "rising to the challenge"

Marko Banovic[1,2]* and Ronak Rajani[3,4]

[1]Belgrade Medical Faculty, University of Belgrade, Belgrade, Serbia, [2]Cardiology Clinic, University Clinical Center of Serbia, Belgrade, Serbia, [3]Cardiovascular Directorate, Guy's and St Thomas' NHS Foundation Trust, London, United Kingdom, [4]School of Biomedical Engineering and Imaging Sciences, King's College London, London, United Kingdom

KEYWORDS

valvular disese, imaging, treatment, prognosis, stratifcation

Editorial on the Research Topic
Advances in the imaging and treatment of valvular heart disease: "rising to the challenge"

## Introduction

Valvular heart disease (VHD) is an increasing cause of cardiovascular morbidity and mortality worldwide. This overall burden is set to increase further in future years as the world's population ages and access to diagnostic techniques increase (1). Fortunately, this challenge is being met by renewed interest by the scientific community across the globe into the pathophysiology of valve disease, new potential pharmacotherapeutic agents and novel surgical and minimally invasive techniques to treat this burdensome disease. In this edition of Frontiers, the Editors have collated a series of manuscripts that detail some of the current key advancements in the diagnosis, management, and treatment across the spectrum of aortic, mitral valve and tricuspid and pulmonary valve disease (**Supplementary Table S1**).

## Aortic valve disease

With the rapid global expansion of transcatheter aortic valve replacement (TAVR), it was not surprising that many submissions were received detailing new deployment techniques and strategies to improve clinical outcomes. Lind et al. reported their experience with a new endovascular approach for transcatheter aortic valve replacement (TAVR) combining an axillary prosthetic conduit-based access technique with new-generation balloon-expandable TAVR prostheses. This novel approach offers hope to those patients who otherwise may have been ineligible for surgical aortic valve replacement (SAVR) or TAVR via conventional access routes. In another manuscript, Talmon-Barkar et al. investigated the interaction between transcatheter heart valve selection and valve implantation depth in 2,352 patients with a borderline basal annulus ring size. The authors showed that in these patients, the selection of larger valves resulted in reduced rates of paravalvular leak (PVL) and optimized valve hemodynamics with no increase in procedural complications. Furthermore, to refine the optimal TAVR implantation technique, Maier et al. demonstrated that a cusp-overlap deployment technique is associated with an optimized

implantation depth, leading to fewer permanent conduction disturbances, but at a cost of an increase in radiation doses.

In patients with bicuspid aortic valve stenosis (AS), TAVR has been shown to be a viable treatment option. Although this is associated with increased complication rates, there is a dearth of data comparing how TAVR performs against SAVR in this patient population. To address this unknown, Gaseka et al. conducted a propensity matched cohort study evaluating patients who had undergone TAVR for bicuspid AS compared with TAVR for degenerative AS over a ten-year time frame. The authors showed that TAVR for bicuspid AS had comparable in-hospital mortality, device success, procedural complications, PVL and overall mortality compared to the degenerative AS matched cohort. There was however a higher rate of neurological complications in the TAVR bicuspid AS group. Overall, these results are encouraging but will need to be validated in one or more randomized controlled trials. For those younger patients with calcific severe AS, who are unwilling or unable to undergo SAVR, there are a lack of medical alternatives. In a thought-provoking study by Bernava et al. the potential use of shockwave ultrasound to de-calcify heart valve leaflets in a porcine model was explored. They showed that this treatment has the potential to achieve a partial debridement of calcified leaflets to improve leaflet and hydrodynamic performance. Although this preliminary work offers some hope that alternative treatments to delay the need for AVR may exist, there remains several unanswered questions relating to the use of this technology. Not least its clinical applicability and safety in humans.

There were also several papers addressing the use of imaging in the risk-stratification of patients with aortic valve disease. Kameshima et al. studied the impact of prosthesis-patient mismatch (PPM) on hemodynamics after TAVR using exercise stress-echocardiography. Perhaps unsurprisingly, the authors found that patients with PPM had a disproportionate increase in the transvalvular gradients upon stress echocardiography. This resulted in exercise-induced pulmonary hypertension and indicated a cohort with a higher NYHA functional class. This data stresses the importance of appropriate device selection and sizing in patients undergoing TAVR. Galian-Gay and associates investigated the risk of mortality and need for AVR in patients with paradoxical low-flow low-gradient (LFLG) AS. Of 1,391 patients, 147 (10.5%) had paradoxical LFLG. There was a lower need for AVR compared to a high-gradient group with a similar threshold to the normal-flow low-gradient group with no resultant differences in mortality. The authors concluded that this challenging group of patients with paradoxical LFLG AS have an intermediate clinical risk, which is in-between those patients with high-gradient AS and normal-flow LG AS.

There is increasing attention on the pathophysiology of calcified AS with recent reports suggesting that elevated serum Lipoprotein (a) is associated with the development and progression of aortic stenosis. On this theme, Liu et al. conducted a systematic review to explore this further. Eight studies with 52,931 participants were included of which four were cohort studies and four were case-control studies. The pooled results demonstrated that plasma lp(a) levels ≥50 mg/dl were associated with a 1.76-fold increased risk of calcific aortic valve disease (RR, 1.76; 95% CI, 1.47–2.11). In an experimental research Yang et al. identified ten genes and key signaling pathways through RNA-sequencing dataset and real-time PCR assay as underlying molecular targets for mechanism that may be important in AS. Both of studies indicate a hope for future targeted medical therapies for AS in the future.

## Mitral valve disease

Transcatheter mitral valve (TMV) therapies have made tremendous progress in the last decade (2, 3). Yet, in the group of patients who are eligible for TMV therapies, referral pathways remain deficient and screening failure rates high. To address this, Gill et al. report their experience in setting up a dedicated TMV clinic. The authors show how the integration of relevant experts and the "branding" of a transcatheter mitral valve service within organizations may serve to improve awareness of newer treatments and increase access to care. While TMV replacement itself remains largely in its infancy, percutaneous mitral valve edge-to-edge repair (PMVR) for treating patients with high risk/inoperable severe primary and secondary mitral regurgitation is becoming embedded into many structural interventional services. Recognizing the invaluable role of the cardiac imaging specialist to this procedure Fan et al. detail the latest advancements in transesophageal echocardiography and three-dimensional imaging, together with guide on how to apply them during PMVR procedures. Adding to our knowledge base in this area Neuser et al. demonstrated the ability of right ventricular function to improve following PMVR independent to that being seen with the left ventricle. However, this observation was attenuated in patients being referred late for treatment and in those patients with multiple comorbidities and higher surgical risk scores. This finding suggests that earlier intervention may confer improved clinical outcomes, but this needs to be confirmed in further studies. Another area of emerging interest is the use of transcatheter heart valves to treat degenerative surgical bioprosthesis. In a reasonable sized series of 26 patients Lu et al. demonstrated safety and feasibility of this procedure using the J-Valve System. In this study there was no device-related mortality, device embolization, left ventricular outflow tract obstruction, or mitral valve reintervention. The postprocedural mitral regurgitation was none or trace in all the patients and all patients were in the New York Heart Association (NYHA) class ≤ II at the last follow-up. Although this data is compelling, whether these findings can be attributed to the specific device or careful patients and imaging selection is unknown since there was no comparator device.

Rheumatic heart disease is in decline in developed countries but still affects a significant number of younger and middle-aged patients in developing countries (1). Yu and Wang. retrospectively compared 10-year survival between bioprosthetic and mechanical prosthetic valves in 1,691 middle-aged patients treated at a single center with rheumatic mitral valve disease. The authors observed no difference in all-cause mortality, as

well. Certainly, as bioprosthetic valve utilization rate is increasing in recent years (4) this study demonstrates that mechanical valves are not yet to be dismissed as an option. Even more so as improvements in access to home monitoring kits increase and dedicated anticoagulation clinics expand (5).

## Tricuspid and pulmonary valve

The value of global longitudinal strain (GLS) and some of its surrogates in assessing LV function in patients with valvular diseases is well documented (6, 7). On the other hand, isolated surgical intervention to the tricuspid valve (TV) is relatively uncommon, and if performed, it should be ideally done before right ventricular (RV) dysfunction ensues. To address this issue, Kim et al. investigated the prognostic implications of biventricular global longitudinal strain in 111 patients receiving isolated tricuspid valve surgery and who underwent echocardiography before and after TV surgery. With a primary outcome being comprised of a composite of cardiovascular death, heart failure hospitalization, redo TV surgery, and heart transplantation, the authors showed an RV-GLS < 17.2% to be associated with a poor outcome during a mean follow-up of 3.8 years, and biventricular GLS < 34.0%, to be also associated with a poor prognosis. Transcatheter pulmonary valve replacement (TPVR) is a new and less invasive alternative to surgical valve replacement with acceptable long-term outcome (8). Yet, a large size transcatheter pulmonary valve could cause potential coronary artery compression and/or incomplete expansion of the stent which may increase the transvalvular gradient, and impact upon durability accelerated valve failure. To address this issue, Shang et al. explored the safety and efficacy of the Med-Zenith PT-Valve for the treatment of patients with severe pulmonary regurgitation (PR) and significantly enlarged RV outflow tract (RVOT). Successful valve implantations were achieved in all patients without noticeable device malposition, coronary artery compression, pulmonary branch obstruction or paravalvular leak. At 1-year follow-up, the RV end diastolic volume index reduced from the baseline $181.6 \pm 29.0$ to $123.4 \pm 31.2$ ml/m$^2$, and the 6-min walk distance increased from $416.6 \pm 97.9$ to $467.8 \pm 61.2$ m ($p < 0.05$ for all), demonstrating both, feasibility, and efficacy for the Med-Zenith PT-Valve in the treatment of severe PR with significantly enlarged RVOT.

## Approach to valvular heart disease

Undoubtedly, there have been notable improvements in cardiac imaging techniques, multidisciplinary team structures and new devices that are making a sizeable impact on how we identify, evaluate, and treat patients with VHD. A comprehensive review by Patel et al. showcases some of the current indications and potential future roles of cardiac CT in the assessment of aortic and mitral valves for transcatheter interventions, prosthetic valve complications such as thrombosis and endocarditis, and assessment of the myocardium. Equally important is the role of the patient in shared decision making on the management of patients with VHD which is explored by Saeed et al. Here the authors focus on the importance of patient reported outcome measures based on their own experience from specialist valve clinics and emphasize how this approach may improve post-intervention quality of life, as well as maintain the efficacy of the provided treatment.

## Conclusions

The prevalence of heart valve disease across the globe is increasing and with-it cardiovascular morbidity and mortality. As our understanding of the pathophysiology of HVD increases, so does our access to advanced imaging, new surgical and transcatheter techniques and integrated patient pathways. Despite significant developments over the last twenty years, there remain several unmet needs. These relate to better methods of identifying asymptomatic patients, predicting symptom onset and the development and implementation of new pharmacotherapeutic agents and medical devices. As we approach an era where computer processing power and artificial intelligence is reaching the clinical domain, the next twenty years are likely to witness a quantum leap in how we approach and manage patients with heart valve disease. If 10 years ago we thought that the future came quickly (9), then it will seem mild compared to how quickly new advances are coming to us.

## Author contributions

MB: Conceptualization, Writing – original draft. RR: Writing – review & editing.

## Conflict of interest

The authors declare that the research was conducted in the absence of any commercial or financial relationships that could be construed as a potential conflict of interest.

## Publisher's note



## Supplementary material

The Supplementary Material for this article can be found online at: https://www.frontiersin.org/articles/10.3389/fcvm.2023.1276202/full#supplementary-material

# References


1. Iung B, Delgado V, Rosenhek R, Price S, Prendergast B, Wendler O, et al. Contemporary presentation and management of valvular heart disease: the EURObservational research programme valvular heart disease II survey. *Circulation*. (2019) 140(14):1156–69. doi: 10.1161/CIRCULATIONAHA.119.041080

2. Mack M, Carroll JD, Thourani V, Vemulapalli S, Squiers J, Manandhar P, et al. Transcatheter mitral valve therapy in the United States: a report from the STS/ACC TVT registry. *Ann Thorac Surg*. (2022) 113(1):337–65. doi: 10.1016/j.athoracsur.2021.07.030

3. Banovic M, DaCosta M. Degenerative mitral stenosis: from pathophysiology to challenging interventional treatment. *Curr Probl Cardiol*. (2019) 44(1):10–35. doi: 10.1016/j.cpcardiol.2018.03.004

4. Gammie JS, Sheng S, Griffith BP, Peterson ED, Scott Rankin J, O'Brien SM, et al. Trends in mitral valve surgery in the United States: results from the society of thoracic surgeons adult cardiac database. *Ann Thorac Surg*. (2009) 87:1431–9. doi: 10.1016/j.athoracsur.2009.01.064

5. Levine MA, Shao W, Klein D. Monitoring of international normalized ratios: comparison of community nurses with family physicians. *Can Fam Physician*. (2012) 58:e465–71.

6. Stokke TM, Hasselberg NE, Smedsrud MK, Sarvari SI, Haugaa KH, Smiseth OA, et al. Geometry as a confounder when assessing ventricular systolic function: comparison between ejection fraction and strain. *J Am Coll Cardiol*. (2017) 70 (8):942–54. doi: 10.1016/j.jacc.2017.06.046

7. Banovic M, Mileva N, Moya A, Paolisso P, Beles M, Boskovic N, et al. Myocardial work predicts outcome in asymptomatic severe aortic stenosis: subanalysis of the randomized AVATAR trial. *JACC Cardiovasc Imaging*. (2023) 16(5):708–10. doi: 10.1016/j.jcmg.2022.10.019

8. Cheatham JP, Hellenbrand WE, Zahn EM, Jones TK, Berman DP, Vincent JA, et al. Clinical and hemodynamic outcomes up to 7 years after transcatheter pulmonary valve replacement in the US melody valve investigational device exemption trial. *Circulation*. (2015) 131:1960–70. doi: 10.1161/CIRCULATIONAHA.114.013588

9. Banovic M, Nikolic S, Putnik S. A randomized trial in patients with asymptomatic severe aortic stenosis: a future has begun!. *J Am Coll Cardiol*. (2016) 67(16):1970–1. doi: 10.1016/j.jacc.2016.01.068

frontiers in Cardiovascular Medicine

ORIGINAL RESEARCH
published: 13 January 2022
doi: 10.3389/fcvm.2021.795263

# The Transaxillary Approach *via* Prosthetic Conduit for Transcatheter Aortic Valve Replacement With the New-Generation Balloon-Expandable Valves in Patients With Severe Peripheral Artery Disease

*Alexander Lind*[1]*, *Alina Zubarevich*[2], *Arjang Ruhparwar*[2], *Matthias Totzeck*[1], *Rolf Alexander Jánosi*[1], *Tienush Rassaf*[1] *and Fadi Al-Rashid*[1]

[1] Department of Cardiology and Vascular Medicine, West-German Heart and Vascular Center Essen, University of Duisburg-Essen, Essen, Germany, [2] Department of Heart Surgery, West-German Heart and Vascular Center Essen, University of Duisburg-Essen, Essen, Germany

OPEN ACCESS

**Edited by:**
Marko Banovic,
University of Belgrade, Serbia

**Reviewed by:**
Stéphane Cook,
Université de Fribourg, Switzerland
Masahiko Asami,
Mitsui Memorial Hospital, Japan

***Correspondence:**
Alexander Lind
alexander.lind@uk-essen.de

**Specialty section:**
This article was submitted to Heart Valve Disease, a section of the journal Frontiers in Cardiovascular Medicine

**Received:** 14 October 2021
**Accepted:** 14 December 2021
**Published:** 13 January 2022

**Citation:**
Lind A, Zubarevich A, Ruhparwar A, Totzeck M, Jánosi RA, Rassaf T and Al-Rashid F (2022) The Transaxillary Approach via Prosthetic Conduit for Transcatheter Aortic Valve Replacement With the New-Generation Balloon-Expandable Valves in Patients With Severe Peripheral Artery Disease. Front. Cardiovasc. Med. 8:795263. doi: 10.3389/fcvm.2021.795263

**Background:** The left subclavian artery (LSA) is an infrequently used alternative access route for patients with severe peripheral artery disease (PAD) in patients who underwent transcatheter aortic valve replacement (TAVR). We report a new endovascular approach for TAVR combining an axillary prosthetic conduit-based access technique with new-generation balloon-expandable TAVR prostheses.

**Methods and Results:** Between January 2020 and December 2020, 251 patients underwent TAVR at the West German Heart and Vascular Center. Of these, 10 patients (3.9%) were deemed to be treated optimally by direct surgical exposure of the left or right axillary artery *via* a surgically adapted prosthetic conduit. All procedures were performed under general anesthesia. One procedural stroke occurred due to severe calcification of the aortic arch. No specific complications of the subclavian access site (vessel rupture, vertebral, or internal mammary ischemia) were reported. Two minor bleedings from the access site could be treated conservatively. No surgical revision was necessary.

**Conclusion:** The axillary prosthetic conduit-based access technique using new-generation balloon-expandable valves allows safe and successful TAVR in a subgroup of patients with a high risk of procedural complications due to severe peripheral vascular disease. Considering the increasing number of patients referred for TAVR, this approach could represent an alternative for patients with limited access sites.

**Keywords: TAVR, axillary access, conduit, prosthetic, Dacron, balloon-expandable prosthesis, percutaneous-methods**

## INTRODUCTION

Transcatheter aortic valve replacement (TAVR) continues to expand rapidly as a less invasive option for the treatment of severe aortic stenosis (AS) in patients considered at intermediate or high risk during surgical aortic valve replacement (1, 2). Delivery systems have evolved, corresponding sheath sizes have also diminished to facilitate higher rates of transfemoral (TF-)

TAVR. Therefore, TF access is the state-of-the-art access route for TAVR procedures with documented low periprocedural complications enabling early mobilization and discharge (3). However, a growing number of patients requiring TAVR may have femoral access issues, usually related to severe peripheral artery disease (PAD), small iliofemoral arteries, and comorbidities, such as hostile aortoiliac segment occlusive disease (3, 4). Initially, the transapical (TA) and transaortic (TAo) approaches were used whenever a TF approach was not anatomically feasible. However, the use of these non-arterial accesses was associated with worse outcomes, partially because of the need for thoracotomy (4–6). Due to the disappointing outcomes associated with these more traditional alternative access routes, alternative access sites, including transaxillary (TAx), trans-subclavian (TS), transcarotid, and transcaval access, have been developed (7–10). The TAx approach is considered the second option in many centers when TF-TAVR is not feasible. Within the more popular TAx and TS approaches, procedural techniques vary widely and most of the interventions using the TAx access have been performed with self-expanding valve platforms considering the necessity of assembling the balloon-expandable valve system in the ascending aorta (11–14).

Vessel access is gained either *via* open surgical access through an infraclavicular incision and direct insertion of a large-bore sheath directly into the axillary artery (15) or alternatively through direct percutaneous access of the vessel. However, the vascular complication rate is relatively high with up to 29.2% resulting in endovascular stent-graft implantation due to closure device failure (8).

A new option to facilitate surgical cut-down is a "chimney approach" using an end-to-side anastomosed prosthetic conduit for vessel access (16). This access facilitates the introduction of large self-expanding sheaths into the axillary artery and simplifies the valve mounting maneuver of the balloon-expandable system in the ascending aorta. The chimney approach overcomes access site complications and bleedings from overstretched self-expandable sheaths and is often used for central implanted mechanical circulatory support systems in the case of PAD (17, 18).

We here describe a series of patients treated with TAVR using a TAx approach with a Dacron graft (Terumo Vascular System Corp, Ann Arbor, MI, USA) in combination with a balloon-expandable aortic valve prosthesis.

# METHODS

## Patient Population

Between January 2020 and December 2020, 251 patients underwent TAVR at our center (19). In total, 210 patients underwent TF-TAVR (83.7%), 10 patients (3.9%) with severe AS and severe PAD underwent TAVR using the TAx approach, and 31 Patients (12.4%) underwent TA-TAVR due to small subclavian arteries or previous coronary artery bypass graft (CABG). Written informed consent was obtained from each patient following comprehensive assessment and discussion in the multidisciplinary Heart Valve Team meeting and was deemed best managed with TAVR. This retrospective single-center observational study was performed in accordance with the Declaration of Helsinki. The study protocol was approved by the ethics committee of the Faculty of Medicine of the University of Duisburg-Essen (no. 16-6894-BO). All parameters were analyzed anonymously.

Aortic stenosis severity was assessed using transthoracic echocardiography (TTE) according to the joint *European Society of Echocardiography* recommendations (20). Pre-operative imaging was performed in all patients using electrocardiogram-gated multidetector contrast CT angiography. Image analysis, including three-dimensional (3D) reconstructions extending from the aortic annulus to the superficial femoral artery, was performed using *3mensio Structural Heart* software version 9.1 (Pie Medical Imaging, Maastricht, Netherlands).

## Patient Selection

All patients admitted to the department of cardiology were primarily screened for femoral accessibility evaluating the planning CT angiogram using 3D reconstructions. Particular attention was paid to the caliber of the femoral arteries, the anatomical relationships of the side branches to the femoral head, the presence and extension of atherosclerotic plaques and calcifications, and the degree and extension of tortuosity. Severe bilateral occlusive PAD of the iliac and femoral arteries with a caliber $<5.5$ mm was considered as a contraindication for the TF approach. In this case, the TAx access was considered the second-best access route, and the right and left subclavian and axillary arteries were assessed on the planning CT angiograms using 3D reconstructions. Particular attention was paid to the aortic take-off of the subclavian artery, a typical site of atherosclerotic calcific plaque apposition (21). The presence of a patent right or left internal mammary artery to right coronary artery or left anterior descending artery was a contraindication for the use of this access due to the increased risk of vascular complication leading to the potentially lethal acute graft occlusion. Additionally, Doppler ultrasound (DUS) of the subclavian artery was performed visualizing and assessing the axillary portion of the vessel to control for pre- or post-interventional vessel stenosis, vessel occlusion, or local hematoma. Assessment of the proximal subclavicular portion of the vessel was only possible using 3D reconstructions of the vessel. Thereafter, all patients were discussed at a multidisciplinary Heart Valve Team meeting, and the TAx approach was deemed to be the most appropriate management strategy in each case.

## TAVR Procedure and Operative Technique

In all cases, general anesthesia was obtained. Central venous access is obtained *via* the left or right internal jugular vein to place a pacemaker for right atrium pacing. A left-sided 6F femoral arterial sheath was placed for pigtail placement.

After detailed skin disinfection, identification of the infraclavicular site and skin incision, the pectoralis minor was divided as required, and the brachial plexus cords were preserved (**Figure 1A**). The second part of the left or right axillary artery was identified, and proximal and distal controls were obtained. Unfractionated heparin was administered during the procedure. The initial heparin dose was 70 U/kg, and the

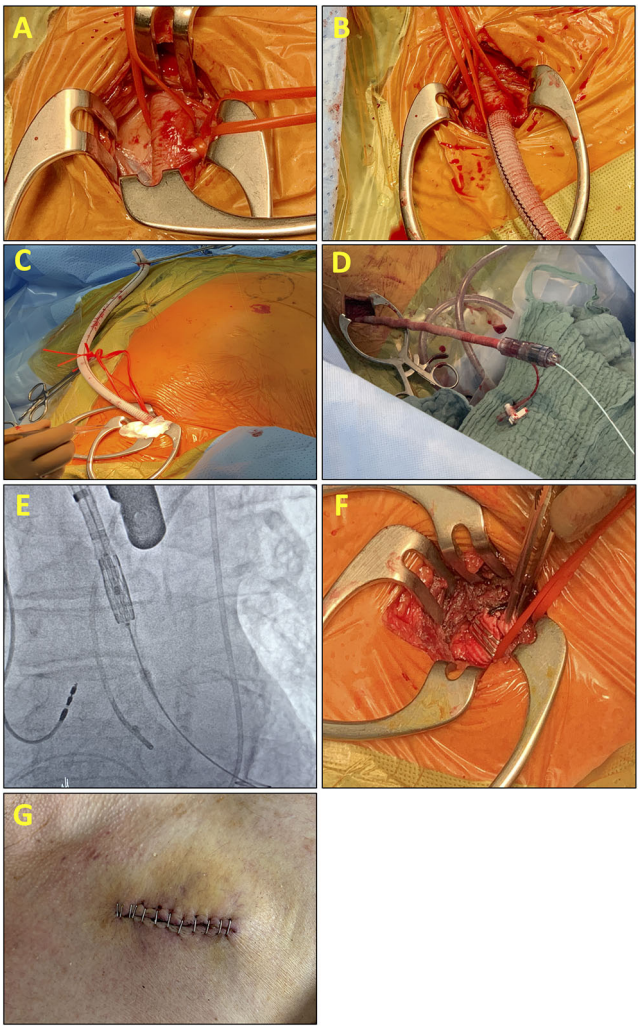


**FIGURE 1 |** Intraoperative pictures and fluoroscopic images explain the steps of the transaxillary (Tax) end-to-side prosthetic conduit for vessel access. **(A)** Preparation of the axillary artery with **(B)** end-to-side anastomosis of an 8-mm Dacron graft to the axillary artery. **(C)** Final position and length of the Dacron graft before the introduction of the eSheath. **(D)** eSheath is placed through the Dacron graft into the ascending aorta. **(E)** Fluoroscopic-guided advancement of the valve system through the subclavian artery with the Confida wire in the left ventricle. After valve implantation, the e-Sheath is retracted. **(F)** Postinterventional situs: Cut and clipped Dacron graft. **(G)** The wound is closed in a standard fashion with or without a drainage tube according to the preferences of the surgeon.

activated clotting time (ACT) was measured the latest before the insertion of the valve. If not being >250 s, an additional heparin bolus according to body weight was administered.

In nine patients, an 8-mm Dacron graft was anastomosed end-to-side to the axillary artery with a running 6-0 polypropylene suture, leaving the full length of the Dacron graft available to the introducer system (**Figure 1B**). In one patient, a 10-mm Dacron graft was used (22) (**Figure 1C**). The 14 French Edwards expandable introducer sheath (eSheath) (Edwards Lifescience Inc., Irvine, CA, USA) guided by a standard 180 cm 0.035 guidewire was inserted in the Dacron graft (**Figure 1D**). Advancement of the eSheath under fluoroscopic guidance facing the expandable part of the eSheath toward the superior wall of the vessel in line with the axillary artery and the subclavian artery was necessary to avoid increasing trauma to the vessel. The hydrophilic coating of the Edwards introducer system attached itself to the Dacron graft as soon as the complete insertion of the introducer system was finished. Under fluoroscopic guidance, an Amplatzer Left 1 catheter and a straight tipped wire was used to cross the aortic valve. A pigtail catheter was then used to exchange to a Confida Brecker guidewire (Medtronic, Minneapolis, MN, USA) into the left ventricle. Balloon aortic valvuloplasty was not required prior to implant in any patients (**Figure 1E**).

The technical challenge of deploying an Edwards TAVR *via* the axillary artery is that there is only limited space within the ascending aorta for the preparation of the valve. The critical step is to advance the sheath into the aortic arch just proximal to the entry into the left or right subclavian artery. In three cases with a short ascending aorta, the nose cone of the Commander Delivery System (Edwards Lifescience Inc., Irvine, CA, USA) was passed through the aortic valve into the left outflow tract. With the nose cone beyond the aortic annular plane, it is important to keep the delivery sheath in place to prevent the valve system from moving further into the left ventricle increasing the risk for ventricular rupture by a guidewire or nose cone displacement. Thereafter, the valve system is mounted as described in the instruction for use (IFU) of the Edwards Valve System. Mounting the valve system must be done quickly to prevent prolonged aortic regurgitation from worsening hemodynamics. Finally, the assembly is advanced together into the deployment position. The right sided axillary approach is technical even more challenging due to steeper angle between the subclavian artery and the ascending aorta compared to the left subclavian artery. Additionally, the distance from the ostium of the subclavian artery to the annular plane is shorter leading to increasing the risk of ventricular rupture and worsening hemodynamics due to prolonged mounting maneuvers.

When satisfactory positioning was achieved, rapid pacing was initiated, and the valve is deployed using the identical technique as that during routine implantation *via* the femoral artery. After valve implantation, the delivery system is withdrawn into the sheath and an angiogram is taken to confirm the correct positioning of the valve. A transthoracic echocardiogram was used to assess hemodynamic parameters (**Table 2**). The delivery system was then removed from the body under fluoroscopic guidance (**Figure 1F**). At the end of the procedure, the Dacron graft was clipped close to the subclavian artery, cut-off just distally of the clip, and the cut was sewn over (**Figure 1G**). Tight banding was not necessary.

## Anticoagulation Regime Before and After TAVR

If percutaneous coronary intervention (PCI) was performed before TAVR dual antiplatelet therapy (DAPT) was continued for up to 6 months post-PCI and thereafter reduced to single

antiplatelet therapy (SAPT) consisting of aspirin monotherapy lifelong. In patients without previous PCI, a loading dose of clopidogrel (600 mg per os) was administered after completion of the TAVR procedure and continued for 6 months according to 2017 guideline recommendations (20). In patients with the need for oral anticoagulation (OAK) being on vitamin K antagonist (VKA) before TAVR anticoagulation was paused until the International Normalized Ratio (INR) of 2.0 was reached. If necessary, bridging with intravenous (i.v.) full-dose unfractionated heparin (FDUH) was started before TAVR when INR was below 2.0. Heparin was paused 6 h before TAVR. Novel Oral Anticoagulants (NOACs) were stopped at least 48 h before the TAVR and resumed on the day after the procedure. Patients with the need for OAK and PCI before TAVR were continued on OAK and DAPT for 4 weeks. Bridging with FDUH was resumed on the first day after TAVR. VKA was simultaneously started. NOAC was re-initiated on the first post-operative day if the access site was uneventful. Thereafter, the anticoagulation regime was reduced to lifelong OAK and single platelet inhibition for 5 more months.

## Endpoint Definition

Peri- and post-procedural complications were evaluated according to the Valve Academic Research Consortium 3 (VARC-3) (23) (**Supplementary Table S1**).

## Statistics

All continuous data are reported as a mean, with or without SD. All categorical data are reported as percentages of the group. All statistical analyses were performed with SPSS 27.0.1.0 (IBM, Armonk, NY, USA).

# RESULTS

## Patient Population and Anatomic Data

The mean age was 79.8 ± 4.0 years. The mean aortic pressure gradient was 42.7 ± 20.1 mmHg, and the pre-procedural calculated aortic valve area was 0.75 ± 0.2 $cm^2$. The mean left ventricular ejection fraction was 42.0 ± 10.8% (range: 28–60%), the logistic European System for Cardiac Operative Risk Evaluation (EuroSCORE) was 18.4 ± 9.7% (STS Score 4.3 ± 2.4%), and 90% of the patients were in New York Heart Association functional class III or IV. Patient characteristics are summarized in **Table 1**.

**TABLE 1 |** Baseline characteristics of the study group.

| Variables | Overall ($n$ = 10) |
|---|---|
| Age (years) | 79.9 ± 4.0 |
| Male patients | 7 (70) |
| Body mass index ($kg/m^2$) | 24.9 ± 4.8 |
| NYHA III/IV | 9 (90) |
| Coronary artery disease | 9 (90) |
| Prior coronary artery bypass graft | 0 |
| Prior percutaneous coronary intervention | 6 (60) |
| Atrial fibrillation | 5 (50) |
| Previous cerebrovascular event | 1 (10) |
| Peripheral vascular disease prohibiting TF-TAVR | 10 (100) |
| Cerebral vascular disease | 1 (10) |
| Diabetes mellitus | 26 (31.3) |
| Renal insufficiency (GFR<60 $ml/min/m^2$) | 5 (50) |
| GFR ($ml/min/^2$) | 54.5 ± 24.3 |
| Logistic EuroScore (%) | 18.4 ± 9.7 |
| EuroScore II (%) | 5.5 ± 4.0 |
| Society of thoracic surgeons score (%) | 4.3 ± 2.4 |
| Left ventricular ejection fraction (%) | 42.0 ± 10.8 |
| Aortic valve area ($cm^2$) | 0.75 ± 0.2 |
| Mean aortic pressure gradient (mmHg) | 42.7 ± 20.1 |
| Mean diameter axillary artery (mm) | 6.7 ± 0.79 |

*Data are presented as mean ± SD or number (%); NYHA, New York Heart Association; GFR, glomerular filtration rate; TF-TAVR, transfemoral TAVR.*

## Procedural Success and 30-Day Major Adverse Cardiac and Cerebrovascular Events

Transcatheter aortic valve replacement was performed using the left axillary artery in nine patients. In one case, the right axillary artery was used. The mean diameter of the axillary arteries was 6.7 ± 0.8 mm. In nine patients, an 8-mm Dacron graft was used to match with the 14F and 16F Edwards eSheath, respectively. In one patient, a 10-mm Dacron graft was used. In this case, a thick silk suture was needed to prevent blood loss from the distal part of the graft. Calcification was absent in eight patients, one patient had mild calcification, severe calcification was present in one patient, respectively. DUS was performed before TAVI procedure and confirmed pre-interventional computed tomography (CT) findings. However, assessment of vessel calcification with DUS was not possible in the proximal subclavicular portion of the subclavian artery.

The incision-suture time was 91 ± 36 min (range 49–169 min). TAVR procedure time was 34 ± 16 min (range 15–34 min). Procedural device success according to the Valve Academic Research Consortium (VARC-3) criteria (23) was achieved in all patients (**Table 2**). Conversion to open-heart surgery was not necessary for any patient.

Obstruction of the coronary arteries by the valve prosthesis was not observed. The invasive mean postprocedural aortic transvalvular gradient was 11.5 ± 4.2 mmHg. Mild postprocedural aortic regurgitation was present in two patients (20%), trivial or no aortic regurgitation was seen in eight patients (80%). Periprocedural fatal stroke occurred in one patient (10%). The patient was presented with severe calcification of the left subclavian ostium, calcification of the aortic arch, and plaque of both carotid arteries. TAVR-access site was the LSA. Postinterventional CT showed ischemic infarction in the territory of the anterior cerebral artery and in the left posterior cerebellar artery with subsequent hemiplegia of the left hand. This patient had subsequently died 24 d later due to severe respiratory insufficiency based on severe pneumonia. Two bleeding complications (VARC-3 Type 2) were detected in patients on OAK. Bleedings were located at the cut-down site leading to minor vascular complications (VARC-3 minor)

**TABLE 2 |** Procedural details and adverse events.

| Variables | Overall $n = 10$ |
|---|---|
| Device success | 10 (100) |
| Incision-suture time (min) | 91.5 ± 36.3 |
| Procedure time TAVR (min) | 34.5 ± 16.3 |
| Fluoroscopy time (min) | 8.0 ± 1.5 |
| Contrast (ml) | 116.0 ± 39.8 |
| Mean aortic pressure gradient post-TAVR (mmHg) | 11.5 ± 4.2 |
| Length of postoperative hospital stay (days) | 9.2 ± 6.4 |
| Total hospital stay (days) | 18.8 ± 9.0 |
| Conscious sedation | 0 |
| Prior valvuloplasty | 0 |
| Annular rupture | 0 |
| Coronary obstruction | 0 |
| Valve size edwards sapien 3 (mm) | |
| 23 | 2 |
| 26 | 6 |
| 29 | 2 |
| New permanent pacemaker | 1 (10) |
| *VARC-3 complications* | |
| VARC-3 bleeding complications (BARC-Bleeding complications) | |
| Type 1 (BARC 2) | 2 (20) |
| Type 2 (BARC 3a) | 0 |
| Type 3 (BARC 3b, 3c) | 0 |
| Type 4 (BARC 5a, 5b) | 0 |
| VARC-3 vascular complications | |
| Minor | 1 (10) |
| Major | 0 |
| Periprocedural severe fatal Stroke (VARC-3) | 1 (10) |

*Data are presented as mean ± SD or number (%); NYHA, New York Heart Association; GFR, Glomerular filtration rate; BARC, Bleeding Academic Research Consortium; VARC-3, Valve Academic Research Consortium.*

and could be handled in both patients conservatively (20%). No blood transfusions due to bleeding complications were necessary (**Table 2**). No ischemic complication due to distal thromboembolism was detected.

Doppler ultrasound before discharge showed no stenosis or occlusion of axillary arteries in any patient. Permanent pacemaker implantation due to new onset of complete or high-grade atrioventricular was necessary for one patient (10%).

## DISCUSSION

This case series describes the first-time procedural steps and postprocedural results of TAVR with new-generation balloon-expandable valves using a surgical cut-down and a prosthetic conduit ("chimney approach") for axillary artery access.

The use of TAx TAVR is well-known for years and was described in 2008 for the first time (15). Since then, several technical improvements and increased operator familiarity with the method contributed to making this approach the second choice in many TAVR centers (24). Most subclavian registries, describing the subclavian approach, were technically TAx given the infraclavicular approach. The largest study to report TAx access with balloon-expandable valves was a single-center experience, including 100 cases of various valve types (25). Only limited case reports have been published using the newest generation balloon-expandable platform, the SAPIEN 3 Ultra (Edwards Lifescience, Irvine, California, USA), from a TAx approach (9, 26).

The end-to-side anastomosis of a Dacron vascular graft was described previously only using self-expandable second-generation valves (16). Some studies are promoting the completely percutaneous use of the TAx-TAVR technique. However, implantation rates of covered stents due to vascular complications or insufficient closure with vascular closure devices are observed in up to 50% of the patients, promoting further stent-related complications and driving interventional costs (24, 26–28).

We started to combine TAx surgical cut-down and end-to-side anastomosis of a Dacron vascular graft to facilitate save vessel access and valve preparation of the Edwards balloon-expandable valves in the ascending aorta. This modified technique avoids extensive manipulation of the artery in case of borderline vascular diameter allowing safe implantation even in patients with patent left or right internal mammary artery to the left anterior descending or right coronary artery compared to the direct open axillary access.

Transaxillary access was applied in only 3.9% of our TAVI population. This is in contrast to previous studies using the TAx approach in 5–10% of the cases when TF TAVR is not feasible (29). Considering the high proportion of patients who underwent TA-TAVR (12.4%) in our center and considering the necessity of thoracotomy leading to delayed mobilization and prolonged hospitalization, increased use of the TAx access seems to be reasonable.

The end-to-side anastomosis of a vascular graft allows prolonged manipulation of large sheaths inside the axillary and subclavian artery and completely accommodates the expandable Edwards eSheath (Edwards Lifescience Inc., Irvine, CA, USA) in different sizes outside the body in the Dacron graft simplifying the valve mounting maneuver of the Edwards Sapien S3 valve in the ascending aorta. Additionally, it is possible to keep the introducer sheath of the TAVR system above the aortic valve due to the "concertina effect" of the Dacron graft while hosting the eSheath of the Edwards Valve System. Applying this combination of Dacron vascular end-to-side graft with surgical cut-down and new-generation balloon-expandable valves led to a 100% implantation success rate.

The TAx approach is routinely used for other vascular interventions, such as complex aortic pathology with fenestrated endografts and extra-anatomic bypasses, while other traditional upper extremity access routes, such as the brachial artery, have problems due to sheath size limitations or frequent complications, such as thrombosis and risk of peripheral neurologic deficits (30). In this series, we were able to show a low peri- and post-interventional access site complication rate. We performed DUS to assess pre- and post-interventional vessel states. Compared to CT, DUS is radiation free and does not expose the patient to contrast agents. Hereby, we could exclude

any access site stenosis, vessel occlusion, or vessel thrombosis. Two minor cut-down site bleeding complications (VARC-3 Type 2 bleeding) were detected in our cohort in patients on OAK and could be treated conservatively by tight compression bandage. No blood transfusions due to bleeding complications were necessary. This contrasts with other studies promoting a complete percutaneous approach. These studies documented higher major access site complications ranging from 14 to 30% (25, 27). Postinterventional monitoring is particularly important. In studies describing direct percutaneous access, stent rate is high to resolve access site complications, such as bleeding with long-term stent complications, i.e., deformation and stent thrombosis in up to 18%.

Specific local access site complications described before, such as brachial plexus injury due to the axillary approach at the deltopectoral groove, could not be found in our series. This is in line with other studies suggesting low peripheral neurological complications (27, 31). The rate of periprocedural stroke is significantly higher in patients receiving TAVR through a TAx approach compared to the TF approach as described in a meta-analysis (OR 1.53 (95% CI, 1.05–2.22) (26, 32). However, these studies included only patients where the TAx approach was performed through a direct surgical cut-down without Dacron end-to-side graft. We observed one fatal stroke in a patient with severe calcification of the aortic arch and the ostium of the LSA. This is in line with previous studies emphasizing the need to identify the anatomic characteristics, such as severe calcifications of the axillary artery, the proximal part of the subclavian artery, and the aortic arch, which may lead to embolization of atheromatous plaque during the sheath transfer into the ascending aorta (32).

Bleeding control during the intervention and before TAVR positioning is of paramount importance for surgical access. Unfractionated heparin with an initial bolus of 5,000 IE units and an additional bolus according to weight were administered during the procedure to achieve an ACT target >250 s. Normalization of peri-interventional heparin anticoagulation with protamine was not necessary. Insertion of a drain because of peri-interventional bleeding was not necessary for any patient. Surgical site infection is an ever-present danger. To tackle this issue, all procedures must be performed under sterile conditions. In our study, no access site infection was observed. Therefore, mobilization of patients was possible on the next day after intervention with the goal to keep postinterventional hospitalization as short as possible. Postinterventional length of hospitalization was 9.2 ± 6.4 d, ranging from 4 to 24 days. This seems to be higher compared to other studies. However, our patient cohort includes urgent inpatients in whom complete pre-TAVR screening was performed and a postinterventional rehabilitation facility or a nursing home was to be organized during the hospitalization. However, our study group is rather small to draw definitive conclusions.

### Study Limitations

The present case series has several limitations that should be acknowledged. Most of the patients qualify for TF-TAVR. Therefore, the sample size is relatively limited (3.9%) and a larger series may improve technique and results. Additionally, multiple patients did not present at the outpatient clinic at 3-month or 1-year follow-up, resulting in an inability to report on VARC-3 adverse events beyond 30 days.

## CONCLUSION

In patients with high or prohibitive risk and no suitable femoral access site, TAx-TAVR using the end-to-side anastomosis of a prosthetic conduit offers a valuable alternative to TF-TAVR after a detailed evaluation of the axillary anatomy.

## DATA AVAILABILITY STATEMENT

The original contributions presented in the study are included in the article/**Supplementary Material**, further inquiries can be directed to the corresponding author.

## ETHICS STATEMENT

The studies involving human participants were reviewed and approved by Ethics Committee of the Faculty of Medicine of the University of Duisburg-Essen. The patients/participants provided their written informed consent to participate in this study.

## AUTHOR CONTRIBUTIONS

AL, FA-R, and RJ: conceptualization and writing—original draft preparation. AL, AZ, and FA-R: formal analysis. TR and AR: data curation. AL, RJ, MT, and FA-R: writing—review and editing. All authors have read and agreed to the published version of the manuscript.

## SUPPLEMENTARY MATERIAL

The Supplementary Material for this article can be found online at: https://www.frontiersin.org/articles/10.3389/fcvm.2021.795263/full#supplementary-material

## REFERENCES

1. Smith CR, Leon MB, Mack MJ, Miller DC, Moses JW, Svensson LG, et al. Transcatheter versus surgical aortic-valve replacement in high-risk patients. *N Engl J Med.* (2011) 364:2187–98. doi: 10.1056/NEJMoa1103510
2. Leon MB, Smith CR, Mack MJ, Makkar RR, Svensson LG, Kodali SK, et al. Transcatheter or surgical aortic-valve replacement in intermediate-risk patients. *N Engl J Med.* (2016) 374:1609–20. doi: 10.1056/NEJMoa1514616
3. Del Val D, Ferreira-Neto AN, Asmarats L, Maes F, Guimaraes L, Junquera L, et al. Transcatheter aortic valve replacement: relative safety and efficacy of the

procedure with different devices. *Expert Rev Med Devices.* (2019) 16:11–24. doi: 10.1080/17434440.2019.1552132
4. Holmes DR Jr, Nishimura RA, Grover FL, Brindis RG, Carroll JD, et al. Annual outcomes with transcatheter valve therapy: from the STS/ACC TVT registry. *J Am Coll Cardiol.* (2015) 66:2813–23. doi: 10.1016/j.jacc.2015.10.021
5. Thourani VH, Jensen HA, Babaliaros V, Suri R, Vemulapalli S, Dai D, et al. Transapical and transaortic transcatheter aortic valve replacement in the United States. *Ann Thorac Surg.* (2015) 100:1718–26. doi: 10.1016/j.athoracsur.2015.05.010
6. Elmariah S, Fearon WF, Inglessis I, Vlahakes GJ, Lindman BR, Alu MC, et al. Transapical transcatheter aortic valve replacement is associated with increased cardiac mortality in patients with left ventricular dysfunction: insights from the PARTNER I Trial. *JACC Cardiovasc Interv.* (2017) 10:2414–22. doi: 10.1016/j.jcin.2017.09.023
7. Greenbaum AB, Babaliaros VC, Chen MY, Stine AM, Rogers T, O'Neill WW, et al. Transcaval access and closure for transcatheter aortic valve replacement: a prospective investigation. *J Am Coll Cardiol.* (2017) 69:511–21. doi: 10.1016/j.jacc.2016.10.024
8. Schäfer U, Ho Y, Frerker C, Schewel D, Sanchez-Quintana D, Schofer J, et al. Direct percutaneous access technique for transaxillary transcatheter aortic valve implantation: "the Hamburg Sankt Georg approach". *JACC Cardiovasc Interv.* (2012) 5:477–86. doi: 10.1016/j.jcin.2011.11.014
9. Dahle TG, Castro NJ, Stegman BM, Dutcher JR, Teskey JM, Schmidt WT, et al. Supraclavicular subclavian access for sapien transcatheter aortic valve replacement- a novel approach. *J Cardiothorac Surg.* (2018) 13:16. doi: 10.1186/s13019-018-0706-9
10. Mylotte D, Sudre A, Teiger E, Obadia JF, Lee M, Spence M, et al. Transcarotid transcatheter aortic valve replacement. *JACC.* (2016) 9:472–80. doi: 10.1016/j.jcin.2015.11.045
11. Gleason TG, Schindler JT, Hagberg RC, Deeb GM, Adams DH, Conte JV, et al. Subclavian/axillary access for self-expanding transcatheter aortic valve replacement renders equivalent outcomes as transfemoral. *Ann Thorac Surg.* (2018) 105:477–83. doi: 10.1016/j.athoracsur.2017.07.017
12. Ciuca C, Tarantini G, Latib A, Gasparetto V, Savini C, Di Eusanio M, et al. Trans-subclavian versus transapical access for transcatheter aortic valve implantation: A multicenter study. *Catheter Cardiovasc Interv.* (2016) 87:332–8. doi: 10.1002/ccd.26012
13. Fröhlich GM, Baxter PD, Malkin CJ, Scott DJ, Moat NE, Hildick-Smith D, et al. Comparative survival after transapical, direct aortic, and subclavian transcatheter aortic valve implantation (data from the UK TAVI registry). *Am J Cardiol.* (2015) 116:1555–9. doi: 10.1016/j.amjcard.2015.08.035
14. Muensterer A, Mazzitelli D, Ruge H, Wagner A, Hettich I, Piazza N, et al. Safety and efficacy of the subclavian access route for TAVI in cases of missing transfemoral access. *Clin Res Cardiol.* (2013) 102:627–36. doi: 10.1007/s00392-013-0575-0
15. Ruge H, Lange R, Bleiziffer S, Hutter A, Mazzitelli D, Will A, et al. First successful aortic valve implantation with the corevalve revalving system via right subclavian artery access: a case report. *Heart Surg Forum.* (2008) 11:E323–4. doi: 10.1532/HSF98.20081021
16. Biasco L, De Backer O, Holme S, Søndergaard L, Jönsson A. The "chimney approach" for transcatheter aortic valve implantation: a strategy for trans axillarian bareback approach in patients with no other access options. *Catheter Cardiovasc Interv.* (2015) 86:E167–73. doi: 10.1002/ccd.25840
17. Abu Saleh WK, Mason P, Jabbari OA, Samir H, Bruckner BA. Successful use of surgically placed impella 5.0 and central extracorporeal membrane oxygenation circuit in a patient with postcardiotomy shock. *Tex Heart Inst J.* (2015) 42:569–71. doi: 10.14503/THIJ-14-4873
18. Stamou SC, Lin N, James T, Rothenberg M, Lovitz L, Faber C, et al. Alternative access versus transfemoral transcatheter aortic valve replacement in nonagenarians. *J Invasive Cardiol.* (2019) 31:171–5.
19. Rassaf T, Heusch G. The West German heart and vascular center at university medicine essen. *Euro Heart J.* (2021) 42:963–4. doi: 10.1093/eurheartj/ehaa980
20. Baumgartner HC, Hung JC-C, Bermejo J, Chambers JB, Edvardsen T, Goldstein S, et al. Recommendations on the echocardiographic assessment of aortic valve stenosis: a focused update from the European Association of Cardiovascular Imaging and the American Society of Echocardiography. *Eur Heart J Cardiovasc Imaging.* (2017) 18:254–75. doi: 10.1093/ehjci/jew335
21. Biasco L, Ferrari E, Pedrazzini G, Faletra F, Moccetti T, Petracca F, et al. Access sites for TAVI: patient selection criteria, technical aspects, and outcomes. *Front Cardiovasc Med.* (2018) 5:88. doi: 10.3389/fcvm.2018.00088
22. Poelman JE, van der Werf RW, Douglas YL, van den Heuvel AF, de Smet BJ, Mariani MA. Percutaneous aortic valve replacement using a subclavian artery graft. *Ann Thorac Surg.* (2012) 94:e95–6. doi: 10.1016/j.athoracsur.2012.03.017
23. Généreux P, Piazza N, Alu MC, Nazif T, Hahn RT, Pibarot P, et al. Valve academic research consortium 3: updated endpoint definitions for aortic valve clinical research. *J Am College Cardiol.* (2021) 77:2717–46. doi: 10.1016/j.jacc.2021.02.038
24. Tagliari AP, Saadi RP, Ferrari E, Taramasso M, Saadi EK. The role of the axillary artery as a second access choice in TAVI procedures. *Braz J Cardiovasc Surg.* (2021) 36:237–43. doi: 10.21470/1678-9741-2020-0343
25. Schäfer U, Deuschl F, Schofer N, Frerker C, Schmidt T, Kuck KH, et al. Safety and efficacy of the percutaneous transaxillary access for transcatheter aortic valve implantation using various transcatheter heart valves in 100 consecutive patients. *Int J Cardiol.* (2017) 232:247–54. doi: 10.1016/j.ijcard.2017.01.010
26. Dahle TG, Kaneko T, McCabe JM. Outcomes following subclavian and axillary artery access for transcatheter aortic valve replacement. *JACC.* (2019) 12:662–9. doi: 10.1016/j.jcin.2019.01.219
27. Ooms JF, Van Wiechen MP, Hokken TW, Goudzwaard J, De Ronde-Tillmans MJ, Daemen J, et al. Simplified trans-axillary aortic valve replacement under local anesthesia - A single center early experience. *Cardiovasc Revasc Med.* (2021) 23:7–13. doi: 10.1016/j.carrev.2020.11.025
28. Pisaniello AD, Fraser DGW, Colville H, Hasan R. Transcatheter aortic valve replacement via the right subclavian artery approach: a case series. *Innovations.* (2021) 16:188–91. doi: 10.1177/1556984520984436
29. Di Mario C, Eltchaninoff H, Moat N, Goicolea J, Ussia GP, Kala P, et al. The 2011-12 pilot European Sentinel Registry of Transcatheter Aortic Valve Implantation: in-hospital results in 4,571 patients. *EuroIntervention.* (2013) 8:1362–71. doi: 10.4244/EIJV8I12A209
30. Alvarez-Tostado JA, Moise MA, Bena JF, Pavkov ML, Greenberg RK, Clair DG, et al. The brachial artery: a critical access for endovascular procedures. *J Vasc Surg.* (2009) 49:378–85. doi: 10.1016/j.jvs.2008.09.017
31. Modine T, Obadia JF, Choukroun E, Rioufoul G, Sudre A, Laborde JC, et al. Transcutaneous aortic valve implantation using the axillary/subclavian access: Feasibility and early clinical outcomes. *J Thoracic Cardiovasc Surg.* (2011) 141:487–91.e1. doi: 10.1016/j.jtcvs.2010.01.044
32. Faroux L, Junquera L, Mohammadi S, Del Val D, Muntané-Carol G, Alperi A, et al. Femoral versus nonfemoral subclavian/carotid arterial access route for transcatheter aortic valve replacement: a systematic review and meta-analysis. *J Am Heart Assoc.* (2020) 9:17460. doi: 10.1161/JAHA.120.017460

**Conflict of Interest:** The authors declare that the research was conducted in the absence of any commercial or financial relationships that could be construed as a potential conflict of interest.

frontiers in Cardiovascular Medicine

ORIGINAL RESEARCH
published: 20 January 2022
doi: 10.3389/fcvm.2021.783507

# Transcatheter Mitral Valve-in-Valve Implantation With a New Transcatheter Heart Valve for Bioprosthetic Degeneration

*Yuntao Lu[1,2†], Ye Yang[1,2†], Wenshuo Wang[1,2†], Jinmiao Chen[1,2†], Minyan Yin[3], Liqi Huang[1,2], Lili Dong[4], Chunsheng Wang[1,2*] and Lai Wei[1,2,5*]*

[1] Department of Cardiac Surgery, Zhongshan Hospital, Fudan University, Shanghai, China, [2] Shanghai Engineering Research Center of Heart Valve, Shanghai, China, [3] Shanghai Institute of Medical Imaging, Shanghai, China, [4] Department of Echocardiography, Zhongshan Hospital, Fudan University, Shanghai, China, [5] Department of Cardiac Surgery, Shanghai Public Health Clinical Center, Shanghai, China

OPEN ACCESS

**Edited by:**
Ronak Rajani,
Guy's and St Thomas' NHS Foundation Trust, United Kingdom

**Reviewed by:**
Paolo Denti,
San Raffaele Hospital (IRCCS), Italy
Ganesh Manoharan,
Belfast Health and Social Care Trust, United Kingdom

***Correspondence:**
Lai Wei
wei.lai@zs-hospital.sh.cn
Chunsheng Wang
wangchunsheng@fudan.edu.cn

[†] These authors have contributed equally to this work and share first authorship

**Specialty section:**
This article was submitted to Heart Valve Disease, a section of the journal Frontiers in Cardiovascular Medicine

**Received:** 26 September 2021
**Accepted:** 16 December 2021
**Published:** 20 January 2022

**Citation:**
Lu Y, Yang Y, Wang W, Chen J, Yin M, Huang L, Dong L, Wang C and Wei L (2022) Transcatheter Mitral Valve-in-Valve Implantation With a New Transcatheter Heart Valve for Bioprosthetic Degeneration. Front. Cardiovasc. Med. 8:783507. doi: 10.3389/fcvm.2021.783507

**Background:** Transcatheter mitral valve-in-valve (TMVIV) procedure with aortic transcatheter heart valves has recently become a less invasive alternative for patients with mitral bioprosthetic dysfunction. This study reports the initial experience of TMVIV implantation using the J-Valve System (JieCheng Medical Technology Corporation Ltd., Suzhou, China).

**Methods:** A retrospective observational multicenter study was conducted to evaluate the short-term outcomes of TMVIV. In total, 26 consecutive patients with symptomatic bioprosthetic failure at eight hospitals underwent TMVIV using the J-Valve System between May 2019 and June 2021. Procedural results and clinical outcomes were analyzed using the Mitral Valve Academic Research Consortium criteria.

**Results:** The mean age was 75.3 ± 7.1 years and 69.2% of patients were female. The mean Society of Thoracic Surgeons Predicted Risk of Mortality score was 12.3 ± 8.3%. The technical success rate was 96.2%. Nine of the 26 patients (34.6%) were implanted with a J-Valve of a size equal to the internal diameters of the deteriorated prostheses. At the 30-day and 1-year follow-ups, all-cause mortality was 3.8 and 16.0% and the stroke rates were 0 and 12.0%, respectively. Device-related mortality was 0% and the mean mitral valve gradient was 6.4 ± 2.7 mm Hg. No patient experienced device embolization, left ventricular outflow tract obstruction, or mitral valve reintervention. Postprocedural mitral regurgitation was none or trace in all the patients. All the patients were in the New York Heart Association (NYHA) class ≤ II at the last follow-up.

**Conclusion:** Transcatheter implantation of the J-Valve System in high-risk patients with mitral bioprosthetic dysfunction was found to be a reasonable alternative and associated with good short-term outcomes.

**Keywords: bioprosthetic degeneration, valve-in-valve, J-Valve, transapical, mitral valve**

## INTRODUCTION

Mitral valve disease is the most prevalent form of valvular disease, affecting 10% of patients over the age of 75 years (1). Bioprosthetic valves have become more common in the treatment of mitral valve disease. Consequently, structural valve deterioration is the most prevalent problem and reoperation is required in as many as 35% of patients within the first 10 years after mitral valve surgery (2). Redo mitral valve surgery is associated with high perioperative morbidity and mortality (3, 4) due to repeat sternotomy, cardiopulmonary bypass, the older age of patients, and severe comorbidities. Nevertheless, transcatheter mitral valve-in-valve (TMVIV) implantation has been developed as a feasible and safe treatment for high-risk and inoperable patients (5–7). In TMVIV, an oversizing strategy is preferred due to the risk of embolization resulting from high gradient pressure between the ventricle and atrium. However, excessive oversizing may be unfavorable, as it leads to under expansion of the transcatheter heart valve (THV) device, which increases the risk of leaflet pin-wheeling, device thrombosis, and decreased durability (8).

The J-Valve System (JieCheng Medical Technology Corporation Ltd., Suzhou, China) is a low-profile, self-expanding THV (**Figures 1A,B**). Excellent short-term outcomes, such as 4.7% all-cause mortality, 2% new permanent pacemaker implantation, 0% coronary artery obstruction, and 0% myocardial infarction at the 1-year follow-up, have demonstrated the efficacy and safety of the J-Valve in the treatment of patients with aortic stenosis and/or insufficiency (9–12). While the J-Valve was originally designed to treat aortic stenosis and/or insufficiency (12), its specific self-positioning design is also favorable in TMVIV implantation. Inspired by the Sapien prosthesis (Edwards Lifesciences Incorporation, Irvine, California, USA) to initially perform transapical mitral valve-in-valve by crimping the valve into the delivery catheter in the opposite direction, we attempted to treat high-risk or inoperable patients with degenerative mitral bioprostheses using the J-Valve System.

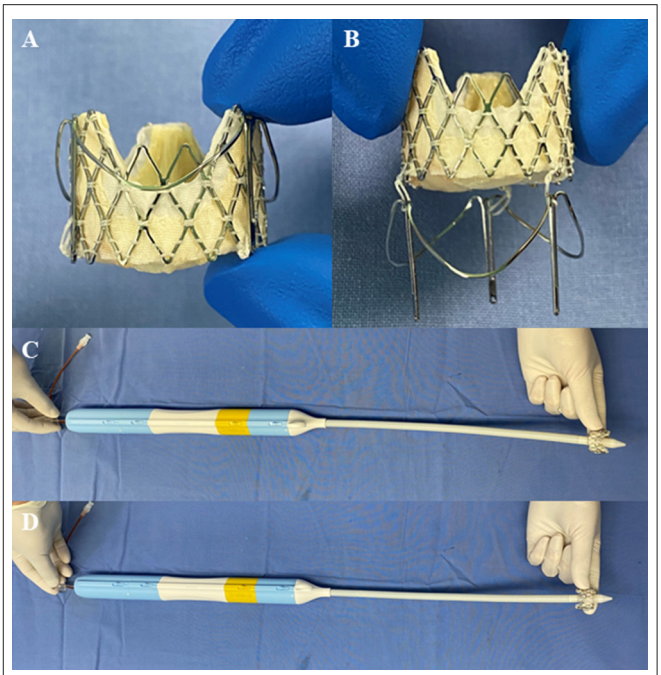


**FIGURE 1 |** The J-Valve system (JieCheng Medical Technology Corporation Ltd., Suzhou, China). **(A)** The prosthesis was combined with locators after release. **(B)** Movable connection between prosthesis and locators. **(C)** Prosthesis orientation for the transapical aortic valve replacement using the J-Valve system. **(D)** Prosthesis orientation for the transapical mitral valve-in-valve implantation using the J-Valve system.

## METHODS

### Patient Population

We conducted a retrospective observational analysis for all the consecutive patients who underwent TMVIV with the J-Valve System for the treatment of a degenerated mitral bioprosthesis at eight medical centers between May 2019 and June 2021. Indications for redo mitral valve replacement were based on the 2014 American College of Cardiology/American Heart Association Guideline for the Management of Patients with Valvular Heart Disease (13). All the patients were evaluated by a multidisciplinary heart team and found to have high surgical risk scores and/or severe comorbidity precluding redo valve surgery with cardiopulmonary bypass. The only exception was a 50-year-old patient whose symptoms could not be controlled by drugs. We strongly advised him to choose conventional surgery, but he still declined it and opted for TMVIV surgery as the preferred choice. The exclusion criteria for the TMVIV procedure were active endocarditis, prosthetic valve endocarditis, left atrial and/or left ventricular thrombosis, moderate or severe mitral paravalvular leakage, a true internal diameter (ID) of mitral bioprostheses $< 20$ mm, a requirement for concomitant coronary artery bypass graft, and high risk for TMVIV-induced left ventricular outflow tract (LVOT) obstruction.

### Ethics

All the patients or their legal representatives were fully informed about the procedure and signed written consent prior to surgery. The study protocol was approved by the Ethics Committee of Zhongshan Hospital, Fudan University.

### Devices

The J-Valve System is composed of a bioprosthetic valve and a transapical delivery catheter (**Figure 1C**). The bioprosthetic valve is a porcine valve supported by a self-expanding nitinol structure of different sizes: external diameters of 21, 23, 25, 27, and 29 mm. The size of the J-Valve mentioned below refers to the external diameter. A set of 3 "U" -shaped nitinol hoops were designed to surround the aortic valve as locators to position the device to sit in three aortic sinuses to facilitate accurate positioning of the implanted valve and fix it to the native valve (10). Valve sizes of 21, 23, and 25 mm were crimped into the

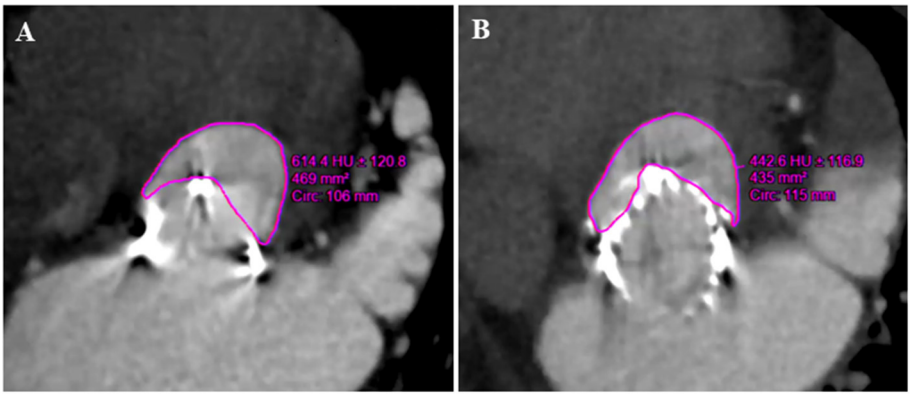


**FIGURE 2 |** Preoperative and postoperative multidetector CT in the assessment of neo-LVOT (Patient number 23). **(A)** The predicted area of neo-LVOT was 469 $mm^2$ before the J-Valve implantation. **(B)** The postoperative area of neo-LVOT was 435 $mm^2$. LVOT, left ventricular outflow tract.

27 F delivery catheter and 33 F catheter for valve sizes of 27 and 29 mm.

## Procedures

Before the procedure, all the patients underwent transthoracic echocardiography and contrast-enhanced multislice CT to assess (1) the severity and types of bioprosthetic failure; (2) the bioprosthesis dimensions for the sizing of the J-Valve; (3) the mitral valve, left ventricle, and aortic root anatomy to evaluate the risk of LVOT obstruction; and (4) the coronary vessels or bypass grafts for significant coronary artery disease.

The neo-LVOT surface area was estimated on CT images in systole (**Figure 2A**) using Vitrea software (version 6.5.3, Vital Images Incorporation, Minnetonka, Minnesota, USA). We used a predicted surface area $<200$ $mm^2$ as a cutoff value to identify patients at risk for TMVIV-induced LVOT obstruction.

The size of the J-Valve and the balloon used for valvuloplasty were selected based on the true ID of the surgical heart valves (SHVs) from CT measurements and/or the "valve-in-valve" app according to the manual of the manufacturer. In 15 patients, we oversized the implanted valves. A 23-mm J-Valve was implanted in only one patient with an SHV ID measuring 25 mm because of severe calcification of the leaflets. For the remaining patients, we implanted the J-Valve with the strategy of "true sizing" meaning that the size of the THV is equal to the ID of the SHV. The J-Valve prosthesis and three locators were preloaded into the delivery system direction opposite to that used for aortic valve replacement (**Figures 1C,D**).

With patients under general anesthesia, all the surgeries were performed in a hybrid operating room with cardiopulmonary bypass on standby. During the procedure, the C-arm was directed at a specific angle, so that any two of the three stent posts of the SHV totally overlapped under fluoroscopy. The transapical approach was used in all the cases. A limited left thoracotomy was made. Two 3–0 polypropylene (Ethicon, Somerville, New Jersey, USA) Teflon-reinforced mattress sutures were placed on the left ventricular apex and the patient was administered heparin to maintain an activated clotting time $>$ 250 s. A guidewire was inserted from the middle of the suture to reach the left atrium through the SHV. Balloon valvuloplasty was performed only in cases of mitral bioprosthetic stenosis before J-Valve implantation during rapid ventricular pacing (160–180 beats/min). The J-Valve delivery system was then inserted into the left ventricle and atrium *via* a guidewire. The three locators were released first and the delivery catheter was gently advanced toward the atrium to help the three locators accurately sit in the SHV "sinuses" among the three struts. Then, the J-Valve was released and deployed with the aid of the locators, so that it was fixed in the middle of the SHV after self-expansion (**Figure 3**). Finally, postimplant balloon valvuloplasty was performed in all the cases to ensure that the THV fully fit within the SHV (**Supplementary Video**). A vitamin

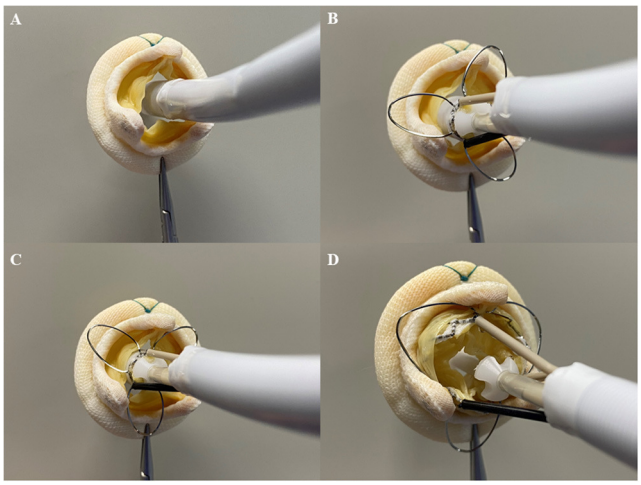


**FIGURE 3 |** Process of transapical mitral valve-in-valve implantation with the J-Valve system *in vitro*. **(A)** The delivery system was inserted into the surgical mitral prosthesis. **(B)** The locators were released. **(C)** The locators were placed in "sinuses" of the surgical mitral prosthesis. **(D)** The transcatheter prosthesis was released and the surgical mitral prosthesis was fixed between the transcatheter prosthesis and locators.

K antagonist was initiated on the day following the procedure with a target international normalized ratio of 2 to 3 for 6 months.

## Definitions and Study Endpoints

We used standardized endpoint criteria according to the Mitral Valve Academic Research Consortium (MVARC) for the data collection (14). The endpoints of this study included technical success at the exit from the procedure room as well as all-cause mortality. Other clinical endpoints, including device-related mortality, device embolization (the device moves during or after deployment such it loses contact with its initial position), LVOT obstruction, echocardiographic hemodynamic parameters, access site complications, myocardial infarction, stroke, permanent pacemaker implantation, bleeding, acute kidney injury, and rehospitalization at the 30-day follow-up and last clinical follow-up, were also evaluated. LVOT obstruction in this study was defined as a severe hemodynamic compromise. In addition, we collected data on procedure details, length of postprocedural hospital stay, and the New York Heart Association (NYHA) class at 30 days and last follow-up.

All the patients underwent transesophageal echocardiography examinations during the procedure and were followed-up using transthoracic echocardiography at discharge, 1 month, 3–6 months, 1 year, and once every year.

## Statistical Methods

Categorical variables are expressed as numbers and percentages. Normal variables are expressed as the mean ±SD. Nonnormally distributed parameters are presented using medians (interquartile ranges). The Kaplan–Meier survival curves were used to analyze survival. Statistical analysis was conducted using the SPSS software (version 20.0; SPSS Incorporation, Chicago, Illinois, USA).

# RESULTS

## Baseline Clinical Characteristics

Between May 2019 and June 2021, 26 consecutive patients (18 female; mean age 75.3 ± 7.1 years) with symptomatic bioprosthetic mitral valve dysfunction (regurgitation and/or stenosis) at eight centers underwent TMVIV. The indications for the TMVIV procedure were severe prosthetic stenosis in four patients, severe regurgitation in 21 patients, or a combination of stenosis and regurgitation in one patient. The mean Society of Thoracic Surgeons Predicted Risk of Mortality score was 12.3 ± 8.3%. Furthermore, the mean pulmonary artery systolic pressure was 61.8 ± 17.3 mm Hg and the mean left ventricular ejection fraction was 63.4 ± 5.8%. All the patients had heart failure symptoms with the NYHA classification III or IV at admission. The baseline characteristics of 26 patients are shown in **Table 1**.

**TABLE 1 |** Baseline clinical characteristics.

| Variables | *N* = 26 |
|---|---|
| Age, years | **75.3 ± 7.1** |
| Female | **18 (69.2)** |
| Body mass index, Kg/m$^2$ | **22.8 ± 3.6** |
| NYHA class III | **15 (57.7)** |
| NYHA class IV | **11 (42.3)** |
| STS, % | **12.3 ± 8.3** |
| Hypertension | **16 (61.5)** |
| Diabetes mellitus | **6 (23.1)** |
| Stroke | **3 (11.5)** |
| Atrial fibrillation | **17 (65.4)** |
| Chronic lung disease | **1 (3.8)** |
| Anemia | **8 (30.8)** |
| Prior CABG | **1 (3.8)** |
| Second redo cardiac surgery | **1 (3.8)** |
| Pulmonary Edema | **2 (7.7)** |
| ECMO | **1 (3.8)** |
| Emergency surgery | **3 (11.5)** |
| Mitral bioprosthetic dysfunction | |
| Duration, years | **11.0 ± 2.6** |
| Regurgitation | **21 (80.8)** |
| Stenosis | **4 (15.4)** |
| Combination | **1 (3.8)** |
| Tricuspid regurgitation | |
| Moderate | **7 (26.9)** |
| Severe | **9 (34.6)** |
| LA diameter, mm | **54.8 ± 10.0** |
| PASP, mmHg | **61.8 ± 17.3** |
| LVEF, % | **63.4 ± 5.8** |

*NYHA, New York Heart Association; STS, Society of Thoracic Surgeons; CABG, coronary artery bypass grafting; ECMO, extracorporeal membrane oxygenation; LA, left atrium; PASP, pulmonary artery systolic pressure; LVEF, left ventricular ejection fraction. Values are mean ± SD or n (%).*

## Procedure Details

Detailed characteristics of the failed bioprostheses and valve-in-valve procedure are shown in **Table 2**. The average duration from surgical valve replacement to bioprosthetic failure was 11.0 ± 2.6 years. Transapical valve-in-valve implantation was performed for all the patients. Balloon dilatation was performed in five prosthetic stenosis cases before J-Valve implantation (patient numbers 3, 4, 10, 13, and 15), and balloon dilatation was performed in all the patients after J-Valve implantation.

Other procedural results and 30-day outcomes are shown in **Table 3**. The technical success rate was 96.2%, as defined by the MVARC. One patient (patient number 14) needed second J-Valve implantation because one prolapsed leaflet of the SHV occluded the inflow tract after the first J-Valve implantation. Transcatheter aortic valve replacement (TAVR) with the J-Valve was simultaneously performed in one patient (patient number 14).

## 30-Day Outcomes

One patient (3.8%) died of pulmonary infection 8 days after the TMVIV procedure. No device embolization, LVOT obstruction, mitral valve reintervention, or neurological complications occurred. One patient (3.8%) developed acute kidney injury and renal function had recovered at discharge. One patient (3.8%) needed surgery *via* the left

**TABLE 2 |** Detailed characteristics of the failed bioprostheses and valve-in-valve procedure.

| Pt | Failed prosthesis type | Age year | Failure Mode | Label Size mm | True ID mm | S3 size by app | J-Valve size mm | Oversizing mm | | Balloon Dilatation | | Peak/Mean transvalvular gradient, mmHg | | MR grade (0–4) | |
|---|---|---|---|---|---|---|---|---|---|---|---|---|---|---|---|
| | | | | | | | | S3 | J-Valve | Pre | Post | Pre | Post | Pre | Post |
| 1 | Hancock II | 10 | MR | 27 | 22 | 23 | 25 | +1 | +3 | NO | YES | 34/14 | 10/5 | 4 | 1 |
| 2 | Perimount | 10 | MR | 25 | 23 | 26 | 23 | +3 | 0 | NO | YES | 29/14 | 14/5 | 4 | 1 |
| 3 | Hancock II | 10 | MS | 27 | 22 | 23 | 25 | +1 | +3 | YES | YES | 50/27 | 18/9 | 2 | 1 |
| 4 | Epic | 10 | MS | 29 | 25 | 26 | 27 | +1 | +2 | YES | YES | 45/21 | 11/7 | 1 | 0 |
| 5 | Hancock II | 12 | MR | 27 | 22 | 23 | 23 | +1 | +1 | NO | YES | 25/9 | 10/6 | 4 | 1 |
| 6 | CE Standard | 7 | MR | 27 | 23 | 26 | 23 | +3 | 0 | NO | YES | 27/14 | 10/6 | 4 | 1 |
| 7 | Hancock II | 10 | MR | 29 | 24 | 26 | 25 | +2 | +1 | NO | YES | NA | 7/5 | 4 | 1 |
| 8 | Hancock II | 13 | MR | 29 | 24 | 26 | 25 | +2 | +1 | NO | YES | 21/9 | 7/3 | 4 | 1 |
| 9 | Hancock II | 11 | MR | 27 | 22 | 23 | 25 | +1 | +3 | NO | YES | 38/NA | 28/NA | 4 | 0 |
| 10 | Perimount | 15 | MS | 27 | 25 | 26 | 25 | +1 | 0 | YES | YES | 41/NA | 14/NA | 2 | 1 |
| 11 | Hancock II | 11 | MR | 27 | 22 | 23 | 25 | +1 | +3 | NO | YES | NA | 6/4 | 4 | 0 |
| 12 | Hancock II | 10 | MR | 29 | 24 | 26 | 25 | +2 | +1 | NO | YES | 29/6 | 11/4 | 4 | 0 |
| 13 | Perimount | 17 | MS + MR | 27 | 25 | 26 | 23 | +1 | −2 | YES | YES | 29/NA | 9.0/NA | 2 | 1 |
| 14 | Epic | 14 | MR | 29 | 25 | 26 | 25 + 23 | +1 | 0 | NO | YES | 38/13 | 22/9 | 4 | 1 |
| 15 | Perimount | 15 | MS | 27 | 25 | 26 | 25 | +1 | 0 | YES | YES | 40/23 | 6/3 | 1 | 1 |
| 16 | CE Standard | 9 | MR | 29 | 25 | 26 | 25 | +1 | 0 | NO | YES | 15/7 | 6/4 | 4 | 1 |
| 17 | Epic | 8 | MR | 27 | 23 | 26 | 25 | +3 | +2 | NO | YES | 21/9 | 7/4 | 4 | 1 |
| 18 | Epic | 11 | MR | 27 | 23 | 26 | 23 | +3 | 0 | NO | YES | 19/8 | 12/7 | 4 | 1 |
| 19 | Hancock II | 11 | MR | 27 | 22 | 23 | 23 | +1 | +1 | NO | YES | 19/7 | 10/5 | 4 | 1 |
| 20 | Hancock II | 10 | MR | 29 | 24 | 26 | 25 | +2 | +1 | NO | YES | NA | NA/4 | 4 | 1 |
| 21 | Hancock II | 13 | MR | 29 | 24 | 26 | 25 | +2 | +1 | NO | YES | 13/7 | 9/4 | 4 | 1 |
| 22 | Epic | 6 | MR | 27 | 23 | 26 | 23 | +3 | 0 | NO | YES | 16/9 | 11/6 | 4 | 1 |
| 23 | Perimount | 15 | MR | 27 | 25 | 26 | 25 | +1 | 0 | NO | YES | 16/7 | 13/5 | 4 | 1 |
| 24 | Hancock II | 10 | MR | 27 | 22 | 23 | 23 | +1 | +1 | NO | YES | 18/10 | 16/9 | 4 | 1 |
| 25 | CE Standard | 8 | MR | 29 | 25 | 26 | 25 | +1 | 0 | NO | YES | 29/9 | 10/4 | 4 | 1 |
| 26 | Hancock II | 10 | MR | 25 | 20.5 | 23 | 23 | +2.5 | +2.5 | NO | YES | 16/7 | 13/9 | 4 | 1 |

*PT, patient; ID, internal diameter; S3, Sapien 3 (Edwards Lifesciences Incorporation, Irvine, California, USA); THV, transcatheter heart valve; MR, mitral regurgitation; CE, Carpentier-Edwards; NA, not available; MS, mitral stenosis; grade (0–4): 0 = none; 1 = trace; 2 = mild; 3 = moderate; 4 = severe.*

**TABLE 3 |** Procedural details and 30-day outcomes.

| Variables | *N* = 26 |
|---|---|
| Procedural details | |
| Transapical access | 26 (100) |
| J-Valve | 26 (100) |
| THV size strategy | |
| Oversizing | 15 (57.7) |
| "True sizing" | 9 (34.6) |
| Downsizing | 1 (3.8) |
| MVARC technical success | 25 (96.2) |
| Simultaneously TAVR | 1 (3.8) |
| Contrast dose, ml | 40 (20,140) |
| Procedural complications | 1 (3.8) |
| Conversion to surgery | 0 |
| Need for second THV implantation | 1 (3.8) |
| Dislocation | 0 |
| LVOT obstruction | 0 |
| Left ventricular perforation | 0 |
| 30-day outcomes | |
| Peak MVG, mmHg | 11.1 ± 5.1 |
| Mean MVG, mmHg | 5.8 ± 2.7 |
| Mitral valve regurgitation ≥ mild | 0 |
| Death | 1 (3.8) |
| Device-related death | 0 |
| Myocardial infarction | 0 |
| Stroke | 0 |
| Permanent pacemaker implantation | 0 |
| Access site complication | 1 (3.8) |
| Life-threatening Bleeding | 1 (3.8) |
| Acute kidney injury | 1 (3.8) |
| Stage 1 | 1 (3.8) |
| Stage 2 or 3 | 0 |
| Length of post-procedural hospital stay, days | 8 (4,30) |
| Cardiovascular rehospitalization | 0 |
| Noncardiovascular rehospitalization | 1 (3.8) |
| NYHA class ≥ III | 0 |

*THV, transcatheter heart valve; "true size: the size of transcatheter heart valve equal to the internal diameter of a deteriorated prosthesis; MVARC, Mitral Valve Academic Research Consortium; TAVR, transcatheter aortic valve replacement; LVOT, left ventricular outflow tract; MVG, mitral valve gradient; NYHA, New York Heart Association. Values are mean ± SD, n (%) or median (min, max).*

thoracic incision for life-threatening bleeding. One patient (3.8%) was rehospitalized because of pneumonia. The median length of the postprocedural hospital stay was 8 days (range, 4–30). Heart failure symptoms were significantly reduced and all the patients were at the NYHA II or less at the 30-day follow-up.

The peak mitral valve gradient (MVG) was 11.1 ± 5.1 mm Hg and the mean MVG was 5.8 ± 2.7 mm Hg. In total, 14 of 23 (60.9%) patients had a mean gradient of 5 mm Hg or less. The severity of paravalvular leakage or regurgitation was ≤ mild for all the patients. Notably, all the patients showed heart function improvement and were in the NYHA class ≤ II.

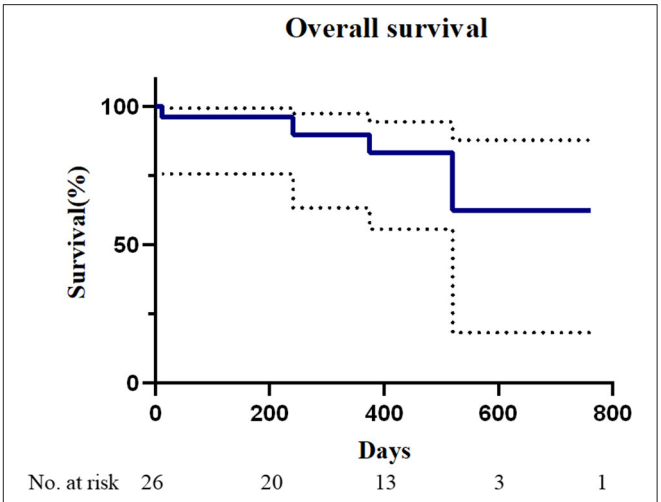


**FIGURE 4 |** Mortality after transapical mitral valve-in-valve implantation. The Kaplan–Meier analysis of overall survival in patients who underwent transapical mitral valve-in-valve (*n* = 26).

## 1-Year Follow-Up Outcomes

The median follow-up time was 370 days (range, 8–762 days). Only one patient had a postoperative follow-up time of less than 3 months. All-cause mortality was 16.0% and device-related mortality was 0%. The overall survival during follow-up is given in **Figure 4**. One patient (patient number 11) developed a hemorrhagic stroke from vitamin K antagonist overdose 251 days after TMVIV and she died of central nervous system infection 15 days after emergency lateral ventricular drainage. Another patient (patient number 13) with atrial fibrillation died of severe hemorrhagic stroke 375 days after TMVIV. One patient (patient number 3) died of pneumonia 520 days after implantation. One patient (patient number 5) with atrial fibrillation developed ischemic stroke from insufficient anticoagulation 228 days after TMVIV and had recovered without disability at the last visit. One patient (patient number 2) needed rehospitalization for tachycardia from atrial fibrillation. No patient experienced valve-related reintervention, device embolization, myocardial infarction, dialysis, or new pacemaker implantation.

The peak MVG was 16.9 ± 5.2 mm Hg and the mean MVG was 6.4 ± 2.7 mm Hg. Postprocedural mitral regurgitation was none or trace in all the patients. The mean left ventricular ejection fraction was 63.2 ± 4.6% and all the patients were in the NYHA class ≤ II. The last follow-up clinical outcomes are shown in **Table 4**.

# DISCUSSION

This study demonstrates the feasibility of the J-Valve for use in TMVIV in patients with degenerated mitral bioprostheses to treat mitral regurgitation, mitral stenosis, or a combination of the two. The MVARC-defined technical success rate with the J-Valve was 96.2%, which is comparable to that reported in the TMVIV multicenter registry study of 94.6% (7). TMVIV using

**TABLE 4 |** One-year outcomes.

| Variables | *N* = 25 |
|---|---|
| All-cause death | 4 (16.0) |
| Device-related death | 0 |
| Stroke | 3 (12.0) |
| Ischemic stroke | 1 (4.0) |
| Hemorrhagic stroke | 2 (8.0) |
| Access site complication | 1 (4.0) |
| Valve-related reintervention | 0 |
| Device embolization | 0 |
| New dialysis requirement | 0 |
| New pacemaker implantation | 0 |
| Mitral valve regurgitation ≥ mild | 0 |
| Peak MVG, mmHg | 16.9 ± 5.2 |
| Mean MVG, mmHg | 6.4 ± 2.7 |
| LVEF, | 63.2 ± 4.6 |
| PASP, mmHg | 42.4 ± 10.4 |
| Cardiovascular rehospitalization | 1 (4.0) |
| NYHA class ≥ III | 0 |

*MVG, mitral valve gradient; LVEF, left ventricular ejection fraction; PASP, pulmonary artery systolic pressure; NYHA, New York Heart Association. Values are mean ± SD or n (%).*

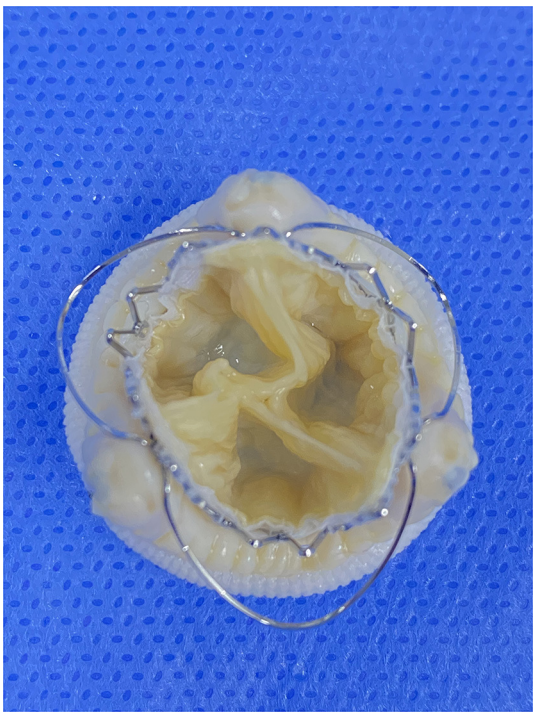

**FIGURE 5 |** The oversizing transcatheter heart valves implantation inside different surgical heart valves *in vitro*. Pinwheel-like leaflets of underexpanded transcatheter heart valves. A 23-mm J-Valve inside a 25-mm epic (internal diameter of 21 mm).

the J-Valve was also associated with good short-term outcomes. This study showed 3.8% all-cause mortality at the 30-day follow-up and 16.0% at 1-year follow-up, whereas the 30-day and 1-year all-cause mortality in the Transcatheter Valve Therapy Registry (5) were 5.4 and 16.7%, respectively. The stroke rates were 0 and 12.0% at the 30-day and 1-year follow-ups, respectively, and 1.1 and 3.3% in the previous report (5). No device-related death, device embolization, or LVOT obstruction occurred. All the patients experienced a clinically important improvement in heart failure symptoms during follow-up. The hemodynamic performance was acceptable after the TMVIV procedure with the J-Valve. The mean MVG was 5.8 mm Hg and 6.4 mm Hg at the 30-day and 1-year follow-ups, respectively, which is comparable to those in the TMVIV multicenter registry study of 7.3 mm Hg and 7.0 mm Hg, respectively (7). No patient had more than mild mitral regurgitation or required valve-related reintervention after TMVIV during follow-up.

In the TAVR procedure, the J-Valve System can fix the native aortic valves in the middle of its locators and frame, which can offer robust support to reduce the risk of left ventricular dislocation (10, 11). In addition, the J-Valve is the low-profile THV that is suitable for TMVIV implantation. In *in vitro* test, the locators could be deployed in the "sinuses" of the SHVs (**Figure 3**). The construction of the J-Valve with the locators could also reduce the risk of embolization, as it works in the aortic position. Inspired by these features, we initially applied the J-Valve in the TMVIV procedure as a second choice in the treatment of high-risk surgical patients with mitral bioprosthetic deterioration.

Currently, the Sapien 3 (Edwards Lifesciences Incorporation, Irvine, California, USA) is used as the standard THV for most TMVIV interventions with good short-term outcomes (7, 15). To avoid embolization, it is important to avoid parallel deployment and achieve conical deployment with an oversizing strategy (8). Unlike with the Sapien XT (Edwards Lifesciences Incorporation, Irvine, California, USA) (16), interventionists tend to select the proper Sapien 3 size selection following a slightly oversizing principle for its favorable extensibility. In the early exploration of the J-Valve system, interventionalists also performed the TMVIV procedure using an oversizing strategy that would lead to under expansion of the leaflets (**Figure 5**). Nevertheless, the J-Valve can be sized according to the ID of the SHV for the robust fixation of locators to reduce the risk of dislocation (**Figures 6A–P**). In this analysis cohort, 34.6% of patients underwent TMVIV according to the principle of "true sizing." Notably, 13 of the deteriorated SHVs in these patients were the Hancock II (Medtronic, Minneapolis, Minnesota, USA) whose label sizes of 29, 27, and 25 mm were corresponded to IDs of 24, 22, and 20.5 mm, respectively. Therefore, "true sizing" was unlikely to occur in patients with a Hancock II (**Table 2**). When the SHVs of the Hancock II were excluded, nine of 13 patients (69.2%) underwent TMVIV with the principle of "true sizing" (**Table 2**). No patient had experienced valve dislocation by the last follow-up. Therefore, TMVIV with a J-Valve system of "true sizing" may be feasible and would theoretically result in fully unfolded leaflets (**Figures 6A,I,M**), a lower gradient, and longer durability.

Left ventricular outflow tract obstruction is a potentially disastrous complication of TMVIV and predicting this condition still poses a challenge. The expected neo-LVOT area measured from cardiac CT is used to assess the risk of LVOT obstruction

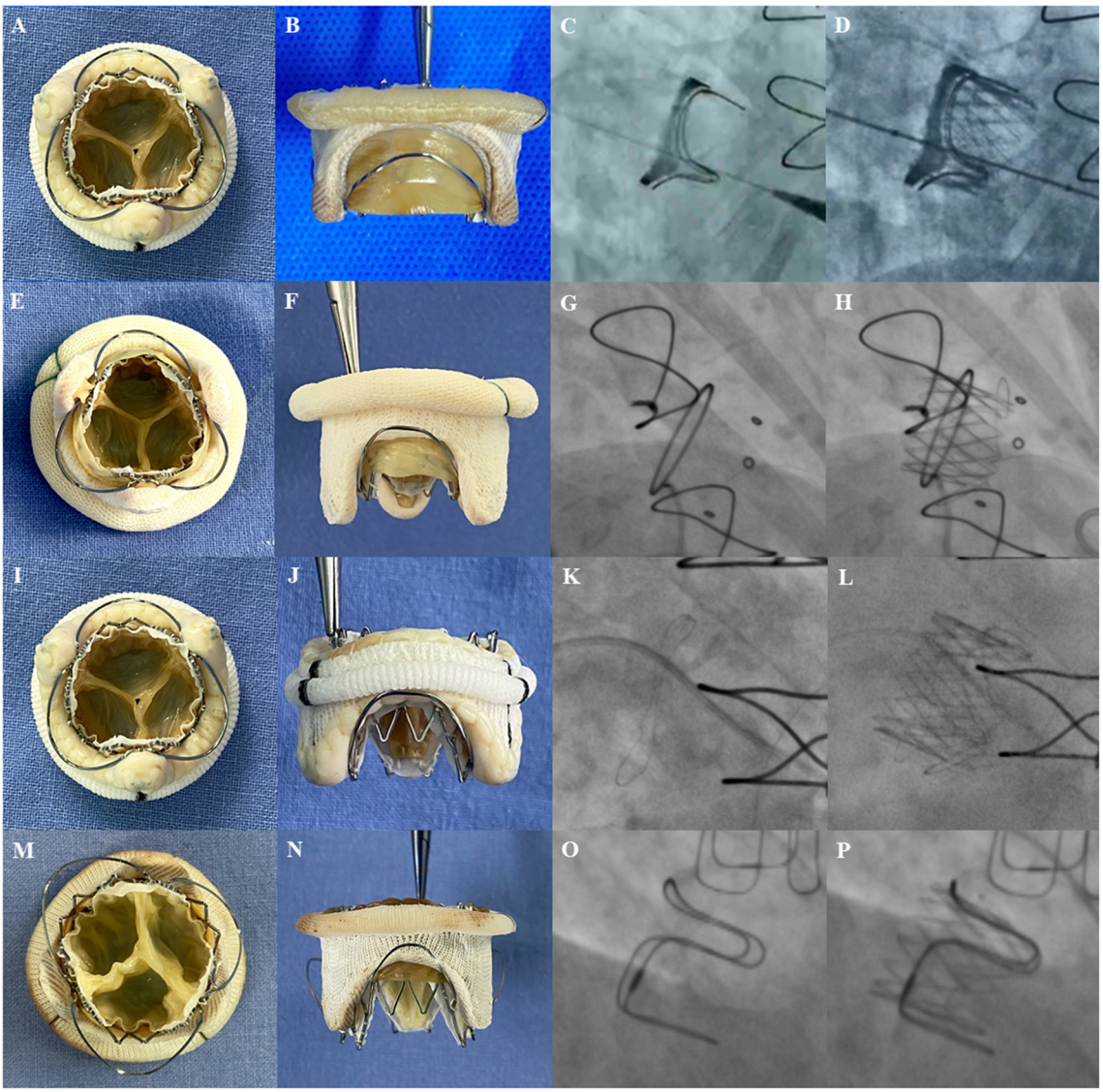


**FIGURE 6 |** The transcatheter heart valves implantation inside the different surgical heart valves. Photos of surgical bioprosthetic mitral valves with J-Valve implantation *in vitro* (left 2 panels) and fluoroscopic images before (third panel) and after (fourth panel) implantation. **(A,B)** A 23-mm J-Valve inside a 25-mm Perimount (internal diameter of 23 mm). **(C,D)** A 25-mm J-Valve inside a 27-mm Perimount (internal diameter of 25 mm); **(E,F)** A 21-mm J-Valve inside a 25-mm Mosaic (internal diameter of 20.5 mm); **(G,H)** A 25-mm J-Valve inside a 29-mm Hancock II (internal diameter of 24 mm); **(I,J)** A 21-mm J-Valve inside a 25 mm Epic (internal diameter of 21 mm); **(K,L)** A 23-mm J-Valve inside a 27-mm Epic (internal diameter of 23 mm). **(M,N)** A 25-mm J-Valve inside a 29-mm Carpentier-Edwards porcine (internal diameter of 25 mm). **(O,P)** A 25-mm J-Valve inside a 29-mm Carpentier-Edwards supra-annular valve (internal diameter of 25 mm).

caused by transcatheter mitral valve replacement (17, 18). All the patients in this study underwent multislice CT to evaluate the risk of LVOT obstruction and no patient in this study had a predicted neo-LVOT area $< 200$ mm$^2$ (**Figures 2A,B**).

At the time of surgical implantation, most surgeons prefer orienting SHVs such that two posts straddle the LVOT rather than the posterior annulus so that there is no strut occluding the LVOT. However, the SHV orientation does not influence the risk of LVOT obstruction during a TMVIV procedure with Sapien valves because the height of the skirt is lower than the leaflets of the SHV (19). In contrast, the frame and skirt of the J-Valve are wavelike (**Figure 1A**) and with the fixation of the locators, the struts of the J-Valve usually overlap the struts of the SHV (**Figures 6B,F,J,N**). This characteristic would not increase the risk of LVOT obstruction. However, the length of the bovine pericardial leaflets of the Perimount (SHV; Edwards Lifesciences Incorporation, Irvine, California, USA) is longer than J-Valve's frame (**Figure 6B**) or the other THVs, which might increase the risk of LVOT obstruction.

Previous studies have demonstrated transfemoral MVIV to be safer than transapical implantation with fewer complications and lower mortality (7, 15). The J-Valve system was primarily designed for transapical TAVR and the transfemoral J-Valve system is still under clinical trials. We had to perform the

procedure *via* transapical access rather than transvenous access. Similar to transapical aortic valve replacement, transapical TMVIV offers short and straight access to the degenerated SHV with good coaxial alignment. However, the transapical approach in this study still promoted less safe 30-day outcomes than the transfemoral approach in a large TMVIV study (7).

A previous study by Sung-Han Yoon et al. showed a high incidence of valve thrombosis after TMVIV (15). Nevertheless, anticoagulation therapy after TMVIV surgery is still controversial. Given the high proportion of atrial fibrillation (65.4%) in this cohort and the complex configuration of valve-in-valve, anticoagulation with warfarin was recommended for these patients for at least 6 months. However, two patients had a hemorrhagic stroke and one patient had an ischemic stroke during a 1-year follow-up. A retrospective review of the visit data of the three patients revealed that the two patients with hemorrhagic stroke both failed to regularly monitor prothrombin time. This may be the main reason why the stroke rate is obviously higher than that reported in other studies (7, 15) and it also suggests that anticoagulation education for the elderly should be improved.

Although TMVIV is becoming a promising therapy in high-risk patients with mitral bioprosthetic dysfunction and should be considered a therapeutic option (7), patients with small SHVs or low-risk patients may likely undergo redo surgical mitral valve replacement. This is because elevated valve gradients, the durability of the THVs, the optimal management of concomitant TR, and optimal anticoagulation strategies are still unknown and require further study (20).

## LIMITATION

In addition to the inherent bias of observational studies, the major limitation was that this study had a small sample size and short-term follow-up, as it included only 26 patients with a median follow-up time of 370 days (range, 8–762 days). Moreover, the leaflets of the surgical valves in **Figure 4** did not deteriorate. Thus, these simulations could not authentically represent valve-in-valve implantation *in vivo*.

## CONCLUSION

Transcatheter implantation of the J-Valve system within a degenerated mitral bioprosthesis *via* the transapical route is feasible and associated with good short-term outcomes in high-risk surgical patients. All the patients experienced improvements in heart failure after discharge. Owing to the locator units, the J-Valve system may be a good alternative to the TMVIV procedure and its use may shed light on new devices customized for valve-in-valve procedures.

## DATA AVAILABILITY STATEMENT

The original contributions presented in the study are included in the article/**Supplementary Material**, further inquiries can be directed to the corresponding authors.

## ETHICS STATEMENT

The studies involving human participants were reviewed and approved by Ethics Committee of Zhongshan Hospital, Fudan University. The patients/participants provided their written informed consent to participate in this study.

## AUTHOR CONTRIBUTIONS

YL, YY, WW, JC, CW, and LW contributed to the study conception and design. MY, LH, and LD performed material preparation, data collection, and analysis. YL, YY, and JC wrote the draft of the manuscript. All the authors have read and approved the final version of the manuscript.

## FUNDING

This study was supported by the National Natural Science Foundation of China (Grant Number: 81974272) and Shanghai Engineering Technology Research Center for Cardiac Intervention (Grant Number: 19DZ2250300).

## ACKNOWLEDGMENTS

We thank Dr Xue Yang for the consultation on neo-LVOT.

## SUPPLEMENTARY MATERIAL

The Supplementary Material for this article can be found online at: https://www.frontiersin.org/articles/10.3389/fcvm.2021.783507/full#supplementary-material

**Supplementary Video |** Transapical mitral valve-in-valve using the J-Valve system. The J-Valve delivery system was inserted into the left ventricle and atrium *via* a guidewire. The three locators were released first and the delivery catheter was gently advanced toward the atrium to help the three locators accurately sit in the "sinuses" of the surgical heart valve among the three structs. Then, the J-Valve was released and deployed with the aid of the locators, so that the J-Valve was fixed in the middle of the surgical prosthesis after self-expansion. Finally, postimplant balloon valvuloplasty was performed to ensure that the J-Valve fully fit within the failed prosthesis.

## REFERENCES

1. Nkomo VT, Gardin JM, Skelton TN, Gottdiener JS, Scott CG, Enriquez-Sarano M. Burden of valvular heart diseases: a population-based study. *Lancet.* (2006) 368:1005–11. doi: 10.1016/S0140-6736(06)69208-8
2. Thourani VH, Weintraub WS, Guyton RA, Jones EL, Williams WH, Elkabbani S et al. Outcomes and long-term survival for patients undergoing mitral valve repair versus replacement: effect of age and concomitant coronary artery bypass grafting. *Circulation.* (2003) 108:298–304. doi: 10.1161/01.CIR.0000079169.15862.13
3. Jones JM, O'Kane H, Gladstone DJ, Sarsam MA, Campalani G, MacGowan SW et al. Repeat heart valve surgery: risk factors for operative mortality. *J Thorac Cardiovasc Surg.* (2001) 122:913–8. doi: 10.1067/mtc.2001.116470

4. Jamieson WR, Burr LH, Miyagishima RT, Janusz MT, Fradet GJ, Lichtenstein SV et al. Reoperation for bioprosthetic mitral structural failure: risk assessment. *Circulation.* (2003) 108 Suppl 1:II98–102. doi: 10.1161/01.cir.0000089184.46999.f4
5. Guerrero M, Vemulapalli S, Xiang Q, Wang DD, Eleid M, Cabalka AK et al. Thirty-day outcomes of transcatheter mitral valve replacement for degenerated mitral bioprostheses (valve-in-valve), failed surgical rings (valve-in-ring), and native valve with severe mitral annular calcification (valve-in-mitral annular calcification) in the united states: data from the society of thoracic surgeons/american college of cardiology/transcatheter valve therapy registry. *Circ Cardiovasc Interv.* (2020) 13:e008425. doi: 10.1161/CIRCINTERVENTIONS.119.008425
6. Takagi H, Hari Y, Kawai N, Ando T. A meta-analysis of valve-in-valve and valve-in-ring transcatheter mitral valve implantation. *J Interv Cardiol.* (2018) 31:899–906. doi: 10.1111/joic.12564
7. Whisenant B, Kapadia SR, Eleid MF, Kodali SK, McCabe JM, Krishnaswamy A et al. One-year outcomes of mitral valve-in-valve using the SAPIEN 3 transcatheter heart valve. *JAMA Cardiol.* (2020). doi: 10.1001/jamacardio.2020.2974
8. Pirelli L, Hong E, Steffen R, Vahl TP, Kodali SK, Bapat V. Mitral valve-in-valve and valve-in-ring: tips, tricks, and outcomes. *Ann Cardiothorac Surg.* (2021) 10:96–112. doi: 10.21037/acs-2019-mv-169
9. Liu H, Yang Y, Wang W, Zhu D, Wei L, Guo K et al. Transapical transcatheter aortic valve replacement for aortic regurgitation with a second-generation heart valve. *J Thorac Cardiovasc Surg.* (2018) 156:106–16. doi: 10.1016/j.jtcvs.2017.12.150
10. Zhu L, Guo Y, Wang W, Liu H, Yang Y, Wei L et al. Transapical transcatheter aortic valve replacement with a novel transcatheter aortic valve replacement system in high-risk patients with severe aortic valve diseases. *J Thorac Cardiovasc Surg.* (2018) 155:588–97. doi: 10.1016/j.jtcvs.2017.09.015
11. Liu H, Liu S, Lu Y, Wang W, Yang Y, Zhu L et al. Transapical transcatheter aortic valve implantation for predominant aortic regurgitation with a self-expandable valve. *J Thorac Dis.* (2020) 12:538–49. doi: 10.21037/jtd.2020.01.04
12. Wei L, Liu H, Zhu L, Yang Y, Zheng J, Guo K et al. A New Transcatheter aortic valve replacement system for predominant aortic regurgitation implantation of the J-Valve and early outcome. *JACC Cardiovasc Interv.* (2015) 8:1831–41. doi: 10.1016/j.jcin.2015.08.021
13. Nishimura RA, Otto CM, Bonow RO, Carabello BA, Erwin JP, Guyton RA et al. 2014 AHA/ACC guideline for the management of patients with valvular heart disease: executive summary: a report of the American College of Cardiology/American Heart Association Task Force on practice guidelines. *Circulation.* (2014) 129:2440–92. doi: 10.1161/CIR.0000000000000029
14. Stone GW, Adams DH, Abraham WT, Kappetein AP, Généreux P, Vranckx P et al. Clinical trial design principles and endpoint definitions for transcatheter mitral valve repair and replacement: part 2: endpoint definitions: a consensus document from the mitral valve academic research consortium. *J Am Coll Cardiol.* (2015) 66:308–21. doi: 10.1016/j.jacc.2015.05.049
15. Yoon SH, Whisenant BK, Bleiziffer S, Delgado V, Dhoble A, Schofer N et al. Outcomes of transcatheter mitral valve replacement for degenerated bioprostheses, failed annuloplasty rings, and mitral annular calcification. *Eur Heart J.* (2019) 40:441–51. doi: 10.1093/eurheartj/ehy590
16. Bapat VV, Khaliel F, Ihleberg L. Delayed migration of Sapien valve following a transcatheter mitral valve-in-valve implantation. *Catheter Cardiovasc Interv.* (2014) 83:E150–4. doi: 10.1002/ccd.25076
17. Wang DD, Eng M, Greenbaum A, Myers E, Forbes M, Pantelic M et al. Predicting LVOT obstruction after TMVR. *JACC Cardiovasc Imaging.* (2016) 9:1349–52. doi: 10.1016/j.jcmg.2016.01.017
18. Wang DD, Eng MH, Greenbaum AB, Myers E, Forbes M. Karabon k et al. Validating a prediction modeling tool for left ventricular outflow tract (LVOT) obstruction after transcatheter mitral valve replacement (TMVR) Catheter. *Cardiovasc Interv.* (2018) 92:379–87. doi: 10.1002/ccd.27447
19. Little SH, Bapat V, Blanke P, Guerrero M, Rajagopal V, Siegel R. Imaging guidance for transcatheter mitral valve intervention on prosthetic valves, rings, and annular calcification. *JACC Cardiovasc Imaging.* (2020) 14:22–40. doi: 10.1016/j.jcmg.2019.10.027
20. Asgar AW. Transcatheter mitral valve-in-valve-A plausible option but questions remain. *JAMA Cardiol.* (2020). doi: 10.1001/jamacardio.2020.2993. [Epub ahead of print].


**Conflict of Interest:** The authors declare that the research was conducted in the absence of any commercial or financial relationships that could be construed as a potential conflict of interest.

**Publisher's Note:** All claims expressed in this article are solely those of the authors and do not necessarily represent those of their affiliated organizations, or those of the publisher, the editors and the reviewers. Any product that may be evaluated in this article, or claim that may be made by its manufacturer, is not guaranteed or endorsed by the publisher.

frontiers in Cardiovascular Medicine

ORIGINAL RESEARCH
published: 31 January 2022
doi: 10.3389/fcvm.2021.799285

# Impact of Prosthesis-Patient Mismatch on Hemodynamics During Exercise in Patients With Aortic Stenosis After Transcatheter Aortic Valve Implantation With a Balloon-Expandable Valve

*Haruka Kameshima[1], Masaki Izumo[1], Tomomi Suzuki[1], Hiroshi Ohara[2], Yukio Sato[1], Mika Watanabe[1], Shingo Kuwata[1], Kazuaki Okuyama[1], Ryo Kamijima[1], Manabu Takai[1], Seisyou Kou[1], Yasuhiro Tanabe[1], Tomoo Harada[1] and Yoshihiro J. Akashi[1]**

[1] Division of Cardiology, Department of Internal Medicine, St. Marianna University School of Medicine, Kawasaki, Japan, [2] Division of Cardiovascular Medicine, Department of Internal Medicine, Toho University Faculty of Medicine, Tokyo, Japan

OPEN ACCESS

**Edited by:**
*Marko Banovic,*
*University of Belgrade, Serbia*

**Reviewed by:**
*Alessandro Iadanza,*
*University of Siena, Italy*
*Tanja Katharina Rudolph,*
*Heart and Diabetes Center North Rhine-Westphalia, Germany*

***Correspondence:**
*Yoshihiro J. Akashi*
*johnny@marianna-u.ac.jp*

**Specialty section:**
*This article was submitted to Heart Valve Disease, a section of the journal Frontiers in Cardiovascular Medicine*

**Received:** *21 October 2021*
**Accepted:** *21 December 2021*
**Published:** *31 January 2022*

**Citation:**
*Kameshima H, Izumo M, Suzuki T, Ohara H, Sato Y, Watanabe M, Kuwata S, Okuyama K, Kamijima R, Takai M, Kou S, Tanabe Y, Harada T and Akashi YJ (2022) Impact of Prosthesis-Patient Mismatch on Hemodynamics During Exercise in Patients With Aortic Stenosis After Transcatheter Aortic Valve Implantation With a Balloon-Expandable Valve. Front. Cardiovasc. Med. 8:799285. doi: 10.3389/fcvm.2021.799285*

**Background:** There is no evidence of hemodynamic performance during exercise in patients with aortic stenosis (AS) after transcatheter aortic valve implantation (TAVI). This study aimed to investigate the changes in kinematic hemodynamics during exercise and determine the impact of prosthesis-patient mismatch (PPM) on the hemodynamics of transcatheter heart valves using exercise stress echocardiography (ESE) in AS patients after TAVI.

**Methods and Results:** This study enrolled 77 consecutive patients (mean age 82 ± 5 years, 50.6% male) who underwent ESE 3–6 months after TAVI with a balloon-expandable valve. The effective orifice area index at rest was significantly correlated with the mean pressure gradient (PG) during exercise ($p$ <0.001). The patients were divided into two groups according to the presence of PPM (PPM and non-PPM groups). During exercise, the patients with PPM had a higher left ventricular ejection fraction (74.6 ± 6.1% vs. 69.7 ± 9.6%, $p = 0.048$), a lower stroke volume index (47.2 ± 14.0 ml/m$^2$ vs. 55.6 ± 14.5 ml/m$^2$, $p = 0.037$), a significantly higher mean transvalvular PG (21.9 ± 9.1 mmHg vs. 12.2 ± 4.9 mmHg, $p = 0.01$) and an increased mean PG from rest to exercise (5.7 ± 3.5 mmHg vs. 2.3 ± 2.8 mmHg, $p$ <0.001) compared with patients without PPM. Patients with PPM had a higher pulmonary artery systolic pressure (SPAP) during exercise (57.3 ± 13.8 mmHg vs. 49.7 ± 10.9 mmHg, $p = 0.021$) and a higher incidence of exercise-induced pulmonary hypertension (43.8 vs. 15.0%, $p = 0.037$) than patients without PPM. PPM was strongly associated with exercise-induced pulmonary hypertension (hazard ratio: 3.570, $p = 0.013$).

**Conclusions:** AS patients with PPM after TAVI showed a disproportionate increase in the transvalvular PG and SPAP during exercise, and PPM was associated with exercise-induced pulmonary hypertension.

**Keywords: prosthesis-patient mismatch (PPM), aortic stenosis (AS), transcatheter aortic valve implantation (TAVI), exercise induced pulmonary hypertension, exercise stress echocardiography**

## INTRODUCTION

Aortic stenosis (AS) has become a common public health problem in the aging society. Transcatheter aortic valve implantation (TAVI) has changed the paradigm of care for AS patients and is currently being assessed for use in patients with a low surgical risk (1). As the indications for TAVI expand, the age of patients eligible for this type of treatment is decreasing and their level of activity in daily life is increasing accordingly. As a result, transcatheter heart valves (THVs) should have longer durability and better hemodynamic performance.

Prosthesis-patient mismatch (PPM) was first defined in 1978 to describe the mismatch between the hemodynamics of a valve prosthesis and the patient requirements for cardiac output (CO) (2). PPM occurs when the effective orifice area (EOA) of the prosthetic valve is very small in relation to the body surface area (BSA) of the patient, thus resulting in high residual postoperative pressure gradients (PGs) across the prosthesis. This problem is associated with postoperative prognosis (3–6) and prosthetic valve durability (7), and more recently, severe PPM has also been reported to be associated with prognosis after TAVI (6, 8, 9). However, to the best of our knowledge, there is no evidence of changes in hemodynamic performance during exercise in AS patients after TAVI. Therefore, the purpose of this study was to investigate the kinematic hemodynamics during exercise and determine the impact of PPM on the hemodynamics of THVs using exercise stress echocardiography (ESE) in AS patients after TAVI.

## MATERIALS AND METHODS

### Study Population and Study Design

This study retrospectively reviewed 256 consecutive patients who underwent TAVI with a balloon-expandable valve between January 2016 and December 2018 at the St. Marianna University School of Medicine Hospital. The Balloon-expandable valve devices were Sapien XT and Sapien 3 (Edwards Lifesciences, Irvine, CA, USA). Among these, 77 patients who underwent ESE 3–6 months after TAVI were enrolled in our study. **Figure 1** is a flow diagram of this study. All TAVI procedures were performed under general anesthesia. The study was performed in accordance with the Declaration of Helsinki and was approved by the Institutional Review Board of the St. Marianna University School of Medicine, Japan (No. 1288). Written informed consent was obtained from all the patients.

### Exercise Stress Protocol

Exercise was performed using the symptom-limited bicycle exercise test in the semi-supine position on a dedicated tilting exercise table at an initial workload of 10 Watt for 3 min, followed by a 10 Watt increase in workload every 3 min. Two-dimensional imaging and Doppler echocardiography data were obtained throughout the exercise test. The endpoints for terminating exercise were as follows: target heart rate reached, symptoms developed; blood pressure of $<80$ or $>220$ mmHg; ischemic electrocardiogram changes; ventricular arrhythmia; and rapid atrial tachycardia.

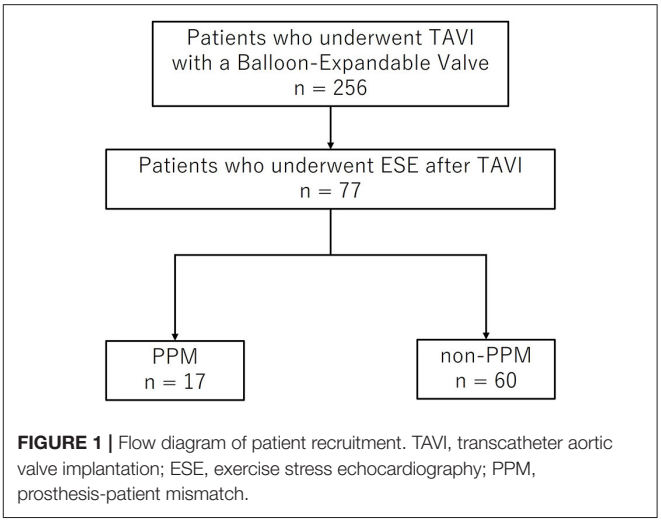


**FIGURE 1 |** Flow diagram of patient recruitment. TAVI, transcatheter aortic valve implantation; ESE, exercise stress echocardiography; PPM, prosthesis-patient mismatch.

### Transthoracic Echocardiography

Transthoracic echocardiography (Vivid E9; GE Vingmed Milwaukee, WI, USA) was performed at rest and during exercise. All images were digitally stored for offline analysis (EchoPAC, version 12; GE Vingmed Milwaukee, WI, USA), and they included standard two-dimensional, color, pulsed, and continuous-wave Doppler acquisitions according to the current American Society of Echocardiography guidelines (10). Left ventricular (LV) end-diastolic and end-systolic volumes and LV ejection fraction (LVEF) were measured from the standard apical views, according to Simpson's disk summation method. Stroke volume (SV) was measured in the left ventricular outflow tract (LVOT) using the Doppler method, and it was related to the BSA. The CO was obtained by multiplying the SV with heart rate. LV mass was calculated using two-dimensional images and the area-length method (10). To assess LV diastolic function, transmitral early (E-wave) and late (A-wave) velocities were measured using pulsed-wave Doppler imaging at the mitral leaflet tips. The peak early diastolic velocities of the septal mitral annulus (e') were measured using pulsed-wave tissue Doppler imaging from the apical 4-chamber view, and the E/e' ratio was calculated. Suspected pulmonary artery pressure (SPAP) was estimated based on the Doppler spectral signal of the tricuspid regurgitation jet. Pulmonary hypertension (PH) was defined as an SPAP of $\geq$40 mmHg at rest, and exercise-induced PH was defined as an SPAP of $\geq$60 mmHg during exercise. PPM was defined as an EOA index (EOAi) of $\leq$0.85 $cm^2/m^2$. The EOA of the THVs was calculated using the continuity equation, according to the current consensus document (11). From a zoomed parasternal long-axis view, the LVOT diameter was measured just below the apical border, i.e., from the outer border to the outer border of the stent or ring. To measure the LVOT flow velocity, the pulsed-wave Doppler was placed immediately below the apical border of the stent, with no valve opening or closing clicks visible. The transprosthetic flow velocity was determined by continuous-wave Doppler imaging with multiwindow interrogation, including the apical and right

parasternal windows. The valvulo-arterial impedance (Zva) was calculated using the following formula (12): Zva (mmHg/ml/$m^2$) = (mean transvalvular PG [mean PG] + systolic blood pressure)/(SV/BSA). Paravalvular leak was evaluated according to the Valve Academic Research Consortium 3 (13). The patients were divided into two groups according to the presence of PPM (PPM and non-PPM groups).

## Computed Tomography

Preprocedural multidetector computed tomography was performed, and aortic annulus area was measured from 3-dimensional reconstruction recommended by the Society of Cardiovascular Computed Tomography guidelines (14).

## Clinical Outcomes

The primary endpoint of this study was composite outcomes, including all-cause mortality, cardiovascular mortality, cardiovascular event, and heart failure-related hospitalization. The events were determined by reviewing the patients' medical reports or via direct telephonic contact with the patients' families.

## Statistical Analysis

All analyses were performed using SPSS (version 26.0.0, IBM Corporation, Somers, New York). Continuous variables are presented as mean ± standard deviation and were tested for differences using the Student's *t*-test. Categorical variables are presented as frequencies and percentages. The chi-squared and Fisher's exact tests were used to compare the PPM and non-PPM groups. The relationship between the preoperative and postoperative mean PG and the EOAi was evaluated using a simple inverse regression analysis, with r-values (Pearson's correlation coefficient). Survival was estimated using Kaplan-Meier analysis and compared using the two-sided log-rank test. The effects of clinical and echocardiographic parameters were assessed using the Cox proportional hazard model. Statistical significance was set at $p < 0.05$.

# RESULTS

## Clinical and Pre-procedural Echocardiographic Characteristics

Patients with PPM accounted for 17 (22.1%) of the total 77 patients, which included 15 (19.5%) patients with moderate

**TABLE 1 |** Procedural results and baseline characteristics.

| | All ($n = 77$) | PPM ($n = 17$) | Non-PPM ($n = 60$) | *p*-value (PPM vs. non-PPM) |
|---|---|---|---|---|
| Age, years | 82 ± 5 | 80 ± 6 | 83 ± 4 | 0.003 |
| Men, *n* (%) | 39 (50.6) | 7 (41.2) | 32 (53.3) | 0.742 |
| Body surface area, $m^2$ | 1.50 ± 0.17 | 1.50 ± 0.13 | 1.50 ± 0.18 | 0.855 |
| Hypertension, *n* (%) | 65 (84.4) | 12 (15.6) | 53 (88.3) | 0.085 |
| Diabetes, *n* (%) | 16 (20.8) | 3 (17.6) | 13 (21.7) | 0.507 |
| Hypercholesterolemia, *n* (%) | 51 (66.2) | 11 (64.7) | 40 (66.7) | 0.548 |
| Chronic kidney disease, *n* (%) | 51 (66.2) | 10 (58.8) | 41 (68.3) | 0.325 |
| Atrial fibrillation, *n* (%) | 31 (40.3) | 6 (35.3) | 25 (41.7) | 0.428 |
| Coronary artery disease, *n* (%) | 27 (35.1) | 3 (17.6) | 24 (40.0) | 0.075 |
| Myocardial infarction, *n* (%) | 6 (7.8) | 2 (11.8) | 4 (6.7) | 0.397 |
| Pre procedure NYHA class | | | | 0.554 |
| II, *n* (%) | 47 (61.0) | 12 (70.6) | 35 (58.3) | |
| III-IV, *n* (%) | 28 (36.4) | 5 (29.4) | 23 (38.3) | |
| Post procedure NYHA class | | | | 0.467 |
| I, *n* (%) | 64 (83.1) | 13 (76.5) | 51 (85.0) | |
| II, *n* (%) | 13 (16.9) | 4 (23.5) | 9 (15.0) | |
| III-IV, *n* (%) | 0 (0) | 0 (0) | 0 (0) | |
| STS score | 5.01 ± 2.64 | 4.45 ± 2.21 | 5.17 ± 2.74 | 0.324 |
| Annulus area, $mm^2$ | 425 ± 89 | 365 ± 64 | 442 ± 89 | 0.001 |
| **THV size** | | | | 0.001 |
| 20 mm, *n* (%) | 5 (6.5) | 3 (17.6) | 2 (3.3) | |
| 23 mm, *n* (%) | 36 (46.8) | 13 (76.5) | 23 (38.3) | |
| 26 mm, *n* (%) | 31 (40.3) | 1 (5.9) | 30 (50.0) | |
| 29 mm, *n* (%) | 5 (6.5) | 0 (0) | 5 (8.3) | |
| **Approach** | | | | 0.276 |
| Trans-femoral, *n* (%) | 72 (93.5) | 17 (100) | 55 (91.7) | |

*Data presented as mean ± standard deviation or n (%). PPM, prosthesis-patient mismatch; CABG, coronary artery bypass grafting; NYHA, New York Heart Association; STS, The Society of Thoracic Surgeons; THV, transcatheter heart valve.*

PPM (EOAi of 0.65 $cm^2/m^2$ < and ≤0.85 $cm^2/m^2$) and 2 (2.6%) patients with severe PPM (which was defined as an EOAi of ≤0.65 $cm^2/m^2$.) The baseline characteristics of the study patients and the procedural characteristics of TAVI are summarized in **Table 1** and **Supplementary Table 1**. The mean age of the study patients was 82 ± 5 years, and 50.6% of the patients were men. The mean Society of Thoracic Surgeons score was 5%, which indicates an intermediate surgical risk. Balloon-expandable THVs of 23 or 26 mm size were used in most patients. Patients with PPM were younger than patients without PPM, and no significant differences were found in sex between the PPM and non-PPM groups. Although the preoperative functional status in terms of the New York Heart Association (NYHA) functional class was similar between the groups, the post-procedure NYHA functional class tended to be higher in patients with PPM than in those without PPM; however, the

**TABLE 2 |** Preoperative echocardiography characteristics.

| | All ($n = 77$) | PPM ($n = 17$) | Non-PPM ($n = 60$) | *p*-value (PPM vs. non-PPM) |
|---|---|---|---|---|
| LVEDV, ml | 85 ± 33 | 78 ± 21 | 87 ± 36 | 0.349 |
| LVESV, ml | 32 ± 23 | 26 ± 11 | 34 ± 25 | 0.263 |
| LVEF, % | 65.4 ± 10.1 | 66.9 ± 6.6 | 64.9 ± 10.9 | 0.465 |
| SVi, $ml/m^2$ | 42.0 ± 11.7 | 41.0 ± 8.3 | 42.3 ± 12.5 | 0.687 |
| LVMi, $g/m^2$ | 108 ± 30 | 109 ± 28 | 108 ± 31 | 0.883 |
| E/A | 0.87 ± 0.90 ($n = 61$) | 0.87 ± 0.59 ($n = 14$) | 0.87 ± 0.98 ($n = 47$) | 0.977 |
| E/e' | 16.6 ± 7.2 | 16.7 ± 7.7 | 16.6 ± 7.1 | 0.961 |
| SPAP, mmHg | 32.1 ± 9.6 | 33.0 ± 10.1 | 31.8 ± 9.5 | 0.645 |
| Peak velocity, m/s | 4.3 ± 1.1 | 4.8 ± 1.4 | 4.1 ± 1.0 | 0.030 |
| Mean PG, mmHg | 44.9 ± 23.9 | 56.1 ± 32.3 | 41.7 ± 20.1 | 0.097 |
| AVA, $cm^2$ | 0.64 ± 0.19 | 0.57 ± 0.16 | 0.66 ± 0.19 | 0.087 |
| AVAi, $cm^2/m^2$ | 0.42 ± 0.12 | 0.38 ± 0.10 | 0.44 ± 0.12 | 0.064 |

*Data presented as mean ± standard deviation or n (%). LVEF, left ventricular ejection fraction; LVEDV, left ventricular end-diastolic volume; LVESV, left ventricular end-systolic volume; SVi, stroke volume index; CO, cardiac output; LVMi, left ventricular mass index; SPAP, systolic pulmonary artery pressure; Mean PG, mean transvalvular pressure gradient; AVA, aortic valve area; AVAi, aortic valve area index. The other abbreviations are shown in* ***Table 1****.*

**TABLE 3 |** Resting echocardiography data.

| | All ($n = 77$) | PPM ($n = 17$) | Non-PPM ($n = 60$) | *p*-value (PPM vs. non-PPM) |
|---|---|---|---|---|
| Systolic BP, mmHg | 139 ± 22 | 141 ± 25 | 138 ± 21 | 0.596 |
| Diastolic BP, mmHg | 68 ± 15 | 72 ± 14 | 68 ± 16 | 0.361 |
| Heart rate, beats/min | 67 ± 11 | 66 ± 10 | 68 ± 10 | 0.620 |
| LVMi, $g/m^2$ | 84 ± 24 | 84 ± 21 | 83 ± 24 | 0.889 |
| LVEDV, ml | 85 ± 29 | 77 ± 20 | 88 ± 31 | 0.211 |
| LVESV, ml | 31 ± 19 | 25 ± 8 | 33 ± 21 | 0.099 |
| LVEF, % | 65.4 ± 10.1 | 67.4 ± 8.1 | 63.6 ± 8.8 | 0.110 |
| SVi, $ml/m^2$ | 49.2 ± 12.3 | 43.2 ± 11.9 | 50.9 ± 12.0 | 0.023 |
| CO, ml/min | 4.9 ± 1.2 | 4.2 ± 1.0 | 5.0 ± 1.1 | 0.008 |
| E/A | 0.72 ± 0.18 ($n = 58$) | 0.79 ± 0.17 ($n = 14$) | 0.79 ± 0.18 ($n = 44$) | 0.105 |
| E/e' | 21.8 ± 9.9 | 23.0 ± 9.3 | 21.5 ± 10.1 | 0.575 |
| SPAP, mmHg | 29.4 ± 7.9 | 32.5 ± 8.0 | 28.0 ± 7.7 | 0.070 |
| TAPSE/SPAP | 0.64 ± 0.26 | 0.57 ± 0.24 | 0.66 ± 0.26 | 0.228 |
| Pulmonary hypertension, *n* (%) | 7 (9.1) | 3 (17.6) | 4 (6.7) | 0.182 |
| Peak velocity, m/s | 2.3 ± 0.46 | 2.7 ± 0.52 | 2.2 ± 0.37 | <0.001 |
| Mean PG, mmHg | 11.3 ± 5.0 | 16.2 ± 6.4 | 9.9 ± 3.5 | 0.001 |
| Zva, $mmHg/ml/m^2$ | 3.2 ± 0.81 | 3.8 ± 0.96 | 3.0 ± 0.67 | <0.001 |
| PVL | 1.3 ± 0.98 | 0.91 ± 1.0 | 1.4 ± 0.95 | 0.066 |
| EOAi, $cm^2/m^2$ | 1.08 ± 0.31 | 0.74 ± 0.07 | 1.17 ± 0.28 | <0.001 |

*Data presented as mean ± standard deviation or n (%). BP, blood pressure; TAPSE, tricuspid annular plane systolic excursion; Mean PG, mean transvalvular pressure gradient; Zva, valvulo-arterial impedance; PVL, para-valvular leak; EOA, effective orifice area; EOAi, effective orifice area index. The other abbreviations are shown in* ***Tables 1****,* ***2****.*

**TABLE 4 |** Exercise stress echocardiography data.

| | All ($n = 77$) | PPM ($n = 17$) | Non-PPM ($n = 60$) | *p*-value (PPM vs. non-PPM) |
|---|---|---|---|---|
| Exercise duration, min | 10.3 ± 3.6 | 9.7 ± 2.4 | 10.5 ± 3.9 | 0.274 |
| Peak watt, Watt | 32 ± 14 | 32 ± 10 | 32 ± 14 | 0.876 |
| Systolic BP, mmHg | 180 ± 30 | 187 ± 21 | 178 ± 32 | 0.153 |
| Diastolic BP, mmHg | 76 ± 16 | 84 ± 15 | 74 ± 16 | 0.015 |
| Heart rate, beats/min | 104 ± 18 | 107 ± 21 | 103 ± 17 | 0.354 |
| LVEDV, ml | 93 ± 31 | 82 ± 23 | 95 ± 32 | 0.128 |
| LVESV, ml | 29 ± 20 | 21 ± 10 | 31 ± 22 | 0.094 |
| LVEF, % | 70.8 ± 9.1 | 74.6 ± 6.1 | 69.7 ± 9.6 | 0.048 |
| SVi, ml/m$^2$ | 53.7 ± 14.7 | 47.2 ± 14.0 | 55.6 ± 14.5 | 0.037 |
| CO, ml/min | 8.2 ± 2.5 | 7.5 ± 2.5 | 8.4 ± 2.5 | 0.216 |
| E/A | 1.00 ± 0.24 ($n = 49$) | 0.99 ± 0.22 ($n = 13$) | 1.00 ± 0.26 ($n = 36$) | 0.853 |
| E/e' | 21.9 ± 7.9 | 23.2 ± 9.2 | 21.5 ± 7.6 | 0.465 |
| SPAP, mmHg | 51.5 ± 12.0 | 57.3 ± 13.8 | 49.7 ± 10.9 | 0.021 |
| TAPSE/SPAP | 0.48 ± 0.15 | 0.44 ± 0.10 | 0.49 ± 0.16 | 0.230 |
| Exercise-induced pulmonary hypertension, *n* (%) | 16 (20.8) | 7 (43.8) | 9 (15.0) | 0.037 |
| Peak velocity, m/s | 2.5 ± 0.58 | 3.0 ± 0.7 | 2.4 ± 0.5 | <0.001 |
| Mean PG, mmHg | 14.3 ± 7.3 | 21.9 ± 9.1 | 12.2 ± 4.9 | 0.001 |
| Δ Mean PG, mmHg | 3.1 ± 3.2 | 5.7 ± 3.5 | 2.3 ± 2.8 | <0.001 |
| Zva, mmHg/ml/m$^2$ | 3.9 ± 1.2 | 4.9 ± 1.8 | 3.6 ± 0.92 | 0.010 |
| Δ Zva, mmHg/ml/m$^2$ | 0.69 ± 1.1 | 1.1 ± 1.7 | 0.57 ± 0.89 | 0.243 |

*Data presented as mean ± standard deviation or n (%). Δ Zva, meant the change in Zva from rest to exercise. The other abbreviations are shown in* ***Tables 1***, ***2***.

difference was not statistically significant. The device size used in the PPM group was smaller than that used in the non-PPM group.

**Table 2** presents the preoperative echocardiographic findings. The mean LVEF was not significantly different between patients with PPM and those without PPM. The LV end-diastolic volume and LV mass index were smaller in patients with PPM than in those without PPM. Although the peak velocity was higher in patients with PPM (4.8 ± 1.4 m/s vs. 4.1 ± 1.0 m/s, $p = 0.030$), mean PG and aortic valve area index were not significantly different between the two groups.

## Impact of PPM on Hemodynamics at Rest and During Exercise

The hemodynamic characteristics at rest and during exercise are summarized in **Tables 3**, **4** and in **Figures 2**, **3**. The relationship between the mean PG and EOAi was curvilinear, with a correlation coefficient ($r$) of 0.421 ($p < 0.001$) at rest and 0.440 ($p < 0.001$) during exercise (**Figure 2**). Exercise capacity was slightly higher in patients without PPM than in those with PPM, although the difference was not statistically significant. At rest, patients with PPM demonstrated a higher peak transvalvular velocity and mean PG than patients without PPM (both $p \leq 0.001$). Zva and the changes in the mean PG from rest to exercise were significantly greater in patients with PPM than in patients without PPM (Zva: 4.9 ± 1.8 mmHg/ml/m$^2$ vs. 3.6 ± 0.92 mmHg/ml/m$^2$, Δ mean PG: 5.7 ± 3.5 mmHg vs. 2.3 ± 2.8 mmHg, both $p \leq 0.001$, **Figures 3A,B**). Although there were no significant differences in the SPAP and the prevalence of PH at rest between patients with and without PPM, patients with PPM had a higher SPAP and a higher prevalence of exercise-induced PH than patients without PPM (**Figure 3C**; **Table 4**).

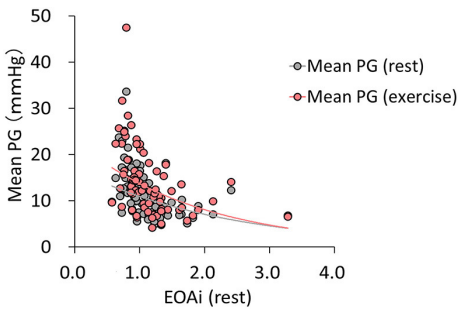


**FIGURE 2 |** The relationship between the mean PG and EOAi at rest and during exercise. Inverse simple regression analysis of the mean PG and EOAi at rest ($r = 0.421$; $p < 0.001$) and during exercise ($r = 0.440$; $p < 0.001$). Mean PG, mean transvalvular pressure gradient; EOAi, effective orifice area index.

The results of univariate Cox proportional hazard analyses for the prediction of exercise-induced PH are presented in **Table 5**. Age and preoperative aortic valve area index (AVAi) were associated with exercise-induced PH. PPM was strongly associated with exercise-induced PH. Although there was no significant association between exercise-induced PH and mean PG, Zva, E/e' and blood pressure were associated with exercise-induced PH both at rest and during exercise. The

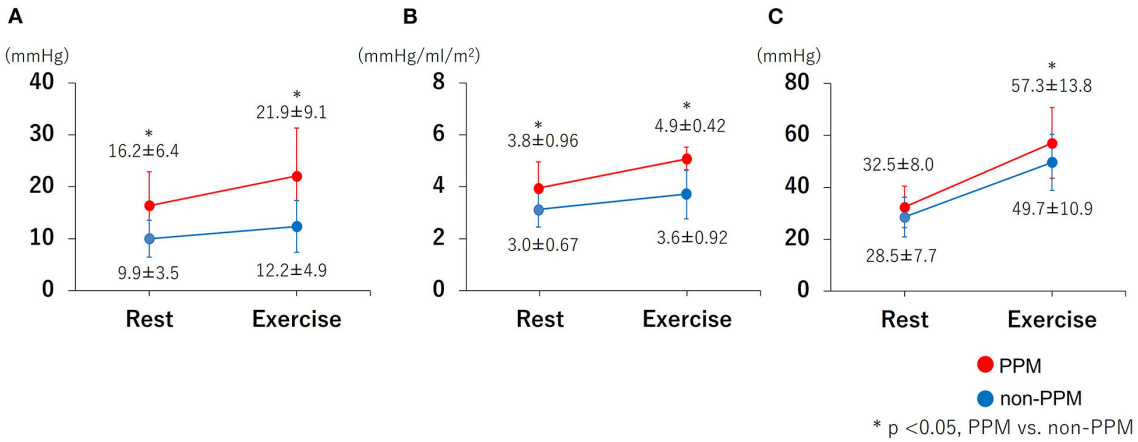


**FIGURE 3 |** The changes in the mean PG, Zva and SPAP from rest to exercise. **(A)** mean PG increase from rest to exercise; **(B)** Zva increase from rest to exercise; **(C)** SPAP increase from rest to exercise. The increase in the mean PG and Zva from rest to exercise was greater in patients with PPM than in those without PPM. Patients with PPM had a higher SPAP increase than patients without PPM (57.3 ± 13.8 mmHg vs. 49.7 ± 10.9 mmHg). PPM = prosthesis-patient mismatch; Mean PG, mean transvalvular pressure gradient; Zva, valvulo-arterial impedance; SPAP, systolic pulmonary artery pressure. *P*-value, PPM vs. non-PPM.

**TABLE 5 |** Univariate models of Cox regression analysis for exercise induced pulmonary hypertension.

| | Univariate | | |
|---|---|---|---|
| | **HR** | **95% CI** | ***p*-value** |
| **Patient characteristics** | | | |
| Female sex | 1.020 | 0.375–2.769 | 0.970 |
| Age | 0.902 | 0.824–0.987 | 0.024 |
| Atrial fibrillation | 0.816 | 0.281–2.367 | 0.708 |
| **Preoperative echocardiography** | | | |
| SVi | 0.986 | 0.943–1.031 | 0.529 |
| SPAP | 1.019 | 0.976–1.063 | 0.401 |
| E/A | 1.120 | 0.575–2.184 | 0.738 |
| E/e' | 1.064 | 0.993–1.140 | 0.078 |
| AVAi | 0.006 | 0.000–0.909 | 0.046 |
| Mean PG | 1.010 | 0.995–1.026 | 0.199 |
| **Exercise echocardiography** | | | |
| Rest systolic BP | 1.038 | 1.013–1.063 | 0.003 |
| Rest diastolic BP | 1.031 | 1.008–1.054 | 0.007 |
| Rest SVi | 1.002 | 0.957–1.048 | 0.942 |
| Rest CO | 0.923 | 0.554–1.537 | 0.758 |
| Rest SPAP | 1.063 | 1.019–1.110 | 0.005 |
| Rest E/A | 35.132 | 3.062–403.1 | 0.004 |
| Rest E/e' | 1.082 | 1.019-1.148 | 0.009 |
| PPM | 3.570 | 1.304–9.778 | 0.013 |
| Rest Mean PG | 1.058 | 0.997–1.123 | 0.064 |
| Rest Zva | 2.025 | 1.108–3.701 | 0.022 |
| Peak systolic BP | 1.040 | 1.015–1.065 | 0.001 |
| Peak diastolic BP | 1.091 | 1.044–1.140 | <0.001 |
| SVi during exercise | 0.985 | 0.953–1.019 | 0.386 |
| CO during exercise | 0.994 | 0.834–1.183 | 0.943 |
| E/A during exercise | 1.112 | 0.086–14.41 | 0.935 |
| E/e' during exercise | 1.087 | 1.019–1.159 | 0.011 |
| Mean PG during exercise | 1.039 | 0.998–1.082 | 0.066 |
| Zva during exercise | 1.728 | 1.179–2.534 | 0.005 |

*HR, hazard ratio; CI, confidence interval. The other abbreviations are shown in* ***Tables 1–3****.*

echocardiographic parameters of right-side heart function, such as tricuspid annular plane systolic excursion or tricuspid annular plane systolic excursion/SPAP, were similar in the PPM and non-PPM groups.

The CO at rest was lower in patients with PPM than in patients without PPM, although the difference was not statistically significant during exercise. **Figure 4** depicts the relationship between the SPAP and CO at rest and during exercise. According to the diagram, the CO tended to be lower and the SPAP was higher in patients with PPM than in those without PPM both at rest and during exercise. The slopes showed that the ratio of the change in the SPAP and the change in the CO (ΔSPAP/ΔCO) was higher in patients with PPM than in those without PPM, but the difference was not statistically significant (23.9 ± 45.9 vs. 8.9 ± 14.4, $p = 0.202$).

## Prognostic Impact of PPM

During the 28 ± 10 months follow-up period, 19 patients reported the primary composite endpoint and five patients had the secondary endpoint of heart failure-related hospitalization. Kaplan-Meier survival curves (**Figure 5**) did not show any significant differences in both primary and secondary endpoints between patients with and without PPM (primary endpoint: log-rank $\chi^2 = 0.210$, $p = 0.647$; secondary endpoints: log-rank $\chi^2 = 0.181$, $p = 0.671$).

# DISCUSSION

The major findings of this study are as follows: (1) The EOAi at rest correlated well with the mean PG at rest and during exercise; (2) patients with PPM showed a disproportionate increase in the transvalvular PG, LV afterload, and SPAP during exercise compared with patients without PPM; (3) the prevalence of exercise-induced PH after TAVI was higher in the PPM group than in the non-PPM group, and the improvement of symptoms tended to be poor in the PPM

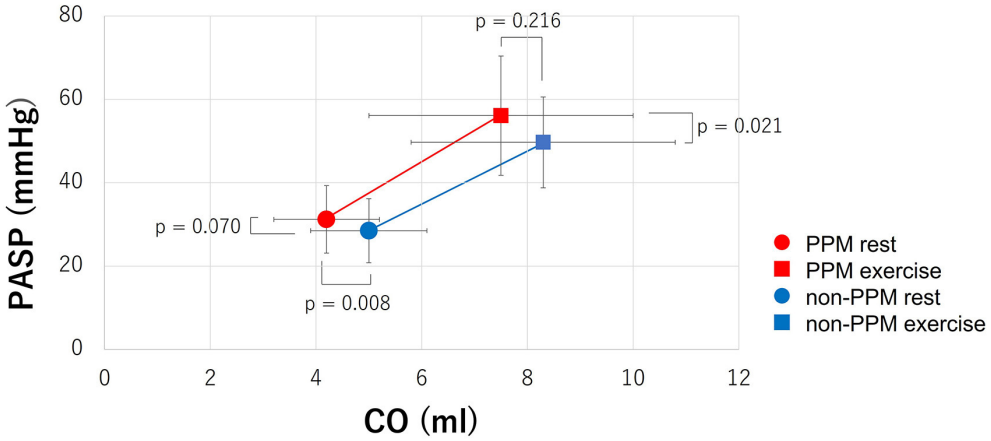


**FIGURE 4 |** The relationship between the SPAP and CO at rest and during exercise. The CO tended to be lower and the SPAP was higher in patients with PPM than in those without PPM both at rest and during exercise. The slopes showed that ΔSPAP/ΔCO was higher in patients with PPM than in those without PPM, but the difference was not statistically significant (23.9 ± 45.9 vs. 8.9 ± 14.4, $p = 0.202$).SPAP = systolic pulmonary artery pressure; CO, cardiac output; PPM, prosthesis-patient mismatch; ΔSPAP/ΔCO, the ratio of the change in SPAP and the change in CO.

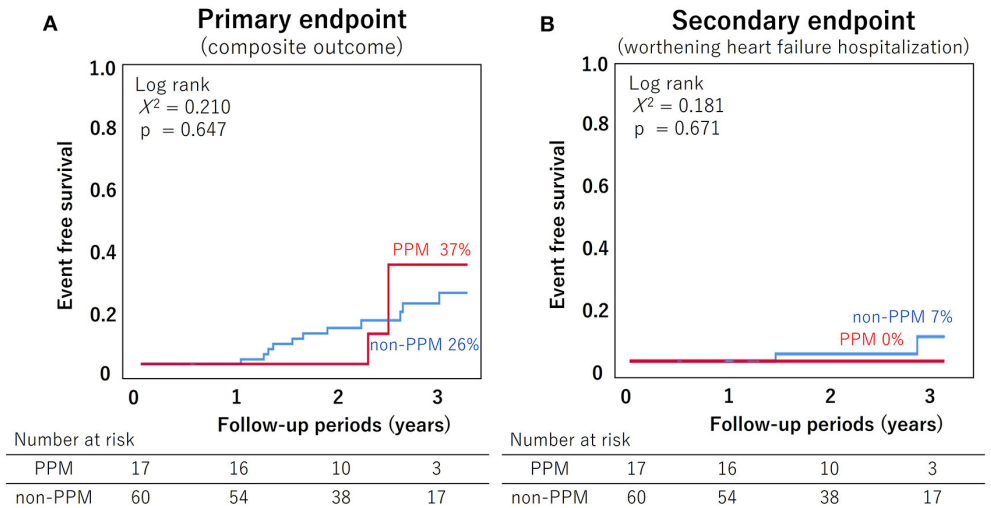


**FIGURE 5 |** The Kaplan-Meier survival curves for all-cause mortality and heart failure-related hospitalization. **(A)** Primary endpoint (composite outcomes including all-cause mortality, cardiovascular mortality, cardiovascular event, and heart failure-related hospitalization); **(B)** Secondary endpoint (heart failure-related hospitalization). There were no differences in the primary and secondary endpoints between the PPM and non-PPM groups. PPM, prosthesis-patient mismatch.

group; and (4) PPM was not associated with all-cause mortality or heart failure-related hospitalization during 2 years in this cohort.

## Hemodynamic Changes During Exercise

Some previously published reports (15–17) have addressed the hemodynamic characteristics of various surgical aortic prosthetic valves during exercise. To the best of our knowledge, this is the first study to assess the hemodynamic characteristics of THVs during exercise using ESE. Pibarot (15, 16) reported that PPM is associated with a marked increase in the mean PG and the prevalence of PH, whereas a normal functional prosthetic valve shows a minimal increase in the mean PG. These findings regarding surgical prosthesis were consistent with the major findings of our study that included AS patients after TAVI. O'Sullivan et al. (18) demonstrated that postcapillary PH (left-sided PH) is the most common form of PH among patients with severe symptomatic AS undergoing TAVI. In postcapillary PH, the increased SPAP is mainly thought to be due to the passive backward transmission of an increased LV filling pressure (19, 20). Although the SPAP usually correlates with the CO, our study also found that patients with PPM had a higher SPAP during exercise despite a lower CO than patients without PPM. These findings suggest that the LV afterload during exercise was higher in the PPM group than in the non-PPM group and that the impaired LV diastolic function, increased LV filling and left atrial

pressure are causes of disproportionate increase in pulmonary artery pressure. However, no statistically significant difference was noted in the diastolic function parameters, including the E/A ratio in our study. Despite of the fact that the mitral variables the mitral variables of the E/A ratio are the main parameters for evaluating diastolic function, many studies reported there is a weak correlation between the echocardiographic indices of the LV diastolic function and the LV filling pressure in patients with LV hypertrophy (21–23). In addition, the presence of mitral annular calcification reportedly underestimates the e' value (24, 25) in this study, mitral annular calcification was observed in ∼30% of the patients, which is considered to be one of the reasons for the lack of difference in the E/e' ratio.

### Clinical Impact of PPM

Many studies have documented the negative clinical impact of PPM after surgical aortic valve replacement (SAVR) and TAVI, focusing on clinical outcomes such as survival (3–6, 8, 9), heart failure worsening (8), LV mass regression (5, 6), and valve durability (7). Bleiziffer S (17) reported that the presence of PPM significantly influences the percentage of predicted exercise capacity and impairs the quality of life in patients. Although no statistically significant difference was found in our study in terms of adverse events, the post-procedure NYHA functional class was higher in patients with PPM than in patients without PPM. The transvalvular PG and SPAP were higher in patients with PPM than in patients without PPM, and the prevalence of exercise-induced PH was higher in patients with PPM (**Figure 3**), which resulted in a higher NYHA functional class. We speculated that an increased hemodynamic burden due to higher gradients in patients with PPM could explain this phenomenon. Another possible explanation is that PPM may limit the increase in the CO (**Figure 4**). This may, in turn, limit the capacity of cardiac function to match the increasing metabolic demand during exercise.

In our study, there were no differences in the hard endpoints between the PPM and non-PPM groups (**Figure 5**). The reasons for this possibly include the short follow-up period, elderly patients, and inclusion of exercisable patients only. It is important to estimate the postoperative EOA and predict PPM from preoperative cardiac imaging. In this study, prosthetic valve EOA tended to increase with preoperative annulus area, and each value was similar to the previously reported valve area in the CoreLab analysis (26) (**Supplementary Table 1**). It is desirable to predict prosthetic valve size and determine the predicted EOA and PPM from preoperative imaging data and select treatment strategy accordingly.

A previous study with a similar follow-up in AS patients after TAVI reported that only severe PPM was associated with prognosis (6, 8). Moreover, Schofer et al. (9) reported that in patients with low LVEF (<40%), severe PPM was associated with increased risk of mortality. In our study, severe PPM was noted in only two patients, and no patient had low LVEF or severe PPM.

## LIMITATIONS

This study was performed with a relatively small number of patients. Nonetheless, our findings are new, and important implications were made regarding the behavior of the transcatheter aortic valve during exercise. In this study, only balloon-expandable THV was examined, and the study of hemodynamics during exercise in patients with Self-expandable THVs and comparison with prosthetic valve types is warranted. It is unknown whether ESE performed at 3–6 months after TAVI is valid in terms of the time period for evaluating the impact of PPM on hemodynamics. Most patients in our study were elderly; therefore, it was difficult to perform ESE in such patients after long periods. Some patients, including young and low-risk patients, in previous studies (17) underwent ESE from 5 to 12 months after SAVR. Further studies are necessary to investigate PPM in post-TAVI patients after longer periods.

## CONCLUSION

AS patients with PPM after TAVI showed a disproportionate increase in the transvalvular gradient and SPAP during exercise. In addition, PPM was associated with exercise-induced PH.

## DATA AVAILABILITY STATEMENT

The original contributions presented in the study are included in the article/**Supplementary Material**, further inquiries can be directed to the corresponding author/s.

## ETHICS STATEMENT

The studies involving human participants were reviewed and approved by Institutional Review Board of the St. Marianna University School of Medicine. The patients/participants provided their written informed consent to participate in this study.

## AUTHOR CONTRIBUTIONS

MI contributed to conception and design of the study. HK performed the statistical analysis. HK and MI wrote the manuscript. YA helped revise the manuscript. All authors organized the database and read and approved the submitted version.

## SUPPLEMENTARY MATERIAL

The Supplementary Material for this article can be found online at: https://www.frontiersin.org/articles/10.3389/fcvm.2021.799285/full#supplementary-material

## REFERENCES


1. Mack MJ, Leon MB, Thourani VH, Makkar R, Kodali SK, Russo M, et al. Transcatheter aortic-valve replacement with a balloon-expandable valve in low-risk patients. *N Engl J Med.* (2019) 380:1695–705. doi: 10.1056/NEJMoa1814052
2. Rahimtoola SH. The problem of valve prosthesis-patient mismatch. *Circulation.* (1978) 58:20–4. doi: 10.1161/01.CIR.58.1.20
3. Blais C, Dumesnil JG, Baillot R, Simard S, Doyle D, Pibarot P. Impact of valve prosthesis-patient mismatch on short-term mortality after aortic valve replacement. *Circulation.* (2003) 108:983–8. doi: 10.1161/01.CIR.0000085167.67105.32
4. Head SJ, Mokhles MM, Osnabrugge RL, Pibarot P, Mack MJ, Takkenberg JJ, et al. The impact of prosthesis–patient mismatch on long-term survival after aortic valve replacement: a systematic review and meta-analysis of 34 observational studies comprising 27 186 patients with 133 141 patient-years. *European heart journal.* (2012) 33:1518–29. doi: 10.1093/eurheartj/ehs003
5. Dayan V, Vignolo G, Soca G, Paganini JJ, Brusich D, Pibarot P. Predictors and outcomes of prosthesis-patient mismatch after aortic valve replacement. *JACC: Cardiovasc Imaging.* (2016) 9:924–33. doi: 10.1016/j.jcmg.2015.10.026
6. Pibarot P, Weissman NJ, Stewart WJ, Hahn RT, Lindman BR, McAndrew T, et al. Incidence and sequelae of prosthesis-patient mismatch in transcatheter versus surgical valve replacement in high-risk patients with severe aortic stenosis: a PARTNER trial cohort-A analysis. *J Am Coll Cardiol.* (2014) 64:1323–34. doi: 10.1016/j.jacc.2014.06.1195
7. Flameng W, Herregods MC, Vercalsteren M, Herijgers P, Bogaerts K, Meuris B. Prosthesis-patient mismatch predicts structural valve degeneration in bioprosthetic heart valves. *Circulation.* (2010) 121:2123–9. doi: 10.1161/CIRCULATIONAHA.109.901272
8. Herrmann HC, Daneshvar SA, Fonarow GC, Stebbins A, Vemulapalli S, Desai ND, et al. Prosthesis–patient mismatch in patients undergoing transcatheter aortic valve replacement: from the STS/ACC TVT registry. *J Am Coll Cardiol.* (2018) 72:2701–11. doi: 10.1016/j.jacc.2018.09.001
9. Schofer N, Deuschl F, Rubsamen N, Skibowski J, Seiffert M, Voigtlander L, et al. Prosthesis-patient mismatch after transcatheter aortic valve implantation: prevalence and prognostic impact with respect to baseline left ventricular function. *EuroIntervention.* (2019) 14:1648–55. doi: 10.4244/EIJ-D-18-00827
10. Lang RM, Badano LP, Mor-Avi V, Afilalo J, Armstrong A, Ernande L, et al. Recommendations for cardiac chamber quantification by echocardiography in adults: an update from the American Society of Echocardiography and the European Association of Cardiovascular Imaging. *Eur Heart J Cardiovasc Imaging.* (2015) 16:233–70. doi: 10.1093/ehjci/jev014
11. Lancellotti P, Pibarot P, Chambers J, Edvardsen T, Delgado V, Dulgheru R, et al. Recommendations for the imaging assessment of prosthetic heart valves: a report from the European Association of Cardiovascular Imaging endorsed by the Chinese Society of Echocardiography, the Inter-American Society of Echocardiography, and the Brazilian Department of Cardiovascular Imaging. *Eur Heart J Cardiovasc Imaging.* (2016) 17:589–90. doi: 10.1093/ehjci/jew025
12. Baumgartner H, Hung J, Bermejo J, Chambers JB, Edvardsen T, Goldstein S, et al. Recommendations on the echocardiographic assessment of aortic valve stenosis: a focused update from the European Association of Cardiovascular Imaging and the American Society of Echocardiography. *J Am Soc Echocardiogr.* (2017) 30:372–92. doi: 10.1016/j.echo.2017.02.009
13. Pibarot P, Hahn RT, Weissman NJ, Monaghan MJ. Assessment of paravalvular regurgitation following TAVR: a proposal of unifying grading scheme. *JACC Cardiovasc Imaging.* (2015) 8:340–60. doi: 10.1016/j.jcmg.2015.01.008
14. Achenbach S, Delgado V, Hausleiter J, Schoenhagen P, Min JK, Leipsic JA. SCCT expert consensus document on computed tomography imaging before transcatheter aortic valve implantation (TAVI)/transcatheter aortic valve replacement (TAVR). *J Cardiovasc Comp Tomogr.* (2012) 6:366–80. doi: 10.1016/j.jcct.2012.11.002
15. Pibarot P, Dumesnil JG, Jobin J, Cartier P, Honos G, Durand LG. Hemodynamic and physical performance during maximal exercise in patients with an aortic bioprosthetic valve: comparison of stentless versus stented bioprostheses. *J Am Coll Cardiol.* (1999) 34:1609–17. doi: 10.1016/S0735-1097(99)00360-5
16. Pibarot P, Dumesnil JG, Jobin J, Lemieux M, Honos G, Durand LG. Usefulness of the indexed effective orifice area at rest in predicting an increase in gradient during maximum exercise in patients with a bioprosthesis in the aortic valve position. *Am J Cardiol.* (1999) 83:542–6. doi: 10.1016/S0002-9149(98)00910-2
17. Bleiziffer S, Eichinger WB, Hettich I, Ruzicka D, Wottke M, Bauernschmitt R, et al. Impact of patient-prosthesis mismatch on exercise capacity in patients after bioprosthetic aortic valve replacement. *Heart.* (2008) 94:637–41. doi: 10.1136/hrt.2007.116673
18. O'Sullivan CJ, Wenaweser P, Ceylan O, Rat-Wirtzler J, Stortecky S, Heg D, et al. Effect of pulmonary hypertension hemodynamic presentation on clinical outcomes in patients with severe symptomatic aortic valve stenosis undergoing transcatheter aortic valve implantation: insights from the new proposed pulmonary hypertension classification. *Circ Cardiovasc Interventions.* (2015) 8:e002358. doi: 10.1161/CIRCINTERVENTIONS.114.002358
19. Guazzi M, Borlaug BA. Pulmonary hypertension due to left heart disease. *Circulation.* (2012) 126:975–90. doi: 10.1161/CIRCULATIONAHA.111.085761
20. Bossone E, D'Andrea A, D'Alto M, Citro R, Argiento P, Ferrara F, et al. Echocardiography in pulmonary arterial hypertension: from diagnosis to prognosis. *J Am Soc Echocardiogr.* (2013) 26:1–14. doi: 10.1016/j.echo.2012.10.009
21. Nishimura RA, Appleton CP, Redfield MM, Ilstrup DM, Holmes DR, Tajik AJ. Noninvasive Doppler echocardiographic evaluation of left ventricular filling pressures in patients with cardiomyopathies: a simultaneous Doppler echocardiographic and cardiac catheterization study. *J Am Coll Cardiol.* (1996) 28:1226–33. doi: 10.1016/S0735-1097(96)00315-4
22. Nagueh SF, Lakkis NM, Middleton KJ, Spencer III WH, Zoghbi WA, Quinones MA. Doppler estimation of left ventricular filling pressures in patients with hypertrophic cardiomyopathy. *Circulation.* (1999) 99:254–61. doi: 10.1161/01.CIR.99.2.254
23. Geske JB, Sorajja P, Nishimura RA, Ommen SR. Evaluation of left ventricular filling pressures by Doppler echocardiography in patients with hypertrophic cardiomyopathy: correlation with direct left atrial pressure measurement at cardiac catheterization. *Circulation.* (2007) 116:2702–8. doi: 10.1161/CIRCULATIONAHA.107.698985
24. Soeki T, Fukuda N, Shinohara H, Sakabe K, Onose Y, Sawada Y, et al. Mitral inflow and mitral annular motion velocities in patients with mitral annular calcification: evaluation by pulsed Doppler echocardiography and pulsed Doppler tissue imaging. *Eur J Echocardiogr.* (2002) 3:128–31. doi: 10.1053/euje.2001.0137
25. Abudiab MM, Chebrolu LH, Schutt RC, Nagueh SF, Zoghbi WA. Doppler echocardiography for the estimation of LV filling pressure in patients with mitral annular calcification. *JACC Cardiovasc Imaging.* (2017) 10:1411–20. doi: 10.1016/j.jcmg.2016.10.017
26. Hahn RT, Leipsic J, Douglas PS, Jaber WA, Weissman NJ, Pibarot P, et al. Comprehensive echocardiographic assessment of normal transcatheter valve function. *JACC Cardiovasc Imaging.* (2019) 12:25–34. doi: 10.1016/j.jcmg.2018.04.010


**Conflict of Interest:** MI is a screening proctor for Edwards Lifesciences.

The remaining authors declare that the research was conducted in the absence of any commercial or financial relationships that could be construed as a potential conflict of interest.

frontiers in Cardiovascular Medicine

CASE REPORT
published: 07 February 2022
doi: 10.3389/fcvm.2022.790098

# Usefulness of Intra-Aortic Balloon Pump Off Test With Echocardiography for Decision Making in Secondary Ischemic Mitral Regurgitation: A Case Report

*Noriko Shiokawa*[1], *Masaki Izumo*[2]*, *Shingo Kuwata*[2] and *Yoshihiro J. Akashi*[2]

[1] Department of Ultrasound Center, St. Marianna University Hospital, Kawasaki, Japan, [2] Division of Cardiology, Department of Internal Medicine, St. Marianna University School of Medicine, Kawasaki, Japan

Our patient was a 60-year-old male with myocardial infarction. Urgent percutaneous coronary intervention was performed with intra-aortic balloon pump (IABP) support. Despite successful revascularization, the patient suffered from cardiogenic shock and heart failure. Secondary mitral regurgitation (MR) was mild and seemed unlikely to be the cause of heart failure. However, when IABP was temporarily stopped (IABP-OFF), secondary MR was aggravated; therefore, we decided to perform transcatheter mitral valve repair. Thereafter, only mild residual MR was observed after IABP removal, and hemodynamic stability was achieved. This case presents IABP-OFF test with echocardiography as a useful method to assess secondary MR.

**Keywords: mitral regurgitation, heart failure, intra-aortic balloon pump, transcatheter mitral valve repair, echocardiogaphy**

OPEN ACCESS

***Edited by:***
*Ronak Rajani,*
*Guy's and St Thomas' NHS Foundation Trust, United Kingdom*

***Reviewed by:***
*Carlo Fino,*
*Papa Giovanni XXIII Hospital, Italy*
*Mohammad Abdelghani,*
*Al-Azhar University, Egypt*

***Correspondence:**
*Masaki Izumo*
*heartizumo@yahoo.co.jp;*
*m2izumo@marianna-u.ac.jp*

***Specialty section:***
*This article was submitted to Cardiovascular Imaging, a section of the journal Frontiers in Cardiovascular Medicine*

***Received:*** *06 October 2021*
***Accepted:*** *05 January 2022*
***Published:*** *07 February 2022*

***Citation:***
*Shiokawa N, Izumo M, Kuwata S and Akashi YJ (2022) Usefulness of Intra-Aortic Balloon Pump Off Test With Echocardiography for Decision Making in Secondary Ischemic Mitral Regurgitation: A Case Report. Front. Cardiovasc. Med. 9:790098. doi: 10.3389/fcvm.2022.790098*

## INTRODUCTION

A 60-year-old male with a history of hypertension and dyslipidemia was transported to another hospital due to chest pain and loss of consciousness. On admission, electrocardiogram showed ST elevation in leads V 1 ∼ 5, II, III, and aVF. Emergency coronary angiography was performed under the diagnosis of ST elevation myocardial infarction. Coronary angiography showed complete occlusion of the left main trunk, it was diagnosed as a culprit lesion and primary PCI was performed under IABP support. Drug eluting stent was placed from the left main trunk to the left anterior descending artery. Upon urgent coronary angiography, acute myocardial infarction of the main trunk of the left coronary artery was diagnosed. Approximately 1 month after the primary PCI, heart failure and cardiogenic shock were observed at the previous hospital. Percutaneous intervention (PCI) was then urgently performed with intra-aortic balloon pumping (IABP) support. The patient was transferred to our hospital with IABP inserted to treat cardiogenic shock and heart failure. We performed IABP on/off test with echocardiography the day after he was transferred to our hospital. Transthoracic echocardiography (TTE) revealed the following: left ventricular ejection fraction (LVEF), 32%; left ventricular end-diastolic volume (LVEDV), 175 mL; left ventricular end-systolic volume (LVESV), 120 mL; and left atrial volume index (LAVi), 55 mL/m$^2$. The severity of secondary mitral regurgitation (MR) was mild to moderate (**Figures 1A,B**, **Supplementary Videos 1**, **2**) under IABP support, with an effective regurgitant orifice area

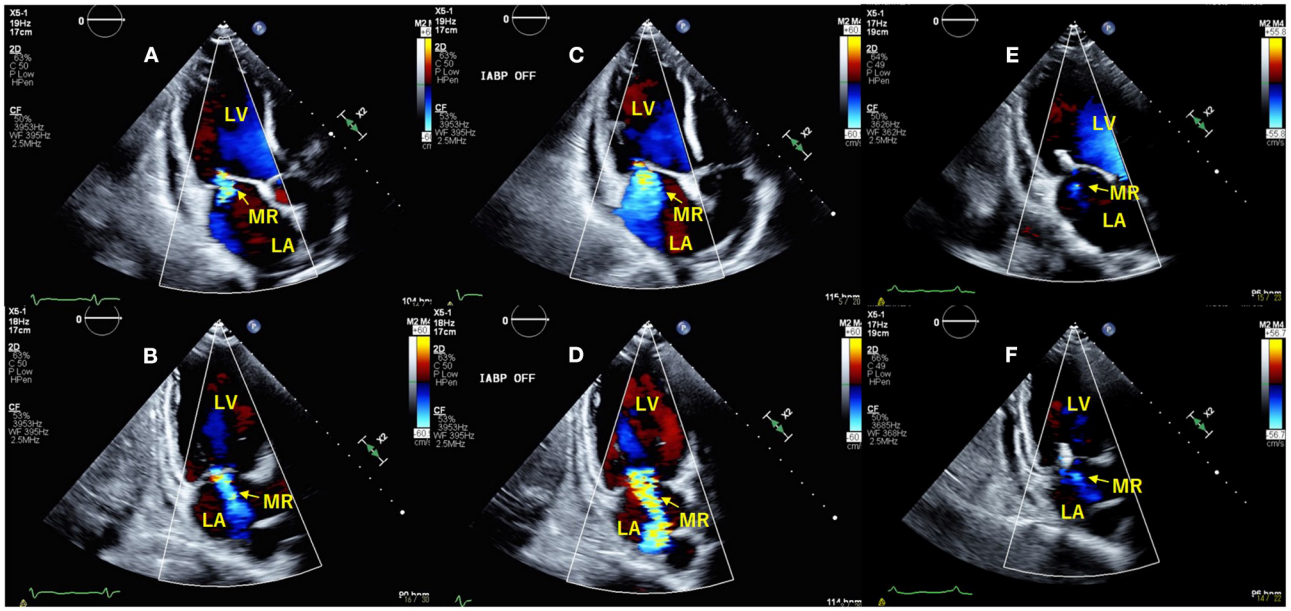


**FIGURE 1 |** Transthoracic echocardiography with intra-aortic balloon pump (IABP)-ON **(A,B)** and -OFF **(C,D)**. The apical long-axis view **(A,C)** and two-chamber view **(B,D)** show that mitral regurgitation is significantly increased from IABP-ON to IABP-OFF. After intervention with the MitraClip™, secondary MR was significantly decreased **(E,F)**. LV, left ventricle; LA, left atrium.

(EROA) of 0.24 $cm^2$, regurgitant volume (RV) of 16 mL, and vena contracta width (VCW) in two-chamber view of 4.6 mm. The coaptation length of the mitral valve was 2.9 mm, and the mitral annular diameter was 29.6 mm. IABP support was temporarily stopped (IABP-OFF) to assess possible changes in the patient's status. The coaptation length shortened to 1.7 mm, and the mitral annular diameter increased to 32.5 mm. MR significantly worsened with EROA of 0.37 $cm^2$, RV of 29 ml, and VCW of 12.7 mm; this indicated MR aggravation compared to what was observed on IABP-ON (**Figures 1C,D**, **Supplementary Videos 3**, **4**). The velocity time integral at the left ventricular outflow tract was 8 cm in IABP-ON and 7 cm in IABP-OFF; thus, a decrease in forward cardiac output was evident. Based on these findings, we concluded the need for intervention to secondary MR. We decided to perform mitral valve intervention by a transcatheter edge-to-edge repair with a MitraClip™ (Abbott Vascular,. Abbott Park, IL). The G4-XTW was placed in the A2P2 region, resulting in a reduction of MR to the degree of trivial MR. The hemodynamics, including the left atrial pressure, also improved to be within the tolerance of the mitral valve mean pressure gradient of 3 mm Hg. After transcatheter mitral valve repair with the MitraClip™, only mild residual MR (**Figures 1E,F**, **Supplementary Videos 5**, **6**) was observed after removal of the IABP, and hemodynamic stability was achieved. Intraprocedural transesophageal echocardiography showed mild secondary MR even after discontinuation of IABP. We inserted a pigtail catheter into the left atrium during MitraClip, and performed the procedure while monitoring the LA pressure (1). The mean LA pressure decreased from 44 to 33 mmHg before and after MitraClip. IABP was removed during the operation. After the MitraClip, heart failure and cardiogenic shock improved, and the patient was discharged 8 days after the MitraClip.

## DISCUSSION

This is a case of acute myocardial infarction complicated by cardiogenic shock, wherein the IABP-OFF test revealed that secondary MR was one of the causes of cardiogenic shock and heart failure. The closure position of the mitral valve leaflet is normally determined by the balance between the closing force from the left ventricular pressure during systole and the tethering force from the chordae tendineae. However, in secondary MR, remodeling of the left ventricle occurs after myocardial infarction, and the valve leaflet shifts posteriorly and/or apically due to myocardial damage around the papillary muscle. This causes valvular apex malfunction, enhanced tethering, and exacerbated MR in patients with dilated left ventricle and decreased left ventricular function (2). Compared with chronic secondary MR, loss of mitral valve coaptation and hemodynamic loading in the acute phase may result in significant secondary MR despite relatively small mitral valve tethering (3). In IABP support, the balloon inflates during diastole to increase diastolic pressure and coronary flow. During systole, the balloon contracts, reducing ventricular afterload, and myocardial oxygen consumption. This effect results in temporary reverse remodeling of the left ventricle, improved mitral coaptation, and decreased MR. Eliaz et al. reported that reduced mitral annulus diameter and increased mitral valve leaflet coaptation were observed in patients with severe MR and with IABP support (4). In this

case, IABP-OFF resulted in an expanded mitral annulus diameter, shortened coaptation length, and increased MR. As far as we know, this case is the first case of utility of IABP off-test for decision making of secondary MR. Further studies are needed to investigate the severity assessment of secondary MR using IABP off-test with echocardiography.

## CONCLUSIONS

This case shows that the IABP ON-OFF test with transthoracic echocardiography is a non-invasive method that can evaluate the severity of MR and the morphology of the mitral valve in patients with difficulty in weaning from IABP support. It is considered to be a useful method for diagnosing the severity of secondary MR and deciding whether to perform mitral valve intervention.

## DATA AVAILABILITY STATEMENT

The original contributions presented in the study are included in the article/**Supplementary Material**, further inquiries can be directed to the corresponding author/s.

## AUTHOR CONTRIBUTIONS

NS and MI contributed data collection and writing the manuscript. SK and YA contributed to the critical revision of the manuscript. All authors contributed to the article and approved the submitted version.

## SUPPLEMENTARY MATERIAL

The Supplementary Material for this article can be found online at: https://www.frontiersin.org/articles/10.3389/fcvm.2022.790098/full#supplementary-material

**Supplementary Video 1 |** The apical long axis view with intra-aortic balloon pump (IABP)-ON.

**Supplementary Video 2 |** The two-chamber view with IABP-ON.

**Supplementary Video 3 |** The apical long axis view with IABP-OFF.

**Supplementary Video 4 |** The two-chamber view with IABP-OFF.

**Supplementary Video 5 |** The apical long axis view after transcatheter mitral valve repair.

**Supplementary Video 6 |** The two-chamber view after transcatheter mitral valve repair.

## REFERENCES

1. Kuwata S, Taramasso M, Czopak A, Luciani M, Pozzoli A, Ho E, et al. Continuous direct left atrial pressure: intraprocedural measurement predicts clinical response following MitraClip therapy. *J Am Coll Cardiol Intv.* (2019) 12:127–36. doi: 10.1016/j.jcin.2018.07.051
2. Nishino S, Watanabe N, Kimura T, Kuriyama N, Shibata Y. Acute versus chronic ischemic mitral regurgitation: an echocardiographic study of anatomy and physiology. *Circ Cardiovasc Imaging.* (2018) 11:e007028. doi: 10.1161/CIRCIMAGING.117.007028
3. Otsuji Y, Handschumacher MD, Schwammenthal E, Jiang L, Song JK, Guerrero JL, et al. Insights from three-dimensional echocardiography into the mechanism of functional mitral regurgitation: direct *in vivo* demonstration of altered leaflet tethering geometry. *Circulation.* (1997) 96:1999–2008. doi: 10.1161/01.CIR.96.6.1999
4. Eliaz R, Turyan A, Beeri R, Shuvy M. Utilization of intra-aortic balloon pump to allow MitraClip procedure in patients with non-coapting mitral valve leaflets: a case series. *Europ Heart J Case Rep.* (2019) 3:1–7. doi: 10.1093/ehjcr/ytz045

**Conflict of Interest:** MI and SK are training faculty of Abbott Medical Japan.

The remaining authors declare that the research was conducted in the absence of any commercial or financial relationships that could be construed as a potential conflict of interest.

frontiers in Cardiovascular Medicine

ORIGINAL RESEARCH
published: 09 March 2022
doi: 10.3389/fcvm.2022.847259

# Impact of Valve Size on Paravalvular Leak and Valve Hemodynamics in Patients With Borderline Size Aortic Valve Annulus

*Yeela Talmor-Barkan[1,2], Ran Kornowski[1], Noam Bar[2], Jeremy Ben-Shoshan[3], Hanna Vaknin-Assa[1], Ashraf Hamdan[1], Boris Kruchin[1], Israel M. Barbash[4], Haim Danenberg[5], Gidon Y. Perlman[5], Maayan Konigstein[3], Ariel Finkelstein[3], Arie Steinvil[3], Ilan Merdler[3], Amit Segev[4], Alon Barsheshet[1] and Pablo Codner[1]**

[1] Rabin Medical Center, Sackler Faculty of Medicine, Tel-Aviv University, Tel-Aviv, Israel, [2] Department of Computer Science and Applied Mathematics, Weizmann Institute of Science, Rehovot, Israel, [3] Tel-Aviv Medical Center, Sackler Faculty of Medicine, Tel-Aviv University, Tel-Aviv, Israel, [4] Chaim Sheba Medical Center, Sackler Faculty of Medicine, Tel-Aviv University, Tel Aviv, Israel, [5] Hadassah Medical Center, Hebrew University, Jerusalem, Israel

**Background:** Transcatheter heart valve (THV) selection for transcatheter aortic valve implantation (TAVI) is crucial to achieve procedural success. Borderline aortic annulus size (BAAS), which allows a choice between two consecutive valve sizes, is a common challenge during device selection. In the present study, we evaluated TAVI outcomes in patients with BAAS according to THV size selection.

**Methods:** We performed a retrospective study including patients with severe aortic stenosis (AS) and BAAS, measured by multi-detector computed tomography (MDCT), undergoing TAVI with self-expandable (SE) or balloon-expandable (BE) THV from the Israeli multi-center TAVI registry. The aim was to evaluate outcomes of TAVI, mainly paravalvular leak (PVL) and valve hemodynamics, in patients with BAAS (based on MDCT) according to THV sizing selection in between 2 valve sizes. In addition, to investigate the benefit of shifting between different THV types (BE and SE) to avoid valve size selection in BAAS.

**Results:** Out of 2,352 patients with MDCT measurements, 598 patients with BAAS as defined for at least one THV type were included in the study. In BAAS patients treated with SE-THV, larger THV selection was associated with lower rate of PVL, compared to smaller THV (45.3 vs. 64.5%; pv = 0.0038). Regarding BE-THV, larger valve selection was associated with lower post-procedural transvalvular gradients compared to smaller THV (mean gradient: 9.9 ± 3.7 vs. 12.5 ± 7.2 mmHg; $p = 0.019$). Of note, rates of mortality, left bundle branch block, permanent pacemaker implantation, stroke, annular rupture, and/or coronary occlusion did not differ between groups.

OPEN ACCESS

**Edited by:**
Ronak Rajani,
Guy's and St Thomas' NHS Foundation Trust, United Kingdom

**Reviewed by:**
Hiroyuki Kamiya,
Asahikawa Medical University, Japan
Antonio Popolo Rubbio,
IRCCS San Donato Polyclinic, Italy

***Correspondence:**
Pablo Codner
drpablocodner@gmail.com

**Specialty section:**
This article was submitted to Heart Valve Disease, a section of the journal Frontiers in Cardiovascular Medicine

**Received:** 01 January 2022
**Accepted:** 01 February 2022
**Published:** 09 March 2022

**Citation:**
Talmor-Barkan Y, Kornowski R, Bar N, Ben-Shoshan J, Vaknin-Assa H, Hamdan A, Kruchin B, Barbash IM, Danenberg H, Perlman GY, Konigstein M, Finkelstein A, Steinvil A, Merdler I, Segev A, Barsheshet A and Codner P (2022) Impact of Valve Size on Paravalvular Leak and Valve Hemodynamics in Patients With Borderline Size Aortic Valve Annulus. Front. Cardiovasc. Med. 9:847259. doi: 10.3389/fcvm.2022.847259

**Conclusion:** BAAS is common among patients undergoing TAVI. Selection of a larger THV in these patients is associated with lower rates of PVL and optimized THV hemodynamics with no effect on procedural complications. Additionally, shift from borderline THV to non-borderline THV modified both THV hemodynamics and post-dilatation rates.

**Keywords: borderline aortic annulus, transcatheter aortic valve implantation, paravalvular leak, valve hemodynamics, multi-detector computed tomography**

# INTRODUCTION

Aortic valve stenosis (AS) is the most common valvular heart disease among elderly (1). Transcatheter aortic valve implantation (TAVI) has become an established and effective therapeutic procedure for symptomatic patients with severe AS regardless of procedural risk (2, 3), and recently is offered to a younger and lower risk population. These changes in TAVI candidates emphasize the need for optimal transcatheter heart valve (THV) implantation to achieve procedural success and prolonged durability. The selection of an appropriately sized THV is a crucial component of the TAVI procedure. Valve undersizing may lead to paravalvular leak (PVL), valve embolization and poor hemodynamics. Oversizing may result in coronary occlusion, atrioventricular block, mitral valve injury, periaortic hematoma, septal or annular rupture (4).

Multi-detector computed tomography (MDCT) is the gold standard method for pre-procedural planning and annular sizing of both balloon-expandable (BE) and self-expanding (SE) THV (5). THVs are currently available in a limited number of sizes and the manufacturer's sizing guidelines allow for a gray area with considerable overlap, where patients with borderline aortic annulus size (BAAS) may be candidates for either of the two suitable THV sizes (smaller or larger). Recently, study from the PARTNER 3 (Placement of Aortic Transcatheter Valves 3) trial demonstrated that in selected patients with annular dimensions in between 2 valve sizes, the larger THV device oversized to both the annular area and perimeter reduced PVL and optimized THV hemodynamics (6). Meanwhile, BAAS remains a common challenge during device size selection and the most effective THV selection strategy for these patients remains unclear.

The aim of the present study was to evaluate outcomes of TAVI, mainly PVL and valve hemodynamics, in patients with BAAS (based on MDCT) according to THV sizing selection in between 2 valve sizes. In addition, to investigate the benefit of shifting between different THV types (BE and SE) to avoid valve size selection in BAAS.

# METHODS

## Study Design and Methodology

We performed a retrospective analysis from the Israeli multi-center TAVI registry, including patients with severe symptomatic AS and BAAS, measured by MDCT, undergoing TAVI with SE-THV (CoreValve, Evolut R and Evolut PRO) or BE-THV (Sapien XT, Sapien 3) during the years 2015–2019, at 1 of 4 tertiary centers in Israel: Rabin Medical Center, Sheba Medical Center, Tel-Aviv Sourasky Medical Center, and Hadassah Medical Center. The study was approved by the institutional review board of each of the participating centers.

Eligibility for TAVI was established after a multi-disciplinary approach as indicated by the current recommendations. The preoperative workout included MDCT scan to plan the most appropriate route of intervention and to establish the aortic size and dimensions. Aortic sizing and valve measurements were performed by the local team in each center. All centers adopted a transfemoral-first approach policy; other vascular accesses (trans-apical, trans-subclavian, etc.) were considered in cases in which the transfemoral access was not feasible. According to the local policy, TAVIs were performed under local or general anesthesia. The selection of prosthesis type and size was at the discretion of the treating physicians at each center. Pre-specified clinical and laboratory data were collected for all patients at baseline before the procedure, immediately after the procedure, during the index hospitalization, and during long-term follow-up. Collected data included medical history, electrocardiogram, echocardiography studies, MDCT measurements, laboratory tests, and clinical outcomes. Outcomes were collected according to the Valve Academic Research Consortium (VARC) 2 consensus document (7).

BAAS was defined based on THV manufacturer sizing instructions; size cut-off $\pm 1$ mm for SE-THV (62.8 $\pm$ 1 mm for valve size of 23 vs. 26; 72.3 $\pm$ 1 for 26 vs. 29; 81.7 $\pm$ 1 for 29 vs. 34 mm) and borderline range for BE-THV (330–350 $mm^2$ for valve size of 20 vs. 23 mm; 420–440 $mm^2$ for 23 vs. 26 mm; 530–560 $mm^2$ for 26 vs. 29 mm) (**Figure 1**) (8). Patients who underwent valve in valve or valve in ring procedures were excluded from the study.

## Study Devices

The Evolut R SE valve is constituted by a nitinol frame mounting three porcine pericardial leaflets. The valve is repositionable, partially recapturable, and it is deliverable using a dedicated delivery system 14/16-Fr compatible depending on valve size. The Evolut PRO device represents an evolution of its predecessor and features a porcine pericardial outer wrap that contributes to reduce the risk of residual PVL. Evolut R covers a wide range of sizes and is available in 23, 26, 29, and 34 mm sizes (9); the PRO valve is available in 23, 26, and 29 mm sizes (10).

**Sizing Chart for BE/SE-THV in BAAS Patients**

| Area ($mm^2$) | Perimeter (mm) | BE-THV (mm) | | | | SE-THV (mm) | | | |
|---|---|---|---|---|---|---|---|---|---|
| | | 20 | 23 | 26 | 29 | 23 | 26 | 29 | 34 |
| 303 | 61.8 | | | | | | | | |
| 310 | 62.8 | | | | | | | | |
| 323 | 63.8 | | | | | | | | |
| 404 | 71.3 | | | | | | | | |
| 420 | 72.6 | | | | | | | | |
| 430 | 73.5 | | | | | | | | |
| 440 | 74.3 | | | | | | | | |
| 520 | 80.7 | | | | | | | | |
| 530 | 81.7 | | | | | | | | |
| 544 | 82.7 | | | | | | | | |
| 550 | 83.1 | | | | | | | | |
| 560 | 83.9 | | | | | | | | |

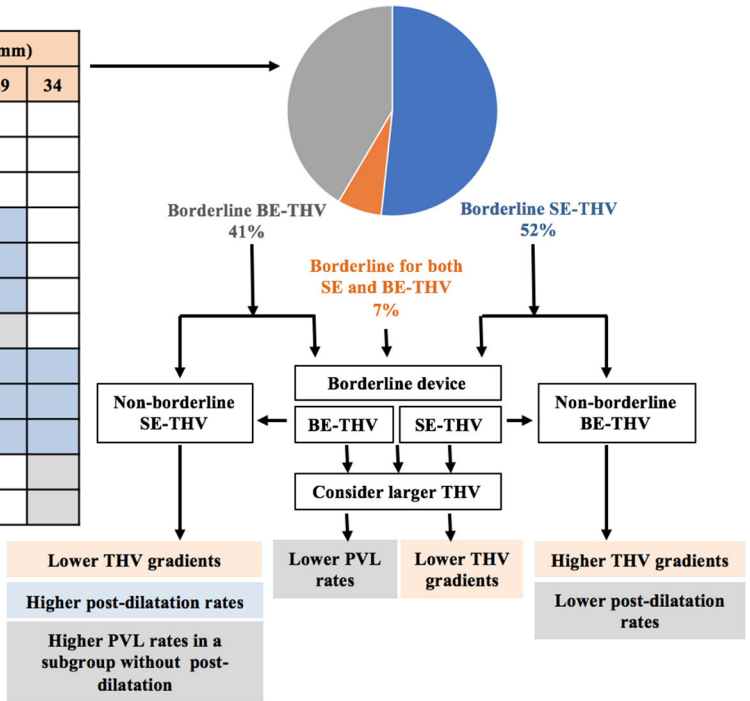


**FIGURE 1 |** Valve selection in BAAS patients. BE, balloon-expandable; SE, self-expandable; THV, transcatheter heart valve; BAAS, borderline aortic annulus size; PVL, paravalvular leak.

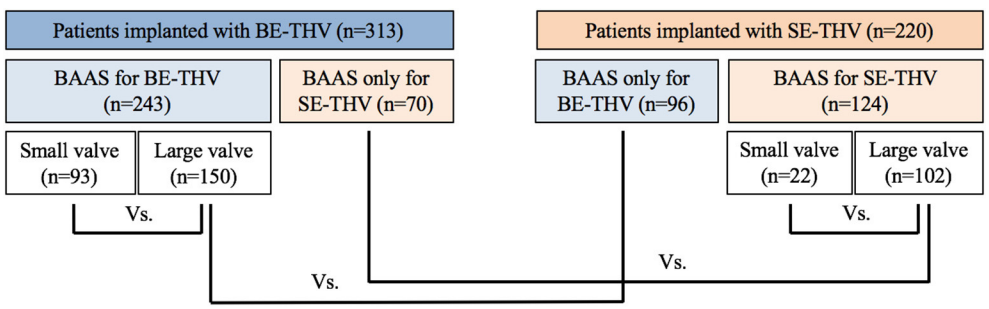


**FIGURE 2 |** Flow chart for study cohort. BE, balloon-expandable; SE, self-expandable; THV, transcatheter heart valve, BAAS, borderline aortic annulus size.

The Sapien XT/3 BE valve incorporates a cobalt chromium stent that mounts bovine pericardial leaflets. Sapien 3, has both an inner and an outer polyethylene terephthalate fabric seal to minimize the risk of paravalvular leaks. The delivery system has an active 3-dimensional coaxial positioning catheter and a 16-Fr expandable sheath (11).

## Statistical Methods

Continuous variables were expressed as mean ± standard deviation and as median and interquartile range (IQR) and compared using Mann-Whitney test. Categorical variables were compared using Chi-square or Fisher's exact tests as needed. All analyses were conducted using Python version 3.5, $p < 0.05$ was considered statistically significant.

# RESULTS

Out of 2,352 patients following implantation of SE-THV (CoreValve, Evolut R and Evolut PRO) or BE-THV (Sapien XT, Sapien 3) with pre-procedural MDCT measurements, 124 were excluded due to valve in valve, valve in ring, or mitral valve interventions. Additional 38 patients with BAAS and an annulus area of 330–350 $mm^2$ who were implanted with BE-THV were excluded from the analysis since the smaller valve size of 20 mm was not implanted. Eventually, 598 patients with BAAS as defined for at least one THV type, 309 for SE-THV, 248 for BE-THV and 41 patients for both devices were included in the analysis. Of them, 367 (61.4%) patients were implanted with borderline valves, while all others were implanted with

**TABLE 1A |** Baseline clinical characteristics of patients with BAAS for SE-THV, implanted with SE or non-borderline BE-THV.

| | **Smaller borderline-SE-THV (*n* = 93)** | **Larger borderline-SE-THV (*n* = 150)** | **Non- borderline BE-THV (*n* = 70)** | ***p*-value*** | ***p*-value[#]** |
|---|---|---|---|---|---|
| Female (%) | 52 (56) | 88 (58) | 50 (71) | 0.69 | 0.07 |
| DM (%) | 31 (33) | 55 (36) | 30 (42) | 0.68 | 0.55 |
| BMI kg/m$^2$ | 27.6 ± 5.4 [27.3, 6.6] | 27 ± 4.6 [26.7, 6.3] | 27.9 ± 4.2 [27.3, 4.7] | 0.21 | 0.09 |
| STS score | 4.2 ± 2.3 [3.79, 2.8] | 4.3 ± 3.3 [3.45, 2.8] | 4.48 ± 2.86 [4.18, 3.2] | 0.29 | 0.28 |
| PR interval (ms) | 179.7 ± 40 [170, 49] | 171 ± 44 [161, 34.5] | 179 ± 38.7 [169, 24.5] | 0.13 | 0.09 |
| QRS interval (ms) | 120 ± 33 [108, 52] | 112 ± 35 [99, 35] | 104 ± 33 [95, 45] | 0.08 | 0.36 |
| NYHA functional class: | | | | 0.03 | 0.38 |
| I | 0 (0) | 2 (1.4) | 1 (1.4) | | |
| II | 29 (33) | 31 (22) | 21 (31) | | |
| III | 51(58) | 78 (55) | 37 (54.4) | | |
| IV | 8 (9) | 30 (21) | 9 (13.2) | | |

*Values are mean ± SD or [median, interquartile range (IQR)] or n (%). DM, diabetes mellitus; BMI, body mass index; STS score, the society of thoracic surgeons scores; NYHA, New York Heart Association; SE, self-expandable; BE, balloon-expandable; THV, transcatheter heart valve. *Smaller borderline-SE-THV vs. larger borderline-SE-THV. [#]Larger borderline-SE-THV vs. non-borderline-BE.*

**TABLE 1B |** Baseline clinical characteristics of patients with BAAS for BE-THV, implanted with BE or non-borderline SE-THV.

| | **Smaller borderline-BE-THV (*n* = 22)** | **Larger borderline-BE-THV (*n* = 102)** | **Non-borderline SE-THV (*n* = 96)** | ***p*-value*** | ***p*-value[#]** |
|---|---|---|---|---|---|
| Female (%) | 10 (45.4) | 24 (23.5) | 61 (63.5) | 0.06 | 1.40e-08 |
| DM (%) | 10 (45.4) | 43 (42.1) | 43 (44.8) | 1 | 0.24 |
| BMI kg/m$^2$ | 28.6 ± 3.7 [27.4, 4.6] | 27.5 ± 4.4 [26.9, 5.4] | 28 ± 4.9 [27.8, 6.9] | 0.12 | 0.23 |
| STS score | 4 ± 4.5 [2.6, 2.1] | 3.4 ± 2.25 [2.7, 2.1] | 4.2 ± 2.4 [3.6, 2.6] | 0.36 | 0.003 |
| PR interval (ms) | 185 ± 60 [189, 33.5] | 181 ± 34 [182, 48.5] | 174 ± 34.18 [171, 36.5] | 0.42 | 0.12 |
| QRS duration (ms) | 135 ± 30 [148, 44] | 121 ± 33 [107, 59] | 106.9 ± 28 [100, 32] | 0.11 | 0.05 |
| NYHA functional class: | | | | 0.18 | 0.1 |
| I | 1 (4.5) | 0 (0) | 2 (2.2) | | |
| II | 5 (22.7) | 22 (21.5) | 29 (31.5) | | |
| III | 12 (54.5) | 61 (59.8) | 44 (47.8) | | |
| IV | 4 (18) | 13 (12.7) | 17 (18.5) | | |

*Values are mean ± SD or [median, interquartile range (IQR)] or n (%). DM, diabetes mellitus; BMI, body mass index; STS score, the society of thoracic surgeons scores; NYHA, New York Heart Association; SE, self-expandable; BE, balloon-expandable; THV, transcatheter heart valve. *Smaller borderline-BE-THV vs. larger borderline-BE-THV. [#]Larger borderline-BE-THV vs. non-borderline-SE.*

non-borderline valves due to shift from SE-THV to BE-THV, or vice versa. The SE-THV group included 93 patients implanted with smaller valves, and 150 patients implanted with larger valves. In the BE-THV group, 22 patients were implanted with smaller valves, and 102 patients with larger valves (**Figure 2**).

In BAAS patients implanted with SE-THV, the baseline clinical characteristics of both groups (smaller and larger valves) did not differ, except for the New York Heart Association (NYHA) functional class (**Table 1A**). In addition, no significant differences were observed in imaging (echocardiography and MDCT) measurements (**Table 2A**). In BAAS patients implanted with BE-THV, differences were noted in left ventricular function (**Table 2B**). Other measured baseline clinical and imaging characteristics did not differ between smaller and larger valves implantation (**Tables 1B**, **2B**).

Baseline clinical and imaging characteristics of patients with borderline annulus for SE devices implanted with borderline large SE-THV or non-borderline BE-THV did not differ,

**TABLE 2A |** Baseline echocardiography and MDCT characteristics of patients with BAAS for SE-THV implanted with SE or non-borderline BE-THV.

| | Smaller borderline-SE-THV (*n* = 93) | Larger borderline-SE-THV (*n* = 150) | Non- borderline BE-THV (*n* = 70) | *p* value* | *p* value# |
|---|---|---|---|---|---|
| Distance of LM (mm) | 12.4 ± 3.2 [12, 4.1] | 12.6 ± 2.6 [12.35, 3.6] | 12.6 ± 2.7 [12, 2.5] | 0.26 | 0.39 |
| Distance of RCA (mm) | 14.8 ± 3 [15, 3.9] | 15.19 ± 2.9 [14.8, 3.7] | 14.9 ± 2.8 [15, 4.1] | 0.44 | 0.27 |
| AVA $cm^2$ | 0.65 ± 0.13 | 0.74 ± 0.17 | 0.7 ± 0.19 | 0.3 | 0.3 |
| AV mean pressure (mmHg) | 45 ± 15 [42, 21] | 44 ± 14 [42, 21] | 48 ± 12 [46, 16.5] | 0.4 | 0.02 |
| LV Function | | | | 0.189 | 0.52 |
| Normal (>55%) | 65 (70.6) | 120 (82) | 58 (84) | | |
| Mild (45–54%) | 7 (7.6) | 8 (5.4) | 6 (8.6) | | |
| Mild-moderate (40–44%) | 6 (6.5) | 4 (2.7) | 2 (2.8) | | |
| Moderate (35–39%) | 3 (3.2) | 7 (4.7) | 1 (1.4) | | |
| Moderate-severe (30–34%) | 5 (5.4) | 3 (2) | 2 (2.8) | | |
| Severe (<29%) | 6 (6.5) | 4 (2.7) | 0 (0) | | |

*Values are mean ± SD or [median, interquartile range (IQR)] or n (%). LM, left main; RCA, right coronary artery; AV, aortic valve; AVA, aortic valve area; SE, self-expandable; BE, balloon-expandable; THV, transcatheter heart valve; LV, left ventricular. *Smaller borderline-SE-THV vs. larger borderline-SE-THV. #Larger borderline-SE-THV vs. non-borderline-BE.*

**TABLE 2B |** Baseline echocardiography and MDCT characteristics of patients with BAAS for BE-THV implanted with BE or non-borderline SE-THV.

| | Smaller borderline-BE-THV (*n* = 22) | Larger borderline-BE-THV (*n* = 102) | Non- borderline SE-THV (*n* = 96) | *p*-value* | *p*-value# |
|---|---|---|---|---|---|
| Distance of LM (mm) | 13.8 ± 2.7 [14.1, 3.2] | 13.69 ± 3 [13.5, 3.9] | 12.45 ± 2.49 [12.2, 3.7] | 0.36 | 0.0006 |
| Distance of RCA (mm) | 15.66 ± 3.2 [15, 3.7] | 16 ± 3.6 [16, 4.6] | 14.5 ± 3.12 [14, 4.9] | 0.25 | 0.0003 |
| AVA $cm^2$ | 0.7 ± 0.16 | 0.76 ± 0.17 | 0.7 ± 0.19 | 0.55 | 0.144 |
| AV mean pressure (mmHg) | 45 ± 12.86 [48, 18] | 41 ± 16 [41, 20.2] | 44.2 ± 17.4 [40,21.5] | 0.17 | 0.35 |
| LV function | | | | 0.0192 | 0.35 |
| Normal (>55%) | 10 (47.6) | 68 (70.8) | 76 (80.8) | | |
| Mild (45–54%) | 3 (14.2) | 14 (14.5) | 12 (12.7) | | |
| Mild-moderate (40–44%) | 5 (23.8) | 4 (4.1) | 3 (3.2) | | |
| Moderate (35–39%) | 0 (0) | 3 (3.1) | 2 (2.1) | | |
| Moderate-severe (30–34%) | 1 (4.7) | 5 (5.2) | 1 (1) | | |
| Severe (<29%) | 2 (9.5) | 2 (2) | 0 (0) | | |

*Values are mean ± SD or [median, interquartile range (IQR)] or n (%). LM, left main; RCA, right coronary artery; AV, aortic valve; AVA, aortic valve area; SE, self-expandable; BE, balloon-expandable; THV, transcatheter heart valve; LV, left ventricular. *Smaller borderline-BE-THV vs. larger borderline-BE-THV. #Larger borderline-BE-THV vs. non-borderline-SE.*

except for aortic valve mean pressure gradient (**Table 2A**). Comparison between non-borderline SE-THV implantation to large BE-borderline valves implantation in patients with borderline annulus for BE devices showed more females and higher Society of Thoracic Surgeons (STS) score in patients implanted with non-borderline SE-THV compared to large BE-borderline valves (**Table 1B**). In addition, in patients implanted with non-borderline SE-THV the left main (LM) and right coronary artery (RCA) heights were shorter compared with patients implanted with larger BE-borderline valves (**Table 2B**).

In the present cohort, favorable outcomes were observed while using larger valves in BAAS patients. For SE-THV, selection of larger valves compared to smaller valves was accompanied with significantly lower rates of PVL measured by both echocardiography (none: 54.6 vs. 35.5%, mild: 36 vs. 54.8%, mild to moderate: 7.3 vs. 6.4%, moderate: 2 vs. 2.1%, moderate to severe: 0 vs. 1%; pv = 0.0282; **Figure 3**; **Table 3**) and angiography (none: 85.3 vs. 68.8%, mild: 13.3 vs. 27.9%, moderate: 1.3 vs. 3.2%; pv = 0.0088; **Table 3**) and a trend toward lower gradients across the THV (7.9 ± 5.4 vs. 10.2 ± 10.8; pv = 0.083; **Figure 4**; **Table 3**); for BE-THV, selection of larger valves compared to smaller valves resulted in better hemodynamics with lower gradients across the THV (9.9 ± 3.7 vs. 12.5 ± 7.2; pv = 0.019; **Figure 4**; **Table 3**). In BE-THV no significant differences were demonstrated in PVL rates while comparing larger to

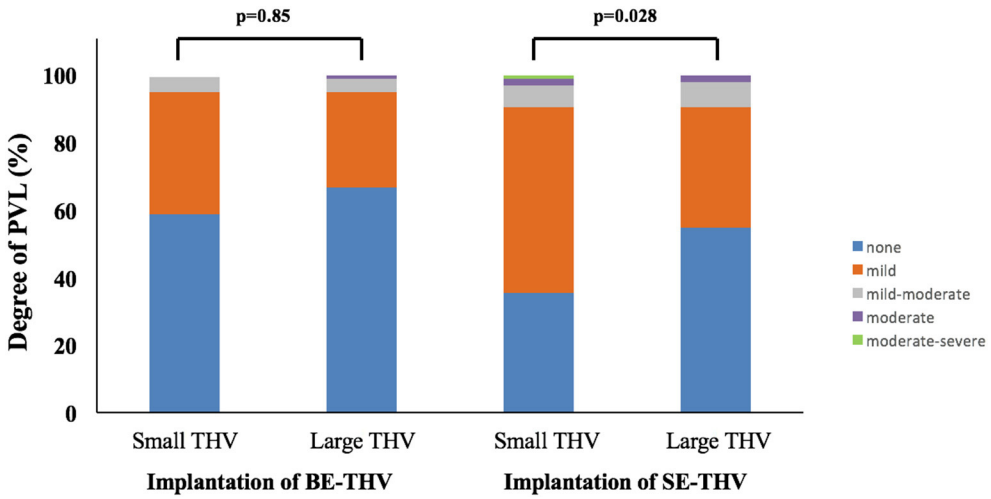


**FIGURE 3 |** Incidence of paravalvular leak in patients with BAAS. BE, balloon-expandable; SE, self-expandable; THV, transcatheter heart valve; BAAS, borderline aortic annulus size; PVL, paravalvular leak.

smaller valves implantation in BAAS patients (**Figure 2**; **Table 3**). Selection of larger valves (either SE or BE) in BAAS patients did not change the rate of post-dilatation as well as adverse clinical outcomes such as new left bundle branch block (LBBB), rate of new pacemaker implantation, stroke or transient ischemic attack (TIA), annular rupture, coronary occlusion, or mortality (**Table 3**).

Shift from large borderline SE-THV to non-borderline BE-THV was associated with higher gradients across the THV (7.98.5 ± 5.46.3 vs. 12.11 ± 4.53; pv < 0.0001; **Figure 4**; **Table 4**); However, lower rates of post-dilatation were observed (38 vs. 12.8%; pv = 0.0001; **Table 4**), but without significant differences in PVL rates (**Table 4**). In a subgroup of patients who didn't undergo post-dilatation the PVL rates also did not differ (**Table 4**). Shift from large borderline BE-THV to non-borderline SE-THV resulted in lower gradients (9.9 ± 3.7 vs. 7.8 ± 3.5, pv < 0.001; **Figure 4**; **Table 4**), and increased rates of post-dilatation (7.8 vs. 35.4%, pv < 0.001; **Table 4**) with a trend toward increased overall PVL rated per echocardiography (33 vs. 45.8%, pv = 0.08; **Table 4**). In a subgroup of patients who didn't undergo post-dilation the PVL rates were increased in non-borderline SE-THV compared to large borderline BE-THV (none: 35.8 vs. 72%, mild: 51.2 vs. 25.8%, mild to moderate: 10.2 vs. 3.37%, moderate: 3 vs. 0%, pv = 0.001; **Table 4**).

## DISCUSSION

Borderline annulus size (annular dimensions in between 2 valve sizes) is common among patients undergoing TAVI, however, the most effective THV selection strategy for these patients remains unclear. The present study of 598 patients with severe symptomatic AS undergoing TAVI based on the ISRAELI-TAVI registry is the largest observational study to date comparing clinical outcomes according to size selection of SE-THV and BE-THV in patients with BAAS. The main findings of our study (**Figure 1**) are as follows:

- In patients with BAAS, the larger THV device reduced PVL rates and optimized THV hemodynamics.
- Selection of a larger valve in BAAS patients did not increase adverse clinical outcomes such as new LBBB, rate of new pacemaker implantation, stroke or TIA, annular rupture, coronary occlusion or mortality.
- Shift from borderline THV to non-borderline THV modified THV hemodynamics and post dilatation rates. Shift from borderline SE-THV to non-borderline BE-THV was associated with lower post dilatation rates, but with higher gradients. Shift from borderline BE-THV to non-borderline SE-THV led to optimized THV hemodynamics, but with increased post-dilatation rates; In addition, in a subgroup of patients in whom post-dilatation was not performed, increased PVL rates were observed.

Large size THV implantation was previously shown to be associated with favorable hemodynamics and lower PVL rate, both are important determinants of clinical outcomes in AS patients following TAVI (4, 12). In fact, evidence shows deleterious prognostic effects even with mild residual PVL after TAVI, including increased mortality (13, 14). In addition, higher post-TAVI transaortic gradients are associated with decreased THV long-term durability (15). The advantages of implanting larger, over smaller, devices were indeed reflected in our cohort of BAAS patients by reduced PVL rates and optimized THV hemodynamics. These findings are particularly important in the current era, in which younger and relatively healthier patients are being treated with TAVI and in whom the durability of the device is extremely important to minimize the need for future reintervention. Importantly, the use of a larger THV in BAAS patients was not associated with increased adverse outcomes commonly encountered with large prostheses, such

**TABLE 3 |** Comparison of procedural and post-procedural outcomes between BAAS patients implanted with smaller vs. larger valves (SE or BE).

| | SE-borderline THV | | *p*-value | BE-borderline THV | | *p*-value |
|---|---|---|---|---|---|---|
| | **Smaller (*n* = 93)** | **Larger (*n* = 150)** | | **Smaller (*n* = 22)** | **Larger (*n* = 102)** | |
| Need for post-dilatation | 37 (40) | 57 (38) | 0.786 | 1 (4.7) | 8 (7.8) | 1 |
| device success (VARC-2) (%) | 91 (97) | 146 (97) | 1 | 22 (100) | 101(99) | 1 |
| Need for a second valve (%) | 2 (2) | 2 (1.3) | 0.638 | 0 (0) | 2 (1.9) | 1 |
| Valve malposition (%) | 2 (2) | 2 (1.3) | 0.638 | 0 (0) | 0 (0) | |
| Valve migration (%) | 2 (2) | 1 (0.6) | 0.565 | 0 (0) | 0 (0) | |
| Ischemic stroke/TIA (%) | 3 (3.2) | 2 (0.1) | 0.616 | 2 (9) | 0 (0) | 0.12 |
| Endocarditis (%) | 2 (2) | 0 (0) | 1 | 0 (0) | 1 (0.98) | 1 |
| Procedural mortality (%) | 1 (1) | 2 (0.1) | 0.599 | 0 (0) | 0 (0) | |
| Coronary obstruction (%) | 0 (0) | 0 (0) | | 0 (0) | 0 (0) | |
| New LBBB (%) | 21 (23) | 34 (23) | 0.882 | 4 (18.1) | 29 (28) | 0.471 |
| New pacemaker (%) | 16 (17) | 17 (11.3) | 0.4 | 2 (9) | 21 (20) | 0.521 |
| AV mean pressure (mmHg) | 10.2 ± 10.8 [8, 4.1] | 7.9 ± 5.4 [7, 4] | 0.083 | 12.5 ± 7.2 [12, 5.7] | 9.9 ± 3.7 [9.6,5] | 0.019 |
| PVL per angiogram | | | 0.0088 | | | 0.403 |
| None | 64 (68.8) | 128 (85.3) | | 21 (95.4) | 88 (86) | |
| Mild | 26 (27.9) | 20 (13.3) | | 1 (4.5) | 14 (13.7) | |
| Moderate | 3 (3.2) | 2 (1.3) | | 0 (0) | 0 (0) | |
| PVL per echo | | | 0.028 | | | 0.856 |
| None (%) | 33 (35.5) | 82 (54.6) | | 13 (59) | 68 (66.6) | |
| Mild (%) | 51 (54.8) | 54 (36) | | 8 (36) | 29 (28.4) | |
| Mild-mod (%) | 6 (6.4) | 11 (7.3) | | 1 (4.5) | 4 (3.9) | |
| Moderate (%) | 2 (2.1) | 3 (2) | | 0 (0) | 1 (0.98) | |
| Moderate-severe (%) | 1 (1) | 0 (0) | | 0 (0) | 0 (0) | |

*Values are mean ± SD or [median, interquartile range (IQR)] or n (%). VARC, valve academic research consortium; TIA, transient ischemic attack; LBBB, left bundle branch block; AV, aortic valve; PVL, paravalvular leak; echo, echocardiography; SE, self-expandable; BE, balloon-expandable; THV, transcatheter heart valve. Post-procedural outcomes (during index hospitalization) were endocarditis and new pacemaker implantation.*

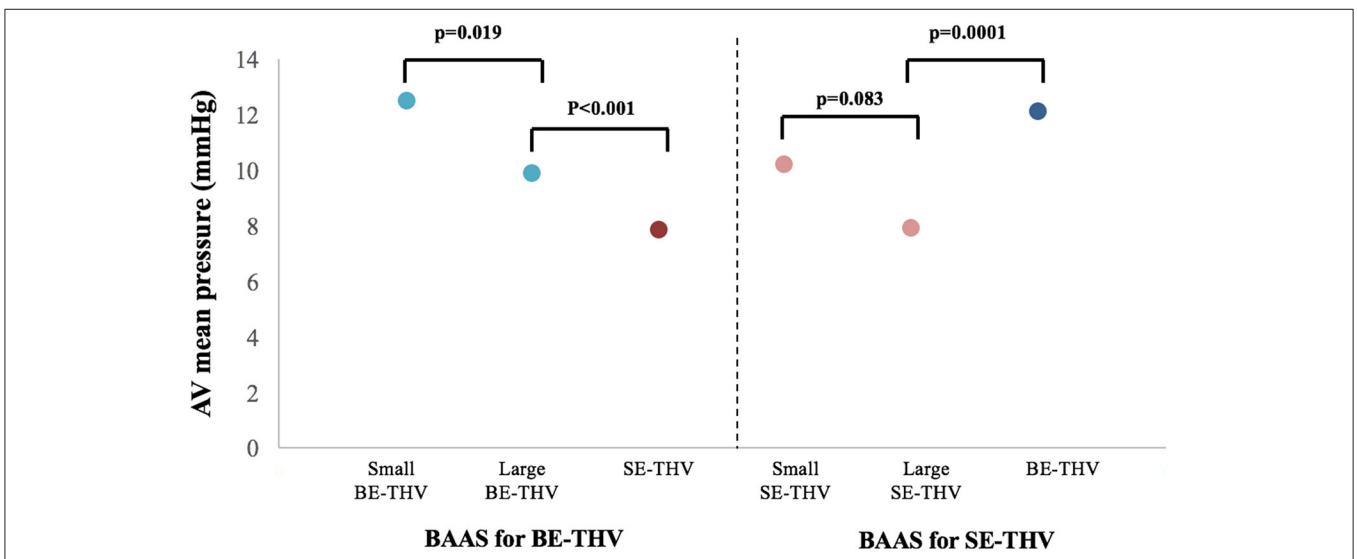


**FIGURE 4 |** Transcatheter heart valve hemodynamics in patients with BAAS. AV, aortic valve; BE, balloon-expandable; SE, self-expandable; THV, transcatheter heart valve, BAAS, borderline aortic annulus size.

**TABLE 4 |** Comparison of procedural and post-procedural outcomes between patients implanted with large borderline-SE vs. non-borderline-BE devices; or large borderline-BE vs. non-borderline-SE devices.

| | **BAAS only for SE device** | | ***p*-value** | **BAAS only for BE device** | | ***p*-value** |
|---|---|---|---|---|---|---|
| | **Large SE-borderline valve (*n* = 150)** | **BE- non-borderline valve (*n* = 70)** | | **Large BE-borderline valve (*n* = 102)** | **SE- non-borderline valve (*n* = 96)** | |
| Need for post dilatation | 57 (38) | 9 (12.8) | 0.0001 | 8 (7.8) | 34 (35.4) | 2.97e-06 |
| Device success (VARC-2) (%) | 146 (97) | 70 (100) | 0.554 | 101 (99) | 93 (96.8) | 0.11 |
| Need for a second valve (%) | 2 (1.3) | 0 (0) | 1 | 2 (1.9) | 2 (2) | 1 |
| Valve malposition (%) | 2 (1.3) | 0 (0) | 1 | 0 (0) | 1 (1) | 1 |
| Valve migration (%) | 1 (0.6) | 0 (0) | 1 | 0 (0) | 0 (0) | |
| Ischemic stroke/TIA (%) | 2 (0.1) | 0 (0) | 1 | 0 (0) | 2 (2) | 0.508 |
| Endocarditis (%) | 0 (0) | 1 (1.4) | 0.36 | 1 (0.98) | 1 (1) | 1 |
| Procedural mortality (%) | 2 (0.1) | 0 (0) | 0.528 | 0 (0) | 1 (1.6) | 0.927 |
| Coronary obstruction (%) | 0 (0) | 2 (3.3) | 0.166 | 0 (0) | 1 (1.6) | 0.927 |
| New LBBB (%) | 34 (23) | 17 (28.3) | 0.615 | 29 (28) | 27 (28.1) | 0.737 |
| New pacemaker (%) | 17 (11.3) | 9 (15) | 0.579 | 21 (20) | 17 (17.7) | 0.499 |
| AV mean pressure (mmHg) | 7.9 ± 5.4 (7, 4) | 12.1 ± 4.5 (12, 8) | 1.70e-10 | 9.9 ± 3.7 [9.6, 5] | 7.8 ± 3.5 (7, 5) | 3.90e-05 |
| PVL per echo$^{+}$ | | | 0.246 | | | 0.191 |
| None (%) | 82 (54.6) | 47 (67.1) | | 68 (66.6) | 52 (54) | |
| Mild (%) | 54 (36) | 20 (28.5) | | 29 (28.4) | 36 (37.5) | |
| Mild-mod (%) | 11 (7.3) | 3 (4.3) | | 4 (3.9) | 6 (6.25) | |
| Moderate (%) | 3 (2) | 0 (0) | | 1 (0.98) | 2 (2) | |
| Moderate-severe (%) | 0 (0) | 0 (0) | | 0 (0) | 0 (0) | |
| Overall PVL per echo$^{+}$ | 68 (45.3) | 23 (32.8) | 0.106 | 34 (33) | 44 (45.8) | 0.0818 |
| | **Large SE-borderline valve (*n* = 93)** | **BE- non-borderline valve (*n* = 32)** | | **Large BE-borderline valve (*n* = 94)** | **SE- non-borderline valve (*n* = 39)** | |
| PVL per echo$^{+}$ | | | 0.699 | | | 0.0015 |
| None (%) | 42 (45.1) | 16 (50) | | 68 (72.3) | 14 (35.8) | |
| Mild (%) | 40 (45.9) | 14 (43.7) | | 23 (25.8) | 20 (51.2) | |
| Mild-moderate (%) | 10 (11.4) | 2 (6.25) | | 3 (3.37) | 4 (10.2) | |
| Moderate (%) | 1 (1.1) | 0 (0) | | 0 (0) | 1 (3) | |
| Moderate-severe (%) | 0 (0) | 0 (0) | | 0 (0) | 0 (0) | |
| Overall PVL per echo$^{+}$ | 51 | 16 | 0.413 | 26 | 25 | 0.0003 |

*Values are mean ± SD or [median, interquartile range (IQR)] or n (%). VARC, valve academic research consortium; TIA, transient ischemic attack; LBBB, left bundle branch block; AV, aortic valve; PVL, paravalvular leak; SE, self-expandable; BE, balloon-expandable; THV, transcatheter heart valve; echo, echocardiography. $^{+}$subgroup of patients who did undergo post-dilatation. Post-procedural outcomes (during index hospitalization) were endocarditis and new pacemaker implantation.*

as conduction disturbances, annular rupture and coronary occlusion (16, 17). Given the above results, the present study strengthens recent results from the PARTNER 3 trial (6) and advocates the selection of a large THV for BAAS patients undergoing TAVI with either SE or BE prostheses.

In our cohort of BAAS patients, 93% of cases were defined as BAAS for one device only (i.e., either BE or SE). In these patients, it is thus conceivable to apply a strategy of selecting the non-borderline device whenever possible. In fact, non-borderline devices were selected over borderline devices in 38.6% of patients in our cohort. We found that selection of non-borderline SE-THV over borderline BE-THV led to lower gradients. On the other hand, selection of non-borderline BE-THV over borderline SE-THV was associated with lower rates of post-dilatation, but at the cost of increased gradients. This trade-off between PVL and higher gradients was repeatedly described in comparative studies between BE and SE devices both in tricuspid and bicuspid AS patients (18, 19). These changes were mainly attributed to THV mechanical characteristics, such as annular/supra-annular valve position, radial forces, and the presence of outer skirt (15). Therefore, our findings point out that similar considerations taken while selecting THV type for non-BAAS patients (including calcifications, coronary height, sinus of valsalva dimensions), should be applied also in BAAS patients.

We acknowledge several limitations of our study. The main limitation is the observational nature of the study. Therefore, undocumented factors, such as sinus of valsalva diameter or calcium score, may have affected device selection. In addition, potential impact of unknown or unmeasured confounding factors on study outcomes cannot be excluded. The low number

of patients implanted with smaller BE-valve may affect the significance of the results and even necessitated the exclusion of patients with annulus measurements of 330–350 $mm^2$ from the analysis. BE-TVH over or under-sizing by over or under-inflation of the valve balloon in order to fine tune the valve dimensions was not registered and might have affected *in-situ* valve size. Nevertheless, the practice of over/under-inflation in the four centers was according to a known algorithm proposed by the company.

The results of the present study support, for both devices (BE and SE), the selection of larger valves for TAVI candidates with BAAS. Shifting from borderline devices to non-borderline devices resulted in significant changes in post-dilatation, PVL, and gradients across the THV. Therefore, our findings point out that the same consideration taken while selecting THV type for non-BAAS patients, should be applied in BAAS patients, and whenever a borderline device is selected the larger valve device should be recommended.

## CONCLUSIONS

The results of the present study support, for both devices (BE and SE), the selection of larger valves for TAVI candidates with BAAS. Shifting from borderline devices to non-borderline devices resulted in significant changes in PVL and THV hemodynamics. Therefore, our findings point out that the same consideration taken while selecting THV type for non-BAAS patients, should be applied in BAAS patients, and whenever a borderline device is selected the larger valve device is recommended.

## DATA AVAILABILITY STATEMENT

The original contributions presented in the study are included in the article/supplementary materials, further inquiries can be directed to the corresponding author.

## AUTHOR CONTRIBUTIONS

YT-B, RK, JB-S, and PC conceived the project, designed and interpreted the results, and wrote the manuscript. NB conducted all analyses and interpreted the results. HV-A, AH, BK, HD, GP, MK, AF, ASt, IM, ASe, and AB coordinated and designed data collection and interpreted the results. All authors contributed to the article and approved the submitted version.

## REFERENCES


1. Nkomo VT, Gardin JM, Skelton TN, Gottdiener JS, Scott CG, Enriquez-Sarano M. Burden of valvular heart diseases: a population-based study. *Lancet*. (2006) 368:1005–11. doi: 10.1016/S0140-6736(06)69208-8
2. Mack MJ, Leon MB, Thourani VH, Makkar R, Kodali SK, Russo M, et al. Transcatheter aortic-valve replacement with a balloon-expandable valve in low-risk patients. *N Engl J Med*. (2019) 380:1695–705. doi: 10.1056/NEJMoa1814052
3. Leon MB, Smith CR, Mack MJ, Makkar RR, Svensson LG, Kodali SK, et al. Transcatheter or surgical aortic-valve replacement in intermediate-risk patients. *N Engl J Med*. (2016) 374:1609–20. doi: 10.1056/NEJMoa1514616
4. Popma JJ, Gleason TG, Yakubov SJ, Harrison JK, Forrest JK, Maini B, et al. Relationship of annular sizing using multidetector computed tomographic imaging and clinical outcomes after self-expanding CoreValve transcatheter aortic valve replacement. *Circ Cardiovasc Interv*. (2016) 9:3282. doi: 10.1161/CIRCINTERVENTIONS.115.003282
5. Blanke P, Weir-McCall JR, Achenbach S, Delgado V, Hausleiter J, Jilaihawi H, et al. Computed tomography imaging in the context of transcatheter aortic valve implantation (tavi)/transcatheter aortic valve replacement (TAVR): an expert consensus document of the society of cardiovascular computed tomography. *JACC Cardiovasc Imaging*. (2019) 12:1–24. doi: 10.1016/j.jcmg.2018.12.003
6. Ihdayhid AR, Leipsic J, Hahn RT, Pibarot P, Thourani V, Makkar R, et al. Impact of annular oversizing on paravalvular regurgitation and valve hemodynamics: new insights from PARTNER 3. *JACC Cardiovasc Interv*. (2021) 14:2158–69. doi: 10.1016/j.jcin.2021.07.018
7. Kappetein AP, Head SJ, Généreux P, Piazza N, van Mieghem NM, Blackstone EH, et al. Updated standardized endpoint definitions for transcatheter aortic valve implantation: the Valve Academic Research Consortium-2 consensus document. *Eur Heart J*. (2012) 33:2403–18. doi: 10.1093/eurheartj/ehs255
8. Todaro D, Picci REA, Barbanti M. *Current TAVR Devices*. Wayne, PA: Cardiac interventions today.
9. Grube E, Van Mieghem NM, Bleiziffer S, Modine T, Bosmans J, Manoharan G, et al. Clinical outcomes with a repositionable self-expanding transcatheter aortic valve prosthesis: the international forward study. *J Am Coll Cardiol*. (2017) 70:845–53. doi: 10.1016/j.jacc.2017.06.045
10. Forrest JK, Mangi AA, Popma JJ, Khabbaz K, Reardon MJ, Kleiman NS, et al. Early outcomes with the evolut PRO repositionable self-expanding transcatheter aortic valve with pericardial wrap. *JACC Cardiovasc Interv*. (2018) 11:160–8. doi: 10.1016/j.jcin.2017.10.014
11. Wendler O, Schymik G, Treede H, Baumgartner H, Dumonteil N, Neumann F-J, et al. 3: 1-year outcomes post-transcatheter aortic valve implantation using the latest generation of the balloon-expandable transcatheter heart valve. *Eur Heart J*. (2017) 38:2717–26. doi: 10.1093/eurheartj/ehx294
12. Willson AB, Webb JG, Labounty TM, Achenbach S, Moss R, Wheeler M, et al. 3-dimensional aortic annular assessment by multidetector computed tomography predicts moderate or severe paravalvular regurgitation after transcatheter aortic valve replacement: a multicenter retrospective analysis. *J Am Coll Cardiol*. (2012) 59:1287–94. doi: 10.1016/S0735-1097(12)60326-X
13. Kodali SK, Williams MR, Smith CR, Svensson LG, Webb JG, Makkar RR, et al. Two-year outcomes after transcatheter or surgical aortic-valve replacement. *N Engl J Med*. (2012) 366:1686–95. doi: 10.1056/NEJMoa1200384
14. Kodali S, Pibarot P, Douglas PS, Williams M, Xu K, Thourani V, et al. Paravalvular regurgitation after transcatheter aortic valve replacement with the Edwards sapien valve in the PARTNER trial: characterizing patients and impact on outcomes. *Eur Heart J*. (2015) 36:449–56. doi: 10.1093/eurheartj/ehu384
15. Abdel-Wahab M, Landt M, Neumann F-J, Massberg S, Frerker C, Kurz T, et al. 5-year outcomes after TAVR with balloon-expandable versus self-expanding valves: results from the CHOICE randomized clinical trial. *JACC Cardiovasc Interv*. (2020) 13:1071–82. doi: 10.1016/j.jcin.2019.12.026
16. Lin S-I, Miura M, Tagliari AP, Lee Y-H, Shirai S, Puri R, et al. Intraventricular conduction disturbances after transcatheter aortic valve implantation. *Interv Cardiol*. (2020) 15:e11. doi: 10.15420/icr.2020.07
17. Pasic M, Unbehaun A, Buz S, Drews T, Hetzer R. Annular rupture during transcatheter aortic valve replacement: classification, pathophysiology, diagnostics, treatment approaches, and prevention. *JACC Cardiovasc Interv*. (2015) 8:1–9. doi: 10.1016/j.jcin.2014.07.020
18. Van Belle E, Vincent F, Labreuche J, Auffret V, Debry N, Lefèvre T, et al. Balloon-expandable versus self-expanding transcatheter aortic valve replacement: a propensity-matched comparison from the FRANCE-TAVI registry. *Circulation*. (2020) 141:243–59. doi: 10.1161/CIRCULATIONAHA.120.047270
19. Mangieri A, Tchetchè D, Kim W-K, Pagnesi M, Sinning J-M, Landes U, et al. Balloon versus self-expandable valve for the

treatment of bicuspid aortic valve stenosis: insights from the BEAT international collaborative registrys. *Circ Cardiovasc Interv.* (2020) 13:e008714. doi: 10.1161/CIRCINTERVENTIONS.119.008714

**Conflict of Interest:** The authors declare that the research was conducted in the absence of any commercial or financial relationships that could be construed as a potential conflict of interest.

**Publisher's Note:** All claims expressed in this article are solely those of the authors and do not necessarily represent those of their affiliated organizations, or those of the publisher, the editors and the reviewers. Any product that may be evaluated in this article, or claim that may be made by its manufacturer, is not guaranteed or endorsed by the publisher.

frontiers in Cardiovascular Medicine

REVIEW
published: 11 March 2022
doi: 10.3389/fcvm.2022.849032

# Challenges in Diagnosis and Functional Assessment of Coronary Artery Disease in Patients With Severe Aortic Stenosis

*Srdjan Aleksandric*[1,2]*, *Marko Banovic*[1,2] and *Branko Beleslin*[1,2]

[1] Cardiology Clinic, University Clinical Center of Serbia, Belgrade, Serbia, [2] Faculty of Medicine, University of Belgrade, Belgrade, Serbia

More than half of patients with severe aortic stenosis (AS) over 70 years old have coronary artery disease (CAD). Exertional angina is often present in AS-patients, even in the absence of significant CAD, as a result of oxygen supply/demand mismatch and exercise-induced myocardial ischemia. Moreover, persistent myocardial ischemia leads to extensive myocardial fibrosis and subsequent coronary microvascular dysfunction (CMD) which is defined as reduced coronary vasodilatory capacity below ischemic threshold. Therefore, angina, as well as noninvasive stress tests, have a low specificity and positive predictive value (PPV) for the assessment of epicardial coronary stenosis severity in AS-patients. Moreover, in symptomatic patients with severe AS exercise testing is even contraindicated. Given the limitations of noninvasive stress tests, coronary angiography remains the standard examination for determining the presence and severity of CAD in AS-patients, although angiography alone has poor accuracy in the evaluation of its functional severity. To overcome this limitation, the well-established invasive indices for the assessment of coronary stenosis severity, such as fractional flow reserve (FFR) and instantaneous wave-free ratio (iFR), are now in focus, especially in the contemporary era with the rapid increment of transcatheter aortic valve replacement (TAVR) for the treatment of AS-patients. TAVR induces an immediate decrease in hyperemic microcirculatory resistance and a concomitant increase in hyperemic flow velocity, whereas resting coronary hemodynamics remain unaltered. These findings suggest that FFR may underestimate coronary stenosis severity in AS-patients, whereas iFR as the non-hyperemic index is independent of the AS severity. However, because resting coronary hemodynamics do not improve immediately after TAVR, the coronary vasodilatory capacity in AS-patients treated by TAVR remain impaired, and thus the iFR may overestimate coronary stenosis severity in these patients. The optimal method for evaluating myocardial ischemia in patients with AS and co-existing CAD has not yet been fully established, and this important issue is under further investigation. This review is focused on challenges, limitations, and future perspectives in the functional assessment of coronary stenosis severity in these patients, bearing in mind the complexity of coronary physiology in the presence of this valvular heart disease.

**Keywords: aortic stenosis, coronary artery disease, myocardial ischemia, transcatheter aortic valve replacement, fractional flow reserve, instantaneous wave-free ratio**

OPEN ACCESS

***Edited by:***
*Sanjeev Bhattacharyya,*
*Barts Heart Centre, United Kingdom*

***Reviewed by:***
*Kush Patel,*
*Barts Heart Centre, United Kingdom*
*Yosuke Miyazaki,*
*Yamaguchi University, Japan*

***Correspondence:**
*Srdjan Aleksandric*
*srdjanaleksandric@gmail.com*

***Specialty section:***
*This article was submitted to Cardiovascular Imaging, a section of the journal Frontiers in Cardiovascular Medicine*

***Received:*** *05 January 2022*
***Accepted:*** *16 February 2022*
***Published:*** *11 March 2022*

***Citation:***
*Aleksandric S, Banovic M and Beleslin B (2022) Challenges in Diagnosis and Functional Assessment of Coronary Artery Disease in Patients With Severe Aortic Stenosis. Front. Cardiovasc. Med. 9:849032. doi: 10.3389/fcvm.2022.849032*

## INTRODUCTION

Degenerative aortic stenosis (AS) is the most common valvular heart disease in both western and developed countries, affecting mainly individuals older than 60 years (1–4). Co-existing coronary artery disease (CAD) is present in more than 50% of patients with severe AS over 70 years of age and in more than 65% of patients with severe AS over 80 years of age (2, 3, 5). Both conditions are strongly associated with age and risk factors for degenerative AS are similar to those seen in atherosclerosis including male sex, smoking, hypertension, diabetes, low-density lipoprotein (LDL) cholesterol, and C-reactive protein (2, 4–6). According to current guidelines of the European Society of Cardiology (ESC) and of the American College of Cardiology/American Heart Association (ACC/AHA), coronary artery bypass grafting (CABG) is recommended (class I, level of evidence C) in addition to surgical aortic valve replacement (SAVR) during the same surgical procedure in patients with a severe symptomatic AS and concomitant coronary stenosis ≥70% diameter stenosis (DS) or ≥50% DS in case of left main (LM) stenosis, whereas CABG should be considered in AS-patients with concomitant stenosis ≥50–70% DS in non-LM coronary arteries (class IIa, level of evidence C) (7–9). Two large studies demonstrated that significant CAD which was not revascularized at the time of SAVR was associated with increased risk of adverse short- and long-term outcomes (10–12). In contrast, several surgical nonrandomized studies identified concomitant CABG as an independent predictor of short and long-term mortality among patients undergoing SAVR, especially in elderly patients above 80 years old (5, 10, 13–19). Accordingly, over the last decade, transcatheter aortic valve replacement (TAVR) has been established as the treatment of choice for patients with severe symptomatic AS who are deemed inoperable or at high-risk for SAVR. These high-risk AS-patients are frequently elderly with different comorbidities beyond CAD, such as chronic kidney disease, diabetes, hypertension, or impaired left ventricle (LV) systolic and/or diastolic function (5). Thus, the prevalence of CAD is extremely high in this patient population, ranging up to 75% (5). In recent years, published large randomized trials and meta-analyses demonstrated non-inferiority and even superiority concerning major adverse cardiac events (MACE) favoring TAVR over SAVR across the spectrum of AS-patients, irrespective of baseline surgical risk (20–24). In addition, recently presented the Aortic Valve ReplAcemenT vs. Conservative Treatment in Asymptomatic SeveRe Aortic Stenosis (AVATAR) randomized trial demonstrated benefit of early SAVR in asymptomatic patients with severe AS and normal LV ejection fraction (25). Expert consensus opinion (class IIa, level of evidence C) highlights that percutaneous coronary intervention (PCI) should be considered in AS-patients with a primary indication to undergo TAVR who have stenosis of at least 70% DS in the proximal segments of epicardial coronary arteries that subtend a large area of myocardium at risk (7, 10). This has been recently challenged with the results from the Assessing the Effects of Stenting in Significant Coronary Artery Disease Prior to Transcatheter Aortic Valve Implantation (ACTIVATION) trial (26). Obviously, the optimal management of AS-patients with concomitant CAD in patients undergoing TAVR remains controversial due to the heterogeneity of available data, and the clinical relevance of PCI performed before or immediately after TAVR remains to be determined (2, 5, 27–29). Yet, the purpose of this review is to focus on challenges, limitations, and future perspectives in the functional assessment of coronary artery stenosis in patients with AS, bearing in mind the complexity of coronary physiology in the presence of this valvular heart disease.

## CORONARY ARTERY DISEASE ASSESSMENT IN PATIENTS WITH AORTIC STENOSIS

Exertional angina is the most common presenting symptom in patients with obstructive CAD (2, 4, 6). However, angina is also often present in patients with severe AS, even in the absence of obstructive CAD, as LV oxygen demand exceeds supply (2, 4, 6). The presence of AS increases LV afterload and wall stress resulting in concentric LV hypertrophy as a compensatory mechanism to normalize LV wall stress and maintain LV systolic function (30). Consequently, cardiac output in most of these patients is preserved for many years despite an elevated LV afterload. Hence, the LV oxygen demand is increased by LV afterload, LV hypertrophy, inotropic state and prolonged systolic ejection phase, particularly in the LV subendocardium (2, 4, 6, 30). In such condition, resting coronary blood flow is sustained due to vasodilation of intramyocardial arterioles induced by autoregulation phenomenon. However, coronary blood flow is a significantly diminished during exercise or tachycardia which is usually documented by reduced coronary flow reserve (CFR) during adenosine-induced maximal hyperemia (2, 4, 6, 30). There are 3 possible mechanisms for impaired CFR during exercise or tachycardia in AS-patients with LV hypertrophy: (1) reduced diastolic filling time with subsequent low coronary perfusion pressure; (2) elevated LV diastolic filling pressure with subsequent compression of the LV endocardium and subendocardial hypoperfusion; and (3) arteriolar remodeling, perivascular fibrosis and relative decline in myocardial capillary density as a consequence of prolonged LV hypertrophy (2, 4, 6, 30–33). These mechanisms are responsible for the diminished LV oxygen supply in these patients, especially during exercise or tachycardia (2, 4, 6, 30–33). As a result of concomitant increased LV oxygen demand and diminished LV oxygen supply, exercise-induced myocardial ischemia and exertional angina may occur. Moreover, persistent myocardial ischemia leads to extensive myocardial fibrosis and subsequent coronary microvascular dysfunction (CMD) which is defined as reduced coronary vasodilatory capacity below ischemic threshold (2, 4, 6). Therefore, angina, as well as non-invasive stress tests, have a low specificity and positive predictive value (PPV) for the assessment of epicardial coronary stenosis severity in AS-patients (2, 4, 6). A case in point, approximately 20% of patients with severe AS and non-ischemic exercise-testing have significant CAD at subsequent coronary angiography defined as the visually assessed

coronary stenosis >70% DS or 50–70% DS with fractional flow reserve (FFR) $\leq$ 0.80 (34).

In patients with severe AS, the conventional exercise-stress test and thallium-201 exercise-scintigraphy are generally found to be inaccurate with low specificity for CAD assessment since clinical symptoms and baseline ECG abnormalities are neither specific nor sensitive (35–41). Exercise-induced myocardial ischemia may occur in these patients, even in the absence of CAD (35–41). While exercise-stress testing is contraindicated for symptomatic patients with severe AS, it has clinical relevance for identifying those asymptomatic AS-patients who are at high-risk of poor prognosis (8, 9, 35–41). Pharmacological stress tests such as single photon emission computed tomography (SPECT), positron emission tomography (PET) or cardiac magnetic resonance (CMR) with different vasodilators (adenosine, dipyridamole or regadenoson) have been shown to be a valuable alternative to exercise-stress testing for the CAD assessment in these patients (35–41). These pharmacological tests were found to be safer and more accurate for identifying functionally significant CAD compared to exercise-stress testing in AS-patients (35–41). However, due to its limited specificity and PPV, a more sophisticated diagnostic tools were developed for assessing the coronary stenosis severity in these patients. Given the limitations of noninvasive stress tests, invasive coronary angiography remains the standard examination for determining the presence and severity of CAD in AS-patients, although angiography alone has poor accuracy in the evaluation of its functional severity (5, 6, 28). Current ESC and ACC/AHA guidelines for the management of patients with valvular heart disease recommend coronary angiography before aortic valve replacement (AVR) in symptomatic men and premenopausal women with at least one CAD risk factor >35 years old, in all asymptomatic men >45 years old and in all women >55 years old (8, 9).

Several studies suggest that coronary computed tomography angiography (CCTA) is a reasonable alternative to invasive coronary angiography for assessing CAD before AVR in AS-patients who have a low probability of CAD or in whom invasive coronary angiography is technically not feasible or associated with a high-risk (8–12, 19, 42–57). Compared with invasive coronary angiography, it has been shown that electrocardiogram-gated CCTA has high sensitivity and negative predictive value (Sn: 89–100%; NPV: 91–100%), but low specificity and positive predictive value (Sp: 37–99%; PPV: 8–85%) in detecting angiographically significant coronary stenosis defined as >50% DS (8–12, 19, 42–57). Consequently, CTCA may be useful in excluding angiographically significant stenosis among patients at a low-risk of atherosclerosis (8–12, 19, 42–57). Chieffo et al. demonstrated that using CCTA for CAD screening prior to TAVR reduces the need for invasive coronary angiography by approximately 80%, potentially lowering both overall cost and length of hospitalization without increasing the risk of ischemic cardiovascular events (57). Invasive coronary angiography may therefore be performed when CCTA is contraindicated, fails to assess coronary anatomy, or reveals an angiographically significant proximal coronary artery lesion (8–12, 19, 42–58). However, CCTA alone cannot assess the functional significance of coronary stenosis because it provides only anatomical information about the presence and extent of CAD, and can overestimate stenosis severity, especially in the presence of high calcium scores (59–64). Recently, FFR derived from CCTA ($FFR_{ct}$) has developed as the novel noninvasive method that provides both anatomical and functional evaluation of CAD (59–64). It has been shown that $FFR_{ct}$ has high sensitivity and negative predictive value (Sn: 74–88%; NPV: 90–92%), but low specificity and positive predictive value (Sp: 60–82%; PPV: 41–74%) to identify functionally significant coronary stenosis defined as FFR $\leq$ 0.80 (59–64). In the Computed Tomography-Derived Fractional Flow Reserve in Patients with Severe Aortic Stenosis (CAST-FFR) study similar diagnostic accuracy were observed among patients with severe AS and co-existing CAD in pre-TAVR settings (65). These findings suggest that noninvasively measured $FFR_{ct}$ before TAVR may accurately and safely exclude ischemia-driven coronary lesion and reduce the need for invasive coronary angiography in AS-patients (57–65). Further studies are required to determine the clinical utility of FFRct regarding pre-TAVR diagnostic accuracy and outcomes at longer follow-up in these patients.

## PATHOPHYSIOLOGICAL MECHANISMS OF EXERTIONAL ANGINA IN THE PRESENCE OF AORTIC STENOSIS

Developing exertional angina dramatically worsens the prognosis of patients with AS, which is why AVR is highly indicated in these patients (8, 9, 66–69). Several studies demonstrated that impaired myocardial and/or coronary flow reserve, defined as the maximal hyperemic to resting myocardial or coronary blood flow ratio, is a key mechanism for developing exertional angina in patients with severe AS without obstructive CAD (67–77). Importantly, coronary microvascular function is additionally impaired is patients who have AS and concomitant diabetes, which is a common finding (78, 79). Using adenosine-stress cardiac magnetic resonance (CMR) imaging, Ahn et al. showed that the semiquantitative myocardial perfusion reserve index (MPRI) was significantly lower in the group of symptomatic patients with severe AS and angiographically normal coronary arteries compared to the group of asymptomatic AS-patients, as well as compared to the normal control group (67). Similar findings were observed in other studies evaluating both noninvasive and invasive myocardial and/or coronary flow reserve during adenosine-induced maximal hyperemia (68–77). Likewise, microcirculatory resistance in these patients was significantly higher during maximal hyperemia but significantly lower under baseline conditions in comparison to the control group (68–77). Of note, several previously published studies also noted that myocardial and/or coronary blood flow during hyperemia was markedly reduced in AS-patients who also had LV hypertrophy in comparison to normal subjects, but not at rest (67–77, 80). These findings implicate that the vasodilatory capacity of intramyocardial arterioles in severe AS-patients with LV hypertrophy but without CAD is already exhausted by the autoregulation phenomenon to maintain resting coronary

blood flow in response to increased LV mass and LV oxygen demand, and therefore, the vasodilatory effect of adenosine on microcirculatory resistance is limited during maximal hyperemia (67–77, 80). Hence, a significantly reduced coronary vasodilatory capacity during exercise or stress testing may occur in severe AS-patients even in the absence of CMD, as a result of the increased resting perfusion associated with LV hypertrophy and high-pressure LV overload rather than reduced perfusion during testing (81).

Furthermore, Steadman et al. using adenosine-stress CMR imaging with late-gadolinium enhancement (LGE) identified LV hypertrophy and myocardial fibrosis, rather than the AS severity, as the major determinants of impaired myocardial perfusion reserve (MPR) in symptomatic patients with severe AS (80). Similar findings were observed in the study by Zhou et al. (82). Additionally, MPR was the only independent predictor of reduced aerobic exercise capacity (peak VO2) during cardiopulmonary exercise testing in these patients, whereas echocardiographic and CMR measures of the AS severity were not (80). It is well known that the development of LV hypertrophy in AS-patients is an adaptive and compensatory physiological response to reduce LV wall stress and preserve cardiac output (76, 80). However, LV remodeling is associated with arteriolar remodeling, perivascular fibrosis, and capillary rarefaction, which result in the development of myocardial fibrosis and subsequent CMD at a later stage of the disease (67, 76, 80, 83). Contrary to the previous study, Rajappan et al. found that both hyperemic diastolic filling time and AS severity were more important determinants of MPR in severe AS-patients without CAD compared to LV hypertrophy (76). This study revealed that reduced hyperemic diastolic filling time during stress testing in these patients, which was directly associated with the AS severity quantified as the aortic valve area $<1.0$ cm$^2$, leads to impaired myocardial blood flow in LV subendocardium and subsequent decrease in the subendocardial-to-subepicardial perfusion ratio (76). This inconsistency with previously mentioned studies might be due to a small number of AS-patients (only 20) included in the Rajappan study who were predominantly asymptomatic. Therefore, in patients with severe AS and normal coronary arteries, the impaired subendocardial-to-subepicardial perfusion ratio with an absolute reduction in subendocardial perfusion below the ischemic threshold may occur during exercise or stress testing which simultaneously reduces diastolic filling time and increases LV pressures due to tachycardia and increased LV oxygen demand (81, 82). Additionally, it has been noted that only 60% of symptomatic patients with isolated AS had CMR-quantified MPRI values below the ischemic threshold, and vice-versa, that 60% of those who were asymptomatic had MPRI values above the same threshold (67, 81). Based on these findings, the impaired myocardial and/or coronary flow reserve as the primary cause of myocardial ischemia and exertional angina in AS-patients without CAD may occur not only due to the presence of CMD but also due to different hemodynamic conditions that mainly affects diastolic filling time and diastolic perfusion at subendocardial level (81). Therefore, CMD is not equivalent to a reduced myocardial and/or coronary flow reserve in these patients and is characterized by reduced myocardial perfusion throughout the LV wall (transmural myocardial perfusion) without a subendocardial-to-subepicardial perfusion gradient (81). Invasive measurements of microcirculatory resistance index (IMR) by thermodilution technique (with dual-sensor [pressure and temperature] wire) or hyperemic microcirculatory resistance (HMR) with dual-sensor (Doppler and pressure) wire are the methods of choice for the assessment of CMD (81, 84–88). However, IMR and HMR cannot distinguish the presence of CMD from other hemodynamic disorders that result in subendocardial hypoperfusion and ischemia. For this reason, several authors suggest CMR or PET imaging in AS-patients as a noninvasive diagnostic tool for measuring separately absolute subepicardial and subendocardial perfusion and their ratio (81, 84, 89–94).

Moreover, MPR assessed by PET imaging has been found to further decrease with worsening degrees of LV remodeling and the occurrence of systolic LV dysfunction (82). The study also showed that the annual incidence of major adverse cardiac events (MACE) including death, nonfatal myocardial infarction, hospitalization for heart failure or AVR was significantly higher in the group of AS-patients with impaired MPR regardless of their systolic LV functional status, whereas among patients with normal systolic LV function, those with impaired MPR had a significantly higher rate of MACE (82). In the PRognostic Importance of MIcrovascular Dysfunction in Aortic Stenosis (PRIMID-AS) Study, reduced MPR was found to be an independent predictor of symptom onset in initially asymptomatic patients with moderate-to-severe AS (41). The echocardiographically derived impaired coronary flow reserve (CFR) was also shown to be an independent predictor of adverse outcomes in patients with severe AS and nonobstructive epicardial coronary stenosis (95). The above cited studies suggest that reduced coronary vasodilatory capacity should be used not only as a risk-marker, but also could be used as an early sign of pathologic LV remodeling in AS-patients which indicates subendocardial ischemia at an early stage of the disease (82). Previous findings indicate that subendocardial ischemia is a result of synergistic interaction between increased intracavitary LV pressure and systolic extravascular compression, reduced diastolic filling time, low coronary perfusion pressure, and impaired coronary vasodilatory capacity (82). Likewise, the presence of CMD as a consequence of extensive myocardial fibrosis at an advanced stage of AS is considered to be a key indicator for maladaptive LV remodeling (67, 76, 77, 80, 83). These potential mechanisms underlying myocardial ischemia at early and late stages of AS require clarification in further prospective randomized trials.

## CORONARY HEMODYNAMICS AFTER TRANSCATHETER AORTIC VALVE REPLACEMENT (TAVR)

Wiegerinck et al. demonstrated that TAVR induces an immediate increase in hyperemic coronary flow velocity and a concomitant decrease in HMR, resulting in an immediate increase in CFR (77). However, CFR was significantly lower following TAVR compared

to normal subjects despite high acute procedural success in this study, mainly due to unchanged resting hemodynamics before and after TAVR (77). Two studies regarding coronary wave intensity analysis also found that CFR did not improve immediately after TAVR due to unaltered resting coronary flow velocities (96, 97). Contrary, in the study by Stoller et al., a thermodilution-derived CFR and IMR were not improved immediately after TAVR regardless of the presence of angiographically significant fixed coronary stenosis (>50% DS) (98). These studies showed that changes of both CFR and microcirculatory resistance (HMR or IMR) are not associated with the acute reduction of LV afterload and outflow gradient in patients with severe AS following TAVR (77, 98, 99). It seems that autoregulatory microvascular tone in response to LV hypertrophy remains unaffected immediately after TAVR, despite an immediate decrease in both LV afterload and extravascular compression of the intramyocardial arterioles (77, 98). Hence, it is believed that complete restoration of coronary vasodilatory capacity could be improved only several months or even years after TAVR following the regression of LV hypertrophy (70, 77, 98). This was supported by several studies revealing that significant improvement in CFR was achieved only with longer-term follow-up after TAVR following LV hypertrophy regression (70, 99–103). In two of these studies, significant improvement in CFR at 6 and 30 months after AVR was mainly attributable to an increase in coronary blood flow during maximal hyperemia, whereas resting coronary flow remained similar before and after TAVR or SAVR, respectively (100, 102). The small prospective study by Vendrik et al. regarding the longer-term effects of TAVR on invasively measured coronary hemodynamics by dual-sensor (Doppler and pressure) wire revealed an ongoing increase in hyperemic coronary flow as well as in CFR immediately after TAVR and 6 months after the procedure compared with pre-TAVR values (103). Hyperemic microcirculatory resistance was simultaneously continued to decrease in a similar manner as the CFR increased during 6 months follow-up (103). On the other hand, resting coronary flow as well as resting microcirculatory resistance remain unchanged (103). Contrary, in the other two studies, significant improvement in CFR at 12 months after AVR was closely related to decreasing in resting coronary blood flow after SAVR, whereas hyperemic coronary flow remained equivalent (70, 99). Rajappan et al. also demonstrated that a decrease in resting coronary blood flow and subsequent improvement in CFR 12 months after SAVR was primarily associated with the reduction in extravascular compression and concomitant prolongation of hyperemic diastolic filling time with improvement in diastolic myocardial perfusion rather than the regression of LV hypertrophy (99). This hypothesis is supported by the findings that patients with AS experience relief of anginal symptoms immediately after AVR, even before LV hypertrophy regression has occurred (99). Accordingly, acute anginal symptoms relief immediately after AVR could not be explained by the CFR changes alone due to its limited improvement. Rajappan et al. also noted that CFR changes before and after TAVR significantly correlate with changes in hyperemic diastolic filling time, rather than with changes in LV mass (76, 99). They concluded that the diastolic filling time is an important determinant of CFR and its interaction with AS severity might contribute to the development of myocardial ischemia and/or angina in AS-patients (76, 99). This hypothesis is supported in previously published study by Ferro et al. who found that the diastolic filling time at ischemic threshold during exercise- or pacing-induced tachycardia may indirectly predict the functional significance of coronary stenosis in patients without AS (104). Authors noted that the occurrence of myocardial ischemia and/or angina in these patients is mostly determined by the interaction between reduced diastolic filling time and coronary stenosis severity (104). Considering all these findings, it appears that anginal symptoms relief immediately after AVR is a result of acute diminish in LV oxygen demand driven by decrease in LV afterload, shortened systolic ejection phase and extravascular decompression of microcirculation, and concomitant acute increase in LV oxygen supply driven by mechanical relief of aortic valve obstruction, prolonged diastolic filling time and limited improvement in coronary blood flow and myocardial perfusion, particularly during exercise or tachycardia (30, 76, 77, 96–98). Contrary, while the LV hypertrophy persists following AVR, its regression may continue for months or years thereafter leading to a progressive restoration of coronary vasodilation capacity and CFR (77, 81, 99–103). However, in those AS-patients with extensive myocardial fibrosis, coronary vasodilatory capacity may not be resolved despite LV hypertrophy regression. Having in mind that diastolic filling time is a major determinant of myocardial ischemia and/or angina in AS-patients, it would be of great importance to develop a test that could identify its critically short duration that causes ischemia (30). The predefined critically short diastolic perfusion time could be potentially used as a guide for timing AVR and further studies with AS-patients should be conducted to examine this hypothesis.

In coronary wave intensity analysis studies, the prompt symptoms relief after TAVR could be explained by two concomitant pathophysiological mechanisms. First, early- and mid-systolic forward compression wave (the dominant forward-traveling pushing wave) is depressed and delayed in the presence of AS and promptly regained after TAVR (97). Ahmad et al. found that systolic coronary blood flow is reduced at rest and during hyperemia due to concomitant obstruction of LV ventricular emptying by the stenotic aortic valve, decrease aortic flow and high extravascular compression of microcirculation caused by an increase in LV afterload (105–107). After TAVR, systolic coronary blood flow is improved at rest and during hyperemia as a result of better LV ventricular emptying through the repaired aortic valve, increase aortic flow and extravascular decompression of microcirculation due to lower LV afterload (105, 108). Second, the magnitude of early-diastolic suction wave (the dominant backward-traveling suction wave) at rest was found to be significantly higher in AS-patients with accompanied LV hypertrophy compared with normal subjects, and it increased further with increasing AS severity (96, 97). The higher magnitude of resting early-diastolic suction wave in AS-patients is mainly related to improved propagation of this wave caused by microcirculatory vasodilation in response to LV hypertrophy and high LV oxygen demand (96, 97). During tachycardia in the presence of severe AS, this wave paradoxically

decreases due to the decoupling of regulatory mechanisms for maintenance of normal coronary blood flow and myocardial perfusion (96). Immediately after TAVR, the early-diastolic suction wave decreases at rest, and increases during tachycardia, as a result of an abrupt decrease in LV afterload, extravascular decompression of microcirculation and recoupling of regulatory mechanisms of normal myocardial perfusion (96). However, despite significant improvement of the early-diastolic suction wave at rest and during hyperemia, CFR immediately after TAVR remains unaltered or slightly increased primarily due to high LV end-diastolic pressure associated with LV hypertrophy affecting diastolic myocardial perfusion (77, 96). Accordingly, it seems that the improvement of systolic coronary blood flow has a dominant role in instant angina symptom relief after TAVR as a result of decreased systolic subendocardial compression due to lower LV afterload and perfusion redistribution from nonischemic to subendocardial ischemic areas, which consequently improved subendocardial ischemia (97, 105).

## THE ASSESSMENT OF CORONARY STENOSIS SEVERITY IN AS PATIENTS

To overcome limitations of noninvasive tests and coronary angiography regarding the functional assessment of coronary stenosis severity in AS-patients, the well-established invasive physiological indices, such as FFR and instantaneous wave-free ratio (iFR), are now in focus, especially in the contemporary era with a rapid increment of TAVR. Based on large clinical trials, current guidelines recommend both hyperemic and nonhyperemic indices as a reference invasive physiologic measurement for the assessment of coronary stenosis severity (7, 109, 110). The use of these physiological indices to guide coronary revascularization in patients with CAD improves clinical outcomes compared with treatment based on angiography alone (111–115). However, the optimal method for evaluating myocardial ischemia in patients with AS and co-existing CAD has not yet been fully established, and this important issue is under further investigation. Studies evaluating the use of FFR and iFR in patients with severe AS and co-existing CAD before and after TAVR are summarized in **Table 1**.

Both FFR and iFR are pressure-derived indices which means that their measurements are based on a linear relationship between pressure and coronary flow under conditions of stable, constant and minimized intracoronary resistance (109, 110). Fractional flow reserve, estimated as the ratio of mean distal intracoronary to mean aortic pressure during hyperemia, is a hyperemic index measured over the whole cardiac cycle and includes systolic coronary flow (109). The use of adenosine as the most potent vasodilator of the intramyocardial arterioles, either as an intracoronary bolus at a dose of 150 to 250 μg or intravenous infusion at a dose of 140 μg/kg/min for at least 1 min, is safe and well-tolerated regarding adverse side effects in AS-patients with co-existing CAD (77, 103, 105, 116–124). Of note, a mild decrease in microcirculatory resistance and a moderate increase in coronary blood flow were documented during adenosine-induced maximal hyperemia in the coronary artery segment distal to the intermediate stenosis immediately after TAVR compared with pre-TAVR conditions (77, 105). Contrary, these coronary hemodynamics at rest remain unaltered following TAVR due to compensatory vasodilation of intramyocardial arterioles as a response to longstanding LV hypertrophy and subsequent capillary rarefaction (77, 105). Hence, the coronary vasodilatory capacity remains impaired after TAVR compared with normal subjects, but may be fully regained in the coming months or years with accompanying LV hypertrophy regression (77, 105). Moreover, the moderate improvement in hyperemic coronary blood flow after TAVR is mainly driven by an increase in hyperemic systolic coronary blood flow, which leads to a higher hyperemic whole-cycle flow and therefore lower FFR values compared with the pre-TAVR values (77, 105). As a result, any physiological index that includes the systolic phase of cardiac cycle will be affected by TAVR (105). These findings suggest the following mechanisms that may contribute to the higher FFR values in severe AS-patients before TAVR: (1) the presence of low resting microcirculatory resistance as a response to LV hypertrophy and increased LV oxygen demand to maintain resting coronary blood flow which means that vasodilatory capacity of microcirculation is already exhausted by the autoregulation phenomenon; (2) the presence of high hyperemic microcirculatory resistance due to structural and functional changes of the microcirculation (arteriolar remodeling, perivascular fibrosis, and capillary rarefaction); and (3) the high levels of circulating vasoconstrictors due to hyperactivation of sympathetic adrenergic and renin-angiotensin-aldosterone systems to increase vascular tone and maintain systemic arterial blood pressure, which may block or attenuate the vasodilatory effect of adenosine on microcirculation (67–69, 76, 77, 80, 105). Accordingly, the effect of adenosine is attenuated in the presence of AS, and therefore the blunted FFR before TAVR may underestimate coronary stenosis severity in patients with AS (67–69, 76, 77, 80, 105). Similarly, Pesarini et al. found that the mean FFR value was significantly lower after TAVR in patients with severe AS and co-existing intermediate-to-severe coronary stenosis defined as >50% DS assessed by quantitative coronary analysis (0.84 ± 0.12 vs. 0.82 ± 0.16; $p = 0.02$) (116). In contrast, mean FFR value remained unchanged after TAVR in AS-patients with angiographically non-significant coronary stenosis (<50% DS) (0.90 ± 0.07 vs. 0.91 ± 0.09; $p = 0.69$) (116). In the group of AS-patients and coronary stenosis with positive FFR values (below ischemic threshold ≤ 0.80) before TAVR, FFR was found to further deteriorate immediately after TAVR (0.71 ± 0.11 vs. 0.66 ± 0.14), whereas in those with negative FFR values (>0.80) before TAVR, it was slightly improved (0.92 ± 0.06 vs. 0.93 ± 0.07) (116). These variations in FFR values after TAVR crossed the threshold of 0.80 and changed the revascularization strategy in only 6% of patients with AS and coronary stenosis (116). Accordingly, the study suggests that FFR measured immediately after TAVR could be more suitable for the functional evaluation of coronary stenosis severity in these patients compared with FFR obtained in pre-TAVR clinical settings (116). However, it is questionable whether FFR may be reliably index for the functional assessment of coronary stenosis several days or

**TABLE 1 |** Studies evaluating the use of fractional flow reserve (FFR) and instantaneous wave-free ratio (iFR) in patients with severe aortic stenosis (AS) and co-existing coronary artery disease (CAD) before and after transcatheter aortic valve replacement (TAVR).

| Authors (Ref #) | Citation | Study design | Number of patients and coronary lesions | Conclusion |
|---|---|---|---|---|
| Wiegerinck et al. (77) | Circ. Cardiovasc. Interv. 2015. | Prospective, observational study: intracoronary pressure and flow velocity were simultaneously assessed at rest and during maximal hyperemia (ic. bolus of adenosine 40–60 μg) in patients with severe AS and unobstructed coronary arteries before and immediately after TAVR | 27 symptomatic patients with severe AS and unobstructed CAD were included and compared with 28 patients without AS and unobstructed CAD (control group) | TAVR induces an immediate decrease in hyperemic microcirculatory resistance and an immediate increase in hyperemic flow velocity, whereas resting hemodynamics remain unaltered |
| Pesarini et al. (116) | Circ. Cardiovasc. Interv. 2016. | Prospective, observational study: the functional relevance of coronary lesions was simultaneously assessed by FFR using ic. bolus of adenosine 150–250 μg in patients with severe AS before and immediately after TAVR | 54 symptomatic patients with severe AS and obstructive CAD were included | Post-TAVR functional assessment with conventional FFR cut-off may change the indication to perform PCI in around 15% of patients with CAD undergoing TAVR. Therefore, functional assessment with FFR may be more reliable after TAVR |
| Scarsini et al. (117) | Int. J. Cardiol. 2017 | Prospective, observational study: the study aimed to compare the diagnostic performance of FFR and iFR in patients with severe AS and obstructive CAD. The iFR-FFR diagnostic agreement has been tested using the conventional FFR cut-off 0.80 | 85 patients with severe AS and 179 coronary lesions were included and compared with a control group formed by 167 patients (290 lesions) with stable CAD and without AS | The conventional iFR cut-off has lower diagnostic accuracy in the group of AS patients for detecting coronary lesion with FFR ≤ 0.80 in the group of CAD patients. The best diagnostic iFR cut-off was lower in the group of AS patients compared with the cut-off point observed in CAD patients (0.83 vs 0.89) |
| Scarsini et al. (118) | EuroIntervention 2018 | Prospective, observational study: iFR and FFR using ic. bolus of adenosine 150–250 μg were measured in patients with severe AS and CAD before and immediately after TAVR | 66 patients with severe AS and 145 coronary lesions were included | Higher iFR variation occurred mostly in patients with more severe aortic valve gradient and higher post-TAVR transaortic gradient drop. The iFR-FFR classification agreement is generally poorer in coronary stenosis with more severe angiographic and functional characteristics |
| Scarsini et al. (119) | Cardiovasc. Revasc. Med. 2018 | Prospective, observational study: iFR and FFR using ic. bolus of adenosine 150–250 μg were measured in patients with severe AS and CAD before and immediately after TAVR. All decisions about revascularization were based on post-TAVR FFR assessment with a conventional cut-off 0.80. | 62 patients with severe AS and concomitant CAD were included | A "defer iFR value" >0.93 yielded a NPV of 98% to exclude FFR non-significant stenosis (>0.80), and a "treatment iFR value" <0.83 had a PPV of 91% to identify FFR-significant stenosis (≤ 0.80). This hybrid decision-making strategy spared 63% of patients from adenosine, while maintaining 97% overall agreement with FFR lesions classification |
| Scarsini et al. (120) | Int. J. Cardiol. 2019 | Prospective, observational study: FFR using iv. infusion of adenosine 140 μg/kg/min, iFR and adenosine-stress myocardial perfusion on SPECT were performed in patients with severe AS and borderline coronary lesions before TAVR | 28 patients with severe AS and 41 borderline coronary lesions were included | FFR with conventional cut-off 0.80 was a better predictor of myocardial ischemia on SPECT (PPV 73%, NPV 95%) in comparison to iFR with conventional cut-off 0.89 (PPV 47%, NPV 91%). Using a lower iFR cut-off of 0.82 significantly improved its categorial agreement with the presence of myocardial ischemia on SPECT (from 59 to 73%) with an insignificant loss of its NPV (from 91 to 86%) |
| Ahmad et al. (105) | J. Am. Coll. Cardiol. Intv. 2018 | Prospective, observational study: iFR, FFR, whole-cycle flow, systolic flow, wave-free period flow, microcirculatory resistance, at rest and during maximal hyperemia (ic. bolus of adenosine 150 μg) in patients with severe AS and CAD before and immediately after TAVR | 28 patients with severe AS and 41 coronary lesions were included | Systolic and hyperemic coronary flow velocity increased significantly immediately after TAVR. Thus, hyperemic physiological indices that include systole underestimated coronary stenosis severity in patients with severe AS. After TAVR, iFR values remain unchanged, whereas FFR decreases significantly |
| Yamanaka et al. (121) | J. Am. Coll. Cardiol. Intv. 2018 | Prospective, observational study: the study aimed to assess the diagnostic performance of iFR with adenosine-stress myocardial perfusion on SPECT and FFR cut-off ≤0.80 using iv. infusion of adenosine 140 μg/kg/min, in patients with severe AS and CAD | 95 patients with severe AS and 116 intermediates coronary stenoses were included | iFR with a lower cut-off 0.82 could be a reliable diagnostic tool for indicating reversible myocardial perfusion defects on SPECT as well as FFR ≤ 0.80, in patients with severe AS |
| Vendrik et al. (103) | J Am. Heart. Assoc. 2020 | Prospective, observational study: iFR FFR, whole-cycle flow, systolic flow, wave-free period flow, microcirculatory resistance, at rest and during maximal hyperemia (ic. bolus of adenosine 100–200 μg) in patients with severe AS and CAD before TAVR, immediately after TAVR and 6-months after TAVR | 13 patients with severe AS and moderate-severe coronary lesions were included | Hyperemic coronary flow velocity increases immediately after TAVR and continues to rise to 6-month follow-up. This rise in flow causes both acute and long-term declines in FFR values, leading FFR to underestimate coronary stenosis severity in the presence of severe AS. Resting diastolic flow and consequently iFR are is not affected by severe AS and remain unchanged pre-TAVR, post-TAVR, and at 6-month follow-up. |

*NPV, negative predictive value; PPV, positive predictive value; PCI, percutaneous coronary intervention; SPECT, single-photon emission computed tomography.*

months after TAVR because it has been shown that complete restoration of coronary vasodilatory capacity could be achieved only with longer-term post-TAVR following LV hypertrophy regression (70, 77, 98–102). Vendrik et al. also found an ongoing decrease in FFR immediately after TAVR and 6 months after the procedure compared with pre-TAVR values, whereas iFR and resting Pd/Pa remain unchanged (103). These findings suggest that FFR is a less reliable physiological index for the assessment of coronary lesion severity in patients with severe AS for at least 6 months after AVR (70, 77, 98–103). However, it remains unknown whether FFR could be suitable for the functional assessment of coronary lesions beyond 6 months after AVR.

Unlike FFR, resting coronary hemodynamics including resting coronary flow and resting microcirculatory resistance during the whole diastole as well as during the wave-free period of diastole are not significantly affected by the presence of severe AS and remain unaltered before TAVR, immediately after TAVR, and at 6 months follow-up (77, 96, 97, 103, 105). Accordingly, it has been shown that iFR as a non-hyperemic index is independent of both AS severity and TAVR in short- and long-term follow-up (103, 105). The iFR is defined as the ratio of mean distal intracoronary to mean aortic pressure measured under resting conditions during a specific wave-free period of diastole when microcirculatory resistance is stable and minimized (110). Coronary blood flow during this period occurs when the aortic valve is closed while the myocardium is completely relaxed and without contraction (103). Therefore, it is reasonable to believe that iFR is a more reliable physiological index for the assessment of coronary stenosis severity in the presence of AS (77, 96, 97, 103, 105). Scarsini et al. also found that mean iFR values did not change before and after TAVR, although individual iFR measurements showed high and inconsistent variations following TAVR in around 15% of coronary lesions, mainly in AS-patients with angiographically intermediate severity (37–70% DS) (118). Both negative (iFR $>$0.89) and positive iFR values (iFR $\leq$0.89) before TAVR crossed below or above the ischemic threshold 0.89 after TAVR in similar percent of coronary lesions (6.9% vs. 7.3%, respectively) and, thereby, changed the revascularization strategy (118). These high iFR variations occurred mostly in patients with more severe aortic valve gradients and higher post-TAVR transaortic gradient drops reminding that iFR measurements must be carefully taken in this subgroup of AS-patients (118). The same study also showed that iFR with a conventional cut-off of 0.89 had a high NPV in both pre-TAVR and post-TAVR settings (99% vs. 97%) for excluding without risk the presence of functionally significant coronary lesions defined as FFR $\leq$ 0.80 (118). However, the low PPV of iFR for the detection of significant coronary lesions in AS-patients in both settings (44% vs. 60%, respectively) indicates that predefined ischemic threshold of 0.89 for the assessment of FFR-defined lesion severity may not be appropriate (27, 118). The same authors also presented a high NPV and a low PPV of iFR with a conventional cut-off of 0.89 (91% and 47%) for identifying myocardial ischemia on SPECT in the presence of AS (120). Discordance between iFR and SPECT was found in 41% of patients and 95% of them had false-positive iFR values (negative SPECT and iFR $\leq$ 0.89) (120). The higher rate of false-positive iFR values in severe AS-patients could be explained by increased resting coronary blood flow in response to the increased LV oxygen demand due to higher LV afterload and LV hypertrophy (77, 99, 120). Consequently, a higher pressure gradient occurs across the coronary lesion leading to a lower CFR as well as iFR (120). Hence, the iFR may overestimate coronary stenosis severity in patients with severe AS. To overcome these limitations of iFR, several authors proposed a lower ischemic threshold to achieve a higher positive predictive value in the presence of AS (27, 118). The other study conducted by the same authors revealed that shifting the iFR cut-off from 0.89 to 0.83 in patients with severe AS and co-existing CAD significantly increase its categorial agreement with FFR using cut-off $\leq$ 0.80 measured in patients with CAD but without AS (control group), from 76% to 91%, while maintaining its NPV (95%) (117). Yamanaka et al. evaluated the diagnostic performance of iFR in 95 patients with severe AS and concomitant intermediate coronary lesions, as compared with myocardial perfusion scintigraphy and with FFR as reference (121). They demonstrated that the optimal cut-off value of iFR for detecting the presence of myocardial ischemia on myocardial perfusion scintigraphy was 0.82 (AUC: 0.84). Similarly, the same iFR cut-off was optimal for indicating an FFR $\leq$ 0.75 and $\leq$ 0.80 with an AUC of 0.92 and 0.82, respectively (121). The study concluded that iFR with a lower ischemic threshold of 0.82 has excellent reproducibility and could be used as a reliable physiological index for the assessment of coronary lesion severity in the presence of severe AS (121). Scarsini et al. also noted that using a lower iFR ischemic threshold of 0.82 in these patients significantly improved its categorial agreement with the presence of myocardial ischemia on SPECT (from 59% to 73%) with an insignificant loss of its NPV (from 91% to 86%) (120). However, they regained the use of FFR with a lower cut-off 0.78 as a more accurate physiological index for detecting myocardial ischemia in patients with severe AS and CAD compared with iFR using cut-off 0.82 (AUC: 88% vs. 73%; NPV: 92% vs. 86%; PPV: 81% vs. 73%) (120). This study is hampered by the fact that FFR has not been so far validated in the presence of AS and the conventional or lower FFR threshold (0.80 vs. 0.78) might not accurately reflect the coronary stenosis severity (120). The same authors proposed a new iFR-FFR "hybrid approach" with the iFR measurements before TAVR as the first choice for the functional assessment of coronary stenosis in the presence of severe AS (119). They found that the iFR threshold $>$0.93 had an NPV of 98% to exclude significant stenosis defined as post-TAVR FFR $\leq$0.80. Contrary, iFR threshold $<$0.83 had a PPV of 91% to identify FFR-defined significant stenosis after TAVR (119). Accordingly, FFR was used only when iFR values were between 0.83 and 0.93 (119). This "hybrid" approach enables the assessment of coronary stenosis severity without vasodilatory provocation in 63% of patients with severe AS while maintaining 97% overall agreement with FFR lesions classification (**Figure 1**) (119).

In summary, to determine the optimal FFR and iFR ischemic thresholds in patients with severe AS and co-existing CAD, additional prospective randomized trials are needed with a larger number of patients. Both physiological indices must be

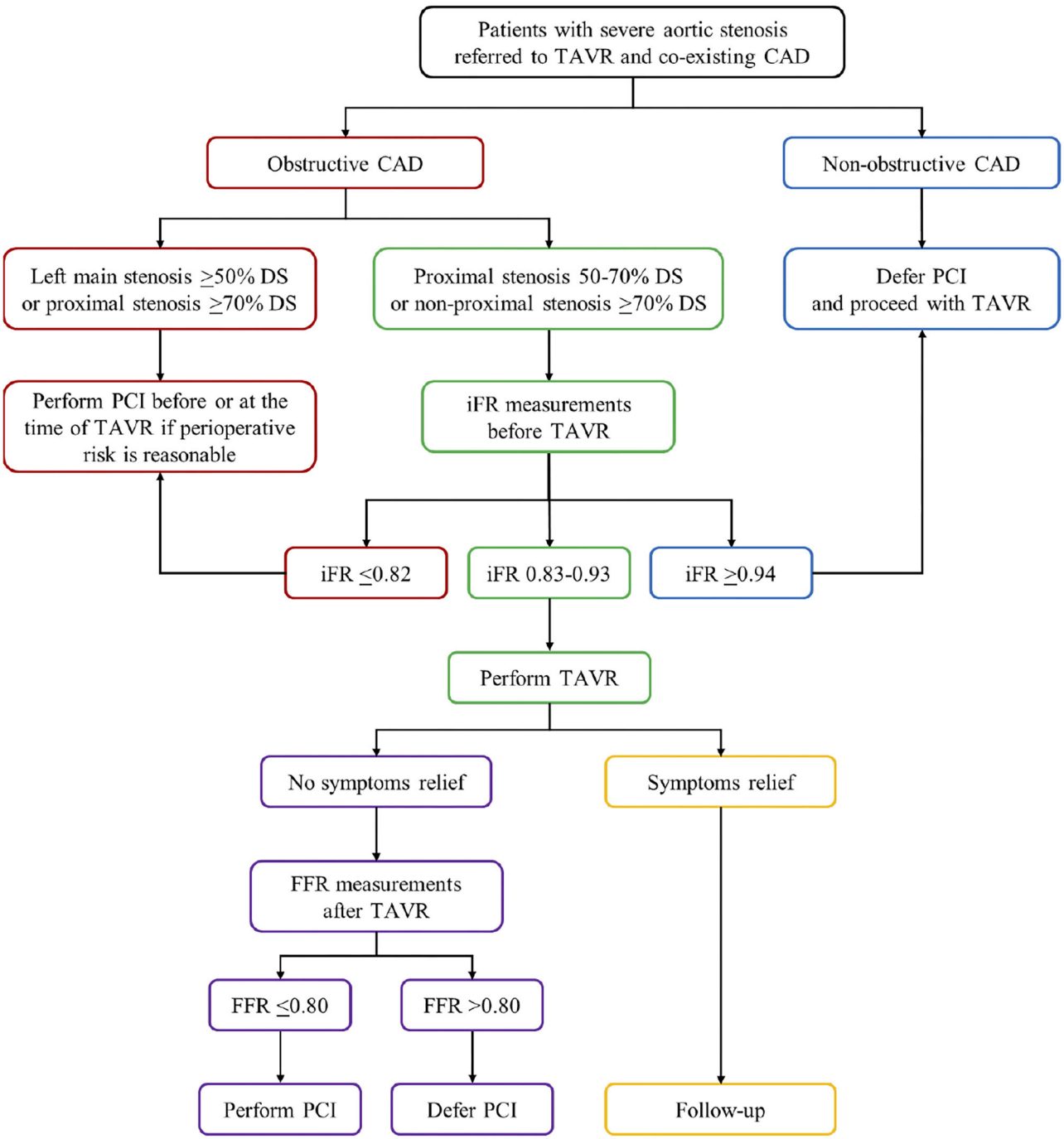


**FIGURE 1 |** The proposed flow chart illustrates the myocardial revascularization strategy in patients with severe aortic stenosis undergoing TAVR. Obstructive CAD is defined as coronary artery stenosis ≥50% DS. CAD, coronary artery disease; DS, diameter stenosis; FFR, fractional flow reserve; iFR, instantaneous wave-free ratio; PCI, percutaneous coronary intervention; TAVR, transcatheter aortic valve replacement.

validated with cardiovascular events during long-term follow-up by randomized trials comparing FFR-guided and/or iFR-guided myocardial revascularization with angiographically-guided therapy in patients with severe AS [FAITAVI (Functional Assessment in TAVI; NCT03360591) trial]. Furthermore, the prognostic relevance of PCI before or after TAVR remains controversial, and several clinical trials regarding optimal time for PCI in patients referred to TAVR are still

ongoing [the NOTION-3 (Nordic Aortic Valve Intervention-3; NCT03058627) trial; the REVIVAL (Revascularization After Transcatheter Aortic Valve Implantation; NCT03283501) trial; the TCW (The TransCatheter Valve and Vessels Trial; NCT03424941) trial; the TAVI-PCI (Optimal Timing of Transcatheter Aortic Valve Implantation and Percutaneous Coronary Intervention; NCT04310046) trial].

## AUTHOR CONTRIBUTIONS

SA and MB: conceptualization. SA: resources and writing—original draft preparation. MB and BB: writing—review and editing. BB: supervision. All authors participated in writing and critically reviewing this manuscript. All authors have read and agreed to the published version of the manuscript.

## REFERENCES


1. Di Gioia G, Bartunek J, Tesorio T, Vukcevic V, Aleksandric S, Dobric M, et al. Pathophysiology, diagnosis, and treatment of patients with concomitant severe aortic stenosis and coronary artery disease: a closer look to the unresolved perplexity. *J Clin Med.* (2021) 10:1617. doi: 10.3390/jcm10081617
2. Paradis JM, Labbé B, Rodés-Cabau J. Coronary artery disease and transcatheter aortic valve replacement: current treatment paradigms. *Coron Artery Dis.* (2015) 26:272–8. doi: 10.1097/MCA.0000000000000210
3. Virk SA, Tian DH, Liou K, Pathan F, Villanueva C, Akhunji Z, et al. Systematic review of percutaneous coronary intervention and transcatheter aortic valve implantation for concomitant aortic stenosis and coronary artery disease. *Int J Cardiol.* (2015) 187:453–5. doi: 10.1016/j.ijcard.2015.03.391
4. Sawaya F, Liff D, Stewart J, Lerakis S, Babaliaros V. Am. *J Med Sci.* (2012) 343:490–6. doi: 10.1097/MAJ.0b013e3182539d70
5. Stefanini GG, Stortecky S, Meier B, Windecker S, Wenaweser P. Severe aortic stenosis and coronary artery disease. *EuroIntervention.* (2013) 9:S63–68. doi: 10.4244/EIJV9SSA12
6. Pepe M, Larosa C, Rosa I, Biondi-Zoccai G, Nestola PL, Di Cillo O, et al. Degenerative severe aortic stenosis and concomitant coronary artery disease: what is changing in the era of the "transcatheter revolution"? *Curr Atheroscler Rep.* (2020) 22:17. doi: 10.1007/s11883-020-0835-1
7. Neumann FJ, Sousa-Uva M, Ahlsson A, Alfonso F, Banning AP, et al. 2018 ESC ESC/EACTS Guidelines on myocardial revascularization. *Eur Heart J.* (2019) 40:87–165. doi: 10.1093/eurheartj/ehy855
8. Vahanian A, Beyersdorf F, Praz F, Milojevic M, Baldus S, Bauersachs J, et al. 2021 ESC/EACTS Guidelines for the management of valvular heart disease. *Eur Heart J.* (2022) 43:561–632. doi: 10.1093/eurheartj/ehab395
9. Otto CM, Nishimura RA, Bonow RO, Carabello BA, Erwin III JP, Gentile F, et al. 2020 ACC/AHA guideline for the management of patients with valvular heart disease: a report of the American College of Cardiology/ American Heart Association Joint Committee on Clinical Practice Guidelines. *J Am Coll Cardiol.* (2021) 77:e25–e197. doi: 10.1161/CIR.0000000000000923
10. Goel SS, Ige M, Tuzcu ME, Ellis SG, Stewart WJ, Svensson LG, et al. Severe aortic stenosis and coronary artery diseased implications for management in the transcatheter aortic valve replacement era. Comprehensive review. *J Am Coll Cardiol.* (2013) 62:1–10. doi: 10.1016/j.jacc.2013.01.096
11. Lund O, Nielsen TT, Pilegaard HK, Magnussen K, Knudsen MA. The influence of coronary artery disease and bypass grafting on early and late survival after valve replacement for aortic stenosis. *J Thorac Cardiovasc Surg.* (1990) 100:327–37. doi: 10.1016/S0022-5223(19)35524-2
12. Mullany CJ, Elveback LR, Frye RL, Pluth JR, Edwards WD, Orszulak TA, et al. Coronary artery disease and its management: influence on survival in patients undergoing aortic valve replacement. *J Am Coll Cardiol.* (1987) 10:66–72. doi: 10.1016/S0735-1097(87)80161-4
13. Beach JM, Mihaljevic T, Svensson LG, Rajeswaran J, Marwick T, Griffin B, et al. Coronary artery disease and outcomes of aortic valve replacement for severe aortic stenosis. *J Am Coll Cardiol.* (2013) 61:837–48. doi: 10.1016/j.jacc.2012.10.049
14. Kvidal P, Bergstrom R, Horte LG, Stahle E. Observed and relative survival after aortic valve replacement. *J Am Coll Cardiol.* (2000) 35:747–56. doi: 10.1016/S0735-1097(99)00584-7
15. Alexander KP, Anstrom KJ, Muhlbaier LH, Grosswald RD, Smith PK, Jones RH, et al. Outcomes of cardiac surgery in patients > or = 80 years: results from the National Cardiovascular Network. *J Am Coll Cardiol.* (2000) 35:731–8. doi: 10.1016/S0735-1097(99)00606-3
16. Hannan EL, Wu C, Bennett EV, Carlson RE, Culliford AT, Gold JP, et al. Risk index for predicting in-hospital mortality for cardiac valve surgery. *Ann Thorac Surg.* (2007) 83:921–9. doi: 10.1016/j.athoracsur.2006.09.051
17. Nowicki ER, Birkmeyer NJ, Weintraub RW, Leavitt BJ, Sanders JH, Dacey LJ, et al. Multivariable prediction of in-hospital mortality associated with aortic and mitral valve surgery in northern New England. *Ann Thorac Surg.* (2004) 77:1966–77. doi: 10.1016/j.athoracsur.2003.12.035
18. Kuduvalli M, Grayson AD, Au J, Grotte G, Bridgewater B, Fabri BM, et al. multi-centre additive and logistic risk model for in-hospital mortality following aortic valve replacement. *Eur J Cardiothorac Surg.* (2007) 31:607–13. doi: 10.1016/j.ejcts.2006.12.035
19. Iung B, Drissi MF, Michel PL, de Pamphilis O, Tsezana R, Cormier B, et al. Prognosis of valve replacement for aortic stenosis with or without coexisting coronary heart disease: a comparative study. *J Heart Valve Dis.* (1993) 2:430–9.
20. Leon MB, Smith CR, Mack MJ, Makkar RR, Svensson LG, Kodali SK, et al. PARTNER 2 Investigators. *N Engl J Med.* (2016) 374:1609–20.
21. Reardon MJ, Van Mieghem NM, Popma JJ, Kleiman NS, Søndergaard L, Mumtaz M, et al. SURTAVI investigators. *N Engl J Med.* (2017) 376:1321–31. doi: 10.1056/NEJMoa1700456
22. Mack MJ, Leon MB, Thourani VH, Makkar R, Kodali SK, Russo M, et al. PARTNER 3 investigators. *N Engl J Med.* (2019) 380:1695–705. doi: 10.1056/NEJMoa1814052
23. Popma JJ, Deeb GM, Yakubov SJ, Mumtaz M, Gada H, O'Hair D, et al. Evolut low risk trial investigators. *N Engl J Med.* (2019) 380:1706–15.
24. Siontis G, Overtchouk P, Cahill TJ, Modine T, Prendergast B, Praz F, et al. Transcatheter aortic valve implantation vs. surgical aortic valve replacement for treatment of symptomatic severe aortic stenosis: an updated meta-analysis. *Eur Heart J.* (2019) 40:3143–53. doi: 10.1093/eurheartj/ehz275
25. Banovic M, Putnik S, Penicka M, Doros G, Deja MA, Kockova R, et al. Aortic Valve ReplAcemenT versus Conservative Treatment in Asymptomatic SeveRe Aortic Stenosis: The AVATAR Trial. *Circulation.* (2021). doi: 10.1161/CIRCULATIONAHA.121.057639. [Epub ahead of print].
26. Patterson T, Clayton T, Dodd M, Khawaja Z, Claude-Morice M, Wilson K, et al. ACTIVATION (PercutAneous Coronary inTervention prIor to transcatheter aortic VAlve implantaTION): a randomized clinical trial. *J Am Coll Cardiol Cardiovasc Interv.* (2021) 14:1965–74. doi: 10.1016/j.jcin.2021.06.041
27. Faroux L, Guimaraes L, Wintzer-Wehekind J, Junquera L, Ferreira-Neto AN, Del Val D, et al. Coronary artery disease and transcatheter aortic valve replacement: JACC state-of-the-art review. *J Am Coll Cardiol.* (2019) 74:362–72. doi: 10.1016/j.jacc.2019.06.012
28. D'Ascenzo F, Verardi R, Visconti M, Conrotto F, Scacciatella P, Dziewierz A, et al. Independent impact of extent of coronary artery disease and percutaneous revascularization on 30-day and one-year mortality after TAVI: a meta-analysis of adjusted observational results. *EuroIntervention.* (2018) 14:e1169–77. doi: 10.4244/EIJ-D-18-00098
29. Sankaramangalam K, Banerjee K, Kandregula K, Mohananey D, Parashar A, Jones BM, et al. Impact of coronary artery disease on 30-day and 1-year mortality in patients undergoing transcatheter aortic valve replacement: a meta-analysis. *J Am Heart Assoc.* (2017) 11:e006092. doi: 10.1161/JAHA.117.006092
30. Gould LK, Carabello BA. Why angina in aortic stenosis with normal coronary arteriograms? *Circulation.* (2003) 107:3121–3. doi: 10.1161/01.CIR.0000074243.02378.80
31. Gould LK. Why angina pectoris in aortic stenosis. *Circulation.* (1997) 95:790–2. doi: 10.1161/01.CIR.95.4.790
32. Dunn RB, Griggs DM. Ventricular filling pressure as a determinant of coronary blood flow during ischemia. *Am J Physiol Heart Circ Physiol.* (1983) 244:H429–36. doi: 10.1152/ajpheart.1983.244.3.H429

33. Breisch EA, Houser SR, Carey RA, Spann JF, Bovel AA. Myocardial blood flow and capillary density in chronic pressure overload of the feline left ventricle. *Cardiovasc Res.* (1980) 14:469–75. doi: 10.1093/cvr/14.8.469
34. Banovic M, Iung B, Brkovic V, Nikolic S, Mitrovic P, Van Camp G, et al. Silent coronary artery disease in asymptomatic patients with severe aortic stenosis and normal exercise testing. *Coron Artery Dis.* (2020) 31:166–73. doi: 10.1097/MCA.0000000000000801
35. Hussain N, Chaudhry W, Ahlberg AW, Amara RS, Elfar A, Parker MW, et al. An assessment of the safety, hemodynamic response, and diagnostic accuracy of commonly used vasodilator stressors in patients with severe aortic stenosis. *J Nucl Cardiol.* (2017) 24:1200–13. doi: 10.1007/s12350-016-0427-1
36. Cremer PC, Khalaf S, Lou J, Rodriguez L, Cerqueira MD, Jaber WA. Stress positron emission tomography is safe and can guide coronary revascularization in high-risk patients being considered for transcatheter aortic valve replacement. *J Nucl Cardiol.* (2014) 21:1001–10. doi: 10.1007/s12350-014-9928-y
37. Patsilinakos SP, Spanodimos S, Rontoyanni F, Kranidis A, Antonelis IP, Sotirellos K, et al. Adenosine stress myocardial perfusion tomographic imaging in patients with significant aortic stenosis. *J Nucl Cardiol.* (2004) 11:20–5. doi: 10.1016/j.nuclcard.2003.10.003
38. Demirkol MO, Yaymaci B, Debeş H, Başaran Y, Turan F. Dipyridamole myocardial perfusion tomography in patients with severe aortic stenosis. *Cardiology.* (2002) 97:37–42. doi: 10.1159/000047417
39. Samuels B, Kiat H, Friedman JD, Berman DS. Adenosine pharmacologic stress myocardial perfusion tomographic imaging in patients with significant aortic stenosis. Diagnostic efficacy and comparison of clinical, hemodynamic and electrocardiographic variables with 100 age-matched control subjects. *J Am Coll Cardiol.* (1995) 25:99–106. doi: 10.1016/0735-1097(94)00317-J
40. Huikuri HV, Korhonen UR, Ikäheimo MJ, Heikkilä J, Takkunen JT. Detection of coronary artery disease by thallium imaging using a combined intravenous dipyridamole and isometric handgrip test in patients with aortic valve stenosis. *Am J Cardiol.* (1987) 59:336–40. doi: 10.1016/0002-9149(87)90809-5
41. Singh A, Greenwood JP, Berry C, Dawson DK, Hogrefe K, Kelly DJ, et al. Comparison of exercise testing and CMR measured myocardial perfusion reserve for predicting outcome in asymptomatic aortic stenosis: the PRognostic Importance of MIcrovascular Dysfunction in Aortic Stenosis (PRIMID AS) Study. *Eur Heart J.* (2017) 38:1222–9. doi: 10.1093/eurheartj/ehx001
42. Iung B. Interface between valve disease and ischaemic heart disease. *Heart.* (2000) 84:47–52. doi: 10.1136/heart.84.3.347
43. Bonow RO, Kent KM, Rosing DR, Lipson LC, Borer JS, McIntosh CL, et al. Aortic valve replacement without myocardial revascularization in patients with combined aortic valvular and coronary artery disease. *Circulation.* (1981) 63:243–51. doi: 10.1161/01.CIR.63.2.243
44. Eltchaninoff H, Prat A, Gilard M, Leguerrier A, Blanchard D, Fournial G, et al. Transcatheter aortic valve implantation: early results of the FRANCE (FRench Aortic National CoreValve and Edwards) registry. *Eur Heart J.* (2011) 32:191–7. doi: 10.1093/eurheartj/ehq261
45. Rodes-Cabau J, Webb JG, Cheung A, Ye J, Dumont E, Feindel CM, et al. Transcatheter aortic valve implantation for the treatment of severe symptomatic aortic stenosis in patients at very high or prohibitive surgical risk: acute and late outcomes of the multicenter Canadian experience. *J Am Coll Cardiol.* (2010) 55:1080–90. doi: 10.1016/j.jacc.2009.12.014
46. de Azevedo Filho AFB, Accorsi TAD, Ribeiro HB. Coronary Artery Disease in Patients with Aortic Stenosis and Transcatheter Aortic Valve Implantation: Implications for Management. *Eur Cardiol Rev.* (2021) 16:e49. doi: 10.15420/ecr.2021.27
47. Pontone G, Andreini D, Bartorelli AL, Annoni A, Mushtaq S, Bertella E, et al. Feasibility and accuracy of a comprehensive multidetector computed tomography acquisition for patients referred for balloon-expandable transcatheter aortic valve implantation. *Am Heart J.* (2011) 161:1106–13. doi: 10.1016/j.ahj.2011.03.003
48. Andreini D, Pontone G, Mushtaq S, Bartorelli AL, Ballerini G, Bertella E, et al. Diagnostic accuracy of multidetector computed tomography coronary angiography in 325 consecutive patients referred for transcatheter aortic valve replacement. *Am Heart J.* (2014) 168:332–9. doi: 10.1016/j.ahj.2014.04.022
49. Hamdan A, Wellnhofer E, Konen E, Kelle S, Goitein O, Andrada B, et al. Coronary CT angiography for the detection of coronary artery stenosis in patients referred for transcatheter aortic valve replacement. *J Cardiovasc Comput Tomogr.* (2015) 9:31–41. doi: 10.1016/j.jcct.2014.11.008
50. Harris BS, De Cecco CN, Schoepf UJ, Steinberg DH, Bayer RR, Krazinski AW, et al. Dual-source CT imaging to plan transcatheter aortic valve replacement: accuracy for diagnosis of obstructive coronary artery disease. *Radiology.* (2015) 275:80–8. doi: 10.1148/radiol.14140763
51. Opolski MP, Kim WK, Liebetrau C, Walther C, Blumenstein J, Gaede L, et al. Diagnostic accuracy of computed tomography angiography for the detection of coronary artery disease in patients referred for transcatheter aortic valve implantation. *Clin Res Cardiol.* (2015) 104:471–80. doi: 10.1007/s00392-014-0806-z
52. Matsumoto S, Yamada Y, Hashimoto M, Okamura T, Yamada M, Yashima F, et al. CT imaging before transcatheter aortic valve implantation (TAVI) using variable helical pitch scanning and its diagnostic performance for coronary artery disease. *Eur Radiol.* (2017) 27:1963–70. doi: 10.1007/s00330-016-4547-4
53. Strong C, Ferreira A, Teles RC, Mendes G, Abecasis J, Cardoso G, et al. Diagnostic accuracy of computed tomography angiography for the exclusion of coronary artery disease in candidates for transcatheter aortic valve implantation. *Sci Rep*. (2019) 9:19942. doi: 10.1038/s41598-019-56519-3
54. Meier D, Depierre A, Topolsky A, Roguelov C, Dupré M, Rubimbura V, et al. Computed tomography angiography for the diagnosis of coronary artery disease among patients undergoing transcatheter aortic valve implantation. *J Cardiovasc Transl Res.* (2021) 14:894–901. doi: 10.1007/s12265-021-10099-8
55. van den Boogert TPW, Vendrik J, Claessen BEPM, Baan J, Beijk MA, Limpens J, et al. CTCA for detection of significant coronary artery disease in routine TAVI work-up: a systematic review and meta-analysis. *Neth Heart J.* (2018) 26:591–9. doi: 10.1007/s12471-018-1149-6
56. van den Boogert TPW, Claessen BEPM, Opolski MP, Kim WK, Hamdan A, Andreini D, et al. DEtection of ProxImal Coronary stenosis in the work-up for Transcatheter aortic valve implantation using CTA (from the DEPICT CTA collaboration). *Eur Radiol.* (2022) 32:143–51. doi: 10.1007/s00330-021-08095-2
57. Chieffo A, Giustino G, Spagnolo P, Panoulas VF, Montorfano M, Latib A, et al. Routine screening of coronary artery disease with computed tomographic coronary angiography in place of invasive coronary angiography in patients undergoing transcatheter aortic valve replacement. *Circ Cardiovasc Interv.* (2015) 8:e002025. doi: 10.1161/CIRCINTERVENTIONS.114.002025
58. Rossi A, De Cecco CN, Kennon SRO, Zou L, Meinel FG, Toscano W, et al. CT angiography to evaluate coronary artery disease and revascularization requirement before trans-catheter aortic valve replacement. *J Cardiovasc Comput Tomogr.* (2017) 11:338–46. doi: 10.1016/j.jcct.2017.06.001
59. Min JK, Koo BK, Erglis A, Doh JH, Daniels DV, Jegere S, et al. Usefulness of noninvasive fractional flow reserve computed from coronary computed tomographic angiograms for intermediate stenoses confirmed by quantitative coronary angiography. *Am J Cardiol.* (2012) 110:971–6. doi: 10.1016/j.amjcard.2012.05.033
60. Thompson AG, Raju R, Blanke P, Yang TH, Mancini GB, Budoff MJ, et al. Diagnostic accuracy and discrimination of ischemia by fractional flow reserve CT using a clinical use rule: results from the Determination of Fractional Flow Reserve by Anatomic Computed Tomographic Angiography study. *J Cardiovasc Comput Tomogr.* (2015) 9:120–8. doi: 10.1016/j.jcct.2015.01.008
61. Lu MT, Ferencik M, Roberts RS, Lee KL, Ivanov A, Adami E, et al. Noninvasive FFR derived from coronary CT angiography: management and outcomes in the PROMISE trial. *JACC Cardiovasc Imaging.* (2017) 10:1350–8. doi: 10.1016/j.jcmg.2016.11.024
62. Coenen A, Rossi A, Lubbers MM, Kurata A, Kono AK, Chelu RG, et al. Integrating CT myocardial perfusion and CT-FFR in the work-up of coronary artery disease. *JACC Cardiovasc Imaging.* (2017) 10:760–70. doi: 10.1016/j.jcmg.2016.09.028
63. Koo BK, Erglis A, Doh JH, Daniels DV, Jegere S, Kim HS, et al. Diagnosis of ischemia-causing coronary stenoses by noninvasive fractional flow reserve

computed from coronary computed tomographic angiograms. Results from the prospective multicenter DISCOVER-FLOW (Diagnosis of Ischemia-Causing Stenoses Obtained Via Noninvasive Fractional Flow Reserve) study. *J Am Coll Cardiol.* (2011) 58:1989–97. doi: 10.1016/j.jacc.2011.06.066

64. Nakazato R, Park HB, Berman DS, Gransar H, Koo BK, Erglis A, et al. Noninvasive fractional flow reserve derived from computed tomography angiography for coronary lesions of intermediate stenosis severity: results from the DeFACTO study. *Circ Cardiovasc Imaging.* (2013) 6:881–9. doi: 10.1161/CIRCIMAGING.113.000297
65. Michail M, Ihdayhid AR, Comella A, Thakur U, Cameron JD, McCormick LM, et al. Feasibility and validity of computed tomography-derived fractional flow reserve in patients with severe aortic stenosis: the CAST-FFR study. *Circ Cardiovasc Interv.* (2021) 14:e009586. doi: 10.1161/CIRCINTERVENTIONS.120.009586
66. Otto CM. Calcific aortic valve disease: outflow obstruction is the end stage of a systemic disease process. *Eur Heart J.* (2009) 30:1940–2. doi: 10.1093/eurheartj/ehp175
67. Ahn JH, Kim SM, Park SJ, Jeong DS, Woo MA, Jung SH, et al. Coronary microvascular dysfunction as a mechanism of angina in severe AS. Prospective adenosine-stress CMR study. *J Am Coll Cardiol.* (2016) 67:1412–22. doi: 10.1016/j.jacc.2016.01.013
68. Julius BK, Spillmann M, Vassalli G, Villari B, Eberli FR, Hess OM. Angina pectoris in patients with aortic stenosis and normal coronary arteries. Mechanisms and pathophysiological concepts. *Circulation.* (1997) 95:892–8. doi: 10.1161/01.CIR.95.4.892
69. Marcus ML, Doty DB, Hiratzka LF, Wright CB, Eastham CL. Decreased coronary reserve: a mechanism for angina pectoris in patients with aortic stenosis and normal coronary arteries. *N Engl J Med.* (1982) 307:1362–6. doi: 10.1056/NEJM198211253072202
70. Eberli FR, Ritter M, Schwitter J, Bortone A, Schneider J, Hess OM, et al. Coronary reserve in patients with aortic valve disease before and after successful aortic valve replacement. *Eur Heart J.* (1991) 12:127–38. doi: 10.1093/oxfordjournals.eurheartj.a059858
71. Nemes A, Balazs E, Csanady M, Forster T. Long term prognostic role of coronary flow reserve in patients with aortic valve stenosis-insights from the SZEGED study. *Clin Physiol Funct Imaging.* (2009) 29:447–52. doi: 10.1111/j.1475-097X.2009.00893.x
72. Garcia D, Camici PG, Durand LG, Rajappan K, Gaillard E, Rimoldi OE, et al. Impairment of coronary flow reserve in aortic stenosis. *Appl Physiol.* (2009) 106:113–21. doi: 10.1152/japplphysiol.00049.2008
73. Banovic M, Vujisic-Tesic B, Kujacic V, Callahan MJ, Nedeljkovic IP, Trifunovic DD, et al. Coronary flow reserve in patients with aortic stenosis and nonobstructed coronary arteries. *Acta Cardiol.* (2011) 66:743–9. doi: 10.1080/AC.66.6.2136958
74. Meimoun P, Germain AL, Elmkies F, Benali T, Boulanger J, Espanel C, et al. Factors associated with noninvasive coronary flow reserve in severe aortic stenosis, J. *Am Soc Echocardiogr.* (2012) 25:835–41. doi: 10.1016/j.echo.2012.05.020
75. Gutiérrez-Barrios A, Gamaza-Chulián S, Agarrado-Luna A, Ruiz-Fernández D, Calle-Pérez G, Marante-Fuertes E, et al. Invasive assessment of coronary flow reserve impairment in severe aortic stenosis and ecochadiographic correlations. *Int J Cardiol.* (2017) 236:370–4. doi: 10.1016/j.ijcard.2017.01.150
76. Rajappan K, Rimoldi O, Dutka DP, Ariff B, Pennell DJ, Sheridan DJ, et al. Mechanism of coronary microcirculatory dysfunction in patients with aortic stenosis and angiographically normal coronary arteries. *Circulation.* (2002) 105:470–6. doi: 10.1161/hc0402.102931
77. Wiegerinck EM, van de Hoef TP, Rolandi MC, Yong Z, van Kesteren F, Koch KT, et al. Impact of aortic valve stenosis on coronary hemodynamics and the instantaneous effect of transcatheter aortic valve implantation. *Circ Cardiovasc Interv.* (2015) 8:e002443. doi: 10.1161/CIRCINTERVENTIONS.114.002443
78. Banovic M, Brkovic V, Nedeljkovic I, Nedeljkovic M, Popovic D, Djordjevic-Dikic A, et al. Diabetes mellitus and coronary microvascular function in asymptomatic patients with severe aortic stenosis and nonobstructed coronary arteries. *Diab Vasc Dis Res.* (2016) 13:220–7. doi: 10.1177/1479164115627107
79. Banovic M, Athithan L. McCannGP. Aortic stenosis and diabetes mellitus: an ominous combination. *Diab Vasc Dis Res.* (2019) 16:310–23. doi: 10.1177/1479164118820657
80. Steadman CD, Jerosch-Herold M, Grundy B, Rafelt S, Ng LL, Squire IB, et al. Determinants and functional significance of myocardial perfusion reserve in severe aortic stenosis. *JACC Cardiovasc Imaging.* (2012) 5:182–9. doi: 10.1016/j.jcmg.2011.09.022
81. Gould LK, Johnson NP. Imaging Coronary Blood Flow in AS. Let the data talk, again. *J Am Coll Cardiol.* (2016) 67:1423–6. doi: 10.1016/j.jacc.2016.01.053
82. Zhou W, Bajaj N, Gupta A, Sun YP, Divakaran S, Bibbo C, et al. Coronary microvascular dysfunction, left ventricular remodeling, and clinical outcomes in aortic stenosis. *J Nucl Cardiol.* (2021) 28:579–88. doi: 10.1007/s12350-019-01706-y
83. Zelis J|M, Tonino PAL, Pijls NHJ, De Bruyne B, Kirkeeide RL, Gould LK, et al. Coronary microcirculation in aortic stenosis: pathophysiology, invasive assessment, and future directions. *J Interv Cardiol.* (2020) 22:4603169. doi: 10.1155/2020/4603169
84. Del Buono MG, Montone RA, Camilli M, Carbone S, Narula J, Lavie CJ, et al. Coronary microvascular dysfunction across the spectrum of cardiovascular diseases: JACC state-of-the-art review. *J Am Coll Cardiol.* (2021) 78:1352–71. doi: 10.1016/j.jacc.2021.07.042
85. MKC Ng, Yueng AC, Fearon WF. Invasive assessment of the coronary microcirculation: superior reproducibility and less hemodynamic dependence of index of microcirculatory resistance compared with coronary flow reserve. *Circulation.* (2006) 113:2054–61. doi: 10.1161/CIRCULATIONAHA.105.603522
86. Fearon WF, Balsam LB, Farouque HM, Caffarelli AD, Robbins RC, Fitzgerald PJ, et al. Novel index for invasively assessing the coronary microcirculation. *Circulation.* (2003) 107:3129–32. doi: 10.1161/01.CIR.0000080700.98607.D1
87. Mangiacapra F, Peace AJ, Di Serafino L, Pyxaras SA, Bartunek J, Wyffels E, et al. Intracoronary EnalaPrilat to reduce microvascular damage during percutaneous coronary intervention (ProMicro) study. *J Am Coll Cardiol.* (2013) 61:615–21. doi: 10.1016/j.jacc.2012.11.025
88. Xaplanteris P, Fournier S, Keulards DCJ, Adjedj J, Ciccarelli G, Milkas A, et al. Catheter-based measurements of absolute coronary blood flow and microvascular resistance: feasibility, safety, and reproducibility in humans. *Circ Cardiovasc Interv.* (2018) 11:e006194. doi: 10.1161/CIRCINTERVENTIONS.117.006194
89. Schindler TH, Schelbert HR, Quercioli A, Dilsizian V. Cardiac PET imaging for the detection and monitoring of coronary artery disease and microvascular health. *JACC Cardiovasc Imaging.* (2010) 3:623–40. doi: 10.1016/j.jcmg.2010.04.007
90. Larghat AM, Maredia N, Biglands J, Greenwood JP, Ball SG, Jerosch-Herold M, et al. Reproducibility of first-pass cardiovascular magnetic resonance myocardial perfusion. *J Magn Reson Imaging.* (2013) 37:865–74. doi: 10.1002/jmri.23889
91. Thomson LE, Wei J, Agarwal M, Haft-Baradaran A, Shufelt C, Mehta PK, et al. Cardiac magnetic resonance myocardial perfusion reserve index is reduced in women with coronary microvascular dysfunction. A national heart, lung, and blood institute-sponsored study from the women's ischemia syndrome evaluation. *Circ Cardiovasc Imaging.* (2015) 8:e002481. doi: 10.1161/CIRCIMAGING.114.002481
92. Branch KR, Haley RD, Bittencourt MS, Patel AR, Hulten E, Blankstein R. Myocardial computed tomography perfusion. *Cardiovasc Diagn Ther.* (2017) 7:452–62. doi: 10.21037/cdt.2017.06.11
93. Kotecha T, Martinez-Naharro A, Boldrini M, Knight D, Hawkins P, et al. Automated pixel-wise quantitative myocardial perfusion mapping by CMR to detect obstructive coronary artery disease and coronary microvascular dysfunction: validation against invasive coronary physiology. *JACC Cardiovasc Imaging.* (2019) 12:1958–69. doi: 10.1016/j.jcmg.2018.12.022
94. Pelletier-Galarneau M, Dilsizian V. Microvascular angina diagnosed by absolute PET myocardial blood flow quantification. *Curr Cardiol Rep.* (2020) 22:9. doi: 10.1007/s11886-020-1261-2
95. Banovic M, Bosiljka VT, Voin B, Milan P, Ivana N, Dejana P, et al. Prognostic value of coronary flow reserve in asymptomatic moderate or severe aortic stenosis with preserved ejection fraction and nonobstructed coronary arteries. *Echocardiography.* (2014) 31:428–33. doi: 10.1111/echo.12404
96. Davies JE, Sen S, Broyd C, Hadjiloizou N, Baksi J, Francis DP, et al. Arterial pulse wave dynamics after percutaneous aortic valve replacement: fall in coronary diastolic suction with increasing heart rate as a basis for angina symptoms in aortic stenosis. *Circulation.* (2011) 124:1565–72. doi: 10.1161/CIRCULATIONAHA.110.011916

97. Rolandi MC, Wiegerinck EMA, Casadonte L, Yong ZY, Koch KT, Vis M, et al. Transcatheter replacement of stenotic aortic valve normalizes cardiac–coronary interaction by restoration of systolic coronary flow dynamics as assessed by wave intensity analysis. *Circ Cardiovasc Interv.* (2016) 9:e002356. doi: 10.1161/CIRCINTERVENTIONS.114.002356
98. Stoller M, Gloekler S, Zbinden R, Tueller D, Eberli F, Windecker S, et al. Left ventricular afterload reduction by transcatheter aortic valve implantation in severe aortic stenosis and its prompt effects on comprehensive coronary haemodynamics. *EuroIntervention.* (2018) 14:166–73. doi: 10.4244/EIJ-D-17-00719
99. Rajappan K, Rimoldi OE, Camici PG, Bellenger NG, Pennell DJ, Sheridan DJ. Functional changes in coronary microcirculation after valve replacement in patients with aortic stenosis. *Circulation.* (2003) 107:3170–5. doi: 10.1161/01.CIR.0000074211.28917.31
100. Hildick-Smith DJR, Shapiro LM. Coronary flow reserve improves after aortic valve replacement for aortic stenosis: an adenosine transthoracic echocardiography study. *J Am Coll Cardiol.* (2000) 36:1889–96. doi: 10.1016/S0735-1097(00)00947-5
101. Doty DB, Eastham CL, Hiratzka LF, Wright CB, Marcus ML. Determination of coronary reserve in patients with supravalvular aortic stenosis. *Circulation.* (1982) 66:186–92.
102. Camuglia AC, Syed J, Garg P, Kiaii B, Chu MW, Jones PM, et al. Invasively assessed coronary flow dynamics improve following relief of aortic stenosis with transcatheter aortic valve implantation. *J Am Coll Cardiol.* (2014) 63:1808–9. doi: 10.1016/j.jacc.2013.11.040
103. Vendrik J, Ahmad Y, Eftekhari A, Howard JP, Wijntjens GWM, Stegehuis VE, et al. Long-term effects of transcatheter aortic valve implantation on coronary hemodynamics in patients with concomitant coronary artery disease and severe aortic stenosis. *J Am Heart Assoc.* (2020) 9:e015133. doi: 10.1161/JAHA.119.015133
104. Ferro G, Duilio C, Spinelli L, Liucci GA, Mazza F, Indolfi C. Relation between diastolic perfusion time and coronary artery stenosis during stress-induced myocardial ischemia. *Circulation.* (1995) 92:342–7. doi: 10.1161/01.CIR.92.3.342
105. Ahmad Y, Götberg M, Cook C, Howard JP, Malik I, Mikhail G, et al. Coronary hemodynamics in patients with severe aortic stenosis and coronary artery disease undergoing transcatheter aortic valve replacement: implications for clinical indices of coronary stenosis severity. *J Am Coll Cardiol Intv.* (2018) 11:2019–31. doi: 10.1016/j.jcin.2018.07.019
106. Hongo M, Goto T, Watanabe N, Nakatsuka T, Tanaka M, Kinoshita O, et al. Relation of phasic coronary flow velocity profile to clinical and hemodynamic characteristics of patients with aortic valve disease. *Circulation.* (1993) 88:953–60. doi: 10.1161/01.CIR.88.3.953
107. Spaan JA. Mechanical determinants of myocardial perfusion. *Basic Res Cardiol.* (1995) 90:89–102. doi: 10.1007/BF00789439
108. Fujiwara T, Nogami A, Masaki H, Yamane H, Matsuoka S, Yoshida H, et al. Coronary flow velocity waveforms in aortic stenosis and the effects of valve replacement. *Ann Thorac Surg.* (1989) 48:518–22. doi: 10.1016/S0003-4975(10)66853-1
109. Pijls NH, De Bruyne B, Peels K, Van Der Voort PH, Bonnier HJ, Bartunek J et al. Measurement of fractional flow reserve to assess the functional severity of coronary-artery stenoses. *N Engl J Med.* (1996) 334:1703–8. doi: 10.1056/NEJM199606273342604
110. Sen S, Escaned J, Malik IS, Mikhail GW, Foale RA, Mila R, et al. Development and validation of a new adenosine-independent index of stenosis severity from coronary wave-intensity analysis: results of the ADVISE (ADenosine Vasodilator Independent Stenosis Evaluation) study. *J Am Coll Cardiol.* (2012) 59:1392–402. doi: 10.1016/j.jacc.2011.11.003
111. Lee JM, Rhee TM, Choi KH, Park J, Hwang D, Kim J, et al. Clinical outcome of lesions with discordant results among different invasive physiologic indices—resting distal coronary to aortic pressure ratio, resting full-cycle ratio, diastolic pressure ratio, instantaneous wave-free ratio, and fractional flow reserve. *Circ J.* (2019) 83:2210–21. doi: 10.1253/circj.CJ-19-0230
112. van Nunen LX, Zimmermann FM, Tonino PA, Barbato E, Baumbach A, Engstrom T, et al. Fractional flow reserve versus angiography for guidance of PCI in patients with multivessel coronary artery disease (FAME): 5-year follow-up of a randomized controlled trial. *Lancet.* (2015) 386:1853–60. doi: 10.1016/S0140-6736(15)00057-4
113. Xaplanteris P, Fournier S, Pijls NHJ, Fearon WF, Barbato E, Tonino PAL, et al. Five-year outcomes with PCI guided by fractional flow reserve. *N Engl J Med.* (2018) 379:250–9. doi: 10.1056/NEJMoa1803538
114. Davies JE, Sen S, Dehbi HM, Al-Lamee R, Petraco R, Nijjer SS, et al. Use of the instantaneous wave-free ratio or fractional flow reserve in PCI. *N Engl J Med.* (2017) 376:1824–34. doi: 10.1056/NEJMoa1700445
115. Gotberg M, Christiansen EH, Gudmundsdottir IJ, Sandhall L, Danielewicz M, Jakobsen L, et al. Instantaneous wave-free ratio versus fractional flow reserve to guide PCI. *N Engl J Med.* (2017) 376:1813–23. doi: 10.1056/NEJMoa1616540
116. Pesarini G, Scarsini R, Zivelonghi C, Piccoli A, Gambaro A, Gottin L, et al. Functional assessment of coronary artery disease in patients undergoing transcatheter aortic valve implantation: influence of pressure overload on the evaluation of lesions severity. *Circ Cardiovasc Interv.* (2016) 9:e004088. doi: 10.1161/CIRCINTERVENTIONS.116.004088
117. Scarsini R, Pesarini G, Zivelonghi C, Piccoli A, Ferrero V, Lunardi M, et al. Coronary physiology in patients with severe aortic stenosis: Comparison between fractional flow reserve and instantaneous wave-free ratio. *Int J Cardiol.* (2017) 243:40–6. doi: 10.1016/j.ijcard.2017.05.117
118. Scarsini R, Pesarini G, Zivelonghi C, Piccoli A, Ferrero V, Lunardi M, et al. Physiologic evaluation of coronary lesions using instantaneous wave-free ratio (iFR) in patients with severe aortic stenosis undergoing transcatheter aortic valve implantation. *EuroIntervention.* (2018) 13:1512–9. doi: 10.4244/EIJ-D-17-00542
119. Scarsini R, Pesarini G, Lunardi M, Piccoli A, Zanetti C, Cantone R, et al. Observations from a real-time, iFR-FFR "hybrid approach" in patients with severe aortic stenosis and coronary artery disease undergoing TAVI. *Cardiovasc Revasc Med.* (2018) 19:355–9. doi: 10.1016/j.carrev.2017.09.019
120. Scarsini R, Cantone R, Venturi G, De Maria GL, Variola A, Braggio P, et al. Correlation between intracoronary physiology and myocardial perfusion imaging in patients with severe aortic stenosis. *Int J Cardiol.* (2019) 292:162–5. doi: 10.1016/j.ijcard.2019.04.050
121. Yamanaka F, Shishido K, Ochiai T, Moriyama N, Yamazaki K, Sugitani A, et al. Instantaneous wave-free ratio for the assessment of intermediate coronary artery stenosis in patients with severe aortic valve stenosis: comparison with myocardial perfusion scintigraphy. *J Am Coll Cardiol Intv.* (2018) 11:2032–40. doi: 10.1016/j.jcin.2018.07.027
122. Kotronias RA, Scarsini R, Rajasundaram S, De Maria GL, Ciofani JL, Ribichini F, et al. Transcatheter aortic valve replacement influence on coronary hemodynamics: a quantitative meta-analysis and proposed decision-making algorithm. *J Invasive Cardiol.* (2020) 32:37–40.
123. Stundl A, Shamekhi J, Bernhardt S, Starke M, Al-Kassou B, Weber M, et al. Fractional flow reserve in patients with coronary artery disease undergoing TAVI: a prospective analysis. *Clin Res Cardiol.* (2020) 109:746–54. doi: 10.1007/s00392-019-01563-2
124. Stanojevic D, Gunasekaran P, Tadros P, Wiley M, Earnest M, Mehta A, et al. Intravenous adenosine infusion is safe and well tolerated during coronary fractional flow reserve assessment in elderly patients with severe aortic stenosis. *J Invasive Cardiol.* (2016) 28:357–61.


**Conflict of Interest:** The authors declare that the research was conducted in the absence of any commercial or financial relationships that could be construed as a potential conflict of interest.

frontiers in Cardiovascular Medicine

ORIGINAL RESEARCH
published: 17 March 2022
doi: 10.3389/fcvm.2022.830944

# Right Ventricular Function Improves Early After Percutaneous Mitral Valve Repair in Patients Suffering From Severe Mitral Regurgitation

*Jonas Neuser, Hans Julian Buck, Maximiliane Oldhafer, Jan-Thorben Sieweke, Udo Bavendiek, Johann Bauersachs, Julian D. Widder and Dominik Berliner**

*Department of Cardiology and Angiology, Hannover Medical School, Hannover, Germany*

OPEN ACCESS

**Edited by:**
*Ronak Rajani, Guy's and St Thomas' NHS Foundation Trust, United Kingdom*

**Reviewed by:**
*Tanja Katharina Rudolph, Heart and Diabetes Center North Rhine-Westphalia, Germany*
*Tobias Zeus, University Hospital of Düsseldorf, Germany*

***Correspondence:**
*Dominik Berliner*
*berliner.dominik@mh-hannover.de*

**Specialty section:**
*This article was submitted to Heart Valve Disease, a section of the journal Frontiers in Cardiovascular Medicine*

**Received:** *07 December 2021*
**Accepted:** *21 February 2022*
**Published:** *17 March 2022*

**Citation:**
*Neuser J, Buck HJ, Oldhafer M, Sieweke J-T, Bavendiek U, Bauersachs J, Widder JD and Berliner D (2022) Right Ventricular Function Improves Early After Percutaneous Mitral Valve Repair in Patients Suffering From Severe Mitral Regurgitation. Front. Cardiovasc. Med. 9:830944. doi: 10.3389/fcvm.2022.830944*

**Background:** Percutaneous mitral valve edge-to-edge procedure (PMVR) using the MitraClip® system (Abbot Vascular, CA) is an established therapy for severe mitral regurgitation (MR) in patients judged inoperable or at high surgical risk. Besides determining exercise capacity, right ventricular (RV) function has prognostic value in heart failure and after cardiac surgery. We therefore investigated the impact of PMVR on RV function in patients with severe MR.

**Methods and Results:** Sixty-three patients undergoing PMVR at our department were prospectively enrolled. Transthoracic echocardiography was performed before, early (2–12d) after PMVR and after 3 months, including advanced echocardiographic analyses such as 3D imaging and strain analyses. At baseline, all patients presented with advanced heart failure symptoms. Etiology of MR was more often secondary and, if present, left ventricular (LV) dysfunction was predominantly caused by ischemic cardiomyopathy. PMVR substantially reduced MR to a grade $\leq$2 in most patients. Echocardiographic assessment revealed a largely unchanged LV systolic function early after PMVR, while in contrast RV function substantially improved after PMVR [3D RV EF (%): pre 33.7% [27.4; 39.6], post 40.0% [34.5; 46.0] ($p < 0.01$ vs. pre), 3 months 42.8% [38.3; 48.1] ($p < 0.01$ vs. pre); 2D RV GLS (%): pre −12.9% [−14.5; −10.5], post −16.0% [−17.9; −12.6] ($p < 0.01$ vs. pre), 3 months −17.2% [−21.7; −14.9] ($p < 0.01$ vs. pre)]. Factors that attenuated RV improvement were larger ventricular volumes, lower LV function, secondary MR, and a higher STS score (all $p < 0.05$).

**Conclusion:** By using advanced echocardiographic parameters, we discovered an early improvement of RV function after PMVR that is preserved for months, independent from changes in LV function. Improvement of RV function was less pronounced in patients presenting with an advanced stage of heart failure and a higher burden of comorbidities reflected by the STS score.

**Keywords: mitral regurgitation, percutaneous mitral valve repair, right ventricle, ventricular function, echocardiography, right ventricular strain**

## INTRODUCTION

Mitral regurgitation (MR) is the second most common valvular disease within the western world (1, 2). According to the Guidelines of the European Society of Cardiology, percutaneous mitral edge-to-edge procedure (PMVR) may be considered in patients suffering from severe MR, which are judged inoperable or at high surgical risk (2, 3). The EVEREST II trial proved that PMVR led to comparable results as conventional surgery concerning mortality or prevalence of moderate-severe or severe MR after 5 years (4). However, despite of improvement in NYHA functional class, more than 10% of patients die and almost 15% are re-hospitalized due to heart failure within the first year after PMVR using the MitraClip® system (Abbott Vascular, Santa Clara, CA) (5). Parameters such as left ventricular (LV) end-systolic volume and NYHA functional class were shown to predict outcome after PMVR, but there is still a need to identify patients who may or may not benefit from PMVR and which patient require a stringent follow up (5).

Right ventricular (RV) function was shown to determine exercise capacity and to possess prognostic value for heart failure and in cardiac surgery outcome (6–12). Due to chronic volume overload, MR causes structural and hemodynamic changes, such as LV remodeling and pulmonary hypertension. These alterations in turn can lead to an increase in RV afterload causing RV remodeling and dysfunction (13–15). It has been shown that surgical therapy for MR is associated with a higher risk of postoperative RV dysfunction (16–19). There is only limited data available on the impact of MR treatment by PMVR on RV function and results are conflicting (20–23). Recent 2D echocardiographic studies reported that in contrast to surgical mitral valve repair, RV function is preserved or even slightly improved after MitraClip® procedure (24–26). Beyond that, a tricuspid annular plane systolic excursion (TAPSE) <15 mm is associated with worse outcome after PMVR (27, 28). However, assessing the RV is challenging due to its complex geometric structure, retrosternal location, trabeculated endocardial surface and load dependency of function indices (25). Due to new 3D echocardiography-based methods, determination of RV volumes and function has recently become possible more easily (29).

We therefore sought to provide further insight on the influence of PMVR on ventricular function using more advanced echocardiographic methods such as 3D echocardiography and myocardial strain analysis in addition to standard 2D echocardiography in a real-world setting.

## PATIENTS AND METHODS

The study protocol is in accordance with the ethical guidelines of the 1975 declaration of Helsinki and approved by the local ethic committee of Hannover Medical School (#3047-2016). All patients gave written informed consent to participate in this study. We prospectively studied consecutive patients suffering from severe MR undergoing elective PMVR using the MitraClip® system at our department. In advance patients were assessed clinical, by transthoracic as well as transoesophageal echocardiography to evaluate MR severity along with mitral valve (MV) morphology. Coronary angiography was performed in all patients to exclude relevant coronary artery disease requiring revascularization. Patients were referred for PMVR by an interdisciplinary team of interventional cardiologists, cardiac imagine experts, cardiac surgeons, and cardiac anesthesiologists based on current guidelines and MV anatomy.

Patients' characteristics concerning general traits, comorbidities and laboratory values were obtained from medical records. PMVR was performed under general anesthesia and fluoroscopic as well as transoesophageal echocardiographic guidance, as described earlier (30). Preexisting co-medication was continued; so far, no preexistent or new contraindication existed. Follow-up data were obtained from medical records as well as by telephone interview 1 year after PMVR.

Sixty-three patients were initially included in the study. One patient withdrew consent for the study and one for the PMVR procedure. Fourteen patients did not attend the follow-up visit in our outpatient clinic 3 months after PMVR. During the first year, five patients deceased, while one withdrew consent for the study. Five patients were lost to follow up after 1 year, but eight patients, who did not attend the outpatient clinic for their 3 months follow-up visit, could be interviewed by phone 1 year after PMVR.

Transthoracic echocardiography using a PHILIPS EPIQ7 ultrasound machine equipped with a X5-1 transducer (PHILIPS, Amsterdam, Netherlands) was performed before and early after PMVR (2–12d) as well as 3 months after PMVR during routine follow-up in the outpatient clinic. Severity of MR was graded following the technique defined by Foster et al. (31). Images presenting the RV were recorded in standard 4-chamber view (4 CV). Analysis of RV global longitudinal strain (GLS) and fractional area change (FAC) derived from 2D images, LV GLS and global circular strain (GCS) derived from 3D images as well as biventricular 3D ejection fraction (EF) were assessed offline using TomTec Imaging Systems (Unterschleissheim, Germany).

All results are presented as median with interquartile range (IQR) or mean with standard deviation. Qualitative variables were compared using the chi² test. Comparison of quantitative variables between groups were performed using the Mann-Whitney-U-Test. Changes of dependent variables over time were analyzed using a variance analysis by the Friedman method followed by Wilcoxon test in the case of significant results. *P* values were corrected for multiple testing by the Bonferroni method. Cochran's Q test was used for comparison of dependent dichotomous variables. Univariable logistic regression analysis was performed to assess predictors for RV improvement after PMVR. Multivariate analysis was not performed due to the limited number of patients in the subgroups. *P* values <0.05 were considered statistically significant. Statistical analyses were done using IBM SPSS Statistics 26 (IBM, Armonk, NY, USA).

## RESULTS

Most patients presented with secondary etiology of MR (**Figure 1A**). Median age was 80 (IQR 75-84) years and the majority of male gender (73%). Baseline characteristics of the

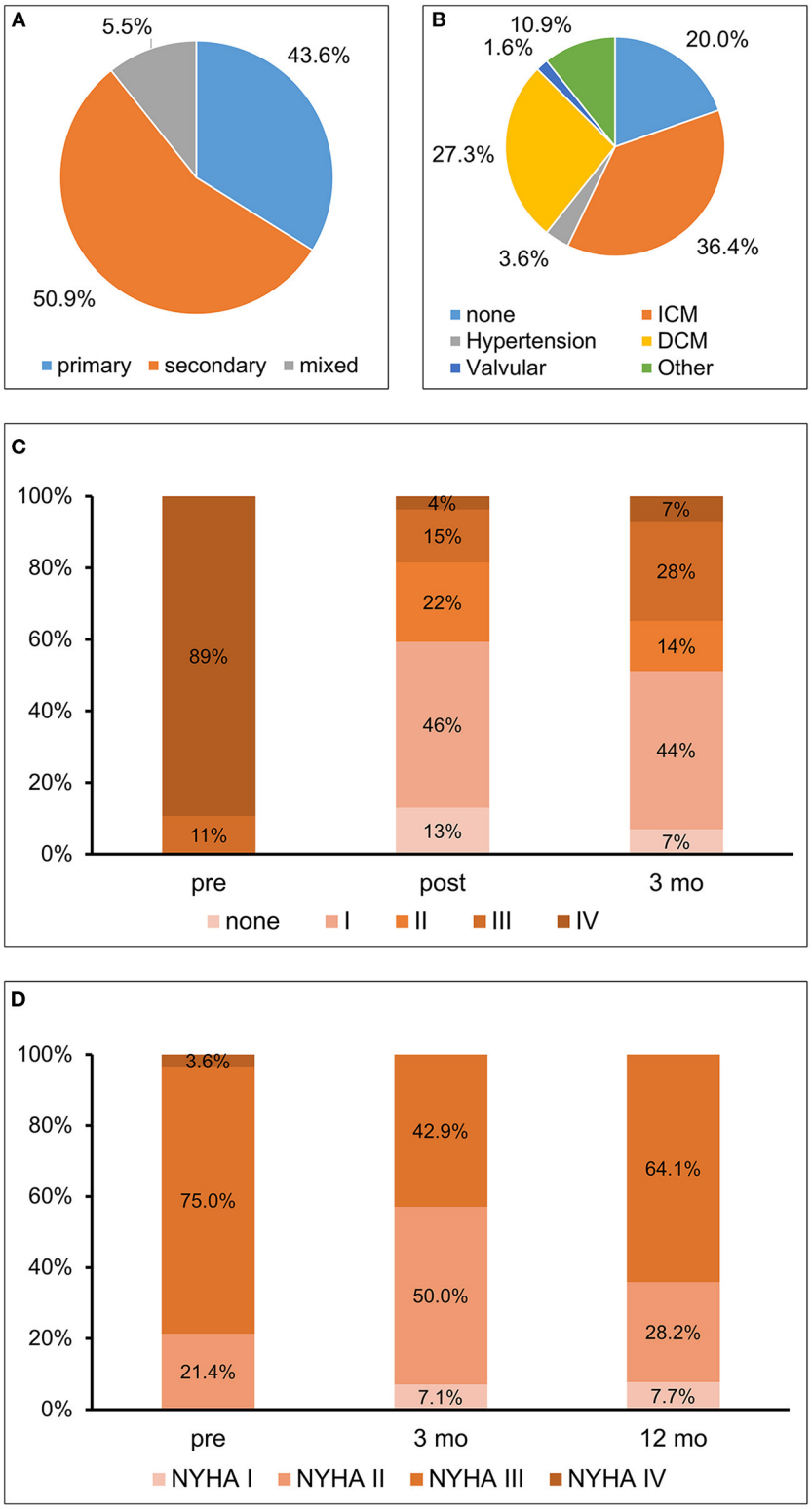


**FIGURE 1 | (A)** Etiology of mitral regurgitation; **(B)** Etiology of left ventricular dysfunction; **(C)** Mitral regurgitation–Severity of mitral regurgitation at baseline (pre), post procedural, i.e., at dismission (post), and 3 months (3 mo) after percutaneous mitral valve repair (PMVR); **(D)** Functional capacity–Assessment by New York Heart Association (NYHA) class before (pre) as well as at 3 months (3 mo) and 1 year (12 mo) after PMVR. ICM, ischemic cardiomyopathy; DCM, dilative cardiomyopathy.

cohort including comorbidities are depicted in **Table 1**. Most patients presented with a high burden of comorbidities and decompensated heart failure had occurred in almost 50%. About one third had suffered from myocardial infarction, more than half of all patients had undergone percutaneous coronary intervention, and in one third coronary bypass graft surgery had been performed. At baseline, all patients presented with symptoms of heart failure (New York Heart Association (NYHA) class ≥II). If present, LV dysfunction was predominantly caused by ischemic cardiomyopathy (**Figure 1B**). The majority of patients with reduced LV function received a sufficient pharmacological heart failure treatment consisting of ACE inhibitor or AT blocker (87.3%), beta-blocker (87.3%), mineralocorticoid receptor antagonists (45.5%) and diuretics (92.7%). Data on the medication during the 12 months of follow up is depicted in **Supplementary Table 1**. There was no significant change in the medication during the observational period. As a marker of heart failure NT-proBNP was elevated to a median of 5,356 (IQR 2028-6971) ng/l.

**TABLE 1 |** Patient characteristics.

| | Median [IQR] or % |
|---|---|
| **Characteristic** | |
| Age (years) | 80 [75; 84] |
| Male gender | 73.2% |
| BMI (kg/m²) | 25.41 [23.18; 29.62] |
| SBP (mmHg) | 122 [107; 134] |
| DBP (mmHg) | 65 [57; 76] |
| Heart rate (bpm) | 72 [62; 86] |
| EuroScore II (%) | 7.04 [5.4; 12.0] |
| STS-Score (Mortality) | |
| Replacement (%) | 5.54 [3.95; 7.03] |
| Repair (%) | 5.31 [3.15; 7.39] |
| **Comorbidities** | |
| Arterial hypertension | 92.9% |
| Diabetes mellitus | 32.1% |
| Hyperlipidemia | 73.2% |
| COPD | 12.5% |
| Renal function | |
| GFR > 90 ml/min | 1.8% |
| GFR 60–90 ml/min | 19.6% |
| GFR 30–60 ml/min | 57.1% |
| GFR 15–30 ml/min | 19.6% |
| GFR < 15 ml/min | 1.8% |
| Atrial fibrillation | 76.8% |
| Pacemaker | 30.4% |
| CRT | 10.7% |
| H/O cerebral ischemia | 14.3% |
| H/O decompensated HF | 50.0% |
| H/O myocardial infarction | 33.9% |
| H/O PTCA | 57.1% |
| H/O CABG | 33.9% |
| **Heart rhythm** | |
| Sinus rhythm | 30.9% |
| Atrial fibrillation | 43.6% |
| Ventricular stimulation | 21.8% |
| Other | 3.6% |
| **Hemodynamics** | |
| Cardiac index (Thermo-Dilution; l/min/m$^2$) | 2.44 [2.24; 3.02] |
| Cardiac index (Fick; l/min/m$^2$) | 2.42 [2.09; 2.63] |
| Mean pulmonary arterial pressure (mmHg) | 30 [23; 37 |
| Pulmonary arterial wedge pressure (mmHg) | 19 [12; 23] |
| Pulmonary vascular resistance (Dynes) | 177 [128; 241] |

*BMI, body mass index; CABG, coronary artery bypass graft; CKD, chronic kidney disease; COPD, chronic obstructive pulmonary disease; CRT, cardiac resynchronization therapy; DBP, diastolic blood pressure; GFR, glomerular filtration rate; H/O, history of; HF, heart failure; IQR, interquartile range; PTCA, percutaneous transluminal coronary angioplasty; PVR, pulmonary vascular resistance; SBP, systolic blood pressure.*

Three months after PMVR MR was reduced and most patients (58.5%) presented with a MR grade ≤2 (**Figure 1C**). No significant difference in the reduction of the MR between patients with secondary or primary MR was detectable ($p = 0.457$). Heart failure burden, evaluated by NYHA functional class, improved at 3 months, with more than one third still being NYHA I or NYHA II after 12 months (**Figure 1D**). During the observational period a total of nineteen hospitalizations had occurred. However, only four of them were due to cardiac decompensation. More than 50% of the events were due to non-cardiovascular causes.

Echocardiographic assessment showed only a temporary trend for a decrease in LV function (3D LVEF) early after PMVR (**Figure 2** and **Table 2**). There were no significant changes of LV volumes (**Table 2**). There was a short-term deterioration of the GLS after PMVR, which was not significant at 3 months follow-up. No changes were detectable in relation to the GCS.

In contrast, various RV function parameters revealed a significant improvement in RV function early after PMVR that was sustained at 3 months follow-up (**Figure 2** and **Table 2**). 3D RVEF, 2D RV GLS, and FAC showed a significant improvement after PMVR (**Table 2**). However, TAPSE, as the probably most widely used RV parameter in clinical routine, did not show any significant changes. 3D calculated RV end systolic (ESV) and end diastolic volumes (ESV) did not change significantly, however, stroke volume significantly increased.

When considering different subpopulations effects on RV function seem to be more pronounced in patients suffering from primary MR. Comparing other subgroups (e.g., existence of ischemic cardiomyopathy), retrieved no significant differences in short term changes of RV function (**Supplementary Tables 1A,B**).

To further elucidate factors of changes in RV function and dimensions following PVMR, we further analyzed the study population by differentiating between relevant RV function improvement and lack of early improvement after PMVR. Patients with reduced RV function at baseline ($n = 36$) were divided into tertiles depending on improvement of 3D RVEF. Being in the lowest tertile (change of <5.2% RVEF) was defined as lack of RV improvement. Patients without relevant improvement of RV function had higher Society of Thoracic Surgeons (STS) scores, more frequently secondary MR, lower LV function (LVEF, GLS) and higher LV volumes, and higher RV diastolic volume with reduced longitudinal function (RV GLS).

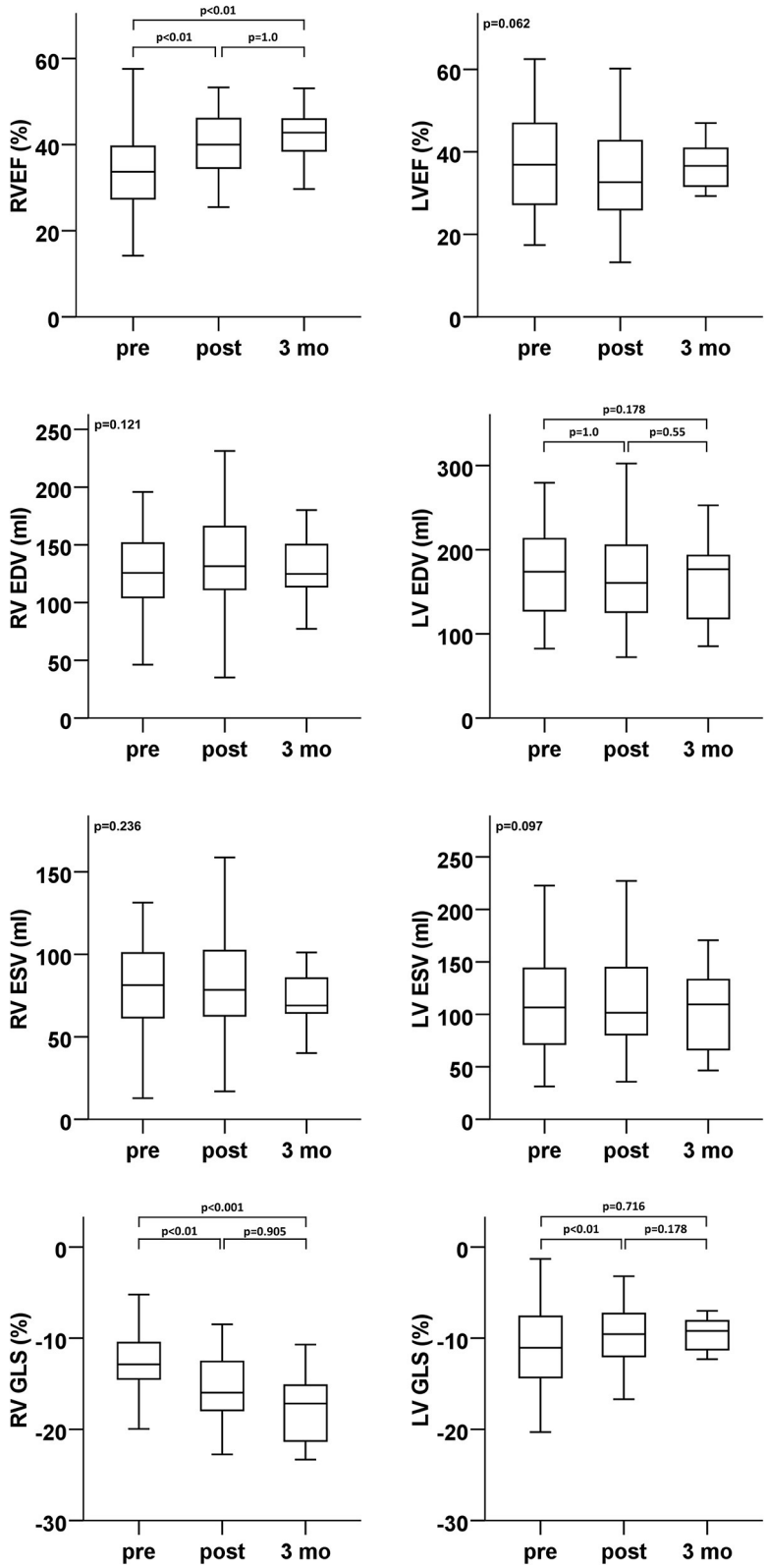


**FIGURE 2 |** Ventricular function (ejection fraction and global longitudinal strain) and volumes (enddiastolic and endsystolic)–echocardiographic analyses of LV (right column) and RV (left column) parameters at baseline (pre), dismission (post), and 3 months after percutaneous mitral valve repair (PMVR). EDV, end diastolic volume; ESV, end systolic volume; GLS, global longitudinal strain; LV, left ventricle; LVEF, left ventricular ejection fraction; RV, right ventricle; RVEF, right ventricular ejection fraction.

**TABLE 2 |** Echocardiographic analyses of LV and RV parameters at baseline, dismission (Post PMVR), and 3 months after percutaneous mitral valve repair (Data presented as inter quartile range).

| | Baseline | Post PMVR | 3 months | *P* |
|---|---|---|---|---|
| **Left ventricle** | | | | |
| 3D LV EDV (ml) | 174.0 [127.6; 213.1] | 160.6 [125.9; 205.4]$^{n.s.}$ | 176.9 [115.3; 197.4]$^{n.s.}$ | **0.045** |
| 3D LV ESV (ml) | 106.6 [71.7; 143.8] | 101.6 [80.7; 144.5] | 109.5 [64.4; 136.5] | 0.097 |
| 3D LV SV (ml) | 57.1 [51.1; 73.5] | 55.6 [44.1; 64.6] $^{n.s.}$ | 57.1 [46.8; 61.7] $^{n.s.}$ | **0.050** |
| 3D LV EF (%) | 36.9 [27.3; 46.9] | 32.7 [26.0; 42.7] | 36.6 [30.9; 41.1] | 0.062 |
| 2D LV GLS (%) | −11.1 [−14.3; −7.6] | −9.6 [−12.0; −7.3]** | −9.2 [−11.4; −7.8] | **0.008** |
| 3D LV GCS (%) | −15.8 [−22.1; −10.4] | −13.0 [−19.3; −11.0] | −17.3 [−19.2; −12.8] | 0.236 |
| 3D LV 3D twist | 8.5 [4.2; 13.3] | 6.7 [2.7; 12.4] | 9.9 [5.4; 13.0] | 0.459 |
| 2D LVEF (Simpson bp; %) | 37 [28; 51] | 34 [25; 46]** | 36 [28; 48]* | **<0.001** |
| E wave (cm/s) | 103.5 [78.4; 119.0] | 136.2 [93.4; 158.0] | 133.8 [101.2; 153.0] | 0.156 |
| A wave (cm/s) | 53.8 [33.6; 88.6] | 108 [84.5; 129.0]* | 114 [68.6; 137.6] | **0.039** |
| Deceleration time (ms) | 170 [150; 195] | 260 [220; 350] | 220 [140; 340] | 0.060 |
| s'lateral (cm/s) | 5.9 [4.6; 6.6] | 5.7 [4.2; 7.2] | 6.1 [5.6; 6.7] | 0.325 |
| e'lateral (cm/s) | 8.25 [6.1; 10.4] | 8.6 [5.6; 9.4] | 7.2 [5.5; 8.4] | 0.417 |
| a'lateral (cm/s) | 5.15 [3.1; 6.3] | 6.6 [3; 7.8] | 6.8 [5.1; 9.1] | 1.000 |
| s'septal (cm/s) | 4.5 [4.0; 5.2] | 4.1 [3.6; 5.3] | 4.95 [3.9; 6.0] | 0.102 |
| e'septal (cm/s) | 4.6 [4.2; 5.8] | 4.1 [3.2; 4.6] | 4.3 [3.5; 5.2] | 0.303 |
| a'septal (cm/s) | 4.3 [3.4; 5.4] | 3.7 [3.7; 4.8] | 6 [4.4; 7.0] | 0.148 |
| E/e' | 16.6 [13.4; 21.5] | 27.0 [16.2; 31.4] | 25.4 [17.8; 33.5] | 0.069 |
| LA volume (ml) | 132.9 [104.6; 154.9] | 128.3 [97.0; 164.4] | 123.15 [96.0; 174.8] | 0.970 |
| **Right ventricle** | | | | |
| 3D RV EDV (ml) | 125.8 [101.9; 151.6] | 131.5 [111.5; 165.8] | 124.8 [111.1; 158.8] | 0.121 |
| 3D RV ESV (ml) | 81.4 [61.7; 101.1] | 78.5 [62.8; 102.3] | 69.0 [63.9; 90.6] | 0.236 |
| 3D RV SV (ml) | 42.0 [30.0; 53.7] | 50.5 [43.8; 58.8]* | 50.0 [46.0; 68.2]** | **0.004** |
| 3D RV EF (%) | 33.7 [27.4; 39.6] | 40.0 [34.5; 46.0]** | 42.8 [38.3; 48.1]** | **0.001** |
| 2D RV GLS (%) | −12.9 [−14.5; −10.5] | −16.0 [−17.9; −12.6]** | −17.2 [−21.7; −14.9]** | **<0.001** |
| 2D RV EDA (cm²) | 25.9 [22.0; 30.2] | 26.9 [22.7; 32.3] | 23.0 [20.3; 28.1] | 0.088 |
| 2D RV ESA (cm²) | 19.6 [15.1; 24.3] | 18.2 [14.2; 24.4] | 15.3 [13.7; 17.9]** | **0.012** |
| 2D RV FAC (%) | 25 [18.4; 31.7] | 31.1 [24.6; 38.5]* | 32.5 [26.5; 40.2]* | **0.007** |
| TAPSE (mm) | 16 [13; 19] | 15 [14; 20] | 15 [11; 18] | 0.348 |
| RV diameter (PLAX) | 3.9 [3.3; 4.4] | 3.95 [3.5; 4.5] | 3.9 [3.4; 4.5] | 0.527 |
| RV diameter (4CV) | 4.4 [3.8; 5.0] | 4.5 [4.1; 5.2] | 4.3 [3.8; 4.8] | 0.175 |
| RV–E wave (cm/s) | 58.1 [44.0; 67.4] | 59.5 [46.2; 74.1] | 54.8 [45.7; 6.02] | 0.905 |
| RV–A wave (cm/s) | 44.2 [31.6; 58.7] | 46.1 [39.2; 53.7] | 62.1 [57.0; 68.6] | 0.135 |
| RV–deceleration time (ms) | 170 [130; 220] | 200 [150; 260] | 170 [140; 240] | 0.097 |
| RV–s'(cm/s) | 9.4 [7.7; 11.3] | 10.2 [8.4; 11.8] | 11.3 [8.3; 12.9] | 0.103 |
| RV–e'(cm/s) | 8.6 [6.1; 12.1] | 8.3 [5.9; 10.1] | 9 [5.7; 13.0] | 0.584 |
| RV–a'(cm/s) | 9.7 [4.8; 13.9] | 11.3 [8.3; 14.4] | 13.4 [10.0; 15.8] | 0.867 |
| RA area (cm²) | 28.6 [24.8; 33.9] | 28.6 [21.7; 33.5] | 28.0 [21.7; 32.6] | 0.334 |
| Estimated sPAP (mmHg) | 43.1 [37.2; 53.0] | 47.7 [38.5; 57.1] | 46.2 [37.7; 49.7] | 0.607 |

*2D, 2-dimensional; 3D, 3-dimensional; 4CV, 4 chamber view; EDA, end diastolic area; EDV, end diastolic volume; EF, ejection fraction; ESA, end systolic area; ESV, end systolic volume; FAC, fractional area change; GCS, global circumferential strain; GLS, global longitudinal strain; LA, left atrium; LV, left ventricle; PLAX, parasternal long axis; RV, right ventricle; sPAP, systolic pulmonary artery pressure; SV, stroke volume; TAPSE, tricuspid annular plane systolic excursion; n.s., not significant.*

**p < 0.05 vs. baseline.*

***p < 0.01 vs. baseline.*

*Bold values indicate significance.*

Neither pulmonary artery pressures and the pulmonary vascular resistance before PMVR nor the transmitral gradient after PMVR were shown to be different between the two groups. In summary, respective patients presented with a more advanced stage of disease (**Table 3**). The two groups did not differ significantly concerning factors such as age, NYHA functional class or level of NT-proBNP. Results are shown in **Table 3**. In univariable analysis higher LV- and RV volumes, a more restricted LV GLS, and the existence of functional MR were predictors of a lower probability of RV improvement (**Table 4**).

**TABLE 3 |** Improvement vs. Non-improvement of RV function after percutaneous mitral valve repair (PMVR) in the subgroup of patients with reduced RV function (RVEF ≤ 45%) at baseline ($n = 36$).

| | Lack of relevant RV improvement ($n = 10$) | RV improvement ($n = 26$) | *P* |
|---|---|---|---|
| **Age (years)** | 76 [73; 80] | 80 [75; 83] | 0.393 |
| **NYHA class at baseline** | | | 0.526 |
| I | 0% | 0% | |
| II | 10.0% | 23.1% | |
| III | 90.0% | 73.1% | |
| IV | 0% | 3.8% | |
| **NYHA class at 12 months** | | | 0.111 |
| I | 40.0% | 5.3% | |
| II | 20.0% | 26.3% | |
| III | 40.0% | 68.4% | |
| IV | 0% | 0% | |
| **STS-score** | | | |
| MV-Repair (mortality) | 7.63 [7.3; 16.8] | 4.5 [3.1; 7.2] | **0.015** |
| MV-Repair (morbidity & mortality) | 35.7 [34.1; 36.2] | 24.6 [20.7; 31.4] | **0.049** |
| **Secondary mitral regurgitation** | 90% | 44% | **0.013** |
| **Tricuspid regurgitation** | | | 0.107 |
| Grade I | 11.1% | 32.0% | |
| Grade II | 22.2% | 16.0% | |
| Grade III | 0% | 28.0% | |
| Grade IV | 33.3% | 8.0% | |
| Grade V | 33.3% | 16.0% | |
| **Mean pulmonary artery pressure (mmHg)** | 30 [26; 40] | 30 [26; 36] | 0.823 |
| **PVR (dyn x sec x cm$^{-5}$)** | 211 [151; 376] | 184 [96; 238] | 0.412 |
| **Improvement of MR** | | | 0.775 |
| 1 grade | 40% | 20% | |
| 2 grades | 20% | 28% | |
| 3 grades | 30% | 36% | |
| **2D LVEF (Simpson biplane; %)** | 30 [24; 34] | 36 [25; 51] | 0.288 |
| **3D LVEF (%)** | 24.2 [19.8; 37.0] | 37.6 [27.3; 47.1] | **0.039** |
| **3D LV EDV (ml)** | 237.6 [177.6; 319.2] | 163.5 [127.6] | **0.022** |
| **3D LV ESV (ml)** | 167.2 [122.8; 259.0] | 97.9 [71.7; 134.8] | **0.022** |
| **LV GLS (%)** | −7.3 [−9.3; −4.8] | −11.5 [14.3; −8.4] | **0.005** |
| **TAPSE (mm)** | 15 [13; 19] | 17 [13; 20] | 0.869 |
| **3D RVEF (%)** | 36.3 [32.3; 39.6] | 29.1 [25.8; 41.2] | **0.041** |
| **RV GLS (%)** | −12.96 [−14.33; −11.51] | −16.36 [−17.91; −12.20] | **0.049** |
| **RV FAC (%)** | 24.16 [19.49; 31.3] | 22.04 [13.28; 27.48] | 0.201 |
| **RV EDV (ml)** | 153.4 [130.1; 195.8] | 116.2 [99.7; 149.5] | **0.021** |
| **RV ESV (ml)** | 99.3 [79.9; 131.4] | 82.8 [61.7; 98.7] | 0.053 |
| **RV E (cm/s)** | 74.9 [63.0; 93.8] | 51.9 [41.8; 63.5] | **0.007** |
| **RV E-deceleration time (ms)** | 225 [180; 250] | 160 [120; 190] | **0.012** |
| **RV s' (cm/s)** | 8.7 [7.8; 9.4] | 10.4 [7.4; 12.1] | 0.149 |
| **RV e' (cm/s)** | 8.8 [8.3; 9.1] | 7.4 [5.7; 12.2] | 0.071 |
| **Estimated sPAP (mmHg)** | 42 [34; 53] | 40 [37; 55] | 0.850 |
| **GFR (ml/min)** | 40 [31; 51] | 44 [34; 56] | 0.393 |
| **Urea (mmol/l)** | 15.7 [14.3; 16.7] | 9.3 [6.3; 13.9] | **0.02** |
| **NT-proBNP (ng/l)** | 5,586 [5,356; 7,714] | 4,186 [1,419; 6,971] | 0.714 |
| **Max. transmitral gradient post PMVR** | 10.2 [8.4; 13.4] | 10.8 [8.9; 13.4] | 0.788 |
| **Mean transmitral gradient post PMVR** | 3.5 [2.4; 4.0] | 3.0 [2.7; 4.0] | 1.000 |

*2D, 2-dimensional; 3D, 3-dimensional; EDV, enddiastolic volume; ESV, endsystolic volume; EF, ejection fraction; FAC, fractional area chance; GFR, glomerular filtration rate; GLS, global longitudinal strain; LV, left ventricle; MV, mitral valve; NYHA, New York Heart Association; PVR, pulmonary vascular resistance; RV, right ventricle; sPAP, systolic pulmonary artery pressure (by echocardiography); STS, Society of Thoracic Surgeons; TAPSE, tricuspid annular plane excursion.*

*Improvement of RVEF was divided into tertiles. The lowest tertile was defined as lack of relevant improvement. Bold values indicate significance.*

**TABLE 4 |** Predictors of improvement of right ventricular function after percutaneous mitral valve repair (PMVR) in the subgroup of patients with reduced RV function (RVEF ≤ 45%) at baseline ($n = 36$) in univariable analysis.

| | OR | 95% CI | *P*-value |
|---|---|---|---|
| STS-Score (%)–MV-Repair (mortality) | 0.822 | 0.675–1.002 | 0.052 |
| **Secondary MR** | **0.087** | **0.010–0.797** | **0.031** |
| 3D LVEF (%) | 1.074 | 0.994–1.161 | 0.072 |
| **3D LV EDV (ml)** | **0.982** | **0.967–0.997** | **0.022** |
| **3D LV ESV (ml)** | **0.981** | **0.966–0.997** | **0.017** |
| **LV GLS (%)** | **0.685** | **0.499–0.941** | **0.019** |
| **3D RVEF (%)** | **0.878** | **0.777–0.993** | **0.038** |
| RV GLS (%) | 0.939 | 0.754–1.171 | 0.577 |
| **RV EDV (ml)** | **0.974** | **0.953–0.997** | **0.025** |
| **RV ESV (ml)** | **0.974** | **0.950–1.000** | **0.048** |
| **RV E (cm/s)** | **0.932** | **0.882–0.986** | **0.014** |
| **RV E-deceleration time (ms)** | **0.982** | **0.967–0.998** | **0.030** |
| RV e' (cm/s) | 0.962 | 0.823–1.123 | 0.622 |
| Urea (mmol/l) | 0.688 | 0.457–1.036 | 0.074 |

*3D, 3-dimensional; EDV, enddiastolic volume; ESV, endsystolic volume; EF, ejection fraction; GLS, global longitudinal strain; LV, left ventricle; MR, mitral regurgitation; MV, mitral valve; RV, right ventricle; STS, Society of Thoracic Surgeons.*
*Bold values indicate significance.*

## DISCUSSION

MR is the second most common valvular disease within the western world and PMVR is an increasingly used therapeutic option for patients ineligible or at high perioperative risk for conventional surgical mitral valve repair or replacement (1, 32). However, knowledge on the impact of PMVR on RV function is scarce and conflicting.

The main findings of our study are: (1) RV function improves early after PMVR using the MitraClip® system. (2) This improvement is independent from changes in LV function. (3) The improvement seems to be less pronounced in patients suffering from more advanced heart disease, i.e., higher RV and LV volumes and reduced LV function and secondary MR. (4) Advanced echocardiographic methods like 3D imaging and strain analyses are superior to the standard parameter TAPSE in detecting changes in RV function.

LV function showed a transient marginal significant (only 2D LVEF and 3D LV GLS, not 3D LVEF) decrease early after PMVR. This decline was more prominent in patients with preserved or mildly reduced LVEF (>40%) due to Frank-Starling-mechanism in a volume overload state before PMVR. By reducing MR pressure load is increased, followed by a decline in EF and stroke volume. However, due to reduced volume overload EF ameliorated within the first months after PMVR. Recently, another study found similar long-term results regarding the LV in a group of patients undergoing PMVR (33). Regarding reverse remodeling of the LV involvement of the RV before PMVR (higher RV volumes, higher sPAP) seem to be existent in patient without reverse remodeling. Despite the borderline decline and following amelioration of LV function, RV function improves early after PMVR, and this development continues at 3 months. The change in RV function can be explained by reduced RV afterload after PMVR. Earlier studies report similar observations after 6 months; however, our data indicate an early improvement of RV function within the first days after PMVR, which seems to be preserved at 3 months in our study, respectively 6 months as Vitarrelli et al. describe (34).

The occurrence or presence of reduced RV function has repeatedly been associated with a worsening of patients' prognosis (35–39). For this reason, we analyzed factors that might influence reverse RV remodeling or relevant improvement of RV function. In summary, patients with less improvement of RV function were found to be in an advanced stage of their heart disease including lower LV function and higher biventricular volumes. A less impaired RV GLS was related to a greater degree of improvement of RV function. Only mildly reduced RV GLS might reflect a state of RV function in which recovery is still possible. Recently, a study in patients undergoing surgical mitral valve repair in primary MR also showed the importance of RV GLS and the prognostic impact of its short term development on myocardial recovery and rehospitalization rates (40). In a former study only patients with secondary MR were more likely to undergo reverse remodeling (41). Nevertheless, our data indicate that patients without relevant improvement in RV function more often have secondary MR and patients with primary MR have a higher increase in RVEF and RV SV in short term follow-up. In general patients suffering from secondary MR present with more comorbidities and advanced progression of their heart disease. This is reflected by our analyses revealing patients with higher STS-risk score to be less likely to develop reverse RV remodeling and by our data showing less RV improvement in patients suffering from severe LV impairment. Our data thereby suggest a threshold of LV and RV dysfunction beyond that RV recovery is unachievable. Further studies are needed to identify this threshold and evaluate whether these patients below still profit clinically from PMVR.

In our study improved RV function could be detected using advanced echocardiographic methods, while TAPSE, in turn did not reveal any significant changes. This partly is in line with earlier reports indicating TAPSE to be a less reliable parameter of RV function compared with advanced echocardiographic methods like 3D EF, RV FAC, GLS and free wall strain. However, some reports state significant changes in RV function after PVMR even measured using TAPSE (21, 42, 43), while in contrast other studies did not show any changes. For instance, in patients undergoing cardiac surgery Rong et al. reported that TAPSE in contrast to FAC, GLS and free wall strain did not predict RV dysfunction at chest closure. Grønlykke et al. described a decline in TAPSE after cardiopulmonary bypass while RV output was sustained, which was reflected in unchanged RVEF, RV GLS and FAC. This indicates that TAPSE does not reliably reflect changes in RV function (44, 45). Van Riel et al. reported that most 2D derived indices of RV function did not show any improvement of RV function after PMVR (22). However, these latter data did not encompass strain analysis, and therefore the analyzed parameters might not be sensitive enough to reliably detect changes in RV function adequately. In your study we were able

to detect changes in RV function in the setting of PMVR, but only by using more advanced echocardiographic methods. This is in line with reports showing improvement in 3D RVEF after PVMR (34, 46).

The main limitation of the study is the small sample size that limits the explanatory power of subgroup analyses. Therefore, analyses of subpopulations need to be considered with precaution and require verification in a larger patient cohort. Moreover, a relevant number of patients was lost to follow up and did not attend their appointments in our outpatient clinics for the scheduled echocardiographic examination reflecting a real-world scenario. Furthermore, the follow up period was relatively short regarding ventricular remodeling. However, changes in RV parameters could be seen very early after PMVR, which suggests that long-term follow-up in this regard is neglectable. Finally, the data only derive from one center.

However, we still believe that the presented data are of significant novelty especially concerning the very early change of RV parameters and the use of advanced echocardiographic methods in the evaluation of RV function.

In summary, we could identify an improvement of RV function early after PMVR which is preserved or even pronounced at 3 months and independent from changes in LV function. Factors that reduce the potential of RV recovery after PMVR included higher LV volumes and lower LV systolic function, higher RV diastolic volume and more severely reduced RV GLS, secondary MR and a higher STS score. Our data reveal that advanced echocardiographic methods should be implemented in daily routine for evaluation of RV function since the widely used TAPSE seems to be less sensitive in reflecting RV dysfunction and its improvement and should be interpreted with caution. Further studies are needed to elucidate a threshold of LV and RV impairment beyond patients do not profit from PMVR.

## DATA AVAILABILITY STATEMENT

The original contributions presented in the study are included in the article/**Supplementary Material**, further inquiries can be directed to the corresponding author.

## ETHICS STATEMENT

The studies involving human participants were reviewed and approved by the local Ethics Committee of Hannover Medical School (#3047-2016). The patients/participants provided their written informed consent to participate in this study.

## AUTHOR CONTRIBUTIONS

JN, JB, JW, and DB: substantial contributions to the conception or design of the work. JN, HB, MO, J-TS, UB, and DB: the acquisition, analysis, and interpretation of data for the work. JN and DB: drafting the work. HB, MO, J-TS, UB, JB, and JW: revising it critically for important intellectual content. JN, HB, MO, J-TS, UB, JB, JW, and DB: provide approval for publication of the content and agree to be accountable for all aspects of the work in ensuring that questions related to the accuracy or integrity of any part of the work are appropriately investigated and resolved. All authors contributed to the article and approved the submitted version.

## SUPPLEMENTARY MATERIAL

The Supplementary Material for this article can be found online at: https://www.frontiersin.org/articles/10.3389/fcvm.2022.830944/full#supplementary-material

## REFERENCES


1. Iung B, Vahanian A. Epidemiology of valvular heart disease in the adult. *Nat Rev Cardiol*. (2011) 8:162–72. doi: 10.1038/nrcardio.2010.202
2. Vahanian A, Beyersdorf F, Praz F, Milojevic M, Baldus S, Bauersachs J, et al. 2021 ESC/EACTS Guidelines for the management of valvular heart disease. *Eur J Cardiothorac Surg*. (2021) 60:727–800. doi: 10.1093/ejcts/ezab389
3. Berliner D, Hanselmann A, Bauersachs J. The treatment of heart failure with reduced ejection fraction. *Dtsch Arztebl Int*. (2020) 117:376–86. doi: 10.3238/arztebl.2020.0376
4. Feldman T, Kar S, Elmariah S, Smart SC, Trento A, Siegel RJ, et al. Randomized comparison of percutaneous repair and surgery for mitral regurgitation: 5-year results of EVEREST II. *J Am Coll Cardiol*. (2015) 66:2844–54. doi: 10.1016/j.jacc.2015.10.018
5. Capodanno D, Adamo M, Barbanti M, Giannini C, Laudisa ML, Cannata S, et al. Predictors of clinical outcomes after edge-to-edge percutaneous mitral valve repair. *Am Heart J*. (2015) 170:187–95. doi: 10.1016/j.ahj.2015.04.010
6. Ternacle J, Berry M, Cognet T, Kloeckner M, Damy T, Monin JL, et al. Prognostic value of right ventricular two-dimensional global strain in patients referred for cardiac surgery. *J Am Soc Echocardiogr*. (2013) 26:721–6. doi: 10.1016/j.echo.2013.03.021
7. de Groote P, Millaire A, Foucher-Hossein C, Nugue O, Marchandise X, Ducloux G, et al. Right ventricular ejection fraction is an independent predictor of survival in patients with moderate heart failure. *J Am Coll Cardiol*. (1998) 32:948–54. doi: 10.1016/S0735-1097(98)00337-4
8. Ghio S, Gavazzi A, Campana C, Inserra C, Klersy C, Sebastiani R, et al. Independent and additive prognostic value of right ventricular systolic function and pulmonary artery pressure in patients with chronic heart failure. *J Am Coll Cardiol*. (2001) 37:183–8. doi: 10.1016/S0735-1097(00)01102-5
9. Patel AR, Dubrey SW, Mendes LA, Skinner M, Cupples A, Falk RH, et al. Right ventricular dilation in primary amyloidosis: an independent predictor of survival. *Am J Cardiol*. (1997) 80:486–92. doi: 10.1016/S0002-9149(97)00400-1
10. Sun JP, James KB, Yang XS, Solankhi N, Shah MS, Arheart KL, et al. Comparison of mortality rates and progression of left ventricular dysfunction in patients with idiopathic dilated cardiomyopathy and dilated versus nondilated right ventricular cavities. *Am J Cardiol*. (1997) 80:1583–7. doi: 10.1016/S0002-9149(97)00780-7
11. Magunia H, Dietrich C, Langer HF, Schibilsky D, Schlensak C, Rosenberger P, et al. 3D echocardiography derived right ventricular function is associated with right ventricular failure and mid-term survival after left ventricular assist device implantation. *Int J Cardiol*. (2018) 272:348–55. doi: 10.1016/j.ijcard.2018.06.026
12. Melenovsky V, Hwang SJ, Lin G, Redfield MM, Borlaug BA. Right heart dysfunction in heart failure with preserved ejection fraction. *Eur Heart J*. (2014) 35:3452–62. doi: 10.1093/eurheartj/ehu193

13. Enriquez-Sarano M, Akins CW, Vahanian A. Mitral regurgitation. *Lancet*. (2009) 373:1382–94. doi: 10.1016/S0140-6736(09)60692-9
14. McLaughlin VV, Rich S. Pulmonary hypertension. *Curr Probl Cardiol*. (2004) 29:575–634. doi: 10.1016/j.cpcardiol.2004.04.001
15. Winzelberg GG, Boucher CA, Pohost GM, McKusick KA, Bingham JB, Okada RD, et al. Right ventricular function in aortic and mitral valve disease. *Chest*. (1981) 79:520–8. doi: 10.1378/chest.79.5.520
16. Orde SR, Chung SY, Pulido JN, Suri RM, Stulak JM, Oh JK, et al. Changes in right ventricle function after mitral valve repair surgery. *Heart Lung Circ*. (2020) 29:785–92. doi: 10.1016/j.hlc.2019.06.724
17. Elgharably H, Javadikasgari H, Koprivanac M, Lowry AM, Sato K, Blackstone EH, et al. Right vs. left heart reverse remodelling after treating ischaemic mitral and tricuspid regurgitation. *Eur J Cardiothorac Surg*. (2021) 59:442–50. doi: 10.1093/ejcts/ezaa326
18. Wranne B, Pinto FJ, Hammarstrom E, St Goar FG, Puryear J, Popp RL. Abnormal right heart filling after cardiac surgery: time course and mechanisms. *Br Heart J*. (1991) 66:435–42. doi: 10.1136/hrt.66.6.435
19. Maffessanti F, Gripari P, Tamborini G, Muratori M, Fusini L, Alamanni F, et al. Evaluation of right ventricular systolic function after mitral valve repair: a two-dimensional Doppler, speckle-tracking, and three-dimensional echocardiographic study. *J Am Soc Echocardiogr*. (2012) 25:701–8. doi: 10.1016/j.echo.2012.03.017
20. Ledwoch J, Fellner C, Hoppmann P, Thalmann R, Kossmann H, Dommasch M, et al. Impact of transcatheter mitral valve repair using MitraClip on right ventricular remodeling. *Int J Cardiovasc Imaging*. (2020) 36:811–9. doi: 10.1007/s10554-020-01771-2
21. Godino C, Salerno A, Cera M, Agricola E, Fragasso G, Rosa I, et al. Impact and evolution of right ventricular dysfunction after successful MitraClip implantation in patients with functional mitral regurgitation. *Int J Cardiol Heart Vasc*. (2016) 11:90–8. doi: 10.1016/j.ijcha.2016.05.017
22. van Riel AC, Boerlage-van Dijk K, de Bruin-Bon RH, Araki M, Koch KT, Vis MM, et al. Percutaneous mitral valve repair preserves right ventricular function. *J Am Soc Echocardiogr*. (2014) 27:1098–106. doi: 10.1016/j.echo.2014.06.001
23. Lurz P, Serpytis R, Blazek S, Seeburger J, Mangner N, Noack T, et al. Assessment of acute changes in ventricular volumes, function, and strain after interventional edge-to-edge repair of mitral regurgitation using cardiac magnetic resonance imaging. *Eur Heart J Cardiovasc Imaging*. (2015) 16:1399–404. doi: 10.1093/ehjci/jev115
24. Cecelja M, Chowienczyk P. Role of arterial stiffness in cardiovascular disease. *JRSM Cardiovasc Dis*. (2012) 1:11. doi: 10.1258/cvd.2012.012016
25. Haddad F, Hunt SA, Rosenthal DN, Murphy DJ. Right ventricular function in cardiovascular disease, part I: anatomy, physiology, aging, and functional assessment of the right ventricle. *Circulation*. (2008) 117:1436–48. doi: 10.1161/CIRCULATIONAHA.107.653576
26. Rossi A, Bonapace S, Cicoira M, Conte L, Anselmi A, Vassanelli C. Aortic stiffness: an old concept for new insights into the pathophysiology of functional mitral regurgitation. *Heart Vessels*. (2013) 28:606–12. doi: 10.1007/s00380-012-0295-9
27. Neuss M, Schau T, Schoepp M, Seifert M, Holschermann F, Meyhofer J, et al. Patient selection criteria and midterm clinical outcome for MitraClip therapy in patients with severe mitral regurgitation and severe congestive heart failure. *Eur J Heart Fail*. (2013) 15:786–95. doi: 10.1093/eurjhf/hfs214
28. Kaneko H, Neuss M, Weissenborn J, Butter C. Role of right ventricular dysfunction and diabetes mellitus in N-terminal pro-B-type natriuretic peptide response of patients with severe mitral regurgitation and heart failure after MitraClip. *Int Heart J*. (2017) 58:225–31. doi: 10.1536/ihj.16-255
29. Park JB, Lee SP, Lee JH, Yoon YE, Park EA, Kim HK, et al. Quantification of right ventricular volume and function using single-beat three-dimensional echocardiography: a validation study with cardiac magnetic resonance. *J Am Soc Echocardiogr*. (2016) 29:392–401. doi: 10.1016/j.echo.2016.01.010
30. Feldman T, Foster E, Glower DD, Kar S, Rinaldi MJ, Fail PS, et al. Percutaneous repair or surgery for mitral regurgitation. *N Engl J Med*. (2011) 364:1395–406. doi: 10.1056/NEJMoa1009355
31. Foster E, Wasserman HS, Gray W, Homma S, di Tullio MR, Rodriguez L, et al. Quantitative assessment of severity of mitral regurgitation by serial echocardiography in a multicenter clinical trial of percutaneous mitral valve repair. *Am J Cardiol*. (2007) 100:1577–83. doi: 10.1016/j.amjcard.2007.06.066
32. Vahanian A, Alfieri O. Guidelines on valvular heart disease in clinical practice. EuroIntervention : journal of EuroPCR in collaboration with the Working Group on Interventional Cardiology of the European Society of Cardiology. (2013) 9(Suppl):S11–3. doi: 10.4244/EIJV9SSA3
33. Cimino S, Maestrini V, Cantisani D, Petronilli V, Filomena D, Mancone M, et al. 2D/3D echocardiographic determinants of left ventricular reverse remodelling after MitraClip implantation. *Eur Heart J Cardiovasc Imaging*. (2019) 20:558–64. doi: 10.1093/ehjci/jey157
34. Vitarelli A, Mangieri E, Capotosto L, Tanzilli G, D'Angeli I, Viceconte N, et al. Assessment of biventricular function by three-dimensional speckle-tracking echocardiography in secondary mitral regurgitation after repair with the MitraClip System. *J Am Soc Echocardiogr*. (2015) 28:1070–82. doi: 10.1016/j.echo.2015.04.005
35. Mohammed SF, Hussain I, AbouEzzeddine OF, Takahama H, Kwon SH, Forfia P, et al. Right ventricular function in heart failure with preserved ejection fraction: a community-based study. *Circulation*. (2014) 130:2310–20. doi: 10.1161/CIRCULATIONAHA.113.008461
36. Meyer P, Filippatos GS, Ahmed MI, Iskandrian AE, Bittner V, Perry GJ, et al. Effects of right ventricular ejection fraction on outcomes in chronic systolic heart failure. *Circulation*. (2010) 121:252–8. doi: 10.1161/CIRCULATIONAHA.109.887570
37. Nagata Y, Wu VC, Kado Y, Otani K, Lin FC, Otsuji Y, et al. Prognostic value of right ventricular ejection fraction assessed by transthoracic 3d echocardiography. *Circ Cardiovasc Imaging*. (2017) 10:e005384. doi: 10.1161/CIRCIMAGING.116.005384
38. Purmah Y, Lei LY, Dykstra S, Mikami Y, Cornhill A, Satriano A, et al. Right ventricular ejection fraction for the prediction of major adverse cardiovascular and heart failure-related events: a cardiac mri based study of 7131 patients with known or suspected cardiovascular disease. *Circ Cardiovasc Imaging*. (2021) 14:e011337. doi: 10.1161/CIRCIMAGING.120.011337
39. Naksuk N, Tan N, Padmanabhan D, Kancharla K, Makkar N, Yogeswaran V, et al. Right ventricular dysfunction and long-term risk of sudden cardiac death in patients with and without severe left ventricular dysfunction. *Circ Arrhythm Electrophysiol*. (2018) 11:e006091. doi: 10.1161/CIRCEP.117.006091
40. Chang WT, Wu NC, Shih JY, Hsu CH, Chen ZC, Cheng BC. Right ventricular reserve post mitral valve repair is associated with heart failure hospitalization. *Pulm Circ*. (2020) 10:2045894020943858. doi: 10.1177/2045894020943858
41. Ozturk C, Friederich M, Werner N, Nickenig G, Hammerstingl C, Schueler R. Single-center five-year outcomes after interventional edge-to-edge repair of the mitral valve. *Cardiol J*. (2021) 28:215–22. doi: 10.5603/CJ.a2019.0071
42. Giannini C, Petronio AS, de Carlo M, Guarracino F, Conte L, Fiorelli F, et al. Integrated reverse left and right ventricular remodelling after MitraClip implantation in functional mitral regurgitation: an echocardiographic study. *Eur Heart J Cardiovasc Imaging*. (2014) 15:95–103. doi: 10.1093/ehjci/jet141
43. Hunlich M, Lubos E, Beuthner BE, Puls M, Bleckmann A, Beissbarth T, et al. Acute and long-term hemodynamic effects of MitraClip implantation on a preexisting secondary right heart failure. *Biomed Res Int*. (2018) 2018:6817832. doi: 10.1155/2018/6817832
44. Gronlykke L, Korshin A, Holmgaard F, Kjoller SM, Gustafsson F, Nilsson JC, et al. Severe loss of right ventricular longitudinal contraction occurs after cardiopulmonary bypass in patients with preserved right ventricular output. *Int J Cardiovasc Imaging*. (2019) 35:1661–70. doi: 10.1007/s10554-019-01616-7
45. Rong LQ, Yum B, Abouzeid C, Palumbo MC, Brouwer LR, Devereux RB, et al. Echocardiographic predictors of intraoperative right ventricular dysfunction: a 2D and speckle tracking echocardiography study. *Cardiovasc Ultrasound*. (2019) 17:11. doi: 10.1186/s12947-019-0161-3
46. Sauter RJ, Patzelt J, Mezger M, Nording H, Reil JC, Saad M, et al. Conventional echocardiographic parameters or three-dimensional echocardiography to evaluate right ventricular function in percutaneous edge-to-edge mitral valve repair (PMVR). *Int J Cardiol Heart Vasc*. (2019) 24:100413. doi: 10.1016/j.ijcha.2019.100413


**Conflict of Interest:** JN received travel support for congresses from Orion Pharma, not related to this manuscript. J-TS received travel support for congresses from Abiomed. No conflict of Interest regarding this submission. JB received honoraria for lectures/consulting from Novartis, Vifor, Bayer, Servier, Abiomed, Pfizer, Boehringer Ingelheim, AstraZeneca, Cardior, Daichii Sankyo, CVRx, BMS, MSD, Amgen, Corvia, not related to this article, and research support for the department from Zoll, CVRx, Vifor, Abiomed, not related to this article. JW is a consultant for Biosensor/NVT and Medtronic and reports personal fees from Edwards, Daiichi Sankyo, Biotronik, Volcano/Philips all outside the submitted

work. DB received honoraria or travel support from Abbott, Bayer, Biotronik, Boehringer Ingelheim, Daiichi Sankyo, Novartis, and Orion Pharma, and research support from CVRx, Novartis, and Zoll, all not related to this manuscript.

The remaining authors declare that the research was conducted in the absence of any commercial or financial relationships that could be construed as a potential conflict of interest.

**Publisher's Note:** All claims expressed in this article are solely those of the authors and do not necessarily represent those of their affiliated organizations, or those of the publisher, the editors and the reviewers. Any product that may be evaluated in this article, or claim that may be made by its manufacturer, is not guaranteed or endorsed by the publisher.

frontiers in Cardiovascular Medicine

REVIEW
published: 24 March 2022
doi: 10.3389/fcvm.2022.849540

# Cardiac Computed Tomography: Application in Valvular Heart Disease

*Kush P. Patel[1,2], Sebastian Vandermolen[1,3], Anna S. Herrey[1,2], Emma Cheasty[1], Leon Menezes[1,4,5], James C. Moon[1,2], Francesca Pugliese[1,3] and Thomas A. Treibel[1,2,4]**

*[1] Barts Heart Centre, St Bartholomew's Hospital, London, United Kingdom, [2] Faculty of Population Health Sciences, Institute of Cardiovascular Sciences, University College London, London, United Kingdom, [3] William Harvey Research Institute, Queen Mary University of London, London, United Kingdom, [4] Institute of Nuclear Medicine, University College London, London, United Kingdom, [5] NIHR Biomedical Research Centre, University College London Hospitals NHS Foundation Trust, London, United Kingdom*

The incidence and prevalence of valvular heart disease (VHD) is increasing and has been described as the next cardiac epidemic. Advances in imaging and therapeutics have revolutionized how we assess and treat patients with VHD. Although echocardiography continues to be the first-line imaging modality to assess the severity and the effects of VHD, advances in cardiac computed tomography (CT) now provide novel insights into VHD. Transcatheter valvular interventions rely heavily on CT guidance for procedural planning, predicting and detecting complications, and monitoring prosthesis. This review focuses on the current role and future prospects of CT in the assessment of aortic and mitral valves for transcatheter interventions, prosthetic valve complications such as thrombosis and endocarditis, and assessment of the myocardium.

**Keywords: valvular heart disease, aortic stenosis, TAVR, TMVR, cardiac computed tomography**

OPEN ACCESS

***Edited by:***
*Ronak Rajani, Guy's and St Thomas' NHS Foundation Trust, United Kingdom*

***Reviewed by:***
*Felice Gragnano, University of Campania Luigi Vanvitelli, Italy*
*Francesco Pollari, Nürnberg Hospital, Germany*

***Correspondence:**
*Thomas A. Treibel*
*Thomas.Treibel.12@ucl.ac.uk*

***Specialty section:***
*This article was submitted to Heart Valve Disease, a section of the journal Frontiers in Cardiovascular Medicine*

***Received:*** *06 January 2022*
***Accepted:*** *22 February 2022*
***Published:*** *24 March 2022*

***Citation:***
*Patel KP, Vandermolen S, Herrey AS, Cheasty E, Menezes L, Moon JC, Pugliese F and Treibel TA (2022) Cardiac Computed Tomography: Application in Valvular Heart Disease. Front. Cardiovasc. Med. 9:849540. doi: 10.3389/fcvm.2022.849540*

## INTRODUCTION

Interest in valvular heart disease (VHD) has been invigorated with the advancement in new imaging modalities and pathological insights, and most importantly the advent of transcatheter valve interventions. Transcatheter aortic valve replacement (TAVR) has now overtaken surgical aortic valve replacement (SAVR) in volume in Germany (and the United States) (1) and is driving innovation in transcatheter interventions on other valves (2). Cardiac computed tomography (CT) has become an essential tool for the heart valve team to supplement the assessment by echocardiography, and decision making for suitability and mode of intervention. Technical developments in CT technology have made this possible by providing high temporal, spatial and contrast resolution for imaging one of the most challenging imaging targets of the body. The use of CT is now recommended in guidelines for the pre-procedural work-up for TAVR (3) and is an important tool for the diagnosis of valvular thrombosis (4) and infective endocarditis (5). This has led to its widespread use in the assessment and management of patients with VHD providing additional novel insights into remodeling, pathophysiology, and prognosis. This review article explores its current role, limitations and future prospects in the assessment and

**Abbreviations:** AS, aortic stenosis; AVA, aortic valve area; AVCS, aortic valve calcium score; CAD, coronary artery disease; CT, cardiac computed tomography; CTCA, computed tomography coronary angiogram; LVOT, left ventricular outflow tract; MPR, multi-planar reconstruction; MR, mitral regurgitation; SAVR, surgical aortic valve replacement; TAVR, transcatheter aortic valve replacement; TMVP, transcatheter mitral valve prosthesis; TMVR, transcatheter mitral valve replacement; VHD, valvular heart disease.

management of patients with VHD. It does not cover the technical aspects of CT data acquisition and reconstruction, which can be found elsewhere (3, 4, 6).

## NATIVE AORTIC VALVE ASSESSMENT

Aortic stenosis (AS) is the commonest type of VHD in the developed world (7). Treatment using either SAVR or TAVR is considered for severe AS (8). Determining severity is largely done using echocardiography, with aortic valve area (AVA) being the most commonly used marker of severity. It is calculated using the continuity equation with the incorrect assumption of a circular left ventricular outflow tract (LVOT) (9). Although using a CT derived LVOT area for the continuity equation is more accurate than a 2D echo-based LVOT area, this has not translated into better diagnostic performance (correlation with transvalvular gradients) or mortality prediction (10). However, discordant echocardiographic parameters (discordant AVA and gradient) occur in up to a third of patients, making the quantification of AS severity difficult (11, 12). CT has an important role in determining severity among these patients, especially those with paradoxical low-flow, low-gradient AS (8, 13). Calcification is the cornerstone underlying the pathophysiology of AS in most patients. A sequence of pathological changes involving lipid infiltration of the valve, inflammation, fibrosis and mineralization, leads to AS (14). Using a non-contrast CT, calcification is identified as areas of increased radio-opacity. The commonly used Agatston score method defines calcification where the density is greater than 130 Hounsfield units (HU) (15). CT derived aortic valve calcium score (AVCS) demonstrates high inter- and intra-observer reproducibility (16), correlates well with the severity of AS determined by echocardiography (17, 18) and calcium weight on explanted valves (16), thus making it a very useful marker of AS severity. AVCS is also prognostically important (13, 19) and determines progression of AS, with higher AVCS at baseline correlating with faster progression of AS (20). Compared to men, women have less calcification, but more fibrosis for the same severity of stenosis (21), leading to different recommended thresholds for the definition of severe AS; 1,200 Agatston units (AU) in women and ∼2,000AU in men (22). However, these thresholds may not be applicable in patients with bicuspid AS or rheumatic valve disease due to differences in pathophysiological mechanisms (12).

An alternative method utilizes planimetry of the orifice during systole. This anatomical, rather than functional measurement, correlates poorly with other measurements of AVA and with transvalvular gradients (10). Consequently this is seldom used clinically.

Outcomes in patients with moderate AS are known to be poor, especially if systolic function is compromised (23, 24). An ongoing trial is evaluating whether TAVR has a role in such patients (25). CT may play a role in the future for identifying patients for intervention with less than severe valvular disease as calcification has been shown to correlate with the rate of progression and mortality in patients with less than severe AS (26).

## TAVR PLANNING

The utility of TAVR has seen a dramatic increase over the last decade, with CT being routinely used to facilitate its use, improve efficacy and reduce complications.

### Access Planning

Cardiac computed tomography angiography of the aorta and peripheral vasculature provides a quick and complete dataset for TAVR planning (**Figure 1**). In addition to illustrating the dimensions of the aortic annulus and root, and degree and distribution of aortic valve calcification, CT can demonstrate the degree of iliac vessel wall calcification, tortuosity, ilio-femoral stenosis, presence of aorto-iliac aneurysms, foci of dissection, large penetrating ulcers, and potentially thrombi, as well as previous vascular procedures with grafting/stent implantation—useful considerations for procedural planning (27–29). When a transfemoral access site is unfavorable, CT can provide valuable information regarding alternative sites, such as subclavian, carotid, apical, trans-aortic, and trans-caval (crossing from the inferior vena cava into the abdominal aorta and using a closure device to plug the aortic wall after implantation of the valve) (30). Trans-caval access is increasingly being used and greatly benefits from pre-procedural planning using CT. Using electrocautery, a puncture is made from the inferior vena cava (IVC) to the adjacent descending aorta between the aortic bifurcation and renal arteries. A calcium-free window on the aorta adjacent to the IVC needs to be located using CT and defined by the vertebral level. Additional measurements such as the distance between aorta and IVC, lumen diameters and identification of bail-out access (in case endograft therapy is required) are useful and can be performed using CT (31, 32).

### Implantation Planning

First, using multiplanar reconstructions (MPR), CT can be used to determine the optimum fluoroscopic projection for valve implantation-orthogonal to the aortic valve (29). This has been shown to reduce additional aortograms, procedural time and contrast use (33). Second, CT provides an accurate guide for sizing an aortic bioprosthesis based on aortic valve (AV) annular dimensions, with a resulting reduction in post-TAVR aortic regurgitation (34, 35). Annulus diameters, area and perimeter are typically used to derive the most appropriate transcatheter valve diameter, applying recommendations provided in manufacturers' charts. Third, additional measurements are typically taken at levels of the sinus of Valsalva, sino-tubular junction, ascending aorta and the heights of the coronary ostia from the AV annulus- guiding the procedure and enabling the prediction of complications (**Figure 2**). Low coronary ostial heights and narrow sinuses of Valsalva are associated with a higher risk of coronary obstruction and difficulty in coronary artery engagement for angiography or intervention

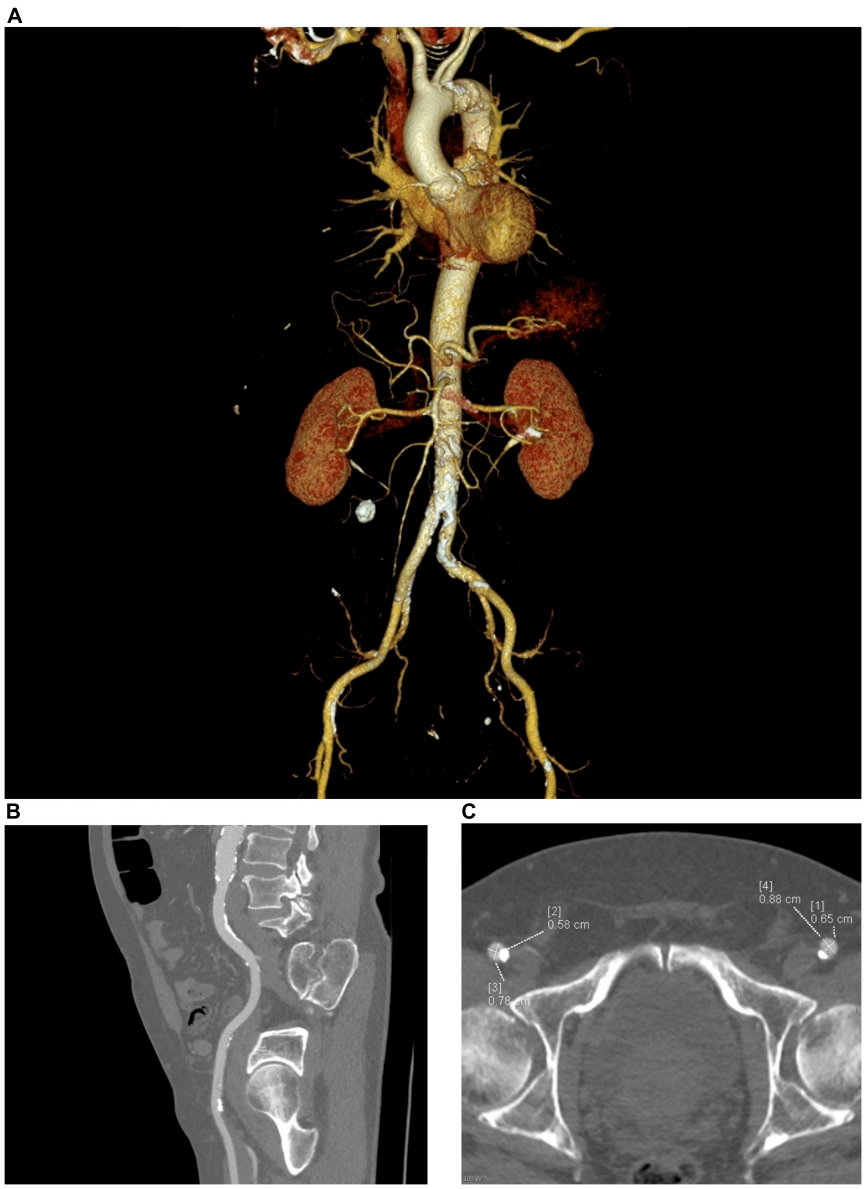


**FIGURE 1 |** Peripheral access planning for TAVR, requires assessment of the size, tortuosity, calcification (both severity and distribution) and any prosthetic material such as stents or pathologies such as aneurysms. **(A)** Multiplanar reconstruction of the vascular tree, **(B)** Sagittal view, **(C)** Axial view.

(36, 37). Correct valve sizing to prevent oversizing is essential to prevent annular rupture, which often results in fatal outcomes (38).

## Predicting Complications

Aortic valve calcification is important to ensure the anchorage of the bioprosthesis and prevent valve migration (aortic root dilatation and the lack of calcification commonly preclude the use of TAVR for aortic regurgitation) (39). However, both an increased burden and bulky eccentric calcification can result in inadequate valve apposition, leading to paravalvular regurgitation, which is poorly tolerated post-TAVR and associated with poor outcomes (40–42).

Conduction abnormalities and permanent pacemaker implantation rates remain high (43). Pacing in TAVR patients is associated with less recovery of left ventricular ejection fraction and a higher rate of heart failure hospitalization (44). Therefore attempts to avoid conduction abnormalities and subsequently pacemaker implantation are important. Device landing zone calcification can predict post-TAVR pacemaker requirement, especially if calcification is located around the LVOT, the basal septum (45, 46) or the mitral annulus (47). Conduction abnormalities can also arise due to a short membranous septum. The bundle of His runs close to the membranous septum and is susceptible to compression by the implanted bioprosthesis. Membranous septal depth is measured from the AV annulus

to the start of the muscular interventricular septum. Depths of <7.8 mm are predictive of high degree atrioventricular block (46).

Calcification in the LVOT, especially below the non-coronary cusp, is associated with annular rupture (area under the ROC curve 0.81), a complication that often leads to death (48). Other factors associated with annular rupture include device oversizing and post-dilatation (38).

The height of the coronary ostia from the aortic annulus is an important parameter to measure as short heights can result in coronary obstruction from the newly implanted prosthesis (29). Coronary ostial heights are considered low if <12 mm. The sinuses of Valsalva that house the coronary ostia are also important when considering coronary occlusion. A mean diameter <30 mm is associated with increased risk as the space between the bioprosthetic valve and coronary ostia is reduced (3, 37). However, these cut-offs have low specificity and are not prohibitive for a TAVR. Additionally, CT allows evaluation of the extent and severity of coronary artery disease, which dictates the need for further assessment and management (3, 49).

## NATIVE MITRAL VALVE ASSESSMENT

The mitral valve, annulus and associated apparatus form a complex 3D structure. Although echocardiography remains the primary imaging modality for mitral assessment, CT can highlight valve pathology, provide clues to its etiology and importantly, assist in planning for valve repair/replacement.

### Mitral Regurgitation

Mitral valve prolapse is a common cause of primary MR, and CT can reliably detect this (50). In these cases, two- and three-chamber views can be used to identify leaflet thickening (>5 mm) and a flail leaflet, both seen in the context of mitral prolapse. Using retrospective ECG gating, multiple phases of the cardiac cycle can be reconstructed, facilitating moving cine images, which is important in recognizing prolapse.

In patients with secondary MR, evaluation of the leaflets, ventricle and coronary arteries will enable both the diagnosis and etiology of the MR. In a study of 151 patients with heart failure and functional mitral regurgitation (FMR), CT was able to identify that those with moderate to severe FMR had significantly increased posterior leaflet angles and mitral valve tenting heights at central and postero-medial levels. These were described as the strongest determinants of FMR severity (51). CT can provide accurate left ventricular dimensions enabling an understanding of left ventricular dilatation (52). Other cardiomyopathies can also result in MR. Systolic anterior motion of the mitral valve can lead to MR and has been described with hypertrophic cardiomyopathy and cardiac amyloidosis.

Cardiac computed tomography may also play a role in quantifying MR. When measuring regurgitant volumes in 49 patients with isolated MR, the severity of regurgitation correlated well with echocardiography findings (53). This can be done by calculating total stroke volume of the left and right ventricles (end-diastolic volume minus end-systolic volume), with the regurgitant volume being the difference between the stroke volumes of the left and right ventricle. However, this is rarely used clinically, but could have a role in patients with poor echo windows and if cardiac magnetic resonance imaging is contraindicated.

### Mitral Stenosis

Echocardiography remains the gold standard for the diagnosis and grading the severity of mitral stenosis (MS). However, CT can confirm the presence of related features such as left atrial enlargement, as well as certain appearances, which point to specific causes of mitral stenosis, such as thickening of the mitral valve leaflets with commissural fusion and calcification, commonly seen in rheumatic mitral stenosis (so-called fish mouth appearance) (54).

## MITRAL INTERVENTION PLANNING

Transcatheter mitral valve interventions include technology for both repair and replacement, each requiring different approaches and techniques. An in-depth review of the various technologies available can be found here (55). Once a decision to intervene has been made, CT plays a vital role in procedural planning.

### Annular Dimensions

Sizing the annulus is important for selecting a transcatheter mitral valve prosthesis. The mitral annulus is saddle-shaped. However, for the purposes of certain transcatheter prostheses, a D-shaped annulus can be assumed; the medial and lateral fibrous trigones are connected via a virtual straight line, and the diameter and area then calculated by "tracing" its perimeter border (56). 3D software packages are then able to recreate the annulus, allowing further measurements to be made. Specifically, the landing zone is an important consideration when choosing a transcatheter MV prosthesis; each prosthesis has a different anchoring mechanism and requires certain anatomical characteristics. For this reason, leaflet length, chordal anatomy, the presence of a myocardial shelf and left ventricular cavity dimensions need to be assessed on CT (57).

### Leaflets

The mitral valve has an anterior and a posterior leaflet, both of which have three scallops. These are identifiable via CT, and seen in both reconstructed short-axis and long-axis views. Although echocardiography remains the primary imaging modality to evaluate the mitral leaflets, numerous geometric measurements can also be estimated from CT, including leaflet length, area, tenting height, and coaptation angle. These measurements are important for understanding the mechanism of MR and guiding intervention. Indeed, comparisons of three-dimensional (3D) transesophageal echocardiography and cardiac CT have shown that both imaging modalities provide good detailing of mitral leaflet morphology (58). In addition, calcification and clefts of the leaflets are important to note as these can preclude adequate transcatheter edge to edge repair (TEER) (59).

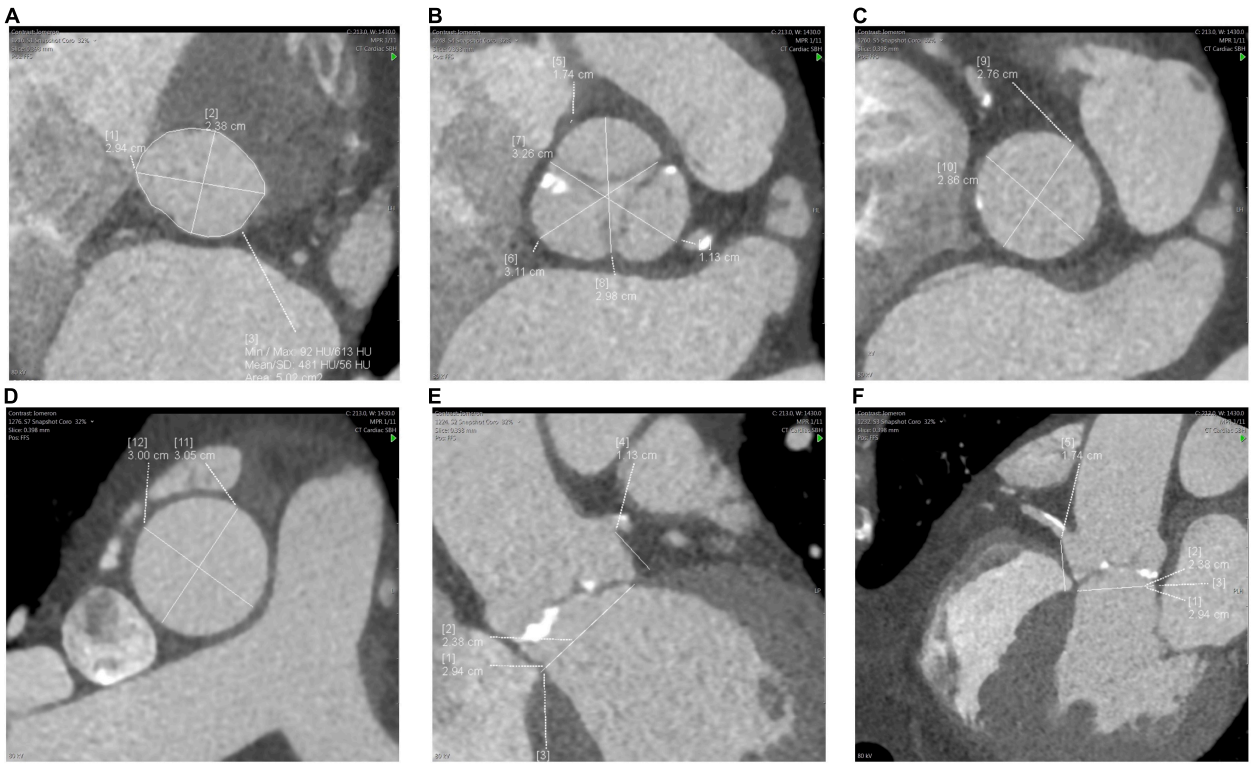


**FIGURE 2 |** Measurements of the aortic root and ascending aorta. **(A)** aortic valve (AV) annulus, **(B)** sinus of Valsalva, **(C)** sino-tubular junction, **(D)** ascending aorta, **(E)** left coronary ostial height from AV annulus, **(F)** right coronary ostial height.

## Left Ventricular Outflow Tract Assessment

Left ventricular outflow tract (LVOT) obstruction is a known complication of TMVR carrying a significant risk of mortality. A new LVOT (termed the "neo-LVOT") is formed from the interventricular septum anteriorly and the native anterior mitral valve leaflet. Pre-procedural CT planning simulating a neo-LVOT can help predict the risk of LVOT obstruction (60). Extrapolation from hypertrophic cardiomyopathy studies initially identified a LVOT area of 2 $cm^2$ as a safe cut-off for TMVR (61). Further studies specific to TMVR suggested a neo-LVOT $< 1.7$ $cm^2$ at end-systole as high risk (60), but more recent evidence has suggested that even smaller areas are safe (62).

Several factors predict LVOT obstruction; device related, remodeling related and native anatomical factors. Of these, the aorto-mitral angulation is important and can be calculated using CT. Defined as the angle between the mitral annular trajectory and LVOT long axis; the smaller the angle, the lower the risk of LVOT obstruction. Coupled with this, the size of the mitral annulus, annulus-to-interventricular septal distance and LVOT and septal shape should also be taken into consideration (57, 60).

## Mitral Annular Calcification

Mitral annular calcification (MAC) has a reported incidence of between 10 and 42% (63, 64) and in patients with co-existent aortic stenosis is found in 50% of patients (47). MAC can be easily identified and its distribution mapped out using CT. MAC increases the technical complexity of surgical intervention, specifically increasing the risk of AV groove disruption, paravalvular leak and increasing pump and clamp times (65, 66). It also increases the risk for percutaneous intervention; performing TMVR in patients with MAC carries substantially more risk of LVOT obstruction than performing it in valve-in-valve or valve-in-ring (60). MAC can make it challenging to recognize the boundary between annulus and blood pool and therefore accurately measure annular dimensions.

Mitral annular calcification itself can serve as a bed on which the new valve can anchor. In procedures involving the implantation of a TAVR prosthesis in the mitral valve position, non-circumferential or thin MAC can result in poor device sealing (67). MAC can also make it difficult to determine the correct position for valve deployment, with 17% of valve-in-MAC cases requiring a second valve deployed in an early study. The population in this study was at high surgical risk (STS score 14.4 $\pm$ 9.5%) and had a 30-day all-cause mortality of 30% (68). In order to plan a TMVR, 3D reconstructions can be created and valve implantation simulated using dedicated off-line software (**Figure 3**).

## Access Planning

The trans-septal approach is increasingly being used to access the mitral valve. With CT, operators are able to determine the

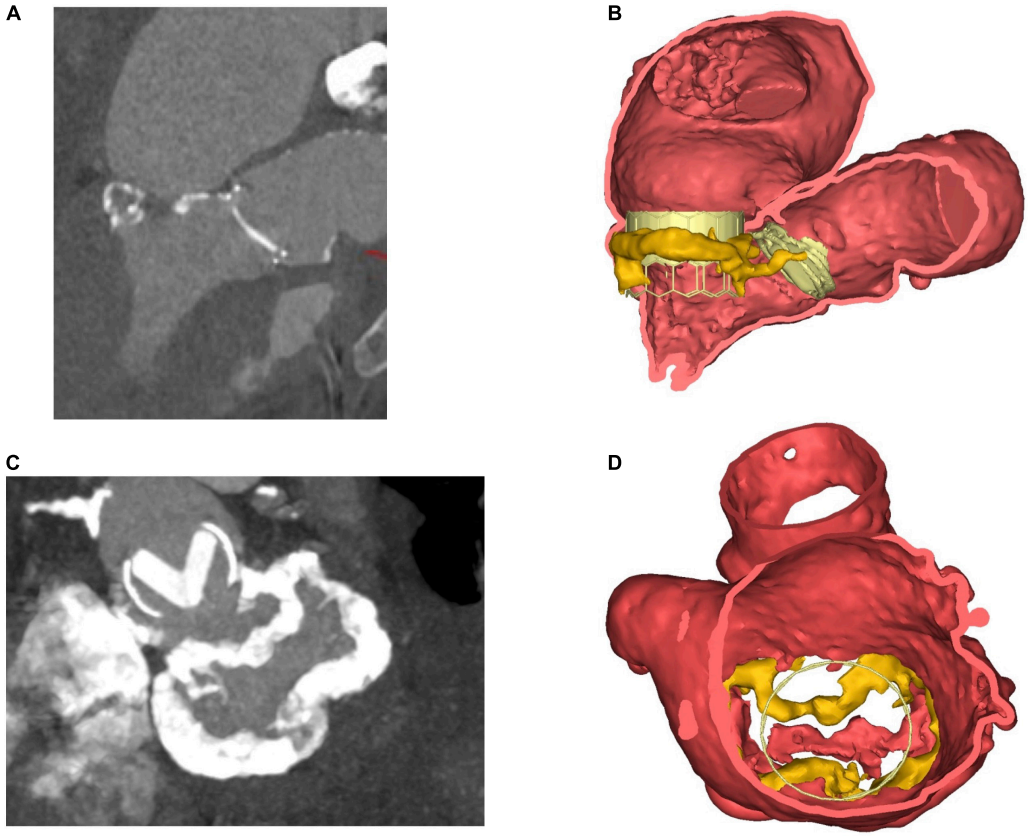


**FIGURE 3 |** Steps in planning for mitral intervention in a patient with a heavily calcified mitral annulus. **(A)** 2D ECG-gated CT scan. Pre-existing TAVR valve in aortic position, with dense calcification of the mitral annulus. **(B)** Coronal view. 3D volume-rendered image of pre-existing TAVR valve *in situ* in aortic position. Cylindrical valve simulated in mitral position, thereby allowing for anatomical and geometrical calculations to be made prior to implantation. **(C)** 2D CT- En-face view of calcification surrounding mitral annulus. Also visible is the TAVR valve in the aortic position. **(D)** 3D volume-rendered en-face image of mitral annulus down through the left atrium. MAC highlighted in yellow. Panels **(B,D)** created courtesy of post-acquisition processing with Mimics Enlight TMVR planner, Beta version, Materialise NV Inc.

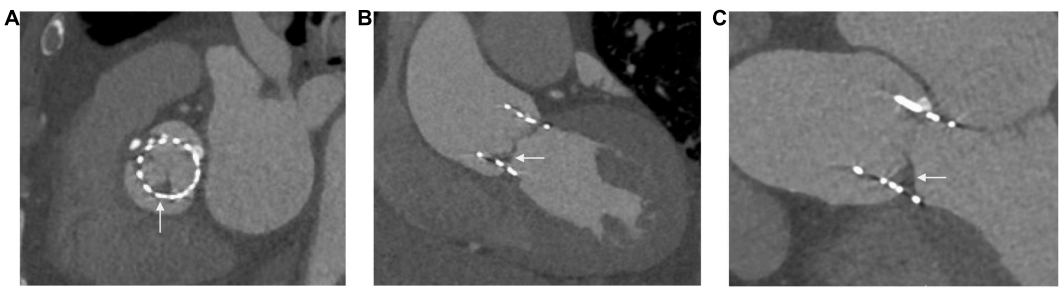


**FIGURE 4 |** Hypo-attenuated leaflet thickening seen in three views of the same patient **(A)** at the level of the sinus of Valsalva, **(B)** left ventricular outflow tract view, **(C)** three chamber view.

precise anatomy of the left atrium and plan the site of trans-septal puncture in order to minimize the risk of complications, including aortic puncture or myocardial perforation (69). Anomalies within the left atrium that can be seen via CT include aneurysms of the inter-atrial septum, patent foramen ovale and atrial septal defects, all requiring a tailored approach for the trans-septal puncture (70).

With respect to trans-apical approach, access requires an intimate knowledge of the position of the apex and its relation to the chest wall. Valve deployment using this approach requires a perpendicular deployment at the level of the mitral annulus. Once the apex is located, CT can identify the position of the papillary muscles, coronary arteries and chords, so as to plan the approach and prevent complications (61, 71).

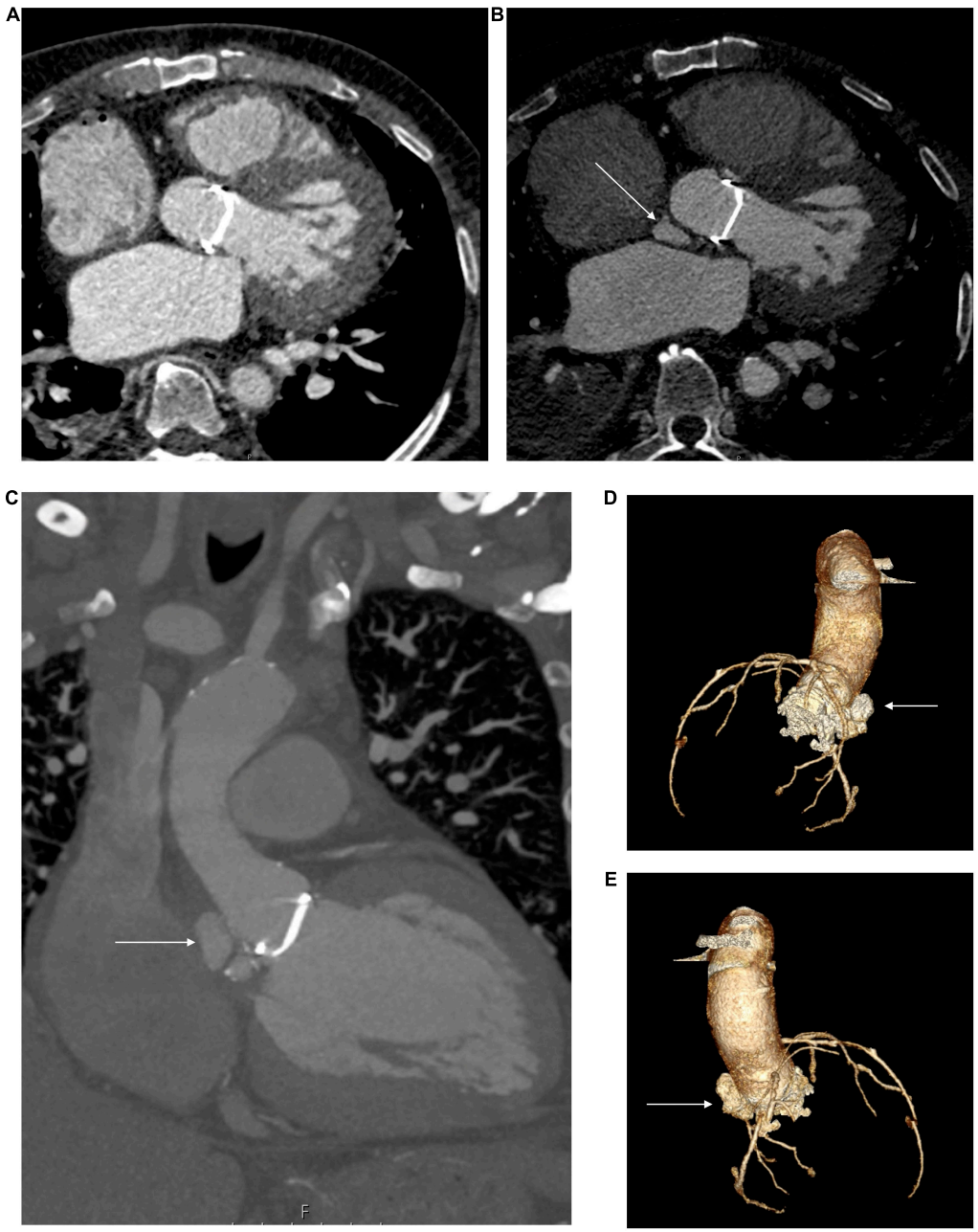


**FIGURE 5 |** Aortic root abscess seen in a patient with a previous metallic surgical aortic valve implanted in 2010. An axial slice from 2013 without an abscess **(A)**, and a similar slice from 2017 showing a root abscess indicated by a white arrow **(B)**. A coronal view **(C)** and 3D reconstructions **(D,E)** illustrate the abscess indicated by the white arrow.

As with TAVR planning, CT for TMVR planning can guide vascular access by defining the anatomy of peripheral vessels, including vessel dimension, tortuosity, location and extent of calcification and any prosthetic material such as stents.

## Pre-surgical Planning

Similar to percutaneous mitral valve interventions, minimal-invasive mitral valve surgery (MIMVS) is being performed with increasing frequency. MIMVS commonly refers to procedures involving mini-thoracotomy, port access and robotic-assisted techniques. Certain differences exist between MIMVS and standard open-heart surgery, including access (various locations and lengths of incisions), vision (direct, video-assisted or endoscopic), and cardio-pulmonary bypass strategies (antegrade vs retrograde), as well as between individual centers and operators.

Cardiac computed tomographic angiography and post-processing 3D reconstructions allow assessment for suitability [suitability for retrograde cannulation, presence

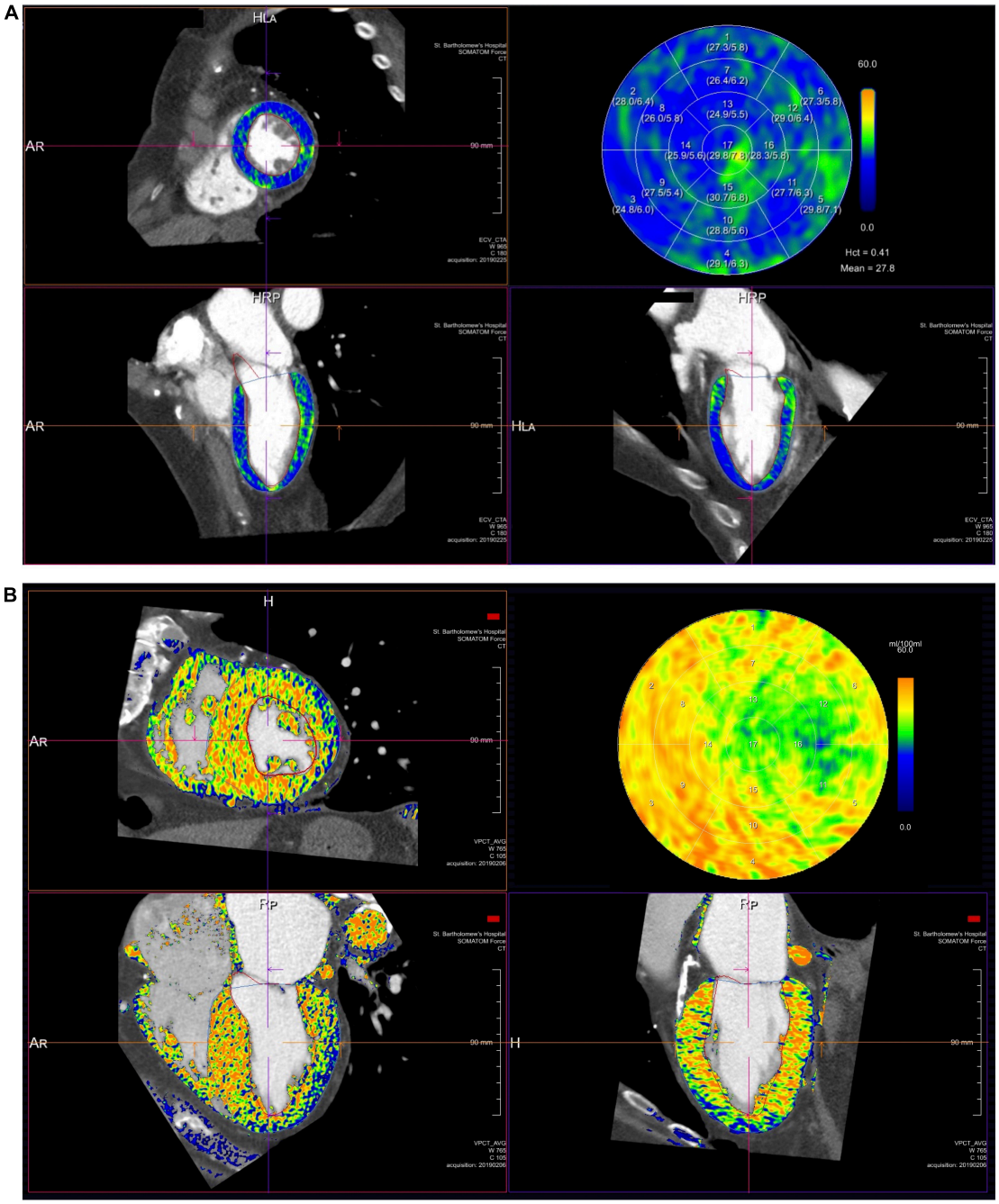


**FIGURE 6 |** Extracellular volume quantification in two patients: **(A)** severe AS and **(B)** severe AS and cardiac transthyretin amyloidosis. Each panel illustrates a short-axis, 4 and 2 chamber views and a bull's eye plot. High extracellular volume seen in panel **(B)** is identified by the yellow/orange coloration compared to lower extracellular volume in panel **(A)** identified by the green/blue areas.

of a heavily-calcified abdominal aorta, vessel tortuosity and pericardial calcification (72)] and access planning for MIMVS (location of mini-thoracotomy to access the left atrium). CT also allows for evaluation of the aortic dimensions. In MIMVS, one popular technique involves the use of an endo-aortic balloon; its safe use and efficacy dependent on aortic dimensions (73). The CT scan protocol can also include a CT coronary angiogram, which allows for accurate assessment of co-existent coronary disease. This is particularly sensitive in MIMVS patients, many of whom are young with few coronary risk factors and thus low risk profiles for coronary disease (74).

## CT FOR GUIDING TRANSCATHETER TRICUSPID VALVE INTERVENTION

Cardiac computed tomography also plays a role in the evaluation of tricuspid valve pathology and the planning of related interventions. As with all right-sided lesions, comprehensive assessment via transthoracic echocardiography can be limited by suboptimal cardiac windows, especially when trying to accurately evaluate the three leaflets of the tricuspid valve (anterior, posterior, and septal) and associated structures. Like MR, tricuspid regurgitation (TR) can be primary, but is more often secondary, related to distortion of the right atrial or ventricular anatomy, and consequent annular dilatation.

Cardiac computed tomography facilitates accurate measurement of dimensions for the tricuspid annulus, right ventricular size and distance from the annulus to right ventricular apex, and thus allows deductions to be made as to the likely etiology of regurgitation.

As annular dilatation is often a key pathological process in TR, the majority of devices focus around annuloplasty (including Trialign, Tricinch, and Cardioband), edge-to-edge repair (Triclip and Forma) or the placement of valves in the vena cava to reduce the damage of the tricuspid regurgitant jet on hepatic and renal vasculature (TricValve).

For procedure planning, determining access to the right heart is key. Vascular access can be clearly defined by CT, including vessel dimensions and tortuosity. For the edge-to-edge repair systems, transfemoral venous access is routinely used, whilst for annuloplasty devices a trans-jugular approach is preferred. Accurate assessment of subclavian and axillary veins can also be done, aiding sheath and device delivery (75).

Annuloplasty-based treatments require delineation of landing zones, be that the tricuspid valve annulus, the inferior vena cava or the commissures. The relation of the landing zone with adjacent structures is also important. The right coronary artery runs along the posterior aspect of the tricuspid annulus along the heart's epicardial surface. Its compression needs to be avoided when securing devices to the tricuspid annulus (76). Calcification along the annulus can also impair percutaneous valve deployment, which can be detected pre-procedurally via CT (77).

## ASSESSMENT OF BIOPROSTHETIC VALVES

### Structural Valve Degeneration

Structural valve degeneration (SVD) is defined as acquired abnormalities affecting the bioprosthetic valve leaflets and/or its supporting structures that eventually results in valve dysfunction (78). One study assessing patients with an assortment of surgical bioprostheses demonstrated at a median follow-up of 10 years, a rate of clinical SVD of 6.6% and subclinical SVD of 30.1% (79). Data on TAVR prostheses have demonstrated a rate of SVD at 1 year of 2.5% (80) and at a median of 5.8 years of 9% with severe SVD affecting <1% (81). CT provides a valuable tool for assessing the structure and mobility of prosthetic valves, but cannot determine transvalvular hemodynamics (78). Therefore the diagnosis and quantification of stenosis or regurgitation is best achieved using echocardiography with CT providing supplementary information.

### Valve Thrombosis

Multi-slice CT angiography has provided important insights into the natural history of prosthetic valves with a particular focus on valve thrombosis. Hypo-attenuated leaflet thickening (HALT) can be found in 10–38% of prosthetic valves (82, 83), with the prevalence possibly higher in TAVR valves (84). Although lacking histological confirmation, this is highly suspected to be thrombus, based on its resolution with anticoagulation (85). HALT usually involves the periphery and bases of a leaflet and extends to a varying degree toward the center of the bioprosthesis (**Figure 4**) (4). HALT can develop as early as 5 days post-TAVR and has been shown to either progress, stabilize or regress over time (82, 83). Progression of HALT can lead to valve dysfunction described as restricted leaflet motion. This causes an increase in echocardiographically defined transvalvular gradients and eventually leads to symptoms of valve dysfunction (83). CT provides a reliable and potentially more sensitive methodology compared to transthoracic echocardiography for identifying and monitoring HALT (86, 84). It can also help determine management; the composition of acute thrombus has a low attenuation <90 HU, whereas chronic thrombus has values of 90–145 HU. Small acute thrombi are amenable to thrombolysis making this differentiation between types of thrombi important (87). 2D MPR provides an axial cross-sectional assessment to identify leaflet abnormalities. 3D volume rendered CT acquired through multiple phases provides confirmation of the leaflet abnormalities. When reconstructed into a movie (4D virtual reality CT), this can reliably illustrate restricted leaflet motion (4, 88, 89). Prophylaxis and treatment of thromboembolic disease associated with prosthetic valves have important implications for anti-thrombotic therapy, which is discussed elsewhere (90).

Additionally, a common and late complication of prosthetic valves is pannus formation, which commonly coexists with thrombus. Differentiation of the two pathologies is important for management. Pannus has a high attenuation >145 HU and the degree to which it is obstructing the valve orifice can be calculated, making CT a useful modality for its detection (87).

## CT IN INFECTIVE ENDOCARDITIS

Although echocardiography is the main imaging modality used to diagnose and monitor infective endocarditis, CT can play a valuable role and its use is advocated by international guidelines (91). CT can provide confirmation of a diagnosis with high accuracy if echocardiography is equivocal. Additionally, CT provides supplementary information such as extra-cardiac foci of infection, abscesses and pseudoaneursyms (5, 92). When combined with positron emission tomography (PET), CT provides diagnostic and prognostic value in prosthetic valve endocarditis for future cardiovascular events (93, 94) (**Figure 5**).

## EXTRACELLULAR VOLUME QUANTIFICATION (ECV) BY CT

VHD causes myocardial remodeling affecting ECV and its composition (95). ECV quantification using cardiac magnetic resonance imaging has been shown to track myocardial fibrosis and provide prognostic value in AS patients (96, 97). Based on similar concepts to cardiac magnetic resonance imaging, ECV can be calculated using CT (98). Certain pathologies such as cardiac amyloidosis result in very high ECV, enabling CT to act as a screening tool (**Figure 6**) (99).

## FUTURE APPLICATIONS

Valvular heart disease directly affects the myocardial structure, function, and perfusion. Therefore, assessing these facets guides both, prognosis and management. CT myocardial perfusion imaging (CT MPI) provides prognostic information that can influence management strategies (100). Additionally the quantification of extracellular volume (ECV) has been shown to provide unique insights into diffuse myocardial fibrosis and cardiac amyloid (101). Fusion imaging using a CT overlay on live fluoroscopy imaging may provide a useful tool for transcatheter interventions enabling more complex and safer procedures (102). Photon counting CT potentially heralds a new era in cardiac CT, improving signal to noise ratio, reducing artifacts and radiation. Its integration into clinical use may improve the utility of CT for valvular heart disease (103).

## CONCLUSION

Cardiac CT has become an irreplaceable adjunct to echocardiography in the clinical assessment of significant aortic stenosis and with the expansion of transcatheter valve intervention, the indications and utility of CT are continually growing. With high spatial resolution, CT allows evaluation of valve anatomy and coronary artery status, aortic pathology and vascular access planning, identification of the risk of likely complications and significant incidental extracardiac findings that influence treatment decisions, prognosis or trigger additional investigations.

## AUTHOR CONTRIBUTIONS

KP and TT were involved in the genesis and planning of this manuscript. All authors contributed to the literature review, figures, text and editing of the final manuscript.

## FUNDING

KP was funded by a University College London-held British Heart Foundation clinical research training fellowship grant (FS/19/48/34523) and has an unrestricted research grant from Edwards Lifesciences. FP had received research support from Siemens Healthineers. TT was supported by British Heart Foundation Intermediate fellowship (FS/19/35/3434). JM and TT were directly and indirectly supported by the UCLH and Barts NIHR Biomedical Research Units.

## REFERENCES

1. Gaede L, Blumenstein J, Liebetrau C, Dörr O, Kim WK, Nef H, et al. Outcome after transvascular transcatheter aortic valve implantation in 2016. *Eur Heart J.* (2018) 39:667–75. doi: 10.1093/eurheartj/ehx688
2. Regueiro A, Granada JF, Dagenais F, Rodés-Cabau J. Transcatheter mitral valve replacement: insights from early clinical experience and future challenges. *J Am Coll Cardiol.* (2017) 2:2175–92. doi: 10.1016/j.jacc.2017.02.045
3. Blanke P, Weir-McCall JR, Achenbach S, Delgado V, Hausleiter J, Jilaihawi H, et al. Computed tomography imaging in the context of transcatheter aortic valve implantation (TAVI)/transcatheter aortic valve replacement (TAVR): an expert consensus document of the society of cardiovascular computed tomography. *JACC Cardiovasc Imaging.* (2019) 12:1–24. doi: 10.1016/j.jcmg.2018.12.003
4. Jilaihawi H, Asch FM, Manasse E, Ruiz CE, Jelnin V, Kashif M, et al. Systematic CT methodology for the evaluation of subclinical leaflet thrombosis. *JACC Cardiovasc Imaging.* (2017) 10:461–70. doi: 10.1016/j.jcmg.2017.02.005
5. Habets J, Tanis W, Van Herwerden LA, Van Den Brink RBA, Mali WPTM, De Mol BAJM, et al. Cardiac computed tomography angiography results in diagnostic and therapeutic change in prosthetic heart valve endocarditis. *Int J Cardiovasc Imaging.* (2014) 30:377–87. doi: 10.1007/s10554-013-0335-2
6. Faggioni L, Gabelloni M, Accogli S, Angelillis M, Costa G, Spontoni P, et al. Preprocedural planning of transcatheter mitral valve interventions by multidetector CT: what the radiologist needs to know. *Eur J Radiol Open.* (2018) 31:131–40. doi: 10.1016/j.ejro.2018.08.005
7. Nkomo VT, Gardin JM, Skelton TN, Gottdiener JS, Scott CG, Enriquez-Sarano M. Burden of valvular heart diseases: a population-based study. *Lancet.* (2006) 368:1005–11. doi: 10.1016/S0140-6736(06)69208-8
8. Baumgartner H, Falk V, Bax JJ, De Bonis M, Hamm C, Holm PJ, et al. 2017 ESC/EACTS guidelines for the management of valvular heart disease. *Eur Heart J.* (2017) 38:2739–86. doi: 10.1093/eurheartj/ehx391
9. Messika-Zeitoun D, Serfaty JM, Brochet E, Ducrocq G, Lepage L, Detaint D, et al. Multimodal assessment of the aortic annulus diameter. Implications for transcatheter aortic valve implantation. *J Am Coll Cardiol.* (2010) 55:186–94. doi: 10.1016/j.jacc.2009.06.063
10. Clavel MA, Malouf J, Messika-Zeitoun D, Araoz PA, Michelena HI, Enriquez-Sarano M. Aortic valve area calculation in aortic stenosis by CT and doppler echocardiography. *JACC Cardiovasc Imaging.* (2015) 8:248–57. doi: 10.1016/j.jcmg.2015.01.009
11. Pibarot P, Dumesnil JG. Low-flow, low-gradient aortic stenosis with normal and depressed left ventricular ejection fraction. *J Am Coll Cardiol.* (2012) 60:1845–53. doi: 10.1016/j.jacc.2012.06.051
12. David M-Z, Guy L. Aortic valve stenosis: evaluation and management of patients with discordant grading. *E J Cardiol Pract.* (2018) 15:N26.
13. Pawade T, Clavel MA, Tribouilloy C, Dreyfus J, Mathieu T, Tastet L, et al. Computed tomography aortic valve calcium scoring in patients with aortic stenosis. *Circ Cardiovasc Imaging.* (2018) 11:e007146. doi: 10.1161/CIRCIMAGING.117.007146
14. Pawade TA, Newby DE, Dweck MR. Calcification in aortic stenosis: the skeleton key. *J Am Coll Cardiol.* (2015) 66:561–77. doi: 10.1016/j.jacc.2015.05.066
15. Agatston AS, Janowitz WR, Hildner FJ, Zusmer NR, Viamonte M, Detrano R. Quantification of coronary artery calcium using ultrafast computed tomography. *J Am Coll Cardiol.* (1990) 15:827. doi: 10.1016/0735-1097(90)90282-T
16. Messika-Zeitoun D, Aubry MC, Detaint D, Bielak LF, Peyser PA, Sheedy PF, et al. Evaluation and clinical implications of aortic valve calcification measured

by electron-beam computed tomography. *Circulation.* (2004) 110:356–62. doi: 10.1161/01.CIR.0000135469.82545.D0
17. Cueff C, Serfaty JM, Cimadevilla C, Laissy JP, Himbert D, Tubach F, et al. Measurement of aortic valve calcification using multislice computed tomography: correlation with haemodynamic severity of aortic stenosis and clinical implication for patients with low ejection fraction. *Heart.* (2011) 97:721–6. doi: 10.1136/hrt.2010.198853
18. Clavel MA, Messika-Zeitoun D, Pibarot P, Aggarwal SR, Malouf J, Araoz PA, et al. The complex nature of discordant severe calcified aortic valve disease grading: new insights from combined Doppler echocardiographic and computed tomographic study. *J Am Coll Cardiol.* (2013) 62:2329–38. doi: 10.1016/j.jacc.2013.08.1621
19. Clavel MA, Pibarot P, Messika-Zeitoun D, Capoulade R, Malouf J, Aggarval S, et al. Impact of aortic valve calcification, as measured by MDCT, on survival in patients with aortic stenosis: results of an international registry study. *J Am Coll Cardiol.* (2014) 64:1202–13. doi: 10.1016/j.jacc.2014.05.066
20. Messika-Zeitoun D, Bielak LF, Peyser PA, Sheedy PF, Turner ST, Nkomo VT, et al. Aortic valve calcification: determinants and progression in the population. *Arterioscler Thromb Vasc Biol.* (2007) 27:642–8. doi: 10.1161/01.ATV.0000255952.47980.c2
21. Aggarwal SR, Clavel MA, Messika-Zeitoun D, Cueff C, Malouf J, Araoz PA, et al. Sex differences in aortic valve calcification measured by multidetector computed tomography in aortic stenosis. *Circ Cardiovasc Imaging.* (2013) 6:40–7. doi: 10.1161/CIRCIMAGING.112.980052
22. Falk V, Baumgartner H, Bax JJ, De Bonis M, Hamm C, Holm PJ, et al. 2017 ESC/EACTS guidelines for the management of valvular heart disease. *Eur J Cardiothorac Surg.* (2017) 52:616–64. doi: 10.1093/ejcts/ezx324
23. Jean G, Van Mieghem NM, Gegenava T, van Gils L, Bernard J, Geleijnse ML, et al. Moderate aortic stenosis in patients with heart failure and reduced ejection fraction. *J Am Coll Cardiol.* (2021) 77:2796–803. doi: 10.1016/j.jacc.2021.04.014
24. Strange G, Stewart S, Celermajer D, Prior D, Scalia GM, Marwick T, et al. Poor long-term survival in patients with moderate aortic stenosis. *J Am Coll Cardiol.* (2019) 74:1851–63. doi: 10.1016/j.jacc.2019.08.004
25. Clinicaltrials.gov Transcatheter Aortic Valve Replacement to UNload the Left Ventricle in Patients with Advanced Heart Failure: A Randomized Trial (TAVR UNLOAD). Available online at: https://clinicaltrials.gov/ct2/show/NCT02661451 (accessed June 12, 2021).
26. Rosenhek R, Klaar U, Schemper M, Scholten C, Heger M, Gabriel H, et al. Mild and moderate aortic stenosis: natural history and risk stratification by echocardiography. *Eur Heart J.* (2004) 25:199–205. doi: 10.1016/j.ehj.2003.12.002
27. Hayashida K, Lefvre T, Chevalier B, Hovasse T, Romano M, Garot P, et al. Transfemoral aortic valve implantation: new criteria to predict vascular complications. *JACC Cardiovasc Interv.* (2011) 4:851–8. doi: 10.1016/j.jcin.2011.03.019
28. Toggweiler S, Gurvitch R, Leipsic J, Wood DA, Willson AB, Binder RK, et al. Percutaneous aortic valve replacement: vascular outcomes with a fully percutaneous procedure. *J Am Coll Cardiol.* (2012) 59:113–8. doi: 10.1016/j.jacc.2011.08.069
29. Achenbach S, Delgado V, Hausleiter J, Schoenhagen P, Min JK, Leipsic JA. SCCT expert consensus document on computed tomography imaging before transcatheter aortic valve implantation (TAVI)/transcatheter aortic valve replacement (TAVR). *J Cardiovasc Comput Tomogr.* (2012) 6:366–80. doi: 10.1016/j.jcct.2012.11.002
30. Biasco L, Ferrari E, Pedrazzini G, Faletra F, Moccetti T, Petracca F, et al. Access sites for TAVI: patient selection criteria, technical aspects, and outcomes. *Front Cardiovasc Med.* (2018) 5:88. doi: 10.3389/fcvm.2018.00088
31. Lederman RJ, Chen MY, Rogers T, Wang DD, Paone G, Guerrero M, et al. Planning transcaval access using CT for large transcatheter implants. *JACC Cardiovasc Imaging.* (2014) 7:1167–71. doi: 10.1016/j.jcmg.2014.05.015
32. Lederman RJ, Greenbaum AB, Rogers T, Khan JM, Fusari M, Chen MY. Anatomic suitability for transcaval access based on computed tomography. *JACC Cardiovasc Interv.* (2017) 10:1–10. doi: 10.1016/j.jcin.2016.09.002
33. Hell MM, Biburger L, Marwan M, Schuhbaeck A, Achenbach S, Lell M, et al. Prediction of fluoroscopic angulations for transcatheter aortic valve implantation by CT angiography: influence on procedural parameters. *Eur Heart J Cardiovasc Imaging.* (2016) 18:906–14. doi: 10.1093/ehjci/jew144
34. Schwarz F, Lange P, Zinsser D, Greif M, Boekstegers P, Schmitz C, et al. CT-angiography based evaluation of the aortic annulus for prosthesis sizing in transcatheter aortic valve implantation (TAVI)-predictive value and optimal thresholds for major anatomic parameters. *PLoS One.* (2014) 9:e103481. doi: 10.1371/journal.pone.0103481
35. Hayashida K, Bouvier E, Lefèvre T, Hovasse T, Morice MC, Chevalier B, et al. Impact of CT-guided valve sizing on post-procedural aortic regurgitation in transcatheter aortic valve implantation. *EuroIntervention.* (2012) 8:546–55. doi: 10.4244/EIJV8I5A85
36. Dvir D, Leipsic J, Blanke P, Ribeiro HB, Kornowski R, Pichard A, et al. Coronary obstruction in transcatheter aortic valve-in-valve implantation. *Circ Cardiovasc Interv.* (2015) 8:e002079. doi: 10.1161/circinterventions.114.002079
37. Ribeiro HB, Webb JG, Makkar RR, Cohen MG, Kapadia SR, Kodali S, et al. Predictive factors, management, and clinical outcomes of coronary obstruction following transcatheter aortic valve implantation: insights from a large multicenter registry. *J Am Coll Cardiol.* (2013) 62:1552–62. doi: 10.1016/j.jacc.2013.07.040
38. Barbanti M, Yang T-H, Cabau JR, Tamburino C, Wood DA, Jilaihawi H, et al. Anatomical and procedural features associated with aortic root rupture during balloon-expandable transcatheter aortic valve replacement. *Circulation.* (2013) 128:244–53. doi: 10.1161/CIRCULATIONAHA.113.002947
39. Van Mieghem NM, Schultz CJ, Van Der Boon RMA, Nuis RJ, Tzikas A, Geleijnse ML, et al. Incidence, timing, and predictors of valve dislodgment during TAVI with the medtronic corevalve system. *Catheter Cardiovasc Interv.* (2012) 79:726–32. doi: 10.1002/ccd.23275
40. Takagi H, Umemoto T. Impact of paravalvular aortic regurgitation after transcatheter aortic valve implantation on survival. *Int J Cardiol.* (2016) 221:46–51. doi: 10.1016/j.ijcard.2016.07.006
41. Delgado V, Ng ACT, Van De Veire NR, Van Der Kley F, Schuijf JD, Tops LF, et al. Transcatheter aortic valve implantation: role of multi-detector row computed tomography to evaluate prosthesis positioning and deployment in relation to valve function. *Eur Heart J.* (2010) 31:1114–23. doi: 10.1093/eurheartj/ehq018
42. Pollari F, Dell'Aquila AM, Söhn C, Marianowicz J, Wiehofsky P, Schwab J, et al. Risk factors for paravalvular leak after transcatheter aortic valve replacement. *J Thorac Cardiovasc Surg.* (2019) 157:1406.e–15.e. doi: 10.1016/j.jtcvs.2018.08.085
43. Kawsara A, Sulaiman S, Alqahtani F, Eleid MF, Deshmukh AJ, Cha Y, et al. Temporal trends in the incidence and outcomes of pacemaker implantation after transcatheter aortic valve replacement in the United States (2012\&\#x2013;2017). *J Am Heart Assoc.* (2020) 9:e016685. doi: 10.1161/JAHA.120.016685
44. Chamandi C, Barbanti M, Munoz-Garcia A, Latib A, Nombela-Franco L, Gutiérrez-Ibanez E, et al. Long-term outcomes in patients with new permanent pacemaker implantation following transcatheter aortic valve replacement. *JACC Cardiovasc Interv.* (2018) 11:301–10. doi: 10.1016/j.jcin.2017.10.032
45. Latsios G, Gerckens U, Buellesfeld L, Mueller R, John D, Yuecel S, et al. "Device landing zone" calcification, assessed by MSCT, as a predictive factor for pacemaker implantation after TAVI. *Catheter Cardiovasc Interv.* (2010) 76:431–9. doi: 10.1002/ccd.22563
46. Hamdan A, Guetta V, Klempfner R, Konen E, Raanani E, Glikson M, et al. Inverse relationship between membranous septal length and the risk of atrioventricular block in patients undergoing transcatheter aortic valve implantation. *JACC Cardiovasc Interv.* (2015) 8:1218–28. doi: 10.1016/j.jcin.2015.05.010
47. Abramowitz Y, Kazuno Y, Chakravarty T, Kawamori H, Maeno Y, Anderson D, et al. Concomitant mitral annular calcification and severe aortic stenosis: prevalence, characteristics and outcome following transcatheter aortic valve replacement. *Eur Heart J.* (2017) 38:1194–203. doi: 10.1093/eurheartj/ehw594
48. Hansson NC, Nørgaard BL, Barbanti M, Nielsen NE, Yang T-H, Tamburino C, et al. The impact of calcium volume and distribution in aortic root injury related to balloon-expandable transcatheter aortic valve replacement. *J Cardiovasc Comput Tomogr.* (2015) 9:382–92. doi: 10.1016/j.jcct.2015.04.002
49. Chieffo A, Giustino G, Spagnolo P, Panoulas VF, Montorfano M, Latib A, et al. Routine screening of coronary artery disease with computed tomographic coronary angiography in place of invasive coronary angiography in patients

undergoing transcatheter aortic valve replacement. *Circ Cardiovasc Interv.* (2015) 8:e002025. doi: 10.1161/CIRCINTERVENTIONS.114.002025
50. Feuchtner GM, Alkadhi H, Karlo C, Sarwar A, Meier A, Dichtl W, et al. Cardiac CT angiography for the diagnosis of mitral valve prolapse: comparison with echocardiography. *Radiology.* (2010) 254:374–83. doi: 10.1148/radiol.2541090393
51. Delgado V, Tops LF, Schuijf JD, de Roos A, Brugada J, Schalij MJ, et al. Assessment of mitral valve anatomy and geometry with multislice computed tomography. *JACC Cardiovasc Imaging.* (2009) 2:556–65. doi: 10.1016/j.jcmg.2008.12.025
52. Palazzuoli A, Cademartiri F, Geleijnse ML, Meijboom B, Pugliese F, Soliman O, et al. Left ventricular remodelling and systolic function measurement with 64 multi-slice computed tomography versus second harmonic echocardiography in patients with coronary artery disease: a double blind study. *Eur J Radiol.* (2010) 73:82–8. doi: 10.1016/j.ejrad.2008.09.022
53. Guo YK, Yang ZG, Ning G, Rao L, Dong L, Pen Y, et al. Isolated mitral regurgitation: quantitative assessment with 64-section multidetector CT – comparison with MR imaging and echocardiography. *Radiology.* (2009) 252:369–76. doi: 10.1148/radiol.2522081714
54. Morris MF, Maleszewski JJ, Suri RM, Burkhart HM, Foley TA, Bonnichsen CR, et al. CT and MR imaging of the mitral valve: radiologic-pathologic correlation. *Radiographics.* (2010) 30:1603–20. doi: 10.1148/rg.306105518
55. Shah M, Jorde UP. Percutaneous mitral valve interventions (Repair): current indications and future perspectives. *Front Cardiovasc Med.* (2019) 6:88. doi: 10.3389/fcvm.2019.00088
56. Blanke P, Dvir D, Cheung A, Ye J, Levine RA, Precious B, et al. A simplified D-shaped model of the mitral annulus to facilitate CT-based sizing before transcatheter mitral valve implantation. *J Cardiovasc Comput Tomogr.* (2014) 8:459–67. doi: 10.1016/j.jcct.2014.09.009
57. Blanke P, Naoum C, Webb J, Dvir D, Hahn RT, Grayburn P, et al. Multimodality imaging in the context of transcatheter mitral valve replacement establishing consensus among modalities and disciplines. *JACC Cardiovasc Imaging.* (2015) 8:1191–208. doi: 10.1016/j.jcmg.2015.08.004
58. Shanks M, Delgado V, Ng ACT, Van Der Kley F, Schuijf JD, Boersma E, et al. Mitral valve morphology assessment: three-dimensional transesophageal echocardiography versus computed tomography. *Ann Thorac Surg.* (2010) 90:1922–9. doi: 10.1016/j.athoracsur.2010.06.116
59. Gössl M, Sorajja P. MitraClip patient selection: inclusion and exclusion criteria for optimal outcomes. *Ann Cardiothorac Surg.* (2018) 7:771–5. doi: 10.21037/acs.2018.08.04
60. Yoon SH, Bleiziffer S, Latib A, Eschenbach L, Ancona M, Vincent F, et al. Predictors of left ventricular outflow tract obstruction after transcatheter mitral valve replacement. *JACC Cardiovasc Interv.* (2019) 12:182–93. doi: 10.1016/j.jcin.2018.12.001
61. Naoum C, Blanke P, Cavalcante JL, Leipsic J. Cardiac computed tomography and magnetic resonance imaging in the evaluation of mitral and tricuspid valve disease. *Circ Cardiovasc Imaging.* (2017) 10:e005331. doi: 10.1161/CIRCIMAGING.116.005331
62. Meduri CU, Reardon MJ, Lim DS, Howard E, Dunnington G, Lee DP, et al. Novel multiphase assessment for predicting left ventricular outflow tract obstruction before transcatheter mitral valve replacement. *JACC Cardiovasc Interv.* (2019) 12:2402–12. doi: 10.1016/j.jcin.2019.06.015
63. Allison MA, Cheung P, Criqui MH, Langer RD, Wright CM. Mitral and aortic annular calcification are highly associated with systemic calcified atherosclerosis. *Circulation.* (2006) 113:861–6. doi: 10.1161/CIRCULATIONAHA.105.552844
64. Barasch E, Gottdiener JS, Marino Larsen EK, Chaves PHM, Newman AB, Manolio TA. Clinical significance of calcification of the fibrous skeleton of the heart and aortosclerosis in community dwelling elderly. the cardiovascular health study (CHS). *Am Heart J.* (2006) 151:39–47. doi: 10.1016/j.ahj.2005.03.052
65. Guerrero M, Urena M, Himbert D, Wang DD, Eleid M, Kodali S, et al. 1-Year outcomes of transcatheter mitral valve replacement in patients with severe mitral annular calcification. *J Am Coll Cardiol.* (2018) 71:1841–53. doi: 10.1016/j.jacc.2018.02.054
66. Okada Y. Surgical management of mitral annular calcification. *Gen Thorac Cardiovasc Surg.* (2013) 61:619–25. doi: 10.1007/s11748-013-0207-7
67. Weir-McCall JR, Blanke P, Naoum C, Delgado V, Bax JJ, Leipsic J. Mitral valve imaging with CT: relationship with transcatheter mitral valve interventions. *Radiology.* (2018) 288:638–55. doi: 10.1148/radiol.2018172758
68. Guerrero M, Dvir D, Himbert D, Urena M, Eleid M, Wang DD, et al. Transcatheter mitral valve replacement in native mitral valve disease with severe mitral annular calcification: results from the first multicenter global registry. *JACC Cardiovasc Interv.* (2016) 9:1361–71. doi: 10.1016/j.jcin.2016.04.022
69. O'Brien B, Zafar H, De Freitas S, Sharif F. Transseptal puncture — review of anatomy, techniques, complications and challenges. *Int J Cardiol.* (2017) 233:12–22. doi: 10.1016/j.ijcard.2017.02.009
70. Yasunaga D, Hamon M. MDCT of interatrial septum. *Diagn Interv Imaging.* (2015) 96:891–9. doi: 10.1016/j.diii.2015.02.011
71. Yu W-L, Omid-Fard N, Arepalli C, Shao M, Hart SL. Weir McCall J, et al. Role of computed tomography in pre-procedural planning of transcatheter mitral valve replacement. *Struct Heart.* (2018) 2:23–9. doi: 10.1080/24748706.2017.1407503
72. Heuts S, Maessen JG, Sardari Nia P. Preoperative planning of left-sided valve surgery with 3D computed tomography reconstruction models: sternotomy or a minimally invasive approach? *Interact Cardiovasc Thorac Surg.* (2016) 22:587–93. doi: 10.1093/icvts/ivv408
73. Czesla M, Mogilansky C, Balan R, Kattner S, van Ingen G, Massoudy P. Evolution of a minimally invasive mitral valve program. *J Vis Surg.* (2016) 2:169. doi: 10.21037/jovs.2016.11.04
74. Morris MF, Suri RM, Akhtar NJ, Young PM, Gruden JF, Burkhart HM, et al. Computed tomography as an alternative to catheter angiography prior to robotic mitral valve repair. *Ann Thorac Surg.* (2013) 95:1354–9. doi: 10.1016/j.athoracsur.2012.12.010
75. Van Praet KM, Kofler M, Montagner M, Heck R, Eggert-Doktor D, Stamm C, et al. Minimally invasive mitral valve repair using external clamping—pearls and pitfalls. *J Vis Surg.* (2020) 6:45.
76. Latib A, Agricola E, Pozzoli A, Denti P, Taramasso M, Spagnolo P, et al. First-in-man implantation of a tricuspid annular remodeling device for functional tricuspid regurgitation. *JACC Cardiovasc Interv.* (2015) 8:e211–4. doi: 10.1016/j.jcin.2015.06.028
77. Winkel MG, Brugger N, Khalique OK, Gräni C, Huber A, Pilgrim T, et al. Imaging and patient selection for transcatheter tricuspid valve interventions. *Front Cardiovasc Med.* (2020) 7:60. doi: 10.3389/fcvm.2020.00060
78. Dvir D, Bourguignon T, Otto CM, Hahn RT, Rosenhek R, Webb JG, et al. Standardized definition of structural valve degeneration for surgical and transcatheter bioprosthetic aortic valves. *Circulation.* (2018) 137:388–99. doi: 10.1161/CIRCULATIONAHA.117.030729
79. Rodriguez-Gabella T, Voisine P, Dagenais F, Mohammadi S, Perron J, Dumont E, et al. Long-term outcomes following surgical aortic bioprosthesis implantation. *J Am Coll Cardiol.* (2018) 71:1401–12. doi: 10.1016/j.jacc.2018.01.059
80. Vemulapalli S, Holmes DR, Dai D, Matsouaka R, Mack MJ, Grover FL, et al. Valve hemodynamic deterioration and cardiovascular outcomes in TAVR: a report from the STS/ACC TVT registry. *Am Heart J.* (2018) 195:1–13. doi: 10.1016/j.ahj.2017.09.005
81. Blackman DJ, Saraf S, MacCarthy PA, Myat A, Anderson SG, Malkin CJ, et al. Long-term durability of transcatheter aortic valve prostheses. *J Am Coll Cardiol.* (2019) 73:537–45. doi: 10.1016/j.jacc.2018.10.078
82. Pache G, Schoechlin S, Blanke P, Dorfs S, Jander N, Arepalli CD, et al. Early hypo-attenuated leaflet thickening in balloon-expandable transcatheter aortic heart valves. *Eur Heart J.* (2016) 37:2263–71. doi: 10.1093/eurheartj/ehv526
83. Sondergaard L, De Backer O, Kofoed KF, Jilaihawi H, Fuchs A, Chakravarty T, et al. Natural history of subclinical leaflet thrombosis affectingmotion in bioprosthetic aortic valves. *Eur Heart J.* (2017) 38:2201–7. doi: 10.1093/eurheartj/ehx369
84. Chakravarty T, Søndergaard L, Friedman J, De Backer O, Berman D, Kofoed KF, et al. Subclinical leaflet thrombosis in surgical and transcatheter bioprosthetic aortic valves: an observational study. *Lancet.* (2017) 17:2383–92. doi: 10.1016/S0140-6736(17)30757-2
85. Ruile P, Neumann F-J. Valve thrombosis after TAVI. *Eur Heart J.* (2017) 38:2700–1. doi: 10.1093/eurheartj/ehx472

86. Leetmaa T, Hansson NC, Leipsic J, Jensen K, Poulsen SH, Andersen HR, et al. Early aortic transcatheter heart valve thrombosis: diagnostic value of contrast-enhanced multidetector computed tomography. *Circ Cardiovasc Interv*. (2015) 8:e001596. doi: 10.1161/CIRCINTERVENTIONS.114.001596
87. Aladmawi MA, Pragliola C, Vriz O, Galzerano D. Use of multidetector-row computed tomography scan to detect pannus formation in prosthetic mechanical aortic valves. *J Thorac Dis*. (2017) 9:s343–8. doi: 10.21037/jtd.2017.04.14
88. Pache G, Blanke P, Zeh W, Jander N. Cusp thrombosis after transcatheter aortic valve replacement detected by computed tomography and echocardiography. *Eur Heart J*. (2013) 34:3546. doi: 10.1093/eurheartj/eht316
89. Makkar RR, Fontana G, Jilaihawi H, Chakravarty T, Kofoed KF, De Backer O, et al. Possible subclinical leaflet thrombosis in bioprosthetic aortic valves. *N Engl J Med*. (2015) 373:2015–24. doi: 10.1056/NEJMoa1509233
90. Calabrò P, Gragnano F, Niccoli G, Marcucci R, Zimarino M, Spaccarotella C, et al. Antithrombotic therapy in patients undergoing transcatheter interventions for structural heart disease. *Circulation*. (2021) 144:1323–43. doi: 10.1161/CIRCULATIONAHA.121.054305
91. Habib G, Lancellotti P, Antunes MJ, Bongiorni MG, Casalta JP, Del Zotti F, et al. 2015 ESC infective endocarditis. *Eur Heart J*. (2015) 36:3075–128. doi: 10.1093/eurheartj/ehv319
92. Feuchtner GM, Stolzmann P, Dichtl W, Schertler T, Bonatti J, Scheffel H, et al. Multislice computed tomography in infective endocarditis. Comparison with transesophageal echocardiography and intraoperative findings. *J Am Coll Cardiol*. (2009) 53:436–44. doi: 10.1016/j.jacc.2008.01.077
93. San S, Ravis E, Tessonier L, Philip M, Cammilleri S, Lavagna F, et al. Prognostic value of 18F-fluorodeoxyglucose positron emission tomography/computed tomography in infective endocarditis. *J Am Coll Cardiol*. (2019) 74:1031–1040. doi: 10.1016/j.jacc.2019.06.050
94. Pizzi MN, Roque A, Fernández-Hidalgo N, Cuéllar-Calabria H, Ferreira-González I, Gonzàlez-Alujas MT, et al. Improving the diagnosis of infective endocarditis in prosthetic valves and intracardiac devices with 18F-fluordeoxyglucose positron emission tomography/computed tomography angiography: initial results at an infective endocarditis referral center. *Circulation*. (2015) 132:1113–26. doi: 10.1161/CIRCULATIONAHA.115.015316
95. Treibel TA, López B, González A, Menacho K, Schofield RS, Ravassa S, et al. Reappraising myocardial fibrosis in severe aortic stenosis: an invasive and non-invasive study in 133 patients. *Eur Heart J*. (2018) 39:699–709. doi: 10.1093/eurheartj/ehx353
96. Treibel TA, Kozor R, Schofield R, Benedetti G, Fontana M, Bhuva AN, et al. Reverse myocardial remodeling following valve replacement in patients with aortic stenosis. *J Am Coll Cardiol*. (2018) 71:860–71. doi: 10.1016/j.jacc.2017.12.035
97. Chin CWL, Everett RJ, Kwiecinski J, Vesey AT, Yeung E, Esson G, et al. Myocardial fibrosis and cardiac decompensation in aortic stenosis. *JACC Cardiovasc Imaging*. (2017) 10:1320–33. doi: 10.1016/j.jcmg.2016.10.007
98. Treibel TA, Bandula S, Fontana M, White SK, Gilbertson JA, Herrey AS, et al. Extracellular volume quantification by dynamic equilibrium cardiac computed tomography in cardiac amyloidosis. *J Cardiovasc Comput Tomogr*. (2015) 9:585–92. doi: 10.1016/j.jcct.2015.07.001
99. Treibel T, Bandula S, Fontana M, White SK, Gilbertson JA, Punwani SA, et al. Quantification cardiac amyloid by cardiac computed tomography. *Eur Heart J Cardiovasc Imaging*. (2015) 9:585–92.
100. Takx RAP, Celeng C, Schoepf UJ. CT myocardial perfusion imaging: ready for prime time? *Eur Radiol*. (2018) 28:1253–6. doi: 10.1007/s00330-017-5057-8
101. Scully PR, Bastarrika G, Moon JC, Treibel TA. Myocardial extracellular volume quantification by cardiovascular magnetic resonance and computed tomography. *Curr Cardiol Rep*. (2018) 20:15. doi: 10.1007/s11886-018-0961-3
102. Mousavi N, Spaziano M. *The Expanding Role of CT in Pre-procedural Planning of Percutaneous Structural Heart Disease Interventions*. Washington, DC: American College of Cardiology (2018).
103. Willemink MJ, Persson M, Pourmorteza A, Pelc NJ, Fleischmann D. Photon-counting CT: technical principles and clinical prospects. *Radiology*. (2018) 289:293–312. doi: 10.1148/radiol.2018172656


**Conflict of Interest:** The authors declare that the research was conducted in the absence of any commercial or financial relationships that could be construed as a potential conflict of interest.

frontiers in Cardiovascular Medicine

ORIGINAL RESEARCH
published: 25 March 2022
doi: 10.3389/fcvm.2022.850393

# Lithotripsy of Calcified Aortic Valve Leaflets by a Novel Ultrasound Transcatheter-Based Device

*Giacomo Bernava[1†], Enrico Fermi[2†], Guido Gelpi[3], Stefano Rizzi[1], Davide Benettin[2], Marianna Barbuto[1], Claudia Romagnoni[3], Domenico Ventrella[4], Maria Chiara Palmieri[2], Marco Agrifoglio[5], Gianluca Polvani[5], Maria Laura Bacci[4], Enrico Pasquino[2] and Maurizio Pesce[1*]*

[1] Unità di Ingegneria Tissutale Cardiovascolare, Centro Cardiologico Monzino, Istituto di Ricovero e Cura a Carattere Scientifico (IRCCS), Milan, Italy, [2] AorticLab S.r.l., Bioindustry Park, Colleretto Giacosa, Italy, [3] ASST Fatebenefratelli Sacco, Milan, Italy, [4] Università Degli Studi di Bologna, Bologna, Italy, [5] Università Degli Studi di Milano, Milan, Italy

The increasing incidence of calcific aortic valve disease necessitates the elaboration of new strategies to retard the progression of the pathology with an innovative solution. While the increasing diffusion of the transcatheter aortic valve replacements (TAVRs) allows a mini-invasive approach to aortic valve substitution as an alternative to conventional surgical replacement (SAVR) in an always larger patient population, TAVR implantation still has contraindications for young patients. In addition, it is liable to undergo calcification with the consequent necessity of re-intervention with conventional valve surgery or repeated implantation in the so-called TAVR-in-TAVR procedure. Inspired by applications for non-cardiac pathologies or for vascular decalcification before stenting (i.e., coronary lithotripsy), in the present study, we show the feasibility of human valve treatment with a mini-invasive device tailored to deliver shockwaves to the calcific leaflets. We provide evidence of efficient calcium deposit ruptures in human calcified leaflets treated *ex vivo* and the safety of the treatment in pigs. The use of this device could be helpful to perform shockwaves valvuloplasty as an option to retard TAVR/SAVR, or as a pretreatment to facilitate prosthesis implantation and minimize the occurrence of paravalvular leak.

**Keywords: calcific aortic valve disease (CAVD), ultrasound, lithotripsy—methods, valve leaflets, valvuloplasty, medical device**

OPEN ACCESS

***Edited by:***
*Ronak Rajani, Guy's and St Thomas' NHS Foundation Trust, United Kingdom*

***Reviewed by:***
*Alexander Sedaghat, University Hospital Bonn, Germany*
*Tanja Katharina Rudolph, Heart and Diabetes Center North Rhine-Westphalia, Germany*

****Correspondence:***
*Maurizio Pesce*
*maurizio.pesce@ccfm.it*

*† These authors have contributed equally to this work*

***Specialty section:***
*This article was submitted to Heart Valve Disease, a section of the journal Frontiers in Cardiovascular Medicine*

***Received:*** *07 January 2022*
***Accepted:*** *21 February 2022*
***Published:*** *25 March 2022*

***Citation:***
*Bernava G, Fermi E, Gelpi G, Rizzi S, Benettin D, Barbuto M, Romagnoni C, Ventrella D, Palmieri MC, Agrifoglio M, Polvani G, Bacci ML, Pasquino E and Pesce M (2022) Lithotripsy of Calcified Aortic Valve Leaflets by a Novel Ultrasound Transcatheter-Based Device. Front. Cardiovasc. Med. 9:850393. doi: 10.3389/fcvm.2022.850393*

## INTRODUCTION

Calcific aortic valve disease (CAVD) is one of the most prevalent pathologies in elderly people with a trend to increase worldwide (1–4), along with sex-specific differences (5). Epidemiological studies show that the prevalence of the pathology exponentially increases with age. In addition, the trend is favored by the generalized and continuously growing increase in life expectancy (6) and the constant rate increase in the world population of around 1.05% per year (Worldometer, 2020 global population data; https://www.worldometers.info/world-population/world-population-by-year/). CAVD and other aging-related disorders are therefore anticipated to have an epidemic diffusion in the next decades.

A main characteristic of CAVD is that it has a biphasic trend. During the first phase, named sclerosis, the valve leaflets undergo a slow progression of lipid accumulation and thickening due to the matrix remodeling activity of valve-resident and recruited inflammatory cells. During this

phase, the change in valve hemodynamics is minimal. The sclerotic phase of CAVD is relatively slow and is followed by a more rapid stenotic phase, during which the resident cells start releasing small calcified microparticles that accumulate in the matrix (especially at the aortic side of the leaflets), giving rise to large calcific nodules. These nodules distort the leaflet geometry and make leaflets less pliable, preventing complete valve closure and giving rise to regurgitation and valve mechanical insufficiency. This progresses rapidly and can lead to death within 2–3 years after the beginning of the calcification process (7–10). For example, mild aortic valve stenosis (AVS) is defined by a peak velocity between 2.5 and 3 m/s, with a mean trans-valvular pressure gradient of less than 20 mmHg and a valve opening $>1.5$ cm$^2$. By contrast, severe AVS is defined by a peak velocity greater than 4 m/s, a mean gradient of 40 mmHg or more and an aortic valve area less than 1 cm$^2$. For several decades, the gold standard treatment of severe aortic stenosis has been surgical aortic valve replacement (SAVR) with mechanical or bio-prosthetic valves. Recently, a new trend has been established by the introduction of transcatheter aortic valve replacements (TAVRs) which has become an optimal solution for patients in the age range of 60–65 to ∼80 years (11) or patients who cannot be operated for concomitant risk conditions (12). At the moment, there are no efficient pharmacological therapies that may retard the rapid calcific progression in the stenotic valve or inhibit the transition from the sclerotic to the stenotic phase–a shortcoming for the management of many young patients worldwide.

Inspired by the use of shockwaves to disintegrate kidney stones or gallstones (13, 14), which was introduced in the mid-'80s in medicine, new applications of high-intensity focused ultrasounds have proven to be effective for other treatments for calcific pathologies, such as tendonitis and other orthopedic applications (15). Lithotripsy has also been successfully used in the cardiovascular pathology area as an adjuvant treatment for better implantation of stents in coronary and peripheral calcified arteries (16–18). Similar to lithotripsy, ultrasounds that are properly modulated in intensity, frequency, and waveform can be used to produce fractures and structural changes in calcific aortic valve deposits. For this application, much less energy density is required to limit soft tissue injury. In this study, we describe the first validation of an innovative device that is tailored to disintegrate the calcific deposits in the human aortic valve leaflets. This device has been conceived to be part of a trans-catheter debridement device (TDD) that uses low-intensity ultrasound shockwaves for the calcium ablation in the native aortic or bioprosthetic valves with the aim of restoring the leaflet pliability to, therefore, regain an adequate trans-valvular flow and reduce pressure gradient. We show that treatment with TDD is able to reduce the calcium deposits in human calcified leaflets *ex vivo* without altering the vitality or affecting the structure and gross morphology of the leaflets, and of pericardium as the most represented material normally employed to manufacture bioprosthetic valves. We also show that the employment of the device is feasible in pigs. Based on our results, we propose TDD as an alternative treatment for young patients not eligible for TAVR. It may also be an alternative to the TAVR-in-TAVR procedure when restoring valve performance in patients with preexisting TAVRs affected by *post*-implant calcification.

# MATERIALS AND METHODS

## Biological Material and Ethics

Human stenotic aortic valves were obtained from a leftover of valve surgery replacement after approval from the Ethical Committee at Centro Cardiologico Monzino for the purpose of the present study. Porcine pericardia were collected from euthanized adult pigs in the experimental piggery facility and the slaughterhouse of the Department of Veterinary Medical Sciences of the University of Bologna. The pig *in vivo* trial was performed at an external facility authorized for the execution of cardiothoracic surgery trials. Animals were treated according to the ethical guidelines approved by the Italian Ministry of Health.

## Description of the TDD Device and of the *ex vivo*/*in vivo* Treatment Protocol

The TDD used in the present study was an evolution of the device we preliminarily tested (19). The theoretical considerations underlying the use of shockwaves is provided for interested readers in the supplementary information. Briefly, the TDD comprised a pulse wave generator that was designed to provide two narrow impulsive electrical signals ranging from 50 to 75V. For the present study, one electrical signal was emitted pulses at 100 kHz and the other emitted at 3MHz to the ablation unit in an alternating pattern, with a time interval of 6 s. The combination of these different frequencies improved the disruptive effects of calcium deposits in the aortic valve cusps, avoiding thermal injury and the breaking of the transducers. The ablation unit was based on two mechanically bound piezoceramic transducers produced by PI Ceramics that had dimensions of 2.7 mm × 8 mm × .7 mm. Each transducer was electrically connected to a Kapton flexible printed circuit and housed in metal support. The metal support was engineered to create a backing effect on the ultrasounds emitted by the transducer as the waves are conveyed in the direction of treatment. To obtain this effect, the thickness of the wall where the transducer was anchored is $\frac{3}{4}\lambda$. The transducer must be electrically isolated to work in a biological environment. The insulating material was a variant of parylene. It is deposited with a thickness of $\frac{\lambda}{4}$ that facilitates the passage of ultrasonic waves as the effects of refraction and reflection are limited. The debridement device used for the execution of the tests that is reported in this article consisted of a clamp whose faces are constituted by two piezoceramic transducers, but the final version of the device also included an artificial temporary valve with a Nitinol support structure intended to be positioned within the native valve to keep it open during the positioning of the transducers. **Figure 1** illustrates the main constructive elements of the TDD and its experimental setup for the removal of calcium deposits in the soft valve tissue. The calcific leaflets were continuously treated for 30 min at alternating frequencies of 3 MHz and 100 KHz, with a switch between the two frequencies every 6 s. The combination of two-frequency ultrasound fields, as indicated in the literature (REF), increases the cavitation effects compared to the use of a single frequency. Hence, it is likely to preserve the integrity of the transducer and reduce the heat emitted.

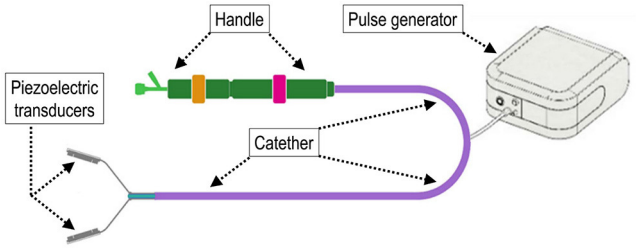


**FIGURE 1 |** Scheme illustrating the main components of the trans-catheter debridement device (TDD) in the configuration as it was employed for the *in vivo* trial. The device consists of two piezoelectric transducers that can be juxtaposed to deliver shockwaves on both sides of the region of treatment. The impulse-transducing cables are inserted into an intravascular catheter and operated by a handle at the other extremity to deploy and de-sheath the device.

## TDD Treatment of Porcine Pericardium

Immediately after gentle isolation of the parietal pericardial membrane, the tissue was immersed in a solution of Phosphate-buffered saline (PBS)-containing antibiotics (penicillin/streptomycin) and stored or shipped at 4°C until the beginning of the experiments. Before the treatment with shockwaves, the remaining fat tissue was removed from the pericardial flap under sterile conditions. Subsequently, it was divided into stripes with a sterile knife and further cut into three samples/stripes. TDD treatment was localized at the center of the samples after marking with a surgical pen for discriminating the treated vs. the untreated portions in subsequent analyses.

## Treatment of Human Valves With TDD

Candidate valves for TDD testing were selected on the basis of the degree of calcification as detected by echocardiographic characteristics before the valve substitution intervention. In general, valves with low or moderate stenosis levels were selected due to the inability of our experimental TDD to ablate nodules with a volume smaller than 100 $mm^3$. The system was mounted with the two piezoelectric transducers clamping the portion of the tissue to be treated before connecting to the system amplifier (**Figure 1**).

## *In vivo* Pig Model

The experimental treatment was carried out in two adult pigs in a fully equipped operating room with a portable angiographic C-arm. Under general anesthesia, the animals were fully heparinized, and the femoral artery was exposed to perform the treatment with TDD using a minimally invasive procedure. The animals were kept anesthetized for the whole duration of the treatments and were immediately euthanized after the procedure to recover the heart and dissect the treated valves. The mean arterial pressure was stable during the entire procedure (mean arterial pressure of 80 mmHg with heart rate of ∼130 beats per min). No moderate to severe aortic regurgitation was ever detected by echocardiographic monitoring during and after TDD treatment. No pacing or rapid pacing was needed for the treatment.

## Histological Characterization

Human and pig valve samples were fixed in 4% paraformaldehyde (4°C overnight), dehydrated in alcoholic scale, and embedded in paraffin. Histological sections (5 μm in thickness) were cut, dewaxed, and stained. Von Kossa staining was performed to evaluate calcium deposits in untreated vs. treated portions of the specimens. Conventional staining (hematoxylin/eosin, Masson's trichrome) was performed to observe in greater detail the structure of the tissue. Images of the tissue sections were acquired using an AxioPlane optical microscope (Carl Zeiss) and analyzed with ZenBlue software.

# RESULTS AND DISCUSSION

## Validation of TDD *in vitro* and *ex vivo*

To preliminarily test the efficiency of calcium deposits debridement in human aortic valves, experiments were performed on explanted and formaldehyde-fixed aortic valve leaflets. Under these conditions, we obtained an average volume reduction of 13.87% with a single piezo and a supply voltage of 55V, which allowed to obtain a peak of acoustic pressure of .2Mpa. The emitted energy is 150 mj/$mm^2$ in the center of the transducer and 80 mj/$mm^2$ at the edges (the shape of the emitted field is pyramidal). Volume reduction was calculated from the post-treatment vs. pre-treatment leaflet by CT scan (**Supplementary Figure S1**).

Since application of shockwaves to tissues can determine mechanical damages to cells, we were prompted to assess the effects on cellular survival and tissue ruptures using our experimental setup. This was done by measuring the vitality of living pericardial membranes from pigs, a tissue that we already employed for engineering valve tissues after recellularization (20) and is the golden standard material for manufacturing valve replacements. As shown in **Figures 2A,B**, the samples, stained with 3-(4.5-dimethylthiazol-2-yl)2,5-diphenyltetrazolium bromide (MTT) and treated with the device, exhibited no differences in the overall vitality of the treated vs. the non-treated areas on both sides of the tissue. The absence of large ruptures and the presence of cells with normal morphology in transversal sections of the treated and untreated areas showed that the type and intensity of the shockwaves delivered by the TDD did not affect, at least macroscopically, the integrity of the tissue (**Figure 2C**). Confirming the macroscopic observations by MTT staining, a normal amount of cells in the treated vs. the non-treated areas were counted in high magnifications of transversal tissue sections of the pericardial material (**Figures 2C,D**). This *bona fide* consolidates the lack of important structural deterioration of a valve-resembling living tissue treated with the device and warrants the safety of the procedure for employment *in vivo*.

To validate the double-piezo device for fragmentation and/or disruption of the calcium deposits in living calcified valves, we employed the TDD to treat calcified areas of human stenotic valves leaflets that were freshly explanted from patients with CAVD who were undergoing surgical valve replacement (**Figure 3A**). Treatments were performed using a 3 MHz ultrasound field combined with a field at a low frequency of

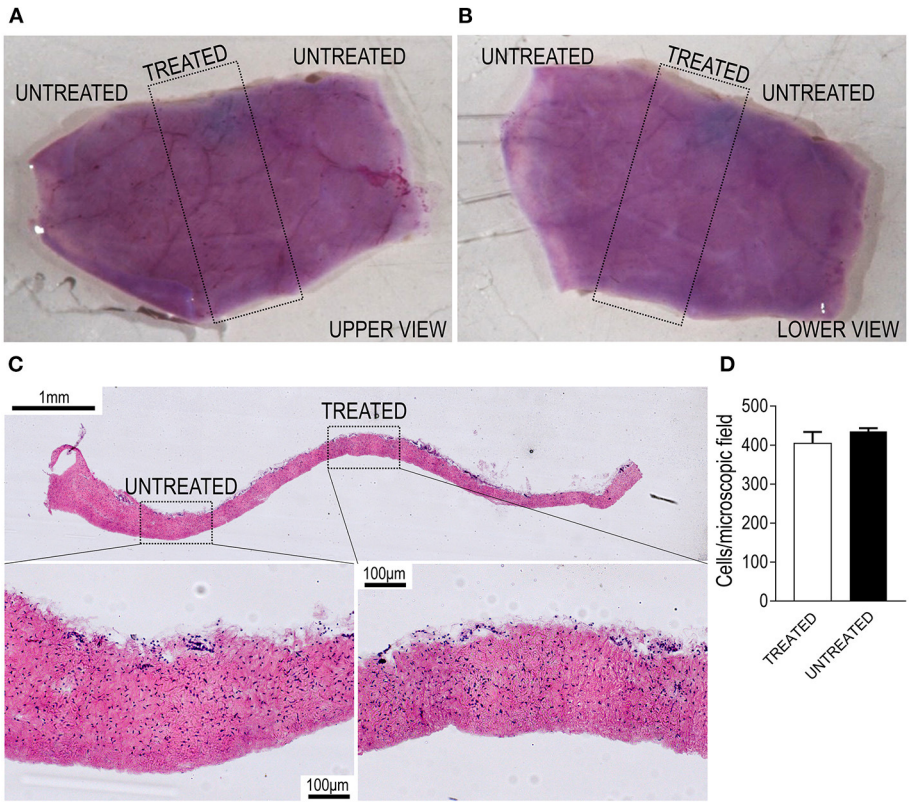


**FIGURE 2 |** Validation of the TDD on living porcine pericardium. **(A,B)** Show the two sides of a pericardial patch stained with 3-(4.5-dimethylthiazol-2-yl)2,5-diphenyltetrazolium bromide (MTT; purple color). The region encircled by the dotted rectangle indicates the part that was exposed to shockwaves and does not exhibit any staining reduction, suggesting maintenance of an excellent vitality of the tissue. **(C)** Shows the transversal section of another section of living pericardium treated with the TDD. It is evident from the high magnifications in the lower part of the panels that cells in the treated regions are in the same amount as in the untreated portions. Quantifications of nuclei are present in **D**, showing no difference in the nuclei counting in treated vs. untreated portions. Bar graph displays the mean and the SE of data ($n = 3$ independently treated pericardial samples; $p > 0.05$ by paired Student's $t$-test).

100 kHz, which, according to preliminary tests, were found to ensure the most efficient removal of the nodules of intermediate or low size (up to 100 $mm^3$). To this aim, we selected areas of the leaflets that were not characterized by the largest calcific deposits or affected by sclerosis, where, instead, calcium deposition is not involved (21). Leaflets were treated in areas juxtaposed to the visible calcifications with an orientation, as indicated in **Figure 3B.** From the morphological observation of the leaflets after treatment, the tissues, in no case, showed signs of burns or obvious damages. Histology staining was performed after transversally cutting the treated areas to analyze possible microscopic ruptures to the extracellular matrix components (e.g., collagen and elastic fibers) and variations in the dimensions of the calcium nodules. **Figures 3C–F** show representative low or high magnifications of calcifications in control (**Figures 3C,E**) and treated (**Figures 3C,F**, **Supplementary Figure S2**) leaflet sections stained with von Kossa. In treated leaflets, it was evident that a partial fragmentation or disruption of the calcium deposits appeared less compact than in untreated samples, as shown by the reduction of the area covered by the compact bone, and the presence of areas where the calcium appeared pulverized. The elimination of calcium deposits was also macroscopically observed by treating a calcified human valve in a cadaveric heart (**Supplementary Figure S2**). Together, these data macroscopically and microscopically demonstrate the removal of calcium nodules from the calcific leaflets by TDD.

## Safety of TDD Employment *in vivo*

A pigtail catheter, under fluoroscopic guidance, was advanced through a 6 Fr arterial introducer and over a 0.035″ standard wire until the right aortic valve sinus of Valsalva to mark aortic valve plane and leaflet. The TDD, integrated in a transfemoral 21 Fr delivery system, was advanced over a 0.035″ stiff wire through the thoracic aorta and aortic arch to the aortic root (**Figure 4A**, left center, **Supplementary Video 1**). An angiography was performed to highlight the correspondence between the position of the device and the aortic valve plane (**Figure 4A,** right, **Supplementary Video 1**). After opening the device, under intravascular ultrasound control (**Figure 4B**), the active element was correctly positioned by laying on the aortic side of the leaflet. The device only kept in closed position at which the leaflet was lying on, allowing the two other leaflets to normally open and close for the whole

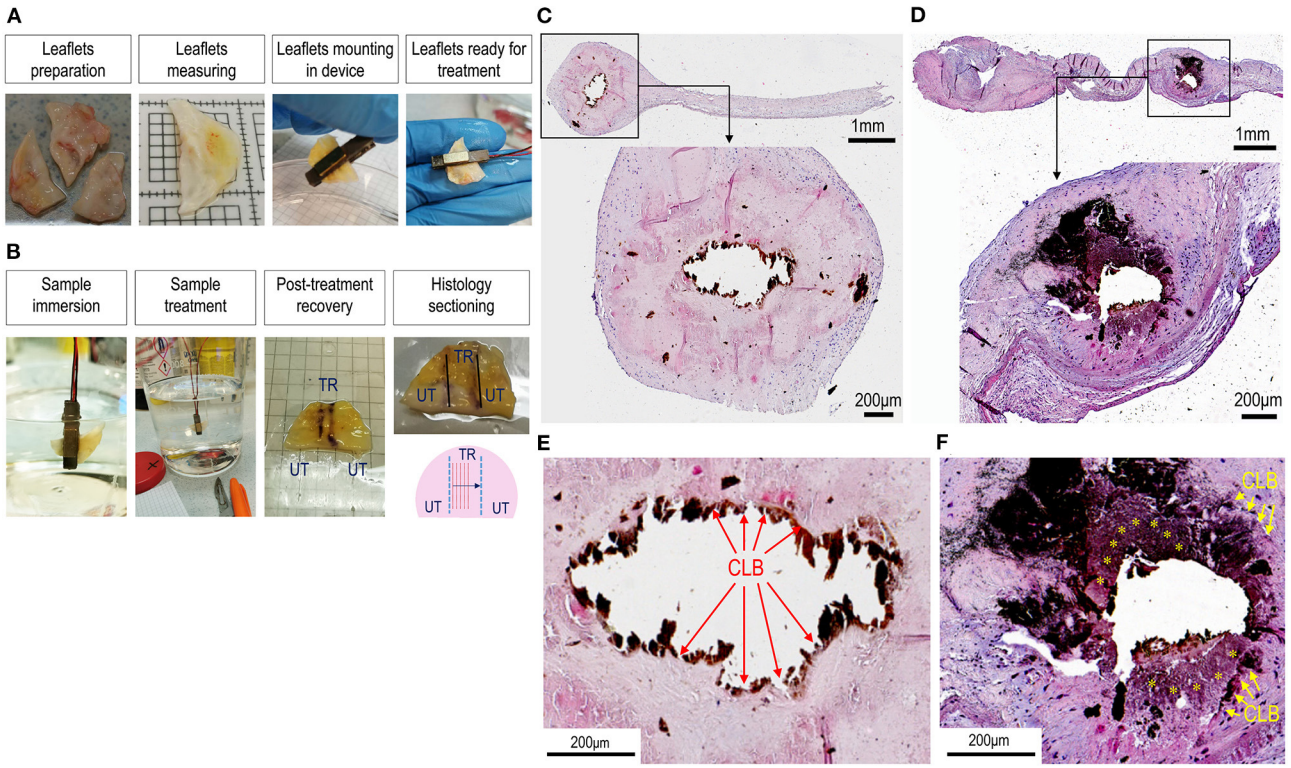


**FIGURE 3 |** Treatment of calcific aortic valve disease (CAVD) leaflets by TDD. **(A,B)** Show the sequence of the human CAVD leaflets mounting in the debridement device. After preparation, leaflets were individually placed among the two piezoelectric transducers and immersed into a phosphate-buffered saline (PBS) solution for the treatment. After treatment, the orientation of the treated zones (TR) was marked with a surgical pen to distinguish them from the untreated portions (UT). These marks were taken as a reference for histological sectioning that occurred in a transversal orientation as indicated in the lower right panel in **(B)**. **(C,D)** And the high magnifications of the histological regions represented therein **(E,F)** show the difference in the aspect of the calcifications in control **(C,E)** vs. the treated calcific leaflets **(D,F)**. It is remarkable that in control tissues there was a net boundary between the calcific lesions (removed by sectioning; CLB) and the surrounding sclerotic tissue (red arrows in **E**). By contrast in treated tissues, the boundaries were less sharp (yellow arrows) and granular-like deposits (yellow asterisks) appeared around the lesions, suggesting a partial debridement of the calcium. See also **Supplementary Figure S1** for another clear example of calcium debridement in a calcific human valve leaflet treated with TDD. Sections in **C–F** stained with von Kossa staining solution.

duration of the treatment (**Figure 4B**, center and right) and after retraction of the TDD from the valve (**Figure 4C** and **Supplementary Video 1**). It was interesting to note that during the activation of the piezo, the TDD ablator interfered with the echo signal. While this suggests an efficient *in vivo* functioning of the device, it also shows that echocardiographic assessment of leaflet motion during ultrasound treatment is not possible, thus leaving to angiographic monitoring the elective way to control the positioning of the piezo during the procedure. Every 10 min, the treatment was interrupted to check the status of the electrical insulation of the device. The check was carried out by pinching the electrical cables connected to the generator, and the piezoelectric capacity was measured with a tester.

After the end of the experiments, the valves were explanted and processed for histological sectioning. Given that the entire valves were available, the three leaflets were individually dissected from the Valsalva sinuses and transversally sectioned in a circumferential direction from commissure to commissure to screen for potential tissue damage. **Figures 5a–c** show the picture of the right, left, and non-coronary leaflets, respectively, of one of the valves treated by the TDD *in vivo*. To identify possible tissue damages, staining with Masson's and Hematoxylin/Eosin (H&E) solutions were performed. The magnifications in each of the panels indicate areas with possible tissue damage due to the treatment. As expected, evident signs of mild/moderate ruptures on the aortic side of the right leaflet (**Figure 5a**), the one that received the ultrasounds according to echocardiography data. These ruptures, however, were found only on the most external surface of the tissue and did not affect the collagenous structure of the *fibrosa* layer, suggesting that the shockwaves were very focused on the area of the tissue localized immediately below the contact point of the piezoelectric transducer to the aortic side of the leaflet. This finding, in keeping with the data obtained in animal pericardium and the human calcific leaflets, shows a localized effect of the TDD that is tailored to fracture the calcific lesions without involving major tissue ruptures.

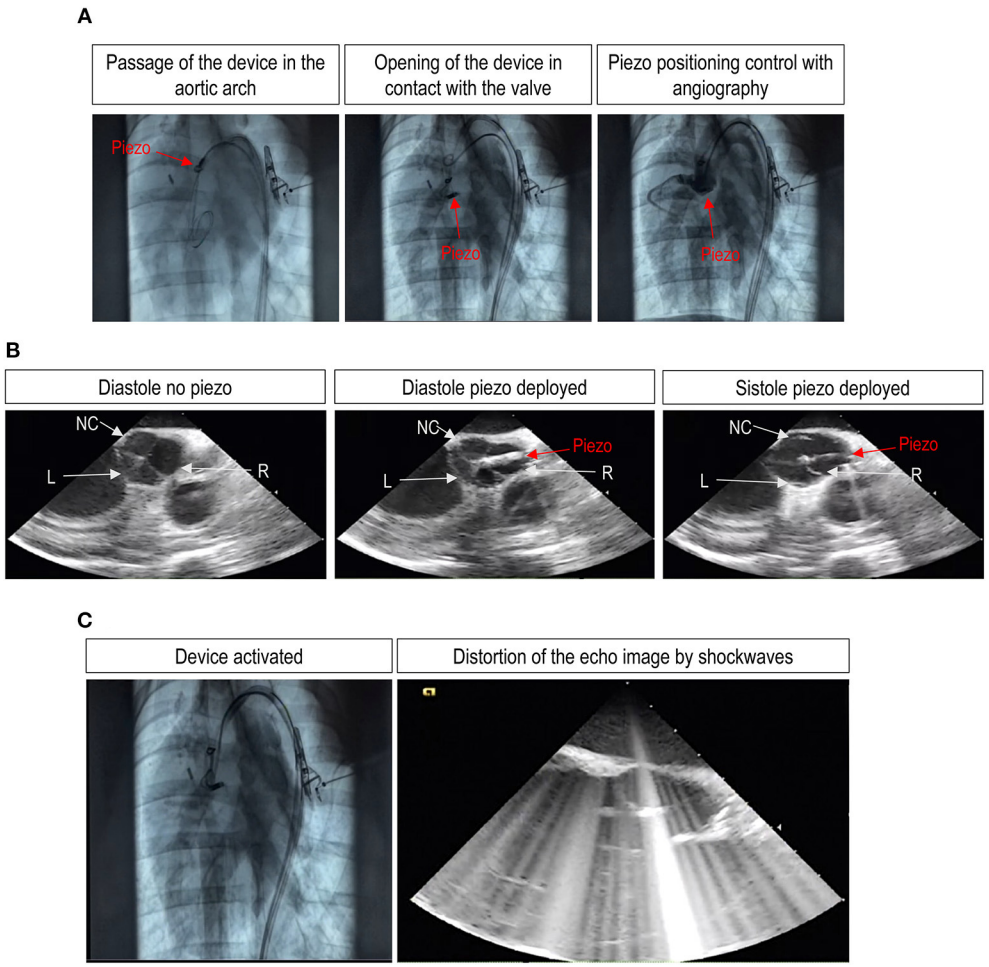


**FIGURE 4 |** Angiographic and echocardiographic assessment of successful TDD deployment and leaflet treatment with a trans-femoral access *in vivo*. **(A)** Shows the deployment of the device through the femoral artery from an initial position at the level of the ascending aorta and down to the positioning of the piezo in the Valsalva sinus of the right aortic valve leaflet. **(B)** Shows three images of an echocardiographic sequence showing the motion of the valve leaflets in the presence of the piezo deployed at the level of the right leaflet. The pictures of the sequence show, respectively, the correct closure of the three leaflets before piezo deployment (left picture), the closure of the valve after piezo deployment (center picture), and the opening of the left (L) and the non-coronary (NC) leaflets or the blockade of the right (R) leaflet by the deployed piezo at systole (right picture). The complete sequence is provided as **Supplementary Video 1**. **(C)** Shows, finally, static images of the angiography and the echocardiographic sequences during activation of the piezo. It is evident on the right the interference of shockwaves with the ultrasounds, making it impossible to distinguish the structure of the valve.

## CONCLUSIONS AND LIMITATIONS

In the present study, we provide the first proof of concept demonstration of a new device specifically tailored to operate with a high level of safety and efficiency. It is a partial debridement of the calcific deposits affecting the aortic valve motion and hydrodynamic performance. Although innovative, this approach is not the first to be employed to this aim. In fact, in recent literature, there are emerging descriptions of lithotripsy application as a preventive strategy to improve the ellipticity index and limit the paravalvular leak of transcatheter aortic valve implantations (TAVIs) (22, 23), to reduce percutaneously the extent of cardiac valves calcifications (24), or as a pretreatment for valvuloplasty (25, 26). On the other hand, the devices employed so far to deliver shockwaves to the valves—expandable lithotripsy balloons tailored for intravascular calcific lesions debridement—are not specifically designed for the scope of shockwave-based valvuloplasty and, therefore, do not have the design specifications to perform debridement of the calcific lesions with the necessary precision and accuracy. The TDD presented in our investigation has been conceived from the beginning as a specific device for treatment of the valve leaflets with calcifications. Compared with the existing lithotripsy balloons, TDD has, for example, the possibility to be placed precisely on the portions of the leaflets to be treated under angiographic and echocardiographic guidance. In addition, although the system employed in our *in vivo* trial consisted of only one piezoelectric transducer, by virtue of the double piezo design that could be implemented in a clinical version, the TDD offers the advantage to treat both sides of the leaflets and

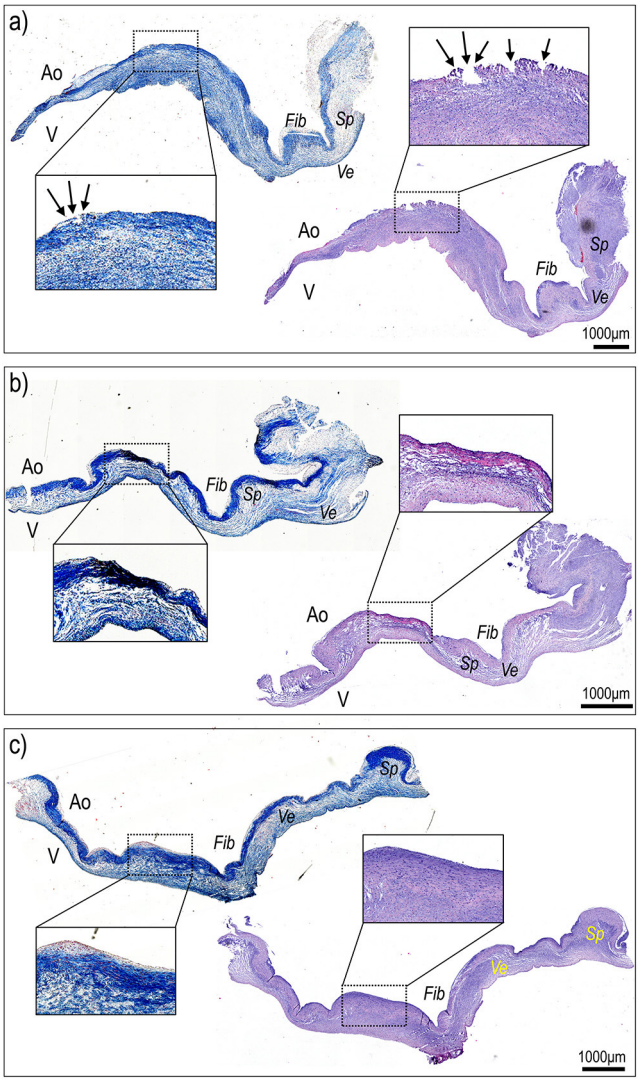


**FIGURE 5 |** Histological sectioning of the right **(a)**, non-coronaric **(b)**, and left **(c)** leaflets of the aortic valve treated with TDD in **Figure 4** from commissure to commissure and along a radial direction stained with hematoxylin/eosin and Masson's staining solutions. The right leaflet, treated with the TDD **(a)**, showed evident signs of superficial damage (arrows in magnification inset) that were contained within the superficial portion of the fibrosa (Fib) identifiable on the aortic (Ao) side of the valve due to its intense blue staining. In no case the ventricular portion (V) or the ventricularis (Ve) or the spongiosa (Sp) layers exhibited signs of tissue damage.

operate with shockwaves with the desired power and frequency to optimize calcium debridement, thereby minimizing tissue damages. Although the system has been designed to reduce the size of the calcium deposits in valves with calcific disease and positively impact on the valve hemodynamics with the recovery of leaflet pliability, another appealing opportunity to employ our system is also to remove calcium deposits from calcified biological prostheses in preparation of TAVR-in-TAVR procedures, to restore leaflets pliability and valve performance in patients with calcified TAVRs, and to reduce the content of the calcium in the valve annulus to reduce paravalvular leak in conventional SAVR with mechanical or bioprosthetic implants. In this regard, the increase in energy delivery (up to 150 V and the presence of a double piezo on both sizes of the leaflets) planned in the next version of the *in vivo* device will help to improve the efficiency of calcium deposits debridement. Accordingly, suitable mechanical tests in a pulse duplicator system will be necessary on treated valves to confirm the variations in hemodynamics after treatment with TDD in its full power configuration.

A possible limitation in the transfer of TDD to the clinics may result from potential pathologic effects of the shockwaves resulting from induction of cellular apoptosis or local or systemic inflammation (27–30) that could lead to rapid tissue re-calcification. In the present study, our primary concern was to demonstrate that delivery of the shockwaves does not determine macroscopic ruptures in the leaflets and the pericardium. Hence, it does not affect the survival of cells inside the treated tissues and performs efficient calcium debridement. Future safety assessment of the TDD will have to be performed *in vivo*, ideally using animal models, i.e., sheep (31), where the possible pathologic evolution of the treated leaflets will be monitored with state-of-the-art systems.

Other important risks that should be considered for clinical implementation of the device are the potential embolization of calcific debris and the thrombogenic effects of possible valve leaflets denudation. Although in the version of the TDD employed in the present study, this component was not present. Our device has been designed to be used with deployment of a distal filter to avoid unwanted debris embolization. To limit the risk due to endothelial denudation and thrombogenicity, tests will finally be conducted with the administration of anticoagulation therapy in animals treated with TDD to monitor the dynamics of reendothelialization of the portions of treated leaflets. In summary, due to the possibility to modulate the frequency and the power of the shockwaves, our new device offers the possibility to promote, at least potentially, *in vivo* valve tissue repair as it has been demonstrated, for example, for the kidney (32).

## DATA AVAILABILITY STATEMENT

The raw data supporting the conclusions of this article will be made available by the authors, without undue reservation.

## ETHICS STATEMENT

The studies involving human participants were reviewed and approved by Ethical Committee - Centro Cardiologico Monzino, IRCCS. The patients/participants provided their written informed consent to participate in this study. The animal study was reviewed and approved by Ministero della Salute.

## AUTHOR CONTRIBUTIONS

EF, DB, MCP, and EP: concieved the device. GB, CR, GG, SR, and MB: performed experiments. DV, MLB, MA, and GP: provided

samples. GB, EF, EP, GG, and MP: revised data and analyzed results. MP: wrote the paper.

## FUNDING

GB, GG, SR, MB, CR, MA, GP, and MP are supported by institutional funding (Ricerca Corrente, Ricerca 5 per mille – Ministero della Salute, Italy). DV and MLB are supported by the local funding program RFO-UNIBO.

## SUPPLEMENTARY MATERIAL

The Supplementary Material for this article can be found online at: https://www.frontiersin.org/articles/10.3389/fcvm.2022.850393/full#supplementary-material

## REFERENCES


1. Coffey S, Roberts-Thomson R, Brown A, Carapetis J, Chen M, Enriquez-Sarano M, et al. Global epidemiology of valvular heart disease. *Nat Rev Cardiol.* (2021) 18:853–64. doi: 10.1038/s41569-021-00570-z
2. Summerhill VI,Moschetta D, Orekhov AN, Poggio P, Myasoedova VA. Sex-specific features of calcific aortic valve disease. *Int J Mol Sci.* (2020) 21:5620. doi: 10.3390/ijms21165620
3. Badiani S, Bhattacharyya S, Aziminia NT, Treibel A, Lloyd G. Moderate aortic stenosis: what is it and when should we intervene? *Interv cardiol.* (2021) 16:e09. doi: 10.15420/icr.2021.04
4. Kanwar A, Thaden JJ, Nkomo VT. Management of patients with aortic valve stenosis. *Mayo Clin Proc.* (2018) 93:488–508. doi: 10.1016/j.mayocp.2018.01.020
5. Porras AM, McCoy CM, Masters KS. Calcific aortic valve disease: a battle of the sexes. *Circ Res.* (2017) 120:604–6. doi: 10.1161/CIRCRESAHA.117.310440
6. Yi B, Zeng W, Lv L, Hua P. Changing epidemiology of calcific aortic valve disease: 30-year trends of incidence, prevalence, and deaths across 204 countries and territories. *Aging.* (2021) 13:12710–32. doi: 10.18632/aging.202942
7. Yutzey KE, Demer LL, Body SC, Huggins GS, Towler DA, Giachelli CM, et al. Calcific aortic valve disease: a consensus summary from the Alliance of Investigators on Calcific Aortic Valve Disease. *Arterioscler Thromb Vasc Biol.* (2014) 34:2387–93. doi: 10.1161/ATVBAHA.114.302523
8. Pellikka PA, Sarano ME, Nishimura RA, Malouf JF, Bailey KR, Scott CG, et al. Outcome of 622 adults with asymptomatic, hemodynamically significant aortic stenosis during prolonged follow-up. *Circulation.* (2005) 111:3290–5. doi: 10.1161/CIRCULATIONAHA.104.495903
9. Lancellotti P, Donal E, Magne J, Moonen M, O'Connor K, Daubert JC, et al. Risk stratification in asymptomatic moderate to severe aortic stenosis: the importance of the valvular, arterial and ventricular interplay. *Heart.* (2010) 96:1364–71. doi: 10.1136/hrt.2009.190942
10. Owens DS, Katz R, Takasu J, Kronmal R, Budoff MJ, O'Brien KD. Incidence and progression of aortic valve calcium in the Multi-ethnic Study of Atherosclerosis (MESA). *Am J Cardiol.* (2010) 105:701–8. doi: 10.1016/j.amjcard.2009.10.071
11. Head SJ, Celik M, Kappetein AP. Mechanical versus bioprosthetic aortic valve replacement. *Eur Heart J.* (2017) 38:2183–91. doi: 10.1093/eurheartj/ehx141
12. Kapadia SR, Leon MB, Makkar RR, Tuzcu EM, Svensson LG, Kodali S, et al. 5-year outcomes of transcatheter aortic valve replacement compared with standard treatment for patients with inoperable aortic stenosis (PARTNER 1): a randomised controlled trial. *Lancet.* (2015) 385:2485–91. doi: 10.1016/S0140-6736(15)60290-2
13. Nahrwold DL. Gallstone lithotripsy. *Am J Surg.* (1993) 165(4):431-4. doi: 10.1016/S0002-9610(05)80935-3
14. Chaussy C, Schmiedt E, Jocham D, Brendel W, Forssmann B, Walther V. First clinical experience with extracorporeally induced destruction of kidney stones by shock waves. *J Urol.* (1982) 127:417–20. doi: 10.1016/S0022-5347(17)53841-0
15. Shrivastava SK, Kailash. Shock wave treatment in medicine. *J Biosci.* (2005) 30:269–75. doi: 10.1007/BF02703708
16. Hill JM, Kereiakes DJ, Shlofmitz RA, Klein AJ, Riley RF, Price MJ, et al. Intravascular lithotripsy for treatment of severely calcified coronary artery disease. *J Am Coll Cardiol.* (2020) 76:2635–46. doi: 10.1016/j.jacc.2020.09.603
17. Forero MNT, Daemen J. The Coronary intravascular lithotripsy system. *Interv cardiol.* (2019) 14:174–81. doi: 10.15420/icr.2019.18.R1
18. Ali ZA, Nef H, Escaned J, Werner N, Banning AP, Hill JM, et al. Safety and effectiveness of coronary intravascular lithotripsy for treatment of severely calcified coronary stenoses: the disrupt CAD II study. *Circ Cardiovasc Interv.* (2019) 12:e008434. doi: 10.1161/CIRCINTERVENTIONS.119.008434
19. Fermi E, Benettin D, Bernava G, Pesce M, Pasquino E. Trans-catheter double-frequency ultrasound ablator for the treatment of aortic valve leaflets calcification. *Biomed J Sci Tech Res.* (2021) 33:25952–57. doi: 10.26717/BJSTR.2021.33.005429
20. Amadeo F, Barbuto M, Bernava G, Savini N, Brioschi M, Rizzi S, et al. Culture into perfusion-assisted bioreactor promotes valve-like tissue maturation of recellularized pericardial membrane. *Front Cardiovasc Med.* (2020) 7:80. doi: 10.3389/fcvm.2020.00080
21. Otto CM, Prendergast B. Aortic-valve stenosis–from patients at risk to severe valve obstruction. *N Engl J Med.* (2014) 371:744–56. doi: 10.1056/NEJMra1313875
22. Sharma A, Bertog S, Mbai M. Transcatheter aortic valve lithotripsy in severely calcified bicuspid aortic stenosis prior to transcatheter aortic valve implantation. *Eur Heart J.* (2021) 42:358. doi: 10.1093/eurheartj/ehaa829
23. Chiam P, Lim Y, Sivathasan C. Transfemoral transcatheter aortic valve implantation facilitated by intravascular ultrasound-guided shockwave lithotripsy: TAVI facilitated by IVUS guided lithotripsy. *AsiaIntervention.* (2021) 7:116–7. doi: 10.4244/AIJ-D-21-00026
24. Sanz-Ruiz R, Gonzalez-Mansilla A, Rivera-Juarez A, Bermejo J, Fernandez-Aviles F. 1-step percutaneous treatment of heavily calcified left-heart valve stenoses. *JACC Cardiovasc Interv.* (2021) 14:e335–7. doi: 10.1016/j.jcin.2021.09.026
25. Sharma A, Kelly R, Mbai M, Chandrashekhar Y, Bertog S. Transcatheter mitral valve lithotripsy as a pretreatment to percutaneous balloon mitral valvuloplasty for heavily calcified rheumatic mitral stenosis. *Circ Cardiovasc Interv.* (2020) 13:e009357. doi: 10.1161/CIRCINTERVENTIONS.120.009357
26. Sardella G, Salvi N, Bruno E, Colantonio R, Mancone M. Lithotripsy-assisted aortic valvuloplasty during TAVR. *JACC Cardiovasc Interv.* (2019) 12:e1312. doi: 10.1016/j.jcin.2019.05.018
27. Zhang B, Zhou H, Cheng Q, Lei L, Hu B. Low-frequency low energy ultrasound combined with microbubbles induces distinct apoptosis of A7r5 cells. *Mol Med Rep.* (2014) 10:3282–8. doi: 10.3892/mmr.2014.2654
28. Zhong W, Sit WH, Wan JM, Yu AC. Sonoporation induces apoptosis and cell cycle arrest in human promyelocytic leukemia cells. *Ultrasound Med Biol.* (2011) 37:2149–59. doi: 10.1016/j.ultrasmedbio.2011.09.012
29. Tabei T, Ito H, Usui K, Kuroda S, Kawahara T, Terao H, et al. Risk factors of systemic inflammation response syndrome after endoscopic combined intrarenal surgery in the modified Valdivia position. *Int J Urol.* (2016) 23:687–92. doi: 10.1111/iju.13124
30. Clark DL, Connors BA, Evan AP, Willis LR, Handa RK, Gao S. Localization of renal oxidative stress and inflammatory response after lithotripsy. *BJU Int.* (2009) 103:1562–8. doi: 10.1111/j.1464-410X.2008.08260.x
31. Gallegos RP, Nockel PJ, Rivard AL, Bianco RW. The current state of in-vivo pre-clinical animal models for heart valve evaluation. *J Heart Valve Dis.* (2005) 14:423–32

32. Klomjit N, Lerman A, Lerman LO. It comes as a shock: kidney repair using shockwave therapy. *Hypertension*. (2020) 76:1696–703. doi: 10.1161/HYPERTENSIONAHA.120.14595

**Conflict of Interest:** EF, DB, MCP, and EP are collaborators of the equity-financed company AorticLab S.r.l. AorticLab S.r.l. is an equity-financed Company for development of the TDD as a novel minimally invasive calcium debridement procedure in human pathologic valves. GG and CR were employed by ASST Fatebenefratelli Sacco.

The remaining authors declare that the research was conducted in the absence of any commercial or financial relationships that could be construed as a potential conflict of interest.

**Publisher's Note:** All claims expressed in this article are solely those of the authors and do not necessarily represent those of their affiliated organizations, or those of the publisher, the editors and the reviewers. Any product that may be evaluated in this article, or claim that may be made by its manufacturer, is not guaranteed or endorsed by the publisher.

frontiers in Cardiovascular Medicine

MINI REVIEW
published: 28 March 2022
doi: 10.3389/fcvm.2022.864341

# Advances in Procedural Echocardiographic Imaging in Transcatheter Edge-to-Edge Repair for Mitral Regurgitation

*Yiting Fan*[1,2], *Jeffrey Shi Kai Chan*[2] *and Alex Pui-Wai Lee*[2*]

[1] Department of Cardiology, Shanghai Chest Hospital, Shanghai Jiao Tong University, Shanghai, China, [2] Laboratory of Cardiac Imaging and 3D Printing, Li Ka Shing Institute of Health Science, The Chinese University of Hong Kong, Hong Kong, China

OPEN ACCESS

**Edited by:**
*Ronak Rajani,*
*Guy's and St Thomas' NHS Foundation Trust, United Kingdom*

**Reviewed by:**
*Robert Siegel,*
*Cedars Sinai Medical Center, United States*
*Alon Shechter,*
*Cedars Sinai Medical Center, United States, in collaboration with reviewer RS*
*Masaki Izumo,*
*St. Marianna University School of Medicine, Japan*
*Kensuke Hirasawa,*
*Leiden University Medical Center, Netherlands*

***Correspondence:**
*Alex Pui-Wai Lee*
*alexpwlee@cuhk.edu.hk*

**Specialty section:**
*This article was submitted to Cardiovascular Imaging, a section of the journal Frontiers in Cardiovascular Medicine*

**Received:** *28 January 2022*
**Accepted:** *07 March 2022*
**Published:** *28 March 2022*

**Citation:**
*Fan Y, Chan JSK and Lee AP-W (2022) Advances in Procedural Echocardiographic Imaging in Transcatheter Edge-to-Edge Repair for Mitral Regurgitation. Front. Cardiovasc. Med. 9:864341. doi: 10.3389/fcvm.2022.864341*

Transcatheter edge-to-edge repair (TEER) therapy is recommended by the American College of Cardiology/American Heart Association (ACC/AHA) guidelines for selected patients with symptomatic severe or moderate-severe mitral regurgitation (MR). Echocardiography, in particular transesophageal echocardiography (TEE), plays a critical role in procedural planning and guidance for TEER. Recent innovations and advances in TEE techniques including three-dimensional (3D) imaging, unlimited x-plane imaging, live 3D multiplanar reconstruction, as well as transillumination imaging with color Doppler and transparency rendering have further enhanced procedural imaging for TEER, especially for complex diseases including commissural defects, clefts, and multi-segment pathologies. This review discusses the technology of these advanced procedural imaging techniques and provides a "step-by-step" guide on how to apply them during the TEER procedure with a focus on their added values in treatment of complex valve lesions.

**Keywords: echocardiography, 3D TEE, TEER, mitral regurgitation, transillumination imaging**

## BACKGROUND

Transcatheter mitral valve (MV) repair is a minimally invasive technique for treatment of selected patients with moderate-severe or severe (3+ or 4+) mitral regurgitation (MR). While several technologies are in clinical development, a transcatheter edge-to-edge repair (TEER) device, the MitraClip™ (Abbott Vascular, Santa Clara, CA, US), is currently the only US Food and Drug Administration approved device for transcatheter MV repair (1–3). Other investigational TEER devices include the PASCAL™ (4) (Edwards Lifesciences, Irvine, CA, US) and the DragonFly™ (5) (Valgen Medical, Hangzhou, China) transcatheter MV repair systems. TEER therapy is recommended by the 2020 ACC/AHA guidelines for selected patients with primary and secondary MR (6). Based on the surgical Alfieri edge-to-edge repair, the MitraClip™ system utilizes a cobalt chromium clip covered with a polypropylene fabric that grasps both the anterior and posterior MV leaflets, thereby reducing MR by increasing the coaptation between the regurgitant valve leaflets. According to the data from the manufacturer, over 100,000 patients have been treated with the MitraClip™ worldwide over the past 17 years. Early experience with the use of TEER therapy was confined to patients with favorable anatomy for the repair procedure, namely, A2-P2 defect, limited flail gap (<10 mm) and width (<15 mm), larger MV area (>4 $cm^2$), long mobile leaflet (≥7 mm), without commissural lesions or clefts (2, 3). With growing implantation experience,

technological improvement in device design, and cumulating outcome data demonstrating clinical benefits, TEER therapy is increasingly used in patients with more complex lesions and less favorable anatomy, including commissural prolapse, multiple lesions, and clefts. Procedural steps common to all TEER systems include analysis of MV anatomy and function, transseptal access to the left atrium (LA), steering of the clip toward MV, and grasping of MV leaflets; these steps are performed under careful procedural imaging guidance, with transesophageal echocardiography (TEE) as the primary imaging modality, and fluoroscopy as adjunct technique. Two-dimensional (2D) TEE has been the standard procedural imaging technique during early clinical experience of the MitraClip$^{TM}$ procedure; the advent of three-dimensional (3D) TEE technology has further enhanced procedural guidance. A combination of 2D and 3D TEE is increasingly used (7–9). The widened spectrum of MV lesions with increased complexity that can now be treated with TEER therapy has stimulated a rapid parallel advances of ultrasound hardware and software to match the increasingly sophisticated procedural imaging demand. In this review, we discuss the technological advances in procedural TEE imaging, and provide a step-by-step guide to applying these new techniques in the TEER procedure.

## ADVANCED TECHNIQUES FOR TEER PROCEDURAL IMAGING—TECHNOLOGICAL CONSIDERATIONS

Introduction of the 3D fully sampled matrix array TEE transducer in the past decade has made possible simultaneous multiplane (or x-plane) and live 3D imaging; more recently, increase in the computing power of ultrasound system and innovations in 3D rendering techniques have led to advances in new imaging techniques. Three new techniques relevant to TEER procedural imaging will be discussed—namely, x-plane imaging with unlimited plane combination, live 3D multiplanar reconstruction (MPR), and transillumination imaging (TI).

## X-PLANE IMAGING WITH UNLIMITED PLANE COMBINATION

X-plane imaging displays two views from the same heartbeat utilizing one acoustic window. The default images are orthogonal (90°) to each other. Typically, the left sector displays the reference imaging plane (A plane) and the right sector displays an adjustable plane (B plane) on which the elevation, lateral tilt, and rotation can be manipulated. X-plane imaging allows visualization of anatomic structures and devices from different imaging planes simultaneously, leading to improved accuracy of measurement and device positioning. In the earlier versions of x-plane imaging offered by most vendors, however, there was a limited combination of plane tilting and rotation—the scan planes are forced to align orthogonal when B plane is tilted and tilting always resets when B plane is rotated (10). This limitation becomes important when commissural MR is treated, as the proper clip arm orientation is rotated to maintain perpendicularity to the line of coaptation at the commissures, where the bicommissural view and the optimal leaflet grasping views are non-orthogonal. In the recently updated version of x-plane imaging, combination of plane tilting and rotation is unlimited, allowing flexible multiplane evaluation with scan planes aligned to cardiac structures with non-orthogonal views when required (11) (**Supplementary Figure 1**).

## LIVE 3D MPR

The 3D data set can be sliced to generate multiple 2D views (as orthogonal planes, parallel slices, or rotated around a common rotation axis)—a process known as MPR (9). MPR allows 2D visualization of cardiac structures which are difficult (sometimes impossible) to obtain directly from traditional 2D imaging. Conventional MPR is performed offline after the 3D data sets are acquired and stored. Live 3D MPR is a new 3D visualization tool that allows free MPR manipulation during real-time imaging for structure/device alignment and measurements (11, 12). Use of live 3D MPR allows simultaneous display of multiple imaging planes (typically two long-axis views and one short-axis view), as well as a 3D en face view, without or with color Doppler. MPR orientation is typically displayed on the volume data as reference view lines. There are several advantages for using live 3D MPR in the guidance of the TEER procedure: (1) the errors of parallax (perceived shift in position of a structure when it is viewed from different angles on 3D echocardiography) can be minimized by simultaneously displaying the 2D views and 3D images; (2) 2D views that are physically impossible to obtain with conventional 2D imaging as a result of the limitation of physical angle of insonation can be reconstructed and displayed; and (3) the need to change views and probe positions for complete assessment can be avoided.

## PHOTOREALISTIC TRANSILLUMINATION IMAGING AND TRANSPARENCY RENDERING

Optimal methods for displaying 3D images are critical for the perception of depth and to provide a clinically useful, high-fidelity images of cardiac structures and devices. Conventional 3D rendering uses shading techniques to encode voxels based on their distance, gray-level gradient, and texture to generate a 3D display of cardiac structures; these techniques do not consistently provide images with adequate detail definition and depth perception. A novel rendering technique known as transillumination imaging (TI) adds a virtual light source and simulates light-tissue interactions, including absorption, scattering and reflection, resulting in a photorealistic image with shadows that highlight structures and enhance depth perception (13, 14). The light source is freely movable within the volume to illuminate specific structures. It has been shown that TI enhances the sense of depth and space, producing images that appear more realistic to the human eye, which facilitates the detection of subtle structures and pathologies, such as ruptured chordae

and clefts. TI with transparency rendering is a modification of the TI technique that highlights interface between tissue and blood within the 3D data set (15). TI with transparency displays tissue as transparent while showing the blood/tissue border as a colored contour, allowing the operator to adjust the degree of transparency in order to provide better delineation of cardiac anatomy and devices. Additionally, TI has the ability to superimpose 3D color Doppler onto 3D anatomic data with tissue transparency in order to refine the visualization of MR jet origin before and after the TEER procedure (16).

## PROCEDURAL IMAGING IN TEER USING ADVANCED ECHOCARDIOGRAPHIC TECHNIQUES—STEP-BY-STEP

Procedural imaging in TEER should follow a standard protocol involving the following steps: preprocedural analysis of the MV anatomy and function, transseptal puncture, introduction of the steerable guide into the LA, steering and positioning of the clip, grasping, leaflet insertion assessment, and pre-deployment evaluation. An integrative imaging approach combining the proper use of 2D, Doppler, and advanced 3D techniques as indicated by the imaging goal of each procedural step should be adopted. This review highlights the steps in which the abovementioned advanced imaging techniques have added value, especially for complex lesions, and describes the practical steps to apply them during the procedure.

## PRE-PROCEDURAL ANALYSIS OF VALVE ANATOMY AND FUNCTION

Procedural imaging for TEER starts with pre-procedural planning of clips strategy (location, size, and numbers of clip to be implanted) with detail analysis of the valve anatomy and function. The Carpentier nomenclature of the MV scallops divides the valve into 6 segments (A1, A2, A3, P1, P2, and P3). Live 3D MPR is particularly suited for segmental analysis of leaflet edge anatomy. Typically, the reconstructed bicommissural view, long-axis view, short-axis MV view, and a 3D en face image are displayed. By positioning the long-axis plane at each leaflet segment, the leaflet edge anatomy and function of each segment is systematically evaluated along the whole line of coaptation (**Figure 1A**); any prolapse, flail, billowing, tethering, clefts, and calcifications are documented. In fact, as the lesion location and the optimal clip implantation position can vary by only a few millimeters, a TEER-specific nomenclature dividing the leaflets into more, smaller segments may be required for more precise localization and communication (e.g., the lateral 1/3 of P2 can be called P2L). Segmental analysis with live 3D MPR is particularly important for treating complex lesions with multi-segment pathologies. In degenerative MR due to diffuse myxomatous disease, it is important to differentiate prolapsing from billowing segments, as the former has genuine loss of leaflet edge coaptation (hence becomes the MR origin) and could be the primary target site for clip implantation (1, 17, 18). Pure billowing, on the other hand, does not contribute to MR and may not require clipping. Calcifications of leaflet grasping zone may preclude clip implantation in the relevant segment, and clefts or deep indentations may need specialized clips strategy (19). The added advantage of live 3D MPR over plain 2D (including simultaneous biplane) imaging is the simultaneous display of 2D planes and 3D views, allowing guided alignment of the reconstructed long-axis 2D plane to be perpendicular to the line of coaptation; this technique allows the length of leaflet segment available for grasping to be measured with improved accuracy. Similarly, the flail width, flail gap, and MV area can be measured with higher accuracy by adjusting the 2D planes to the correct positions according to the anatomy (20, 21). Importantly, interrogation of a smaller 3D volume can be performed during 3D imaging to compensate for the relative reduction of spatial resolution and frame rates, reducing measurement error. The 3D image of the MV should be viewed from both the atrial (**Figure 1B**) and ventricular (**Figure 1C**) perspectives for visualization of leaflet clefts or indentations, which can be better appreciated with the use of TI (**Figures 1B,C**). TI with color Doppler and transparency rendering could enhance 3D visualization of the origin(s) of the MR jet(s) (16) (**Figure 1D**).

## TRANSSEPTAL PUNCTURE

The goal of transseptal puncture is to ensure the clip delivery system crosses the atrial septum at an appropriate distance (the transseptal height) from mitral annular level according to leaflet anatomy and function. An optimal transseptal height allows appropriate alignment of the clip to adequate trajectory toward the mitral leaflets for proper grasping. Typically, transseptal puncture is performed at the superior and posterior-mid aspect of the fossa ovalis to achieve a transseptal height of 4–4.5 cm (**Supplementary Figure 2**). The bicaval (∼90°) view and short-axis (∼45°) view guide transseptal puncture in, respectively, superoinferior and anteroposterior direction by monitoring tenting of fossa ovalis by the Brockenbrough™ needle. It is important to have the aortic valve visualized in the 45° short-axis view to ensure puncture is performed away from the aorta. However, bi-caval and short-axis planes are in fact ∼45° (non-orthogonal) to each other; in the previous version of x-plane imaging, when A plane is used to show the bi-caval view, tilting of B plane to "chase" the needle resets the short-axis B plane to 0°, and aorta becomes out of sight. The new x-plane imaging with unlimited plane combination has important added advantage by allowing tilting of B plane without resetting its rotation to allow visualization of aorta throughout the puncture process and minimizes the chance of aortic injury (**Supplementary Figure 3**). Fine adjustment of transseptal height (±5 mm) may be required according to leaflet anatomy and function: flail leaflets or prolapse requires a higher while functional MR with tethered leaflets requires a lower transseptal height, owing to the different level of leaflet coaptation relative to the annulus. On the other hand, transseptal height should be higher for medial and lower for lateral commissural MR, because the clip delivery system gains height as it travels laterally. Moreover, the medial commissure is more caudal and the lateral

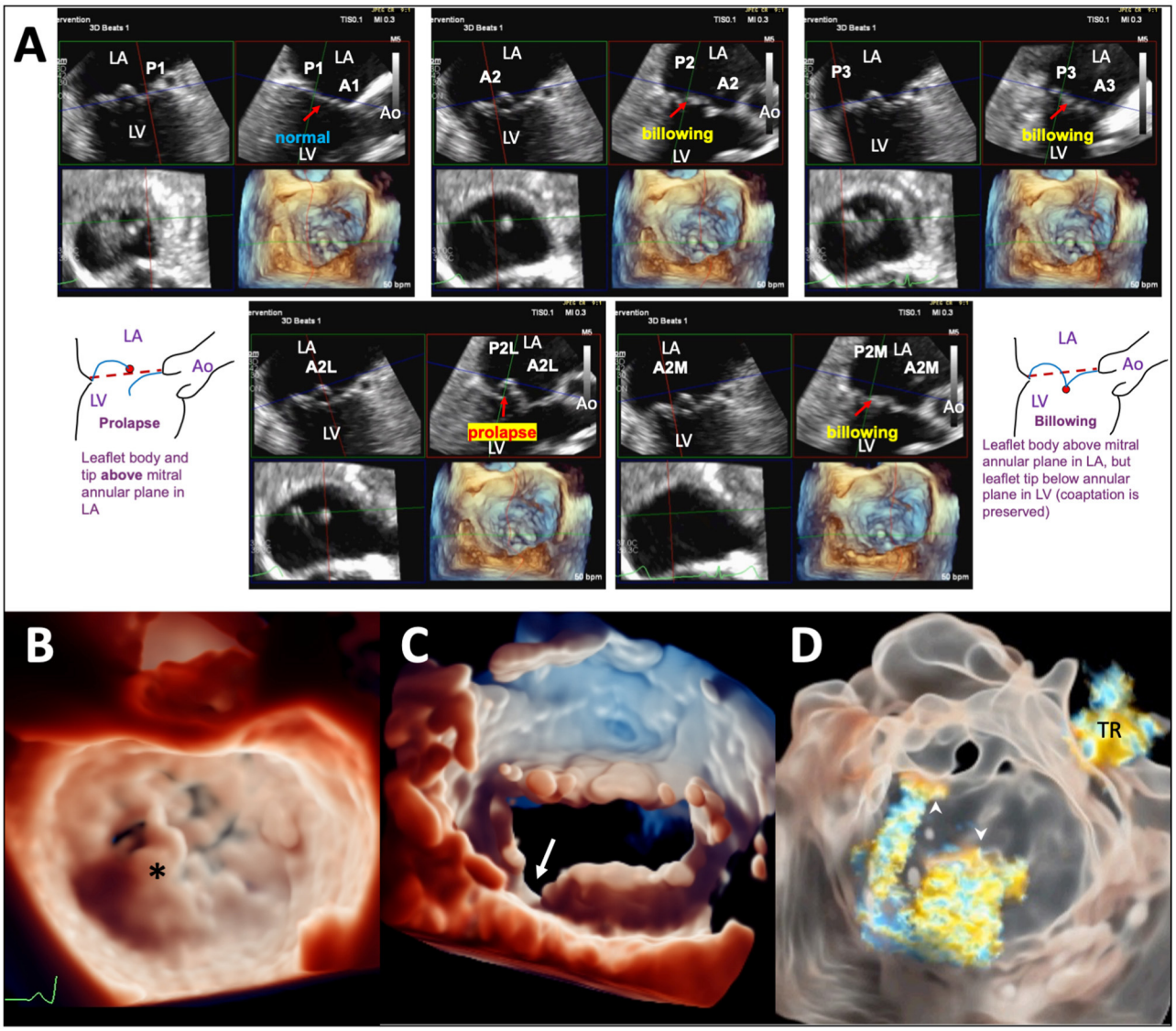


**FIGURE 1 |** Pre-TEER analysis of MV anatomy and function using advanced TEE imaging techniques. **(A)** Segmental analysis of leaflet edge anatomy using live 3D MPR on 3D TEE data set of a patients with diffuse myxomatous MV disease. Prolapse is seen in the lateral part of the A2 segment (A2L); other segments show either leaflet billowing or normal leaflet motion. **(B)** TI in a patient with a flail P2 segment (*). **(C)** TI of the MV viewed from the LV perspective highlighting a leaflet cleft/deep indentation (arrow) between P2 and P3. **(D)** TI with transparency rendering in a patient with MR of mixed etiologies showing the origins of 2 separate MR jets (arrowheads), one at A2-P2 (secondary MR component) and another from a perforation of the anterior leaflet near the left trigone (primary MR component). A tricuspid regurgitation (TR) jet is also visualized. Ao, aorta; LA, left atrium; LV, left ventricle; A2L, lateral 1/3 of A2; A2M, medial 1/3 of A2; P2L, lateral 1/3 of P2; P2M, medial 1/3 of P2.

commissure more cephalic; therefore, supero-inferior position of transseptal puncture may need to be adjusted accordingly for treatment of commissural MR (19). Unfortunately, it is difficult to appreciate the relationship between transseptal puncture site and MV commissures on 2D imaging; 3D imaging has added value by demonstrating the distance and position of transseptal puncture relative to mitral commissures and leaflets in the 3D en face view (**Figure 2A**). Furthermore, TI with lighting source behind fossa ovalis is valuable for assessing soft tissue thickness and enhances 3D perception of anatomic relations with mitral leaflets, providing additional information for guiding transseptal puncture (**Figure 2B**).

## CLIP STEERING AND POSITIONING

Once the guide catheter is correctly positioned, the clip delivery system is inserted and advanced through the guide into the LA. As movement of the clip delivery system in LA is 3-dimensional (antero-posterior, septo-lateral, and deflection toward MV), 3D

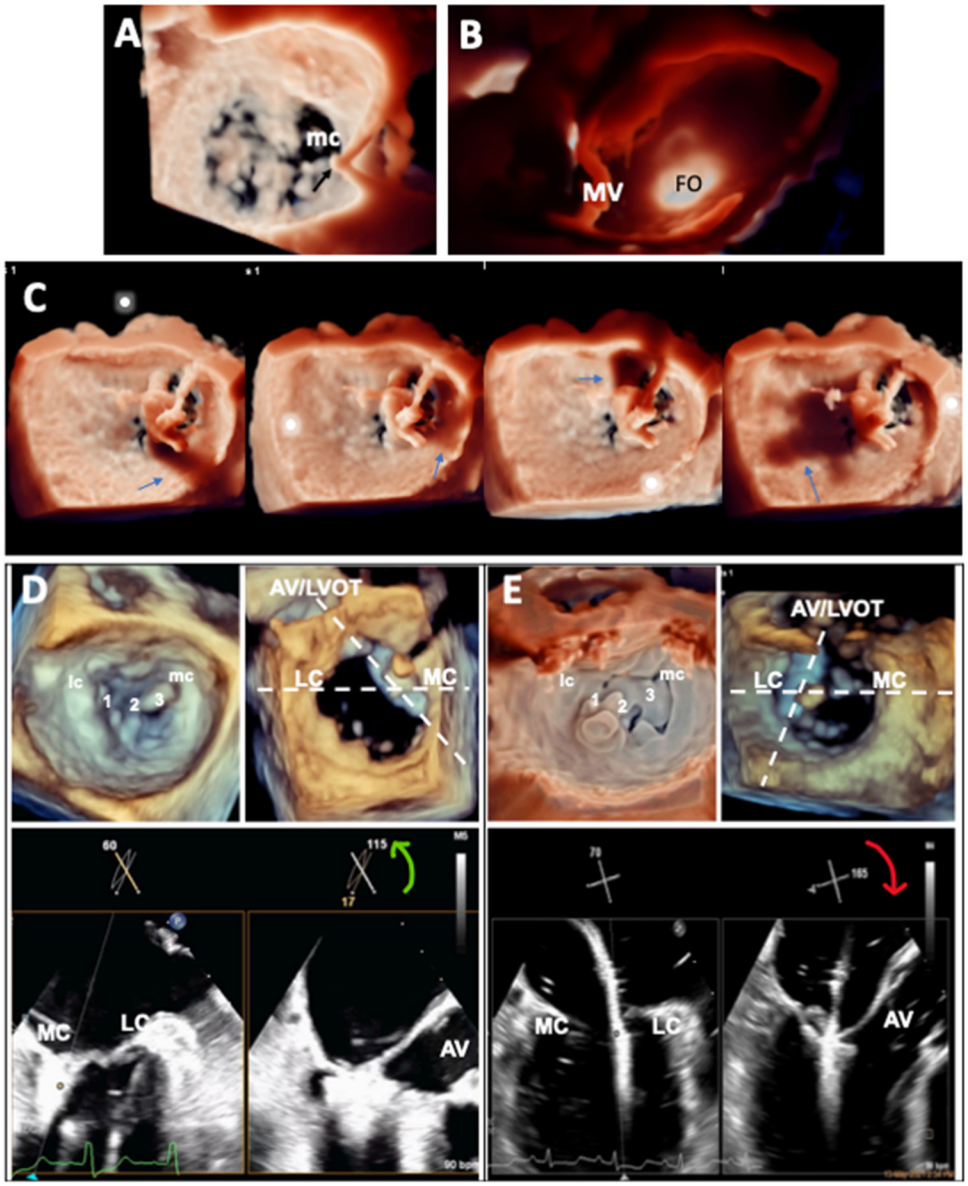


**FIGURE 2 |** Application of advanced TEE imaging in the guidance of mitral TEER procedure. **(A)** 3D en face view of the MV showing the position of tenting of the atrial septum by the transseptal puncture needle and its relationship with the medial commissure (mc) of the MV. **(B)** TI of the atrial septum showing the position of the fossa ovalis (FO) and its relationship with the MV. **(C)** TI with the virtual light source at different positions in the LA casting shadows (arrows) of the clip to enhance 3D perception of distance of the clip from adjacent structures during clip steering. **(D,E)** X-plane imaging (bicommissural and long-axis views) with simultaneous independent tilting and rotation facilitating leaflet grasping for medial **(D)** and lateral **(E)** commissural prolapse.

imaging is superior to 2D imaging in guiding the steering process without needing to change views (22). Additionally, TI with lighting source in LA enhances 3D perception by casting shadows of the clip on surrounding structures, and helps to confirm the clip is free from LA wall and valve tissue to avoid cardiac injury (**Figure 2C**). The goals of steering are to align the clip to a trajectory perpendicular to the plane of the MV and to position the clip to the target lesion/MR origin. X-plane imaging with simultaneous display of the bicommissural and long-axis views, combined with fluoroscopy, is often used to check clip trajectory. However, 2D imaging may occasionally be difficult to confirm axiality of clip trajectory as the clip path may be out of plane despite meticulous probe manipulation. This may be more likely in complex procedures, such as treatment of commissural MR or when the LA is severely dilated. Live 3D MPR has a unique advantage by displaying simultaneously the reconstructed 2D bicommissural plane (M/L alignment) and long-axis plane (A/P alignment), as well as the 3D en face view

of the MV (clip arms perpendicularity to line of coaptation); orientations of MPR can be aligned co-axial to the delivery catheter shaft (**Supplementary Video 1**) and clip trajectory can be observed and adjusted in real-time (23). Failure to confirm that the clip arms are perpendicular to the line of coaptation may result in loss of leaflet capture and insertion. Clip arms perpendicularity is best confirmed on 3D imaging. In the en face "surgeon view", the open clip arms are oriented 12-6 o'clock (with aortic valve at 12 o'clock) to be perpendicular to the coaptation line at A2/P2; but for peripheral or commissural defects, because the coaptation line is curved like "smiley face" the clip arms should be rotated clockwise or counterclockwise to achieve perpendicularity for, respectively, lateral (A1/P1/lateral commissural) or medial (A3/P3/medial commissural) defects.

## LEAFLET GRASPING AND PRE-DEPLOYMENT EVALUATION

After verification of axial trajectory and clip arms perpendicularity, the clip is advanced into LV; after rechecking clip orientation below the MV, the clip is partially closed and brought up to grasp the leaflets. Leaflet grasping is best performed by using x-plane imaging (bicommissural and long-axis) (24, 25). Proper grasping requires both clip arms to be seen within the long-axis grasping plane. The intersection angles between the bicommissural and grasping planes at the peripheral segments are non-orthogonal (26). For lateral defects (A1/P1/lateral commissure), lateral tilt and clockwise rotation of B plane should get the proper grasping view; for medial defects (A3/P3/medial commissure) medial tilt and counterclockwise rotation will be needed. One easier way to remember which way to rotate is that the B plane rotation follows the same direction as clip rotation to achieve perpendicularity on the 3D *en face* image (**Figures 2D,E**). Similarly, live 3D MPR can be useful to display the proper bicommissural and grasping plane to monitor leaflet capture in patients whose 2D planes are not easy or possible to obtain with x-plane imaging (27). The orientations of the live-reconstructed 2D planes can be adjusted to follow the device direction and position during real-time grasping (23). Specific structures can be identified and located correctly on the 3D image, which is particularly helpful when multiple clips are implanted (**Supplementary Video 2**). Leaflet insertion and MR reduction should be confirmed before clip deployment. MPR is helpful in confirming leaflet insertion (23, 28) by calculating the difference of the leaflet length outside the clip measured in the long-axis plane on the clip and the entire leaflet length measured in the parallel planes just beside the clip (**Supplementary Figure 4**). In addition to the bicommissural/long-axis x-plane imaging, 3D color-Doppler imaging using TI with tissue transparency adds visual information of localization of any residual MR jet origin (16) (**Supplementary Video 3**).

## CONCLUSION AND FUTURE PERSPECTIVES

Advanced procedural TEE 3D imaging and related techniques have incremental practical value in procedural guidance for TEER especially in complex procedures. New hybrid, or fusion, imaging technology allows for 3D TEE to be overlaid on fluoroscopy to provide the most pertinent information from both imaging modalities on a single screen, and may improve safety and efficacy of the TEER procedure (29). In future, technological improvement in 3D imaging especially on resolution and frame rates (30), as well as the advent of full-volume 3D intracardiac echocardiography technique (12), will likely further enhance the use of 3D echocardiography in procedural imaging to simplify and optimize procedural guidance for structural heart interventions.

## AUTHOR CONTRIBUTIONS

YF and JC were responsible for drafting of the manuscript. AL was responsible for conceptualization and revision of the manuscript. All authors contributed to the article and approved the submitted version.

## FUNDING

This work was supported by the Hong Kong Health and Medical Research Fund (05160976).

## SUPPLEMENTARY MATERIAL

The Supplementary Material for this article can be found online at: https://www.frontiersin.org/articles/10.3389/fcvm.2022.864341/full#supplementary-material

## REFERENCES

1. Lee AP, Fan Y, Baig FN, Lam YY. Mechanisms of mitral regurgitation. *JACC Asia*. (2021) 1:115–6. doi: 10.1016/j.jacasi.2021.04.004
2. Feldman T, Foster E, Glower DD, Kar S, Rinaldi MJ, Fail PS, et al. Percutaneous repair or surgery for mitral regurgitation. *N Engl J Med*. (2011) 364:1395–406. doi: 10.1056/NEJMoa1009355
3. Stone GW, Lindenfeld J, Abraham WT, Kar S, Lim DS, Mishell JM, et al. Transcatheter mitral-valve repair in patients with heart failure. *N Engl J Med*. (2018) 379:2307–18. doi: 10.1056/NEJMoa1806640
4. Szerlip M, Spargias KS, Makkar R, Kar S, Kipperman RM, O'Neill WW, et al. 2-Year outcomes for transcatheter repair in patients with mitral regurgitation from the CLASP study. *JACC Cardiovasc Interv*. (2021) 14:1538–48. doi: 10.1016/j.jcin.2021.04.001
5. Liu X, Pu Z, Lim DS, Wang J. Transcatheter mitral valve repair in a high-surgical risk patient with severe degenerative mitral regurgitation using the novel DragonFly Transcatheter Repair device-First in man implantation in China. *Catheter Cardiovasc Interv*. (2021) 99:518–21. doi: 10.1002/ccd.29687
6. Otto CM, Nishimura RA, Bonow RO, Carabello BA, Erwin JP III, Gentile F, et al. 2020 ACC/AHA guideline for the management of patients with valvular heart disease: a report of the American College of Cardiology/American Heart Association joint committee on clinical practice guidelines. *Circulation*. (2021) 143:e35–71. doi: 10.1161/CIR.0000000000000923

7. Wunderlich NC, Siegel RJ. Peri-interventional echo assessment for the MitraClip procedure. *Eur Heart J Cardiovasc Imaging*. (2013) 14:935–49. doi: 10.1093/ehjci/jet060
8. Biner S, Perk G, Kar S, Rafique AM, Slater J, Shiota T, et al. Utility of combined two-dimensional and three-dimensional transesophageal imaging for catheter-based mitral valve clip repair of mitral regurgitation. *J Am Soc Echocardiogr*. (2011) 24:611–7. doi: 10.1016/j.echo.2011.02.005
9. Lee AP, Lam YY, Yip GW, Lang RM, Zhang Q, Yu CM. Role of real time three-dimensional transesophageal echocardiography in guidance of interventional procedures in cardiology. *Heart*. (2010) 96:1485–93. doi: 10.1136/hrt.2009.190025
10. Katz WE, Conrad Smith AJ, Crock FW, Cavalcante JL. Echocardiographic evaluation and guidance for MitraClip procedure. *Cardiovasc Diagn Ther*. (2017) 7:616–32. doi: 10.21037/cdt.2017.07.04
11. Hahn RT, Saric M, Faletra FF, Garg R, Gillam LD, Horton K, et al. Recommended standards for the performance of transesophageal echocardiographic screening for structural heart intervention: from the American Society of Echocardiography. *J Am Soc Echocardiogr*. (2022) 35:1–76. doi: 10.1016/j.echo.2021.07.006
12. Patzelt J, Schreieck J, Camus E, Gawaz M, Seizer P, Langer HF. Percutaneous mitral valve edge-to-edge repair using volume intracardiac echocardiography-first in human experience. *CASE*. (2017) 1:41–3. doi: 10.1016/j.case.2017.01.006
13. Genovese D, Addetia K, Kebed K, Kruse E, Yamat M, Narang A, et al. First clinical experience with 3-dimensional echocardiographic transillumination rendering. *JACC Cardiovasc Imaging*. (2019) 12:1868–71. doi: 10.1016/j.jcmg.2018.12.012
14. Fan Y, Kam K, So K, Lam YY, Lee AP. Imaging for transcatheter edge-to-edge repair for tricuspid regurgitation in Ebstein anomaly. *Circ Cardiovasc Imaging*. (2021) 14:e013327. doi: 10.1161/CIRCIMAGING.121.013327
15. Karagodin I, Addetia K, Singh A, Dow A, Rivera L, DeCara JM, et al. Improved delineation of cardiac pathology using a novel three-dimensional echocardiographic tissue transparency tool. *J Am Soc Echocardiogr*. (2020) 33:1316–23. doi: 10.1016/j.echo.2020.08.005
16. Barreiro-Perez M, Cruz-González I, Martin-Moreiras J, Diaz-Pelaez E, Nuñez Jean C, Luengo-Mondéjar P, et al. Transillumination and tissue-transparency photo-realistic echocardiography imaging during percutaneous mitral valve interventions. *JACC Cardiovasc Interv*. (2021) 14:919–22. doi: 10.1016/j.jcin.2021.01.034
17. Lancellotti P, Tribouilloy C, Hagendorff A, Popescu BA, Edvardsen T, Pierard LA, et al. Recommendations for the echocardiographic assessment of native valvular regurgitation: an executive summary from the European Association of Cardiovascular Imaging. *Eur Heart J Cardiovasc Imaging*. (2013) 14:611–44. doi: 10.1093/ehjci/jet105
18. Lee AP, Hsiung MC, Salgo IS, Fang F, Xie JM, Zhang YC, et al. Quantitative analysis of mitral valve morphology in mitral valve prolapse with real-time 3-dimensional echocardiography: importance of annular saddle shape in the pathogenesis of mitral regurgitation. *Circulation*. (2013) 127:832–41. doi: 10.1161/CIRCULATIONAHA.112.118083
19. Gavazzoni M, Taramasso M, Zuber M, Russo G, Pozzoli A, Miura M, et al. Conceiving MitraClip as a tool: percutaneous edge-to-edge repair in complex mitral valve anatomies. *Eur Heart J Cardiovasc Imaging*. (2020) 21:1059–67. doi: 10.1093/ehjci/jeaa062
20. Bushari LI, Reeder GS, Eleid MF, Chandrasekaran K, Eriquez-Sarano M, Rihal CS, et al. Percutaneous transcatheter edge-to-edge mitraclip technique: a practical "Step-by-step" 3-dimensional transesophageal echocardiography guide. *Mayo Clin Proc*. (2019) 94:89–102. doi: 10.1016/j.mayocp.2018.10.007
21. Zhong X, Chen W, Shi Z, Huan Z, Ma L, Liu W, et al. Three-dimensional transesophageal echocardiography measurement of mitral valve area in patients with rheumatic mitral stenosis: multiplanar reconstruction or 3D direct planimetry? *Int J Cardiovasc Imaging*. (2021) 37:99–107. doi: 10.1007/s10554-020-01950-1
22. Altiok E, Becker M, Hamada S, Reith S, Marx N, Hoffmann R. Optimized guidance of percutaneous edge-to edge repair of the mitral valve using real-time 3-D transesophageal echocardiography. *Clin Res Cardiol*. (2011) 100:675–81. doi: 10.1007/s00392-011-0296-1
23. Harb SC, Krishnaswamy A, Kapadia SR, Miyasaka RL. The added value of 3D real-time multiplanar reconstruction for intraprocedural guidance of challenging MitraClip cases. *JACC Cardiovasc Imaging*. (2020) 13:1809–14. doi: 10.1016/j.jcmg.2019.11.014
24. Ancona F, Stella S, Capogrosso C, Melillo F, Ingallina G, Boccellino A, et al. Intraprocedural guidance in percutaneous mitral valve repair. *Mini Invasive Surg*. (2020) 4:79. doi: 10.20517/2574-1225.2020.80
25. Hahn RT. Transcathether valve replacement and valve repair: review of procedures and intraprocedural echocardiographic imaging. *Circ Res*. (2016) 119:341–56. doi: 10.1161/CIRCRESAHA.116.307972
26. Estevez-Loureiro R, Franzen O, Winter R, Sondergaard L, Jacobsen P, Cheung G, et al. Echocardiographic and clinical outcomes of central versus noncentral percutaneous edge-to-edge repair of degenerative mitral regurgitation. *J Am Coll Cardiol*. (2013) 62:2370–7. doi: 10.1016/j.jacc.2013.05.093
27. Wang TKM, Harb SC, Miyasaka RL, Wagener J, Krishnaswamy A, Reed GK, et al. Live three-dimensional multiplanar reconstruction imaging guidance for concomitant mitral and tricuspid valve repairs using the MitraClip. *CASE*. (2020) 4:119–26. doi: 10.1016/j.case.2020.01.002
28. Melillo F, Ancona F, Calvo F, Fisicaro A, Stella S, Capogrosso C, et al. Loss of leaflet insertion after percutaneous mitral valve repair requiring left ventricular assist device implantation: usefulness of 3D multiplanar reconstruction. *J Invasive Cardiol*. (2019) 31:E274–6.
29. Faletra FF, Pozzoli A, Agricola E, Guidotti A, Biasco L, Leo LA, et al. Echocardiographic-fluoroscopic fusion imaging for transcatheter mitral valve repair guidance. *Eur Heart J Cardiovasc Imaging*. (2018) 19:715–26. doi: 10.1093/ehjci/jey067
30. Faletra FF, Pedrazzini G, Pasotti E, Muzzarelli S, Dequarti MC, Murzilli R, et al. 3D TEE during catheter-based interventions. *JACC Cardiovasc Imaging*. (2014) 7:292–308. doi: 10.1016/j.jcmg.2013.10.012


**Conflict of Interest:** AL is a speaker and consultant for Abbott Structural and Philips Healthcare.

The remaining authors declare that the research was conducted in the absence of any commercial or financial relationships that could be construed as a potential conflict of interest.

frontiers | Frontiers in Cardiovascular Medicine

ORIGINAL RESEARCH
published: 01 April 2022
doi: 10.3389/fcvm.2022.852954

# Prognosis of Paradoxical Low-Flow Low-Gradient Aortic Stenosis: A Severe, Non-critical Form, With Surgical Treatment Benefits

*Laura Galian-Gay[1], Roxana Andreina Escalona Silva[1], Gisela Teixidó-Turà[1], Guillem Casas[1], Elena Ferrer-Sistach[2], Cristina Mitroi[3], Susana Mingo[3], Vanessa Monivas[3], Daniel Saura[4], Bàrbara Vidal[5], Livia Trasca[5], Sergio Moral[6], Francisco Calvo[7], Maria Castiñeira Busto[7], Violeta Sánchez[8], Ariana Gonzalez[9], Gabriela Guzman[10], Marta Noris Mora[11], MiguelÁngel Arnau Vives[12], Jesús Peteiro[13], Alberto Bouzas[13], Aleksandra Mas-Stachurska[14], Teresa González-Alujas[1], Laura Gutiérrez[1], Rubén Fernandez-Galera[1], Filipa Valente[1], Andrea Guala[1], Aroa Ruiz-Muñoz[1], Cesar Augusto Sao Avilés[1], José F. Rodríguez Palomares[1], Ignacio Ferreira[1]* and Artur Evangelista[1]**

[1] Department of Cardiology, Hospital Universitari Vall d'Hebron, CIBER-CV, Universitat Autònoma de Barcelona, Barcelona, Spain, [2] Department of Cardiology, Hospital Universitari Germans Tries i Pujol, Badalona, Spain, [3] Department of Cardiology, Hospital Puerta de Hierro - Majadahonda, Madrid, Spain, [4] Department of Cardiology, CIBER-CV, Hospital Clínico Universitario Virgen de la Arrixaca, Murcia, Spain, [5] Department of Cardiology, Hospital Clínic de Barcelona, Barcelona, Spain, [6] Department of Cardiology, Hospital Josep Trueta, Girona, Spain, [7] Department of Cardiology, Hospital Alvaro Cunqueiro, Vigo, Spain, [8] Department of Cardiology, CIBER-CV, Hospital Universitario 12 de Octubre, Madrid, Spain, [9] Department of Cardiology, Hospital Ramón y Cajal, Madrid, Spain, [10] Department of Cardiology, Hospital Universitario La Paz, Madrid, Spain, [11] Department of Cardiology, Hospital Universitario Son Espases, IdISBa, Mallorca, Spain, [12] Department of Cardiology, Hospital Universitario y Politécnico La Fe, Valencia, Spain, [13] Department of Cardiology, CIBER-CV, Complexo Hospitalario Universitario A Coruña, Coruña, Spain, [14] Department of Cardiology, Hospital del Mar – Parc de Salut Mar, Barcelona, Spain

**Objectives:** To determine the risk of mortality and need for aortic valve replacement (AVR) in patients with low-flow low-gradient (LFLG) aortic stenosis (AS).

**Methods:** A longitudinal multicentre study including consecutive patients with severe AS (aortic valve area [AVA] $< 1.0$ cm$^2$) and normal left ventricular ejection fraction (LVEF). Patients were classified as: high-gradient (HG, mean gradient $\geq 40$ mmHg), normal-flow low-gradient (NFLG, mean gradient $< 40$ mmHg, indexed systolic volume (SVi) $> 35$ ml/m²) and LFLG (mean gradient $< 40$ mmHg, SVi $\leq 35$ ml/m²).

**Results:** Of 1,391 patients, 147 (10.5%) had LFLG, 752 (54.1%) HG, and 492 (35.4%) NFLG. Echocardiographic parameters of the LFLG group showed similar AVA to the HG group but with less severity in the dimensionless index, calcification, and hypertrophy. The HG group required AVR earlier than NFLG ($p < 0.001$) and LFLG ($p < 0.001$), with no differences between LFLG and NFLG groups ($p = 0.358$). Overall mortality was 27.7% (*CI* 95% 25.3–30.1) with no differences among groups ($p = 0.319$). The impact of AVR in terms of overall mortality reduction was observed the most in patients with HG (hazard ratio [*HR*]: 0.17; 95% *CI*: 0.12–0.23; $p < 0.001$), followed by patients with LFLG (*HR*: 0.25; 95% *CI*: 0.13–0.49; $p < 0.001$), and finally patients with NFLG (*HR*: 0.29; 95% *CI*: 0.20–0.44; $p < 0.001$), with a risk reduction of 84, 75, and 71%, respectively.

OPEN ACCESS

**Edited by:**
Ronak Rajani,
Guy's and St Thomas' NHS Foundation Trust, United Kingdom

**Reviewed by:**
Choon Hwai Yap,
Imperial College London, United Kingdom
Chiara De Biase,
Centro Sanitario Locale Napoli 1 Centro, Italy

***Correspondence:**
Artur Evangelista
arturevangelistamasip@gmail.com
Ignacio Ferreira
nachoferreira@secardiologia.es

**Specialty section:**
This article was submitted to Heart Valve Disease, a section of the journal Frontiers in Cardiovascular Medicine

**Received:** 11 January 2022
**Accepted:** 07 February 2022
**Published:** 01 April 2022

**Citation:**
Galian-Gay L, Escalona Silva RA, Teixidó-Turà G, Casas G, Ferrer-Sistach E, Mitroi C, Mingo S, Monivas V, Saura D, Vidal B, Trasca L, Moral S, Calvo F, Castiñeira Busto M, Sánchez V, Gonzalez A, Guzman G, Mora MN, Arnau Vives M, Peteiro J, Bouzas A, Mas-Stachurska A, González-Alujas T, Gutiérrez L, Fernandez-Galera R, Valente F, Guala A, Ruiz-Muñoz A, Avilés CAS, Palomares JFR, Ferreira I and Evangelista A (2022) Prognosis of Paradoxical Low-Flow Low-Gradient Aortic Stenosis: A Severe, Non-critical Form, With Surgical Treatment Benefits. *Front. Cardiovasc. Med.* 9:852954. doi: 10.3389/fcvm.2022.852954

**Conclusions:** Paradoxical LFLG AS affects 10.5% of severe AS, and has a lower need for AVR than the HG group and similar to the NFLG group, with no differences in mortality. AVR had a lower impact on LFLG AS compared with HG AS. Therefore, the findings of the present study showed LFLG AS to have an intermediate clinical risk profile between the HG and NFHG groups.

**Keywords: aortic stenosis, paradoxical low-flow low-gradient, echocardiography, aortic valve surgery, heart valve disease**

## INTRODUCTION

Degenerative aortic stenosis (AS) is the most common valve disease in developed countries and, owing to aging of the population, threatens to become a true epidemic in coming decades (1). Paradoxical low-flow low-gradient (LFLG) AS poses diagnostic challenges and uncertainties regarding the true severity of the disease and appropriate therapeutic decision-making. Initial studies considered LFLG AS to be an entity with worse prognosis than high-gradient (HG) AS and could thus benefit from surgical or percutaneous treatment as or earlier than in HG AS (2–4). However, recent meta-analyses questioned these results, considering that LFLG AS probably behaves in an intermediate manner between moderate and severe AS (5–8). The present study aimed to assess, in a large and contemporary cohort of patients with AS, the natural history and prognosis of LFLG AS in comparison with HG and normal-flow low-gradient (NFLG) AS, as well as the impact of aortic valve replacement (AVR) in each subgroup.

## MATERIALS AND METHODS

A retrospective longitudinal observational study was conducted of consecutive patients from 14 tertiary hospitals nationwide diagnosed between 2008 and 2016 with severe AS (aortic valve area (AVA) $<1.0$ cm$^2$) with left ventricular ejection fraction (LVEF) $\geq$ 50% on the transthoracic ECG (**Figure 1**). Exclusion criteria were: age $<18$ years, atrial fibrillation or pacemaker rhythm, aortic regurgitation more than mild, other valvular heart disease more than mild, left ventricular outflow tract dynamic gradient exceeding a velocity $>1$ m/s, previous heart surgery, suboptimal echocardiographic window, poor blood pressure control, and comorbidities at baseline that could themselves cause an alteration in functional grade or prognosis (e.g., severe chronic obstructive pulmonary disease [COPD]).

The approval for the study was obtained from the Ethics Committee of the Vall d'Hebron Hospital (PR (AG) 60/2018). The study protocol conformed to the ethical guidelines of the Declaration of Helsinki 1975 as reflected in the Ethics Committee approval.

Baseline demographic and clinical data were collected. The presence of coronary artery disease was defined when a history of acute myocardial infarction, significant ischaemic or the presence of coronary artery disease were documented. The presence of baseline symptoms was considered when the functional status of the New York Heart Association was $\geq$ II, or syncope or angina was reported in clinical reports. Follow-up clinical data, such as the need for surgery or TAVI, status (alive/deceased), and cause of death (cardiovascular/non-cardiovascular) were also obtained. AVR was indicated at the participating centers according to current guideline indications (9).

Echocardiographic studies were performed in all patients by expert imaging cardiologists at the participating centers. Measurements were obtained following European Association of Cardiovascular Imaging (EACVI) standards and were validated by a senior expert from each center. AVA was calculated through continuity equation. The degree of aortic valve calcification and stenosis was established semi-quantitatively as recommended by current guidelines (10). Patients were classified into 3 groups according to baseline ECG data regarding the gradient and indexed systolic volume (SVi) as recommended by current guidelines (10): high-gradient (HG) if mean gradient $\geq$ 40 mmHg, normal-flow low-gradient (NFLG) if mean gradient $<$40 mmHg and SVi $>$ 35 ml/m$^2$, and LFLG if mean gradient $<$ 40 mmHg and SVi $\leq$ 35 ml/m$^2$. Patients were not involved in the design, conducting, reporting, or dissemination plans of our research.

All analyses were made with Stata software version 13.1. Continuous variables were expressed as mean and SD when the normality assumptions were met and as median and interquartile range (IQR) otherwise. Categorical variables were expressed as absolute numbers and percentages. Demographic, echocardiographic, and AVR variables were evaluated among the different groups using ANOVA test, chi-square test, or Fisher's exact test, as appropriate. Kaplan–Meier analysis was used for time-to-event variables (time-mortality and time-AVR) and the log-rank test to compare survival and time-AVR curves among groups. A multivariate Cox regression analysis was used to identify independent variables associated with the response variable (predictors of mortality and AVR), such as variables with statistical significance ($p < 0.20$) in the univariate analysis or with significant clinical relevance.

## RESULTS

### Baseline Clinical and Demographic Characteristics

In this study, 1,391 patients with baseline ECG with AVA $<$ 1 cm$^2$ and normal LVEF from 14 tertiary hospitals (**Figure 1**), mean age 74.5 (10.9) years and 53.6% women were included.

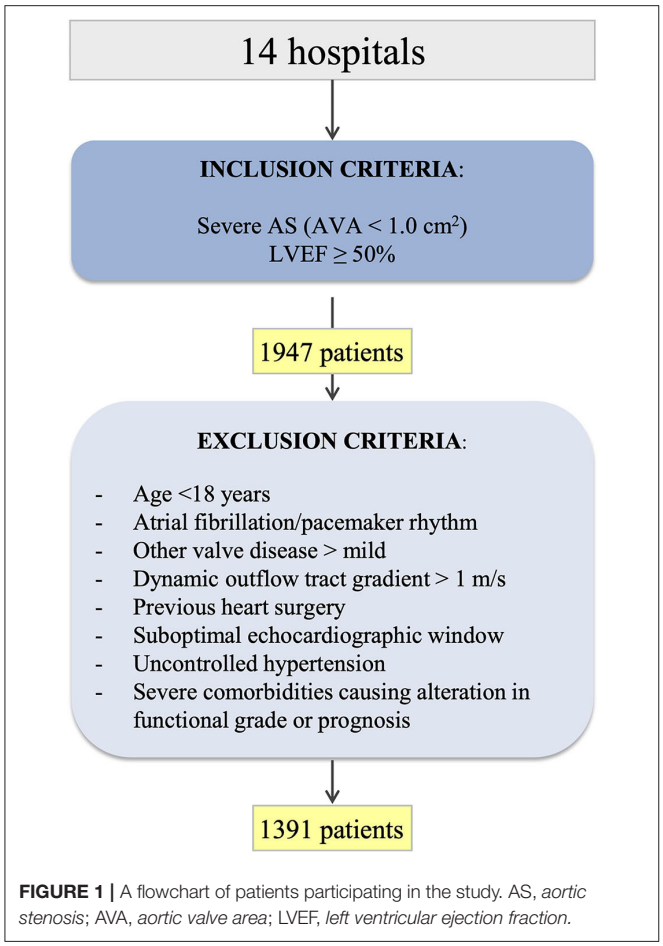


**FIGURE 1 |** A flowchart of patients participating in the study. AS, *aortic stenosis*; AVA, *aortic valve area*; LVEF, *left ventricular ejection fraction.*

In the whole cohort, 752 (54.1%) were classified as HG, 492 (35.4%) as NFLG, and 147 (10.5%) as LFLG. No significant differences were observed among groups regarding age, sex, or cardiovascular risk factors, except for smoking and body weight (**Table 1**). The mean total follow-up time was 59.0 months (IQR 39.7–82.9 months), with no significant differences among groups.

## Baseline Echocardiographic Characteristics

The echocardiographic data of each AS subtype are shown in **Table 2**. Remarkably, AVA of the LFLG group was similar to AVA of the HG group [0.74 (0.14) vs. 0.73 (0.16) $cm^2$; $p$ = NS] and significantly lower than that of the NFLG group [0.89 (0.09), $p < 0.001$]. However, the dimensionless index (ratio between LVOT VTI and aortic VTI) value in the LFLG group was intermediate between the HG group [0.25 (0.06) vs. 0.22 (0.05); $p < 0.001$] and the NFLG group [0.25 (0.06) vs. 0.27 (0.04); $p < 0.001$], with differences between the HG and NFLG groups also being significant [0.22 (0.05) vs. 0.27 (0.04); $p < 0.001$]. Left ventricular hypertrophy was significantly lower in patients of the LFLG group compared with the HG group and similar to the NFLG group (**Table 2**). Severe valve calcification in the LFLG group was lower than in the HG group and showed no significant differences with the NFLG group.

## AVR Indication According to AS Subgroups at Baseline

In total, 1,248 patients had complete data related to AVR (676 (54.2%) with HG, 450 (36.0%) with NFLG and 122 (9.8%) with LFLG). Throughout the follow-up, 857 patients (68.7%, *CI* 95% 66.0–71.2) underwent AVR [685 surgery and 172 Transcater Aortic Valve Implantation (TAVI)]: 529 with HG (78.2%, *CI* 95% 75.0–81.3; median time: 17.7 months, IQR 5.5–43.4 months), 74 with LFLG (60.6%, *CI* 95% 51.4–69.4; median time: 41.0 months, IQR 13.6–78.9 months) and 254 with NFLG (56.4%, *CI* 95% 51.7–61.1; median time: 46.9 months, IQR: 26.0–70.0 months) (**Figure 2**) with differences among groups in the estimated survival free from AVR that persisted after adjustment for age, smoking, diabetes mellitus, presence of symptoms, and LVEF ($p < 0.001$). In HG AS, AVR was indicated earlier compared with NFLG (log-rank $p < 0.001$) and LFLG AS (log-rank $p < 0.001$). No significant differences were observed between the LFLG and NFLG groups (log-rank $p = 0.358$).

On multivariate analysis, indication of AVR was inversely associated with age (hazard ratio [*HR*] 0.99, *CI* 95%: 0.98–0.99; $p = 0.002$); nevertheless, the presence of symptoms (*HR* 1.82, 95% *CI*: 1.57–2.01; $p < 0.001$) and coronary artery disease (*HR* 1.21, 95% *CI*: 1.03–1.43; $p = 0.018$) were independently related to AVR indication. Regarding echocardiographic parameters, AVA (AVA $< 0.8$ $cm^2$: *HR* 1.25, 95% *CI*: 1.04–1.48; $p = 0.014$), mean gradient (mean gradient $\geq$ 40 mmHg: *HR* 1.95, 95% *CI*: 1.67–2.29, $p < 0.001$), dimensionless index (dimensionless index $\leq$ 0.25: *HR* 1, 39, 95% *CI*: 1.18–1.65, $p < 0.001$), and LVEF 50–55% (*HR* 1.52, 95% *CI*: 1.21–1.91, $p < 0.001$) were also independently associated to AVR indication (**Supplementary Table 1**).

## Mortality According to AS Subgroup at Baseline

Overall mortality during follow-up was 27.7% (385 patients, *CI* 95% 25.3–30.1): 46 of the LFLG group (31.3%, *CI* 95% 23.9–39.5; median time: 50.8 months, IQR: 29.6–75.8), 205 of the HG group (27.3%, *CI* 95% 24.1–30.6; median time: 56.1 months, IQR: 33.8–83.7), and 134 of the NFLG group (27.2%, *CI* 95% 23.3–31.4; median time: 53.2 months, IQR: 31.0–76.9). Kaplan–Meier survival curves showed no significant differences among groups (**Figure 3**, log-rank $p = 0.319$). Early mortality after AVR (<30 days) was 6.5% (25 patients, *CI* 95% 1.2–2.6) with no differences among groups.

Death from cardiovascular cause occurred in 195 cases (14%, *CI* 95% 12.2–16.0) representing a 50.6% of overall mortality: 28 patients with LFLG (19%, *CI* 95% 13.0–26.3; median time: 50.9 months, ICR: 32.0–75.9), 95 patients with HG (12.6%, *CI* 10.3–15.2; median time: 56.1 months, ICR: 33.8–83.7), and 72 patients with NFLG (14.6%, *CI* 95% 11.6–18.1; median time: 52.5 months,

**TABLE 1 |** Clinical and demographic data according to aortic stenosis (AS) subgroups at baseline.

| | All patients *n* = 1,391 | HG *n* = 752 (54.1%) | NFLG *n* = 492 (35.4%) | LFLG *n* = 147 (10.5%) | *p*-value |
|---|---|---|---|---|---|
| Females, *n (%)* | 744 (53.6) | 393 (52.3) | 272 (55.4) | 79 (54.5) | 0.560 |
| Age, *years* [mean (SD), *median, IQR*] | 74.5 (10.9) *77 (70–82)* | 74.3 (10.8) *76 (69–82)* | 74.4 (11.3) *77 (70–81)* | 76.0 (10.4) *78 (73–82)* | 0.155 |
| Body surface area, $Kg/m^2$ | 1.8 (0.2) | 1.8 (0.2) | 1.7 (0.2) | 1.8 (0.2) | 0.834 |
| Weight, *Kg* | 72.7 (13.3) | 73.0 (13.3) | 71.1 (12.1) | 76.6 (15.6) | <0.001 |
| Height, *cm* | 160.3 (9.6) | 160.6 (9.9) | 159.7 (8.8) | 160.3 (10.3) | 0.264 |
| Hypertension, *n* (%) | 1,120 (80.5) | 601 (79.9) | 403 (81.9) | 116 (78.9) | 0.584 |
| Dyslipidaemia, *n* (%) | 799 (57.4) | 431 (57.3) | 284 (57.7) | 84 (57.1) | 0.987 |
| Diabetes, *n* (%) | 456 (32.8) | 254 (33.8) | 147 (29.9) | 55 (37.4) | 0.157 |
| Smoking status, *n* (%) | 270 (19.4) | 169 (22.5) | 80 (16.3) | 21 (14.3) | 0.007 |
| Coronary disease, *n* (%) | 320 (23.0) | 165 (22.0) | 121 (24.6) | 34 (23.1) | 0.550 |
| COPD, *n* (%) | 172 (12.4) | 93 (12.4) | 65 (13.2) | 14 (9.5) | 0.513 |
| Baseline symptoms, *n (%)* | 777 (55.9) | 438 (58.2) | 256 (52.0) | 83 (56.5) | 0.097 |
| Follow-up, *months (IQR)* | 59.0 (39.7–82.9) | 59.3 (38.4–84.6) | 59.4 (43.5–79.8) | 55.6 (36.6–76.5) | 0.286 |

*AS, aortic stenosis; COPD, chronic obstructive pulmonary disease; HG, high gradient; IQR, interquartile range; LFLG, low-flow low-gradient; NFLG, normal-flow low-gradient; SD, standard deviation. For continuous variables mean and SD was expressed [mean (SD)].*

**TABLE 2 |** Echocardiographic data according to the AS subgroup at baseline.

| | All patients *n* = 1391 | HG *n* = 752 (54.1%) | NFLG *n* = 492 (35.4%) | LFLG *n* = 147 (10.5%) | *p*-value |
|---|---|---|---|---|---|
| Maximum aortic jet velocity, *m/s* | 4.4 (0.3) | 5.1 (0.7) | 3.6 (0.3) | 3.5 (0.4) | $0.035^{a.b}$ |
| Mean aortic gradient, *mmHg* | 42.0 (14.0) | 51.6 (11.5) | 31.2 (5.4) | 29.2 (6.7) | $<0.001^{a.b}$ |
| LVOT, *mm* | 2.04 (0.17) | 2.04 (0.17) | 2.04 (0.15) | 1.97 (0.18) | $<0.001^{b.c}$ |
| LVOT VTI, *cm* | 23.3 (4.7) | 24 (5.0) | 23.6 (3.8) | 18.4 (3.7) | $<0.001^{a.b}$ |
| SVi, $ml/m^2$ | 43.2 (9.1) | 44.7 (9.6) | 44.5 (6.2) | 30.8 (3.3) | $<0.001^{b.c}$ |
| AVA, $cm^2$ | 0.79 (0.16) | 0.73 (0.16) | 0.89 (0.09) | 0.74 (0.14) | $<0.001^{a.c}$ |
| Dimensionless index | 0.24 (0.05) | 0.22 (0.05) | 0.27 (0.04) | 0.25 (0.06) | $<0.001^{a.b.c}$ |
| Severe aortic valve calcification, *n* (%) | 717 (54.1) | 488 (67.7) | 186 (38.7) | 4 (35.0) | $<0.001^{a.b}$ |
| Bicuspid aortic valve. *n* (%) | 156 (11.5) | 88 (11.9) | 59 (12.3) | 9 (6.5) | $0.008^{b.c}$ |
| LVEDD, *mm* | 46.0 (6.7) | 46.3 (6.8) | 45.7 (6.0) | 45.2 (7.5) | 0.059 |
| LVESD, *mm* | 29.0 (6.2) | 29.2 (6.2) | 28.8 (6.0) | 29.2 (6.6) | 0.062 |
| IVS, *mm* | 13.7 (2.4) | 14.2 (2.4) | 13.1 (2.4) | 13.4 (2.5) | $<0.001^{a.b}$ |
| PW, *mm* | 12.3 (2.1) | 12.6 (2.1) | 11.8 (2.0) | 12.1 (2.2) | $<0.001^{a.b}$ |
| LVEF, *%* | 64.8 (7.2) | 65.0 (7.3) | 64.5 (7.1) | 64.6 (7.7) | 0.228 |
| LVEF 50–55%, *n* (%) | 63 (4.5%) | 31 (4.1) | 21 (4.3) | 11 (7.5) | 0.200 |
| LV mass, $g/m^2$ | 130.5 (42.5) | 139.7 (41.7) | 120.9 (41.7) | 118.1 (38.8) | $<0.001^{a.b}$ |
| E/e' | 14.7 (7.4) | 14.6 (8.0) | 14.8 (7.3) | 14.7 (5.4) | 0.881 |
| LA volume, *ml* | 72.5 (36.7) | 71.6 (26.0) | 73.8 (49.6) | 74.0 (40.7) | 0.510 |

*AS, aortic stenosis; AVA, aortic valve area; COPD, chronic obstructive pulmonary disease; HG, high gradient; IQR, interquartile range; IVS, interventricular septum; LA, left atrium. LFLG, low-flow low-gradient; LVEDD, left ventricle end diastolic diameter; LVEF, left ventricular ejection fraction; LVESD, left ventricle end systolic diameter; LVOT, left ventricle outflow tract; NFLG, normal-flow low-gradient. PW, posterior wall; SD, standard deviation; SVi, indexed systolic volume; VTI, velocity-time integral. For continuous variables mean and SD was expressed [mean (SD)]. a, significant differences between HG and NFLG; b, significant differences between HG and LFLG; c, significant differences between NFLG and LFLG.*

ICR: 29.0–76.9), with no significant differences among groups (**Figure 4**, log-rank $p = 0.061$).

In patients undergoing AVR, no significant differences in mortality were observed among groups (log-rank $p = 0.612$) after adjustment for significant clinical variables and AVA. However, in non-operated patients, differences were observed among groups (log-rank $p = 0.004$), with low event-free survival in the HG group compared with the NFLG group (log-rank $p = 0.001$), with no significant differences between the LFLG and HG groups (log-rank $p = 0.354$) or between the LFLG and NFLG groups (log-rank $p = 0.171$).

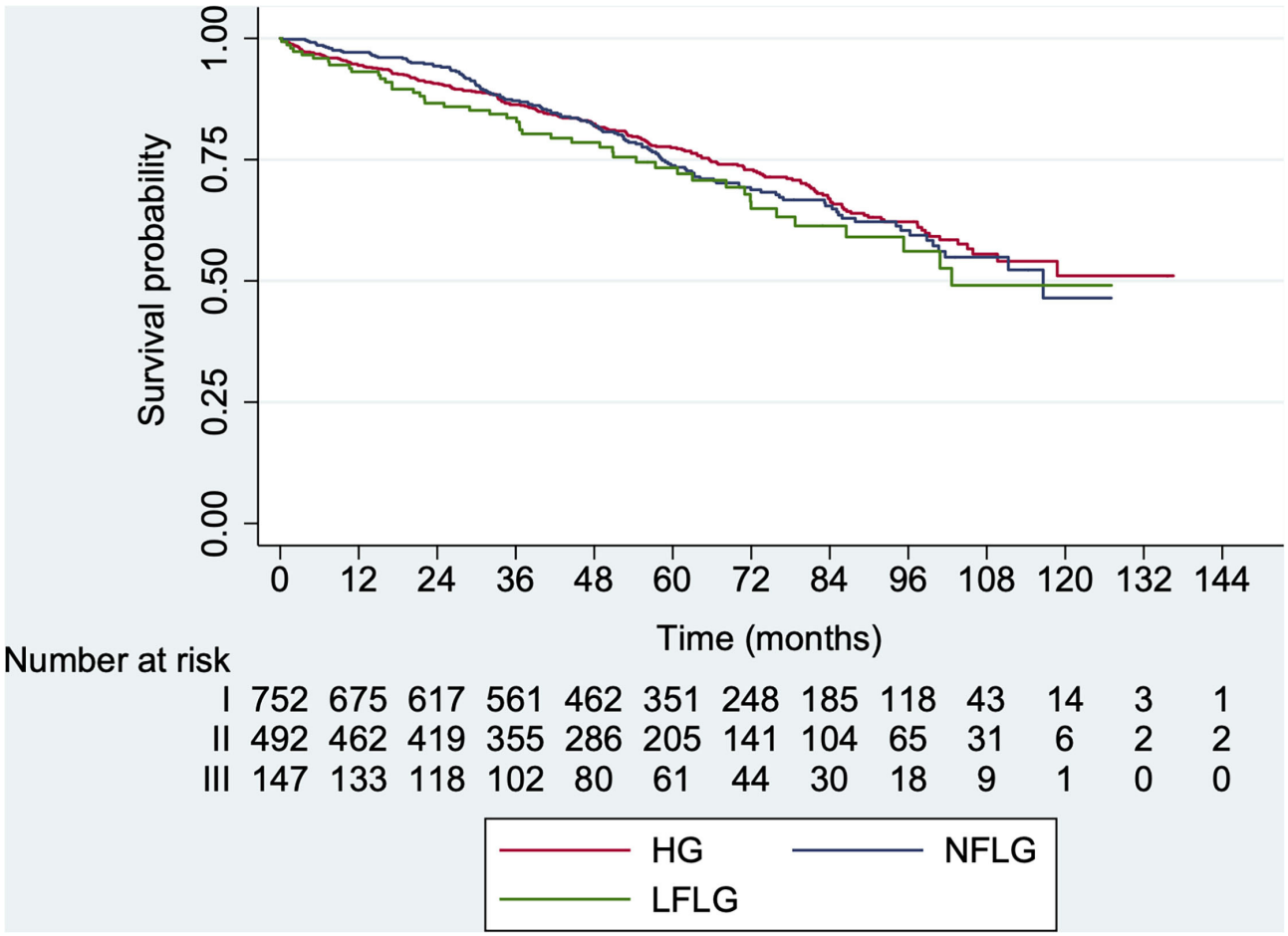


**FIGURE 2 |** Kaplan–Meier aortic valve replacement (AVR)-free survival curves according to AS subtype at baseline. HG, *high-gradient*; LFLG, *low-flow low-gradient*; NFLG, *normal-flow low-gradient* (log-rank $p < 0.001$).

In the multivariate analysis, age (*HR* 1.06, 95% *CI*: 1.04–1.08; $p < 0.001$), diabetes mellitus (*HR* 1.52; 95% *CI*: 1.23–1.89; $p < 0.001$), smoking (*HR*: 1.77, 95% *CI*: 1.32–2.37; $p < 0.0001$), COPD (*HR* 1.45, 95% *CI*: 1.09–1.92; $p = 0.010$), and the presence of symptoms (*HR* 1.48, 95% *CI*: 1.18–1.85; $p = 0.001$) were clinical variables associated to overall mortality (**Supplementary Table 2**). Echocardiographic variables independently associated with mortality were mean gradient > 50 mmHg (*HR* 1.56, 95% *CI*: 1.17–2.08; $p = 0.002$) and LVEF 50–55% (*HR* 1.68, 95% *CI*: 1.07–2.63; $p = 0.023$).

## Impact of AVR on Mortality Reduction

Overall mortality was higher in those patients who did not undergo AVR. The impact of AVR on mortality reduction in the whole population with AS was significant (*HR*: 0.22; 95% *CI*: 0.18–0.28; $p < 0.001$) after adjustment for significant clinical variables and AVA. AVR reduced mortality risk by 83% in patients with HG AS (*HR*: 0.17; 95% *CI*: 0.12–0.23; $p < 0.001$), 75% in patients with LFLG (*HR*: 0.25; 95% *CI*: 0.13–0.49; $p < 0.001$), and 71% in patients with NFLG AS (*HR*: 0.29; 95% *CI*: 0.20–0.44; $p < 0.001$; **Figure 5**).

# DISCUSSION

In this large multicentre retrospective cohort of consecutive patients with AS and normal ejection fraction and sinus rhythm, the prevalence of paradoxical LFLG AS was 10%. Echocardiographic parameters showed a similar AVA in comparison with HG and NFLG groups, but less severity in the dimensionless index, valve calcification, and LV hypertrophy than in HG AS. However, overall/cardiovascular mortality and the impact of AVR on mortality reduction were similar to patients with HG AS.

## Echocardiographic Characterization of LFLG AS

In the present series, patients with LFLG AS had a similar AVA value to the HG group and lower than NFLG group. However, in the remaining echocardiographic parameters, such as left ventricular hypertrophy and degree of valve calcification, LFLG did not significantly differ from NFLG AS. Interestingly, the dimensionless index in LFLG AS laid between HG and

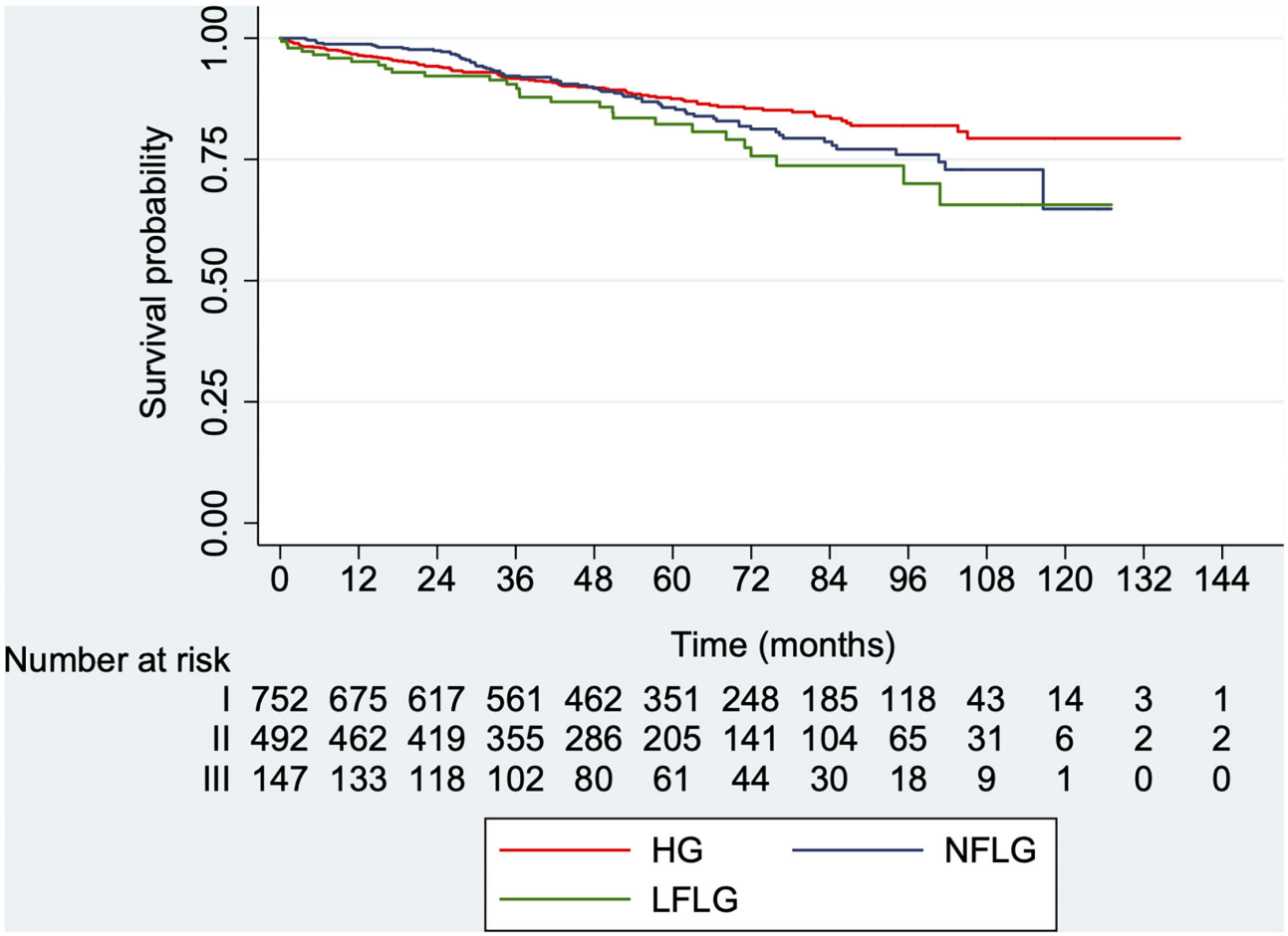


**FIGURE 3 |** Kaplan–Meier survival curves for overall mortality according to AS subtype at baseline. HG, *high-gradient*; LFLG, *low-flow low-gradient*; NFLG, *normal-flow low-gradient* (log-rank $p = 0.319$).

NFLG AS. Thus, LFLG AS presented intermediate-severity echocardiographic parameters between HG and NFLG AS. Other series yielded similar results (4). Clavel et al. in a series of 561 patients with AS, found LFLG patients to have significantly lower velocity and transaortic gradients than HG AS while AVA was practically the same (11). Several studies reported that this entity was associated with small ventricles and a high degree of hypertrophy (2); however, the present LFLG group had a significantly lower degree of hypertrophy than patients with HG AS but similar to those with NFLG AS. Other studies using echocardiography or CMR stated that patients with LFLG AS do not have a greater degree of hypertrophy than HG AS, but lower or similar to NFLG AS or moderate AS (4, 5, 12). Few studies analyzed the degree of calcification in LFLG AS by echocardiography or multidetector CT (MDCT), although this is currently one of the more recommended approaches to diagnose severe AS (10, 13). Calcification by MDCT may be highly useful in patients with discordant severity data on echocardiography (13).

## Outcome in LFLG Patients and Protective Effect of AVR

The risk throughout follow-up of undergoing AVR was higher for patients with HG, lower in patients with LFLG AS and comparable to patients with NFLG AS, as previously reported (14). Mortality was 27% and no significant differences were detected between patients with LFLG AS and the other groups. Patients of the three hemodynamic groups who underwent AVR had a similar prognosis, whereas patients who did not undergo surgery had higher mortality in the HG group compared with the NFLG group, with no differences between the LFLG and HG groups. Different series previously reported poorer survival and a higher rate of events in the LFLG population compared with HG AS (3, 11, 15); however, the trend in the more contemporary series has changed the paradigm, suggesting that higher mortality is associated with HG AS, with the behavior of LFLG AS being more similar to moderate AS or intermediate between HG and NFLG AS (8, 16). Recent evidence suggested that moderate forms of AS are not as benign as historically assumed, particularly if

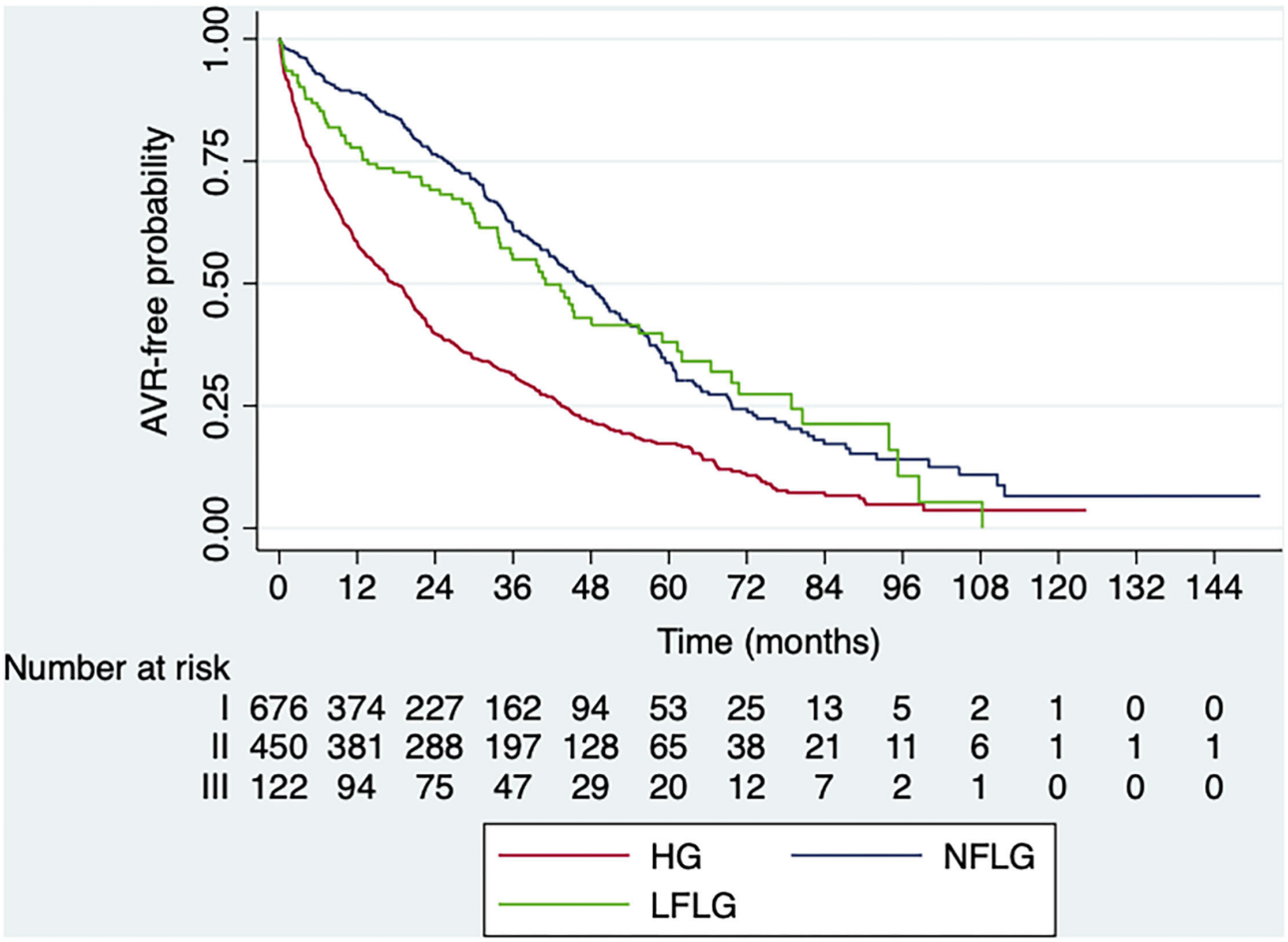


**FIGURE 4 |** Kaplan–Meier survival curves for cardiovascular mortality according to AS subtype at baseline. HG, high-gradient; LFLG, *low-flow low-gradient*; NFLG, normal-flow low-gradient (log-rank $p = 0.061$).

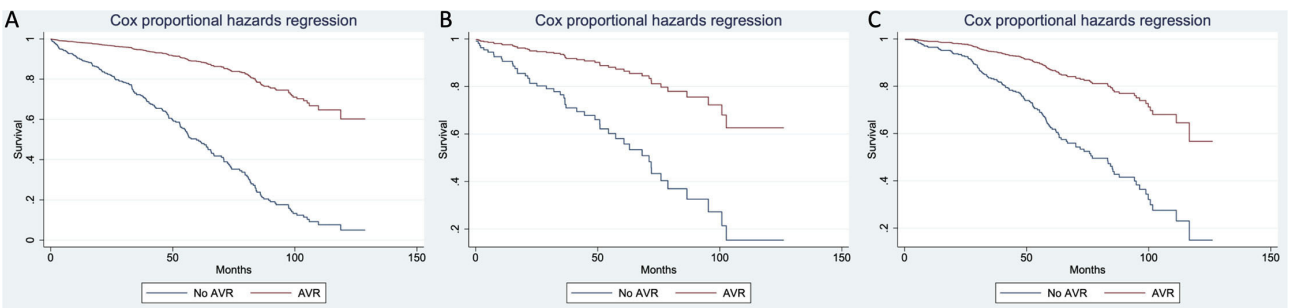


**FIGURE 5 |** Cox survival curves for overall mortality in the population with severe AS according to AVR and AS subtype [**(A)**: HG; **(B)**: LFLG; **(C)**: NFLG)]. AVR, aortic valve replacement.

left ventricular dysfunction is present (17). A recent study analyzing data from the Australian national echocardiography database showed mortality in patients with moderate AS to be similar to severe AS (18). Another contemporary study reported that patients with NFLG who did not undergo surgery had 6.3 times more overall mortality compared with surgically-treated patients, with surgery being associated with a significant increase in survival (19). Taking the results of this study and previous reported findings into account, there may be sufficient reasons to consider AS severity as moderate-severe when the AVA is between 0.8–1.2 $cm^2$ and severe when $< 0.8$ $cm^2$. In moderate-severe patients with

AS, other multimodality parameters, such as calcium score by CT, exercise test, or left ventricle overall strain could help to identify a subgroup of patients in whom AVR would be indicated.

Overall, patients with significant AS benefited from intervention on the AV, and despite the HG AS group benefited the most, both LFLG and NFLG AS also obtained significant benefit. Although few studies failed to show this benefit in patients with LFLG AS (5, 20), most series suggested a beneficial effect of valve replacement in the LFLG population (and even in NFLG and moderate AS) compared with conservative management (4, 18, 19). Thus, evidence of the effectiveness of aggressive treatment (surgical or percutaneous) of AS continues to grow and, though data remain discrepant, the trend is toward a more aggressive approach and in a wider range of the disease.

### Mortality Risk Predictors in Patients With Severe AS

In this study, patients with AS who died were older, more symptomatic, had more cardiovascular risk factors and a smaller AVA. However, the multivariate analysis failed to show AVA to be independently associated with mortality which instead was related to age, risk factors (diabetes, smoking, and COPD), symptoms, mean gradient $>$ 50 mmHg, and LVEF from 50–54%. Some studies showed mortality in AS to be associated with maximum velocity, aortic calcification, and LVEF. Valvular heart disease guidelines recommended as class I an AVR indication in systolic dysfunction (LVEF $<$ 50%) regardless of the presence of symptoms (9, 21). However, recent studies reported that patients with LVEF $<$ 55% had poor prognosis (22–24). All these results suggest that the cut-off point of $<$50% for LVEF could be too low, indicating that left ventricular dysfunction is already present when LVEF is between 50 and 60% and, in fact, recent guidelines recommend that patients with LVEF $<$ 60% on serial studies and severe AS should undergo surgery (21). Cardiac magnetic resonance demonstrated the presence of late gadolinium enhancement and increased extracellular volume in AS patients with normal ejection fraction, which have been related to prognosis (25). Other imaging techniques, such as strain by speckle tracking echocardiography can detect patients with subclinical ventricular dysfunction, (26) with overall longitudinal strain values $<$ $-$15% being associated with worse prognosis (27, 28). Global LV strain values may become one of the markers that will provide additional data to decide whether or not the patient could have a higher risk and deserves surgery. Given that patients with LFLG AS benefit significantly from AVR, they should be followed with caution, with the accuracy in echocardiographic severity evaluation to be maximized to avoid possible errors in SVi quantification. Furthermore, additional information through other imaging techniques (myocardial strain, CMR of calcium score by CT) are likely to be useful to determine whether data support the AS severity and/or suggest incipient ventricular dysfunction, to sustain the choice to treat paradoxical LFLG as HG AS.

## LIMITATIONS

The main limitation of this study was its retrospective nature. In the present series, confirmation of the low-flow state was not requested for inclusion. Exclusion of patients with atrial fibrillation was considered in the design of the study since the continuity equation may be less accurate in AVA calculation. Calcification of the aortic valve was analyzed following the semi-quantitative approach recommended by the current guidelines, although the optimal method is cardiac CT. Myocardial strain would have added complementary information; however, owing to the multicentre nature of the study and the years of inclusion established, variability of the values depending on the different vendors used would have resulted in difficult result analysis.

## CONCLUSIONS

Low-flow low-gradient AS has intermediate echocardiographic severity parameters and clinical outcomes between NFLG and HG AS, with lower AVR requirements than HG AS, but with overall mortality and benefits of surgery similar to the other two haemodynamic groups. Given that patients classified within this group benefited significantly from AVR, they should be followed with caution as in HG AS. The most appropriate option to adequately manage this subgroup may be to maximize the accuracy of the echocardiographic evaluation, provide additional information through other imaging techniques and determine whether there are data supporting the severity of AS or suggestive of incipient ventricular dysfunction, for them to be treated as HG AS.

## DATA AVAILABILITY STATEMENT

The datasets presented in this article are not readily available because further analyses are still underway for other papers awaiting publication. Requests to access these datasets should be directed to LG-G, lauragaliangay@gmail.com.

## ETHICS STATEMENT

The studies involving human participants were reviewed and approved by CEIm - Comitè d'Ètica d'Investigació amb medicaments - VHIR. Informed consent was not available due to the retrospective nature of the study.

## AUTHOR CONTRIBUTIONS

LG-G, GT-T, GC, and AE designed the study. LG-G, RE, GC, EF-S, CM, SMi, VM, DS, BV, LT, SM, FC, MC, VS, AGo, GG, MM, MA, JP, AB, AM-S, TG-A, LG, RF-G, FV, and AR-M contributed to conduction and reporting of the study. LG-G

and AS performed the statistical analysis. AE, AGu, JFP, and IF contributed to manuscript revision. AE and IF are the responsible for the overall content as guarantors. All authors contributed to the article and approved the submitted version.

## FUNDING

AGu has received funding from the Spanish Ministry of Science, Innovation and Universities (IJC2018- 037349-I).

## ACKNOWLEDGMENTS

We wish to thank Christine O'Hara for help with the English version of the manuscript.

## SUPPLEMENTARY MATERIAL

The Supplementary Material for this article can be found online at: https://www.frontiersin.org/articles/10.3389/fcvm.2022.852954/full#supplementary-material

## REFERENCES

1. Osnabrugge RLJ, Mylotte D, Head SJ, Van Mieghem NM, Nkomo VT, LeReun CM, et al. Aortic stenosis in the elderly. *J Am Coll Cardiol.* (2013) 62:1002–12. doi: 10.1016/j.jacc.2013.05.015
2. Hachicha Z, Dumesnil JG, Bogaty P, Pibarot P. Paradoxical low-flow, low-gradient severe aortic stenosis despite preserved ejection fraction is associated with higher afterload and reduced survival. *Circulation.* (2007) 115:2856–64. doi: 10.1161/CIRCULATIONAHA.106.668681
3. Lancellotti P, Magne J, Donal E, Davin L, O'Connor K, Rosca M, et al. Clinical outcome in asymptomatic severe aortic stenosis: Insights from the new proposed aortic stenosis grading classification. *J Am Coll Cardiol.* (2012) 59:235–43. doi: 10.1016/j.jacc.2011.08.072
4. Eleid MF, Sorajja P, Michelena HI, Malouf JF, Scott CG, Pellikka PA. Flow-gradient patterns in severe aortic stenosis with preserved ejection fraction: Clinical characteristics and predictors of survival. *Circulation.* (2013) 128:1781–9. doi: 10.1161/CIRCULATIONAHA.113.003695
5. Tribouilloy C, Rusinaru D, Marchaux S, Castel AL, Debry N, Maizel J, et al. Low-gradient, low-flow severe aortic stenosis with preserved left ventricular ejection fraction: Characteristics, outcome, and implications for surgery. *J Am Coll Cardiol.* (2015) 65:55–66. doi: 10.1016/j.jacc.2014.09.080
6. Jander N, Minners J, Holme I, Gerdts E, Boman K, Brudi P, et al. Outcome of patients with low-gradient severe aortic stenosis and preserved ejection fraction. *Circulation.* (2011) 123:887–95. doi: 10.1161/CIRCULATIONAHA.110.983510
7. Maes F, Boulif J, Piérard S, De Meester C, Melchior J, Gerber B, et al. Natural history of paradoxical low-gradient severe aortic stenosis. *Circ Cardiovasc Imag.* (2014) 7:714–22. doi: 10.1161/CIRCIMAGING.113.001695
8. Rezzoug N, Vaes B, Pasquet A, Gerber B, de Meester C, Van Pottelbergh G, et al. Prevalence and prognostic impact of valve area—gradient patterns in patients ≥80 years with moderate-to-severe aortic stenosis (from the prospective BELFRAIL study). *Am J Cardiol.* (2015) 116:925–32. doi: 10.1016/j.amjcard.2015.05.062
9. Baumgartner H, Falk V, Bax JJ, De Bonis M, Hamm C, Holm PJ, et al. 2017 ESC/EACTS Guidelines for the management of valvular heart disease. *Eur Heart J.* (2017) 38:2739–91. doi: 10.1016/j.rec.2017.12.013
10. Baumgartner H, Hung J, Bermejo J, Chambers JB, Edvardsen T, Goldstein S, et al. Recommendations on the echocardiographic assessment of aortic valve stenosis: a focused update from the european association of cardiovascular imaging and the american society of echocardiography. *J Am Soc Echocardiogr.* (2017) 30:372–92. doi: 10.1016/j.echo.2017.02.009
11. Clavel M-A, Dumesnil JG, Capoulade R, Mathieu P, Sénéchal M, Pibarot P. Outcome of patients with aortic stenosis, small valve area, and low-flow, low-gradient despite preserved left ventricular ejection fraction. *J Am Coll Cardiol.* (2012) 60:1259–67. doi: 10.1016/j.jacc.2011.12.054
12. Barone-Rochette G, Piérard S, Seldrum S, de Meester de. Ravenstein C, Melchior J, Maes F, et al. Aortic valve area, stroke volume, left ventricular hypertrophy, remodeling, and fibrosis in aortic stenosis assessed by cardiac magnetic resonance imaging: comparison between high and low gradient and normal and low flow aortic stenosis. *Circ Cardiovasc Imaging.* (2013) 6:1009–17. doi: 10.1161/CIRCIMAGING.113.000515
13. Clavel M-A, Messika-Zeitoun D, Pibarot P, Aggarwal SR, Malouf J, Araoz PA, et al. The complex nature of discordant severe calcified aortic valve disease grading: new insights from combined Doppler echocardiographic and computed tomographic study. *J Am Coll Cardiol.* (2013) 62:2329–38. doi: 10.1016/j.jacc.2013.08.1621
14. González Gómez A, Fernández-Golfín C, Monteagudo JM, Izurieta C, Hinojar R, García A, et al. Severe aortic stenosis patients with preserved ejection fraction according to flow and gradient classification: prevalence and outcomes. *Int J Cardiol.* (2017) 248:211–5. doi: 10.1016/j.ijcard.2017.06.064
15. Parikh R, Goodman AL, Barr T, Sabik JF, Svensson LG, Rodriguez LL, et al. Outcomes of surgical aortic valve replacement for severe aortic stenosis: Incorporation of left ventricular systolic function and stroke volume index. *J Thorac Cardiovasc Surg.* (2015) 149:1558–66e1. doi: 10.1016/j.jtcvs.2015.03.008
16. Kavianipour M, Farkhooy A, Flachskampf FA. Clinical outcome and functional characteristics of patients with asymptomatic low-flow low-gradient severe aortic stenosis with preserved ejection fraction are closer to high-gradient severe than to moderate aortic stenosis. *Int J Cardiovasc Imaging.* (2017) 34:545–52. doi: 10.1007/s10554-017-1264-2
17. van Gils L, Clavel M-A, Vollema EM, Hahn RT, Spitzer E, Delgado V, et al. Prognostic implications of moderate aortic stenosis in patients with left ventricular systolic dysfunction. *J Am Coll Cardiol.* (2017) 69:2383–92. doi: 10.1016/j.jacc.2017.03.023
18. Strange G, Stewart S, Celermajer D, Prior D, Scalia GM, Marwick T, et al. Poor long-term survival in patients with moderate aortic stenosis. *J Am Coll Cardiol.* (2019) 74:1851–63. doi: 10.1016/j.jacc.2019.08.004
19. Saeed S, Vamvakidou A, Seifert R, Khattar R, Li W, Senior R. The impact of aortic valve replacement on survival in patients with normal flow low gradient severe aortic stenosis: a propensity-matched comparison. *Eur Heart J Cardiovasc Imaging.* (2019) 20:1094–101. doi: 10.1093/ehjci/jez191
20. Zheng Q, Djohan AH, Lim E, Ding ZP, Ling LH, Chan ES, et al. Effects of aortic valve replacement on severe aortic stenosis and preserved systolic function: systematic review and network meta-analysis. *Sci Rep.* (2017) 7:1–9. doi: 10.1038/s41598-017-05021-9
21. Otto CM, Nishimura RA, Bonow RO, Carabello BA, III JPE, Gentile F, et al. 2020 ACC/AHA guideline for the management of patients with valvular heart disease: a report of the American College of Cardiology/American Heart Association joint committee on clinical practice guidelines. *Circulation.* (2021) 143:E72–227. doi: 10.1161/CIR.0000000000000923
22. Dahl JS, Eleid MF, Michelena HI, Scott CG, Suri RM, Schaff H V, et al. Effect of left ventricular ejection fraction on postoperative outcome in patients with severe aortic stenosis undergoing aortic valve replacement. *Circ Cardiovasc Imaging.* (2015) 8:1–8. doi: 10.1161/CIRCIMAGING.114.002917
23. Capoulade R, Le Ven F, Clavel M-A, Dumesnil JG, Dahou A, Thébault C, et al. Echocardiographic predictors of outcomes in adults with aortic stenosis. *Heart.* (2016) 102:934–42. doi: 10.1136/heartjnl-2015-308742

24. Ito S, Miranda WR, Nkomo VT, Connolly HM, Pislaru S V, Greason KL, et al. Reduced left ventricular ejection fraction in patients with aortic stenosis. *J Am Coll Cardiol.* (2018) 71:1313–21. doi: 10.1016/j.jacc.2018.01.045
25. Chin CWL, Everett RJ, Kwiecinski J, Vesey AT, Yeung E, Esson G, et al. Myocardial fibrosis and cardiac decompensation in aortic stenosis. *JACC Cardiovasc Imaging.* (2017) 10:1320–33. doi: 10.1016/j.jcmg.2016.10.007
26. Galli E, Lancellotti P, Sengupta PP, Donal E. LV mechanics in mitral and aortic valve diseases :value of functional assessment beyond ejection fraction. *JACC: Cardiovasc Imaging.* (2014) 7:151–66. doi: 10.1016/j.jcmg.2014.07.015
27. Ng ACT, Prihadi EA, Antoni ML, Bertini M, Ewe SH, Ajmone Marsan N, et al. Left ventricular global longitudinal strain is predictive of all-cause mortality independent of aortic stenosis severity and ejection fraction. *Eur Hear J - Cardiovasc Imaging.* (2018) 19:859–67. doi: 10.1093/ehjci/jex189
28. Magne J, Cosyns B, Popescu BA, Carstensen HG, Dahl J, Desai MY, et al. Distribution and prognostic significance of left ventricular global longitudinal strain in asymptomatic significant aortic stenosis an individual participant data meta-analysis. *JACC: Cardiovasc Imag.* (2019) 12:84–92. doi: 10.1016/j.jcmg.2018.11.005

**Conflict of Interest:** The authors declare that the research was conducted in the absence of any commercial or financial relationships that could be construed as a potential conflict of interest.

frontiers | Frontiers in Cardiovascular Medicine

REVIEW
published: 08 April 2022
doi: 10.3389/fcvm.2022.863040

# Shared Decision-Making and Patient-Reported Outcome Measures in Valvular Heart Disease

*Sahrai Saeed*[1]*, *Elisabeth Skaar*[1], *Andrea Romarheim*[1], *John B. Chambers*[2] and *Øyvind Bleie*[1]

[1] Department of Heart Disease, Haukeland University Hospital, Bergen, Norway, [2] Cardiothoracic Centre, Guy's and Saint Thomas' Hospital, London, United Kingdom

Patient-centered health care emphasizes shared decision-making (SDM), incorporating both clinical evidence and patient preferences and values. SDM is important in heart valve disease, both because there might be more than one treatment option and due to the importance of adherence after intervention. We aimed to describe patient information and involvement in decision-making about care and recording of patient-reported outcome measures (PROMs) in valve interventions. The opinion piece and recommendations are based upon literature review and our own experience from specialist valve clinics. Before a valve intervention, adequate patient information, discussion of the various treatment options and exploring patient preferences, in line with the concept of SDM, may improve post-intervention quality of life. After intervention, patients with prosthetic heart valves require adequate counseling and close follow-up to make them more confident and competent to manage their own health, as well as to maintain the efficacy of treatment provided. PROMs inform SDM before and improve care after valve intervention, focusing on outcomes beyond mortality and morbidity. SDM may improve post-intervention quality of life. Formal PROMs questionnaires inform SDM, quantify patient centered changes and should be used more often in clinical practice and research. A thorough assessment of baseline frailty status in patients scheduled for valve intervention is essential and may affect postoperative outcome.

**Keywords: aortic stenosis, aortic valve replacement, frailty, patient-reported outcome measures, quality of life, shared decision-making, transcatheter aortic valve implantation, valvular heart disease**

OPEN ACCESS

***Edited by:***
*Marko Banovic,*
*University of Belgrade, Serbia*

***Reviewed by:***
*Antonio Greco,*
*University of Catania, Italy*
*Guy Van Camp,*
*OLV Aalst, Belgium*

***Correspondence:**
*Sahrai Saeed*
*sahrai.saeed@helse-bergen.no*

***Specialty section:***
*This article was submitted to Heart Valve Disease, a section of the journal Frontiers in Cardiovascular Medicine*

***Received:*** *26 January 2022*
***Accepted:*** *17 March 2022*
***Published:*** *08 April 2022*

***Citation:***
*Saeed S, Skaar E, Romarheim A, Chambers JB and Bleie Ø (2022) Shared Decision-Making and Patient-Reported Outcome Measures in Valvular Heart Disease. Front. Cardiovasc. Med. 9:863040. doi: 10.3389/fcvm.2022.863040*

## INTRODUCTION

Health policy makers encourage patient-centered health care including shared decision-making (SDM) (https://www.bhvs.org.uk/bhvs-blueprint/). SDM is a collaborative process involving at least a healthcare professional and a patient, where both participate in decision-making (1). The goal is to reach a consensus of decision incorporating best available evidence and patient priorities (2). The purpose of SDM is also to keep a balance in power between patients and physicians or other caregivers (1), and to replace the more traditional authoritarian communication models, in order to reach decisions consistent with patients' goals of care. Evolving from the original focus, SDM also encompasses management, self-care and lifestyle changes (3). In valvular heart disease (VHD), for which surgery or transcatheter interventions are common, this approach can be divided into care before and after the intervention. Before the procedure, there must be adequate information of the patient, discussion of the various treatment options and actively seeking patients' preferences

and involvement. After the valve intervention, sufficient information should be provided for the patient in order to support self-management and take care of their own health. This is particularly important in the period of time after receiving treatment at hospital in order to maintain the efficacy of treatment provided. Patients are also expected to take more responsibility for their own health and get actively involved in the disease management. After the procedure, the patient-centered approach goes beyond the traditional measures of mortality and morbidity to assess patient-reported outcome measures (PROMs).

The aims of this review are to describe: (1) SDM with focus on patient information and involvement in decisions about care and; (2) commonly used instruments for recording PROMs after interventions.

## SHARED DECISION-MAKING BEFORE INTERVENTION

In clinical care, most patients appreciate SDM (4), which alongside careful baseline risk stratification is important for better outcomes after surgical aortic valve replacement (SAVR) (2, 5). Treating depression and modifying negative illness beliefs before surgical intervention may further improve outcomes in these patients (5). Patient preference is cited as the first indication in choosing a biological instead of a mechanical valve for the younger patient (5). However, this choice is made based upon the mutual relationship between patient preferences and medical practice, especially after providing adequate information by the physician or other healthcare professional regarding the two available options: (1) mechanical which are thrombogenic and require lifelong anticoagulation; and (2) biological which has shorter durability and carries risk of degeneration and reoperation in younger patients. Indeed, the 2020 American College of Cardiology (ACC)/American Heart Association (AHA) guidelines on VHD highlight including the patient's values and preferences and the indications for and risks of anticoagulant therapy when making a decision about surgery (6). Similarly, current European guidelines for the management of VHD (7), also reinforce the critical role of the patient's involvement in the mode of intervention, beyond the Heart Teams integration of the clinical, anatomical, and procedural characteristics and conventional scores. Most patients can expect a significant improvement in survival, symptoms, exercise tolerance and disease specific quality of life (QoL) after AVR, but their physical QoL may not return to normal. However, in patients <60 years, mental QoL after biological AVR was significantly better than age-matched control subjects (8), highlighting the importance of pre-intervention SDM in prosthetic valve selection, particularly in younger patients.

Evidence suggests that transcatheter aortic valve implantation (TAVI) compared with conservative treatment improves QoL, symptoms and physical function related to aortic stenosis (AS). However, the psychological or general health benefits appear to be modest (9), particularly if valve intervention is offered late. Frailty, a known predictor of adverse outcome, is defined as a state of reduced physiological reserve and diminished resistance to stressors. There is no consensus on the definition, and the two main models are the accumulation of deficits (adding together an individual's number of impairments and condition) creating a Frailty Index (10) and the specific physical phenotype consisting of 5 possible components (weight loss, exhaustion, weakness, slowness, and reduced physical activity (11).

Older adults, especially those with multiple chronic conditions and frailty, may have different goals of care than younger healthier adults. There may be less focus on survival and more on QoL, including physical function and independence (3). High-risk elderly patients with severe AS being evaluated for TAVI, can define their goals through a simple question "What do you hope to accomplish by having your valve replaced?" (12). Repairing the aortic valve if AS is one of several comorbid conditions may not restore a patient's functional status and QoL (9, 13). SDM does not justify patients demanding futile treatment. The decision to offer valve intervention should be made by the heart valve team, weighing benefit vs. risk, while taking into account comorbidities, life-expectancy, frailty, procedural risk and symptom burden.

Patient preference is the most common reason for selecting medical management in severe symptomatic AS (14). However, patients receiving medical management received less information and felt less engaged by their heart valve physicians than those receiving TAVI or SAVR (14).

A core aim of a valve clinic is to inform patients adequately before intervention is required (15). Exploring patient preferences and values during this process enables SDM over many visits and not during a single consultation immediately before the intervention. However, providing sufficient information is challenging, and there is only patchy availability of reliable literature (15, 16). Some patients may turn first to the internet, but sites may be biased commercially or toward the specialty of the hospital preparing the website (17). A patient's understanding of valve disease may therefore be limited (18–20). In surveys, <20% were aware of heart valve disease and only 7% knew what AS was (19, 20).

Decision aids may improve a patient's understanding of available treatment options (21). These may be written material, charts, graphs presented electronically or as brochures available at hospitals or general practitioner (GP) offices. An experienced patient voluntarily affiliated with a hospital may help new patients (22). Patient preferences can be formalized using questionnaires based on PROMs (18, 23–25). Overall, in health care delivery systems, PROMs-based information is underused, probably because of the perceived lack of time in the clinic (23), and lack of effective educational tools for risk communication. PROMs facilitate symptom monitoring, and improve patient-doctor communication and could be used in individuals or groups (23). Making the PROMs score available through the electronic patient record and dashboards before consultation and preferably to show any changes over several visits, is expected to increase awareness among doctors about the individual patient's needs. Patient-reported health status seems to be a useful supplement to the established physical examination during the clinical assessment (26), and may improve risk assessment

of patients with AS. Aggregated PROMs scores could be used before intervention to guide patients on their likely outcomes beyond mortality and morbidity (23). In some countries it has become mandatory to collect and report PROMs for surgical interventions. However, decision aids, written material and brochures are not a substitute for direct communication between the physician and older patients with multiple conditions (for example reduced cognition or frailty).

## PATIENT-REPORTED OUTCOME MEASURES (PROMS) AFTER INTERVENTION

The main objectives in treating VHD is to decrease the rate of premature death and improve clinical outcomes including QoL. Both SAVR and TAVI lead to recovery of LV function, LV mass regression and improved survival and symptoms. However, QoL is not routinely assessed and this is obviously of paramount importance to the patient. PROMs represents a strategy of evaluating health status by the patients themselves, for example assessing QoL after SAVR and TAVI (**Table 1**) (27–29), which require the use of optimal QoL instruments. There is, therefore, increasing work on PROMs.

The Minnesota Living with Heart Failure Questionnaire (MLHFQ) includes 21 formal questions and describes physical, emotional and socioeconomic aspects of QoL (30). It is a cardiac-specific health status questionnaire, in which 13 of 21 items are summated into two subscale scores: emotional and physical. Lower scores indicate better disease-specific health status. The SF-12 is a widely used instrument consisting of 12 items that capture eight domains of self-rated health generating a physical component summary and a mental component summary scores (31, 32). The SF-12 scores are converted into a norm-based score ranging from 0 to 100, in which 50 represents the mean score of the overall US normal population, and 10 points correspond to one standard deviation (SD). Higher scores indicate better health status in the preceding month. The minimum clinically important difference for the summary scores is 2.0–2.5 points. The EuroQol (EQ-5D) is a generic instrument, commonly used in Europe and provides a five dimension scale scoring usual activity, mobility, self-care, pain/discomfort and anxiety/depression. Each dimension is scored in five levels with a lower score indicating a better QoL (28). The World Health Organization Quality of Life Instrument Abbreviated (WHOQOL-BREF, an abbreviated version of the WHOQOL-100) is designed to measure overall perspective of QoL (**Table 1**) (33).

**TABLE 1 |** List of commonly used Questionnaires to assess patient-reported outcome measures (PROMs) as useful aids in shared-decision making in surgical practice and other areas of therapeutic medicine.

| No | Type of instruments | Health status assessed |
|---|---|---|
| 1 | The Minnesota Living with Heart Failure Questionnaire (MLHFQ).<br>Includes 21 formal questions and describes physical, emotional and socioeconomic aspects of quality of life related to a specific disease. Emotional (five questions; range 0–25), physical (eight question; range 0–40). | Cardiac- or disease-specific |
| 2 | Medical Outcomes Study Short Form-12 (SF-12) questionnaire.<br>Includes 12 items capturing eight domains of self-rated health status of physical component summary (PCS) and a mental component summary (MCS). | Generic |
| 3 | EuroQol 5 Domains (EQ-5D)<br>Provides information on patient's general health status involving usual activity, mobility, self-care, pain, anxiety and depression, as well as visual analogue scale as a second component. | Generic |
| 4 | The World Health Organization Quality of Life Instrument WHOQOL-BREF (an abbreviated version of the WHOQOL-100).<br>Responses illustrate experiences in the preceding 2 weeks. | Global perspective of quality of life |

In a small prospective observational study of 84 patients with VHD who underwent surgery, both the EuroQol (EQ-5D) and MLHFQ were effective for assessing QoL over a limited 6–12 week follow-up (34). A non-randomized Norwegian study of 143 patients (mean age 83 $\pm$ 2.7 years, 57% women) with AS undergoing TAVI (45%) or SAVR assessed PROMs and frailty status before and 6 month after intervention (35). The PROMs used were: (1) Medical Outcomes Study Short Form-12 questionnaire (SF-12) to assess generic aspect of self-rated health; (2) The MLHFQ to assess cardiac-specific health status; and (3) Two questions from the WHOQOL-BREF assessing the global perspective of self-reported health and QoL: "How would you rate your quality of life?" and "How satisfied are you with your health?" Patients had improved self-rated health after AVR. After TAVI, patients who were frail at baseline reported lower overall QoL and self-rated health compared with patients in the SAVR arm. The same trend was also observed at 6-months follow-up.

Frailty may affect predictions of improvement after intervention depending on its causes. If frailty is caused mainly by the VHD, patients are expected to improve after TAVI with an increase in the physical component summary score from 30.0 to 36.2 points and the mental summary component score from 42.2 to 49.6 points. After SAVR, the increase in physical component summary score was more pronounced (increased from 33.6 to 41.4), but there was no significant improvement in the mental summary component score (increased from 47.1 to 47.5 points). However, if frailty is dominated by coexistent pathology, for example chronic obstructive pulmonary disease (COPD) (36), the benefits of interventions for VHD may then be blunted. Not only will the risk of intervention be higher but also the likelihood of improvement on QoL afterwards will be lower. In situations where there is doubt about benefit, SDM exploring patients' values and preferences are even more important than usual. Some definitions include impaired cognition as a part of frailty. For patients with cognitive impairment or dementia, the concept of SDM is even more challenging and goes beyond the scope of this paper.

Nearly 20% of patients are frail at discharge following heart valve surgery and this is associated with poor self-reported

health (37). International guidelines on the management of VHD recommend formal assessment of frailty status before surgery for risk stratification (38). Irrespective of the choice of valve intervention (TAVI vs. SAVR), frail patients have worse self-reported health compared with non-frail patients (39, 40). However, it is also important to highlight that following valve intervention some patients may improve in frailty status and achieve better scores on questionnaires evaluating disease-specific health status (35).

After cardiac surgery, patients with prosthetic heart valves require adequate counseling and close follow-up to make them more confident and competent to manage their own health (41). Hence, patient participation is not only essential in preoperative SDM, but also in rehabilitation programs following cardiac surgery. Experience from nurse-led clinics shows that outcomes are improved when patients are offered help to ensure guideline adherence and to identify important clinical symptoms (42, 43).

Further research focusing on values and preferences of patients with VHD, particularly AS undergoing SAVR vs. TAVI, as well as overall valve intervention vs. conservative treatment, is warranted. PROMs instruments should be used more often in research studies exploring the efficacy of intervention for patients with VHD in order to refine treatment options. In future, larger, well-designed prospective studies are needed to explore the impact of pre-intervention SDM on post-intervention outcomes including QoL, and to explore the performance of the individual PROMS instruments.

## CONCLUSIONS

Patient-centered health care places patient's autonomy, values and preferences at the core of shared decision making. Formal PROMs questionnaires encourage this process and should be used more often in daily clinical practice and in research.

## REVIEW CRITERIA

- This review is based on literature and our own experience from specialist heart valve clinics.
- A comprehensive search strategy using keywords shared decision-making (SDM), patient-reported outcome measures (PROMs) and quality of life was designed.
- Bibliographic database PubMed and Embase were searched for articles published over the past 2 decades.

## MESSAGE FOR THE CLINIC

- Pre-intervention SDM may improve post-intervention outcomes including quality of life.
- PROMS should be used to inform SDM for patients with heart valve disease.
- Formal PROMs questionnaires encourage communication between patient and physician and may lead to better outcomes after valve interventions.
- SDM is especially important in a clinical setting where benefit/risk is uncertain due to patients characteristics like frailty or comorbid conditions.
- In older adults, objective frailty testing is recommended to inform decision-making.
- It is important to inform patients with frailty and several comorbid conditions that repairing the valve may improve disease-specific symptoms, but may not restore the patient's functional status or quality of life.

## AUTHOR CONTRIBUTIONS

SS, ES, AR, and JC conducted the literature search. SS, ES, and AR drafted the manuscript. JC and ØB critically revised the manuscript. All authors read and approved the final version before submission.

## REFERENCES


1. Charles C, Gafni A, Whelan T. Shared decision-making in the medical encounter: what does it mean? (or it takes at least two to tango). *Soc Sci Med.* (1997) 44:681–92. doi: 10.1016/S0277-9536(96)00221-3
2. Lauck SB, Lewis KB, Borregaard B, de Sousa I. "What Is the Right Decision for Me?" Integrating patient perspectives through shared decision-making for valvular heart disease therapy. *Can J Cardiol.* (2021) 37:1054–63. doi: 10.1016/j.cjca.2021.02.022
3. Backman WD, Levine SA, Wenger NK, Harold JG. Shared decision-making for older adults with cardiovascular disease. *Clin Cardiol.* (2020) 43:196–204. doi: 10.1002/clc.23267
4. Korteland NM, Bras FJ, van Hout FMA, Kluin J, Klautz RJ, Bogers AJ, et al. Prosthetic aortic valve selection: current patient experience, preference and knowledge. *Open Heart.* (2015) 2:e000237. doi: 10.1136/openhrt-2015-000237
5. Rimington HM, Weinman J, Chambers JB. Predicting outcome after valve replacement. *Heart.* (2010) 96:118–23. doi: 10.1136/hrt.2008.160010
6. Otto CM, Nishimura RA, Bonow RO, Carabello BA, Erwin JP III, Gentile F, et al. 2020 ACC/AHA Guideline for the management of patients with valvular heart disease: a report of the American College of Cardiology/American Heart Association Joint Committee on clinical practice guidelines. *Circulation.* (2021) 143:e72–227. doi: 10.1161/CIR.0000000000000955
7. Vahanian A, Beyersdorf F, Praz F, Milojevic M, Baldus S, Bauersachs J, et al. 2021 ESC/EACTS Guidelines for the management of valvular heart disease. *Eurointervention.* (2022) 17:e1126–96. doi: 10.4244/EIJ-E-21-00009
8. Petersen J, Krogmann H, Reichenspurner H, Girdauskas E. Long-term outcome and quality of life after biological aortic valve replacement in nonelderly adults. *Ann Thorac Surg.* (2021) 111:142–9. doi: 10.1016/j.athoracsur.2020.04.097
9. Kim CA, Rasania SP, Afilalo J, Popma JJ, Lipsitz LA, Kim DH. Functional status and quality of life after transcatheter aortic valve replacement: a systematic review. *Ann Intern Med.* (2014) 160:243–54. doi: 10.7326/M13-1316
10. Rockwood K, Mitnitski A. Frailty defined by deficit accumulation and geriatric medicine defined by frailty. *Clin Geriatr Med.* (2011) 27:17–26. doi: 10.1016/j.cger.2010.08.008
11. Fried LP, Tangen CM, Walston J, Newman AB, Hirsch C, Gottdiener J, et al. Frailty in older adults: evidence for a phenotype. *J Gerontol A Biol Sci Med Sci.* (2001) 56:M146–56. doi: 10.1093/gerona/56.3.M146
12. Coylewright M, Palmer R, O'Neill ES, Robb JF, Fried TR. Patient-defined goals for the treatment of severe aortic stenosis: a qualitative analysis. *Health Expect.* (2016) 19:1036–43. doi: 10.1111/hex.12393
13. Kim DH. incorporating quality of life prediction in shared decision making about transcatheter aortic valve replacement. *Circ Cardiovasc Qual Outcomes.* (2018) 11:e005097. doi: 10.1161/CIRCOUTCOMES.118.005097

14. Dharmarajan K, Foster J, Coylewright M, Green P, Vavalle JP, Faheem O, et al. The medically managed patient with severe symptomatic aortic stenosis in the TAVR era: patient characteristics, reasons for medical management, and quality of shared decision making at heart valve treatment centers. *PLoS ONE.* (2017) 12:e0175926. doi: 10.1371/journal.pone.0175926
15. Lancellotti P, Rosenhek R, Pibarot P, Iung B, Otto CM, Tornos P, et al. Heart valve clinics: organisation, structure and experiences. *Eur Heart J.* (2013) 34:1597–606. doi: 10.1093/eurheartj/ehs443
16. Bhattacharyya S, Pavitt C, Lloyd G, Chambers JB. Provision, organization and models of heart valve clinics within the United Kingdom. *Quart J Med.* (2015) 108:113–7. doi: 10.1093/qjmed/hcu164
17. Lai MY, McDermott H, Chambers JB. Aortic valve surgery: how reliable are health information websites? *Brit J Gen Pract Open.* (2017) 1:BJGP-2017–0665. doi: 10.3399/bjgpopen17X100665
18. Lytvyn L, Guyatt GH, Manja V, Siemieniuk RA, Zhang Y, Agoritsas T, et al. Patient values and preferences on transcatheter or surgical aortic valve replacement therapy for aortic stenosis: a systematic review. *BMJ Open.* (2016) 6:e014327. doi: 10.1136/bmjopen-2016-014327
19. Gaede L, Di Bartolomeo R, van der Kley F, Elsässer A, Iung B, Möllmann H. Aortic valve stenosis: what do people know? A heart valve disease awareness survey of over 8,800 people aged 60 or over. *Eurointervention.* (2016) 12:883–9. doi: 10.4244/EIJY16M06_02
20. Gaede L, Aarberge L, Brandon Bravo Bruinsma G, Macarthy P, Musumeci F, Zamorano P, et al. Heart Valve Disease Awareness Survey 2017: what did we achieve since 2015? *Clin Res Cardiol.* (2019) 108:61–7. doi: 10.1007/s00392-018-1312-5
21. Stacey D, Legare F, Col NF, Bennett CL, Barry MJ, Eden KB, et al. Decision aids for people facing health treatment or screening decisions. *Cochrane Database Syst Rev.* (2014) 4:CD001431. doi: 10.1002/14651858.CD001431.pub4
22. *Mike Higginbottom's Heart Valve Disease Story*. (2016). Available online at: https://www.heart-surgeon.biz/expertise
23. Damman OC, Jani A, de Jong BA, Becker A, Metz MJ, de Bruijne MC, et al. The use of PROMs and shared decision-making in medical encounters with patients: an opportunity to deliver value-based health care to patients. *J Eval Clin Pract.* (2020) 26:524–40. doi: 10.1111/jep.13321
24. Briffa N. The employment of Patient-Reported Outcome Measures to communicate the likely benefits of surgery. *Patient Relat Outcome Meas.* (2018) 9:263–6. doi: 10.2147/PROM.S132746
25. *International Patient Decision Aids Standards (IPDAS) Collaboration*. Available online at: http://ipdas.ohri.ca/index.html (accessed December 30, 2017).
26. Oterhals K, Haaverstad R, Nordrehaug JE, Eide GE, Norekvål TM. Self-reported health status, treatment decision and survival in asymptomatic and symptomatic patients with aortic stenosis in a Western Norway population undergoing conservative treatment: a cross-sectional study with 18 months follow-up. *BMJ Open.* (2017) 7:e016489. doi: 10.1136/bmjopen-2017-016489
27. Supino PG, Borer JS, Franciosa JA, Preibisz JJ, Hochreiter C, Isom OW, et al. Acceptability and psychometric properties of the Minnesota living with heart failure questionnaire among patients undergoing heart valve surgery: validation and comparison with SF-36. *J Card Fail.* (2009) 15:267–77. doi: 10.1016/j.cardfail.2008.10.003
28. The EuroQol Group. EuroQol-a new facility for the measurement of health-related quality of life. *Health Policy.* (1990) 16:199–208. doi: 10.1016/0168-8510(90)90421-9
29. Spaziano M, Carrier M, Pellerin M, Choinière M. Quality of life following heart valve replacement in the elderly. *J Heart Valve Dis.* (2010) 19:524–32.
30. Rector T, Cohn J. Assessment of patient outcome with the Minnesota Living with Heart Failure questionnaire: reliability and validity during a randomized, double-blind, placebo- controlled trial of pimobendan. Pimobendan Multicenter Research Group. *Am Heart J.* (1992) 124:1017–25. doi: 10.1016/0002-8703(92)90986-6
31. Ware JJ, Kosinski M, Keller SD. A 12-Item Short-Form Health Survey: construction of scales and preliminary tests of reliability and validity. *Med Care.* (1996) 34:220–33. doi: 10.1097/00005650-199603000-00003
32. Ware J, Kosinski M, Bjorner JB, Turner-Bowkes DM, Gandek B, Maruish ME. Determining important differences in scores. In: *User's Manual for the SF-36v2® Health Survey*. 2nd ed. Lincoln, NE: Quality Metric (2007). p. 125–33.
33. Skevington SM, Lotfy M, O'Connel KA. The World Health Organisa tion's WHOQOL - BREF quality of life assessment: psychometric properties and results of the international field trial A Report from the WHOQOL Group. *Qual Life Res.* (2004) 13:299–310. doi: 10.1023/B:QURE.0000018486.91360.00
34. Holmes C, Briffa N. Patient-Reported Outcome Measures (PROMS) in patients undergoing heart valve surgery: why should we measure them and which instruments should we use? *Open Heart.* (2016) 3(1):e000315. doi: 10.1136/openhrt-2015-000315
35. Frantzen AT, Eide LSP, Fridlund B, Haaverstad R, Hufthammer KO, Kuiper KKJ, et al. Frailty status and patient-reported outcomes in octogenarians following transcatheter or surgical aortic valve replacement. *Heart Lung Circ.* (2021) 30:1221–31. doi: 10.1016/j.hlc.2020.10.024
36. Hogan DB. Models, definitions, and criteria for frailty. In: *Conn's Handbook of Models for Human Aging.* Alberta: Elsevier (2018). p. 35–44.
37. Borregaard B, Dahl JS, Lauck SB, Ryg J, Berg SK, Ekholm O, et al. Association between frailty and self-reported health following heart valve surgery. *Int J Cardiol Heart Vasc.* (2020) 31:100671. doi: 10.1016/j.ijcha.2020.100671
38. Baumgartner H, Falk V, Bax JJ, De Bonis M, Hamm C, Holm PJ, et al. 2017 ESC/EACTS Guidelines for the management of valvular heart disease. *Euro Heart J.* (2017) 38:2739–86. doi: 10.1093/eurheartj/ehx470
39. Kotajarvi BR, Schafer MJ, Atkinson EJ, Traynor MM, Bruce CJ, Greason KL, et al. The impact of frailty on patient-centered outcomes following aortic valve replacement. *J Gerontol A Biol Sci Med Sci.* (2017) 72:917–21. doi: 10.1093/gerona/glx038
40. Henry L, Halpin L, Barnett SD, Pritchard G, Sarin E, Speir AM. Frailty in the cardiac surgical patient: comparison of frailty tools and associated outcomes. *Ann Thorac Surg.* (2019) 108:16–22. doi: 10.1016/j.athoracsur.2019.03.009
41. Oterhals K, Fridlund B, Nordrehaug JE, Haaverstad R, Norekvål TM. Adapting to living with a mechanical aortic heart valve: a phenomenographic study. *J Adv Nurs.* (2013) 69:2088–98. doi: 10.1111/jan.12076
42. Anscomb A, Cadet J. Follow-up of patients after heart valve surgery: setting up a nurse-led clinic. *Br J Cardiac Nurs.* (2008) 3:320–3. doi: 10.12968/bjca.2008.3.7.30503
43. McLachlan A, Sutton T, Ding P, Kerr A. A nurse practitioner clinic: a novel approach to supporting patients following heart valve surgery. *Heart Lung Circ.* (2015) 24:1126–33. doi: 10.1016/j.hlc.2015.04.064


**Conflict of Interest:** The authors declare that the research was conducted in the absence of any commercial or financial relationships that could be construed as a potential conflict of interest.

frontiers | Frontiers in Cardiovascular Medicine

BRIEF RESEARCH REPORT
published: 15 April 2022
doi: 10.3389/fcvm.2022.862471

# Anatomy of a Transcatheter Mitral Valve Service

*Harminder Gill*[1,2], *Heath S. L. Adams*[1], *Omar Chehab*[1], *Christopher Allen*[1], *Jane Hancock*[1], *Pablo Lamata*[2], *Gianluca Lucchese*[1], *Bernard Prendergast*[1], *Simon Redwood*[1], *Tiffany Patterson*[1] *and Ronak Rajani*[1,2]*

[1] Cardiovascuar Directorate, Guy's and St Thomas' Hospitals, London, United Kingdom, [2] School of Biomedical Engineering and Imaging Sciences Engineering, King's College London, London, United Kingdom

Transcatheter mitral therapies offer treatment options to selected patients who are unable to undergo open procedures due to prohibitive surgical risk. Data detailing the design and structure of transcatheter mitral services to ensure appropriate patient selection and tailored management strategies is lacking. We report our initial experience of developing and running a purpose-built transcatheter mitral service. The nature and number of referral sources, the multi-disciplinary make-up of the dedicated Mitral Heart Team and the use of integrative imaging assessment with incorporation of computational solutions are discussed. In addition, a summary of the clinical decision-making process is presented. This report sets out a framework from which future clinics can evolve to improve and streamline the delivery of transcatheter mitral therapies.

**Keywords: transcatheter mitral valve replacement, mitral regurgitation, Heart Team, mitral edge-to-edge repair, indirect annuloplasty, mitral stenosis**

OPEN ACCESS

***Edited by:***
*Verena Veulemans, University Hospital of Düsseldorf, Germany*

***Reviewed by:***
*Hoda Hatoum, Michigan Technological University, United States*
*Antonio Popolo Rubbio, IRCCS San Donato Polyclinic, Italy*

***Correspondence:**
*Ronak Rajani*
*ronak.rajani@gstt.nhs.uk*

***Specialty section:***
*This article was submitted to Heart Valve Disease, a section of the journal Frontiers in Cardiovascular Medicine*

***Received:*** *25 January 2022*
***Accepted:*** *22 March 2022*
***Published:*** *15 April 2022*

***Citation:***
*Gill H, Adams HSL, Chehab O, Allen C, Hancock J, Lamata P, Lucchese G, Prendergast B, Redwood S, Patterson T and Rajani R (2022) Anatomy of a Transcatheter Mitral Valve Service. Front. Cardiovasc. Med. 9:862471. doi: 10.3389/fcvm.2022.862471*

## INTRODUCTION

The application of the Heart Team to facilitate transcatheter aortic valve replacement (TAVR) in patients with aortic stenosis is now established in routine clinical practice with well-defined patient pathways (1). It is appealing to consider that the application of this model to patients' inoperable mitral valve (MV) disease would be equally efficacious. Although up to 10% of patients above the age of 75 years have significant MR, only 15% undergo surgical treatment (2). This suggests that a substantial group of patients may be eligible for transcatheter mitral valve therapies (TMVT). Despite this, the number of patients being referred for TMVT is small and screening failure rates remain high, suggesting that alternative strategies are needed to best identify and treat these patients. In the following report we detail our experience in delivering a dedicated Transcatheter Mitral Valve (TMV) Service consisting of a dedicated TMV clinic alongside a specialist multi-disciplinary Heart Team meeting.

## STRUCTURE OF THE TMV CLINIC

A one-stop TMV clinic was run by five Cardiologists. The first two (RR and JH) were imaging cardiologists (echocardiography and cardiac CT) with experience in managing patients with complex valve disease and heart failure, and the third, fourth and fifth were structural interventional cardiologists (TP, BP, and SR) with experience in transcatheter aortic and mitral therapies. Discussion at a Mitral Heart Team meeting comprising of a heart failure/imaging specialist, cardiac surgeon and interventional cardiologist was undertaken for all patients entering the TMT pathway. If treatment was indicated, but surgical options were deemed high risk, then assessment in the

TMV clinic was organized. For other patients a clinic review was arranged to ensure transcatheter options were explored prior to resorting to medical therapy alone or palliation. Following approval for review, patients were seen in a purpose-designed, specialist TMV clinic. Integral to the clinic was the availability of a spectrum of TMVT devices. These comprised (1) transcatheter mitral valve replacement (TMVR) with an Intrepid (Medtronic, MN, USA) or Sapien-3 (Edwards Lifesciences, CA, USA) for cases valve in mitral-annular-calcification (VIMAC), valve-in-valve (VIV) or valve-in-ring (VIR), (2) transcatheter edge-edge repair (TEER) with MitraClip (Abbott, IL, USA) or Pascal (Edwards Lifesciences, CA, USA) for primary or secondary MR, and (3) indirect annuloplasty (IA) with an ARTO (MVRx, CA, USA) device. The clinic was implemented as a one-stop service where patients underwent clinical assessment, a 12-lead electrocardiogram, blood tests and echocardiogram. At this stage, one of the following recommendations was made: (A) no treatment required, (B) optimisation of medical therapy and referral for assessment by the heart failure specialist team, (C) device therapy, (D) re-discussion at the mitral Heart team meeting, or (E) for transcatheter mitral treatment if the prior conditions had been met. If at this stage the preferred strategy was felt to be TEER (i.e., primary or secondary mitral regurgitation with favorable anatomy for TEER), a same day transoesophageal echocardiogram was performed (**Figure 1**). For all other patients (VIMAC, VIV or VIR TMVR and IA), a multiphase ECG-gated CT and transoesophageal echocardiogram were planned for a subsequent visit. Following completion of clinical and imaging assessment, patients were discussed at a dedicated structural Heart Team meeting where patients were either approved for treatment or referred for further advanced imaging. Advanced processing included (A) collaboration with academic partners (King's College London) for cardiac CT 4D flow simulation to predict left ventricular outflow tract gradients following TMVR, (B) finite element modeling (FEM; FEops, Ghent, Belgium) for VIMAC predictions, and (C) preparation of imaging for CT-fluroscopic or CT-echocardiographic fusion for the intended procedure (**Figures 1D–G**) (3, 4).

As awareness of the TMV clinic grew, there was a rapid increase in referrals which was only interrupted by the Coronavirus-19 pandemic (**Figure 2A**). The clinic reviewed 141 patients for TMVT from May 2017 to November 2021. Seventy-nine (56%) patients were referred internally by cardiologists or surgeons, whereas 42.5% were received from external clinicians (**Figure 2B**), including those from geographically distant locations (**Figure 3A**). There were two cases of direct referral by primary care physicians.

## OUR EXPERIENCE

Baseline characteristics are recorded in **Table 1**. The mean age was 77.5 years (range 46.9–95.3 years), of whom 74 (52.8%) were men. NYHA class III-IV symptoms were present in 125 (88.6%) of patients. Etiologies of mitral regurgitation are shown in **Figure 2C**. There was substantial mortality within the cohort and 8 (6%) patients died whilst awaiting assessment or treatment. Procedural management was delivered to a total of 66 (46.8%) patients. Surgical repair was the preferred strategy in 19 patients (13.4%), with repair in 11 patients, and replacement in 8. Transcatheter management was delivered in the remaining 47 patients: 27 patients underwent TEER (19.1%), 13 TMVR (9.2%), 3 IA (2.1%) and 1 Hybrid procedure (TEER + IA) (0.07%). Successful procedural outcomes were recorded in 44 patients (93.6%), with failure of 2 TEER and 1 IA procedures. Additionally, 3 patients suffering with MS were treated with balloon mitral valvuloplasty (BMV). In total, 18 (13%) patients were declined procedural treatment owing to minimal symptoms or scope for further medical optimisation. In 18 (12.7%) patients who met clinical criteria for treatment, there were no surgical or TMVT options available following appropriate imaging assessment (prohibitive surgical risk, small LV cavity, risk of LVOT obstruction, degree of MAC). A multitude of reasons prevented patients receiving definitive management and these are summarized in **Table 2**. An overview of the pathway is summarized in **Figure 3B**.

## DISCUSSION

There are several important observations from our experience in establishing a dedicated TMV service. The proportion of patients receiving comprehensive TMVT assessment increased from 9 in 2017 to 41 in 2021, despite a significant downturn in 2020 and early 2021 due to the COVID-19 pandemic, signaling a growing awareness and demand for the service. Moreover, participation in the clinic resulted in definitive procedural management for 46.8% of these patients. A modest increase in transcatheter therapy was noted, reflecting similar (but amplified) trends from US registry data (5). Our data demonstrate that the delivery of transcatheter therapies outstripped surgery (**Figure 2D**), which is unsurprising considering the cohort was already selected to favor TMVT by virtue of referral to the service.

The structure of our TMVs model was strategically designed to streamline the clinical decision-making process. Patients were often referred once symptomatic with substantial baseline comorbidity and frailty equating to poor physiological reserve. In such cases, rapid assessment and treatment is vital. To achieve this, we positioned a mix of specialists in the clinic as an entry point to the pathway with same day diagnostics for the majority of patients. We believe this bestowed greater referrer confidence in the clinic and increased referrals to the service. The incorporation of MV surgeons earlier in the pathway increased surgical confidence in the TMV clinic, enabling bilateral referral pathways with MV surgeons operating on patients initially deemed to be at high surgical risk, and patients who were not ideal for surgery being referred to the TMV clinic. The positioning of an imaging specialist at the fulcrum of the pathway enabled faster decision making and facilitated access to bioengineering solutions for pre-procedural planning and modeling.

Management of MR is complex, and a multitude of factors are considered when deciding the optimum management strategy (**Figure 4**). Clinical decision-making requires collaboration

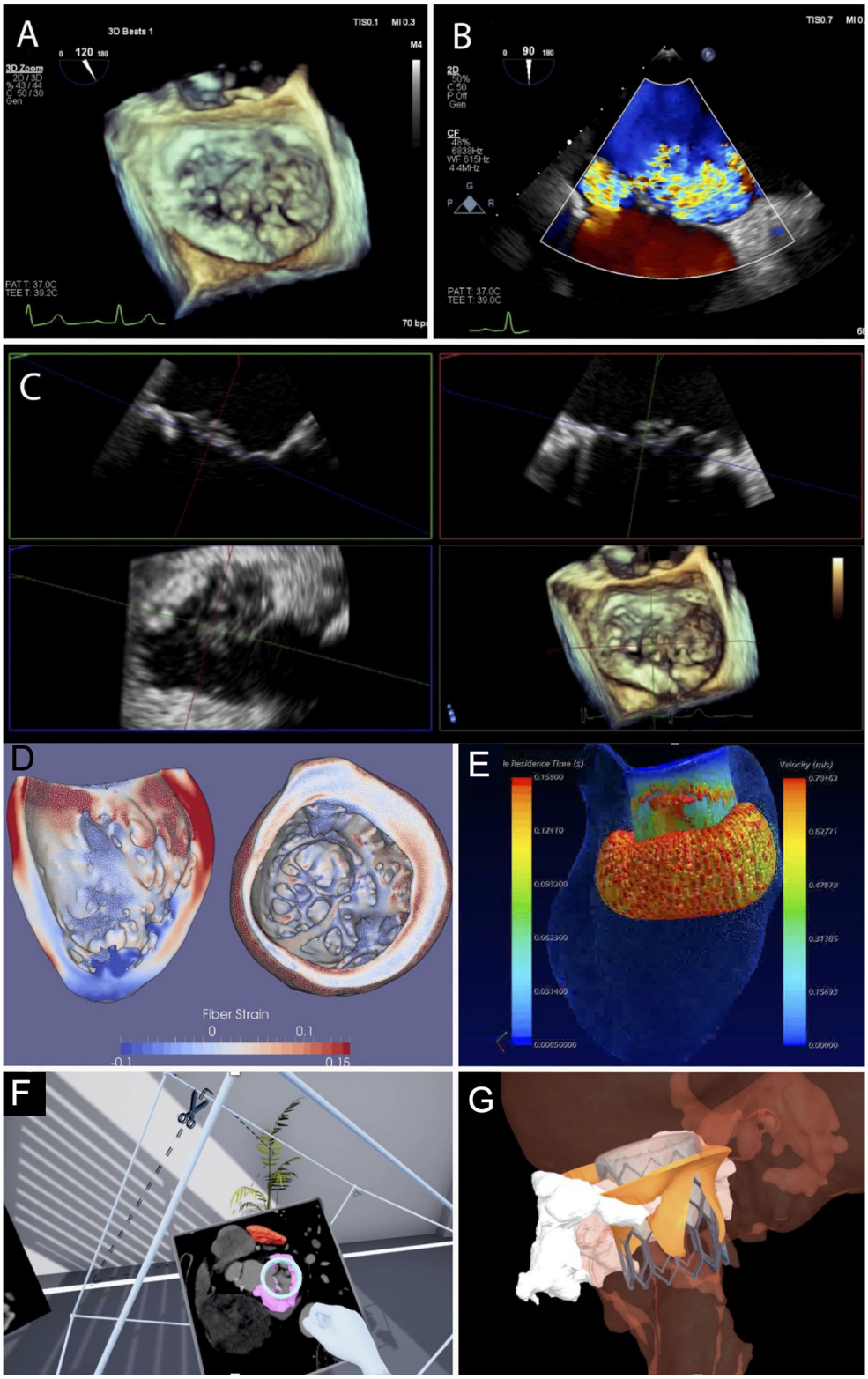


**FIGURE 1 |** Transoesophageal echocardiogram for edge-edge mitral valve leaflet repair. **(A)** Shows 3D imaging, **(B)** Demonstrates Doppler and **(C)** Dual plane imaging. Advanced imaging processing techniques used within the TMVC. **(D)** Shows myocardial fiber strain from CT. **(E)** Demonstrates 4D CT flow to predict blood residence time within the left ventricle following TMVR device deployment. **(F)** Is an example of virtual reality. **(G)** Demonstrates virtual implantation and modeling. 3D, 3-dimensional; TMVC, transcatheter mitral valve clinic; CT, computed tomography; TMVR, transcatheter mitral valve replacement.

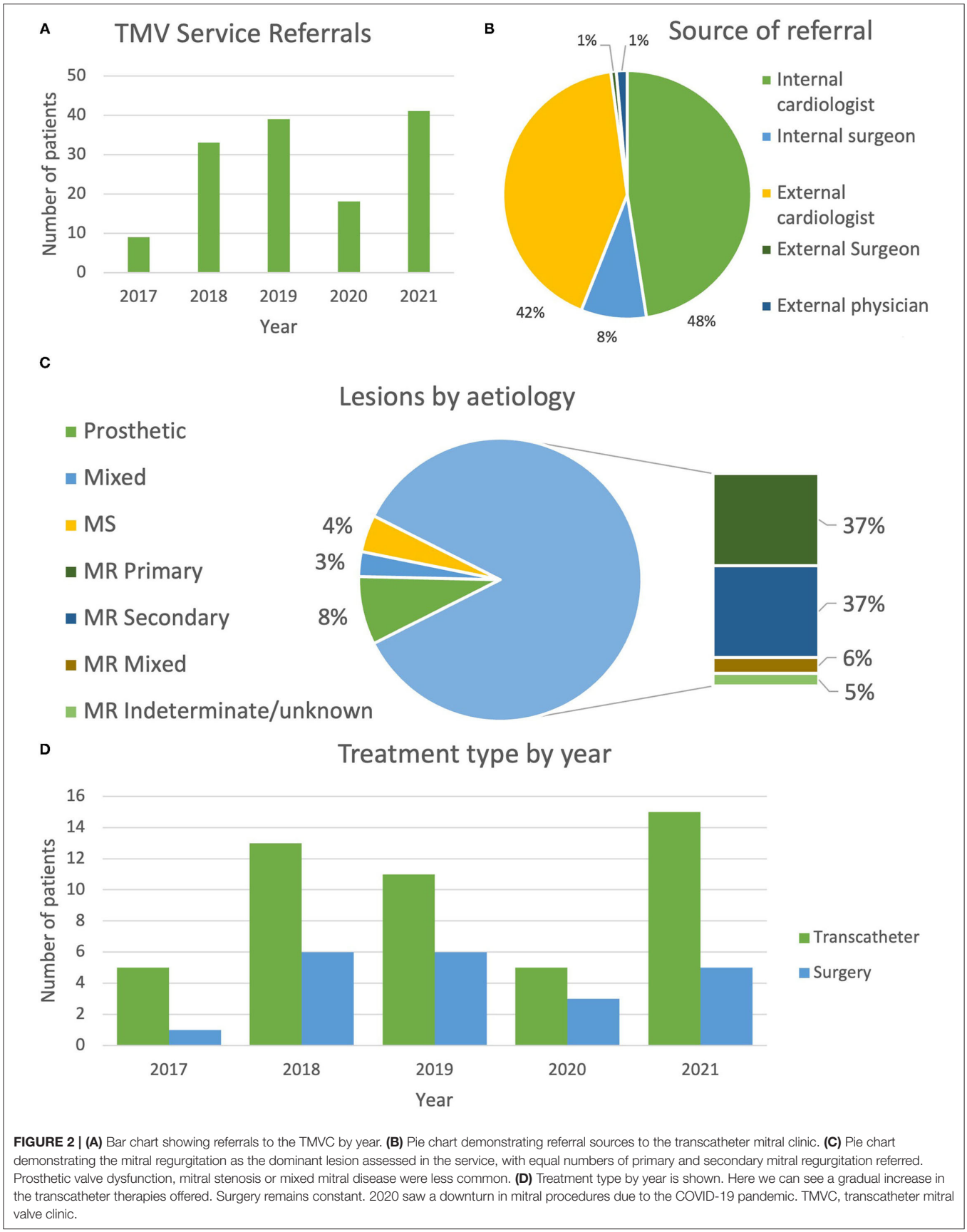


**FIGURE 2 | (A)** Bar chart showing referrals to the TMVC by year. **(B)** Pie chart demonstrating referral sources to the transcatheter mitral clinic. **(C)** Pie chart demonstrating the mitral regurgitation as the dominant lesion assessed in the service, with equal numbers of primary and secondary mitral regurgitation referred. Prosthetic valve dysfunction, mitral stenosis or mixed mitral disease were less common. **(D)** Treatment type by year is shown. Here we can see a gradual increase in the transcatheter therapies offered. Surgery remains constant. 2020 saw a downturn in mitral procedures due to the COVID-19 pandemic. TMVC, transcatheter mitral valve clinic.

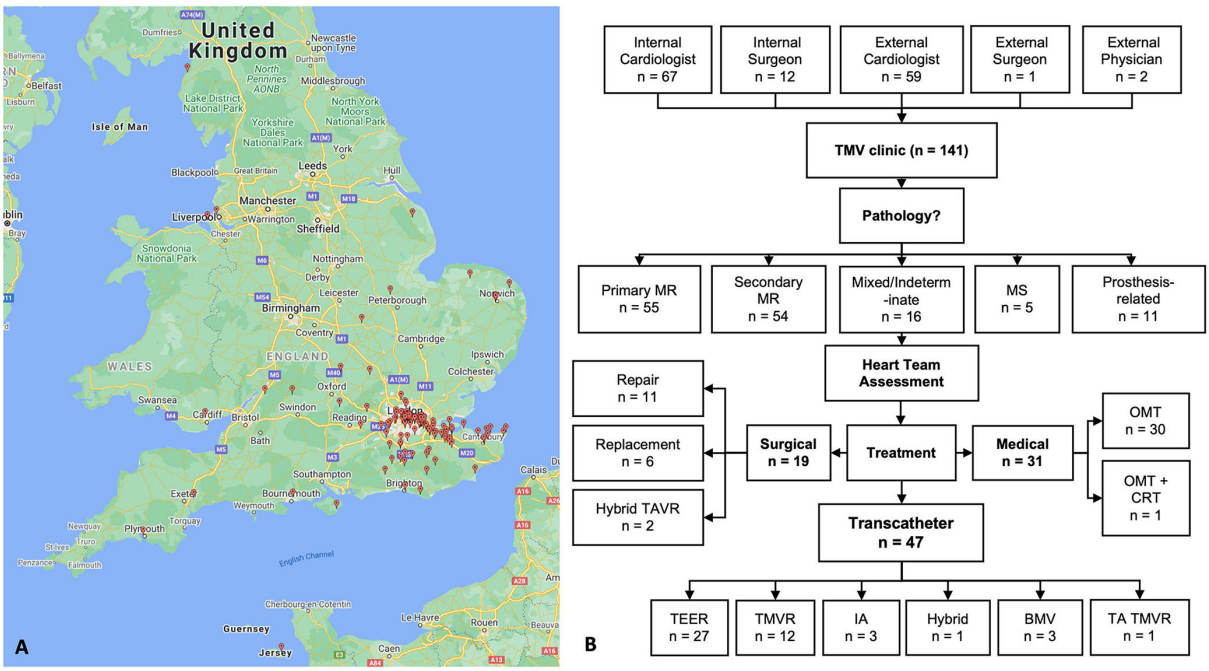


**FIGURE 3 | (A)** Geographical referral sources that developed upon establishment of the TMV service in London. **(B)** Overview of the pathway from referral to assessment and treatment. TMV, transcatheter mitral valve; MR, mitral regurgitation; MS, mitral stenosis; TAVR, transcatheter aortic valve replacement; OMT, optimum medical therapy; CRT, cardiac resynchronisation therapy; TEER, transcatheter edge-edge repair; TMVR, transcatheter mitral valve replacement; IA, indirect annuloplasty; BMV, balloon mitral valvuloplasty; TA TMVR, transapical transcatheter mitral valve.

within the Heart Team to integrate patient-related factors such as symptomatic status, lesion severity and concurrent cardiac disease, in the context of procedure-related factors such as procedural risk, operator experience and anatomic suitability.

The means to assessing patient symptomatic status and lesion severity are well-established, however interpreting these findings in the context of concurrent cardiac comorbidity is vital. MR (especially SMR) is frequently accompanied by concurrent significant tricuspid regurgitation (TR). In the COAPT cohort, greater than moderate TR conferred an additional mortality and morbidity risk (6). Therefore, management of concurrent TR is an important consideration for patients undergoing treatment for MR. Severe pulmonary hypertension, significant (>moderate) right ventricular (RV) dysfunction, or TR requiring operation were exclusion criteria for the COAPT trial and similarly patients within our pathway were not managed procedurally where severe pulmonary hypertension or significant RV dysfunction were present (6). Isolated treatment of MR results in reduction of TR, however whether this result is maintained long-term is unclear (7). Interestingly, Besler et al. reported improved haemodynamic (LV and RV stroke volume and cardiac index), biochemical (reduction in N-terminal pro-brain natriuretic peptide) and symptomatic (NYHA class, 6 min walk test) indices after combined mitral and tricuspid TEER compared to isolated mitral TEER, with no significant difference in mortality (8). Retrospective analysis of patients from the TriValve and TRAMI registries suggested a mortality benefit at 1-year of a combined procedure rather than isolated MR

**TABLE 1 |** Patient baseline characteristics.

| | | TEER | TMVR | Surgery | OMT |
|---|---|---|---|---|---|
| | *n* | 26 | 13 | 19 | 31 |
| Demographic | Age | 80.1 | 76 | 72.1 | 76.1 |
| | Male | 18 | 8 | 12 | 16 |
| | Female | 9 | 5 | 7 | 15 |
| Etiology | Primary MR | 10 | 0 | 9 | 15 |
| | Secondary MR | 12 | 1 | 8 | 12 |
| | Mixed MR | 5 | 0 | 2 | 2 |
| | Prosthetic | 0 | 10 | 0 | 0 |
| | MS | 0 | 2 | 0 | 1 |
| Echocardiography | LVIDD (mm) | 56.0 | 53.2 | 54.2 | 53.2 |
| | LVEF (%) | 50.3 | 48.0 | 53.2 | 51.9 |
| | Significant TR (%) | 64 | 40 | 59 | 43 |
| | Estimated PASP (mmhg) | 51.3 | 50.8 | 51.1 | 53.9 |
| Comorbidity | Hypertension (%) | 38.5 | 25.0 | 47.0 | 43.4 |
| | Coronary artery disease (%) | 36.0 | 38.5 | 35.3 | 60.0 |
| | Atrial fibrillation (%) | 51.9 | 66.7 | 47.4 | 63.3 |
| | Diabetes (%) | 4.0 | 16.7 | 10.5 | 6.7 |
| | CVA/TIA (%) | 27.0 | 8.3 | 5.3 | 6.7 |
| | Dialysis (%) | 0.0 | 3.8 | 5.3 | 0.0 |
| | Hb (g/dl) | 118.3 | 123.2 | 123.5 | 126.0 |
| | eGFR (ml/min) | 51.8 | 64.0 | 71.2 | 51.0 |

*TTE, transthoracic echocardiogram; TEER, transcatheter edge-edge repair; TMVR, transcatheter mitral valve replacement; MR, mitral regurgitation; MS, mitral stenosis; LVIDD, left ventricular internal diameter end diastole; TR, tricuspid regurgitation (significant defined as moderate or greater); PASP, pulmonary artery systolic pressure; CVA, cerebrovascular accident; TIA, transient ischaemic attack; Hb, hemoglobin; eGFR, estimated glomerular filtration rate; OMT, optimum medical therapy.*

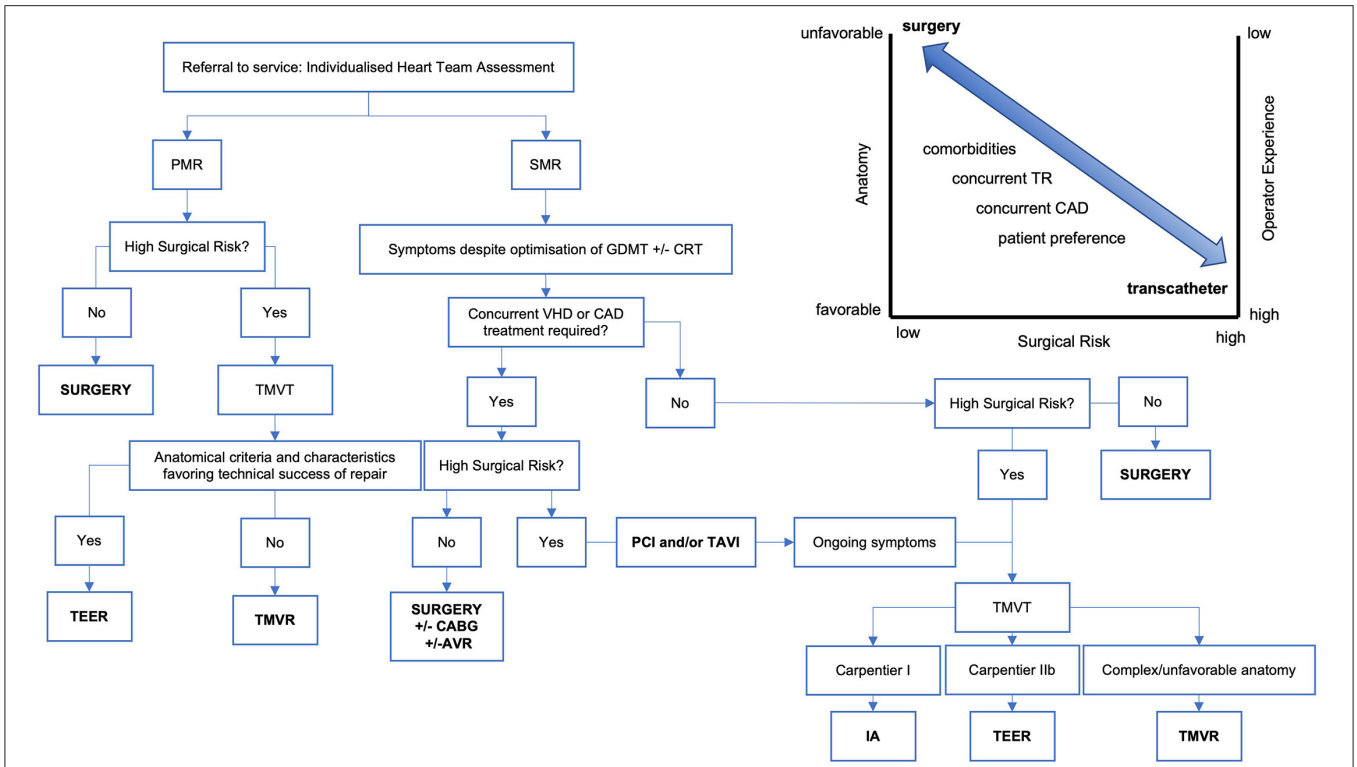


**FIGURE 4 |** A simplified flowchart demonstrating the processes underpinning the patient journey to therapy for mitral regurgitation. The inset graphic illustrates surgical and transcatheter treatment lying on a continuum and how this decision is influenced by surgical risk, anatomic suitability, and operator experience with additional consideration given to concurrent cardiovascular conditions and patient preference. TMVT, transcatheter mitral valve therapy; PMR, primary mitral regurgitation; SMR, secondary mitral regurgitation; VHD, valvular heart disease; TAVR, transcatheter aortic valve replacement; GDMT, guideline-directed medical therapy; CRT, cardiac resynchronisation therapy; TEER, transcatheter edge-edge repair; TMVR, transcatheter mitral valve replacement; IA, indirect annuloplasty; CABG, coronary artery bypass grafting; PCI, percutaneous coronary intervention; AVR, aortic valve replacement.

**TABLE 2 |** Reasons for not receiving procedural management.

| Reasons for not receiving procedural management | Number of patients |
|---|---|
| Treatment awaited pending clinician decision | 4 |
| Treatment awaited pending patient decision | 1 |
| Medical optimization and reassessment required | 2 |
| Clinic assessment or investigations awaited | 3 |
| Treatment awaited | 6 |
| Patient died before assessment | 4 |
| Patient died before treatment | 4 |
| No procedural treatment options after Heart Team Assessment | 18 |
| No indication for treatment | 16 |
| Treatment transferred to alternative center | 4 |
| Patient did not attend for appointment | 4 |
| Patient declined the treatment offered | 9 |

or TR treatment (9). Further work is required to clarify the importance of managing TR in the context of MR in larger scale, randomized trials.

Treatment of concurrent coronary artery disease (CAD) is another important factor in the management of MR, and particularly relevant in ischaemic MR, and warrants address prior to definitive valve treatment (10). Within our pathway, if revascularisation was indicated but surgical risk was prohibitive, percutaneous coronary intervention was undertaken, with subsequent reassessment of the patient clinical status, symptoms and severity of MR. Alternatively, individuals with acceptable surgical risk, would be offered combined CABG and surgical MV where appropriate.

Whilst primary mitral regurgitation (PMR) requires treatment of the valve by repair or replacement once thresholds are met, pharmacotherapy is a core component of secondary mitral regurgitation (SMR) management. Within our cohort, 30% patients received optimum medical therapy, with one patient additionally receiving cardiac resynchronisation therapy (CRT). Optimisation of medical therapy yields improvements in LV function, severity of mitral regurgitation and LV geometry (11). This has a notable benefit in mortality and remains a bastion of SMR management. However, the shortfall in achieving target doses of prognostic medications in the undifferentiated heart failure population has been well documented. For instance, in the CHAMP-HF registry, where the key inclusion criteria was an EF $< 40\%$, target doses were achieved in 18.7, 10.8, and 2% of the cohort for beta blockers, angiotensin converting enzyme inhibitors/angiotensin receptor blockers and anti-neprolysin

**TABLE 3 |** Indication and cautions for transcatheter mitral therapies.

| | Transcatheter edge-edge repair | Indirect annuloplasty | Transcatheter mitral valve replacement |
|---|---|---|---|
| Devices | Mitraclip™ (Abbot)<br>Pascal™ (Edwards) | Arto™ (MVRx) | Sapien 3™ (Edwards)<br>Intrepid™ (Medtronic) |
| Indications | PMR, SMR | SMR | PMR, SMR |
| Anatomic considerations | MVA > 3 $cm^2$<br>Central A2/P2<br>No calcification Grasping length > 10 mm<br>Tenting Height < 10 mm<br>For a flail segment: flail width < 15 mm, flail gap < 10 mm, LVESD > 55 mm*<br>For tethering: coaptation length < 11 mm, overlap length > 2 mm | Annular Dilatation<br>Predetermined by the core lab/PI<br>Coronary sinus proximity and coplanarity | MVA 1.0–3.0 $cm^2$<br>Multi-segment disease<br>Commissural Disease<br>Perforations<br>Clefts<br>Valve-in-ring<br>Valve-in-valve<br>Valve-in-MAC |
| Functional considerations | Mean gradient < 4 mmHg | | LVEF ≥ 30%<br>Mean gradient 5–10 mmHg<br>Low risk for LVOT obstruction |
| Cautions and contraindications | Leaflet perforation or clefts<br>Severe calcification of the annulus or leaflets<br>Barlow/rheumatic valve<br>Flail width > 15 mm<br>Flail gap >10 mm<br>LVESD > 55 mm in PMR, or greater > 70 mm in SMR<br>MS<br>MVA < 3.0 $cm^2$<br>Mean gradient > 5 mmHg | Severe annular calcification | Access constraints<br>Cardiomyopathy<br>LVEDD > 70 mmHg<br>Severe MS<br>Fused commissures<br>Severe MAC<br>Bleeding/coagulation disorders<br>RV dysfunction<br>Severe LV dysfunction<br>Significant CAD |

*PMR, primary mitral regurgitation; SMR, secondary mitral regurgitation; MS, mitral stenosis; LVOT, left ventricular; MAC, mitral annular calcification; MVA, mitral valve area; RV, right ventricle; LV, left ventricle; CAD, coronary artery disease; PI, principal investigator; LVESD, left ventricular end-systolic diameter, outflow tract; LVEDD, left ventricular end-diastolic diameter.*

inhibitors, respectively, despite there being no contraindication or hypotension to prevent administration (12). This shows that barriers remain in achieving optimum medical therapy despite clear target doses, and comorbidity and patient tolerance are important limiting factors. Similarly, the impact of CRT in SMR to restore both local and global coordinated contraction has been reported to increase coaptation forces, reduce tethering forces, improve annular geometry and reduce diastolic MR (13). Whilst resulting in a modest reduction in MR, an improvement confers a mortality benefit, whereas failure to respond is associated with poorer outcomes (11).

Treatment strategy is dependent upon the accurate delineation of anatomic suitability. Careful assessment using transthoracic and/or transoesophageal echocardiography is indicated. Aside from important but generic information on the LV/RV volumes and function, valuable information impacting feasibility for TMVT is obtained. This includes coaptation height, tenting area, leaflet tethering, calcification, posterior leaflet height, annulus geometry and valve area. Important anatomical criteria along with cautions for different TMVT are included in **Table 3**.

Assessment of surgical risk presented an additional challenge when administering the TMV service. Within our institution, surgical risk was estimated by Heart Team consensus, as suggested in ESC guidance (10). In our team's experience, the STS and Euroscore overestimate risk and serve as deterrent to offering procedural management; contributing to the widely reported undertreatment of MR. There is sparse data to underpin the best approach to assessing overall operative risk specific to transcatheter procedures, with surgical scores tending to overlook frailty of patients, and missing important features that impact transcatheter procedures (e.g., access, etc.). For example, Compagnogne et al. showed that Log Euroscore, Euroscore II and STS overestimated risk and were unable to stratify 30-day mortality in patients undergoing TAVR (14). German registry data suggests that the performance of conventional surgical risk scores is mediocre for patients undergoing TAVR with a tendency to overestimate risk, but even specialized transcatheter risk scores demonstrated only moderate performance at predicting 30-day mortality (15). Although this offers some insight into the limitations of such scores, both the pathogenesis of aortic stenosis and the procedural techniques differ and therefore the findings cannot be extrapolated unreservedly. The Mitral Regurgitation International Database (MIDA) score developed for risk stratification in degenerative mitral regurgitation successfully predicted 2-year all-cause mortality and heart-failure hospitalization in patients undergoing TEER in a multicentre, observational study, irrespective of mitral regurgitation etiology, with hazard of all-cause mortality increasing by 13% (95% CI 3–25%) for each additional point on the 12 point scale (16). Further work is required in prospective studies to assess the utility of this score. Ultimately, this highlights the importance of individualized risk assessment, provided by careful evaluation by experienced members of the Heart Team. Evaluation of current and novel risk stratifying methods for TMVT remains an area to be explored.

There is mounting evidence that operator experience and institutional case load influences the technical success and clinical outcomes of TMVT (17). For instance, analysis of 24,709 patients undergoing TEER in the German **TRA**nscatheter **MI**tral (TRAMI) registry, revealed that centers performing TEER in <25 patients/year had comparable in-hospital mortality to those performing >25 procedures/year and that this was the case with cut-offs at 10 and 50 procedures a year (18). However, analysis over the entire 7-year period showed that centers performing <300 TEER, had a range of in-hospital mortality of 0–20%, whereas in those undertaking >300 TEER, the in-hospital mortality ranged 0.9–5.5% (18). Evaluation of the US TVT registry demonstrated a higher likelihood of procedural success, reduced procedure times and fewer complications with increasing institutional case experience (19). This highlights the importance of achieving the requisite volume and suggests that TMVT is best administered in larger, centralized cardiac centers.

Novel approaches to Heart Team dynamics may enable greater access to treatment and improved outcomes for patients with MV disease being considered for TMVT. Further evaluation of TMVC models is needed to confirm this hypothesis.

## DATA AVAILABILITY STATEMENT

The datasets presented in this article are not readily available since they would permit patient identification. Requests to access the datasets should be directed to ronak.rajani@gstt.nhs.uk.

## ETHICS STATEMENT

Ethical review and approval was not required for the study on human participants in accordance with the local legislation and institutional requirements. Written informed consent for participation was not required for this study in accordance with the national legislation and the institutional requirements.

## AUTHOR CONTRIBUTIONS

HG, HA, BP, and RR: concept, design, and drafting. HG and RR: database and analysis. OC, CA, JH, PL, GL, BP, SR, and TP: critical review, editing, and revising manuscript. All authors contributed to the article and approved the submitted version.

## FUNDING

This study was supported by BHF Translational Award Ref: TG/17/3/33406; EU's Horizon 2020 R&I program under the Marie Skłodowska-Curie g.a. No. 764738; Wellcome Trust/EPSRC Centre for Medical Engineering (WT 203148/Z/16/Z). PL holds a Wellcome Trust Senior Research Fellowship (209450/Z/17/Z).

## REFERENCES

1. Jones DR, Chew DP, Horsfall MJ, Sinhal AR, Joseph MX, Baker RA, et al. Impact of surgical and transcatheter aortic valve replacement on frailty score. *Heart Lung Circ.* (2022) 31:566–74. doi: 10.1016/j.hlc.2021.09.014
2. Mirabel M, Iung B, Baron G, Messika-Zeitoun D, Détaint D, Vanoverschelde J-L, et al. Clinical research what are the characteristics of patients with severe, symptomatic, mitral regurgitation who are denied surgery? *Eur Heart J.* (2007) 28:1358–65. doi: 10.1093/eurheartj/ehm001
3. Karády J, Ntalas I, Prendergast B, Blauth C, Niederer S, Maurovich-Horvat P, et al. Transcatheter mitral valve replacement in mitral annulus calcification – "The art of computer simulation". *J Cardiovasc Comput Tomogr.* (2018) 12:153–7. doi: 10.1016/j.jcct.2017.12.007
4. de Vecchi A, Marlevi D, Nordsletten DA, Ntalas I, Leipsic J, Bapat V, et al. Left ventricular outflow obstruction predicts increase in systolic pressure gradients and blood residence time after transcatheter mitral valve replacement. *Sci Rep.* (2018) 8:1–11. doi: 10.1038/s41598-018-33836-7
5. Mack M, Carroll JD, Thourani V, Vemulapalli S, Squiers J, Manandhar P, et al. Transcatheter mitral valve therapy in the united states: a report from the STS-ACC TVT registry. *J Am College Cardiol.* (2021) 78:2326–53. doi: 10.1016/j.jacc.2021.07.058
6. Hahn RT, Asch F, Weissman NJ, Grayburn P, Kar S, Lim S, et al. Impact of tricuspid regurgitation on clinical outcomes: the COAPT trial. *J Am College Cardiol.* (2020) 76:1305–14. doi: 10.1016/j.jacc.2020.07.035
7. Kavsur R, Iliadis C, Spieker M, Brachtendorf BM, Tiyerili V, Metze C, et al. Predictors and prognostic relevance of tricuspid alterations in patients undergoing transcatheter edge-to-edge mitral valve repair. *Eurointervention.* (2021) 17:827–34. doi: 10.4244/EIJ-D-20-01094
8. Besler C, Orban M, Rommel KP, Braun D, Patel M, Hagl C, et al. Predictors of procedural and clinical outcomes in patients with symptomatic tricuspid regurgitation undergoing transcatheter edge-to-edge repair. *JACC Cardiovasc Interv.* (2018) 11:1119–28. doi: 10.1016/j.jcin.2018.05.002
9. Mehr M, Karam N, Taramasso M, Ouarrak T, Schneider S, Lurz P, et al. combined tricuspid and mitral versus isolated mitral valve repair for severe MR and TR: an analysis from the TriValve and TRAMI registries. *JACC Cardiovasc Interv.* (2020) 13:543–50. doi: 10.1016/j.jcin.2019.10.023
10. Vahanian A, Beyersdorf F, Praz F, Milojevic M, Baldus S, Bauersachs J, et al. 2021 ESC/EACTS guidelines for the management of valvular heart disease developed by the task force for the management of valvular heart disease of the European Society of Cardiology (ESC) and the European Association for Cardio-Thoracic Surgery (EACTS). *Eur Heart J.* (2021) 43:561–632. doi: 10.1093/eurheartj/ehab395
11. Coats AJS, Anker SD, Baumbach A, Alfieri O, von Bardeleben RS, Bauersachs J, et al. The management of secondary mitral regurgitation in patients with heart failure: a joint position statement from the Heart Failure Association (HFA), European Association of Cardiovascular Imaging (EACVI), European Heart Rhythm Association (EHRA), and European Association of Percutaneous Cardiovascular Interventions (EAPCI) of the ESC. *Eur Heart J.* (2021) 42:1254–69. doi: 10.1093/eurheartj/ehab086
12. Peri-Okonny PA, Mi X, Khariton Y, Patel KK, Thomas L, Fonarow GC, et al. Target doses of heart failure medical therapy and blood pressure: insights from the CHAMP-HF registry. *JACC Heart Fail.* (2019) 7:350–8. doi: 10.1016/j.jchf.2018.11.011
13. Spartera M, Galderisi M, Mele D, Cameli M, D'Andrea A, Rossi A, et al. Role of cardiac dyssynchrony and resynchronization therapy in functional mitral regurgitation. *Eur Heart J Cardiovasc Imaging.* (2016) 17:471–80. doi: 10.1093/ehjci/jev352
14. Compagnone M, Moretti C, Marcelli C, Taglieri N, Ghetti G, Corsini A, et al. Surgical risk scores applied to transcatheter aortic valve implantation: friends or foes? Short-term and long-term outcomes from a single-center registry. *J Invasive Cardiol.* (2019) 31:E282–8.

15. Wolff G, Shamekhi J, Al-Kassou B, Tabata N, Parco C, Klein K, et al. Risk modeling in transcatheter aortic valve replacement remains unsolved: an external validation study in 2946 German patients. *Clin Res Cardiol.* (1234) 110:368–76. doi: 10.1007/s00392-020-01731-9
16. Kavsur R, Spieker M, Iliadis C, Metze C, Transier M, Tiyerili V, et al. Mitral regurgitation international database (Mida) score predicts outcome in patients with heart failure undergoing transcatheter edge-to-edge mitral valve repair. *J Am Heart Assoc.* (2021) 10:19548. doi: 10.1161/JAHA.120.019548
17. Taramasso M, Gavazzoni M, Nickenig G, Maisano F. Transcatheter mitral repair and replacement: which procedure for which patient? *EuroIntervention.* (2019) 15:867–74. doi: 10.4244/EIJ-D-19-00743
18. Keller K, Hobohm L, Schmidtmann I, Münzel T, Baldus S, Stephan Von Bardeleben R. Centre procedural volume and adverse in-hospital outcomes in patients undergoing percutaneous transvenous edge-to-edge mitral valve repair using MitraClip® in Germany. *Eur J Heart Fail.* (2021) 23:1380–9. doi: 10.1002/ejhf.2162
19. Chhatriwalla AK, Vemulapalli S, Holmes DR, Dai D, Li Z, Ailawadi G, et al. Institutional experience with transcatheter mitral valve repair and clinical outcomes: insights from the TVT registry. *Cardiovasc Interv.* (2019) 12:1342–52. doi: 10.1016/j.jcin.2019.02.039

**Conflict of Interest:** The authors declare that the research was conducted in the absence of any commercial or financial relationships that could be construed as a potential conflict of interest.

frontiers | Frontiers in Cardiovascular Medicine

SYSTEMATIC REVIEW
published: 25 April 2022
doi: 10.3389/fcvm.2022.877140

# Association Between Lipoprotein(a) and Calcific Aortic Valve Disease: A Systematic Review and Meta-Analysis

*Qiyu Liu[1,2†], Yanqiao Yu[1,2†], Ruixi Xi[1], Jingen Li[3], Runmin Lai[1], Tongxin Wang[1,2], Yixuan Fan[1,2], Zihao Zhang[1,2], Hao Xu[1*] and Jianqing Ju[1*]*

[1] National Clinical Research Center for Chinese Medicine Cardiology, Xiyuan Hospital, China Academy of Chinese Medical Sciences, Beijing, China, [2] Graduate School, Beijing University of Chinese Medicine, Beijing, China, [3] Dongzhimen Hospital, Beijing University of Chinese Medicine, Beijing, China

OPEN ACCESS

**Edited by:**
Ronak Rajani,
Guy's and St Thomas' NHS Foundation Trust, United Kingdom

**Reviewed by:**
Simon Kraler,
University of Zurich, Switzerland
Amin Polzin,
University Hospital of Düsseldorf, Germany

***Correspondence:**
Hao Xu
xuhaotcm@hotmail.com
Jianqing Ju
jujianqing@163.com

[†] These authors have contributed equally to this work

**Specialty section:**
This article was submitted to Heart Valve Disease, a section of the journal Frontiers in Cardiovascular Medicine

**Received:** 16 February 2022
**Accepted:** 28 March 2022
**Published:** 25 April 2022

**Citation:**
Liu Q, Yu Y, Xi R, Li J, Lai R, Wang T, Fan Y, Zhang Z, Xu H and Ju J (2022) Association Between Lipoprotein(a) and Calcific Aortic Valve Disease: A Systematic Review and Meta-Analysis. Front. Cardiovasc. Med. 9:877140. doi: 10.3389/fcvm.2022.877140

**Background:** Preliminary studies indicated that enhanced plasma levels of lipoprotein(a) [lp(a)] might link with the risk of calcific aortic valve disease (CAVD), but the clinical association between them remained inconclusive. This systematic review and meta-analysis were aimed to determine this association.

**Methods:** We comprehensively searched PubMed, Embase, Web of Science, and Scopus databases for studies reporting the incidence of CAVD and their plasma lp(a) concentrations. Pooled risk ratio (RR) and 95% confidence interval (95% CI) were calculated to evaluate the effect of lp(a) on CAVD using the random-effects model. Subgroup analyses by study types, countries, and the level of adjustment were also conducted. Funnel plots, Egger's test and Begg's test were conducted to evaluate the publication bias.

**Results:** Eight eligible studies with 52,931 participants were included in this systematic review and meta-analysis. Of these, four were cohort studies and four were case-control studies. Five studies were rated as high quality, three as moderate quality. The pooled results showed that plasma lp(a) levels ≥50 mg/dL were associated with a 1.76-fold increased risk of CAVD (RR, 1.76; 95% CI, 1.47–2.11), but lp(a) levels ≥30 mg/dL were not observed to be significantly related with CAVD (RR, 1.28; 95% CI, 0.98–1.68). We performed subgroup analyses by study type, the RRs of cohort studies revealed lp(a) levels ≥50 mg/dL and lp(a) levels ≥30 mg/dL have positive association with CAVD (RR, 1.70; 95% CI, 1.39–2.07; RR 1.38; 95% CI, 1.19–1.61).

**Conclusion:** High plasma lp(a) levels (≥50 mg/dL) are significantly associated with increased risk of CAVD.

**Keywords: lipoprotein(a), calcific aortic valve disease, aortic valve stenosis, aortic valve calcification, systematic review and meta-analysis**

# INTRODUCTION

Calcific aortic valve disease (CAVD) is one of the most common valve disorders (1). CAVD is characterized by calcification and remodeling of the valve leaflets, which often progresses to aortic sclerosis and stenosis, eventually leading to heart failure, angina, death, and other serious adverse cardiovascular events (2, 3). 2020 VHD guideline recommended the intervention of symptomatic AVS mainly apply to SAVR and TAVI. Surgical treatment is not performed routinely in asymptomatic patients (4). With more and more in-depth studies of pathogenesis, researchers are exploring targeted drugs to delay disease progression (5). A meta-analysis included three RCT and five observational studies to analyze the efficacy of ACEI/ARB to CAVD (6), the results showed that there was no statistically significant difference in all-cause mortality between the two groups, but the AVR rate of the treatment group was lower than that of the control group, which needed large-scale RCT to prove. Multiple rigorous RCTs have shown negative efficacy of statins (7–9). Besides, researchers also explored the targets on phosphate/calcium-metabolism and nitric oxide and IGF-1 signaling pathway, which need to be further proved (5).

Globally, about 10–30% of the population has high lp(a) levels ≥50 mg/dl (10). Epidemiological and genetic evidence suggested that high lp(a) concentration had a direct relationship with cardiovascular disease (11). Previous cytological studies have shown that lipoprotein(a) [lp(a)] played an important role in the pathogenesis of CAVD through increasing inflammation and oxidative stress, promoting calcium deposition of valvular interstitial cells (VICs) (12, 13). Mendelian randomization studies suggested that *LPA* genotype, which could mediate the levels of lp(a), had a strong relationship with CAVD (14). Multiple genome-wide association studies had shown that the rs10455872 genetic variant in *LPA*, which was associated with higher lp(a) levels, was independently related to an augmented risk of CAVD (15, 16). However, evidence from clinical studies was inconsistent. Some studies indicated comparing to those without CAVD, patients with CAVD had significantly higher levels of lp(a) (17, 18), while some studies suggested there were no statistical differences in lp(a) levels between CAVD and controls (19). In response to the lack of systematic and comprehensive evidence on the clinical association between lp(a) and CAVD. We performed an extensive systematic review and meta-analysis to assess whether elevated lp(a) significantly affected the incidence of CAVD.

# METHODS

The systematic review and meta-analysis were performed following the recommendations of the Preferred Reporting Items for Systematic Reviews and Meta-analyses (PRISMA) (20) and Meta-analyses of Observational Studies in Epidemiology (MOOSE) checklist (21). The protocol has been registered in PROSPERO database (registration number: CRD42021273149).

## Search Strategy

Two authors (Liu QY and Yu YQ) systematically searched the electronic databases, including PubMed (MEDLINE), Embase, Web of Science, and Scopus, up to 31 August 2021. Searching terms included ["lipoprotein(a)" or "lp (a)" or "lipoprotein"] and ("calcific aortic valve disease" or "calcific aortic valve stenosis" or "aortic valve stenosis" or "aortic stenosis" or "aortic valve sclerosis" or "aortic sclerosis" or "aortic valve calcification") without language or sample size restrictions. The reference lists of relevant reviews, original reports were also searched for potential eligible records. The initial screening of eligible studies was based on the titles and abstracts.

## Study Selection

All cohort studies and case-control studies that had investigated the association between lp(a) and the risk of CAVD were eligible for inclusion. 2016 ESC/EAS Guidelines suggested that lp(a) ≥50 mg/dL had a significant risk of CVD (22). European Atherosclerosis Society Consensus Panel recommended that 50 mg/dL as the cut-off value of lp(a) elevation to screen the risk of CVD (23). In the U.S, the general cut-off value for lp(a) elevation is 30 mg/dL higher (24). Canadian Guidelines for the Management of Dyslipidemia pointed out that lp(a) ≥30 mg/dL continuously increased the risk of CVD (25). Analyzing Chinese studies on the risk of lp(a) cut-off value, the Expert Statement suggested 30 mg/dl might be the cut point for the increased risk of CVD (26). And lots of studies revealed both two cut-off values might be applicable to assess CAVD risk (27, 28). Therefore, we considered 30 and 50 mg/dL as the cut-off points for grouping and merging as most studies reported lp(a) as a categorical variable. The exclusion criteria were as follows: (1) patients with rheumatic diseases; (2) duplications or conference abstracts; (3) missing data and data that were impossible to extract or calculate from the published results. The eligibility of the included studies was assessed by two reviewers (Liu QY and Yu YQ) independently. Any disputes were resolved by consensus with all the authors.

## Data Extraction

Data extraction was completed by two reviewers (Liu QY and Lai RM) independently. If there were disagreements, a third reviewer would be consulted (Ju JQ). Information extracted from each included study comprised first author's name, publication year, country or region where it was performed, study design, and follow-up duration. Demographic data included the number of participants and primary characteristics were obtained.

## Qualitative Assessment

Both cohort studies and case-control studies were estimated the risk of bias according to the Newcastle–Ottawa quality assessment scale (NOS), with a maximum score of 9 (29). The summary scores in 0–3, 4–6, 7–9 scale were classified into high, medium, and low quality. Qualitative assessment was assessed independently by two reviewers (Wang TX and Fan YX). Any disputes were evaluated by the third author (Xi RX).

## Statistical Analysis

The pooled CAVD prevalence was compared between individuals with lp(a) levels <50 vs. ≥50 mg/dL and with lp(a) levels <30 vs. ≥30 mg/dL, respectively. Adjusted risk estimates of CAVD reported directly in the included studies were extracted, including odds ratios (ORs), hazard ratio (HRs), and risk ratios (RRs). Adjusted factors were currently identified risk factors related to the occurrence and development of CAVD, including age, sex, hypertension, smoking, dyslipidemia, BNP, diabetes, and obesity, and at least one of them was required to be adjusted in advance (30). And plasma Lp(a) concentration is primarily genetically determined by variation in the LPA gene (17). Studies without adjusted values were replaced with unadjusted values. Given the incidence of CAVD is <20%, the OR was approximately equal to RR (31, 32). Therefore, RRs and 95% CIs were used to estimate the combined effects.

The overall effect was calculated by a *Z*-test, and a two-tailed $P < 0.05$ was deemed statistically significant. Chi-square Cochran's *Q*-test and I square statistics were used to assess potential heterogeneity among studies. In detail, I square >50% was defined as high statistical heterogeneity, I square of 0–50% indicates low heterogeneity, I square = 0% indicates no heterogeneity, respectively (33). Considering the potential heterogeneity of the included studies, we employed a random-effects model to calculate the pooled RR estimates, and heterogeneity assessment with $P \leq 0.10$ was considered as a significance set (34).

Subgroup analysis was performed to investigate the source of heterogeneity, based on study types, countries, and the level of adjustment (the number of covariates). Potential publication and small sample bias were evaluated by Egger's and Begg's test (35). The funnel plot was provided for visual inspection of any bias. Statistical

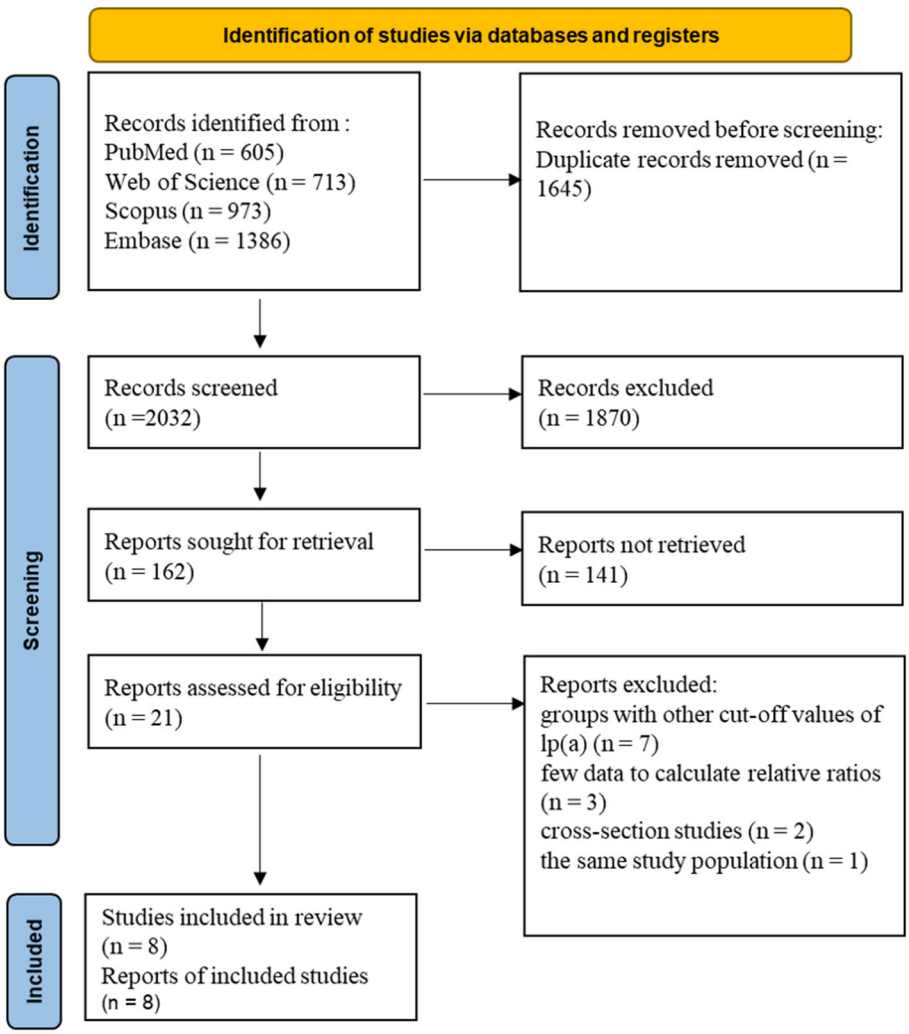


**FIGURE 1 |** Flow diagram of studies.

analyses were accomplished with Stata (Version 12.0, College Station, Texas).

# RESULTS

## Search Results and Study Characteristics

A total of 2,032 articles were identified in four databases. After the final full-text screening, eight eligible studies were included for systematic review and meta-analysis (27, 28, 36–41). There were seven studies assessing the association of lp(a) concentration >50 mg/dL with CAVD, five studies assessing the association of lp(a) concentration >30 mg/dL with CAVD. **Figure 1** shows a detailed flow diagram.

Of the eight included studies, four were cohort studies, and four were case-control studies. Three included studies originated from America, four from Europe, and the remaining one study was unknown. The age of participants ranged from 51 to 75 years. The proportion of females was 35–57%. Five studies evaluated the association between AVS and lp(a), three estimated associations between aortic valve calcification (AVC) and lp(a). In the four included cohort studies, outcome events occurred in 1,383 of 52,134 participants during follow-up. The case-control studies comprised 425 cases and 372 controls. Characteristics of the included studies are displayed in **Table 1**. As shown in **Table 2**, seven studies reported the association using the cut-off value of 50 mg/dL of plasma lp(a), and five studies reported the association using the cut-off value of 30 mg/dL. The adjusted covariates which affected the relationship between lp(a) and CAVD in analyses are provided in **Supplementary Table 1**. The cardiovascular biomarkers of included studies are shown in **Supplementary Table 2**.

## Quality Assessment

The NOS quality assessment scores ranged from 5 to 8 in cohort studies and 6 to 7 in case-control studies. Two out of four cohort studies were identified as high quality, two as moderate quality. Three out of four case-control studies were identified as high quality, one as moderate quality. Scoring details are provided in **Supplementary Table 3**.

## Meta-Analysis

Lp(a) 50 mg/dL group analysis We extracted all the effect estimates of CAVD from seven studies grouped with 50 mg/dL of lp(a) level. One study used the Cox regression to calculate the HR. The rest of the studies used logistic regression and reported ORs and RRs.

Transforming the effect estimates into RRs as described previously, we performed two analyses by study types. The summarized result of the risk ratio was 1.76 (95% CI, 1.47–2.11), which suggested elevated lp(a) level might increase the risk of CAVD by 76% ($P < 0.001$). And lp(a) ≥50 mg/dL might be a risk indicator for CAVD. However, the included studies had substantial statistical heterogeneity (I square = 59.2%), which needed further analysis. The association between lp(a) ≥50 mg/dL and CAVD were

**TABLE 2 |** The statistics of included studies.

| lp(a) 50 mg/dL group | | lp(a) 30 mg/dL group | |
|---|---|---|---|
| **Source** | **Risk estimates (95% CI)** | **Source** | **Risk estimates (95% CI)** |
| Makshood et al. (40) | OR 1.55 (0.71–3.37) | Makshood et al. (40) | OR 1.45 (0.77–2.74) |
| Afshar et al. (36) | RR 1.95 (1.94–1.97) | Cao et al. (27) | RR 1.38 (1.18–1.62) |
| Cao et al. (27) | RR 1.44 (1.21–1.72) | Glader et al. (37) | OR 1.7 (0.8–3.9) |
| Zheng et al. (28) | HR 1.70 (1.33–2.19) | Vongpromek et al. (38) | OR 1.80 (0.88–3.70) |
| Glader et al. (37)[a] | OR 3.4 (1.1–11.2) | Wilkinson et al. (39) | RR 0.93 (0.78–1.15) |
| Vongpromek et al. (38) | OR 2.03 (0.80–5.18) | | |
| Nsaibia et al. (41) | OR 4.19 (0.88–19.89) | | |

*RR, risk ratio; HR, hazard ratio; OR, odds ratio; 95%CI, 95% confidence interval.*
*[a] This study used 48 mg/dl as the threshold values, we classified it as lp(a) 50 mg/dl group.*

**TABLE 1 |** The characteristics of included studies.

| Source | Country | Age, mean | Female,% | Median of follow-up | Participants | Events (cases) | Specific outcome | Diagnosis of CAVD |
|---|---|---|---|---|---|---|---|---|
| **Cohort study** | | | | | | | | |
| Makshood et al. (40) | America | 59.3 | 57 | 5 | 695 | 74 | AVC | CT |
| Afshar et al. (36) | Denmark | 58 | 56 | 5 | 29,016 | 324 | AVS | ICD-8,−10 code |
| Cao et al. (27) | America | 61.5 | 53.7 | – | 4,678 | 582 | AVC | CT |
| Zheng et al. (28) | UK | 59.2 | 55.1 | 19.8 | 17,745 | 403 | AVS | ICD-10 code |
| **Case-control study** | | | | | | | | |
| Glader et al. (37) | Sweden | 60 | 40.6 | – | 202 | 101 | AVS | AVR |
| Vongpromek et al. (38) | Netherlands | 51 | 37.2 | – | 129 | 50 | AVC | CT |
| Nsaibia et al. (41) | NA | 71 | 35 | – | 300 | 150 | AVS | NA |
| Wilkinson et al. (39) | America | 75 | 47 | – | 166 | 124 | AVS | Echocardiography |

*CAD, coronary artery disease; AVC, aortic valve calcification; AVS, aortic valve stenosis; AVR, aortic valve replacement; NA, information not available.*

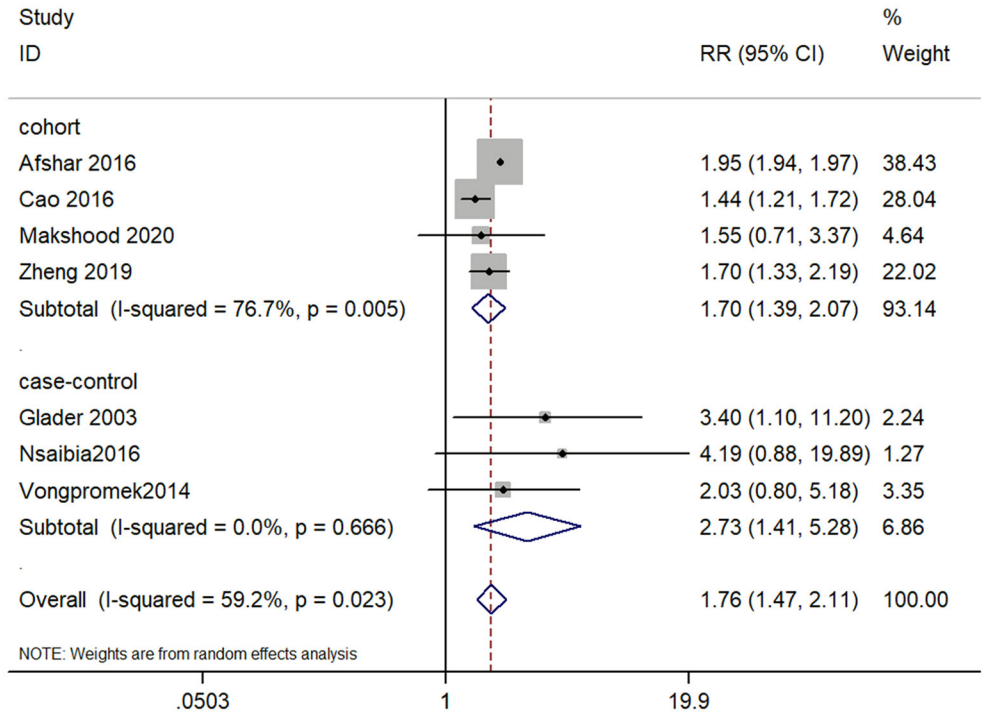


**FIGURE 2 |** Forest plot for examining the association between lp(a) ≤50 mg/dL and CAVD.

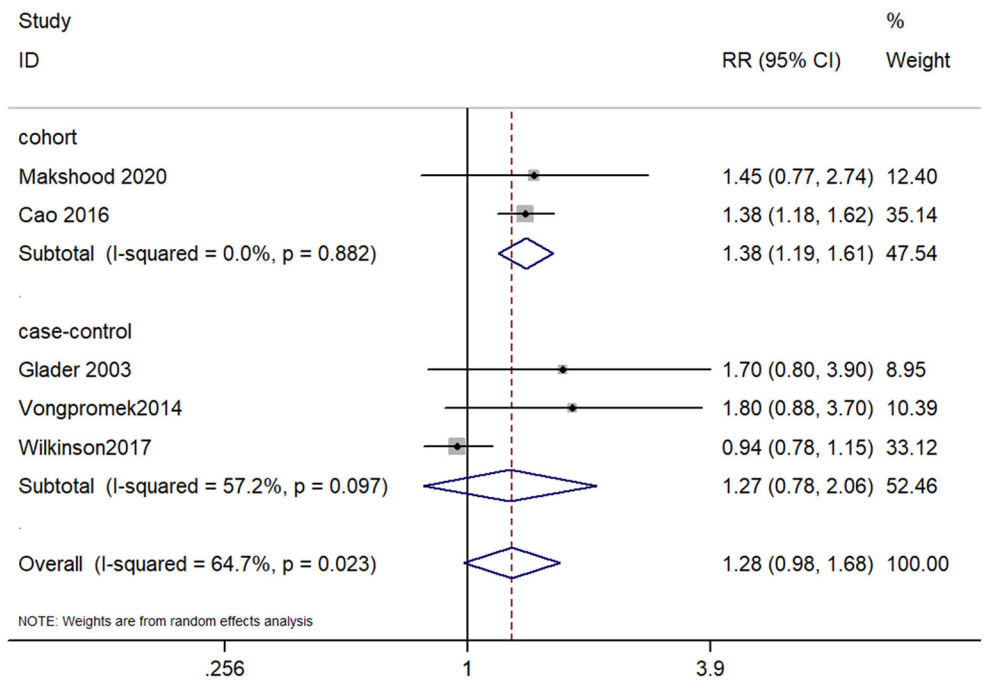


**FIGURE 3 |** Forest plot for examining the association between lp(a) ≤30 mg/dL and CAVD.

significant in both cohort studies (RR, 1.70; 95% CI, 1.39–2.07) and case-control studies (RR, 2.73; 95% CI, 1.41–5.28) (**Figure 2**).

Lp(a) 30 mg/dL group analysis Five studies, which consisted of two cohort studies and three case-control studies, examined the association between lp(a) ≥30 mg/dL and CAVD. The

pooled RR was 1.28 (95% CI, 0.98–1.68), which indicated lp(a) concentration of 30 mg/dL or higher was not significantly associated with CAVD ($P = 0.072$; **Figure 3**). There was significant heterogeneity among studies (I square = 64.7%), which needed further analysis. The result of cohort studies showed that lp(a) ≥30 mg/dL might have an association with the increased risk of CAVD (RR, 1.38; 95% CI, 1.19–1.61). Whereas, the case-control studies showed the association between lp(a) and CAVD was not statistically significant (RR, 1.27; 95% CI 0.78–2.06). In summary, the lp(a) cut-off value of 50 mg/dL seemed more convincing than 30 mg/dL as a risk factor for CAVD.

When we screened the relevant studies, many focused on the relationship between lp(a) and AVC or AVS. AVC and AVS are the preclinical and post-clinical phases of CAVD, regarded as the representative of CAVD. So we analyzed the associations of lp(a) with these two outcomes, respectively. In the lp(a) 50 mg/dL group, four studies reported the association with AVS, three reported the association with AVC. The separate meta-analysis indicated that lp(a) ≥50 mg/dL was significantly correlated with AVC (RR, 1.46; 95% CI, 1.23–1.73) and AVS (RR, 1.95; 95% CI, 1.93–1.96). In the lp(a) 30 mg/dL group, two studies reported the association with AVS, three reported the association with AVC. And the relationship of lp(a) ≥30 mg/dL with AVC (RR, 1.40; 95% CI, 1.20–1.63) is stronger than with AVS (RR, 1.11; 95% CI, 0.66–1.87). As shown in **Table 3**.

**TABLE 3 |** The meta-analyses for the associations of lp(a) with AVC and AVS.

| Outcome | RR (95% CI) | *p*-value | I square |
|---|---|---|---|
| **lp(a) 50 mg/dL group** | | | |
| AVC | 1.46 (1.23, 1.73) | <0.001 | 0.0% |
| AVS | 1.95 (1.93, 1.96) | <0.001 | 0.0% |
| **lp(a) 30 mg/dL group** | | | |
| AVC | 1.40 (1.20, 1.63) | <0.001 | 0.0% |
| AVS | 1.11 (0.66, 1.87) | 0.694 | 50.7% |

## Subgroup Analysis

Subgroup analyses stratified according to study types, countries, and level of adjustment, the statistically significant association between lp(a) ≥50 mg/dL and CAVD risk was observed in all subgroups. When the subgroup analysis was conducted considering the study types in lp(a) 30 mg/dL group, a significant positive effect of lp(a) ≥30 mg/dL on CAVD was noted in the cohort studies (RR, 1.38; 95% CI, 1.19–1.61), while the result of case-control studies had a positive trend without statistical significance (RR, 1.27; 95% CI, 0.78–2.06). A subgroup analysis stratified by different countries, lp(a) ≥30 mg/dL was associated with a higher risk of CAVD in Europe (RR, 1.75; 95% CI, 1.03–2.99), but not in America (RR, 1.19; 95% CI, 0.87–1.63). In a subgroup analysis by the level of adjustment (i.e., the median of the adjusted covariates), the pooled RR in studies adjusted for six or more covariates (RR, 1.39; 95% CI, 1.20–1.62) was more marked than in the less than six covariates group (RR, 1.18; 95% CI, 0.64–2.17). The details are shown in **Table 4**.

## Publication Bias

Publication bias assessment of the above two groups was performed using funnel plots at first. There might be asymmetry in the two diagrams figure (**Supplementary Figure 1**). Therefore, the Egger's test and the Begg's test were carried out for further verification, which suggested these findings might not have publication bias or small sample effect [lp(a)50 mg/dL group: Begg's test, $P = 0.230$; Egger's test, $P = 0.499$; lp(a) 30 mg/dL group: Begg's test, $P > 0.99$; Egger's test, $P > 0.99$].

# DISCUSSION

We evaluated the relationship between elevated plasma lp(a) level and CAVD. The major findings were as follows: (1) The incidence of CAVD was higher in the high lp(a) level group than in the low-level group, as reported by most of the original studies. (2) The pooled results of lp(a) 50 mg/dL group supported that plasma

**TABLE 4 |** Summary risk estimates of the subgroup analyses.

| Subgroup | Design | Study (No.) | RR (95% CI) | *p*-value | Heterogeneity ($I^2$, *p*-value) |
|---|---|---|---|---|---|
| **lp(a) 50 mg/dL group** | | | | | |
| Study types | Cohort studies | 4 | 1.70 (1.39, 2.07) | $p < 0.001$ | 76.7%, $p = 0.005$ |
| | Case-control studies | 3 | 2.73 (1.41, 5.28) | $p = 0.003$ | 0.0%, $p = 0.666$ |
| Countries | America | 2 | 1.45 (1.22, 1.72) | $p < 0.001$ | 0.0%, $p = 0.857$ |
| | Europe | 4 | 1.95 (1.93, 1.96) | $p < 0.001$ | 0.0%, $p = 0.562$ |
| | other | 1 | 4.19 (0.88–19.89) | – | – |
| Level of adjustment | ≥7 | 4 | 1.48 (1.25, 1.75) | $p < 0.001$ | 0.0%, $p = 0.521$ |
| | <7 | 3 | 1.95 (1.88, 2.02) | $p < 0.001$ | 2.2%, $p = 0.360$ |
| **lp(a) 30 mg/dL group** | | | | | |
| Study types | Cohort studies | 2 | 1.38 (1.19, 1.61) | $p < 0.001$ | 0.0%, $p = 0.882$ |
| | Case-control studies | 3 | 1.27 (0.78, 2.06) | $p = 0.339$ | 57.2%, $p = 0.097$ |
| Country | America | 3 | 1.19 (0.87, 1.63) | $p = 0.282$ | 78.7%, $p = 0.009$ |
| | Europe | 2 | 1.75 (1.03, 2.99) | $p = 0.038$ | 0.0%, $p = 0.917$ |
| Level of adjustment | ≥6 | 3 | 1.39 (1.20, 1.62) | $p < 0.001$ | 0.0%, $p = 0.873$ |
| | <6 | 2 | 1.18 (0.64, 2.17) | $p = 0.590$ | 65.9%, $p = 0.087$ |

lp(a) ≥50 mg/dL might be a risk factor for CAVD. Whereas, there was insufficient evidence for the association between plasma lp(a) ≥30 mg/dL and CAVD. Also, substantial heterogeneity between studies was not well-explained by subgroup analysis with a 30 mg/dL lp(a) cut-off value, which called for caution when interpreting the result. (3) Patients with plasma lp(a) ≥50 mg/dL might have a higher risk of CAVD than those with lp(a) ≥30 mg/dL. Therefore, we speculated that the magnitude of lp(a) concentration might have a dose-response relationship with CAVD. (4) The progression of CAVD has multiple stages, including calcification and stenosis, etc. AVC, an independent predictor of cardiovascular events (42), not only may progress to AVS (43), but increases the risk of CAD and all-cause mortality (44, 45). Severe AVS directly correlates with heart failure and death (2). Therefore, the lp(a) effect on AVC and AVS were analyzed separately. The results showed that high plasma lp(a) (≥30 mg/dL and ≥50 mg/dL) was associated with AVC, the relationship of AVS with lp(a) ≥50 mg/dL was significant but not with lp(a) ≥30 mg/dL. (5) The subgroup analysis by study types in lp(a) 30 mg/dL group concluded a positive finding in the cohort studies instead of case-control studies. Included case-control studies have the disadvantages of small sample size and the inherent nature of recall and select bias, which might cause inaccurate reporting of the results (46). And due to the larger sample size, the cohort studies had narrower confidence intervals and higher weight with more accurate estimates. Therefore, large sample cohort studies are needed to further explore the relationship between lp(a) ≥30 mg/dL and CAVD. The analysis result in Europe was more significant than in America, and no meaningful association of lp(a) ≥30 mg/dL was found in America. The participants of two American studies mainly involved Asians, Hispanics, Caucasians and Blacks, and the initial results were inconsistent among different races. However, the race of European studies was relatively homogeneous. Therefore, there are possible ethnic effect factors in the pathogenesis of lp(a)-mediated CAVD (27, 40). And a research article from the MESA study pointed out a possible race/ethnicity-related modification of lp(a) and coronary heart disease events (24). Their findings suggested that the 30 mg/dL cutoff for lp(a) is inappropriate in Caucasian and Hispanic individuals, and the higher 50 mg/dL cutoff should be considered. In contrast, the 30 mg/dL cutoff remains suitable in Black individuals. From the present evidence, the cut-off values of lp(a) differed according to different race/ethnicity groups. But most studies agreed on the cut-off values of 30 and 50 mg/dL. That's why we analyzed using both cut-off values in our meta-analysis. Our subgroup analysis results agree with the findings from Guan et al. (24). (6) The Egger's test and the Begg's test had certified that there was no publication bias in these studies. The number of included studies was <10 and the estimates we used were inherently related to their standard errors, leading to relatively imprecise test power of the funnel plot. Whereas, it was undeniable that selection bias and true heterogeneity might also be related to the asymmetry, such as unavailable unpublished studies, which inevitably lead to publication bias. And we conducted the subgroup analysis to investigate the source of heterogeneity, and this deficiency was made up to some extent.

Besides other conventional risk factors like age, sex, hypertension, and smoking, dyslipidemia played a vital role in calcific aortic valve disease (30). Lipids oxidation may promote chronic low-grade inflammation in the aortic valve, which frequently induces the osteogenic process of VICs (47–49). However, whether LDL-C or HDL-C has casual associations with CAVD remains controversial (50, 51). And two meta-analyses about the effect of statins on aortic valve stenosis demonstrated statins might not retard the progression of valve stenosis even though LDL-C concentration was reduced (52, 53). Instead, attention has turned to lp(a). A rapidly-growing body of evidence demonstrated that lp(a) has a bright prospect in predicting and treating CAVD. A previous systematic review speculated plasma lp(a) might be related to the occurrence and progression of AVS. However, this study did not perform a quantitative meta-analysis (54). Our work, which has been thoroughly searched, rigorously screened and quantitatively analyzed, found that lp(a) ≥50 mg/dL could potentially be a proper risk factor for CAVD. Therefore, lp(a) concentration could be more suitable for assessing the incidence of CAVD, compared with that of LDL-C and HDL-C.

Several plausible mechanisms may account for the underlying pathophysiology of lp(a)-mediated CAVD. Lp(a) is a low-density lipoprotein-like structure, which mainly contains apolipoprotein B (apo B) covalently bound to apolipoprotein(a) [apo(a)] (55, 56), transporting some pro-inflammatory and pro-osteogenic mediators. When aortic valve leaflets are damaged to mechanical or shear stress, excessive lp(a) could infiltrate and accumulate the valve to stimulate inflammation, calcification, and fibrosis (57–59). Oxidized phospholipids (OxPL), primarily carried by lp(a) complexes, has been demonstrated the association with CAVD (60, 61). Zheng et al. have revealed that the high content of lp(a) and OxPL-apoB was independently associated with increased active tissue calcification and clinical events such as AVR or all-cause mortality (12). OxPL might be hydrolyzed to lysophosphatidylcholine (LPC) in the presence of phospholipases, promoting valvular inflammation, thickening and mineralization (62). Lipoprotein-associated phospholipase A2 (Lp-PLA2) and autotaxin (ATX) might be the key phospholipases in the metabolism of lp(a)-OxPL. Lp-PLA2, with a high affinity to lp(a), could convert OxPL into LPC, increasing the expression of phosphate-related genes (63, 64). ATX, mainly combined with apo(a) of lp(a) particles, could transform LPC into LysoPA, which drives the inflammatory and osteogenic program through the NF-κB/IL-6/BMP pathway (41, 65). In addition, lp(a) could directly mediate remodeling and calcification of VICs through inducing MAPKs signaling pathway and the expression of pro-osteogenic factors like bone-specific transcription factor SP7 (osterix), BMP-2, and BMP-4 (66).

Welsh et al. revealed reducing the baseline lp(a) levels by 80%, patients with lp(a) ≥175 nmol/l and baseline CVD could decrease the risk of CVD by 20% (67). And the conclusions of this study suggested that lowering lp(a) levels might be an important way to intervene CAVD. Pharmacotherapies of lp(a) include PCSK9 inhibitor and nucleic acid antisense, etc. In the FOURIER study, it was found that PCSK9 inhibitors could reduce the plasma Lp(a)

level on average 26.9%, and patients with higher Lp(a) levels had a 23% lower risk of major cardiovascular events (68). In the ODYSSEY OUTCOMES trial, the reduction of Lp(a) levels by PCSK9 inhibitors was associated with a decrease in the risk of cardiovascular disease (69). Mipomersen is a 2′-O-methoxyethyl modified second-generation antisense oligonucleotide, which binds to homologous Apo B messenger RNA to inhibit the synthesis of ApoB-100. It can significantly reduce Apo B and Lp(a) levels (70). IONIS-APO(a)Rx, an oligonucleotide targeting lp(a), could reduce lp(a) levels by 66–92%, OxPL-ApoB and OxPL-apo(a) decreased moderately, which play a vital role in pathogenesis of CAVD (71).

There are several strengths of our meta-analysis. Firstly, this is the first meta-analysis assessing the association between lp(a) and CAVD. Secondly, our analysis included a comprehensive search strategy, a considerable number of participants, a subgroup analysis for heterogeneity. And we integrated all relevant cross-sectional and case-control studies, allowing us to determine whether there was a significant relationship between lp(a) and CAVD. Thirdly, most of the included studies have controlled the confounders, which ensured the reliability of the outcomes. Finally, we investigated the relationship between high lp(a) levels ($\geq$50 and $\geq$30 mg/dL) and the incidence of CAVD, respectively, which provided some guidance for patients with elevated plasma lp(a) levels to assess their risk of CAVD. However, heterogeneity was observed in our meta-analysis, even though most of studies had adjusted multiple potential confounders. Therefore, the results of the present analyses should be interpreted with caution.

## CONCLUSION

Based on the current cohort studies and case-control studies, we could conclude that patients with lp(a) $\geq$50 mg/dL were at a significantly high risk of CAVD. However, further large-scale prospective cohort studies with high quality and adequate control for confounders are necessary to draw a firm conclusion on the causality between plasma lp(a) and CAVD.

## DATA AVAILABILITY STATEMENT

The original contributions presented in the study are included in the article/**Supplementary Material**, further inquiries can be directed to the corresponding author/s.

## AUTHOR CONTRIBUTIONS

QL and JJ conceived the study. QL and YY searched the studies, screened the studies, analyzed the data, and wrote the manuscript. QL and RL extracted the data. TW, YF, and RX assessed the risk of bias. JL, JJ, and HX reviewed and revised the manuscript. All authors contributed to the article and approved the submitted version.

## FUNDING

This research was supported by grant CI2021A00917 from the China Academy of Chinese Medical Sciences Innovation Fund, grant ZYYCXTD-C-202007 from the Innovation Team and Talents Cultivation Program of National Administration of Traditional Chinese Medicine, and grant ZZ13-YQ-017 from the Central Public Welfare Research Institutes of China Academy of Chinese Medical Sciences.

## ACKNOWLEDGMENTS

The authors thank Xiyuan Hospital, China Academy of Chinese Medical Sciences, for their support of this work and the reviewers for allowing us to make improvements to the manuscript.

## SUPPLEMENTARY MATERIAL

The Supplementary Material for this article can be found online at: https://www.frontiersin.org/articles/10.3389/fcvm.2022.877140/full#supplementary-material

## REFERENCES

1. Yadgir S, Johnson CO, Aboyans V, Adebayo OM, Adedoyin RA, Afarideh M, et al. Global, regional, and national burden of calcific aortic valve and degenerative mitral valve diseases, 1990-2017. *Circulation.* (2020) 141:1670–80. doi: 10.1161/circulationaha.119.043391
2. Lindman BR, Clavel MA, Mathieu P, Iung B, Lancellotti P, Otto CM, et al. Calcific aortic stenosis. *Nat Rev Dis Prim.* (2016) 2:16006. doi: 10.1038/nrdp.2016.6
3. Dutta P, Lincoln J. Calcific aortic valve disease: a developmental biology perspective. *Curr Cardiol Rep.* (2018) 20:21. doi: 10.1007/s11886-018-0968-9
4. Otto CM, Nishimura RA, Bonow RO, Carabello BA, Erwin JP III, Gentile F, et al. 2020 ACC/AHA guideline for the management of patients with valvular heart disease: executive summary: a report of the American College of Cardiology/American Heart Association Joint Committee on Clinical Practice Guidelines. *Circulation.* (2021). 143:e35–71. doi: 10.1161/cir.0000000000000932
5. Kraler S, Blaser MC, Aikawa E, Camici GG, Lüscher TF. Calcific aortic valve disease: from molecular and cellular mechanisms to medical therapy. *Eur Heart J.* (2022) 43:683–97. doi: 10.1093/eurheartj/ehab757
6. Andersson C, Abdulla J. Is the use of renin-angiotensin system inhibitors in patients with aortic valve stenosis safe and of prognostic benefit? A systematic review and meta-analysis. *Eur Heart J Cardiovasc Pharmacother.* (2017) 3:21–7. doi: 10.1093/ehjcvp/pvw027
7. Chan KL, Teo K, Dumesnil JG, Ni A, Tam J. Effect of Lipid lowering with rosuvastatin on progression of aortic stenosis: results of the aortic stenosis progression observation: measuring effects of rosuvastatin (ASTRONOMER) trial. *Circulation.* (2010) 121:306–14. doi: 10.1161/circulationaha.109.900027
8. Rossebø AB, Pedersen TR, Boman K, Brudi P, Chambers JB, Egstrup K, et al. Intensive lipid lowering with simvastatin and ezetimibe in aortic stenosis. *N Engl J Med.* (2008) 359:1343–56. doi: 10.1056/NEJMoa0804602
9. Dichtl W, Alber HF, Feuchtner GM, Hintringer F, Reinthaler M, Bartel T, et al. Prognosis and risk factors in patients with asymptomatic aortic stenosis and their modulation by atorvastatin (20 mg). *Am J Cardiol.* (2008) 102:743–8. doi: 10.1016/j.amjcard.2008.04.060
10. Enas EA, Varkey B, Dharmarajan TS, Pare G, Bahl VK. Lipoprotein(a): an independent, genetic, and causal factor for cardiovascular disease and acute myocardial infarction. *Indian Heart J.* (2019) 71:99–112. doi: 10.1016/j.ihj.2019.03.004

11. Nordestgaard BG, Langsted A. Lipoprotein (a) as a cause of cardiovascular disease: insights from epidemiology, genetics, and biology. *J Lipid Res.* (2016) 57:1953–75. doi: 10.1194/jlr.R071233
12. Zheng KH, Tsimikas S, Pawade T, Kroon J, Jenkins WSA, Doris MK, et al. Lipoprotein(a) and oxidized phospholipids promote valve calcification in patients with aortic stenosis. *J Am Coll Cardiol.* (2019) 73:2150–62. doi: 10.1016/j.jacc.2019.01.070
13. Yu B, Khan K, Hamid Q, Mardini A, Siddique A, Aguilar-Gonzalez LP, et al. Pathological significance of lipoprotein(a) in aortic valve stenosis. *Atherosclerosis.* (2018) 272:168–74. doi: 10.1016/j.atherosclerosis.2018.03.025
14. Thanassoulis G, Campbell CY, Owens DS, Smith JG, Smith AV, Peloso GM, et al. Genetic associations with valvular calcification and aortic stenosis. *N Engl J Med.* (2013) 368:503–12. doi: 10.1056/NEJMoa1109034
15. Cairns BJ, Coffey S, Travis RC, Prendergast B, Green J, Engert JC, et al. A replicated, genome-wide significant association of aortic stenosis with a genetic variant for lipoprotein(a): meta-analysis of published and novel data. *Circulation.* (2017) 135:1181–3. doi: 10.1161/circulationaha.116.026103
16. Arsenault BJ, Boekholdt SM, Dubé MP, Rhéaume E, Wareham NJ, Khaw KT, et al. Lipoprotein(a) levels, genotype, and incident aortic valve stenosis: a prospective Mendelian randomization study and replication in a case-control cohort. *Circ Cardiovasc Genet.* (2014) 7:304–10. doi: 10.1161/circgenetics.113.000400
17. Kamstrup PR, Tybjærg-Hansen A, Nordestgaard BG. Elevated lipoprotein(a) and risk of aortic valve stenosis in the general population. *J Am Coll Cardiol.* (2014) 63:470–7. doi: 10.1016/j.jacc.2013.09.038
18. Ljungberg J, Holmgren A, Bergdahl IA, Hultdin J, Norberg M, Näslund U, et al. Lipoprotein(a) and the apolipoprotein B/A1 ratio independently associate with surgery for aortic stenosis only in patients with concomitant coronary artery disease. *J Am Heart Assoc.* (2017) 6:e007160. doi: 10.1161/jaha.117.007160
19. Mahabadi AA, Kahlert P, Kahlert HA, Dykun I, Balcer B, Forsting M, et al. Comparison of lipoprotein(a)-levels in patients ≥70 years of age with versus without aortic valve stenosis. *Am J Cardiol.* (2018) 122:645–9. doi: 10.1016/j.amjcard.2018.04.046
20. Moher D, Liberati A, Tetzlaff J, Altman DG. Preferred reporting items for systematic reviews and meta-analyses: the PRISMA statement. *BMJ.* (2009) 339:b2535. doi: 10.1136/bmj.b2535
21. Stroup DF, Berlin JA, Morton SC, Olkin I, Williamson GD, Rennie D, et al. Meta-analysis of observational studies in epidemiology: a proposal for reporting. Meta-analysis Of Observational Studies in Epidemiology (MOOSE) group. *JAMA.* (2000) 283:2008–12. doi: 10.1001/jama.283.15.2008
22. Catapano AL, Graham I, De Backer G, Wiklund O, Chapman MJ, Drexel H, et al. 2016 ESC/EAS guidelines for the management of dyslipidaemias: the task force for the management of dyslipidaemias of the European Society of Cardiology (ESC) and European Atherosclerosis Society (EAS) Developed with the special contribution of the European Association for Cardiovascular Prevention & Rehabilitation (EACPR). *Atherosclerosis.* (2016). 253:281–344. doi: 10.1016/j.atherosclerosis.2016.08.018
23. Nordestgaard BG, Chapman MJ, Ray K, Borén J, Andreotti F, Watts GF, et al. Lipoprotein(a) as a cardiovascular risk factor: current status. *Eur Heart J.* (2010) 31:2844–53. doi: 10.1093/eurheartj/ehq386
24. Guan W, Cao J, Steffen BT, Post WS, Stein JH, Tattersall MC, et al. Race is a key variable in assigning lipoprotein(a) cutoff values for coronary heart disease risk assessment: the Multi-Ethnic Study of Atherosclerosis. *Arterioscler Thromb Vasc Biol.* (2015) 35:996–1001. doi: 10.1161/atvbaha.114.304785
25. Anderson TJ, Grégoire J, Pearson GJ, Barry AR, Couture P, Dawes M, et al. 2016 Canadian Cardiovascular Society Guidelines for the management of dyslipidemia for the prevention of cardiovascular disease in the adult. *Can J Cardiol.* (2016). 32:1263–82. doi: 10.1016/j.cjca.2016.07.510
26. Li JJ, Ma CS, Zhao D, Yan XW, Ye P, Chen H, et al. Expert statement on the relationship between lipoprotein(a) and cardiovascular disease risk and clinical management. *Chin Circu J.* (2021) 36:1158–67. doi: 10.3969/j.issn.1000-3614.2021.12.003
27. Cao J, Steffen BT, Budoff M, Post WS, Thanassoulis G, Kestenbaum B, et al. Lipoprotein(a) levels are associated with subclinical calcific aortic valve disease in white and black individuals: the multi-ethnic study of atherosclerosis. *Arterioscler Thromb Vasc Biol.* (2016) 36:1003–9. doi: 10.1161/atvbaha.115.306683
28. Zheng KH, Arsenault BJ, Kaiser Y, Khaw KT, Wareham NJ, Stroes ESG, et al. apoB/apoA-I ratio and Lp(a) associations with aortic valve stenosis incidence: insights from the EPIC-Norfolk prospective population study. *J Am Heart Assoc.* (2019) 8:e013020. doi: 10.1161/jaha.119.013020
29. Stang A. Critical evaluation of the Newcastle-Ottawa scale for the assessment of the quality of nonrandomized studies in meta-analyses. *Eur J Epidemiol.* (2010) 25:603–5. doi: 10.1007/s10654-010-9491-z
30. Small A, Kiss D, Giri J, Anwaruddin S, Siddiqi H, Guerraty M, et al. Biomarkers of Calcific Aortic Valve Disease. *Arterioscler Thromb Vasc Biol.* (2017) 37:623–32. doi: 10.1161/atvbaha.116.308615
31. Yi B, Zeng W, Lv L, Hua P. Changing epidemiology of calcific aortic valve disease: 30-year trends of incidence, prevalence, and deaths across 204 countries and territories. *Aging.* (2021) 13:12710–32. doi: 10.18632/aging.202942
32. Grant RL. Converting an odds ratio to a range of plausible relative risks for better communication of research findings. *BMJ.* (2014) 348:f7450. doi: 10.1136/bmj.f7450
33. Higgins JP, Thompson SG. Quantifying heterogeneity in a meta-analysis. *Stat Med.* (2002) 21:1539–58. doi: 10.1002/sim.1186
34. Borenstein M, Hedges LV, Higgins JP, Rothstein HR. A basic introduction to fixed-effect and random-effects models for meta-analysis. *Res Synth Methods.* (2010) 1:97–111. doi: 10.1002/jrsm.12
35. Lin L, Chu H. Quantifying publication bias in meta-analysis. *Biometrics.* (2018) 74:785–94. doi: 10.1111/biom.12817
36. Afshar M, Kamstrup PR, Williams K, Sniderman AD, Nordestgaard BG, Thanassoulis G. Estimating the population impact of lp(a) lowering on the incidence of myocardial infarction and aortic stenosis-brief report. *Arterioscler Thromb Vasc Biol.* (2016) 36:2421–3. doi: 10.1161/atvbaha.116.308271
37. Glader CA, Birgander LS, Söderberg S, Ildgruben HP, Saikku P, Waldenström A, et al. Lipoprotein(a), Chlamydia pneumoniae, leptin and tissue plasminogen activator as risk markers for valvular aortic stenosis. *Eur Heart J.* (2003) 24:198–208. doi: 10.1016/s0195-668x(02)00385-8
38. Vongpromek R, Bos S, Ten Kate GJ, Yahya R, Verhoeven AJ, de Feyter PJ, et al. Lipoprotein(a) levels are associated with aortic valve calcification in asymptomatic patients with familial hypercholesterolaemia. *J Intern Med.* (2015) 278:166–73. doi: 10.1111/joim.12335
39. Wilkinson MJ, Ma GS, Yeang C, Ang L, Strachan M, DeMaria AN, et al. The prevalence of lipoprotein(a) measurement and degree of elevation among 2710 patients with calcific aortic valve stenosis in an academic echocardiography laboratory setting. *Angiology.* (2017) 68:795–8. doi: 10.1177/0003319716688415
40. Makshood M, Joshi PH, Kanaya AM, Ayers C, Budoff M, Tsai MY, et al. Lipoprotein (a) and aortic valve calcium in South Asians compared to other race/ethnic groups. *Atherosclerosis.* (2020) 313:14–19. doi: 10.1016/j.atherosclerosis.2020.09.010
41. Nsaibia MJ, Mahmut A, Boulanger MC, Arsenault BJ, Bouchareb R, Simard S, et al. Autotaxin interacts with lipoprotein(a) and oxidized phospholipids in predicting the risk of calcific aortic valve stenosis in patients with coronary artery disease. *J Intern Med.* (2016) 280:509–17. doi: 10.1111/joim.12519
42. Owens DS, Budoff MJ, Katz R, Takasu J, Shavelle DM, Carr JJ, et al. Aortic valve calcium independently predicts coronary and cardiovascular events in a primary prevention population. *JACC Cardiovasc Imaging.* (2012) 5:619–25. doi: 10.1016/j.jcmg.2011.12.023
43. Cueff C, Serfaty JM, Cimadevilla C, Laissy JP, Himbert D, Tubach F, et al. Measurement of aortic valve calcification using multislice computed tomography: correlation with haemodynamic severity of aortic stenosis and clinical implication for patients with low ejection fraction. *Heart.* (2011) 97:721–6. doi: 10.1136/hrt.2010.198853
44. Utsunomiya H, Yamamoto H, Kunita E, Kitagawa T, Ohashi N, Oka T, et al. Combined presence of aortic valve calcification and mitral annular calcification as a marker of the extent and vulnerable characteristics of coronary artery plaque assessed by 64-multidetector computed tomography. *Atherosclerosis.* (2010) 213:166–72. doi: 10.1016/j.atherosclerosis.2010.08.070
45. Blaha MJ, Budoff MJ, Rivera JJ, Khan AN, Santos RD, Shaw LJ, et al. Relation of aortic valve calcium detected by cardiac computed

tomography to all-cause mortality. *Am J Cardiol.* (2010) 106:1787–91. doi: 10.1016/j.amjcard.2010.08.019
46. Setia MS. Methodology Series Module 2: Case-control Studies. *Indian J Dermatol.* (2016) 61:146–51. doi: 10.4103/0019-5154.177773
47. Nadlonek NA, Lee JH, Weyant MJ, Meng X, Fullerton DA. Ox-LDL induces PiT-1 expression in human aortic valve interstitial cells. *J Surg Res.* (2013) 184:6–9. doi: 10.1016/j.jss.2013.05.001
48. Audet A, Côté N, Couture C, Bossé Y, Després JP, Pibarot P, et al. Amyloid substance within stenotic aortic valves promotes mineralization. *Histopathology.* (2012) 61:610–9. doi: 10.1111/j.1365-2559.2012.04265.x
49. Abdelbaky A, Corsini E, Figueroa AL, Subramanian S, Fontanez S, Emami H, et al. Early aortic valve inflammation precedes calcification: a longitudinal FDG-PET/CT study. *Atherosclerosis.* (2015) 238:165–72. doi: 10.1016/j.atherosclerosis.2014.11.026
50. Hofmanis J, Hofmane D, Svirskis S, Mackevics V, Tretjakovs P, Lejnieks A, et al. HDL-C role in acquired aortic valve stenosis patients and its relationship with oxidative stress. *Medicina.* (2019) 55:416. doi: 10.3390/medicina55080416
51. Nazarzadeh M, Pinho-Gomes AC, Bidel Z, Dehghan A, Canoy D, Hassaine A, et al. Plasma lipids and risk of aortic valve stenosis: a Mendelian randomization study. *Eur Heart J.* (2020) 41:3913–20. doi: 10.1093/eurheartj/ehaa070
52. Zhao Y, Nicoll R, He YH, Henein MY. The effect of statins on valve function and calcification in aortic stenosis: a meta-analysis. *Atherosclerosis.* (2016) 246:318–24. doi: 10.1016/j.atherosclerosis.2016.01.023
53. De Vecchis R, Di Biase G, Esposito C, Ciccarelli A, Cioppa C, Giasi A, et al. Statin use for nonrheumatic calcific aortic valve stenosis: a review with meta-analysis. *J Cardiovasc Med.* (2013) 14:559–67. doi: 10.2459/JCM.0b013e3283587267
54. Guddeti RR, Patil S, Ahmed A, Sharma A, Aboeata A, Lavie CJ, et al. Lipoprotein(a) and calcific aortic valve stenosis: a systematic review. *Prog Cardiovasc Dis.* (2020) 63:496–502. doi: 10.1016/j.pcad.2020.06.002
55. Schmidt K, Noureen A, Kronenberg F, Utermann G. Structure, function, and genetics of lipoprotein(a). *J Lipid Res.* (2016) 57:1339–59. doi: 10.1194/jlr.R067314
56. Ehnholm C, Garoff H, Renkonen O, Simons K. Protein and carbohydrate composition of Lp(a)lipoprotein from human plasma. *Biochemistry.* (1972) 11:3229–32. doi: 10.1021/bi00767a015
57. Thanassoulis G. Lipoprotein (a) in calcific aortic valve disease: from genomics to novel drug target for aortic stenosis. *J Lipid Res.* (2016) 57:917–24. doi: 10.1194/jlr.R051870
58. Nielsen LB, Stender S, Kjeldsen K, Nordestgaard BG. Specific accumulation of lipoprotein(a) in balloon-injured rabbit aorta in vivo. *Circ Res.* (1996) 78:615–26. doi: 10.1161/01.res.78.4.615
59. Hsieh G, Rizk T, Berman AN, Biery DW, Blankstein R. The current landscape of lipoprotein(a) in calcific aortic valvular disease. *Curr Opin Cardiol.* (2021) 36:542–8. doi: 10.1097/hco.0000000000000901
60. Kamstrup PR, Hung MY, Witztum JL, Tsimikas S, Nordestgaard BG. Oxidized phospholipids and risk of calcific aortic valve disease: the Copenhagen general population study. *Arterioscler Thromb Vasc Biol.* (2017) 37:1570–8. doi: 10.1161/atvbaha.116.308761
61. Capoulade R, Chan KL, Yeang C, Mathieu P, Bossé Y, Dumesnil JG, et al. Oxidized phospholipids, lipoprotein(a), and progression of calcific aortic valve stenosis. *J Am Coll Cardiol.* (2015) 66:1236–46. doi: 10.1016/j.jacc.2015.07.020
62. Youssef A, Clark JR, Koschinsky ML, Boffa MB. Lipoprotein(a): expanding our knowledge of aortic valve narrowing. *Trends Cardiovasc Med.* (2021) 31:305–311. doi: 10.1016/j.tcm.2020.06.001
63. Stafforini DM. Biology of platelet-activating factor acetylhydrolase (PAF-AH, lipoprotein associated phospholipase A2). *Cardiovasc Drugs Ther.* (2009) 23:73–83. doi: 10.1007/s10557-008-6133-8
64. Vickers KC, Castro-Chavez F, Morrisett JD. Lyso-phosphatidylcholine induces osteogenic gene expression and phenotype in vascular smooth muscle cells. *Atherosclerosis.* (2010) 211:122–9. doi: 10.1016/j.atherosclerosis.2010.04.005
65. Bouchareb R, Mahmut A, Nsaibia MJ, Boulanger MC, Dahou A, Lépine JL, et al. Autotaxin derived from lipoprotein(a) and valve interstitial cells promotes inflammation and mineralization of the aortic valve. *Circulation.* (2015) 132:677–90. doi: 10.1161/circulationaha.115.016757
66. Yu B, Hafiane A, Thanassoulis G, Ott L, Filwood N, Cerruti M, et al. Lipoprotein(a) induces human aortic valve interstitial cell calcification. *JACC Basic Transl Sci.* (2017) 2:358–71. doi: 10.1016/j.jacbts.2017.03.015
67. Welsh P, Welsh C, Celis-Morales CA, Brown R, Ho FK, Ferguson LD, et al. Lipoprotein(a) and cardiovascular disease: prediction, attributable risk fraction, and estimating benefits from novel interventions. *Eur J Prev Cardiol.* (2022) 28:1991–2000. doi: 10.1093/eurjpc/zwaa063
68. Bittner VA, Szarek M, Aylward PE, Bhatt DL, Diaz R, Edelberg JM, et al. Effect of alirocumab on lipoprotein(a) and cardiovascular risk after acute coronary syndrome. *J Am Coll Cardiol.* (2020) 75:133–44. doi: 10.1016/j.jacc.2019.10.057
69. Szarek M, Bittner VA, Aylward P, Baccara-Dinet M, Bhatt DL, Diaz R, et al. Lipoprotein(a) lowering by alirocumab reduces the total burden of cardiovascular events independent of low-density lipoprotein cholesterol lowering: ODYSSEY OUTCOMES trial. *Eur Heart J.* (2020) 41:4245–55. doi: 10.1093/eurheartj/ehaa649
70. Santos RD, Raal FJ, Catapano AL, Witztum JL, Steinhagen-Thiessen E, Tsimikas S. Mipomersen, an antisense oligonucleotide to apolipoprotein B-100, reduces lipoprotein(a) in various populations with hypercholesterolemia: results of 4 phase III trials. *Arterioscler Thromb Vasc Biol.* (2015) 35:689–99. doi: 10.1161/atvbaha.114.304549
71. Viney NJ, van Capelleveen JC, Geary RS, Xia S, Tami JA, Yu RZ, et al. Antisense oligonucleotides targeting apolipoprotein(a) in people with raised lipoprotein(a): two randomised, double-blind, placebo-controlled, dose-ranging trials. *Lancet.* (2016) 388:2239–53. doi: 10.1016/s0140-6736(16)31009-1

**Conflict of Interest:** The authors declare that the research was conducted in the absence of any commercial or financial relationships that could be construed as a potential conflict of interest.

**Publisher's Note:** All claims expressed in this article are solely those of the authors and do not necessarily represent those of their affiliated organizations, or those of the publisher, the editors and the reviewers. Any product that may be evaluated in this article, or claim that may be made by its manufacturer, is not guaranteed or endorsed by the publisher.

frontiers | Frontiers in Cardiovascular Medicine

ORIGINAL RESEARCH
published: 31 May 2022
doi: 10.3389/fcvm.2022.904958

# Bioprosthetic vs. Mechanical Mitral Valve Replacement for Rheumatic Heart Disease in Patients Aged 50–70 Years

*Jun Yu and Wei Wang**

*Department of Structural Heart Disease Centre, Fu Wai Hospital, National Center for Cardiovascular Diseases, Chinese Academy of Medical Sciences and Peking Union Medical College, Beijing, China*

**Background:** Rheumatic heart disease (RHD) is a critical problem in developing countries and is the cause of most of the cardiovascular adverse events in young people. In patients aged 50–70 years with RHD requiring mitral valve replacement (MVR), deciding between bioprosthetic and mechanical prosthetic valves remains controversial because few studies have defined the long-term outcomes.

**Methods:** 1,691 Patients aged 50–70 years with RHD who received mechanical mitral valve replacement (MVRm) or bioprosthetic mitral valve replacement (MVRb) were retrospectively reviewed in Fuwai hospital from 2010 to 2014. Follow-up ended 31/12/2021; median duration was 8.0 years [interquartile range (IQR), 7.7–8.3 years]. Propensity score matching at a 1:1 ratio for 24 baseline features between MVRm and MVRb yielded 300 patient pairs. The primary late outcome was postoperative mid- to long-term all-cause mortality.

**Results:** Ten-year survival after MVR was 63.4% in the MVRm group and 63.7% in the MVRb group (HR, 0.91; 95% CI, 0.69–1.21; $P = 0.528$). The cumulative incidence of mitral valve reoperation was 0.0% in the MVRm group and 1.2% in the MVRb group (HR, 0.92; 95% CI, 0.69–1.21; $P = 0.530$). The cumulative incidence of stroke was 5.5% in the MVRm group and 6.1% in the MVRb group (HR, 0.89; 95% CI, 0.67–1.18; $P = 0.430$). The cumulative incidence of major bleeding events was 3.3% in the MVRm group and 3.4% in the MVRb group (HR, 0.92; 95% CI, 0.70–1.22; $P = 0.560$).

**Conclusions:** In patients aged 50–70 years with RHD who underwent mitral valve replacement, there was no significant difference on survival, stroke, mitral valve reoperation and major bleeding events at 10 years. These findings suggest mechanical mitral valve replacement may be a more reasonable alternative in patients aged 50–70 years with rheumatic heart disease.

**Keywords: bioprosthesis, rheumatic, mechanical valve, mitral valve replacement, heart valve diseases**

OPEN ACCESS

***Edited by:***
*Marko Banovic,*
*University of Belgrade, Serbia*

***Reviewed by:***
*Mayooran Namasivayam,*
*St. Vincent's Hospital Sydney, Australia*
*Giuseppe Santarpino,*
*Nürnberg Hospital, Germany*

***Correspondence:**
*Wei Wang*
*drweiwangfuwai@163.com*

***Specialty section:***
*This article was submitted to Heart Valve Disease, a section of the journal Frontiers in Cardiovascular Medicine*

***Received:*** *26 March 2022*
***Accepted:*** *12 May 2022*
***Published:*** *31 May 2022*

***Citation:***
*Yu J and Wang W (2022) Bioprosthetic vs. Mechanical Mitral Valve Replacement for Rheumatic Heart Disease in Patients Aged 50–70 Years. Front. Cardiovasc. Med. 9:904958. doi: 10.3389/fcvm.2022.904958*

# INTRODUCTION

Rheumatic heart disease (RHD) remains a challenging health problem across the worldwide, especially in developing countries and is a major cause of cardiovascular mortality in young people (1).

Rheumatic heart disease is mainly caused by rheumatic fever. Rheumatic fever is a type of recurrent acute or chronic systemic connective tissue inflammation caused by group a beta-hemolytic streptococcus invasion of genetically susceptible people (2). After an acute attack, heart damage of varying severity is often left; especially valvular disease is the most dangerous, resulting in chronic rheumatic heart disease or rheumatic heart valve disease (3). The mitral valve is most commonly involved in clinical practice. For rheumatic mitral valve disease, the main treatment methods are surgical operations, including mitral valvuloplasty and mitral valve replacement. At present, the best surgical approach for rheumatic mitral valve disease is still controversial, but due to the higher risk of reoperation with mitral valvuloplasty, mitral valve replacement is more commonly used in clinical practice (4).

The artificial valve used in mitral valve replacement can be categorized as mechanical valve and biological valve. Both types of prosthetic valves have advantages and disadvantages. Patients using mechanical valves need to take anticoagulants for life, and are prone to complications such as premature ventricular contractions, thromboembolism, and bleeding (5, 6). However, mechanical valves have better durability and are less likely to undergo secondary surgery. Patients using biological valve do not need long-term anticoagulation, which reduces the risk of bleeding and embolism, but is more prone to structural valve deterioration (SVD) and has a higher risk of mitral valve reoperation. A mechanical valve may be an option when the patient is already on anticoagulation therapy or when the risk of reoperation is high. When patients have poor compliance with anticoagulation therapy, or lack corresponding medical conditions to monitor coagulation index, bioprosthetic valves can be considered. The trade-off between bleeding risk and reoperation is critical and involves many factors. However, age becomes one of the most objective factors in choosing the appropriate valve type (7). For patients requiring mitral valve replacement, the European Society of Cardiology (ESC) recommends a mechanical valve for those under 65 years of age and a biological valve for those over 70 years of age (5). The American Heart Association (AHA) recommends the use of mechanical valves for people under the age of 50, and the use of biological valves for people over 70 years old, and it indicates that uncertainty and debate continue about which type of prosthesis is appropriate for patients 50–70 years of age. There are conflicting data on survival benefit of mechanical vs. bioprosthetic valves in this age group (6). Few studies have explicitly compared mechanical valves and bioprosthetic valves in patients with RHD (8–10). Therefore, current guidelines do not provide a choice of the most appropriate valve type for patients aged 50–70 years with rheumatic heart disease.

Generally, younger patients may be more inclined to use a mechanical mitral valve, but with the development of transcatheter mitral valve replacement, the problem of reoperation after bioprosthetic valve deterioration may not be so difficult. The rise of this technology may also have important implications for the choice of valve type (7). Therefore, we conducted this study to compare long-term survival and incidence of related outcomes for patients aged 50–70 years with rheumatic mitral valve disease.

# METHODS

## Study Design

All patients aged 50–70 years with RHD who underwent primary mitral valve replacement in Fuwai hospital from 01/01/2010 to 31/12/2014 were identified for retrospective cohort study. The Medical Ethics Review Committee of Fuwai Hospital approved this study (No. 2,021–1,545). Informed consent was waived.

Mechanical prosthetic and bioprosthetic valve replacements were differentiated using International Classification of Diseases, Ninth Revision, Clinical Modification (ICD-9-CM) procedure codes 35.23 and 35.24, respectively. The following patients were excluded: (I) patients who had undergone prior replacement of any heart valve; (II) patients who had undergone concomitant replacement of the aortic, pulmonary, or tricuspid valves; repair of the aortic or pulmonary valves; (III) concomitant coronary artery bypass graft surgery; or concomitant thoracic aortic surgery.

To minimize potential selection bias, we calculated a propensity score from selected variables and matched each patient in the bioprosthetic group with each patient in the mechanical prosthetic group. Three hundred patient pairs of the mechanical prosthetic group and bioprosthetic group were identified and were eligible for analysis.

## Outcomes

The primary outcomes of this study were all-cause mortality. In-hospital or 30-day outcomes included all-cause mortality, stroke, major bleeding events, acute kidney injury, respiratory failure, heart failure, readmission, reexploration for bleeding and deep wound infection. Late outcomes included stroke, mitral valve reoperation, thromboembolic events, major bleeding events, infective endocarditis, prosthetic valve endocarditis, readmission for heart failure, and all-cause readmission. Stroke was defined as any cerebrovascular accident documented during the index hospitalization as well as any subsequent hospital admission in which the principal diagnosis was hemorrhagic or ischemic stroke (not including transient ischemic attacks). Reoperation was defined as any subsequent MVR. Major bleeding event was defined as requiring hospitalization or blood transfusion. Patients were censored on 31/12/2021.

## Statistical Analysis

Baseline patient characteristics are represented as means with standard deviations for normally distributed continuous variables, medians and interquartile ranges for non-normal distributed continuous variables, and proportions for categorical variables. Shapiro-Wilk test was used to test normal distribution. To compare baseline differences in

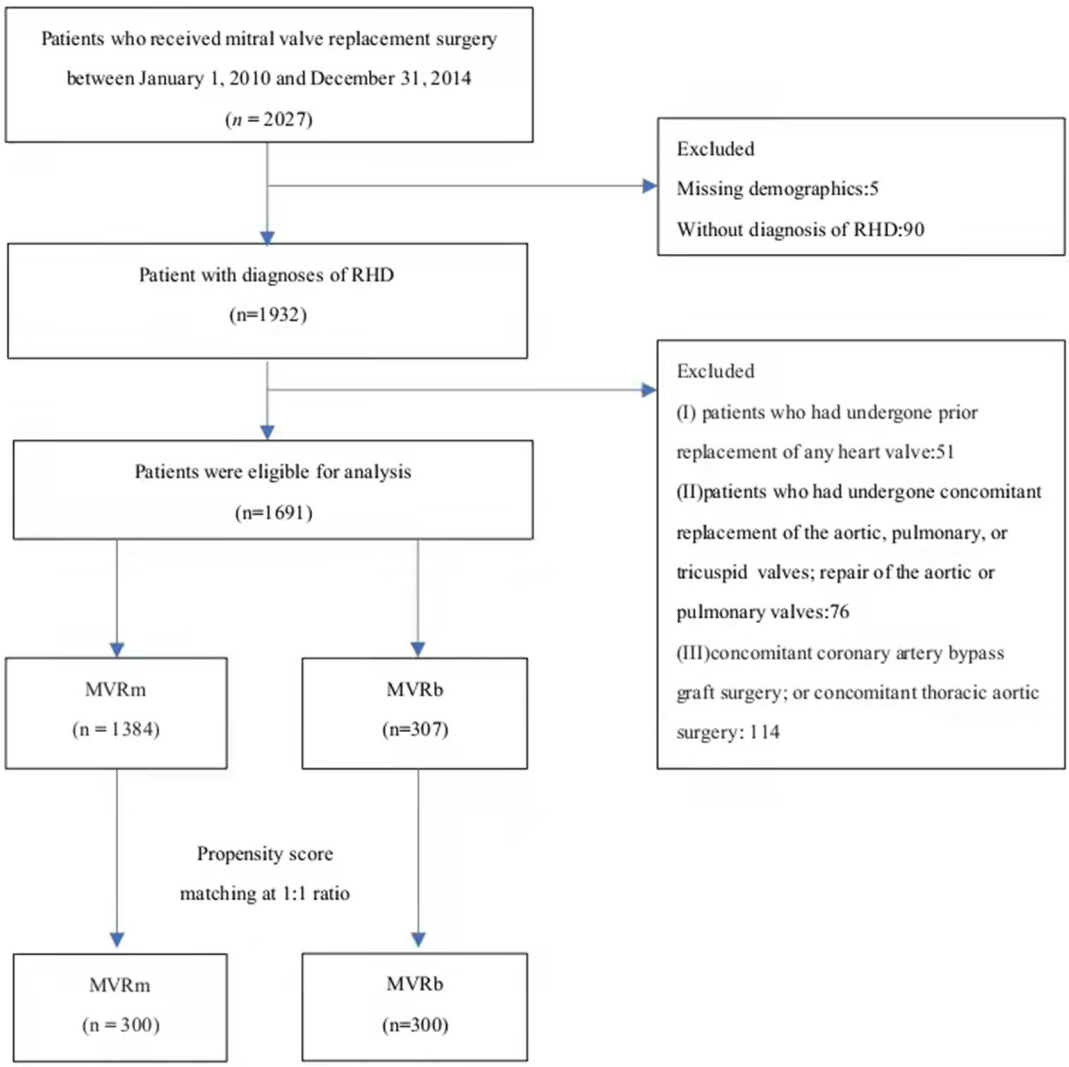


**FIGURE 1 |** The flowchart of patient inclusion and exclusion. RHD, Rheumatic heart disease. MVRm, mechanical mitral valve replacement; MVRb, bioprosthetic mitral valve replacement.

comorbidity between patients receiving mechanical prosthetic and bioprosthetic valves, the Student *t*-test or Mann-Whitey *U*-test was performed for continuous variables, the Pearson $\chi 2$ test or Fisher's exact test was performed for categorical variables, and standardized differences were calculated for all variables.

Confounding due to differences in baseline characteristics was addressed using propensity score matching. To calculate the propensity score, a hierarchical logistic regression model was fitted with bioprosthetic implantation as the outcome. Covariates entered into the model include all measured baseline characteristics: age, sex, year of surgery, New York Heart Association (NYHA) class III to IV, admission urgency, hypertension, diabetes mellitus, hyperlipidaemia, choronic kidney disease, active endocarditis or sepsis, chronic obstructive pulmonary disease, cerebrovascular disease, peripheral vascular disease, coronary artery disease, congestive heart failure, atrial fibrillation, other arrhythmia, liver disease, history of cancer, history of mitral balloon dilatation, mean pulmonary artery systolic blood pressure (greater than or equal to 50 mmHg), concomitant tricuspid valve repair, concomitant radiofrequency ablation of atrial fibrillation, concomitant thrombectomy.

The area under the receiver operating characteristic curve for this model was 0.79. A 1:1 match was then performed using a caliper of 0.4 of the logit of the propensity score computed by this model. The baseline characteristics of the patient pairs matched by propensity score were compared using the paired *t*-test or the Wilcoxon Signed-Rank Test for continuous variables and the McNemar test for categorical variables. Standardized difference that

**TABLE 1 |** Patient baseline characteristics in the overall cohort according to type of mitral valve replacement.

| | All patients ($n$ = 1,691) | MVRm ($n$ = 1,384) | MVRb ($n$ = 307) | SMD, % | $P$-value |
|---|---|---|---|---|---|
| Age, [mean (SD)], y | 58.0 (5.1) | 57.1 (4.8) | 61.9 (4.9) | 98.8 | <0.001 |
| Male sex | 398 (23.5) | 319 (23.0) | 79 (25.7) | 6.1 | 0.353 |
| NYHA class III-IV | 510 (30.2) | 402 (29.0) | 108 (35.2) | 12.8 | 0.040 |
| Emergent or urgent admission status | 339 (20.0) | 286 (20.7) | 53 (17.3) | 9.0 | 0.205 |
| History of mitral valve ballon dilation | 101 (6.0) | 82 (5.9) | 19 (6.2) | 1.1 | 0.965 |
| Hypertension | 286 (16.9) | 217 (15.7) | 69 (22.5) | 16.3 | 0.005 |
| Diabetes mellitus | 132 (7.8) | 98 (7.1) | 34 (11.1) | 12.7 | 0.025 |
| Hyperlipidaemia | 311 (18.4) | 240 (17.3) | 71 (23.1) | 13.7 | 0.022 |
| Endocarditis or sepsis | 2 (0.1) | 2 (0.1) | 0 (0.0) | 4.2 | 1.000 |
| Chronic obstructive pulmonary disease | 17 (1.0) | 12 (0.9) | 5 (1.6) | 6.0 | 0.371 |
| Peripheral vascular disease | 39 (2.3) | 35 (2.5) | 4 (1.3) | 10.8 | 0.278 |
| Cerebrovascular disease | 226 (13.4) | 178 (12.9) | 48 (15.6) | 7.6 | 0.230 |
| Heart failure | 4 (0.2) | 3 (0.2) | 1 (0.3) | 1.9 | 1.000 |
| Chronic kidney disease | 4 (0.2) | 3 (0.2) | 1 (0.3) | 1.9 | 1.000 |
| Liver disease | 17 (1.0) | 15 (1.1) | 2 (0.7) | 5.4 | 0.711 |
| Cancer | 6 (0.4) | 5 (0.4) | 1 (0.3) | 0.6 | 1.000 |
| Pulmonary artery systolic pressure (≥50 mmHg) | 254 (15.0) | 223 (16.1) | 31 (10.1) | 20.0 | 0.010 |
| **Coronary artery disease** | | | | | |
| Without coronary artery disease | 1,636 (96.8) | 1,336 (96.5) | 300 (97.7) | | |
| Without prior revascularization | 52 (3.1) | 45 (3.3) | 7 (2.3) | 9.4 | 0.479 |
| Prior PCI | 3 (0.2) | 3 (0.2) | 0 (0.0) | | |
| **Arrhythmia** | | | | | |
| Atrial fibrillation | 1,217 (72.0) | 1,016 (73.4) | 201 (65.5) | 16.7 | 0.006 |
| Other type of arrhythmia | 103 (6.1) | 83 (6.0) | 20 (6.5) | 2.1 | 0.833 |
| **Concomitant procedures** | | | | | |
| Tricuspid valve repair | 1,300 (76.9) | 1,071 (77.4) | 229 (74.6) | 6.4 | 0.330 |
| Atrial fibrillation radiofrequency ablation | 330 (19.5) | 249 (18.0) | 81 (26.4) | 19.0 | 0.001 |
| Atrial thrombectomy | 328 (19.4) | 270 (19.5) | 58 (18.9) | 1.6 | 0.867 |
| **Year of surgery** | | | | | |
| 2010 | 272 (16.1) | 209 (15.1) | 63 (20.5) | | |
| 2011 | 314 (18.6) | 266 (19.2) | 48 (15.6) | | |
| 2012 | 285 (16.9) | 255 (18.4) | 30 (9.8) | 9.8 | 0.111 |
| 2013 | 414 (24.5) | 362 (26.2) | 52 (16.9) | | |
| 2014 | 406 (24.0) | 292 (21.1) | 114 (37.1) | | |

*Data are given as n (%) except where otherwise noted. MVRm, mechanical mitral valve replacement; MVRb, bioprosthetic mitral valve replacement; SMD, standardized mean difference; PCI, percutaneous coronary intervention; NYHA, New York Heart Association.*

was <0.1 was deemed indicative of acceptable balance. In-hospital or 30-day outcomes rates were compared using the McNemar test.

For the primary end point, survival curves and 10-year estimates were derived from Kaplan-Meier method. For the secondary end points of other time to event outcomes, a competing risk analysis was performed to construct cumulative incidence function curves and to calculate 10-year estimates. For all end points, marginal Cox proportional hazards regression models with robust sandwich variance estimators were fitted with only prosthesis type entered as a covariate. The difference in overall survival was compared using the Cox model, whereas the differences in secondary end points were evaluated using the Gray test. All tests were 2-tailed with an α level of 0.05. All statistical analyses were performed using R software version 4.1.0.

**TABLE 2 |** Baseline characteristics after propensity score matching.

| | MVRm ($n = 300$) | MVRb ($n = 300$) | SMD, % | *P*-value |
|---|---|---|---|---|
| Age, [mean (SD)], y | 61.60 (4.58) | 61.78 (4.82) | 3.8 | 0.627 |
| Male sex | 73 (24.3) | 77 (25.7) | 3.1 | 0.777 |
| NYHA class III-IV | 100 (33.3) | 106 (35.3) | 4.2 | 0.667 |
| Emergent or urgent admission status | 51 (17.0) | 52 (17.3) | 0.9 | 1.000 |
| History of mitral valve ballon dilation | 25 (8.3) | 19 (6.3) | 8.3 | 0.434 |
| Hypertension | 62 (20.7) | 65 (21.7) | 2.4 | 0.842 |
| Diabetes mellitus | 27 (9.0) | 32 (10.7) | 5.3 | 0.583 |
| Hyperlipidaemia | 79 (26.3) | 67 (22.3) | 9.5 | 0.295 |
| Endocarditis or sepsis | 0 (0.0) | 0 (0.0) | 0.0 | 1.000 |
| Chronic obstructive pulmonary disease | 4 (1.3) | 5 (1.7) | 2.6 | 1.000 |
| Peripheral vascular disease | 3 (1.0) | 4 (1.3) | 2.9 | 1.000 |
| Cerebrovascular disease | 53 (17.7) | 47 (15.7) | 5.5 | 0.584 |
| Heart failure | 1 (0.3) | 1 (0.3) | 0.0 | 1.000 |
| Chronic kidney disease | 2 (0.7) | 1 (0.3) | 5.9 | 1.000 |
| Liver disease | 2 (0.7) | 2 (0.7) | 0.0 | 1.000 |
| Cancer | 0 (0.0) | 1 (0.3) | 5.9 | 1.000 |
| Pulmonary artery systolic pressure (≥50 mmHg) | 30 (10.0) | 30 (10.0) | 0.0 | 1.000 |
| **Coronary artery disease** | | | | |
| Without coronary artery disease | 294 (98.0) | 293 (97.7) | | |
| Without prior revascularization | 5 (1.7) | 7 (2.3) | 0.0 | 0.513 |
| Prior PCI | 1 (0.3) | 0 (0.0) | | |
| **Arrhythmia** | | | | |
| Atrial fibrillation | 208 (69.3) | 198 (66.0) | 7.0 | 0.432 |
| Other type of arrhythmia | 14 (4.7) | 20 (6.7) | 8.1 | 0.377 |
| **Concomitant procedures** | | | | |
| Tricuspid valve repair | 233 (77.7) | 224 (74.7) | 6.9 | 0.443 |
| Atrial fibrillation radiofrequency ablation | 80 (26.7) | 78 (26.0) | 1.5 | 0.926 |
| Atrial thrombectomy | 62 (20.7) | 56 (18.7) | 5.1 | 0.608 |
| **Year of surgery** | | | | |
| 2010 | 36 (12.0) | 61 (20.3) | | |
| 2011 | 55 (18.3) | 48 (16.0) | 0.4 | 0.956 |
| 2012 | 56 (18.7) | 29 (9.7) | | |
| 2013 | 78 (26.0) | 51 (17.0) | | |
| 2014 | 75 (25.0) | 111 (37.0) | | |

*Data are given as n (%) except where otherwise noted. MVRm, mechanical mitral valve replacement; MVRb, bioprosthetic mitral valve replacement; SMD, standardized mean difference; PCI, percutaneous coronary intervention; NYHA, New York Heart Association.*

# RESULTS

## Patient Characteristics

Between January 2010 and December 2014, 2,027 patients who underwent MVR were included in this study, among whom 1,932 were diagnosed as having RHD and 1,691 were eligible for inclusion. Among the included patients, 1,384 (81.8%) selected a mechanical valve and 307 (18.2%) selected a bioprosthetic valve (**Figure 1**). The baseline characteristics of the overall cohort are presented in **Table 1**. Patients who received bioprosthetic valve replacement ($n = 307$) compared those who received mechanical valve replacement ($n = 1,384$) were older (61.9 ± 4.9 vs. 57.1 ± 4.8 years, $P < 0.001$), and more likely to have a history of hypertension (22.5 vs. 15.7%, $P = 005$), diabetes mellitus (11.1 vs. 7.1%, $P = 0.025$), NYHA class III-IV (35.2 vs. 29.0, $P = 040$). Patients who received mechanical prosthetic valves were more likely to have cardiovascular morbidity including severe pulmonary hypertension (16.1 vs. 10.1%, $P = 010$), atrial fibrillation (73.4 vs. 65.6%, $P = 0.006$). But patients in MVRb groups were more likely to receive concomitant atrial fibrillation radiofrequency ablation (26.4 vs. 18.0%, $P = 001$). A ratio of 1:1 propensity-score matching produced 300 patient pairs. Age and all baseline comorbidities were balanced with the two groups (**Table 2**).

## In-hospital or 30-Day Outcomes

Among patients matched by propensity score, there was no significant difference in 30-day mortality (0.3% in the

**TABLE 3 |** In-hospital or 30-day outcomes of mitral valve replacement in patients matched by propensity score.

| | MVRm ($n$ = 300) | MVRb ($n$ = 300) | $P$-value |
|---|---|---|---|
| Mortality | 1 (0.3) | 1 (0.3) | 1.000 |
| Stroke | 2 (0.7) | 0 (0.0) | 0.249 |
| Major bleeding events | 2 (0.7) | 0 (0.0) | 0.499 |
| Acute kidney injury | 2 (0.7) | 0 (0.0) | 0.499 |
| Respiratory failure | 3 (1.0) | 0 (0.0) | 0.249 |
| Heart failure | 3 (1.0) | 0 (0.0) | 0.249 |
| Readmission | 2 (0.7) | 2 (0.7) | 1.000 |
| Re-exploration for bleeding | 5 (1.7) | 3 (1.0) | 0.725 |
| Deep wound infection | 3 (1.0) | 3 (1.0) | 1.000 |

*Data are given as n (%) except where otherwise noted. MVRm, mechanical mitral valve replacement; MVRb, bioprosthetic mitral valve replacement.*

bioprosthesis group vs. 0.3% in the mechanical prosthesis group, $P$ = 1.000) after valve replacement. The incidence of 30-day complications and outcomes was comparable between the 2 groups after matching (**Table 3**).

## Late Outcomes

### Survival

Among patients matched by propensity score, there was no significant difference in mid- to long-term survival between MVRm and MVRb [hazard ratio (HR), 0.91 (95% CI, 0.69–1.21), $P$ = 0.528; **Figure 2**]. A total of 98 (32.7%) death occurred in the MVRm group and 92 (30.7%) deaths occurred in the MVRb group. The actuarial survival at 1, 3, 5, and 10 years were 97.7, 89.7, 76.3, and 63.4% in the MVRm group, and 98.7, 91.0, 80.0, and 63.7% in the MVRb group, respectively.

## Mitral Valve Reoperation

There were only 3 patients received a mitral valve reoperation in the MVRb and none in the MVRm. But the difference of the cumulative incidence was not significant [hazard ratio (HR), 0.92 (95% CI, 0.69–1.21), $P$ = 0.530; **Figure 3**] between the 2 groups. The cumulative incidence of mitral valve reoperations at 3, 5, 7, and 10 years were 0.0, 0.0, 0.0, and 0.0% in the MVRm, and 0.0, 0.0, 0.3, and 1.2% in the MVRb, respectively.

## Infective Endocarditis

A total of 2 infective endocarditis occurred in the MVRm and 5 infective endocarditis occurred in the MVRb. There was no significant difference in cumulative incidence of infective endocarditis between the MVRm and the MVRb [hazard ratio (HR), 0.84 (95% CI, 0.63–1.13), $P$ = 250; **Figure 4**]. The cumulative incidence of infective endocarditis at 3, 5, 7, and 10 years were 0.7, 0.7, 0.7, and 0.7% in the MVRm, and 1.0, 1.3, 1.7, and 1.7% in the MVRb, respectively.

## Stroke

A total of 28 strokes occurred during follow-up time, 13 in the MVRm group and 15 in the MVRb group. The cumulative incidence of stroke after MVR was no significant difference between the MVRm and the MVRb [hazard ratio (HR), 0.89 (95% CI, 0.67–1.18), $P$ = 430; **Figure 5**]. Among the 28 patients of stroke, 9 were hemorrhagic and 19 were ischemic. Of the 19 ischemic strokes, 9 occurred in the MVRm group and 10 occurred in the MVRb group.

## Readmission for Heart Failure

A total of 31 and 38 patients occurred readmission for heart failure in the MVRm group and in the MVRb group, respectively. There was no significant difference of readmission for heart failure between the 2 groups [hazard ratio (HR), 0.84 (95% CI, 0.63–1.13), $P$ = 250; **Figure 6**]. The cumulative incidence of readmission for heart failure at 3, 5, 7, and 10 years were 2.3, 4.0, 7.0, and 11.9% in the MVRm group, and 2.3, 4.3, 8.7, and 16.5% in the MVRb group, respectively.

## Readmission for Any Cause

Forty-nine patients occurred readmission for any cause in the MVRm group while 52 patients occurred readmission for any cause in the MVRb group during follow-up period. The cumulative incidence of readmission for any cause after MVR was no significant difference between the MVRm and the MVRb [Hazard Ratio (HR), 0.90 (95% CI, 0.68–1.19), $P$ = 460; **Figure 7**]. The cumulative incidence of readmission for any cause at 3, 5, 7, and 10 years were 4.3, 9.0, 14.0, and 18.3% in the MVRm, and 4.7, 8.0, 13.0, and 21.1% in the MVRb, respectively.

## Thromboembolic Events

A total of 14 thromboembolic events occurred during follow-up period, 8 in the MVRm group and 6 in the MVRb group. No significant difference was observed between the MVRm and the MVRb [hazard ratio (HR), 0.93 (95% CI, 0.70–1.23), $P$ = 610; **Figure 8**]. The cumulative incidence of thromboembolic events at 3, 5, 7 and 10 years were 0.7, 0.7, 1.0, and 4.1% in the MVRm, and 0.7, 1.0, 1.0, and 2.9% in the MVRb, respectively. Among the 14 patients of thromboembolic events, 6 were acute myocardial infarction (5 in the MVRm vs. 1 in the MVRb), 2 were bowel ischemia (1 in the MVRm vs. 1 in the MVRb), 3 were pulmonary embolism (1 in the MVRm vs. 2 in the MVRb) and 3 were systemic thromboembolism (3 in the MVRm vs. 0 in the MVRb).

## Major Bleeding Events

There was no significant difference of major bleeding events in patients with a mechanical or a biological prosthesis [hazard ratio (HR), 0.92 (95% CI, 0.70–1.22), $P$ = 560; **Figure 9**]. The cumulative incidence of major bleeding events at 3, 5, 7, and 10 years were 1.7, 1.7, 2.7, 3.3% in the MVRm, and 0.0, 0.3, 2.0, and 3.4% in the MVRb, respectively. Major bleeding events (10 in the MVRm vs. 8 in the MVRb) were most commonly intracerebral hemorrhage (8 in the MVRm vs. 7 in the MVRb). Of all major bleeding events, 2 were gastrointestinal bleedings (1 in the MVRm vs. 1 in the MVRb).

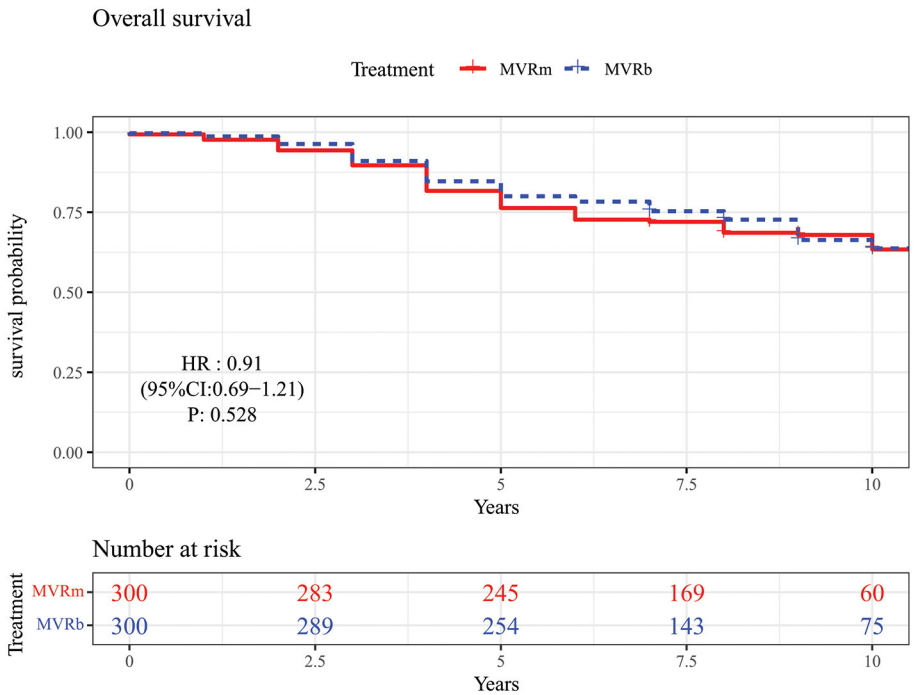


**FIGURE 2 |** Overall survival in patients aged 50–70 years after mitral valve replacement according to prosthetic type. MVRm, mechanical mitral valve replacement; MVRb, bioprosthetic mitral valve replacement.

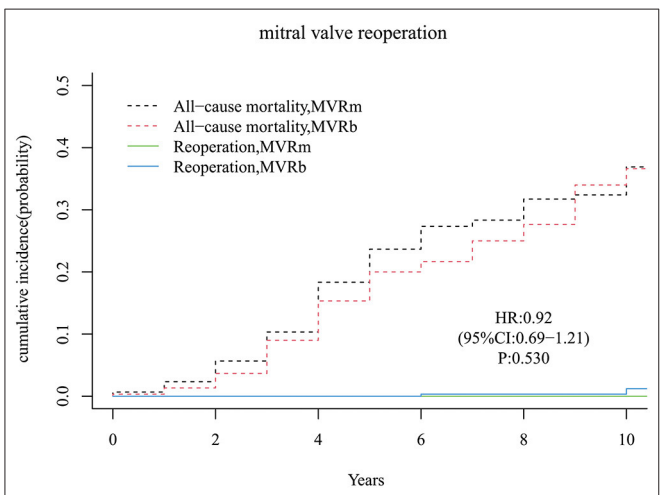


**FIGURE 3 |** Cumulative incidence of reoperation. MVRm, mechanical mitral valve replacement; MVRb, bioprosthetic mitral valve replacement.

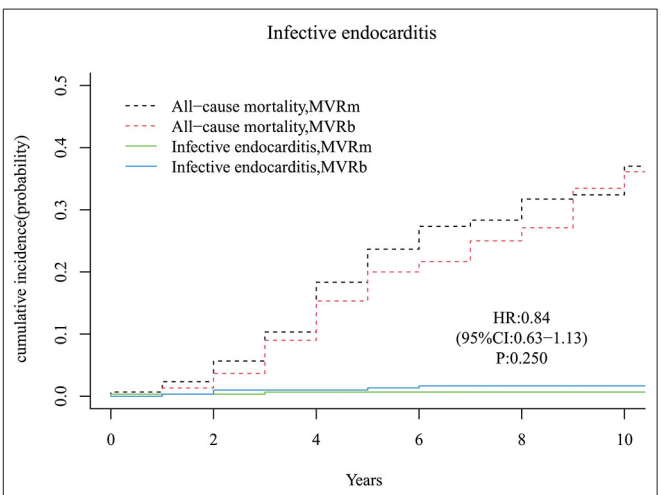


**FIGURE 4 |** Cumulative incidence of infective endocarditis. MVRm, mechanical mitral valve replacement; MVRb, bioprosthetic mitral valve replacement.

## Moderate or Severe Perivalvular Leakage

A total of 8 moderate or severe perivalvular leakage occurred in the MVRm and 17 perivalvular leakage occurred in the MVRb during follow up. There was no significant difference between the 2 groups [hazard ratio (HR), 0.90 (95% CI, 0.68–1.19), $P = 440$; **Figure 10**]. The cumulative incidence of moderate or severe perivalvular leakage at 3, 5, 7, and 10 years were 1.3, 1.7, 2.0, and 3.1% in the MVRm, and 1.3, 2.3, 4.4, and 6.7% in the MVRb, respectively.

## DISCUSSION

There is still much controversy about which type of valve to choose for patients aged 50–70 who need mitral valve

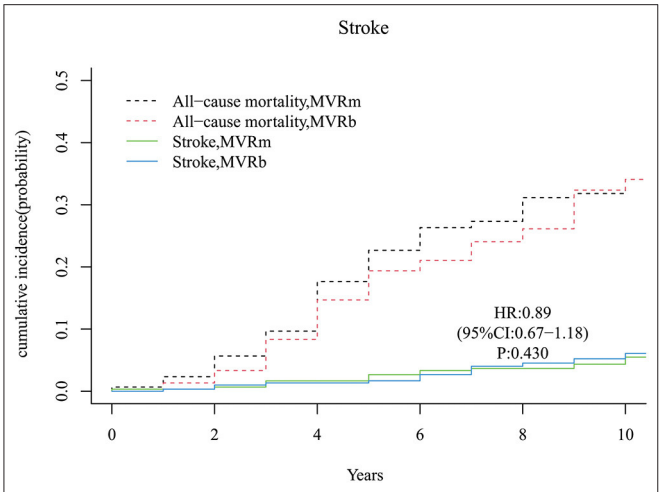


**FIGURE 5 |** Cumulative incidence of stroke. MVRm, mechanical mitral valve replacement; MVRb, bioprosthetic mitral valve replacement.

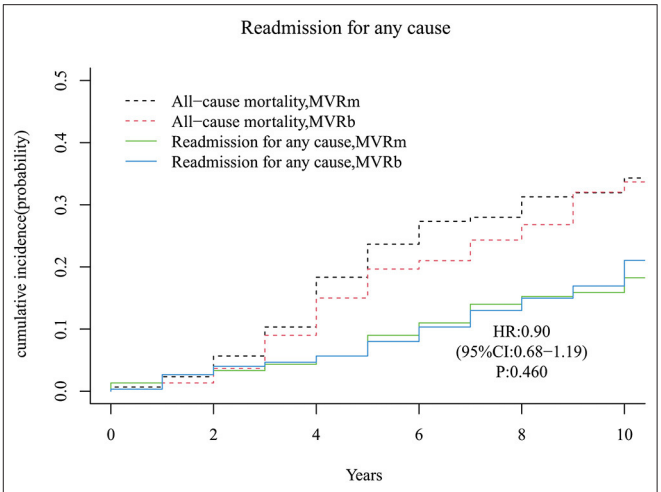


**FIGURE 7 |** Cumulative incidence of readmission for any cause. MVRm, mechanical mitral valve replacement; MVRb, bioprosthetic mitral valve replacement.

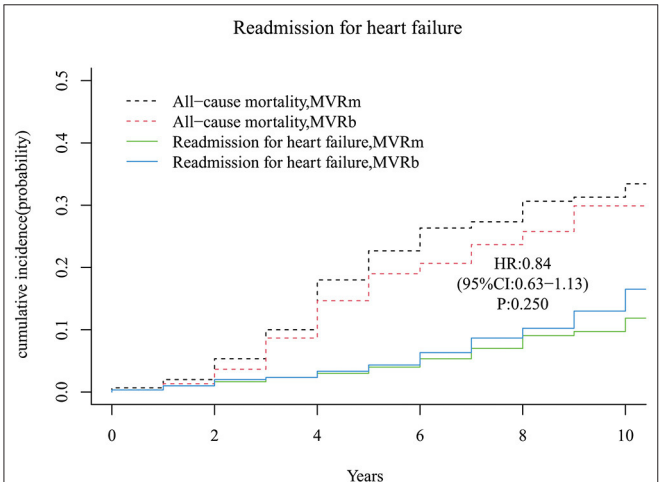


**FIGURE 6 |** Cumulative incidence of readmission for heart failure. MVRm, mechanical mitral valve replacement; MVRb, bioprosthetic mitral valve replacement.

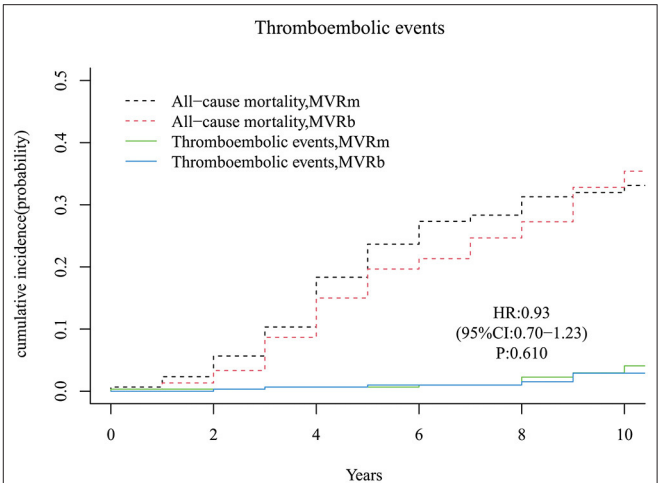


**FIGURE 8 |** Cumulative incidence of thromboembolic events. MVRm, mechanical mitral valve replacement; MVRb, bioprosthetic mitral valve replacement.

replacement in current clinical practice (11). Current guidelines also fail to decide the best options for patients in this age group (6). When we provide advice to patients, we generally consider factors such as age, life expectancy, reoperation risk, anticoagulation related events, and patient preference. However, the specific etiology of valvular disease is rarely considered. Different etiologies of heart valve disease, such as rheumatic, degenerative, and infectious (12), may also affect the clinical prognosis. The study by Goldstone et al. (13) showed that the long-term mortality benefit that was associated with a mechanical prosthesis, as compared with a biologic prosthesis, persisted until 70 years of age among patients undergoing mitral valve replacement. However, Chikwe et al. (14) demonstrates that there was no significant difference in survival at 15-year follow-up between mechanical prosthetic and bioprosthetic mitral valve replacements. Both of the two large studies were conducted in the United States, and neither classified the specific etiology of valvular heart disease. The difference in the etiological composition of valvular heart disease may be one of the underlying reasons for the wide disparity in the results of the two studies. Kulik et al. (15) found that there was no significant difference in late mortality in MVR patients aged 50–65, but an increase in the requirement for reoperation for bioprosthetic valves and an increased risk of thromboembolism for mechanical valves. However, the study did not analyze the specific etiology of valvular heart disease. A study analyzed patients aged 50–70 with infective endocarditis for mitral valve replacement, and the results showed that the long-term mortality and reoperation rates of the biological valve group were significantly higher

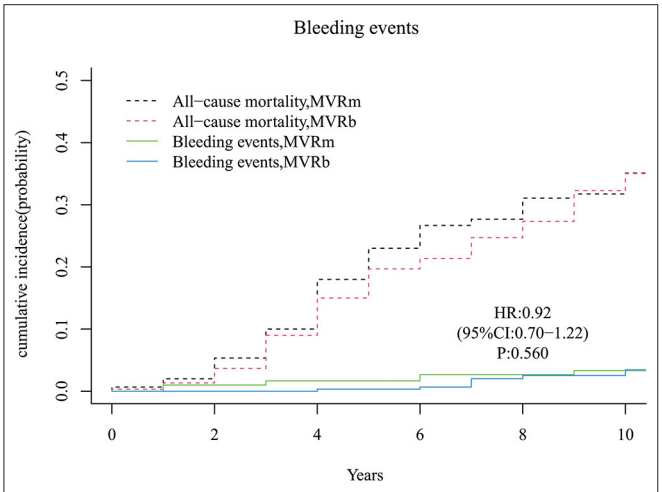


**FIGURE 9 |** Cumulative incidence of major bleeding events. MVRm, mechanical mitral valve replacement; MVRb, bioprosthetic mitral valve replacement.

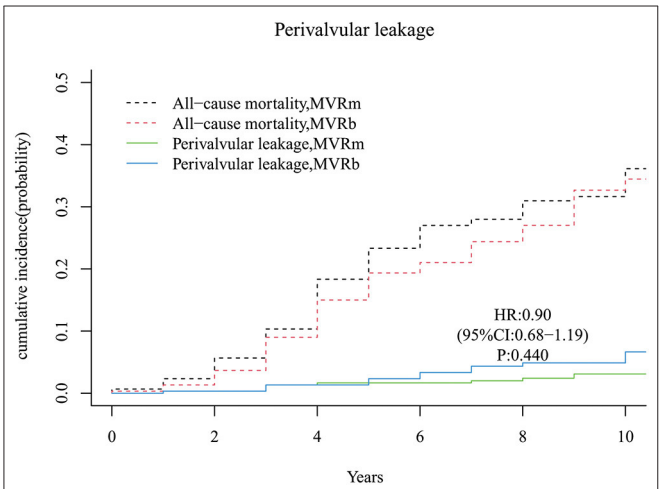


**FIGURE 10 |** Cumulative incidence of perivalvular leakage. MVRm, mechanical mitral valve replacement; MVRb, bioprosthetic mitral valve replacement.

than those of the mechanical valve group. There were no significant differences in stroke and major bleeding events (16). A retrospective study of patients with RHD from Taiwan showed that the all-cause mortality and reoperation rates in the biological valve group were higher than those in the mechanical valve group, no group differences were observed in the risks of stroke, thromboembolic events, and major bleeding events (7). In our study, in patients with RHD aged 50–70 years, there was no significant difference in all-cause mortality and reoperation rates between the MVRb group and the MVRm group. Therefore, whether the specific etiology of valvular heart disease will affect the long-term clinical outcomes after mitral valve replacement requires further clinical trials and newer high-quality evidence.

Our study showed that the bioprosthetic valve utilization rate in our hospital increased from 23.2% in 2010 to 28.1% in 2014. This trend is similar to that of the United States (17). With the increasing use of bioprostheses, the clinical prognosis of patients using bioprostheses has become an issue that we need to pay more attention to. The results of this study showed that there was no significant difference between the bioprosthetic valve group and the mechanical valve group in both primary and secondary outcomes for patients aged 50–70 years with RHD, indicating the use of bioprosthetic valves seems to be a good choice, too. After all, long-term anticoagulation is not required, and the quality of life could be improved. But the follow-up is unfortunately too short to assess the durability of the bioprostheses, that won't be enough time to develop SVD. Mitral valve reoperation rate was higher in MVRb group although the difference was not significant. Our study showed that the mechanical valve group did not increase the incidence of stroke, major bleeding and thromboembolic events compared with the bioprosthetic valve group even if the MVRm group need anticoagulation, suggesting that the use of mechanical valve in patients aged 50–70 years with rheumatic mitral valve disease is a better choice, especially for patients with atrial fibrillation. In this study, 72.0% patients who underwent MVR had atrial fibrillation. And mechanical valve is generally considered more durable than biological valve, reducing the risk of reoperation. During the next years will be quite sure that the MVRb group starts to develop SVD, and the advantage of the MVRm group taking over. With the advent of transcatheter mitral valve technology, some studies have reported that valve-in-valve procedures are associated with better outcomes compared with valve-in-ring procedures (18–20). For high-risk patients who need secondary surgery after SVD, the technology of transcatheter mitral valve replacement can significantly reduce the risk compared with conventional open-heart surgery, providing these patients with a better opportunity to replace the valve, which is of great significance (18). However, we recommend mechanical prostheses in this patient group for the first operation because transcatheter mitral valve-in-valve replacement would not be better in terms of mortality, rehospitalization, and cost-effectiveness, particularly. Besides, with the advancement of science and technology, monitoring INR is more convenient (21, 22). Therefore, the trend of bioprostheses toward younger patients should be tempered according to our study.

## Study Limitations

The main limitation was the nature of the single-center retrospective study. Although we used propensity score matching to minimize measured confounders, potential confounding variables not measured could not be adjusted in this study. There may not have been adequate control for selection bias. The 10-year follow-up was insufficient to fully assess lifetime risks, particularly of SVD and reoperation. However, there were no significant differences in 30-day mortality and morbidity in this cohort, suggesting that the treatment groups were well-matched. Finally, the relatively large sample size and complete follow-up in our study can be considered precise and trustworthy.

## CONCLUSIONS

This propensity score-matched study compared clinical outcomes between mechanical and bioprosthetic MVR in patients aged 50–70 years with rheumatic heart disease. Despite the trend of bioprostheses toward younger patients, mechanical mitral valve replacement may be a more reasonable alternative in this patient group without an increased risk of stroke or major bleeding events.

## PERSPECTIVE STATEMENT

Either a mechanical or bioprosthetic valve is used in patients undergoing mitral valve replacement (MVR). As the development of the transcatheter intervention technologies, the use of bioprosthesis increased during the past decades. But we found that mechanical prosthesis may be a more reasonable alternative in patients aged 50–70 years with rheumatic heart disease.

## DATA AVAILABILITY STATEMENT

The raw data supporting the conclusions of this article will be made available by the authors, without undue reservation.

## ETHICS STATEMENT

The studies involving human participants were reviewed and approved by the Medical Ethics Review Committee of Fuwai Hospital approved this study (No. 2021–1545). Written informed consent for participation was not required for this study in accordance with the national legislation and the institutional requirements.

## AUTHOR CONTRIBUTIONS

JY and WW contributed to conception and design of the study. JY organized the database, performed the statistical analysis, and wrote the first draft of the manuscript. All authors contributed to manuscript revision, read, and approved the submitted version.

## FUNDING

This work was supported by the project of clinical trials in Fuwai Hospital (grant number: 2021-HG34, Beijing, China).

## REFERENCES

1. Marijon E, Mirabel M, Celermajer DS, Jouven X. Rheumatic heart disease. *Lancet.* (2012) 379:953–64. doi: 10.1016/S0140-6736(11)61171-9
2. Leal M, Passos LSA, Guarçoni FV, Aguiar JMS, Silva R, Paula TMN, et al. Rheumatic heart disease in the modern era: recent developments and current challenges. *Rev Soc Bras Med Trop.* (2019) 52:e20180041. doi: 10.1590/0037-8682-0041-2019
3. Liu M, Lu L, Sun R, Zheng Y, Zhang P. Rheumatic heart disease: causes, symptoms, and treatments. *Cell Biochem Biophys.* (2015) 72:861–3. doi: 10.1007/s12013-015-0552-5
4. Chen S, Chen C, Chien-Chia Wu V, Chou A, Cheng Y, Chang S, et al. Mitral valve repair versus replacement in patients with rheumatic heart disease. *J Thorac Cardiovasc Surg.* (2020) S0022-5223:32459–4. doi: 10.1016/j.jtcvs.2020.07.117
5. Vahanian A, Beyersdorf F, Praz F, Milojevic M, Baldus S, Bauersachs J, et al. 2021 ESC/EACTS Guidelines for the management of valvular heart disease. *Eur Heart J.* (2022) 43:561–632. doi: 10.1093/eurheartj/ehab395
6. Nishimura RA, Otto CM, Bonow RO, Carabello BA, Erwin JP, 3rd Fleisher LA et al. 2017 AHA/ACC Focused update of the 2014 AHA/ACC guideline for the management of patients with valvular heart disease: a report of the american college of cardiology/American heart association task force on clinical practice guidelines. *Circulation.* (2017) 135:e1159–95. doi: 10.1161/CIR.0000000000000503
7. Chen CY, Chan YH, Wu VC, Liu KS, Cheng YT, Chu PH, et al. Bioprosthetic vs. mechanical mitral valve replacements in patients with rheumatic heart disease. *J Thorac Cardiovasc Surg.* (2021) S0022-5223:00512–2. doi: 10.1016/j.jtcvs.2021.03.033
8. Travancas PR, Dorigo AH, Simões LC, Fonseca SC, Bloch KV, Herdy GV. Comparison of mechanical and biological prostheses when used to replace heart valves in children and adolescents with rheumatic fever. *Cardiol Young.* (2009) 19:192–7. doi: 10.1017/S1047951109003680
9. Edwin F, Aniteye E, Tettey MM, Tamatey M, Frimpong-Boateng K. Outcome of left heart mechanical valve replacement in West African children—A 15-year retrospective study. *J Cardiothorac Surg.* (2011) 6:57. doi: 10.1186/1749-8090-6-57
10. Tamirat S, Mazine A, Stevens LM, Agwar F, Dejene K, Bedru M, et al. Contemporary outcomes of aortic and mitral valve surgery for rheumatic heart disease in sub-Saharan Africa. *J Thorac Cardiovasc Surg.* (2021) 162:1714–25.e2. doi: 10.1016/j.jtcvs.2020.02.139
11. Nishimura RA, Gentile F, Bonow RO. Guideline update on evaluation and selection of prosthetic valves. *JAMA Cardiol.* (2018) 3:260–1. doi: 10.1001/jamacardio.2017.5123
12. Iung B, Vahanian A. Epidemiology of valvular heart disease in the adult. *Nat Rev Cardiol.* (2011) 8:162–72. doi: 10.1038/nrcardio.2010.202
13. Goldstone AB, Chiu P, Baiocchi M, Lingala B, Patrick WL, Fischbein MP, et al. Mechanical or biologic prostheses for aortic-valve and mitral-valve replacement. *N Engl J Med.* (2017) 377:1847–57. doi: 10.1056/NEJMoa1613792
14. Chikwe J, Chiang YP, Egorova NN, Itagaki S, Adams DH. Survival and outcomes following bioprosthetic vs. mechanical mitral valve replacement in patients aged 50 to 69 years. *JAMA.* (2015) 313:1435–42. doi: 10.1001/jama.2015.3164
15. Kulik A, Bédard P, Lam BK, Rubens FD, Hendry PJ, Masters RG, et al. Mechanical vs. bioprosthetic valve replacement in middle-aged patients. *Eur J Cardiothorac Surg.* (2006) 30:485–91. doi: 10.1016/j.ejcts.2006.06.013
16. Hu X, Jiang W, Xie M, Guo R, Yim WY, Dong N, et al. Bioprosthetic vs. mechanical mitral valve replacement for infective endocarditis in patients aged 50 to 69 years. *Clin Cardiol.* (2020) 43:1093–9. doi: 10.1002/clc.23407
17. Gammie JS, Sheng S, Griffith BP, Peterson ED, Rankin JS, O'Brien SM, et al. Trends in mitral valve surgery in the united states: results from the society of thoracic surgeons adult cardiac database. *Ann Thorac Surg.* (2009) 87:1431–9. doi: 10.1016/j.athoracsur.2009.01.064
18. Schaefer A, Conradi L. Transcatheter mitral valve replacement for degenerated bioprosthetic valves and failed annuloplasty rings. *Surg Technol Int.* (2020) 37:185–90.
19. Paradis JM, Del Trigo M, Puri R, Rodés-Cabau J. Transcatheter valve-in-valve and valve-in-ring for treating aortic and mitral surgical prosthetic dysfunction. *J Am Coll Cardiol.* (2015) 66:2019–37. doi: 10.1016/j.jacc.2015.09.015

20. Yoon SH, Whisenant BK, Bleiziffer S, Delgado V, Dhoble A, Schofer N, et al. Outcomes of transcatheter mitral valve replacement for degenerated bioprostheses, failed annuloplasty rings, and mitral annular calcification. *Eur Heart J.* (2019) 40:441–51. doi: 10.1093/eurheartj/ehy590
21. Murray ET, Fitzmaurice DA, McCahon D. Point of care testing for INR monitoring: where are we now? *Br J Haematol.* (2004) 127:373–8. doi: 10.1111/j.1365-2141.2004.05154.x
22. Levine MA, Shao W, Klein D. Monitoring of international normalized ratios: comparison of community nurses with family physicians. *Can Fam Physician.* (2012) 58:e465–71.

**Conflict of Interest:** The authors declare that the research was conducted in the absence of any commercial or financial relationships that could be construed as a potential conflict of interest.

**Publisher's Note:** All claims expressed in this article are solely those of the authors and do not necessarily represent those of their affiliated organizations, or those of the publisher, the editors and the reviewers. Any product that may be evaluated in this article, or claim that may be made by its manufacturer, is not guaranteed or endorsed by the publisher.

frontiers | Frontiers in Cardiovascular Medicine

ORIGINAL RESEARCH
published: 16 June 2022
doi: 10.3389/fcvm.2022.887886

# The Clinical Trial Outcomes of Med-Zenith PT-Valve in the Treatment of Patients With Severe Pulmonary Regurgitation

*Xiaoke Shang*[1†], *Nianguo Dong*[2†], *Changdong Zhang*[2] *and Yanggan Wang*[1,3*]

[1] *Department of General Medicine and Geriatrics, Zhongnan Hospital of Wuhan University, Wuhan University, Wuhan, China,* [2] *Department of Cardiovascular Surgery, Union Hospital, Tongji Medical College, Huazhong University of Science and Technology, Wuhan, China,* [3] *Medical Research Institute of Wuhan University, Wuhan University, Wuhan, China*

OPEN ACCESS

**Edited by:**
*Marko Banovic,*
*University of Belgrade, Serbia*

**Reviewed by:**
*Gianluca Lucchese,*
*Guy's and St Thomas' NHS Foundation Trust, United Kingdom*
*Gianfranco Butera,*
*Bambino Gesù Children's Hospital (IRCCS), Italy*

***Correspondence:**
*Yanggan Wang*
*wb000813@whu.edu.cn*

[†] *These authors have contributed equally to this work*

**Specialty section:**
*This article was submitted to Heart Valve Disease, a section of the journal Frontiers in Cardiovascular Medicine*

**Received:** *02 March 2022*
**Accepted:** *12 May 2022*
**Published:** *16 June 2022*

**Citation:**
*Shang X, Dong N, Zhang C and Wang Y (2022) The Clinical Trial Outcomes of Med-Zenith PT-Valve in the Treatment of Patients With Severe Pulmonary Regurgitation. Front. Cardiovasc. Med. 9:887886. doi: 10.3389/fcvm.2022.887886*

**Objective:** Nearly 2/3 of patients with dilated right ventricular outflow tract (RVOT) were excluded from pulmonary valves transplantation due to the lack of size-matched valves. Here, we explored the safety and efficacy of the Med-Zenith PT-Valve for the treatment of patients with severe pulmonary regurgitation.

**Methods:** 22 Patients with severe PR (grade 3+,4+) were enrolled based on the anatomical features of native RVOT and the valve design. The immediate, 3-months and 1-year post-procedural follow-up data were analyzed.

**Results:** The baseline mean systolic diameters in the distal main pulmonary artery (MPA), MPA sinus junction, MPA sinus, pulmonary annulus, RVOT aneurysm and muscular outlet measured with computed tomography were 33.6 ± 6.1, 34.0 ± 5.8, 37.9 ± 6.0, 32.4 ± 7.3, 41.9 ± 9.3, and 34.4 ± 8.0 mm, respectively. The PT-Valve landing zone was set within these levels. Successful valve implantations were achieved in all patients without noticeable device malposition, coronary artery compression, pulmonary branch obstruction or paravalvular leak during follow-ups. Post-procedural pulmonary artery diastolic pressure increased from 5.8 ± 3.1 to 11.3 ± 2.5 mmHg. In the 3-month and 1-year follow-up, the right ventricular end diastolic volume index reduced from the baseline 181.6 ± 29.0 to 143.7 ± 29.7 ml/m$^2$ and 123.4 ± 31.2 ml/m$^2$, and the trans-pulmonary valve gradient decreased from 25.6 ± 22.2 to 10.64 ± 3.54 mmHg and 11.16 ± 3.0 mmHg, respectively. The 6-min walk distance increased from 416.6 ± 97.9 to 455.9 ± 64.6 m and 467.8 ± 61.2 m, respectively.

**Conclusion:** This clinical trial revealed favorable outcomes for the safety, efficacy and feasibility of the Med-Zenith PT-Valve in the treatment of severe PR with significantly enlarged RVOT.

**Keywords: transcatheter pulmonary valve, native right ventricular outflow tract, pulmonary regurgitation, Tetralogy of Fallot, coronary artery compression**

## INTRODUCTION

Surgical management of residual pulmonary regurgitation (PR) after initial repair of some congenital heart disease, such as Tetralogy of Fallot (TOF), requires open-heart pulmonary valve replacement with cardiopulmonary bypass. Transcatheter pulmonary valve replacement (TPVR) is a new, less invasive alternative to surgical valve replacement with improved long-term outcome (1–5). However, the current commercially available transcatheter pulmonary valves (TPV) are designed to restore pulmonary valve function in the dysfunctional right ventricle and pulmonary artery (RV-to-PA) conduits (6, 7). To date, the clinical practice of TPV implantation is largely limited to the use of balloon expandable valves, which were only implanted in the native RVOT patients (8). There were reports of several successful implantations of TPV in the native or patched RVOT, with the requirement of landing site diameter less than 29 mm. Because of this limit, about 2/3 of patients with native or patch-expanded dilated RVOT were not suitable for this treatment due to their oversized pulmonary valve annulus. In China, most of the patients underwent surgical reconstruction of the RVOT using a transannular patch technique (9) resulted in a dilated RVOT because the size of annulus usually exceeds the diameter of available percutaneous valves. The need of a device dedicated to the dilated native RVOTs was therefore realized (10–12). However, a large size valve could cause potential coronary artery compression and incomplete expansion of the stent. To prevent the potential risk of coronary artery compression during percutaneous pulmonary valve replacement, 2018 AHA/ACC guideline for the management of adults with congenital heart disease suggested balloon inflation test before transcatheter pulmonary valve placement in the patients with repaired TOF (13). On the other hand, excessive compression or incomplete expansion of the stent could increase the trans-valve gradient, which may affect the durability of the valve and accelerate valve failure (14, 15). To overcome these disadvantages, we reported here the implantations of a novel designed TPV devices (Med-Zenith PT-Valve) and initial outcomes for the treatment of severe PR.

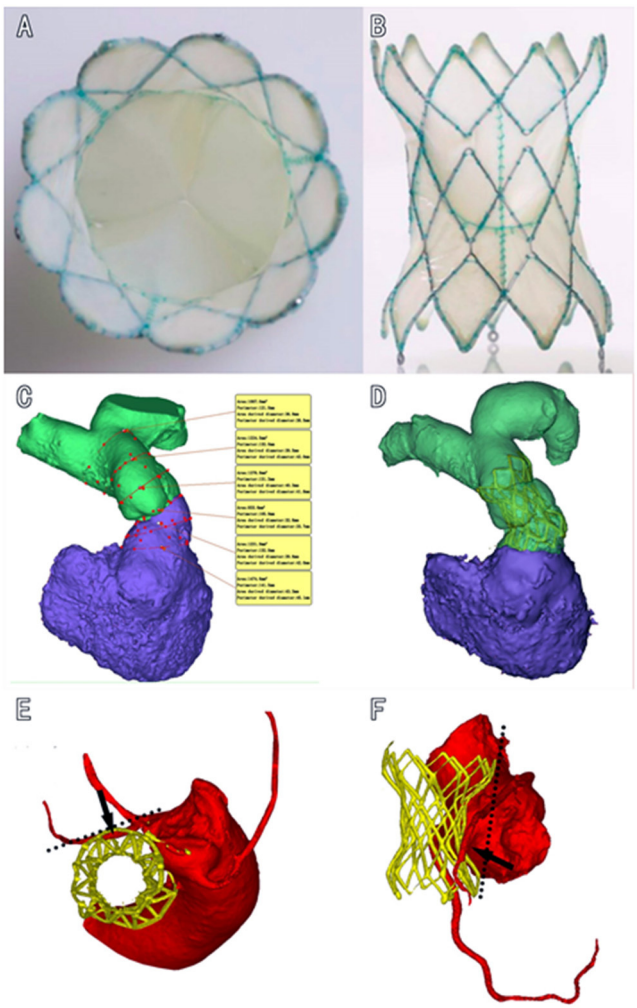


**FIGURE 1 |** Diagram of the dumbbell-shaped Med-Zenith PT-Valve. **(A)**: Cross section view of PT-Valve. **(B)**: Longitudinal view of PT-Valve; **(C)**: Multi-level measurements based on 3D reconstruction of RVOT and MPA. **(D)**: Valve was implanted into the desired position conformed by post-operational CTA, showing that the dumbbell-shape design of PT-Valve provides sufficient contact surface in the dilated pulmonary artery and RVOT without compression of the valve (waist of the frame remains uncompressed), while the tension force of the device lays on the double ends of the frame. **(E,F)**: Left anterior descending artery is away from the out layer of the stent in the cross-sectional and longitudinal views, respectively. RVOT, right ventricular out flow tract; MPA, main pulmonary artery; CTA, computed tomography angiography.

## METHODS

### Ethics Statement and Informed Consent

This study was carried out in accordance with relevant guidelines and regulations. Informed consent was obtained from each of the patients or the parents or legal guardians (for patients under 18 years old). Patient's personal information was kept confidentially. The study complied with the Declaration of Helsinki, and obtained the ethical approval from the Clinical Trial Ethics Committee of Huazhong University of Science and Technology at December 8th 2017 ([2017]ID:S310). This trial was registered in China Clinical Trial Registration Center at Oct 26th,2017.

Registration number: ChiCTR-OPC-17013126.

http://www.chictr.org.cn/showproj.aspx?proj=22502.

### Patient Selection

The patient enrollment standard and valve selection refer to the **Supplemental Materials**.

### Device

The Med-Zenith PT-Valve is a porcine pericardial tissue valve mounted on a self-expanding nitinol frame covered by porcine pericardium (**Figure 1**). The valve frame has five different sizes in order to fit the different morphologies of the RVOT after surgical repair of TOF. The valve frame is made of laser-cut nitinol with a unique symmetrical shape that provides stability and tight seal in the MPA and RVOT to prevent device migration and/or PVL.

The outflow and inflow diameters are the same with sizes of 28, 32, 36, 40, and 44 mm, respectively. The length of the frame varies from 38 to 54 mm. The porcine valve diameters in the middle of the frame are 20, 23, and 26 mm, respectively. The diameter of the valve is smaller than the outflow and inflow diameter of the frame to avoid compression. The TPVs are pretreated with specific alcohol and surfactant to mitigate leaflet calcification.

## RESULTS

The baseline characteristics were shown in **Table 1**. Twenty-two patients were enrolled in this study (17 patients were males). The mean age of the patients was 31.0 ± 9.2 y (weight of 57.9 ± 10.8 kg or 20.7 ± 2.7 kg/m$^2$). Heart function was NYHA III-IV for nine patients and NYHA II for eleven patients. Two patients with baseline NYHA class I were enrolled due to their right ventricular end-diastolic volume index (RVEDVI) >160 ml/m$^2$, which met the criteria recommended by the 2020 ESC guidelines for the management of adult congenital heart disease. The PR was grade 4+ (severe) for 19/22 patients of which 14 patients also had 3+/4+ tricuspid regurgitation. The mean trans-pulmonary valve gradient measured by echocardiography was 25.6 ± 22.2 mmHg. The mean RVEDVI was 181.6 ± 29.0 ml/m$^2$ (measured by cardiac MRI) with RV ejection fraction of 20.3 ± 7.5% and PR fraction of 53.3 ± 13.0%. A large amount of futile circulating in the pulmonary artery aneurysm has been observed in most cases. CTA images showed a substantial variety of RVOT and MPA morphologies with the mean inner diameters (cross section perimeter) at the distal MPA, MPA sinus junction, MPA sinus, pulmonary annulus, RVOT aneurysm and muscular outlet of 33.6 ± 6.1, 34.0 ± 5.8, 37.9 ± 6.0, 32.4 ± 7.3, 41.9 ± 9.3, and 34.4 ± 8.0 mm, respectively (**Figure 2**, **Table 2**). The mean distance from the bifurcation to muscular outlet was 64.3 ± 12.4 mm.

Successful valve implantation was achieved in all patients. Each patient was implanted only one device, of which 7/22 patients used the TPVs with size of 44–26 and 5/22 patients used the TPVs with size 40–26. The other TPVs with sizes of 36–26, 32–23 and 28–20 were implanted in 3/22, 4/22 and 3/22 patients, respectively. The mean procedure time was 66.5 ± 16.3 min. No device malposition, coronary compression, or reduced flow to the PA branches occurred during the procedures. After procedure, the pulmonary artery diastolic pressure increased from 5.8 ± 3.1 mmHg to 11.3 ± 2.5 mmHg ($P < 0.05$), while the invasive trans-valvular gradient decreased from 4.1 ± 7.5 mmHg to 2.3 ± 3.3 mmHg (**Table 3**). No ventricular arrhythmias, valve displacement, regurgitation or PVL above 2+ occurred by

**TABLE 1 |** Baseline demographics.

| Baseline Characteristics ($n$ = 22) | | | | | |
|---|---|---|---|---|---|
| **Male** | **17/22** | **(*n*)** | **Years between TOF repair and TPVR (year)** | **20.4 ± 8.2** | **(*n*)** |
| Age (year) | 31.0 ± 9.2 | | RVOT Type | Native TAP | 17 |
| | 10–20 | 2 | | Conduit | 2 |
| | 21–30 | 8 | | Native Non-TAP | 3 |
| | 31–40 | 10 | Symptoms | Chest tightness | 9 |
| | >40 | 2 | | Edema | 7 |
| Height (cm) | 166.8 ± 9.6 | | | Dyspnea | 13 |
| Weight (kg) | 57.9 ± 10.8 | | | Palpitation | 5 |
| BMI (kg/m$^2$) | 20.7 ± 2.7 | | Atrial fibrillation/atrial flutter | | 7 |
| Diagnosis | PR, rTOF | 8 | Hypertension | | 1 |
| | PR, rPA(TOF) | 3 | Tobacco use | | 3 |
| | PR, rTOF+rVSD | 7 | Diabetes | | 0 |
| | PR, rTOF+TVR | 1 | Chronic obstructive Pulmonary disease | | 0 |
| | PR, rTOF+AVR | 1 | Chronic renal failure | | 0 |
| | PR, rTOF+RVOTO | 2 | Stroke | | 0 |
| rTOF Age (year) | 10.6 ± 9.1 | | Operation time (min) | 66.5 ± 16.3 | |
| | <3 | 5 | Radiation time (min) | 24.9 ± 8.4 | |
| | 3–10 | 9 | Contrast dosage (ml/kg) | 2.0 ± 0.7 | |
| | 11–20 | 6 | Hospital stay (d) | 5.1 ± 1.7 | |
| | >20 | 2 | Valve Size | 44–26 | 7 |
| Surgeries Experienced | 1 | 13 | | 40–26 | 5 |
| | 2 | 6 | | 36–26 | 3 |
| | ≥3 | 3 | | 32–23 | 4 |
| | | | | 28–20 | 3 |

*BMI, body mass index; PR, pulmonary regurgitation; rTOF, repaired Tetralogy of Fallot; rPA, repaired pulmonary atresia; rVSD, residual ventricular septal defect; TVR, tricuspid valve replacement; AVR, aortic valve replacement; RVOTO, right ventricular outflow tract obstruction; RVOT, right ventricular outflow tract; TPVR, transcatheter pulmonary valve replacement; TAP, trans-annular patch.*

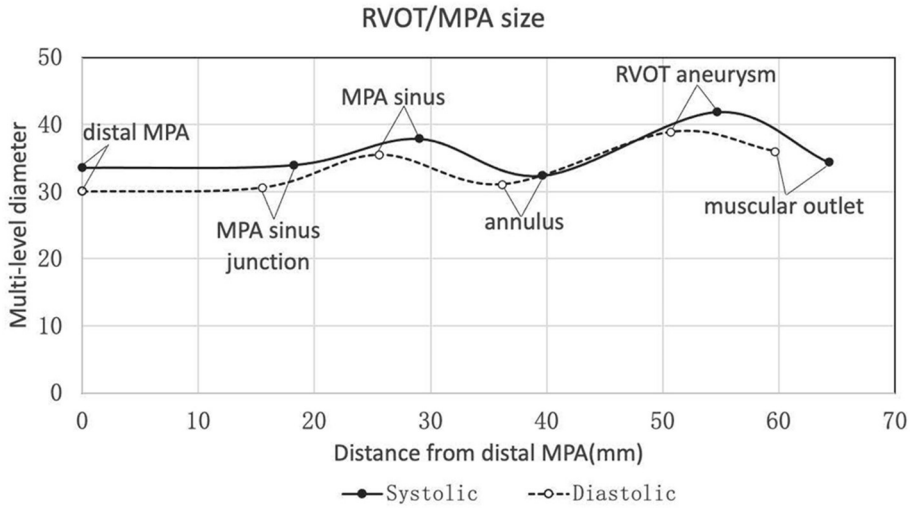


**FIGURE 2 |** Multi-level diameters and distances of right ventricular outflow tract/pulmonary artery measured by three-dimensional CTA reconstruction in the systole and diastole. CTA, computed tomography angiography.

after valve deployment. Prophylactic antibiotics were routinely used for 3 days after procedure, and patients were given dual antiplatelet therapy (Aspirin 100 mg/d + Clopidogrel 75mg/d) for 3 months and aspirin (100 mg/d) alone thereafter for 1 year.

The patients have been followed up for 13–35 months without early valve decay or reintervention. All patients completed related examinations at the time of 3-month and 1-year follow-up. 2+ valvular or para-valvular regurgitation has not been noted. Five patients were diagnosed with grade 1 PVL or PR without requirement of intervention. Echocardiography and MRI revealed regression of right ventricular remodeling and function, manifested by remarkable reduction of RVEDVI (from 181.6 ± 29.0 to 143.7 ± 29.7 ml/m$^2$ at 3 months and 123.4 ± 31.2ml/m$^2$ at 1y follow-up, respectively ($p < 0.05$, **Table 4**). Accordingly, the RV ejection fraction and tricuspid annular plane systolic excursion (TAPSE) were improved (**Table 4**). Furthermore, valve regurgitation and NYHA class, peak $O^2$, 6-min walk distance and NT-proBNP levels were improved continuously after TPVR procedure (**Figure 3**, **Table 4**).

One patient had hemoptysis at conduction of Lunderquist guidewire and healed in one day. No other adverse events occurred in the perioperative period, such as tricuspid valve injury, pulmonary artery rupture, pericardial or thoracic hemorrhage, valve displacement and pulmonary branch obstruction. One patient developed infective endocarditis with miliary vegetations in the prosthetic leaflets. It was cured after two months of anti-infective treatment with vancomycin/cephalosporin. No stent rupture, valve thrombosis, embolism or pseudoaneurysm appeared in any cases.

## DISCUSSION

Severe PR after TOF repair is associated with the progressive RV dilation/ dysfunction and subsequent right heart failure. Restoration of pulmonary valve function is therefore important (6). However, the clinical experience with TPVR is largely limited to the dysfunctional RV-PA conduits using the two-balloon expandable TPV devices, including the Melody TPV (Medtronic, Minneapolis, MN, USA) and the SAPIEN Pulmonic THV (Edwards Life Sciences, California, USA) (7, 16). Compared to the RV-PA conduit repair, it is a great challenge to implant a single self-expanding system to fit the wide variety of post-operative RVOT anatomies (13). Although several new TPV devices have been reported in this setting, the experience is very limited (17, 18). Most TOF patients in China were previously operated using transannular patch technique to reconstruct right ventricular outflow tract, which resulted in severe post-surgery PR, MPA/RVOT dilatation or aneurysm and progressive right heart failure. The size of RVOT could exceed the size of currently available TPV devices, which were therefore not suitable for Chinese TOF patients (15). Balloon expanding valves like Edwards Sapiens series have been used to treat pulmonary regurgitation of native RVOT types, but indications are still largely limited by the diameter of annulus (19).

In this study, we introduced a novel TPV device in the treatment of severe PR that occurred after TOF repair, as introduced in our early reports (20, 21). In this cohort with a variety of sizes and morphologies of native RVOT, the immediate, 3-months and one-y outcomes were very satisfactory in terms of efficacy and safety, without showing any serious complications such as death, device migration, PVL, valve malfunction or coronary compression. Excellent valve stability achieved due to the equally expended distal and proximal ends of the stent. In addition, the extended stent length with a well-matched frame provides support to the valve and prevents the potential risk of valve distortion, early progressive malfunction and PVL. More importantly, the unique feature of this device is the symmetric dumbbell-shape design with equal diameters in the inflow and

**TABLE 2 |** Multi-plane measurement based on 3D construction of CT.

| | Systolic diameter (mm) | Systolic distance from bifurcation (mm) | Diastolic diameter (mm) | Diastolic distance from bifurcation (mm) |
|---|---|---|---|---|
| Distal MPA | 33.6 ± 6.1 | 0 | 30.0 ± 5.6 | 0 |
| MPA sinus junction | 34.0 ± 5.8 | 18.2 ± 7.3 | 30.6 ± 5.9 | 15.5 ± 5.4 |
| MPA sinus | 37.9 ± 6.0 | 29.0 ± 8.5 | 35.5 ± 6.5 | 25.6 ± 7.7 |
| Pulmonary annulus | 32.4 ± 7.3 | 39.6 ± 9.7 | 31.1 ± 7.1 | 36.2 ± 9.7 |
| RVOT aneurysm | 41.9 ± 9.3 | 54.7 ± 10.3 | 38.9 ± 7.8 | 50.7 ± 10.5 |
| Muscular outlet | 34.4 ± 8.0 | 64.3 ± 12.4 | 36.0 ± 7.0 | 59.7 ± 14.0 |

*MPA, main pulmonary artery; RVOT, right ventricular outflow tract.*

**TABLE 3 |** Hemodynamics data in peri-operation.

| | Pre-operation | Post-operation | *t* | *P* |
|---|---|---|---|---|
| RVP/LVP | 0.32 ± 0.08 | 0.26 ± 0.53 | 3.682 | 0.001 |
| PASP (mmHg) | 31.1 ± 5.5 | 32.0 ± 5.5 | 1.082 | 0.292 |
| PADP (mmHg) | 5.8 ± 3.1 | 11.3 ± 2.5 | 6.754 | <0.001 |
| mRAP (mmHg) | 7.7 ± 3.5 | 6.1 ± 2.6 | 2.773 | 0.011 |
| RVEDP (mmHg) | 9.8 ± 3.8 | 7.5 ± 2.4 | 3.138 | 0.005 |
| PA-RV gradient (mmHg) | 4.1 ± 7.5 | 2.3 ± 3.3 | 1.066 | 0.298 |

*RVP, right ventricular pressure; LVP, left ventricular pressure; PASP, pulmonary artery systolic pressure; PADP, pulmonary artery diastolic pressure; mRAP, mean right atrial pressure; RVEDP, right ventricular end diastolic pressure; PA-RV, pulmonary artery-right ventricular.*

outflow portions of the frame and a progressive incremental in the size of the centrally located inner valve. It is different from any other self-expandable TPV designs, such as the Harmony Valve, Venus-P Valve and Pulsta Valve. The symmetric design of the Med-Zenith PT-Valve provides a sufficient contact surface in the dilated pulmonary artery and RVOT without compression of the centrally located valve. This feature ensures the optional hemodynamics and long-term durability of the leaflet and minimizes the risk of coronary artery compression (**Figure 1**).

The dumbbell-shaped design of PT-Valve has many advantages. Different from other products, the size of this valve is no longer restrained by the size of annulus but depends on the diameters of the corolla at the two-ends of frame. The currently available Melody and SAPIEN XT/S3 valves have the maximum allowable annular diameter $\leq$29 mm. Due to this limitation, about 2/3 of patients with native or patch-expanded dilated RVOT have to be excluded from the percutaneous treatment options (10–12). In contrast, the PT-Valve is no longer limited by the diameter of annulus. In fact, most cases in the present study have annulus diameter of 30 mm and above. The PT-Valve significantly extended the valve implantation indication, especially in Chinese patients.

Patients with repaired TOF or abnormal coronary artery anatomy have substantial risk of coronary artery compression during percutaneous pulmonary valve replacement because the left coronary artery usually goes beneath the pulmonary annulus. Coronary artery compression is one of the most serious complications of PPVI (22), which can cause death during operation. To date, several cases of coronary artery occlusion due to compression have been reported in the literature (19). According to current guidelines, in patients with repaired TOF, the trajectories of coronary artery should be determined and the coronary compression test is recommended before percutaneous pulmonary valve replacement (grade Ib) (13). The narrow-waist design in the middle of the PT-Valve leaves no pressure to the annulus and peripheral tissue, thus minimizes the risk of coronary compression. In the present study, our experience demonstrated that with a careful evaluation for the risk of coronary artery compression from the pre-operational CTA while planning the procedure, coronary compression test during the procedure of PT-Valve implantation could often be omitted. Indeed, we only used balloon-inflation coronary artery compression test in 2 patients with RVOT stenosis. Taken together, our results suggest that the unique design of PT-Valve can simplify the procedure of valve implantation and reduce the risk of coronary compression.

Rodriguezgabella et al. (14) reported that excessive compression or incomplete expansion of the stent can increase the trans-valve gradient, resulting in an increased mechanical shear force and asymmetric interaction between the leaflet and the stent, which may affect the durability of the valve and accelerate valve failure. A lowered residual RVOT gradient was associated with the better outcome (15). For the PT-Valve, the valve is in the middle segment of the device, which remains uncompressed after implantation and therefore improves the durability of valves.

Considering the complexity of the native RVOT anatomies, multiple sizes of the frame and valve are required. In the currently

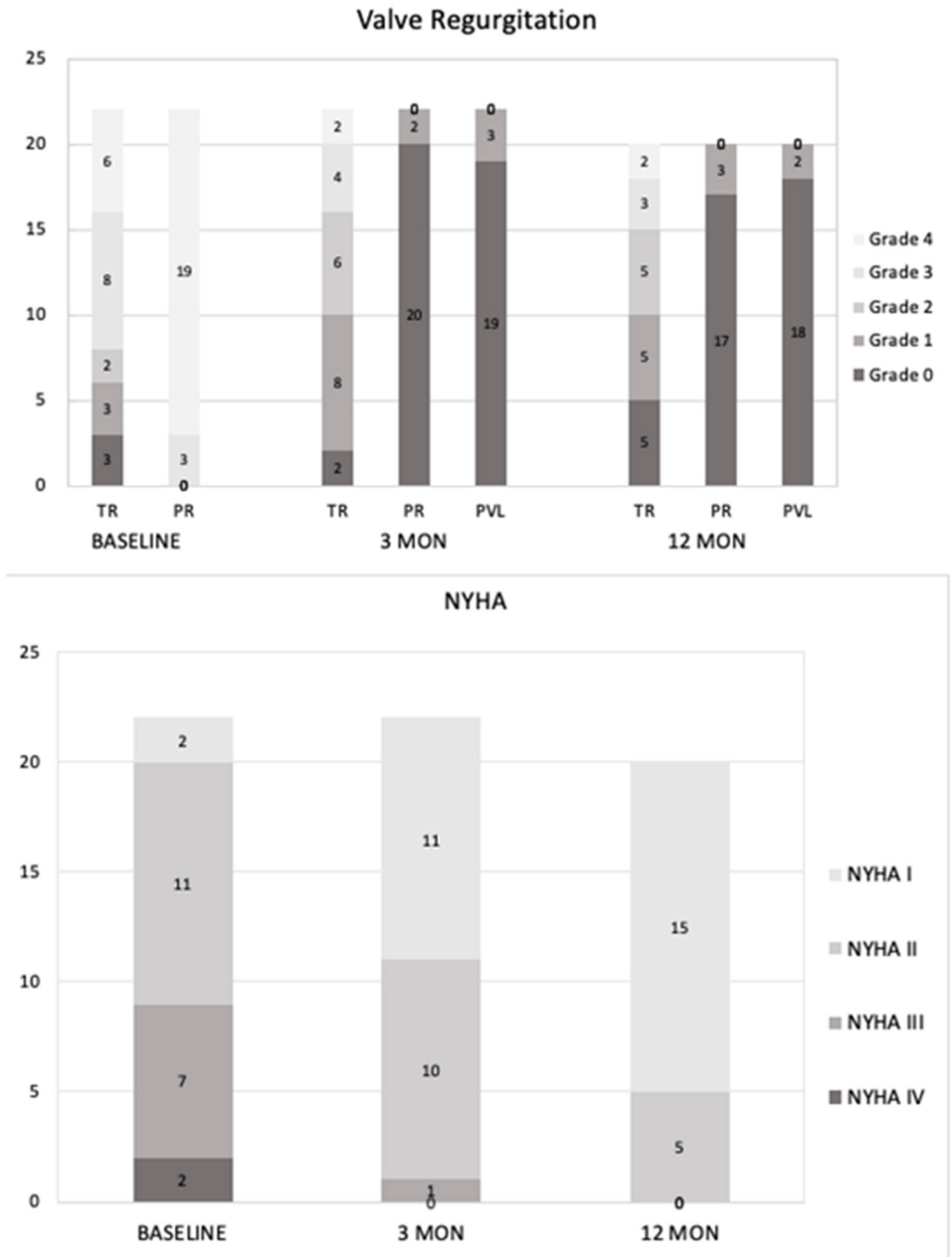


**FIGURE 3 |** Follow-up data after PT-Valve implantation. Upper panel: Tricuspid regurgitation, pulmonary regurgitation, and transcatheter pulmonary perivalvular leakage at baseline, 3-months and 1-year follow-up. Lower panel: The distributions of NYHA classification at baseline, 3-months and 1-year follow-up.

available Med-Zenith PT-Valves, there are five different sizes of frames and three different sizes of valves in combination, which makes a flexible selectivity. For instance, with the 26 mm valve in three different frames (36/40/44 mm), we can treatment patients with severely enlarged RVOT.

Our study has confirmed the anatomic complexity of the native RVOT following congenital heart defect (TOF) repair. Rather than a single measurement, we measured diameters (based on 3D reconstruction) of the distal MPA, MPA sinus junction, MPA sinus, pulmonary annulus, RVOT aneurysm and muscular outlet to guide the device size selection (**Figure 2**, **Table 2**). 3D printing technique was also used for assisting accurate device size selection if necessary. According to the 2020 ESC guidelines for the management of congenital heart disease, transcatheter pulmonary valve implantation (TPVI) is preferred for patients after TOF repair when anatomically feasible (Ic

**TABLE 4 |** Data of pre-operation, 3-months and 1-year follow-up.

| | Pre-operation | 3 months | 1 year | *t1* | *p1* | *t2* | *p2* |
|---|---|---|---|---|---|---|---|
| Peak $O^2$ | 14.5 ± 3.8 | 30.8 ± 9.1 | 34.3 ± 10.4 | 9.902 | <0.001 | 8.333 | <0.001 |
| 6MWD | 416.6 ± 97.9 | 455.9 ± 64.6 | 467.8 ± 61.2 | 3.478 | 0.002 | 4.370 | <0.001 |
| NT-proBNP | 1,256 ± 1,415 | 929 ± 936 | 805 ± 727 | 1.243 | 0.228 | 1.799 | 0.088 |
| QRS duration (ms) | 114.5 ± 21.4 | 111.8 ± 16.2 | 112.4 ± 18.9 | 0.530 | 0.602 | 0.700 | 0.493 |
| Max gradient (mmHg) | 25.6 ± 22.2 | 10.64 ± 3.54 | 11.16 ± 3.0 | 3.351 | 0.003 | 2.953 | 0.008 |
| TAPSE | 1.56 ± 0.38 | 1.68 ± 0.36 | 1.60 ± 0.36 | 1.067 | 0.298 | 0.405 | 0.690 |
| RVD | 5.27 ± 0.90 | 4.66 ± 0.86 | 4.48 ± 0.63 | 4.205 | <0.001 | 4.966 | <0.001 |
| TR velocity | 3.30 ± 0.62 | 3.08 ± 0.47 | 3.00 ± 0.52 | 2.348 | 0.034 | 2.501 | 0.031 |
| RAD | 5.31 ± 1.13 | 4.48 ± 0.80 | 4.49 ± 0.70 | 5.128 | <0.001 | 5.914 | <0.001 |
| RVFAC | 32.8 ± 10.2 | 36.8 ± 10.7 | 37.3 ± 7.9 | 1.823 | 0.083 | 2.314 | 0.032 |
| RVEDVI (ml/$m^2$) | 181.6 ± 29.0 | 143.7 ± 29.7 | 123.4 ± 31.2 | 8.445 | <0.001 | 12.61 | <0.001 |
| RVEF (%) | 20.3 ± 7.5 | 31.6 ± 6.6 | 32.7 ± 4.6 | 9.429 | <0.001 | 10.59 | <0.001 |
| PR fraction (%) | 53.3 ± 13.0 | 1.2 ± 2.4 | 0.7 ± 1.8 | 19.03 | <0.001 | 17.59 | <0.001 |

*6MWD, six-minute walk distance; TAPSE, tricuspid annular plane systolic excursion; RVD, Right ventricular diameter; TR, tricuspid regurgitation; RAD, right atrial diameter; RVFAC, right ventricle fraction of area change; RVEDVI, right ventricular end diastolic volume index; RVEF, right ventricular ejection fraction; PR, pulmonary regurgitation. t1, paired t test of pre-operation vs 3-month follow-up; t2, paired t-test of pre-Implant vs. 12-month follow-up.*

recommendation). This PT-Valve was specially designed adaptive for the anatomic complexity of the native RVOT, and all patients enrolled for the study were anatomically feasible.

In summary, this clinical trial provided the initial, 3-months and 1-year follow-up outcomes for the safety, efficacy and feasibility of the Med-Zenith PT-Valve in the treatment of severe PR. Our results showed that excellent valve function was maintained without progressive PR or PVL, and regression of right ventricular remodeling has been achieved. Long-term following up in these patients is important to assess persist valve function and durability and stent stability/integrity for the safety and efficacy of this TPV. A following study setup for a CFDA approved trial in China with large-scale in multiple centers in 2020.

## Limitations

The sample size in this study is small due to strict inclusion criteria. Although we have achieved 1-year follow-up outcomes, these patients are still in the follow-up process. In addition, the patients with end-stage heart failure were not included in the study. Thus, whether the conclusions from this study apply to those patients needs further study.

## DATA AVAILABILITY STATEMENT

The original contributions presented in the study are included in the article/**Supplementary Material**, further inquiries can be directed to the corresponding author.

## ETHICS STATEMENT

The studies involving human participants were reviewed and approved by Clinical Trial Ethics Committee of Huazhong University of Science and Technology. The patients/participants provided their written informed consent to participate in this study.

## DISCLOSURE

All authors have read and agreed with the content and submission of the manuscript.

## AUTHOR CONTRIBUTIONS

XS and ND made substantial contributions to the patient enrollment and surgical procedures. CZ was responsible for data acquisition and analysis. YW supervised the entire integration, data interpretation, and manuscript revision. He is responsible for the overall content. All authors contributed to the article and approved the submitted version.

## FUNDING

This study was supported by grants from the National Natural Science Foundation of China (NSFC) to YW (Nos. 81420108004, 81270304, 81873507, and 82070348) and grant from the Research Foundation of Commission of Hubei Province to XS (No. WJ2019M173).

## ACKNOWLEDGMENTS

We want to thank Da Zhu, Man Liao, Jun Tian, and Bin Wang for their substantial writing assistance.

## SUPPLEMENTARY MATERIAL

The Supplementary Material for this article can be found online at: https://www.frontiersin.org/articles/10.3389/fcvm.2022.887886/full#supplementary-material

## REFERENCES


1. McElhinney DB, Hellenbrand WE, Zahn EM, Jones TK, Cheatham JP, Lock JE, et al. Short- and medium-term outcomes after transcatheter pulmonary valve placement in the expanded multicenter US melody valve trial. *Circulation.* (2010) 122:507–16. doi: 10.1161/CIRCULATIONAHA.109.921692
2. Cheatham JP, Hellenbrand WE, Zahn EM, Jones TK, Berman DP, Vincent JA, et al. Clinical and hemodynamic outcomes up to 7 years after transcatheter pulmonary valve replacement in the US melody valve investigational device exemption trial. *Circulation.* (2015) 131:1960–70. doi: 10.1161/CIRCULATIONAHA.114.013588
3. Holzer RJ, Hijazi ZM. Transcatheter pulmonary valve replacement: state of the art. *Catheter Cardiovasc Interv.* (2016) 87:117–28. doi: 10.1002/ccd.26263
4. O'Byrne ML, Glatz AC, Mercer-Rosa L, Gillespie MJ, Dori Y, Goldmuntz E, et al. Trends in pulmonary valve replacement in children and adults with tetralogy of fallot. *Am J Cardiol.* (2015) 115:118–24. doi: 10.1016/j.amjcard.2014.09.054
5. Daily JA, Tang X, Angtuaco M, Bolin E, Lang SM, Collins RT 2nd. Transcatheter versus surgical pulmonary valve replacement in repaired tetralogy of fallot. *Am J Cardiol.* (2018) 122:498–504. doi: 10.1016/j.amjcard.2018.04.028
6. Frigiola A, Redington AN, Cullen S, Vogel M. Pulmonary regurgitation is an important determinant of right ventricular contractile dysfunction in patients with surgically repaired tetralogy of Fallot. *Circulation.* (2004) 110:II153–7. doi: 10.1161/01.CIR.0000138397.60956.c2
7. Kenny D, Hijazi ZM, Kar S, Rhodes J, Mullen M, Makkar R, et al. Percutaneous implantation of the Edwards SAPIEN transcatheter heart valve for conduit failure in the pulmonary position: early phase 1 results from an international multicenter clinical trial. *J Am Coll Cardiol.* (2011) 58:2248–56. doi: 10.1016/j.jacc.2011.07.040
8. Zhou D, Pan W, Jilaihawi H, Zhang G, Feng Y, Pan X, et al. A self-expanding percutaneous valve for patients with pulmonary regurgitation and an enlarged native right ventricular outflow tract: one-year results. *EuroIntervention.* (2019) 14:1371–7. doi: 10.4244/EIJ-D-18-00715
9. Chatterjee A, Bajaj NS, McMahon WS, Cribbs MG, White JS, Mukherjee A, et al. Transcatheter pulmonary valve implantation: a comprehensive systematic review and meta-analyses of observational studies. *J Am Heart Assoc.* (2017) 6:e006432. doi: 10.1161/JAHA.117.006432
10. Lurz P, Kister T. Why we need another percutaneous pulmonary valve: if size matters. *EuroIntervention.* (2019) 14:1347–9. doi: 10.4244/EIJV14I13A243
11. Georgiev S, Tanase D, Ewert P, Meierhofer C, Hager A, von Ohain JP. Percutaneous pulmonary valve implantation in patients with dysfunction of a "native" right ventricular outflow tract - Mid-term results. *Int J Cardiol.* (2018) 258:31–5. doi: 10.1016/j.ijcard.2017.11.091
12. Demkow M, Ruzyllo W, Biernacka EK, Kalinczuk L, Spiewak M, Kowalski M, et al. Percutaneous Edwards SAPIEN() valve implantation for significant pulmonary regurgitation after previous surgical repair with a right ventricular outflow patch. *Catheter Cardiovasc Interv.* (2014) 83:474–81. doi: 10.1002/ccd.25096
13. Stout KK, Daniels CJ, Aboulhosn JA, Bozkurt B, Broberg CS, Colman JM, et al. 2018 AHA/ACC Guideline for the Management of Adults With Congenital Heart Disease: Executive Summary: A Report of the American College of Cardiology/American Heart Association Task Force on Clinical Practice Guidelines. *Circulation.* (2019) 139:e637–e697. doi: 10.1161/CIR.0000000000000602
14. Rodriguez-Gabella T, Voisine P, Puri R, Pibarot P, Rodes-Cabau J. Aortic bioprosthetic valve durability: incidence, mechanisms, predictors, and management of surgical and transcatheter valve degeneration. *J Am Coll Cardiol.* (2017) 70:1013–28. doi: 10.1016/j.jacc.2017.07.715
15. Georgiev S, Ewert P, Tanase D, Hess J, Hager A, Cleuziou J, et al. A low residual pressure gradient yields excellent long-term outcome after percutaneous pulmonary valve implantation. *JACC Cardiovasc Interv.* (2019) 12:1594–603. doi: 10.1016/j.jcin.2019.03.037
16. Zahn EM, Hellenbrand WE, Lock JE, McElhinney DB. Implantation of the melody transcatheter pulmonary valve in patients with a dysfunctional right ventricular outflow tract conduit early results from the us clinical trial. *J Am Coll Cardiol.* (2009) 54:1722–9. doi: 10.1016/j.jacc.2009.06.034
17. Bergersen L, Benson LN, Gillespie MJ, Cheatham SL, Crean AM, Hor KN, et al. Harmony feasibility trial: acute and short-term outcomes with a self-expanding transcatheter pulmonary valve. *JACC Cardiovasc Interv.* (2017) 10:1763–73. doi: 10.1016/j.jcin.2017.05.034
18. Cao QL, Kenny D, Zhou D, Pan W, Guan L, Ge J, et al. Early clinical experience with a novel self-expanding percutaneous stent-valve in the native right ventricular outflow tract. *Catheter Cardiovasc Interv.* (2014) 84:1131–7. doi: 10.1002/ccd.25544
19. Virk SA, Liou K, Chandrakumar D, Gupta S, Cao C. Percutaneous pulmonary valve implantation: a systematic review of clinical outcomes. *Int J Cardiol.* (2015) 201:487–9. doi: 10.1016/j.ijcard.2015.08.119
20. Gao Y, Xie M, Wang B, Shang X, Zhang L, Xie Y, et al. First-in-human transcatheter pulmonic valve implantation of Med-Zenith PT-Valve in a stenotic pulmonary conduit. *QJM.* (2020) 113:883–5. doi: 10.1093/qjmed/hcaa133
21. Shang X, Chen S, Zhang C, Wang B, Cheatham SL, Lu R, et al. First-in-Man implantation of med-zenith PT-valve in right ventricular outflow tract for pulmonary regurgitation. *JACC Cardiovasc Interv.* (2019) 12:1989–90. doi: 10.1016/j.jcin.2019.07.036
22. Butera G, Milanesi O, Spadoni I, Piazza L, Donti A, Ricci C, et al. *Catheter Cardiovasc Interv.* (2013) 81:310–6. doi: 10.1002/ccd.24518


**Conflict of Interest:** The authors declare that the research was conducted in the absence of any commercial or financial relationships that could be construed as a potential conflict of interest.

frontiers | Frontiers in Cardiovascular Medicine

ORIGINAL RESEARCH
published: 21 June 2022
doi: 10.3389/fcvm.2022.894497

# Long-Term Mortality After TAVI for Bicuspid vs. Tricuspid Aortic Stenosis: A Propensity-Matched Multicentre Cohort Study

*Aleksandra Gasecka[1†], Michał Walczewski[1*†], Adam Witkowski[2], Maciej Dabrowski[2], Zenon Huczek[1], Radosław Wilimski[1], Andrzej Ochała[3], Radosław Parma[3], Piotr Scisło[1], Bartosz Rymuza[1], Karol Zbroński[1], Piotr Szwed[1], Marek Grygier[4], Anna Olasińska-Wiśniewska[4], Dariusz Jagielak[5], Radosław Targoński[5], Grzegorz Opolski[1] and Janusz Kochman[1]*

[1] 1st Chair and Department of Cardiology, Medical University of Warsaw, Warsaw, Poland, [2] Department of Interventional Cardiology and Angiology, Institute of Cardiology, Warsaw, Poland, [3] Division of Cardiology and Structural Heart Diseases, Medical University of Silesia, Katowice, Poland, [4] Department of Cardiac Surgery and Transplantology, Poznan University of Medical Sciences, Poznan, Poland, [5] Department of Cardiac and Vascular Surgery, Medical University of Gdansk, Gdansk, Poland

**Objectives:** Patients with bicuspid aortic valve (BAV) stenosis were excluded from the pivotal trials of transcatheter aortic valve implantation (TAVI). We compared the in-hospital and long-term outcomes between patients undergoing TAVI for bicuspid and tricuspid aortic valve (TAV) stenosis.

**Methods:** We performed a retrospective registry-based analysis on patients who underwent TAVI for BAV and TAV at five different centers between January 2009 and August 2017. The primary outcome was long-term all-cause mortality. Secondary outcomes were in-hospital mortality, procedural complications, and valve performance.

**Results:** Of 1,451 consecutive patients who underwent TAVI, two propensity-matched cohorts consisting of 130 patients with BAV and 390 patients with TAV were analyzed. All-cause mortality was comparable in both groups up to 10 years following TAVI (*HR* 1.09, 95% *CI*: 0.77–1.51). Device success and in-hospital mortality were comparable between the groups (96 vs. 95%, $p = 0.554$ and 2.3 vs. 2.1%, $p = 0.863$, respectively). Incidence of procedural complications was similar in both groups, with a trend toward a higher rate of stroke in patients with BAV (5 vs. 2%, $p = 0.078$). Incidence of moderate or severe paravalvular leak (PVL) at discharge was comparable in both groups (2 vs. 2%, $p = 0.846$). Among patients with BAV, all-cause mortality was similar in self-expanding and balloon-expandable prostheses (*HR* 1.02, 95% *CI*: 0.52–1.99) and lower in new-generation devices compared to old-generation valves (*HR* 0.27, 95% CI 0.12–0.62).

OPEN ACCESS

**Edited by:**
*Ronak Rajani, Guy's and St Thomas' NHS Foundation Trust, United Kingdom*

**Reviewed by:**
*Masahiko Asami, Mitsui Memorial Hospital, Japan*
*Miralem Pasic, Deutsches Herzzentrum Berlin, Germany*
*Josip A. Borovac, University of Split, Croatia*

***Correspondence:**
*Michał Walczewski*
*walcz.michal@gmail.com*

*[†] These authors have contributed equally to this work and share first authorship*

**Specialty section:**
*This article was submitted to Heart Valve Disease, a section of the journal Frontiers in Cardiovascular Medicine*

**Received:** *11 March 2022*
**Accepted:** *04 May 2022*
**Published:** *21 June 2022*

**Citation:**
*Gasecka A, Walczewski M, Witkowski A, Dabrowski M, Huczek Z, Wilimski R, Ochała A, Parma R, Scisło P, Rymuza B, Zbroński K, Szwed P, Grygier M, Olasińska-Wiśniewska A, Jagielak D, Targoński R, Opolski G and Kochman J (2022) Long-Term Mortality After TAVI for Bicuspid vs. Tricuspid Aortic Stenosis: A Propensity-Matched Multicentre Cohort Study. Front. Cardiovasc. Med. 9:894497. doi: 10.3389/fcvm.2022.894497*

**Conclusion:** Patients who had undergone TAVI for BAV had comparable mortality to patients with TAV up to 10 years after the procedure. The device success, in-hospital mortality, procedural complications, and PVL rate were comparable between the groups. The high rate of neurological complications (5%) in patients with BAV warrants further investigation.

**Keywords: aortic stenosis (AS), bicuspid aortic valve (BAV), transcatheter aortic valve implantation (TAVI), mortality, outcomes**

## INTRODUCTION

Bicuspid aortic valve (BAV) is the most common congenital anomaly in adults, present in 1–2% of the population (1). BAV is associated with accelerated aortic valve degeneration, thoracic aorta dilation, aorta coarctation, and increased risk of infective endocarditis (2–5). Hence, patients with BAV may require aortic valve replacement at an earlier age than those with tricupid aortic valve (TAV). Transcatheter aortic valve implantation (TAVI) has become the established treatment for aortic stenosis (AS) in patients at increased risk of surgery, expanding to intermediate- and low-risk patients (6–8). As bicuspid anatomy has been considered a relative contraindication to TAVI, patients with BAV have been excluded from the hitherto randomized clinical trials (7, 8). The main concerns of TAVI in BAV patients comprised the higher risk of malposition and underexpansion of the device, resulting in significant paravalvular leak (PVL) due to heavy calcification, increased risk for aortic root rupture, coronary occlusion, and faster degeneration of bioprosthesis (9). Using current-generation devices, procedural and 1-year outcomes seem to be comparable following TAVI for bicuspid and tricuspid aortic valve disease, suggesting that TAVI is a viable treatment option for patients with BAV (10, 11). However, the long-term observations after TAVI in BAV patients are not yet available. Considering that TAVI is expanding to the younger and more healthy patients, the long-term observation of TAVI in BAV is of paramount importance (12). The goal of this study was to compare the in-hospital and long-term clinical outcomes between patients undergoing TAVI for bicuspid and tricuspid AS, and compare outcomes between self-expanding vs. balloon-expandable TAVI prostheses and between old- and new-generation devices in BAV patients.

## METHODS

We conducted a multicentre registry-based analysis of patients undergoing TAVI at five experienced academic centers in Poland. The study was formally deemed exempt from Bioethical Medical Committee of Warsaw approval. The study population comprised patients with symptomatic severe AS of the bicuspid or tricuspid valve, who were qualified for TAVI by the local, interdisciplinary Heart Teams comprising a general cardiologist, an interventional cardiologist, and a cardiac surgeon (6). The primary imaging modality for the determination of aortic valve morphology was transoesophageal echocardiography until the year 2013, and multi-slice computed tomography (MSCT) from the year 2014. We excluded all patients with aborted procedures, previous AV replacement, and other valve morphologies (unicuspid, quadricuspid, or uncertain). Participating centers used standardized definitions to collect clinical information such as patient demographics, comorbidities, laboratory data, procedural details, and in-hospital outcomes. Data regarding long-term mortality were obtained from the Polish National Health Service database.

### Outcomes

The primary outcome was long-term all-cause mortality after TAVI for BAV compared to TAV. Secondary outcomes included (i) in-hospital mortality, (ii) incidence of procedural complications (life-threatening or disabling bleeding, major vascular complications, stroke, and new pacemaker implantation), and (iii) valve performance evaluated by the in-hospital echocardiography (mean and peak prosthetic valve gradients, PVL type 3 or 4). The exploratory outcomes included a comparison between self-expanding vs. balloon-expandable TAVI prostheses, as well as between old- and new-generation devices in BAV patients. All adverse outcomes were defined using Valve Academic Research Consortium-2 (VARC-2) definitions.

### Statistical Analysis

Statistical analysis was conducted using IBM SPSS Statistics, version 27.0 (IBM). Categorical variables were presented as numbers and percentages and compared using Chi-square or Fischer exact tests. A Shapiro–Wilk test was used to assess the normal distribution of continuous variables. Continuous variables were presented as mean and standard deviation (SD) or median with interquartile range (IQR) and compared using the two-sample *t*-tests or Mann–Whitney U tests. The long-term mortality rates were presented using Kaplan–Meier curves and compared using the log-rank test. It was anticipated that patients with bicuspid and tricuspid AS would have significantly different baselines and procedural characteristics. To avoid confounding due to these differences, propensity score-based matching was used. Propensity scores were calculated using a logistic regression model based on nine relevant baseline patient characteristics (covariates) with aortic valve type (bicuspid

**Abbreviations:** AS, aortic stenosis; BAV, bicuspid aortic valve; LVEF, left ventricular ejection fraction; MSCT, multi-slice computed tomography; PVL, paravalvular leak; TAV, tricuspid aortic valve; TAVI, transcatheter aortic valve implantation; VARC-2, Valve Academic Research Consortium-2.

or tricuspid aortic stenosis) as the dependent variable. The covariates were age, sex (male), EuroSCORE II, peripheral artery disease, hemoglobin level, estimated glomerular filtration rate, left ventricular ejection fraction (LVEF), access site, and valve size. Missing baseline values were imputed using the Markov Chain Monte Carlo method prior to modeling. The missing procedural outcomes and follow-up data were not imputed. Patients with bicuspid AS were matched in a 1:3 ratio to those with tricuspid AS with a caliper of 0.1, producing two patient cohorts. The results are presented as hazard ratios (*HR*) and with a 95% confidence interval (*CI*). All *p*-values are two-sided, and $p < 0.05$ was considered significant for all tests.

# RESULTS

## Baseline Characteristics

Between January 2009 and August 2017, a total of 1,451 patients underwent TAVI at five participating centers. Aortic valve morphology was determined based on transoesophageal echocardiography in 183 patients, including 34 patients with BAV (35% of the study population), and based on MSCT in 337 patients, including 96 patients with BAV (65% of the study population). The follow-up ended on 30 August 2020. A total of 1,403 patients (139 patients with BAV and 1,264 patients with TAV) were included in the present analysis, producing propensity-matched groups of 130 patients with BAV and 390 patients with TAV (**Figure 1**).

In the unmatched cohort, patients with BAV were younger (median age 79 years, IQR 73–83 years vs. 81 years, IQR76–84 years; $p = 0.002$); they had a lower EuroSCORE II-predicted risk of mortality (3.5%, IQR 2.5–5.2 vs. 4.1%, IQR 2.7–6.8%; $p = 0.04$) and fewer comorbidities. After adjusting with propensity-score matching, baseline characteristics were not significantly different (**Table 1**). The median procedure dates in the matched cohort were 12 November 2014 for the bicuspid AS cohort and 1 September 2014 for the tricuspid AS cohort.

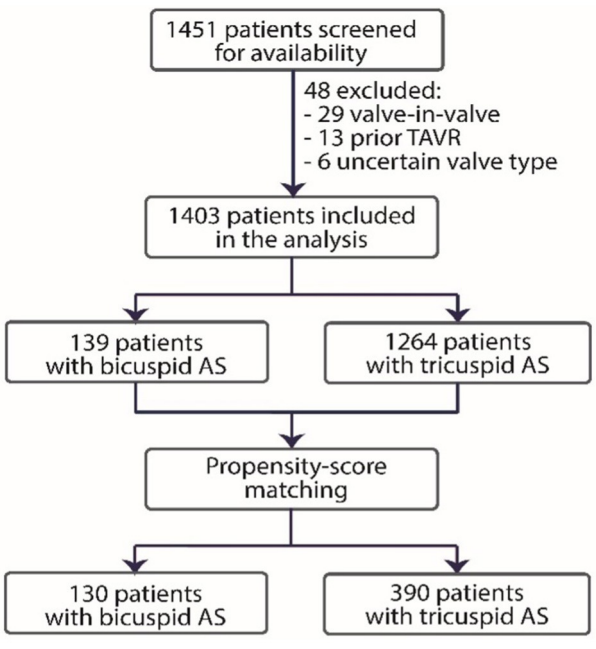


**FIGURE 1 |** Study flowchart. TAVR, transcatheter aortic valve replacement; AS, aortic stenosis.

## Procedural Characteristics and In-hospital Outcomes

All patients in both cohorts completed follow-up at hospital discharge. Among the propensity-score matched patients, there were no procedural differences (**Table 2**). Patients with BAV received larger-size prostheses, with 31 mm prostheses more often used and 26 mm less often in the BAV group compared to the TAV group ($p = 0.003$, $p < 0.001$, respectively). Also, new-generation valves were used more often in patients with BAV (44 vs. 30%, $p < 0.0001$). There were no differences in the use of self-expanding and balloon-expandable valves.

The device success and the in-hospital mortality were comparable between the BAV and TAV groups (96 vs. 95% and 2.3 vs. 2.1%, respectively). The incidence of procedural complications, such as life-threatening or disabling bleeding, major vascular complication and new permanent pacemaker implantation were similar in both groups. There was a trend toward a higher rate of in-hospital stroke in BAV patients (5 vs. 2%, $p = 0.078$).

## Valve Performance

At discharge, there were no differences between the peak and mean aortic valve gradients ($p = 0.097$; $p = 0.165$, respectively). The incidence of moderate or severe PVL (type 3 or 4) was comparable between the groups (2 vs. 2%, $p = 0.846$).

## Long-Term Survival

The median follow-up time was 4.6 years (IQR 3.8–5.5) in the BAV group and 4.8 years (IQR 2.9–5.9) in the TAV group ($p = 0.51$). The longest follow-up time was 10.0 years and 10.2 years in BAV and TAV groups, respectively.

The median survival time was 8.3 years in the BAV group and 8.3 years in the TAV group. There were no significant differences in all-cause mortality between the propensity-matched bicuspid and tricuspid AS groups detected during an observation period of up to 10 years observation period ($p_{\text{logrank}} = 0.63$;*HR* 1.09, 95% *CI*: 0.77–1.5; **Figure 2**).

## Comparison Between Self-Expanding vs. Balloon-Expandable Protheses in BAV Patients

In the BAV group, 96 patients (74%) received self-expanding valve and 34 patients (26%) received balloon-expandable valve. All-cause mortality up to 10 years observation period was comparable in both groups ($p_{\text{logrank}} = 0.956$; *HR* 1.02, 95% *CI*: 0.52–1.99; **Figure 3**).

**TABLE 1 |** Baseline characteristics before and after propensity score matching.

| | Before PS matching | | | After PS matching | | |
|---|---|---|---|---|---|---|
| **Variable** | **TAV ($n$ = 1,264)** | **BAV ($n$ = 139)** | **$p$** | **TAV ($n$ = 390)** | **BAV ($n$ = 130)** | **$p$** |
| **Baseline characteristics** | | | | | | |
| Age (years), | 81 (76–84) | 79 (73–83) | 0.002 | 80 (76–84) | 79 (74–82) | 0.136 |
| Gender (male) | 692 (55%) | 82 (59%) | 0.369 | 198 (51%) | 78 (60%) | 0.068 |
| BMI (kg/m$^2$) | 26.8 (24.0–30.1) | 27.05 (23.9–30.00) | 0.690 | 26.4 (23.6–30.1) | 27.0 (24.0–30.0) | 0.477 |
| **Co-morbidities** | | | | | | |
| Hypertension | 868 (69%) | 90 (65%) | 0.346 | 270 (69%) | 81 (62%) | 0.144 |
| Diabetes mellitus | 445 (35%) | 40 (29%) | 0.130 | 108 (28%) | 45 (35%) | 0.134 |
| Prior stroke/ TIA | 145 (11%) | 16 (12%) | 0.989 | 63 (16%) | 15 (12%) | 0.202 |
| Coronary artery disease | 754 (60%) | 78 (56%) | 0.420 | 219 (56%) | 75 (58%) | 0.094 |
| Myocardial infarction within the last 90 days | 38 (3%) | 1 (1%) | 0.120 | 8 (2%) | 1 (1%) | 0.332 |
| Prior cardiac surgery | 256 (20%) | 27 (19%) | 0.817 | 52 (13%) | 24 (18%) | 0.152 |
| Peripheral artery disease | 343 (27%) | 24 (17%) | 0.012 | 86 (22%) | 24 (18%) | 0.385 |
| Prior pacemaker | 203 (16%) | 16 (12%) | 0.161 | 60 (15%) | 16 (12%) | 0.739 |
| COPD | 233 (18%) | 25 (18%) | 0.897 | 69 (18%) | 31 (24%) | 0.123 |
| Pulmonary hypertension | 175 (14%) | 19 (14%) | 0.955 | 46 (12%) | 19 (15%) | 0.399 |
| Heart failure (NYHA III/IV) | 983 (78%) | 112 (81%) | 0.448 | 300 (77%) | 105 (81%) | 0.360 |
| EuroSCORE II (%) | 4.1% (2.7–6.8%) | 3.5% (2.5–5.2%) | 0.040 | 3.8% (2.8–6.5%) | 3.6% (2.6–5.1%) | 0.171 |
| **Laboratory data** | | | | | | |
| Hemoglobin, g/dL | 12.0 (10.3–13.2) | 12.7 (11.0–13.6) | 0.003 | 12.3 (11.2–13.4) | 12.7 (11.0–13.6 | 0.761 |
| Creatinine, mg/dL | 1.1 (0.9–1.4) | 1.1 (0.9–1.3) | 0.765 | 1.2 (1.0–1.5) | 1.1 (0.9–1.3) | 0.213 |
| Estimated GFR, mL/min/1.73 m$^2$ | 55 (43–65) | 58 (47–73) | 0.020 | 56 (40–65) | 57 (47–74) | 0.101 |
| **Echocardiography before TAVI** | | | | | | |
| Ejection fraction, % | 55 (47–60) | 55 (43–60) | 0.113 | 55 (40–64) | 55 (41–60) | 0.193 |
| Mitral insufficiency (moderate/severe) | 228 (18%) | 43 (31%) | 0.001 | 96 (25%) | 31 (24%) | 0.885 |
| Tricuspid insufficiency (moderate/severe) | 268 (21%) | 32 (23%) | 0.620 | 103 (26%) | 30 (23%) | 0.451 |

## Comparison Between Old-Generation and New-Generation Prostheses in BAV Patients

In the BAV group, 73 patients (56%) received old-generation and 57 patients (44%) received new-generation devices. The median follow-up time in patients with new-generation devices was 4.25 years (IQR 3.79–4.99 years) due to the availability of the new-generation valves on the Polish market since the year 2014. All-cause mortality up to 5 years following TAVI was substantially lower in patients who received new-generation devices compared to old-generation valves ($p_{\text{logrank}} = 0.0016$; *HR* 0.27, 95% *CI* 0.12–0.62; **Figure 4**).

To check whether better outcomes in the new-generation valves were due to between-group differences, we compared baseline and procedural characteristics between patients treated with the new generation and old devices in **Supplementary Tables 1, 2**. There were no major differences between the groups except for a higher rate of moderate/severe tricuspid insufficiency in patients treated with new-generation valves ($p = 0.021$) and a higher rate of prosthesis size 25 mm and 31 mm in patients who received old-generation devices ($p = 0.005$, $p = 0.003$, respectively).

## DISCUSSION

This registry-based study presents the longest hitherto available follow-up in the propensity-matched patients with BAV undergoing TAVI. The main finding of our study is that patients who had undergone TAVI for bicuspid AS had comparable mortality to patients with tricuspid AS up to 10 years after the procedure, with the median follow-up time close to 5 years. The device success, rate of PVL, incidence of procedural complications and in-hospital mortality were comparable between the groups, with a trend toward the higher rate of in-hospital stroke in patients with BAV.

Patients with BAV were excluded from the pivotal trials comparing TAVI vs. surgical aortic valve replacement (SAVR) in AS. However, initial case series and registry data have shown that TAVI might be an efficient and safe alternative to SAVR in patients with BAV stenosis, with the possible caveats of increased PVL and need for permanent pacemaker implantation (13, 14). The higher risk of PVL is caused by the different anatomy of a BAV compared to a normal tricuspid structure, such as (i) asymmetry in the size of leaflets, (ii) higher point of coaptation compared to TAV, (iii) larger dimensions measured at standard anatomic points (aortic annulus, sinus of Valsalva, and ascending aorta), and (iv) higher degree and eccentricity

**TABLE 2 |** Procedural characteristics and in-hospital outcomes.

| Variable | TAV ($n = 390$) | BAV ($n = 130$) | *p* |
|---|---|---|---|
| **Anesthesia** | | | |
| General | 260 (67%) | 89 (68%) | 0.706 |
| Local | 130 (33%) | 41 (32%) | 0.706 |
| **Access site** | | | |
| Transfemoral | 320 (82%) | 112 (86%) | 0.280 |
| Transapical | 35 (9%) | 5 (4%) | 0.057 |
| Other | 35 (9%) | 13 (10%) | 0.726 |
| **Prosthesis size (mm)** | | | |
| 23 | 58 (15%) | 21 (16%) | 0.724 |
| 25 | 9 (2%) | 3 (2%) | 1.000 |
| 26 | 140 (36%) | 26 (20%) | <0.001 |
| 27 | 5 (1%) | 4 (3%) | 0.174 |
| 29 | 158 (41%) | 58 (45%) | 0.411 |
| 31 | 19 (5%) | 16 (12%) | 0.003 |
| 34 | 1 (0.3%) | 2 (1.5%) | 0.094 |
| **Valve type** | | | |
| CoreValve | 144 (37%) | 39 (30%) | 0.152 |
| Boston Lotus | 44 (11%) | 20 (15%) | 0.218 |
| EvolutR | 71 (18%) | 37 (28%) | 0.013 |
| Edwards Sapien | 61 (16%) | 2 (2%) | <0.001 |
| Edwards Sapien XT | 24 (6%) | 8 (6%) | 1.000 |
| Edwards Sapien 3 | 46 (12%) | 24 (18%) | 0.054 |
| Old generation[a] | 273 (70%) | 73 (56%) | <0.001 |
| New generation[b] | 117 (30%) | 57 (44%) | <0.001 |
| Self-expandable[c] | 259 (66%) | 96 (74%) | 0.115 |
| Balloon-expandable[d] | 131 (34%) | 34 (26%) | 0.115 |
| **Device success** | 370 (95%) | 125 (96%) | 0.554 |
| **Procedure complications** | | | |
| Post-dilatation due to PVL | 90 (23%) | 33 (25%) | 0.592 |
| Second valve implantation | 4 (1.0%) | 2 (1.5%) | 0.635 |
| Conversion to surgery | 1 (0.002%) | 0 (0.0%) | 0.563 |
| Annular rupture | 0 (0.0%) | 1 (0.01%) | 0.083 |
| In-hospital mortality | 8 (2.1%) | 3 (2.3%) | 0.863 |
| Life-threatening or disabling bleeding* | 26 (7%) | 7 (5%) | 0.604 |
| Major vascular complication* | 33 (9%) | 7 (5%) | 0.254 |
| Stroke | 9 (2%) | 7 (5%) | 0.079 |
| New pacemaker | 54 (14%) | 20 (15%) | 0.664 |
| **Post-TAVI echocardiography** | | | |
| Ejection fraction, % | 52 (45–60) | 55 (50–60) | 0.101 |
| Peak AV gradient, mm Hg | 19 (14–26) | 17 (12–23) | 0.097 |
| Mean AV gradient, mm Hg | 10 (7–14) | 9 (7–13) | 0.165 |
| Paravalvular leak type 3 or 4 | 7 (2%) | 2 (2%) | 0.846 |

**According to VARC.*
*[a]CoreValve, Boston Lotus, Edwards Sapien, Edwards Sapien XT.*
*[b]EvolutR, Symetis Accurate, Edwards Sapien 3.*
*[c]CoreValve, Boston Lotus, EvolutR.*
*[d]Edwards Sapien, Edwards Sapien XT, Edwards Sapien 3.*

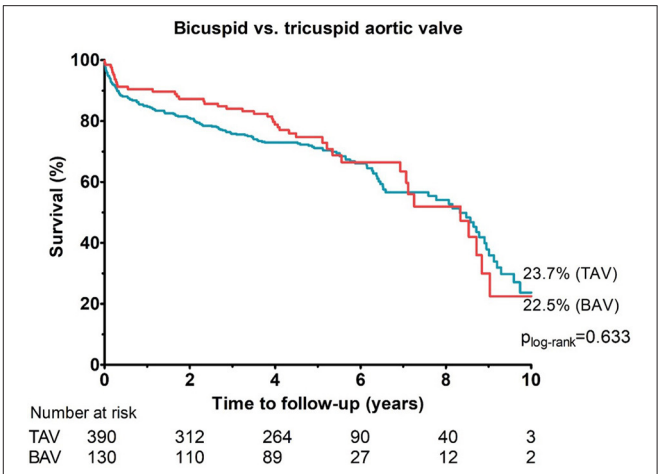


**FIGURE 2 |** Cumulative incidences of all-cause mortality among propensity-matched cohorts with bicuspid and tricuspid aortic valve up to 10 years of follow-up.

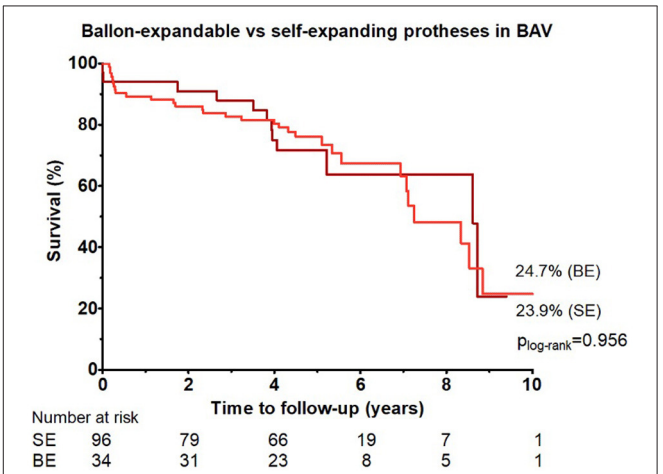


**FIGURE 3 |** Cumulative incidences of all-cause mortality up to 10 years of follow-up among patients with bicuspid aortic valve who received balloon-expandable vs. self-expanding prostheses.

of calcification (15). Since TAVI for bicuspid AS presents both anatomic and clinical challenges, the use of three-dimensional imaging modalities is mandatory to understand the complex and variable anatomy of BAV disease (16). Recently, it was demonstrated that the outcomes of TAVI in bicuspid AS depend on valve morphology, with the calcified raphe and excess leaflet calcification associated with increased risk of procedural complications and 1-year mortality (17). Hence, many studies focused on algorithms for valve sizing in BAV, such as attempts to compare supra-annular valve sizing with the conventional annular sizing (18) and to include the raphe length, calcium burden, and distribution in the pre-procedural evaluation of patients with BAV (19).

Although we did not evaluate the association between valve morphology and outcomes, in all patients since the year 2014 (65% of the total population and 74% of patients with BAV) the bicuspid anatomy was confirmed and valve sizing was facilitated by MSCT, which might at least partly underlie the favorable procedural outcomes. The valve performance at

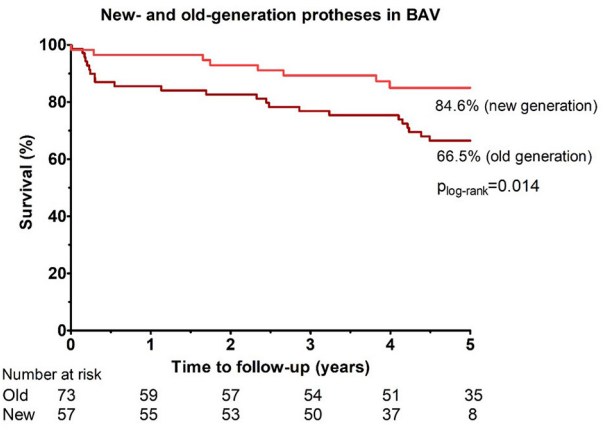


**FIGURE 4 |** Cumulative incidences of all-cause mortality up to 5 years of follow-up among patients with bicuspid aortic valve who received new-generation vs. old-generation prostheses.

hospital discharge and the rate of procedural complications were similar in BAV and TAV groups. In accordance with the previous studies, there was a trend toward a higher rate of in-hospital stroke in BAV patients (11). Importantly, data presented in this analysis largely represent patients who underwent TAVI without the use of cerebral embolic protection. Routine use of embolic protection devices during TAVI has been shown to reduce the incidence of periprocedural strokes and might prove useful, especially in the BAV cohort (20).

The favorable results in our cohort were achieved despite implantation of both old- and new-generation devices. Initial studies suggested that the first-generation TAVI valves had suboptimal outcomes in patients with BAV, but later-generation valves might have outcomes similar to those seen in patients with TAV (21). In the hallmark trial with the third-generation balloon-expandable Edward Sapien 3 valve, the incidence of moderate-to-severe PVL was dramatically reduced compared to older generation valves, with the caveats of relatively high 30-day mortality rate (3.9%), new pacemaker requirement (23.5%), and asymmetrical valve deployment (38%) (22). However, recent large-scale registry-based analyses of patients treated with Edward Sapien 3 valve did not confirm the initial concerns, showing comparable rates of procedural complications in bicuspid and tricuspid AS patients, and similar 1-year rates of stroke and all-cause mortality (11, 23). Similarly, the procedural and 1-year outcomes of TAVI with new-generation self-expanding Evolut R or Evolut PRO valves were similar in patients with BAV and TAV (24). Hence, likely not only the valve generation but also other procedural advancements and improved imaging within the last years, along with the growing operator experience account for improved outcomes in patients with BAV undergoing TAVI.

In our population of intermediate-risk patients, the 2-year survival rates (80–85%) were comparable with those previously reported in the literature (82.0% for BAV vs. 83.4% for TAV) (25). The 10-year survival rate, in turn, was comparable between the bicuspid and tricuspid AS (22.5% in BAV vs. 23.7% in TAV) and higher than previously reported for tricuspid AS patients, treated with the early generation valves only (Cribier-Edwards, Edwards Sapien or CoreValve; 9.4%) (26). Likely, the improved long-term survival in our study is due to the fact that both old- and new-generation devices were used in our cohort, and in the majority of patients, MSCT was used to facilitate the procedural planning.

In our BAV cohort, all-cause mortality up to 5 years following TAVI was lower in patients who received new-generation devices, compared to those treated with old-generation valves (82.3 vs. 50.2%). A recent study that evaluated the outcomes of TAVI in 170,959 patients with bicuspid AV stenosis (3.2%) in comparison with tricuspid AV stenosis (96.7%) demonstrated comparable procedural, post-procedural, and 1-year outcomes following TAVI in both groups when current-generation devices were used (10). Better outcomes with the new-generation devices were also demonstrated in a recent meta-analyses (12, 27). Hence, TAVI seems to be a viable treatment option for patients with BAV, especially with the use of newer-generation devices and careful pre-procedural evaluation by MSCT.

Among BAV patients, there were no differences in the mortality rate up to 10 years in patients who received self-expandable vs. balloon-expanding valves (24.7, 23.9%). Recent registry-based trials and a meta-analysis of seven studies including 706 patients confirmed the feasibility of both balloon-expandable and self-expanding valve implantation in bicuspid AS, with similar rates of 30-day and 1-year mortality and stroke (12, 28). Balloon-expandable valves were associated with lower rates of new pacemaker implantation and PVL but carried a higher risk of annular rupture (12). Further randomized controlled trials are required to compare outcomes between self-expandable vs. balloon-expanding valves in BAV patients.

Our study cohort comprised intermediate-risk patients, as demonstrated by the EuroSCORE II-predicted risk of mortality (3.6 and 3.8% in the propensity-score matched patients with BAV and TAV, respectively). As such, our results suggest that TAVI may be safe and effective not only in high-risk but also intermediate-risk patients with BAV. On the other hand, the high rate of neurological complications (5%) and new pacemaker implantations (12–15%) in patients with BAV are significant drawbacks of TAVI in BAV and warrant further careful investigation. Moreover, our results are not applicable and therefore should not be extrapolated to the low-risk patients with BAV. The ongoing Low-Risk Bicuspid Study designed to evaluate the procedural safety and efficacy of TAVI in patients with BAV at low surgical risk might provide the first evidence-based data regarding the TAVI performance in low-risk BAV patients. The preliminary results of this study such as a total of 150 patients showed favorable 30-day results, with low rates of death and disabling stroke (1.3%), high device success rate (95.3%) and no moderate-to-severe PVL (29). Given that up to 50% of low-risk patients undergoing aortic valve replacement have BAV disease, the results of Low-Risk Bicuspid Study with the planned 10-year follow-up are crucial to determine the optimal interventional treatment method in these patients (29). The next step would be a randomized trial comparing TAVI to SAVR in intermediate- or low-risk BAV stenosis patients. Finally, there

is a need for a prospective study with long-term follow-up such as BAV patients undergoing TAVI with new-generation devices to better understand TAVI valve durability in bicuspid anatomy (30).

## LIMITATIONS

Our study has several limitations. First, the number of patients with BAV was low and does not allow gaining strong clinical and statistical conclusions regarding TAVI in this specific subgroup. The low number of procedures and institutional, learning curve may have influenced the results and therefore the comparisons between the group. However, the number of procedures in both groups gradually increased over the years, with similar slopes on both lines (**Supplementary Figure 1**), implying a comparable impact of the learning curve on TAVI performance in patients with BAV and TAV. Second, there was no independent imaging core laboratory to confirm bicuspid anatomy. Third, the selection of prosthesis was at the operator's discretion, which may have affected the observed outcomes. Fourth, we did not evaluate the incidence of long-term valve performance and major cardiovascular outcomes besides mortality in our cohort. Hence, we cannot draw any conclusions regarding valve durability in BAV patients. Fifth, although propensity-score matching adjusted for the differences in baseline characteristics, it was not possible to adjust for the different degrees of aortic valve calcification. Therefore, a selection bias toward the preference of BAV patients with less calcified valves cannot be excluded. Moreover, our cohort included intermediate-risk patients, and hence our findings are not directly applicable to younger bicuspid patients. Finally, our analysis did not include an additional control group of patients with BAV treated surgically.

## CONCLUSION

In this preliminary, registry-based study of propensity-matched patients who had undergone TAVI for AS, patients with BAV had a similar rate of procedural complications and comparable mortality up to 10 years, compared to patients with TAV. Among BAV patients, the long-term mortality was similar in those who received balloon-expandable vs. self-expanding valves and lower in those who received new-generation valves compared to old-generation valves. However, the high rate of neurological complications and new pacemaker implantations in BAV patients warrant caution regarding TAVI in this subgroup. Further randomized trials are needed to draw firm conclusions regarding the best treatment option in patients with BAV stenosis.

## DATA AVAILABILITY STATEMENT

The raw data supporting the conclusions of this article will be made available by the authors, without undue reservation.

## ETHICS STATEMENT

The studies involving human participants were reviewed and approved by Bioethical Medical Committee of Warsaw. The patients/participants provided their written informed consent to participate in this study.

## AUTHOR CONTRIBUTIONS

AG, JK, MW, and GO: conceptualization. AG, MW, KZ, and MG: data curation. AG, MW, and JK: formal analysis. AG, MW, RW, RP, and PSc: investigation. AG, MW, AW, ZH, RW, AO, GO, and JK: methodology. AG, MW, MD, RP, PSc, and PSz: project administration. AG, MW, BR, MG, AO, and DJ: resources. BR and KZ: software. AW, ZH, AO, GO, and JK: supervision. AG, MW, RT, and DJ: validation. AG and MW: writing—original draft. JK, RT, AW, and GO: writing—review and editing. All authors have read and agreed to the published version of the manuscript.

## SUPPLEMENTARY MATERIAL

The Supplementary Material for this article can be found online at: https://www.frontiersin.org/articles/10.3389/fcvm.2022.894497/full#supplementary-material

## REFERENCES


1. Borger MA, Fedak PWM, Stephens EH, Gleason TG, Girdauskas E, Ikonomidis JS, et al. The American association for thoracic surgery consensus guidelines on bicuspid aortic valve-related aortopathy: executive summary. *J Thorac Cardiovasc Surg.* (2018) 156:473–80. doi: 10.1016/j.jtcvs.2017.10.161
2. Masri A, Kalahasti V, Alkharabsheh S, Svensson LG, Sabik JF, Roselli EE, et al. Characteristics and long-term outcomes of contemporary patients with bicuspid aortic valves. *J Thorac Cardiovasc Surg.* (2016) 151:1650–9. doi: 10.1016/j.jtcvs.2015.12.019
3. Michelena HI, Khanna AD, Mahoney D, Margaryan E, Topilsky Y, Suri RM, et al. Incidence of aortic complications in patients with bicuspid aortic valves. *JAMA.* (2011) 306:1104–12. doi: 10.1001/jama.2011.1286
4. Becerra-Munoz VM, Ruiz-Morales J, Rodriguez-Bailón I, Sánchez-Espin G, López-Garrido MA, Robledo-Carmona J, et al. Infective endocarditis in patients with bicuspid aortic valve: Clinical characteristics, complications, and prognosis. *Enfermedades Infecc y Microbiol Clin.* (2017) 35:645–50. doi: 10.1016/j.eimce.2017.11.007
5. Verma S, Siu SC. Aortic dilatation in patients with bicuspid aortic valve. *N Engl J Med.* (2014) 370:1920–9. doi: 10.1056/NEJMra1207059
6. Baumgartner H, Falk V, Bax JJ, De Bonis M, Hamm C, Holm PJ, et al. 2017 ESC/EACTS guidelines for the management of valvular heart disease. *Eur Heart J.* (2017) 38:2739–91. doi: 10.1093/eurheartj/ehx391
7. Mack MJ, Leon MB, Thourani VH, Makkar R, Kodali SK, Russo M, et al. Transcatheter aortic-valve replacement with a balloon-expandable valve in low-risk patients. *N Engl J Med.* (2019) 380:1695–705. doi: 10.1056/NEJMoa1814052
8. Adams DH, Popma JJ, Reardon MJ, Yakubov SJ, Coselli JS, Deeb GM, et al. Transcatheter aortic-valve replacement with a self-expanding prosthesis. *N Engl J Med.* (2014) 370:1790–8. doi: 10.1056/NEJMoa1400590
9. Philip F, Faza NN, Schoenhagen P, Desai MY, Tuzcu EM, Svensson LG, Kapadia SR. Aortic annulus and root characteristics in severe aortic stenosis due to bicuspid aortic valve and tricuspid aortic valves: implications for

transcatheter aortic valve therapies. *Catheter Cardiovasc Interv*. (2015) 86:E88–98. doi: 10.1002/ccd.25948
10. Halim SA, Edwards FH, Dai D, Li Z, Mack MJ, Holmes DR, et al. Outcomes of transcatheter aortic valve replacement in patients with bicuspid aortic valve disease: a report from the society of thoracic surgeons/American college of cardiology transcatheter valve therapy registry. *Circulation*. (2020) 141:1071–9. doi: 10.1161/CIRCULATIONAHA.119.040333
11. Makkar RR, Yoon S-H, Leon MB, Chakravarty T, Rinaldi M, Shah PB, et al. Association between transcatheter aortic valve replacement for bicuspid vs tricuspid aortic stenosis and mortality or stroke. *JAMA*. (2019) 321:2193–202. doi: 10.1001/jama.2019.7108
12. Ueshima D, Fovino LN, Brener SJ, Fabris T, Scotti A, Barioli A, et al. Transcatheter aortic valve replacement for bicuspid aortic valve stenosis with first-and new-generation bioprostheses: a systematic review and meta-analysis. *Int J Cardiol*. (2020) 298:76–82. doi: 10.1016/j.ijcard.2019.09.003
13. Patel A, Leon MB. Transcatheter aortic valve replacement in patients with bicuspid aortic valves. *J Thorac Dis*. (2018) 10:S3568. doi: 10.21037/jtd.2018.07.122
14. Mentias A, Sarrazin MV, Desai MY, Saad M, Horwitz PA, Kapadia S, et al. Transcatheter versus surgical aortic valve replacement in patients with bicuspid aortic valve stenosis. *J Am Coll Cardiol*. (2020) 75:2518–9. doi: 10.1016/j.jacc.2020.02.069
15. Kochman J, Rymuza B, Huczek Z. Transcatheter aortic valve replacement in bicuspid aortic valve disease. *Curr Opin Cardiol*. (2015) 30:594–602. doi: 10.1097/HCO.0000000000000219
16. Hamdan A, Kornowski R, TAVI. in bicuspid aortic valve stenosis. *Int J Cardiol*. (2020) 298:83–4. doi: 10.1016/j.ijcard.2019.10.018
17. Yoon S-H, Kim W-K, Dhoble A, Milhorini Pio S, Babaliaros V, Jilaihawi H, et al. Bicuspid aortic valve morphology and outcomes after transcatheter aortic valve replacement. *J Am Coll Cardiol*. (2020) 76:1018–30. doi: 10.1016/j.jacc.2020.07.005
18. Weir-McCall JR, Attinger-Toller A, Blanke P, Perlman GY, Sellers SL, Wood D, et al. Annular versus supra-annular sizing for transcatheter aortic valve replacement in bicuspid aortic valve disease. *J Cardiovasc Comput Tomogr*. (2020) 14:407–13. doi: 10.1016/j.jcct.2020.01.008
19. Petronio AS, Angelillis M, De Backer O, Giannini C, Costa G, Fiorina C, et al. Bicuspid aortic valve sizing for transcatheter aortic valve implantation: development and validation of an algorithm based on multi-slice computed tomography. *J Cardiovasc Comput Tomogr*. (2020) 14:452–61. doi: 10.1016/j.jcct.2020.01.007
20. Seeger J, Kapadia SR, Kodali S, Linke A, Wöhrle J, Haussig S, et al. Rate of peri-procedural stroke observed with cerebral embolic protection during transcatheter aortic valve replacement: a patient-level propensity-matched analysis. *Eur Heart J*. (2019) 40:1334–40. doi: 10.1093/eurheartj/ehy847
21. Yoon S-H, Bleiziffer S, De Backer O, Delgado V, Arai T, Ziegelmueller J, et al. Outcomes in transcatheter aortic valve replacement for bicuspid versus tricuspid aortic valve stenosis. *J Am Coll Cardiol*. (2017) 69:2579–89. doi: 10.1016/j.jacc.2017.03.017
22. Guyton RA, Padala M. Transcatheter aortic valve replacement in bicuspid aortic stenosis: early success but concerning red flags. *JACC Cardiovasc Interv*. (2016) 9:825–7. doi: 10.1016/j.jcin.2016.02.042
23. Attinger-Toller A, Bhindi R, Perlman GY, Murdoch D, Weir-McCall J, Blanke P, et al. Mid-term outcome in patients with bicuspid aortic valve stenosis following transcatheter aortic valve replacement with a current generation device: A multicenter study. *Catheter Cardiovasc Interv*. (2020) 95:1186–92. doi: 10.1002/ccd.28475
24. Forrest JK, Kaple RK, Ramlawi B, Gleason TG, Meduri CU, Yakubov SJ, et al. Transcatheter aortic valve replacement in bicuspid versus tricuspid aortic valves from the STS/ACC TVT registry. *Cardiovasc Interv*. (2020) 13:1749–59. doi: 10.1016/j.jcin.2020.03.022
25. Pineda AM, Rymer J, Wang A, Banks AZ, Koweek LH, Plichta R, et al. Transcatheter aortic valve replacement for patients with severe bicuspid aortic stenosis. *Am Heart J*. (2020) 224:105–12. doi: 10.1016/j.ahj.2020.02.003
26. Sathananthan J, Lauck S, Polderman J, Yu M, Stephenson A, Sathananthan G, et al. Ten year follow-up of high-risk patients treated during the early experience with transcatheter aortic valve replacement. *Catheter Cardiovasc Interv*. (2021) 97:E431–7. doi: 10.1002/ccd.29124
27. Quintana RA, Monlezun DJ, DaSilva-DeAbreu A, Sandhu UG, Okwan-Duodu D, Ramirez J, et al. One-year mortality in patients undergoing transcatheter aortic valve replacement for stenotic bicuspid versus tricuspid aortic valves: a meta-analysis and meta-regression. *J Interv Cardiol*. (2019) 2019:8947204. doi: 10.1155/2019/8947204
28. Mangieri A, Tchetchè D, Kim W-K, Pagnesi M, Sinning J-M, Landes U, et al. Balloon versus self-expandable valve for the treatment of bicuspid aortic valve stenosis: insights from the BEAT international collaborative registrys. *Circ Cardiovasc Interv*. (2020) 13:e008714. doi: 10.1161/CIRCINTERVENTIONS.119.008714
29. Waksman R, Rogers T, Torguson R, Gordon P, Ehsan A, Wilson SR, et al. Transcatheter aortic valve replacement in low-risk patients with symptomatic severe aortic stenosis. *J Am Coll Cardiol*. (2018) 72:2095–105. doi: 10.1016/j.jacc.2018.08.1033
30. Tchetche D, Siddiqui S. Percutaneous management of bicuspid aortic valves: still remaining questions. *JACC Cardiovasc Interv*. (2020) 13:1760–2. doi: 10.1016/j.jcin.2020.03.021

**Conflict of Interest:** AW: proctor for Medtronic. ZH: proctor for Medtronic and Abbott. RP: lecture honoraria for Edwards Lifescience. MG: lecture honoraria, proctor and advisory board member of Boston Scientific. DJ: proctor for Edwards Lifesciences. JK: lecture honoraria and proctor for Medtronic, Boston Scientific, Abbott.

The remaining authors declare that the research was conducted in the absence of any commercial or financial relationships that could be construed as a potential conflict of interest.

**Publisher's Note:** All claims expressed in this article are solely those of the authors and do not necessarily represent those of their affiliated organizations, or those of the publisher, the editors and the reviewers. Any product that may be evaluated in this article, or claim that may be made by its manufacturer, is not guaranteed or endorsed by the publisher.

frontiers | Frontiers in Cardiovascular Medicine

CASE REPORT
published: 23 June 2022
doi: 10.3389/fcvm.2022.907168

# Case Report: Posterior Thoracic Window in the Presence of Pleural Effusion in Critical Care Medicine: One More Chance to Image the Aortic Valve

*Francesca Mantovani[1]*, Giovanni Benfari[2], Andrea Barbieri[3], Francesco Manca[1], Vincenzo Guiducci[1], Alessandro Navazio[1] and Marie-Annick Clavel[4]*

*[1] Department of Cardiology, Azienda USL, IRCCS di Reggio Emilia, Reggio Emilia, Italy, [2] Section of Cardiology, Department of Medicine, University of Verona, Verona, Italy, [3] Department of Cardiology, Policlinico Hospital, Modena and Reggio Emilia University, Modena, Italy, [4] Institut Universitaire de Cardiologie et de Pneumologie de Québec (Quebec Heart and Lung Institute), Université Laval, Québec, QC, Canada*

OPEN ACCESS

**Edited by:**
*Ronak Rajani, Guy's and St Thomas' NHS Foundation Trust, United Kingdom*

**Reviewed by:**
*Valeria Pergola, University Hospital of Padua, Italy*
*Birgid Gonska, Ulm University Medical Center, Germany*

***Correspondence:**
*Francesca Mantovani*
*francy_manto@hotmail.com*

**Specialty section:**
*This article was submitted to Cardiovascular Imaging, a section of the journal Frontiers in Cardiovascular Medicine*

**Received:** *29 March 2022*
**Accepted:** *30 May 2022*
**Published:** *23 June 2022*

**Citation:**
*Mantovani F, Benfari G, Barbieri A, Manca F, Guiducci V, Navazio A and Clavel M-A (2022) Case Report: Posterior Thoracic Window in the Presence of Pleural Effusion in Critical Care Medicine: One More Chance to Image the Aortic Valve. Front. Cardiovasc. Med. 9:907168. doi: 10.3389/fcvm.2022.907168*

Good quality echocardiographic images in the setting of critical care medicine may be difficult to obtain for many reasons. We present a case of an 85-year-old woman with acute pulmonary edema and pleural effusion, where transthoracic bedside echocardiographic examination raised a suspicion for significant aortic valve disease. However, given the orthopneic decubitus of the patients, the quality of images was poor. To increase the accuracy of diagnosis, a posterior thoracic view through the pleural effusion in the sitting position was used. This view allowed the diagnosis of mixed aortic valve disease (aortic stenosis and regurgitation) and the quantification of valve disease through multiparametric criteria as recommended by current guidelines. The posterior thoracic view, when feasible, may provide a useful option in the assessment of cardiac structures and further diagnostic information in technically difficult echocardiographic examinations.

**Keywords: case report, posterior thoracic view, aortic stenosis, aortic regurgitation, echocardiography**

## INTRODUCTION

### Case Presentation

An 85-year-old woman was admitted to our institution with acute respiratory distress. Clinical examination revealed a 5/6 systo-diastolic murmur radiating to both carotid arteries and bilateral lung crackles. Laboratory workup was notable for a N-terminal pro-brain natriuretic peptide (NT-proBNP) of 15,000 ng/L (normal range: < 300 ng/L) and a moderate high-sensitive troponin T elevation of 245 ng/L (normal range: < 14 ng/L) with no increase on serial testing. The hemoglobin and renal function were normal. Evaluation by chest X-ray showed bilateral diffuse pulmonary infiltrates consistent with pulmonary edema and bilateral pleural effusion (**Figure 1**). The patient was admitted to CCU. A transthoracic bedside echocardiogram (with EPIQ 7 C, X5-1, Philips Healthcare) was performed, but it was extremely difficult to obtain good quality images from standard views given the orthopneic decubitus of the patient. However, the aortic valve was heavily

calcified, and severe aortic stenosis was documented with a mean gradient of 42 mmHg from the apical 5 chambers view and 35 mmHg from the right parasternal view, with a functional aortic valve area ≈0.6 $cm^2$ (**Figure 2**). The left ventricle showed eccentric hypertrophy with a moderate diffuse reduction of ejection fraction (EF 35–40%). Then, the patient was positioned sitting upright, because the left pleural effusion offered an additional acoustic window—the posterior thoracic window (PTW)—that allowed better alignment of the ultrasound beam with the aortic jet. Mean gradient was recorded definitely higher than that from the standard view at 50 mm Hg (**Figure 2**). Moreover, aortic regurgitation that appeared

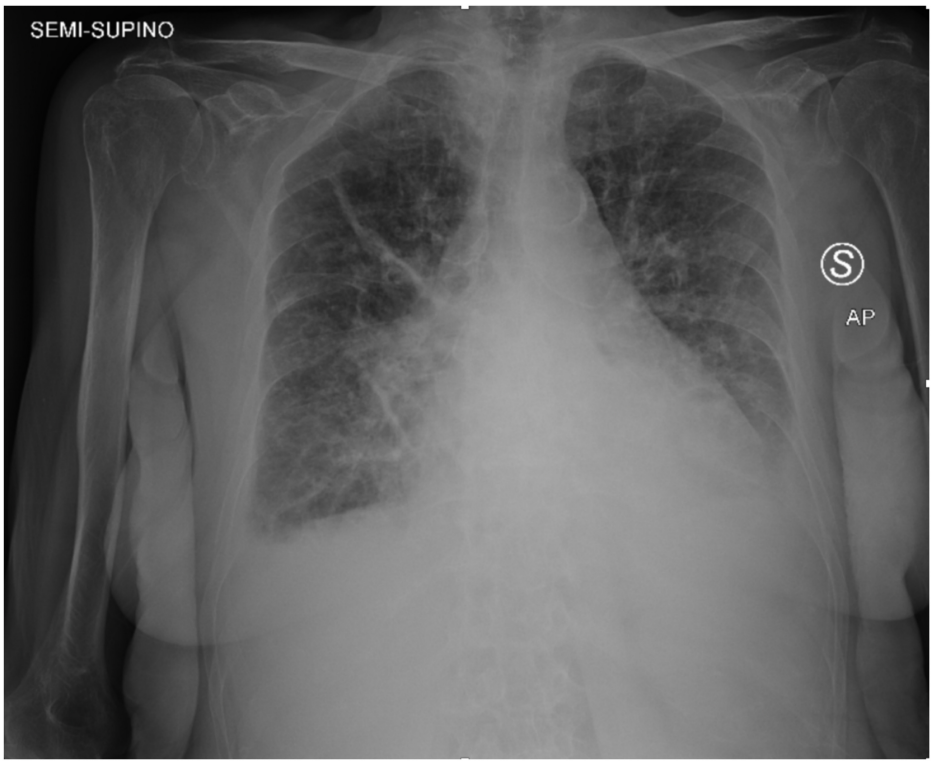


**FIGURE 1 |** Chest X-ray was acquired in the semi-sitting position and showed bilateral diffuse pulmonary infiltrates consistent with pulmonary edema and bilateral pleural effusion.

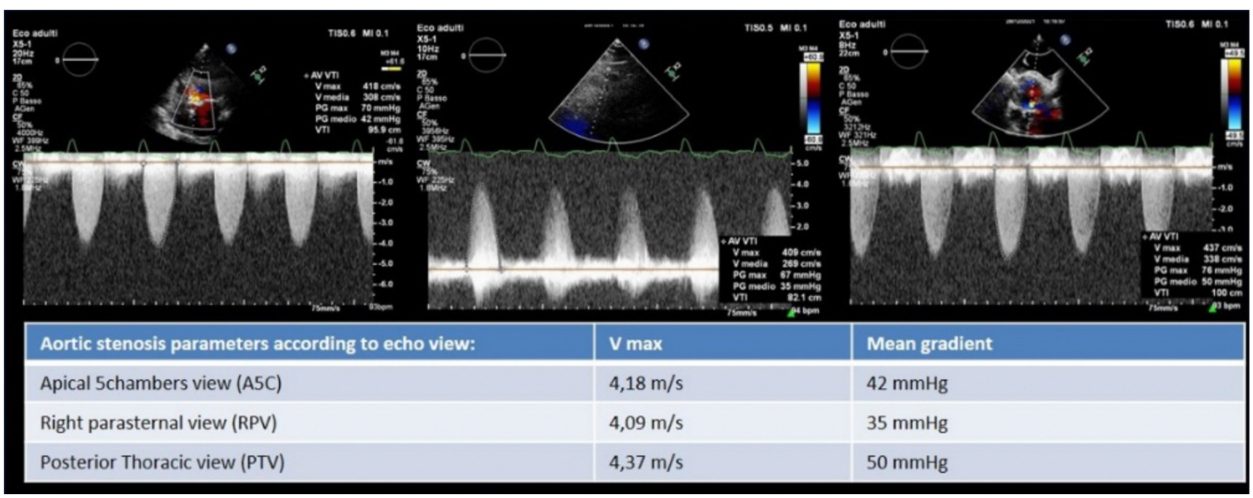

| Aortic stenosis parameters according to echo view: | V max | Mean gradient |
|---|---|---|
| Apical 5chambers view (A5C) | 4,18 m/s | 42 mmHg |
| Right parasternal view (RPV) | 4,09 m/s | 35 mmHg |
| Posterior Thoracic view (PTV) | 4,37 m/s | 50 mmHg |

**FIGURE 2 |** Aortic stenosis severity evaluation by Vmax and mean gradient from apical five chambers, right parasternal, and posterior thoracic view where the latter allowed to record the highest Vmax and mean gradient.

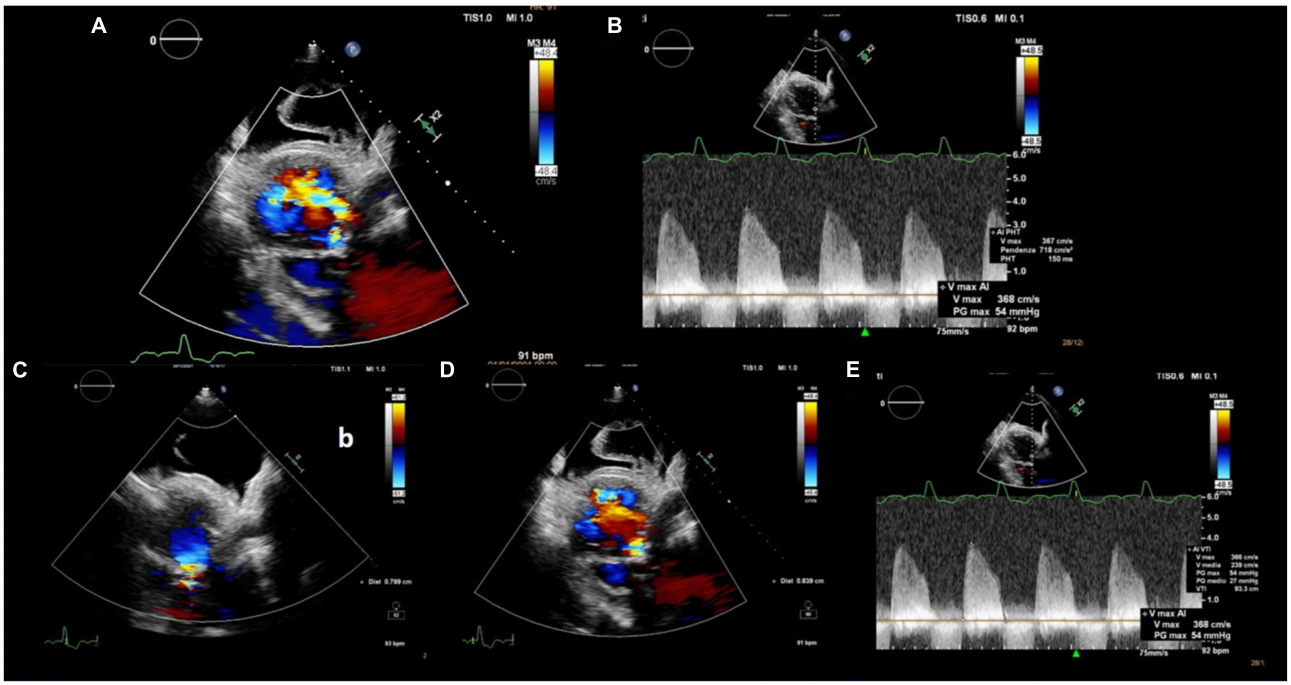


**FIGURE 3 |** Multiparametric evaluation of aortic regurgitation severity: **(A)** Wide color flow regurgitant jet area, **(B)** PHT 150 ms, **(C)** PISA radius 8 mm, **(D)** vena contracta 8 mm, and **(E)** aortic regurgitation VTI 93 cm and Vmax 3.7 cm/s resulting in an EROA 0.52 $cm^2$ and regurgitant volume 50 ml. PHT: pressure half time; PISA: proximal isovelocity surface area; VTI: velocity time integral; EROA: effective regurgitant orifice area.

mild from the standard view was documented as significant from PTW (**Figure 3**). In fact, a proper alignment of the aortic regurgitation jet was feasible from this view with a quantification of severity with multiparameter criteria as suggested by the guidelines (pressure half time 150 ms, vena contracta 8 mm, effective regurgitant orifice area 0.5$cm^2$, regurgitant volume 50 ml; **Figure 3**).

Therefore, the final diagnosis was symptomatic severe mixed aortic valve disease with severe stenosis and severe regurgitation, associated with acute decompensated heart failure. The patient was stabilized by medical therapy and then addressed to transaortic valve replacement (TAVI). At the 6-month follow-up, the patient was asymptomatic with a functional capacity expected for her age.

## DISCUSSION

Obtaining adequate echocardiographic images in critically ill patients is important for accurate diagnosis and treatment. For several reasons, this group of patients remains among the most challenging with regard to the quality of echocardiographic images.

In the presence of pleural effusion, many cardiac structures may be evaluated from PTW (1), also known as subscapular retro cardiac imaging (2). Normally, imaging through the posterior thoracic window is not possible as the lungs overlay the heart and the ultrasound beam is reflected at the tissue-air interface (3), while the presence of a large left pleural effusion minimizes the impedance to ultrasound transmission (4). This view is excellent to adequately assess the native and prosthetic aortic valve velocity/gradients due to the parallel alignment between the ultrasound beam, left ventricular outflow tract, and aortic root (3) (**Figure 4**). Indeed, it is now well established that the "Doppler

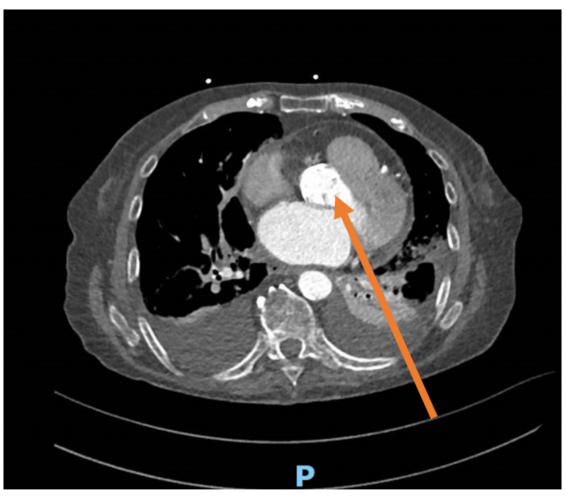


**FIGURE 4 |** CT scan from the same patient showing the alignment of the Doppler beam in the posterior thoracic view toward the aortic valve (arrow). The transducer is positioned between posterior intercostal spaces, parallel to the ribs.

intercept angle," the angle between the ultrasound beam and aortic jet, may strongly influence the hemodynamic assessment of aortic valve stenosis (5). This explains the reason why guidelines not only recommend the use of apical views but also advocate for multiple transducer positions to obtain the most accurate peak velocities across a stenotic aortic valve (6).

Recently, Benfari et al. demonstrated that the right parasternal view is highly feasible and can be crucial to properly assess aortic valve stenosis severity (avoiding misalignment), thereby resolving some inconsistencies between mean gradient and aortic valve area; however, this view is still not routinely used in clinical practice (7, 8).

To the best of our knowledge, only few cases (9) and two case series have been published using PTW in the assessment of native or prosthetic aortic valve (3, 10), but none of them reported a mixed (stenosis and regurgitation) aortic valve disease and the major impact of the PTW in the assessment of both stenosis and regurgitation. Indeed, the present case is unique because PTW allowed to correctly diagnose and quantify not only the highest velocity of aortic stenosis compared with other echocardiographic views but also aortic regurgitation with multiple parameters.

In conclusion, in the presence of pleural effusion and technically difficult echocardiographic examinations, the PTW should always be considered in the assessment of cardiac structures, including the aortic valve as a potentially useful option to provide accurate diagnostic information.

## DATA AVAILABILITY STATEMENT

The original contributions presented in this study are included in the article/supplementary material, further inquiries can be directed to the corresponding author.

## ETHICS STATEMENT

Ethical review and approval was not required for the study on human participants in accordance with the local legislation and institutional requirements. The patients/participants provided their written informed consent to participate in this study. Written informed consent was obtained from the participant for the publication of this case report. Written informed consent was obtained from the individual(s) for the publication of any potentially identifiable images or data included in this article.

## AUTHOR CONTRIBUTIONS

All authors listed have made a substantial, direct, and intellectual contribution to the work, and approved it for publication.

## REFERENCES


1. Parameswaran R, Carr VF, Rao AV, Goldberg H. The posterior thoracic approach in echocardiography. *J Clin Ultrasound.* (1979) 7:461–4. doi: 10.1002/jcu.1870070609
2. Waggoner AD, Baumann CM, Stark PA. "Views from the back" by subscapular retrocardiac imaging: technique and clinical application. *J Am Soc Echocardiogr.* (1995) 8:257–62. doi: 10.1016/s0894-7317(05)80035-5
3. Naqvi TZ, Huynh HK. A new window of opportunity in echocardiography. *J Am Soc Echocardiogr.* (2006) 19:569–77. doi: 10.1016/j.echo.2005.12.028
4. Schutz N, Bendjelid K. Transthoracic echocardiography after heart surgery: could pleural view be of some help? *Eur J Echocardiogr.* (2009) 10:987–8. doi: 10.1093/ejechocard/jep106
5. Martin RP. Clinical implementation of continuous-wave doppler: it made all the difference. *J Am Soc Echocardiogr.* (2018) 31:1323–9.
6. Vahanian A, Beyersdorf F, Praz F, Milojevic M, Baldus S, Bauersachs J, et al. 2021 ESC/EACTS Guidelines for the management of valvular heart disease. *Eur J Cardiothorac Surg.* (2021) 60:727–800.
7. Benfari G, Gori AM, Rossi A, Papesso B, Vassanelli C, Zito GB, et al. Feasibility and relevance of right parasternal view for assessing severity and rate of progression of aortic valve stenosis in primary care. *Int J Cardiol.* (2017) 240:446–51. doi: 10.1016/j.ijcard.2017.04.091
8. Benfari G, Mantovani F, Romero-Brufau S, Setti M, Rossi A, Ribichini FL, et al. The right parasternal window: when Doppler-beam alignment may be life-saving in patients with aortic valve stenosis. *J Cardiovasc Med (Hagerstown).* (2020) 21:831–4. doi: 10.2459/JCM.0000000000000971
9. Giannakopoulos G, Noble S, Rey F, Frei A, Muller H. Left posterior thoracic acoustic window: a forgotten approach for aortic stenosis assessment. *CJC Open.* (2021) 3:838–40. doi: 10.1016/j.cjco.2021.01.015
10. Lee MS, Naqvi TZ. Posterior thoracic echocardiography for assessment of native and prosthetic aortic valves in the presence of pleural effusion. *J Ultrasound Med.* (2014) 33:721–7. doi: 10.7863/ultra.33.4.721


**Conflict of Interest:** The authors declare that the research was conducted in the absence of any commercial or financial relationships that could be construed as a potential conflict of interest.

frontiers | Frontiers in Cardiovascular Medicine

ORIGINAL RESEARCH
published: 03 August 2022
doi: 10.3389/fcvm.2022.908062

# Prognostic Implications of Biventricular Global Longitudinal Strain in Patients With Severe Isolated Tricuspid Regurgitation

*Dae-Young Kim[1], Jiwon Seo[2], Iksung Cho[2], Seung Hyun Lee[3], Sak Lee[3], Geu-Ru Hong[2], Jong-Won Ha[2] and Chi Young Shim[2]**

[1] Department of Cardiology, CHA Bundang Medical Center, CHA University School of Medicine, Seongnam-si, South Korea, [2] Division of Cardiology, Severance Cardiovascular Hospital, Yonsei University College of Medicine, Seoul, South Korea, [3] Division of Cardiovascular Surgery, Department of Thoracic and Cardiovascular Surgery, Severance Cardiovascular Hospital, Yonsei University College of Medicine, Seoul, South Korea

OPEN ACCESS

**Edited by:**
Ronak Rajani,
Guy's and St Thomas' NHS Foundation Trust, United Kingdom

**Reviewed by:**
Yasufumi Nagata,
Massachusetts General Hospital and Harvard Medical School, United States
Valeria Pergola,
University Hospital of Padua, Italy
Osama Soliman,
National University of Ireland Galway, Ireland

***Correspondence:**
Chi Young Shim
cysprs@yuhs.ac

**Specialty section:**
This article was submitted to Heart Valve Disease, a section of the journal Frontiers in Cardiovascular Medicine

**Received:** 30 March 2022
**Accepted:** 14 June 2022
**Published:** 03 August 2022

**Citation:**
Kim D-Y, Seo J, Cho I, Lee SH, Lee S, Hong G-R, Ha J-W and Shim CY (2022) Prognostic Implications of Biventricular Global Longitudinal Strain in Patients With Severe Isolated Tricuspid Regurgitation. Front. Cardiovasc. Med. 9:908062. doi: 10.3389/fcvm.2022.908062

**Background:** Isolated TV surgery can be performed in patients with symptoms caused by severe isolated tricuspid regurgitation (TR), preferably before the onset of significant right ventricular (RV) dysfunction. In patients with severe TR, intrinsic RV dysfunction tends to be masked and promotes left ventricular (LV) mechanical dysfunction. This study investigated the prognostic implications of biventricular global longitudinal strain (GLS) in patients receiving isolated tricuspid valve (TV) surgery.

**Methods:** Among 1,670 patients who underwent TV surgery between January 2000 and December 2020, 111 patients with severe isolated TR who underwent echocardiography before and after TV surgery were analyzed. We assessed LV, RV, and biventricular GLS using speckle tracking echocardiography. Biventricular GLS was defined as the sum of LV-GLS and RV free-wall strain. The primary outcomes were cardiovascular death, heart failure hospitalization, re-done TV surgery, and heart transplantation.

**Results:** During 3.9 ± 3.8 years of follow-up after the postoperative echocardiography, 24 (21.6%) patients experienced a primary outcome. Those patients had more comorbidities and more impaired preoperative RV-GLS and biventricular GLS than those who did not experience a primary outcome, although the two groups did not differ in preoperative LV-GLS. Patients with a primary outcome also showed significantly impaired postoperative RV-GLS, biventricular GLS, and LV-GLS compared those without a primary outcome. In multivariate analyses, both pre- and postoperatively assessed RV-GLS [preoperative; hazard ratio (HR) 0.86, confidence interval (CI) 0.79–0.93, $p < 0.001$, postoperative; HR 0.89, CI 0.82–0.96, $p = 0.004$] and biventricular GLS [preoperative; HR 0.96, CI 0.91–1.00, $p = 0.048$, postoperative; HR 0.94, CI 0.89–0.99, $p = 0.023$] were independently associated with the primary outcomes.

**Conclusion:** In patients with severe isolated TR undergoing TV surgery, the absolute value of RV-GLS under 17.2% is closely associated with a poor prognosis, and that of biventricular GLS under 34.0%, mainly depending on the RV-GLS, is related to the poor prognosis. Further prospective multicenter studies are warranted to establish the risk stratification of isolated TV surgery.

**Keywords: isolated tricuspid regurgitation, global longitudinal strain, left ventricle, right ventricle, surgery, prognosis**

## INTRODUCTION

Isolated tricuspid regurgitation (TR), which is not associated with left-sided heart disease or pulmonary hypertension, has received increased attention because it correlates with early mortality even without any cardiovascular comorbidities (1, 2). It has been recognized that isolated tricuspid valve (TV) surgery could offer prognostic benefit before the development of significant right ventricular (RV) dysfunction or end-organ failure. However, current practice guidelines do not present clear surgical timing for isolated TV surgery due to limited and controversial study results (3, 4).

Most patients with severe isolated TR have chronic RV volume overload, which leads to deteriorating RV function unless intervention is timely (5). Moreover, severe isolated TR can mask intrinsic RV dysfunction. Ultimately, RV dilation and dysfunction promote left ventricular (LV) under-filling, which produces mechanical LV dysfunction (6). Therefore, a comprehensive assessment of both LV and RV function in patients with severe isolated TR is important in predicting prognostic outcomes after isolated TV surgery. However, using echocardiography to evaluate LV and RV function in patients with severe isolated TR is challenging due to the complex anatomic structure of the RV chamber and under-filling of the LV chamber (7). Two-dimensional speckle-tracking echocardiography is more sensitive and less volume-dependent in assessing LV and RV systolic function than conventional transthoracic echocardiography (8–11). However, few reports have used biventricular global longitudinal strain (GLS) to predict the clinical outcomes of patients with severe isolated TR. Therefore, we hypothesized that pre- and postoperative biventricular GLS would provide prognostic information for patients with severe isolated TR.

## MATERIALS AND METHODS

### Study Population

We retrospectively identified 1,670 patients who underwent TV surgery (TV repair or replacement) in a single tertiary center between January 2000 and December 2020. Among them, we excluded patients who had a history of prior TV, aortic valve, or mitral valve surgery, had a cardiovascular implantable electronic device, had concomitant significant (at least moderate) aortic or mitral valve dysfunction, had combined coronary artery bypass surgery, had congenital heart disease, had been diagnosed with pulmonary hypertension (pulmonary artery systolic pressure greater than 50 mmHg), had a primary RV cardiomyopathy such as arrhythmogenic cardiomyopathy, or had an LV ejection fraction (EF) of less than 35%. We also excluded patients who did not undergo preoperative transthoracic echocardiography within 6 months before isolated TV surgery and postoperative echocardiography between 1 and 12 months after isolated TV surgery and those whose echocardiographic images were too poor to analyze ventricular GLS. All patients who had clinical events between TV surgery and the day of postoperative echocardiography were also excluded. After those exclusions, we included 111 patients in this study population (**Figure 1**). Each patient's clinical history, medications, laboratory results, echocardiographic parameters, and clinical outcomes were reviewed retrospectively. The etiology of isolated TR was classified as follows: the primary TR, which included the defect of TV leaflet itself, and the secondary TR, which was related to tricuspid annular dilation with normal leaflet morphology. This study was conducted in accordance with the Declaration of Helsinki, and the study protocol was approved by the Institutional Review Board of Yonsei University Health System (IRB number: 4-2021-0929).

### Follow-Up and Outcomes

After isolated TV surgery, the patients visited the outpatient clinic regularly and were scheduled to undergo postoperative echocardiography between 1 and 12 months later. The index date was defined as the day of the post-op echocardiography. The primary outcomes were cardiovascular-related death, heart failure hospitalization, redone TV surgery, and heart transplantation. Cardiovascular-related death was defined as death from myocardial infarction, aggravation of heart failure, sudden cardiac death, or ischemic stroke. Heart failure hospitalization was defined as symptoms of dyspnea with a New York Heart Association (NYHA) grade of at least 3 requiring medications such as vasodilators or diuretics, elevated N-terminal pro-brain natriuretic peptide, and pulmonary congestion or pleural effusion on a chest X-ray. If a patient had two or more clinical events, only the first event was included as an outcome. The surgical mortality was defined as any cause of death within 30 days after surgery or before hospital discharge. We carefully reviewed medical records to find those outcomes, and follow-up was ended on the last day of April 2021 or whenever a primary outcome event occurred.

### Echocardiography

Standard 2D and Doppler measurements were performed by using a standard commercially available ultrasound machine (Vivid E9 color Doppler ultrasound M5S probe; GE Medical

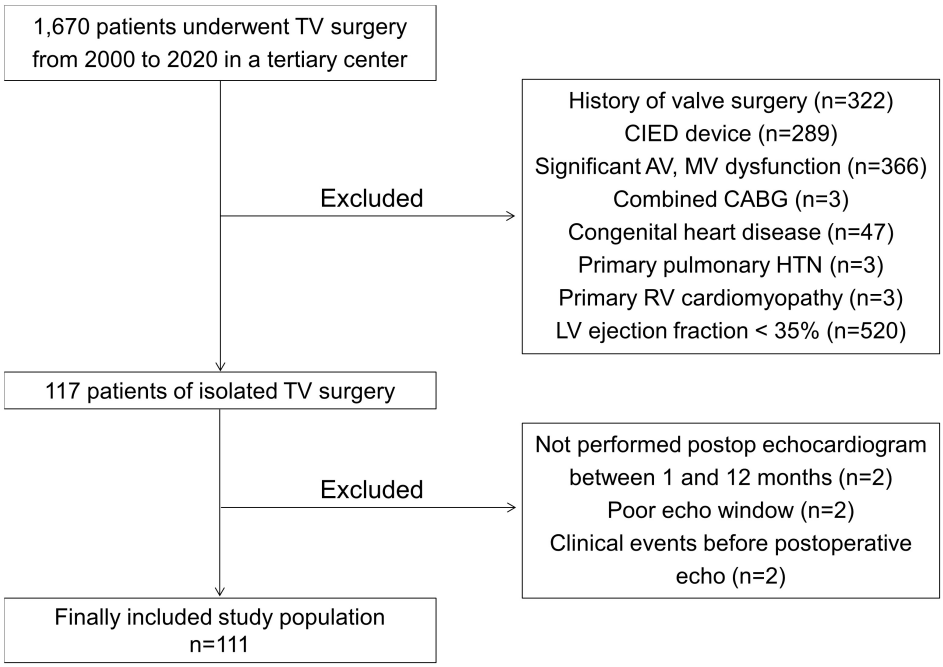


**FIGURE 1 |** A flowchart of this study. TV, tricuspid valve; CIED, cardiovascular implantable electronic devices; AV, aortic valve; MV, mitral valve; CABG, coronary artery bypass graft; HTN, hypertension; RV, right ventricle; LV, left ventricle.

Systems, Chicago, IL; Philips iE33 color Doppler ultrasound X5-1 and S8-3 probe; Philips Healthcare, Netherlands) with a 2.5–3.5 MHz, in accordance with the guidelines of the American Society of Echocardiography (12). To better categorize TR severity, we used a newly proposed grading method that divides severe TR into "severe," "massive," and "torrential" TR (13). Measurements of the RV end-diastolic area (EDA) and end-systolic area (ESA) were obtained from the apical 4-chamber focused RV view at the end-diastolic and end-systolic phases, respectively, and the RV fractional area change (FAC) was calculated as the ratio of the RV EDA and ESA. The vena contracta width was measured at the narrowest portion of the regurgitant jet from the apical 4-chamber focused RV view. The LVEF was calculated by the biplane Simpson's method in the apical 4-chamber and 2-chamber views. The LV end-diastolic dimension (EDD) and end-systolic dimension (ESD) were measured as the distance between the LV interventricular septum and posterior wall from the M-mode at the end-diastolic and end-systolic phases, respectively. Residual TR after TV surgery was defined as at least moderate TR on the post-op echocardiogram.

## Speckle-Tracking Echocardiography

We used the best images from three apical four-, three-, and two-chamber views and the RV-focused apical four-chamber view from both pre- and post-op echocardiographic data for our LV, RV, biventricular, and left atrial (LA) mechanical functional analyses. Those images were stored and exported to an offline storage device, and speckle-tracking echocardiography was performed using a vendor-independent software package (TomTec 2D cardiac performance analysis; Image Arena version 4.6, Munich, Germany). LV- and RV-GLS was measured according to the strain assessment guidelines by expert cardiologists who were blinded to clinical data (14–16). To measure LV-GLS, the LV endocardial borders were traced in apical four-, three-, and two-chamber views at the both the end-diastolic and end-systolic frames, and the TomTec software tracked the speckle on the three LV endocardial borders during a whole cardiac cycle (**Figure 2**). |LV-GLS| was defined as the absolute value of LV-GLS. To measure RV-GLS, the RV endocardial border, which included both the RV free wall and interventricular septum, was traced in the RV-focused apical four-chamber view at both the end-diastolic and end-systolic frames, and the TomTec software tracked the speckle on the RV endocardial borders during a whole cardiac cycle. |RV-GLS| was defined as the absolute value of RV-GLS. RV-free wall longitudinal strain (FWS) was defined as the strain value at the RV free wall. |RV-FWS| was defined as the absolute value of RV-FWS. Biventricular GLS was defined as the sum of LV-GLS and RV-FWS. Biventricular |GLS| was defined as the absolute value of biventricular GLS. To measure LA longitudinal strain, the LA endocardial border was traced in apical four and two-chamber views across the LA appendage and pulmonary veins. Then, the LA longitudinal strain curve through the whole cardiac cycle was analyzed by tracking the speckle on the LA endocardial borders. We selected 20 patients from the study cohort and analyzed the intra- and inter-observer reproducibility of the LV-GLS and RV-GLS measurements using a Bland-Altman analysis. The intra- and inter-class correlation coefficients of |LV-GLS| were 0.957 and 0.962, and those of |RV-GLS| were

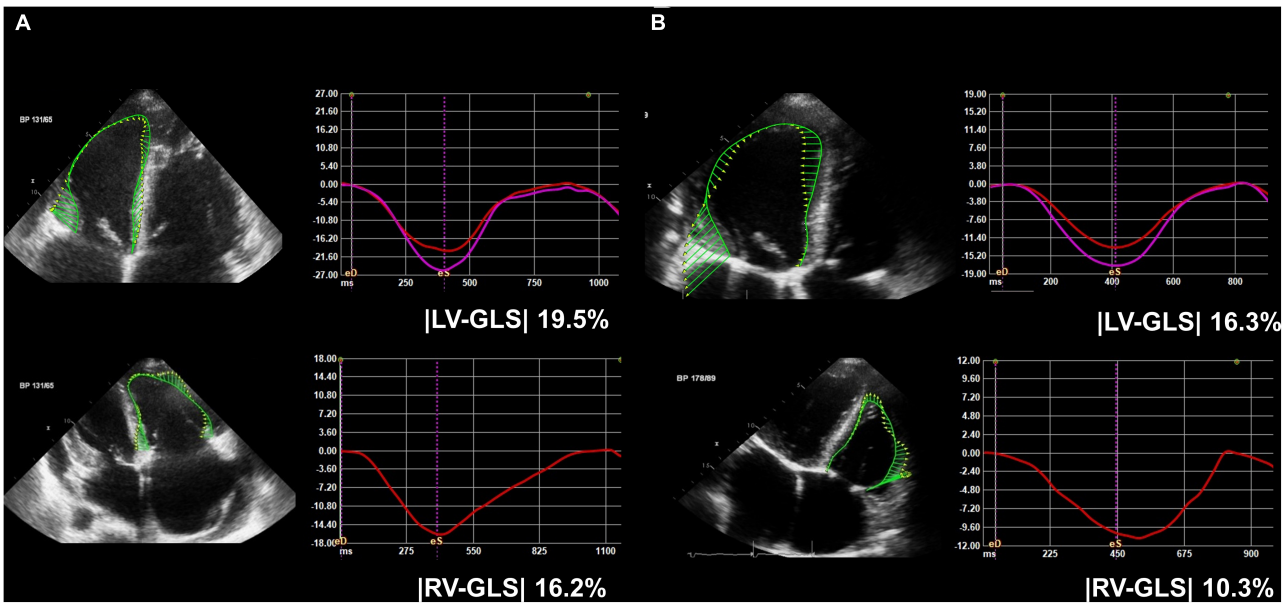


**FIGURE 2 |** Representative figure of **(A)** pre-op and **(B)** post-op LV-GLS and RV-GLS measurements. LV-GLS was calculated from three standard apical images, and RV-GLS was calculated from RV focused apical echocardiographic images. LV, left ventricle; RV, right ventricle; GLS, global longitudinal strain; |LV-GLS|, absolute value of LV-GLS; |RV-GLS|, absolute value of RV-GLS.

0.989 and 0.989, respectively. The Bland-Altman analysis showed the limits of agreement (LOA) across a broad range of |LV-GLS| and |RV-GLS| values; the bias for intra- and inter-observer measurements of |LV-GLS| was 0.39% (range: −0.17 to 0.95%, 95% LOA) and 0.45% (range: 0.07–0.96%), and that of |RV-GLS| was 0.49% (range: −0.07 to 1.04%) and 0.17% (range: −0.39 to 0.73%), respectively.

## Statistical Analysis

Continuous variables are reported as the mean ± standard deviation, and categorical variables are reported as the frequency and percentage. Comparisons of baseline clinical, laboratory and echocardiographic parameters between the two groups (experiencing a primary outcome and not) were performed using Student's *t*-test for continuous data and $\chi^2$ or Fisher's exact test for categorical data. The predictive values of LV-, RV-, and biventricular GLS for the primary outcomes were calculated using a receiver operating characteristics (ROC) analysis. Kaplan-Meier survival analyses and log-rank tests were used to compare the clinical outcomes according to cutoff values for RV- and biventricular GLS during the follow-up period. Predictors of the primary outcomes were analyzed using multivariate nested Cox regression models. EuroSCORE II as a composite of demographic variables and echocardiographic parameters as pre- and post-op GLS of RV and biventricle were analyzed in the multivariate models. EuroSCORE II was included in every four models. Next, pre- and post-op RV-GLS were included in the first and second models. Pre- and post-op biventricular GLS were included in the third and fourth models. Differences were deemed significant at *P*-value $< 0.05$. All statistical analyses were performed using the SPSS software version 25.0 (IBM corporation, Armonk, NY).

# RESULTS

## Baseline Characteristics

During a mean 3.9 ± 3.8 years after the post-op echocardiography, 24 (21.6%) patients experienced one of the primary outcomes. Among them, 5 died from cardiovascular causes, 17 had heart failure hospitalization, 1 had their TV surgery redone, and 1 had a heart transplant. The overall surgical mortality rate was 2.7% ($n = 3$). All of these patients died due to postoperative septic shock before the discharge. The surgery profile, baseline characteristics, medications, and laboratory results of patients with and without the primary outcomes are shown in **Table 1**. Of the total 111 patients, 89 (80.2%) underwent TV repair and 25 (22.5%) had concomitant MAZE operations. In patients with a primary outcome, a previous history of diabetes mellitus, chronic kidney disease, atrial fibrillation, or coronary artery disease was more common than in those without a primary outcome. NYHA class of III and IV were present over half (53.1%) of all patients. In terms of medication, patients with primary outcomes had taken more digoxin, anticoagulants, and diuretics than those without. In the laboratory findings, patients with primary outcomes had a lower level of albumin (3.8 ± 0.7 vs. 4.1 ± 0.5 mg/dL, $p = 0.044$) and a higher level of creatinine (1.1 ± 0.5 vs. 0.8 ± 0.2 mg/dL, $p = 0.013$) than those without primary outcomes. The EuroSCORE II was significantly higher in patients with primary outcomes than the controlled group (3.8 ± 2.3 vs. 1.9 ± 1.1%, $p < 0.001$).

The mean period between preoperative echocardiography and surgery was 1.0 ± 1.2 months and the mean period between surgery and postoperative echocardiography was

**TABLE 1 |** Baseline characteristics.

| | Total (*n* = 111) | With outcome (*n* = 24) | Without outcome (*n* = 87) | *P*-value |
|---|---|---|---|---|
| Age, years | 63.9 ± 12.8 | 67.2 ± 15.1 | 63.0 ± 12.1 | 0.162 |
| Female sex, n (%) | 76 (68.5) | 15 (62.5) | 61 (70.1) | 0.477 |
| BMI, kg/m$^2$ | 23.6 ± 3.3 | 23.9 ± 3.7 | 23.5 ± 3.2 | 0.611 |
| Hypertension, n (%) | 73 (65.8) | 18 (75.0) | 55 (63.2) | 0.282 |
| Diabetes mellitus, n (%) | 19 (17.1) | 8 (33.3) | 11 (12.6) | 0.017 |
| Dyslipidemia, n (%) | 26 (23.4) | 5 (20.8) | 21 (24.1) | 0.735 |
| CKD, n (%) | 11 (9.9) | 5 (20.8) | 6 (6.9) | 0.043 |
| Atrial fibrillation, n (%) | 86 (77.5) | 24 (100.0) | 62 (71.3) | 0.003 |
| CAD, n (%) | 7 (6.3) | 4 (16.7) | 3 (3.4) | 0.018 |
| Chronic lung disease, n (%) | 18 (16.2) | 5 (20.8) | 13 (14.9) | 0.488 |
| Etiology of TR | | | | 0.349 |
| Primary, n (%) | 10 (9.0) | 1 (4.2) | 9 (10.3) | |
| Secondary, n (%) | 101 (91.0) | 23 (95.8) | 78 (89.7) | |
| TV surgery profile | | | | |
| TV replacement, n (%) | 22 (19.8) | 6 (25.0) | 16 (18.4) | 0.472 |
| TV repair, n (%) | 89 (80.2) | 18 (75.0) | 71 (81.6) | |
| Concomitant MAZE, n (%) | 25 (22.5) | 4 (16.7) | 21 (24.1) | 0.438 |
| NYHA class | | | | 0.149 |
| II, n (%) | 52 (46.8) | 8 (33.3) | 44 (50.6) | |
| III, n (%) | 40 (36.0) | 9 (37.5) | 31 (35.6) | |
| IV, n (%) | 19 (17.1) | 7 (29.2) | 12 (13.8) | |
| **Medications, n (%)** | | | | |
| RAAS blockers | 56 (50.5) | 12 (50.0) | 44 (50.6) | 0.960 |
| Beta-blockers | 40 (36.0) | 6 (25.0) | 34 (39.1) | 0.203 |
| CCB | 18 (16.2) | 7 (29.2) | 11 (12.6) | 0.052 |
| Digoxin | 35 (31.5) | 12 (50.0) | 23 (26.4) | 0.028 |
| Statin | 35 (31.5) | 9 (37.5) | 26 (29.9) | 0.477 |
| Antiplatelets | 19 (17.1) | 5 (20.8) | 14 (16.1) | 0.585 |
| Anticoagulants | 76 (68.5) | 21 (87.5) | 55 (63.2) | 0.023 |
| Diuretics | 96 (86.5) | 24 (100.0) | 72 (82.8) | 0.029 |
| Loop diuretics | 84 (75.7) | 20 (83.3) | 64 (73.6) | 0.323 |
| Mineralocorticoid receptor antagonist | 53 (47.7) | 13 (54.2) | 40 (46.0) | 0.477 |
| **Laboratory findings** | | | | |
| Hemoglobin, g/dL | 12.5 ± 2.2 | 11.7 ± 2.8 | 12.8 ± 1.9 | 0.086 |
| Platelet, × 10$^6$ mL | 196.2 ± 83.4 | 183.0 ± 98.5 | 199.9 ± 78.9 | 0.384 |
| Total protein, mg/dL | 6.8 ± 0.8 | 6.6 ± 1.1 | 6.9 ± 0.7 | 0.376 |
| Albumin, mg/dL | 4.0 ± 0.5 | 3.8 ± 0.7 | 4.1 ± 0.5 | 0.044 |
| Creatinine, mg/dL | 0.9 ± 0.3 | 1.1 ± 0.5 | 0.8 ± 0.2 | 0.013 |
| Total bilirubin, mg/dL | 0.8 ± 0.4 | 0.9 ± 0.6 | 0.8 ± 0.4 | 0.190 |
| INR | 1.17 ± 0.4 | 1.25 ± 0.4 | 1.15 ± 0.4 | 0.159 |
| EuroSCORE II, % | 2.3 ± 1.6 | 3.8 ± 2.3 | 1.9 ± 1.1 | < 0.001 |

*BMI, body mass index; CKD, chronic kidney disease; CAD, coronary artery disease; TR, tricuspid regurgitation; NYHA, New York Heart Association; RAAS, renin-angiotensin-aldosterone system; CCB, calcium channel blockers; INR, international normalized ratio.*

**TABLE 2 |** Echocardiographic characteristics.

| | Total (*n* = 111) | With outcome (*n* = 24) | Without outcome (*n* = 87) | *P*-value |
|---|---|---|---|---|
| ***Pre-op TTE*** | | | | |
| TR grade | | | | 0.194 |
| Severe, n (%) | 98 (88.3) | 23 (95.8) | 75 (86.2) | |
| Massive, n (%) | 13 (11.7) | 1 (2.8) | 12 (13.8) | |
| Torrential, n (%) | 0 (0.0) | 0 (0.0) | 0 (0.0) | |
| RV S′, cm/s | 10.6 ± 3.1 | 9.3 ± 2.8 | 11.0 ± 3.1 | 0.023 |
| RV FAC, % | 37.7 ± 10.2 | 31.7 ± 10.5 | 39.4 ± 9.6 | 0.001 |
| \|RV-GLS\|, % | 20.7 ± 6.5 | 16.0 ± 6.2 | 22.0 ± 6.0 | <0.001 |
| \|RV-FWS\|, % | 21.3 ± 8.1 | 17.0 ± 7.4 | 22.5 ± 7.9 | 0.003 |
| RV EDA, mm | 27.5 ± 10.5 | 26.4 ± 11.3 | 27.9 ± 10.3 | 0.537 |
| RV ESA, mm$^2$ | 16.8 ± 6.4 | 17.9 ± 8.1 | 16.6 ± 5.8 | 0.375 |
| VC Width, mm | 9.7 ± 3.0 | 9.8 ± 2.1 | 9.7 ± 3.2 | 0.791 |
| RVSP, mmHg | 42.4 ± 11.2 | 46.0 ± 15.0 | 41.5 ± 9.8 | 0.170 |
| LV EF, % | 61.7 ± 8.6 | 60.2 ± 9.4 | 62.2 ± 8.3 | 0.325 |
| \|LV-GLS\|, % | 18.7 ± 3.9 | 18.0 ± 4.7 | 18.9 ± 3.6 | 0.351 |
| LV EDD, mm | 47.5 ± 6.9 | 50.0 ± 7.7 | 46.8 ± 6.5 | 0.043 |
| LV ESD, mm | 32.6 ± 5.8 | 34.8 ± 6.7 | 32.1 ± 5.4 | 0.039 |
| Biventricular \|GLS\|, % | 40.0 ± 10.1 | 34.9 ± 10.7 | 41.4 ± 9.6 | 0.006 |
| LAVI, mL/m$^2$ | 65.0 ± 47.4 | 74.5 ± 40.6 | 62.4 ± 49.0 | 0.271 |
| E/e' | 11.4 ± 6.7 | 13.6 ± 6.6 | 10.9 ± 6.7 | 0.126 |
| LA reservoir strain, % | 17.4 ± 9.4 | 16.1 ± 8.3 | 17.8 ± 9.7 | 0.434 |
| ***Post-op TTE*** | | | | |
| Residual TR | 29 (26.1) | 9 (37.5) | 20 (23.0) | 0.152 |
| RV FAC, % | 32.2 ± 8.7 | 24.8 ± 9.7 | 34.2 ± 7.2 | <0.001 |
| \|RV-GLS\|, % | 18.3 ± 5.2 | 13.8 ± 5.3 | 19.5 ± 4.4 | <0.001 |
| \|RV-FWS\|, % | 18.7 ± 5.8 | 14.4 ± 6.2 | 19.9 ± 5.1 | <0.001 |
| RV EDA, mm$^2$ | 21.2 ± 6.5 | 22.8 ± 8.1 | 20.8 ± 5.9 | 0.273 |
| RV ESA, mm$^2$ | 14.5 ± 5.1 | 17.2 ± 6.7 | 13.7 ± 4.4 | 0.020 |
| VC Width, mm | 2.9 ± 2.6 | 3.9 ± 3.3 | 2.7 ± 2.3 | 0.105 |
| LV EF, % | 64.1 ± 8.2 | 60.9 ± 11.7 | 65.0 ± 6.8 | 0.114 |
| \|LV-GLS\|, % | 18.4 ± 4.2 | 16.4 ± 5.1 | 19.0 ± 3.7 | 0.024 |
| LV EDD, mm | 49.1 ± 5.6 | 50.0 ± 7.2 | 48.9 ± 5.1 | 0.476 |
| LV ESD, mm | 33.2 ± 5.5 | 34.9 ± 7.8 | 32.8 ± 4.5 | 0.212 |
| \|Biventricular GLS\|, % | 37.1 ± 8.8 | 30.7 ± 10.6 | 38.9 ± 7.5 | <0.001 |
| LAVI, mL/m$^2$ | 61.0 ± 33.3 | 73.5 ± 35.5 | 57.5 ± 32.0 | 0.036 |
| E/e' | 16.2 ± 7.2 | 18.0 ± 4.5 | 15.8 ± 7.6 | 0.298 |
| LA reservoir strain, % | 15.5 ± 10.4 | 8.6 ± 7.0 | 17.4 ± 10.4 | <0.001 |

*RV, right ventricle; FAC, fractional area change; S′, systolic excursion velocity; |GLS|, absolute value of global longitudinal strain; |FWS|, absolute value of free wall strain; EDA, end diastolic area; ESA, end systolic area; VC, vena contracta; HV, hepatic vein; EF, ejection fraction; EDD, end diastolic dimension; ESD, end systolic dimension; LAVI, left atrial volume index; E/e′, ratio of early diastolic mitral inflow velocity to early diastolic mitral annular tissue velocity.*

7.2 ± 4.4 months. The preoperative and postoperative echocardiographic parameters are presented in **Table 2**. In the preoperative echocardiography, 13 of 111 (11.7%) patients were graded with "massive" TR. Patients with primary outcomes had more-dilated LV chambers, lower RV FAC, |RV-GLS|, |RV-FWS|, and biventricular |GLS| than those without primary outcomes. In the postoperative echocardiography, residual TR was reported in 29 (26.1%) patients. Patients with primary outcomes had larger LA and lower RV FAC, |RV-GLS|, |RV-FWS|, |LV-GLS|, biventricular |GLS|, and LA reservoir strain than those without primary outcomes. Changes in strain parameters of the total study population are shown in **Supplementary Figure 1**.

|RV-GLS|, |RV-FWS|, and biventricular |GLS| revealed significant decreases after TV surgery.

## Predictive Value of Global Longitudinal Strain for Primary Outcomes

The ROC analysis for the predictive value of RV-, biventricular, and LV-GLS for the primary outcomes is shown in **Figure 3**. Both pre- and post- echocardiographic strain values showed that |RV-GLS| and biventricular |GLS| had significant predictive value for the primary outcomes. Among the three different GLS values, RV-GLS showed the largest area under the curve for predicting outcomes. The cut-off values of preoperative |RV-GLS| and postoperative |RV-GLS| were 17.2 and 16.3%, respectively, and the cut-off values of pre- and postoperative biventricular |GLS| were 34.0 and 36.6%, respectively. All of those values show acceptable sensitivity and specificity, as shown in **Figure 3**. Interestingly, the preoperative LV-GLS value did not predict the outcomes. Only a postoperative |LV-GLS| lower than 14.1% predicted the outcomes with high specificity.

**Figure 4** shows the Kaplan-Meier survival curves for groups divided by the cut-off values of |RV-GLS| and biventricular |GLS| in both the preoperative and postoperative studies. Regardless of the time point, biventricular mechanical dysfunction, including RV dysfunction, correlated with significant differences in the prognosis of these patients (log rank $p = 0.024$ in preoperative study, log rank $p = 0.001$ in postoperative study). Based on the cut-off values of preoperative |RV-GLS| and |LV-GLS|, we divided the study patients into 4 groups according to whether the RV and LV strain values were preserved and performed another Kaplan-Meier analysis for clinical outcomes (**Supplementary Figure 2**). In the results, patients who had reduced both RV and LV strain on preoperative echocardiography had the worst clinical outcomes ($p = 0.003$).

In the multivariate nested Cox regression models, higher EuroSCORE II was an independent predictor of the primary outcomes in every model. When preoperative |RV-GLS| and postoperative |RV-GLS| were added sequentially in model 1 and model 2, lower preoperative |RV-GLS| [hazard ratio (HR) 0.89, confidence interval (CI) 0.82–0.96, $p = 0.006$] and postoperative |RV-GLS| (HR 0.84, CI 0.78–0.91, $p < 0.001$) were significant independent predictors of the primary outcomes. In the same way, when pre- and postoperative biventricular |GLS| were added sequentially in model 3 and model 4, preoperative biventricular |GLS| was not independently related to primary outcomes (HR 0.97, CI 0.93–1.01, $p = 0.111$). However, lower postoperative biventricular |GLS| (HR 0.93, CI 0.89–0.98, $p = 0.005$) were significant independent predictors of the primary outcomes in model 4 (**Table 3**).

## Incremental Prognostic Value of Right Ventricular and Biventricular Global Longitudinal Strain

The incremental prognostic values of RV and biventricular GLS are shown in **Figure 5**. In the model that included |RV-GLS| for prognosis (**Figure 5A**), the addition of preoperative and postoperative |RV-GLS| to EuroSCORE II significantly improved the model's predictive value for the primary outcomes ($p = 0.002$, $p = 0.001$, respectively) and the preoperative |RV-GLS| had more sensitive predictive value than preoperative FAC ($p = 0.032$). In the model that included biventricular |GLS| for prognosis with EuroSCORE II (**Figure 5B**), preoperative biventricular |GLS| did

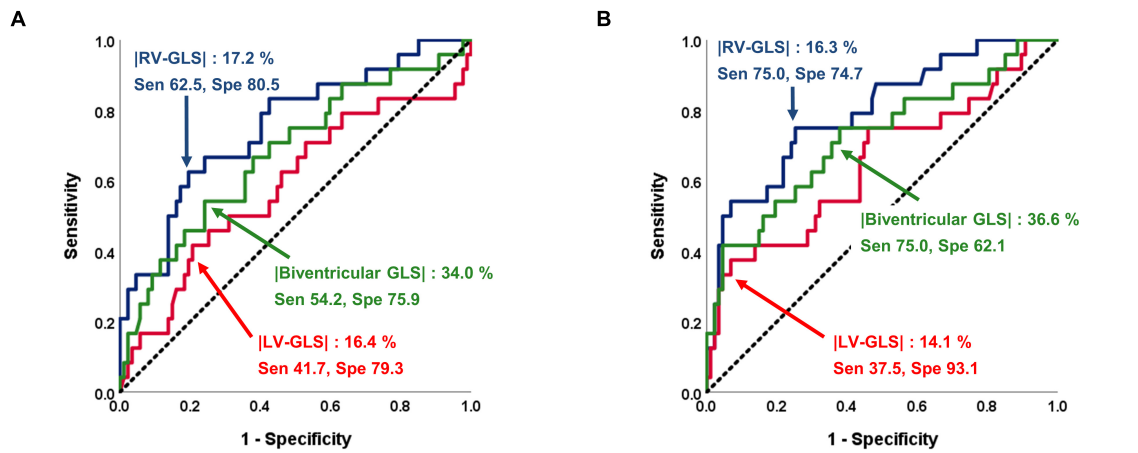


| | AUC | P value |
|---|---|---|
| \|RV-GLS\| | 0.753 | <0.001 |
| \|Biventricular GLS\| | 0.677 | 0.007 |
| \|LV-GLS\| | 0.585 | 0.241 |

| | AUC | P value |
|---|---|---|
| \|RV-GLS\| | 0.796 | <0.001 |
| \|Biventricular GLS\| | 0.722 | 0.001 |
| \|LV-GLS\| | 0.650 | 0.025 |

**FIGURE 3 |** Predictive value of |LV-GLS|, |RV-GLS|, and biventricular |GLS| for the occurrence of negative clinical outcomes. **(A)** On the pre-op echocardiogram, |RV-GLS| and biventricular |GLS| had significant predictive value for clinical outcomes. **(B)** On the post-op echocardiogram, |RV-GLS| showed better predictive value for clinical outcomes than biventricular |GLS| and |LV-GLS|. LV, left ventricle; |GLS|, absolute value of global longitudinal strain; RV, right ventricle.

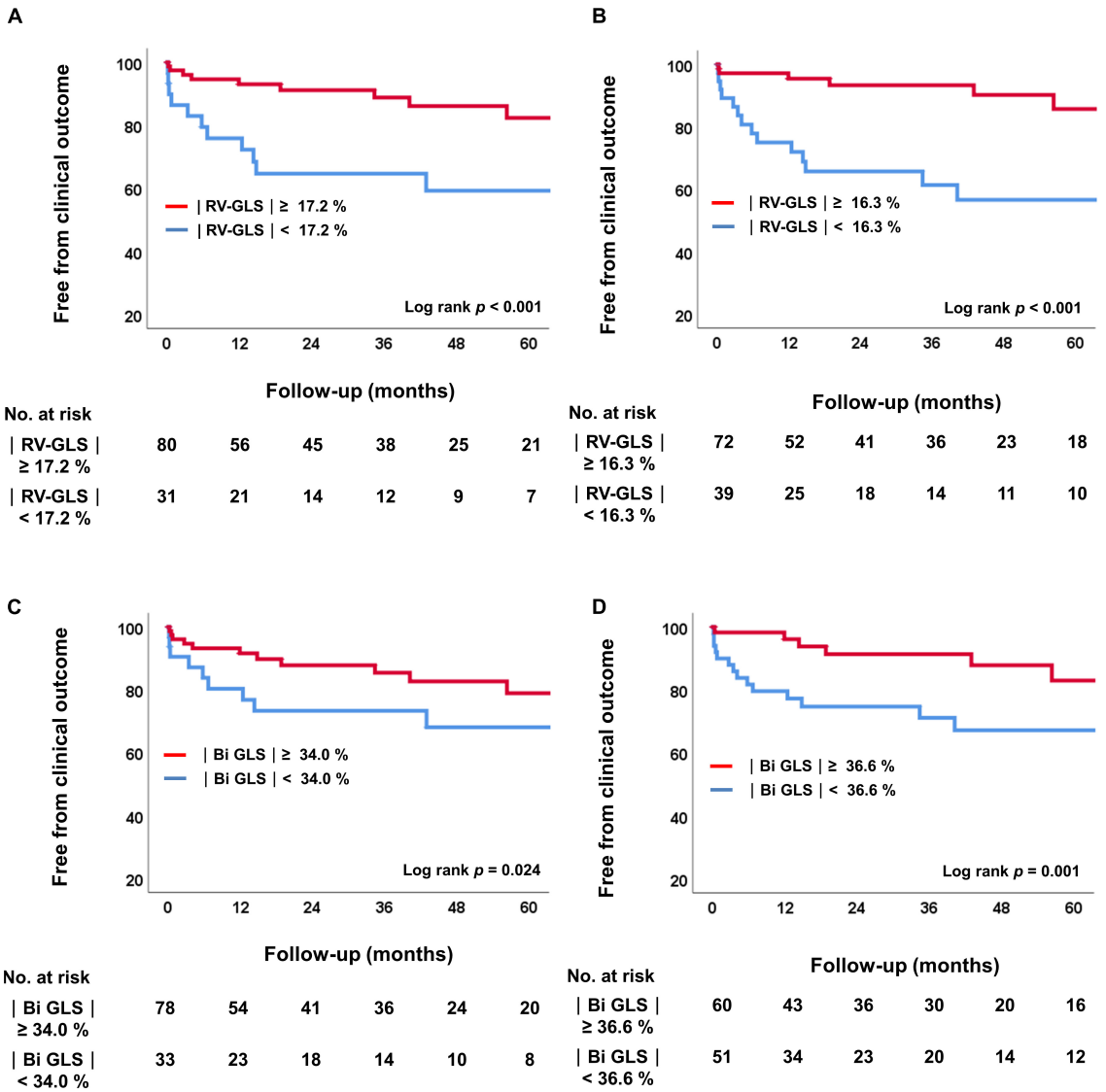


**FIGURE 4 |** Kaplan-Meier analysis of freedom from clinical outcomes. **(A)** Comparison of two groups according to the cutoff value for $|\text{RV-GLS}|_{preop}$. **(B)** Comparison of four groups according to the cutoff value for $|\text{RV-GLS}|_{postop}$. **(C)** Comparison of two groups according to the cutoff value for biventricular $|\text{GLS}|_{preop}$. **(D)** Comparison of four groups according to the cutoff value for biventricular $|\text{GLS}|_{postop}$. RV, right ventricle; |GLS|, absolute value of global longitudinal strain.

not improve the predictive value ($p = 0.981$), but postoperative biventricular |GLS| did ($p = 0.025$).

## DISCUSSION

The principal findings of this study are as follows: (1) Clinical events after isolated TV surgery are common (21.6%), including cardiovascular deaths in 4.5% of patients during a mean 3.9 years. (2) The preoperative GLS value that best predicted the outcomes after isolated TV surgery was |RV-GLS|, which predicted a poor prognosis when it was 17.2% or less. This finding suggests that |RV-GLS| has value in identifying high risk for poorer outcomes after isolated TV surgery. (3) Biventricular GLS, which comprehensively evaluated the mechanical function of both ventricles, also showed predictive value, particularly in the postoperative evaluation. Overall, our findings imply that a GLS evaluation could be used to stratify the risk of post-surgical prognosis of patients with severe isolated TR that could be masking intrinsic ventricular dysfunction.

### Right Ventricular and Left Ventricular Functional Changes in Patients With Severe Isolated Tricuspid Regurgitation

As isolated TR increases in severity, RV volume overload proceeds, and eventually chronic remodeling of the right chambers occurs. Although those phenomena cause intrinsic

**TABLE 3 |** Multivariable Cox regression models for clinical outcomes.

| | Model 1 | | | Model 2 | | |
|---|---|---|---|---|---|---|
| | **HR** | **95% CI** | ***P*-value** | **HR** | **95% CI** | ***P*-value** |
| EuroSCORE II | 1.56 | 1.30–1.88 | <0.001 | 1.59 | 1.32–1.92 | <0.001 |
| Preoperative \|RV-GLS\| | 0.89 | 0.82–0.96 | 0.003 | | | |
| Postoperative \|RV-GLS\| | | | | 0.84 | 0.78–0.91 | <0.001 |
| | **Model 3** | | | **Model 4** | | |
| | **HR** | **95% CI** | ***P*-value** | **HR** | **95% CI** | ***P*-value** |
| EuroSCORE II | 1.64 | 1.37–1.97 | <0.001 | 1.56 | 1.30–1.89 | <0.001 |
| Preoperative \|biventricular GLS\| | 0.97 | 0.93–1.01 | 0.118 | | | |
| Postoperative \|biventricular GLS\| | | | | 0.93 | 0.89–0.98 | 0.005 |

*Model 1: EuroSCORE II + Preoperative |RV-GLS|.*
*Model 2: EuroSCORE II + Postoperative |RV-GLS|.*
*Model 3: EuroSCORE II + Preoperative |biventricular GLS|.*
*Model 4: EuroSCORE II + Postoperative |biventricular GLS|.*
*RV, right ventricle; |GLS|, absolute value of global longitudinal strain.*

RV dysfunction due to stress on the RV myocardium, that RV dysfunction is often masked to some extent due to the volume overload in patients with severe TR (17). Severe isolated TR can also affect the LV chamber. RV overload and consequent RV dysfunction interfere with LV filling by RV dilation and leftward shifting of the interventricular septum by ventricular interdependence. Furthermore, that causes decreased LV distensibility and elastance (6). Therefore, severe TR is often accompanied by LV dysfunction and low stroke volume. In this physiology of underfilled LV, it has limitations on its own function of elastic coil and re-coil of LV myocardial fiber. Therefore, its function might be concealed unless the correction with TV intervention. However, after the correction of severe TR, LV filling is restored, which can unmask left-side heart problems.

With that theoretical background on the change of biventricular function in severe TR, we hypothesized in this study that GLS in both ventricles, which measures the myocardial mechanical function less volume dependently than other tests, would be important in predicting the prognoses of patients with severe isolated TR as they planned surgery. The current guideline does not provide definite timing for TV surgery because of limitations in clinical data, especially in isolated TR, which generally has indolent progression (3, 4). Although severe TR is a strong predictor of poor clinical outcomes, some outcome data from isolated TV surgery have shown poor results, with in-hospital mortality as high as 8–10% (2, 18). Those results are thought to result from the lack of understanding and standards for timing the intervention. In our study results, in-hospital mortality was reported as 2.7% and the results seemed very low. However, considering the 2 patients who dropped out from the strict study inclusion criteria, which excluded the patients who had the clinical events before the postoperative echocardiographic data after at least 1 month of TV surgery, the actual in-hospital mortality was 4.4%. In another previous study that demonstrated the prognostic value of |RV-FWS| in patients who underwent isolated TV surgery (19), the surgical mortality was reported as 5.2% and this result was comparable with our study. That was because of the similarity with the strict cohort criteria of the study, which excluded patients with significant left-sided valve disease, reduced LV systolic function, and primary pulmonary hypertension. With the development of alternative interventional treatments such as trans catheter edge-to-edge repair (20, 21), there is an increasing need to define a reference point for isolated TV surgery.

Therefore, interest in determining optimal surgery timing and analyzing prognostic factors has increased. In 2020, Dreyfus et al. identified the determinants of outcomes after isolated TV surgery in 5,661 patients from French tertiary centers (22). They reported that NYHA class III/IV, at least moderate RV dysfunction, and lower prothrombin time were independent determinants of clinical outcomes. However, they did not quantitatively assess RV function. Another previous study investigated the preoperative predictors of clinical outcomes after isolated TV surgery in 238 patients (23) and found that the TR jet area ($\geq$30 cm$^2$), RA pressure ($\geq$15 mmHg), age, and hemoglobin level were independent predictors of clinical outcomes. Although those factors were calculated by quantitative methods, they have limitations in reflecting RV function. Our study demonstrates the prognostic value of GLS measurements. RV-GLS is a better tool for assessing RV function in isolated TR than conventional echocardiography, which has limitations due to the asymmetrical RV geometry, volume dependency, and difficulty in defining the true endocardial border because of heavy trabeculation (24). In assessing LV function, LV-GLS might be more accurate and sensitive than LVEF under the condition of LV under-filling in severe TR or re-filling after TV surgery (25). There was a similar previous study that performed the analysis of LV function in a group of patients with ventricular interdependence. In the study, LV myocardial function by LV-GLS was evaluated in 54 patients with pulmonary hypertension and 54 control subject (26). The study revealed that patients with pulmonary hypertension had a reduced value of LV-GLS (−18.8 vs. −20.0%, $p = 0.005$) than matched controls, although all the groups had a normal range of LV EF. It showed that LV-GLS reflected the impaired LV

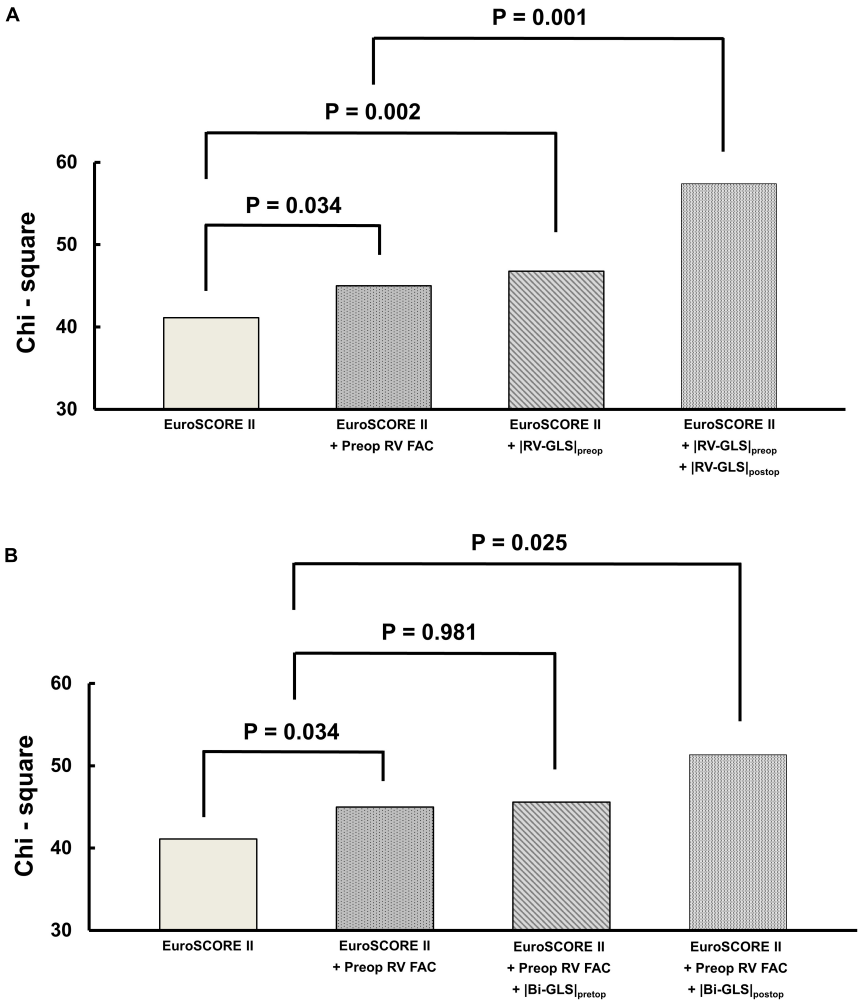


**FIGURE 5 |** Incremental prognostic value of preoperative and postoperative **(A)** |RV-GLS| and **(B)** biventricular |GLS| over EuroSCORE II. RV, right ventricle; FAC, fractional area change; |GLS|, absolute value of global longitudinal strain.

function more accurately than LV EF in patients with ventricular independence. In this study, preoperative |RV-GLS| was the strongest indicator, with a cut-off point of 17.2%, and it would be worth considering as a useful indicator in identifying the risk of post-operative outcomes after TV surgery in other population of isolated TR. On the other hand, preoperative LV-GLS did not meaningfully predict the prognosis of patients after TV surgery. Although biventricular GLS was significantly associated with clinical outcomes, we attribute that to the significance of RV-GLS.

## Biventricular Global Longitudinal Strain in Patients With Severe Isolated Tricuspid Regurgitation

Because isolated TR affects not only the RV but also the LV, integrative functional measurements of both ventricles are needed. We devised an indicator called *biventricular GLS* to comprehensively evaluate the function of both ventricles. It is a combination of RV-FWS and LV-GLS to reflect the functioning of the RV and LV together and can be used to determine the severity of isolated TR. A previous study demonstrated the prognostic value of |RV-FWS| in 115 patients who received isolated TV surgery in 2 tertiary centers between 2005 and 2019 (19). It showed that |RV-FWS| below 24% in pre-op echocardiography was associated with the primary endpoint. Our results in this study are consistent with those in indicating that RV strain is an important imaging prognosticator in patients undergoing isolated TV surgery. However, we are the first to identify the post-surgical prognostic implications of biventricular GLS in patients with severe isolated TR. There have been no other studies that comprehensively assessed the function of both ventricles by summation of GLS, but this trial is thought to provide a considerable foundation for clinical trials related to the prognostic evaluation of other clinical disease spectrums affecting the function of both ventricles and analysis of disease severity. Also, 62.6% of patients in the previous study had had previous left-side valve surgery, whereas we excluded patients who underwent previous left-side valve surgery or open

heart surgery from this study. That is, our study minimized confounding by LV mechanical dysfunction, so we provide clinically important information about the optimal timing for TR intervention and outcome prediction in operation-naïve patients with severe isolated TR. We found that biventricular |GLS| shared a predictive index with |RV-GLS|, and both metrics showed significant correlations before and after surgery. However, both before and after surgery, |RV-GLS| showed higher predictive power than biventricular |GLS|. Thus, we suggest that RV function plays a more important role than LV function in the prognosis of patients after isolated TV surgery.

### Limitations

This study has several limitations. First, this study was designed retrospectively for patients who visited regularly. Intervals of follow-up echocardiography after isolated TV surgery were not consistent in all patients. However, we tried to set the period between the surgery and follow-up echocardiography as consistently as possible to minimize the effects of those limitations. More comprehensive prospective multicenter studies of patients with isolated TR are needed. Second, the entire study cohort was relatively small ($n$ = 111) due to the incidence of isolated TV surgery. However, we selected the patients with isolated TR using strict inclusion and exclusion criteria to identify the exact effects of factors after isolated TV surgery. Third, the echocardiographic parameters of RV and LV strain might be inconsistent because the echocardiography for each patient was not performed on the same equipment. However, we used vendor-independent software to minimize the measurement errors of our expert operators. Fourth, not all the patients did not perform right heart catheterization so the hemodynamic data such as right-sided intracardiac pressures and the cardiac index of the entire study cohorts could not be assessed. Fifth, two patients who had a clinical event from the time of surgery until follow-up echocardiography were excluded and this might introduce selection bias in terms of assessing postoperative prognosis.

## CONCLUSION

In patients with severe isolated TR undergoing TV surgery, |RV-GLS| under 17.2% is closely associated with a poor prognosis, and biventricular |GLS| under 34.0%, mainly depending on the |RV-GLS|, is related to the poor prognosis. Therefore, assessing |RV-GLS| and biventricular |GLS| by speckle-tracking echocardiography could have benefits in identifying high risk of poorer outcomes after TV surgery. Further prospective multicenter studies with better adjustment are warranted to establish the risk stratification of isolated TV surgery.

## DATA AVAILABILITY STATEMENT

The original contributions presented in this study are included in the article/**Supplementary Material**, further inquiries can be directed to the corresponding author/s.

## ETHICS STATEMENT

The studies involving human participants were reviewed and approved by the Institutional Review Board of Yonsei University Health System (IRB number: 4-2021-0929). Written informed consent for participation was not required for this study in accordance with the national legislation and the institutional requirements.

## AUTHOR CONTRIBUTIONS

D-YK and CS contributed to the concept and design of this study. JS, IC, SHL, and SL contributed to acquisition, analysis, and interpretation of the data. G-RH and J-WH contributed to drafting of the manuscript and statistical analysis. D-YK, J-WH, and CS contributed to revision and finalize the manuscript. All authors contributed to the article and approved the submitted version.

## SUPPLEMENTARY MATERIAL

The Supplementary Material for this article can be found online at: https://www.frontiersin.org/articles/10.3389/fcvm.2022.908062/full#supplementary-material

## REFERENCES


1. Dietz MF, Goedemans L, Vo NM, Prihadi EA, van der Bijl P, Gersh BJ, et al. Prognostic implications of significant isolated tricuspid regurgitation in patients with atrial fibrillation without left-sided heart disease or pulmonary hypertension. *Am J Cardiol.* (2020) 135:84–90. doi: 10.1016/j.amjcard.2020.08.034
2. Zack CJ, Fender EA, Chandrashekar P, Reddy YNV, Bennett CE, Stulak JM, et al. National Trends and Outcomes in Isolated Tricuspid Valve Surgery. *J Am Coll Cardiol.* (2017) 70:2953–60. doi: 10.1016/j.jacc.2017.10.039
3. Vahanian A, Beyersdorf F, Praz F, Milojevic M, Baldus S, Bauersachs J, et al. 2021 ESC/EACTS Guidelines for the management of valvular heart disease. *Eur Heart J.* (2021) 43:561–632. doi: 10.1093/ejcts/ezac209
4. Otto CM, Nishimura RA, Bonow RO, Carabello BA, Erwin JP, Gentile F, et al. 2020 ACC/AHA Guideline for the management of patients with valvular heart disease: a report of the American college of cardiology/American heart association joint committee on clinical practice guidelines. *J Am Coll Cardiol.* (2021) 77:e25–197. doi: 10.1016/j.jacc.2020.11.018
5. Fender EA, Zack CJ, Nishimura RA. Isolated tricuspid regurgitation: outcomes and therapeutic interventions. *Heart.* (2018) 104:798–806. doi: 10.1136/heartjnl-2017-311586
6. Haddad F, Doyle R, Murphy DJ, Hunt SA. Right ventricular function in cardiovascular disease, part II: pathophysiology, clinical importance, and management of right ventricular failure. *Circulation.* (2008) 117:1717–31. doi: 10.1161/CIRCULATIONAHA.107.653584
7. Hahn RT, Thomas JD, Khalique OK, Cavalcante JL, Praz F, Zoghbi WA. Imaging Assessment of Tricuspid Regurgitation Severity. *JACC Cardiovasc Imaging.* (2019) 12:469–90. doi: 10.1016/j.jcmg.2018.07.033
8. Kim D, Shim CY, Cho YJ, Park S, Lee CJ, Park JH, et al. Continuous positive airway pressure therapy restores cardiac mechanical function in patients with severe obstructive sleep apnea: a randomized, sham-controlled study. *J Am Soc Echocardiogr.* (2019) 32:826–35. doi: 10.1016/j.echo.2019.03.020

9. Meris A, Faletra F, Conca C, Klersy C, Regoli F, Klimusina J, et al. Timing and magnitude of regional right ventricular function: a speckle tracking-derived strain study of normal subjects and patients with right ventricular dysfunction. *J Am Soc Echocardiogr.* (2010) 23:823–31. doi: 10.1016/j.echo.2010.05.009
10. Kalam K, Otahal P, Marwick TH. Prognostic implications of global LV dysfunction: a systematic review and meta-analysis of global longitudinal strain and ejection fraction. *Heart.* (2014) 100:1673–80. doi: 10.1136/heartjnl-2014-305538
11. Teske AJ, De Boeck BWL, Olimulder M, Prakken NH, Doevendans PAF, Cramer MJ. Echocardiographic assessment of regional right ventricular function: a head-to-head comparison between 2-dimensional and tissue doppler-derived strain analysis. *J Am Soc Echocardiogr.* (2008) 21:275–83. doi: 10.1016/j.echo.2007.08.027
12. Lang RM, Badano LP, Mor-Avi V, Afilalo J, Armstrong A, Ernande L, et al. Recommendations for cardiac chamber quantification by echocardiography in adults: an update from the American society of echocardiography and the European association of cardiovascular imaging. *Eur Heart J Cardiovasc Imaging.* (2015) 16:233–71. doi: 10.1093/ehjci/jev014
13. Hahn RT, Zamorano JL. The need for a new tricuspid regurgitation grading scheme. *Eur Heart J Cardiovasc Imaging.* (2017) 18:1342–3. doi: 10.1093/ehjci/jex139
14. Voigt JU, Pedrizzetti G, Lysyansky P, Marwick TH, Houle H, Baumann R, et al. Definitions for a common standard for 2D speckle tracking echocardiography: consensus document of the EACVI/ASE/Industry Task Force to standardize deformation imaging. *Eur Heart J Cardiovasc Imaging.* (2015) 16:1–11. doi: 10.1093/ehjci/jeu184
15. Negishi K, Negishi T, Kurosawa K, Hristova K, Popescu BA, Vinereanu D, et al. Practical guidance in echocardiographic assessment of global longitudinal strain. *JACC Cardiovasc Imaging.* (2015) 8:489–92. doi: 10.1016/j.jcmg.2014.06.013
16. Badano LP, Kolias TJ, Muraru D, Abraham TP, Aurigemma G, Edvardsen T, et al. Standardization of left atrial, right ventricular, and right atrial deformation imaging using two-dimensional speckle tracking echocardiography: a consensus document of the EACVI/ASE/Industry Task Force to standardize deformation imaging. *Eur Heart J Cardiovasc Imaging.* (2018) 19:591–600. doi: 10.1093/ehjci/jey042
17. Ancona F, Melillo F, Calvo F, Attalla El Halabieh N, Stella S, Capogrosso C, et al. Right ventricular systolic function in severe tricuspid regurgitation: prognostic relevance of longitudinal strain. *Eur Heart J Cardiovasc Imaging.* (2021) 22:868–75. doi: 10.1093/ehjci/jeab030
18. Alqahtani F, Berzingi CO, Aljohani S, Hijazi M, Al-Hallak A, Alkhouli M. Contemporary trends in the use and outcomes of surgical treatment of tricuspid regurgitation. *J Am Heart Assoc.* (2017) 6:e007597. doi: 10.1161/JAHA.117.007597
19. Kim M, Lee HJ, Park JB, Kim J, Lee SP, Kim YJ, et al. Preoperative right ventricular free-wall longitudinal strain as a prognosticator in isolated surgery for severe functional tricuspid regurgitation. *J Am Heart Assoc.* (2021) 10:e019856.
20. Lurz P, Kresoja KP. Tricuspid valve therapies: closing the gap. *JACC Cardiovasc Interv.* (2021) 14:1241–2. doi: 10.1016/j.jcin.2021.04.008
21. Lurz P, Stephan von Bardeleben R, Weber M, Sitges M, Sorajja P, Hausleiter J, et al. Transcatheter Edge-to-Edge Repair for Treatment of Tricuspid Regurgitation. *J Am Coll Cardiol.* (2021) 77:229–39. doi: 10.1016/j.jacc.2020.11.038
22. Dreyfus J, Flagiello M, Bazire B, Eggenspieler F, Viau F, Riant E, et al. Isolated tricuspid valve surgery: impact of aetiology and clinical presentation on outcomes. *Eur Heart J.* (2020) 41:4304–17.
23. Park SJ, Oh JK, Kim SO, Lee SA, Kim HJ, Lee S, et al. Determinants of clinical outcomes of surgery for isolated severe tricuspid regurgitation. *Heart.* (2021) 107:403–10. doi: 10.1136/heartjnl-2020-317715
24. Haddad F, Hunt SA, Rosenthal DN, Murphy DJ. Right ventricular function in cardiovascular disease, part I: anatomy, physiology, aging, and functional assessment of the right ventricle. *Circulation.* (2008) 117:1436–48. doi: 10.1161/CIRCULATIONAHA.107.653576
25. Kovács A, Oláh A, Lux Á, Mátyás C, Németh BT, Kellermayer D, et al. Strain and strain rate by speckle-tracking echocardiography correlate with pressure-volume loop-derived contractility indices in a rat model of athlete's heart. *Am J Physiol Heart Circ Physiol.* (2015) 308:743–8. doi: 10.1152/ajpheart.00828.2014
26. Burkett DA, Slorach C, Patel SS, Redington AN, Ivy DD, Mertens L, et al. Left ventricular myocardial function in children with pulmonary hypertension: relation to right ventricular performance and hemodynamics. *Circ Cardiovasc Imaging.* (2015) 8:e003260. doi: 10.1161/CIRCIMAGING.115.003260


**Conflict of Interest:** The authors declare that the research was conducted in the absence of any commercial or financial relationships that could be construed as a potential conflict of interest.

frontiers | Frontiers in Cardiovascular Medicine

TYPE Original Research
PUBLISHED 31 August 2022
DOI 10.3389/fcvm.2022.847568



OPEN ACCESS

EDITED BY
Ronak Rajani,
Guy's and St Thomas' NHS Foundation Trust, United Kingdom

REVIEWED BY
Tanja Katharina Rudolph,
Heart and Diabetes Center North Rhine-Westphalia, Germany
Guillem Muntané Carol,
Laval University, Canada
Martin Andreas,
Medical University of Vienna, Austria

*CORRESPONDENCE
Verena Veulemans
verenaveulemans@web.de

†These authors have contributed equally to this work

SPECIALTY SECTION
This article was submitted to Heart Valve Disease, a section of the journal Frontiers in Cardiovascular Medicine

RECEIVED 02 January 2022
ACCEPTED 15 August 2022
PUBLISHED 31 August 2022

CITATION
Maier O, Piayda K, Binnebößel S, Berisha N, Afzal S, Polzin A, Klein K, Westenfeld R, Horn P, Jung C, Kelm M, Veulemans V and Zeus T (2022) Real-world experience with the cusp-overlap deployment technique in transcatheter aortic valve replacement: A propensity-matched analysis.
*Front. Cardiovasc. Med.* 9:847568.
doi: 10.3389/fcvm.2022.847568



# Real-world experience with the cusp-overlap deployment technique in transcatheter aortic valve replacement: A propensity-matched analysis

Oliver Maier[1], Kerstin Piayda[2], Stephan Binnebößel[1], Nora Berisha[1], Shazia Afzal[1], Amin Polzin[1], Kathrin Klein[1], Ralf Westenfeld[1], Patrick Horn[1], Christian Jung[1], Malte Kelm[1,3], Verena Veulemans[1*†] and Tobias Zeus[1†]

[1]Department of Cardiology, Pulmonology and Vascular Medicine, Medical Faculty, Heinrich Heine University, Düsseldorf, Germany, [2]CardioVascular Center (CVC) Frankfurt, Frankfurt, Germany, [3]Cardiovascular Research Institute Düsseldorf (CARID), Medical Faculty, Heinrich Heine University, Düsseldorf, Germany

**Background:** The implantation depth (ID) is a critical condition for optimal hemodynamic and clinical outcomes in transcatheter aortic valve replacement (TAVR). The recently recommended cusp-overlap technique (COT) offers optimized fluoroscopic projections facilitating a precise ID. This single-center observational study aimed to investigate short-term clinical performance, safety, and efficacy outcomes in patients undergoing TAVR with self-expandable prostheses and application of COT in a real-world setting.

**Materials and methods:** From September 2020 to April 2021, a total of 170 patients underwent TAVR with self-expandable devices and the application of COT, while 589 patients were treated from January 2016 to August 2020 with a conventional three-cusp coplanar view approach. The final ID and 30-day outcomes were compared after 1:1 propensity score matching, resulting in 150 patients in both cohorts.

**Results:** The mean ID was significantly reduced in the COT cohort (−4.2 ± 2.7 vs. −4.9 ± 2.3 mm; $p$ = 0.007) with an improvement of ID symmetry of less than 2 mm difference below the annular plane (47.3 vs. 57.3%; $p$ = 0.083). The rate of new permanent pacemaker implantation (PPI) following TAVR was effectively reduced (8.0 vs. 16.8%; $p$ = 0.028). While the fluoroscopy time decreased (18.4 ± 7.6 vs. 19.8 ± 7.6 min; $p$ = 0.023), the dose area product increased in the COT group (4951 ± 3662 vs. 3875 ± 2775 Gy × cm$^2$; $p$ = 0.005). Patients implanted with COT had a shorter length of in-hospital stay (8.4 ± 4.0 vs. 10.3 ± 6.7 days; $p$ = 0.007).

**Conclusion:** Transcatheter aortic valve replacement using the cusp-overlap deployment technique is associated with an optimized implantation depth, leading to fewer permanent conduction disturbances. However, our in-depth analysis showed for the first time an increase of radiation dose due to extreme angulations of the gantry to obtain the cusp-overlap view.

KEYWORDS

aortic stenosis, TAVR, implantation depth, cusp-overlap, permanent pacemaker

# Introduction

Transcatheter aortic valve replacement (TAVR) is a fast-growing section in interventional cardiology. In the last decade, TAVR has become a safe and effective alternative to surgical valve replacement (SAVR) to treat symptomatic severe aortic valve stenosis across all surgical risk categories (1–3). Optimized implantation depth (ID) of transcatheter heart valves (THV) is an essential condition for valuable hemodynamic and clinical outcomes. Implantation located too high toward the aorta can result in complicated coronary reaccess, paravalvular leakage, or even valve embolization. In contrast, deep implantation in the left ventricular outflow tract (LVOT) is associated with aortic regurgitation and increased risk of conduction disturbances leading to higher rates of permanent pacemaker implantation (PPI). Despite advanced development of THV design, pre-procedural planning, and progressive implanters' experience, current PPI rates following TAVR–especially with self-expandable valves–have remained high (4, 5).

In 2020, the manufacturer of the self-expandable THV CoreValve Evolut (Medtronic Inc., Minneapolis, MN, United States) introduced new best practice recommendations for valve deployment, including the cusp-overlap technique (COT). This is a series of procedural steps designed to provide optimized angiographic projections for TAVR with self-expandable devices (6). Application of COT during valve deployment has been shown to result in a reduced risk of interaction with the conduction system below the annular plane and significantly lower PPI rates (7–9). However, there is not sufficient evidence showing correlations to the achievement of an optimized ID as well as potential pitfalls of a more complex implantation process regarding prosthesis repositioning, radiation dose or amount of contrast medium used.

Abbreviations: BEV, balloon-expandable valve; COT, cusp-overlap technique; DLZ, device landing zone; ID, implantation depth; LCC, left coronary cusp; MSCT, multislice computed tomography; NCC, non-coronary cusp; PPI, permanent pacemaker implantation; RCC, right coronary cusp; SAVR, surgical aortic valve replacement; SEV, self-expandable valve; TAVR, transcatheter aortic valve replacement; THV, transcatheter heart valve.

Therefore, this single-center observational study aimed to investigate short-term clinical performance, safety, and efficacy outcomes in patients undergoing transfemoral, self-expandable TAVR with newer-generation CoreValve Evolut THV regarding COT during valve deployment in a real-world setting.

# Materials and methods

## Study population

From 1530 consecutive patients who underwent transfemoral TAVR with newer-generation self-expandable CoreValve Evolut system (Medtronic Inc., Minneapolis, MN, United States) from January 2016 to April 2021 at the Heart Center Düsseldorf, 759 patients with completed datasets were included in the analysis (**Figure 1**). Most of the patients excluded from the final analysis due to missing data have lack of documentation in procedural characteristics (pre- and post-dilatation, resheathing, valve dislocation) or post-procedural evaluation of valve function by missing documentation of echocardiography.

The study cohort was further separated into two groups. Patients undergoing TAVR according to Medtronic's new best practice recommendations of 2020 regarding COT for prosthesis deployment and a target ID of 3 mm were analyzed prospectively from September 2020 to April 2021 ($n$ = 170; 22.4%). The control group (Non-COT) treated with former manufacturer's recommendations without COT but with a conventional three-cusp coplanar view and a target ID of 3–5 mm from January 2016 to August 2020 ($n$ = 589; 77.6%) was analyzed retrospectively. To erase potential confounders of the treatment outcome relationship, we performed a 1:1 propensity-score matched analysis resulting in a final study cohort of 150 COT and 150 Non-COT patients (**Figure 2**). All included patients completed a 30-day follow-up examination to evaluate clinical outcome after TAVR based on Valve Academic Research Consortium-2 (VARC-2) definition (10).

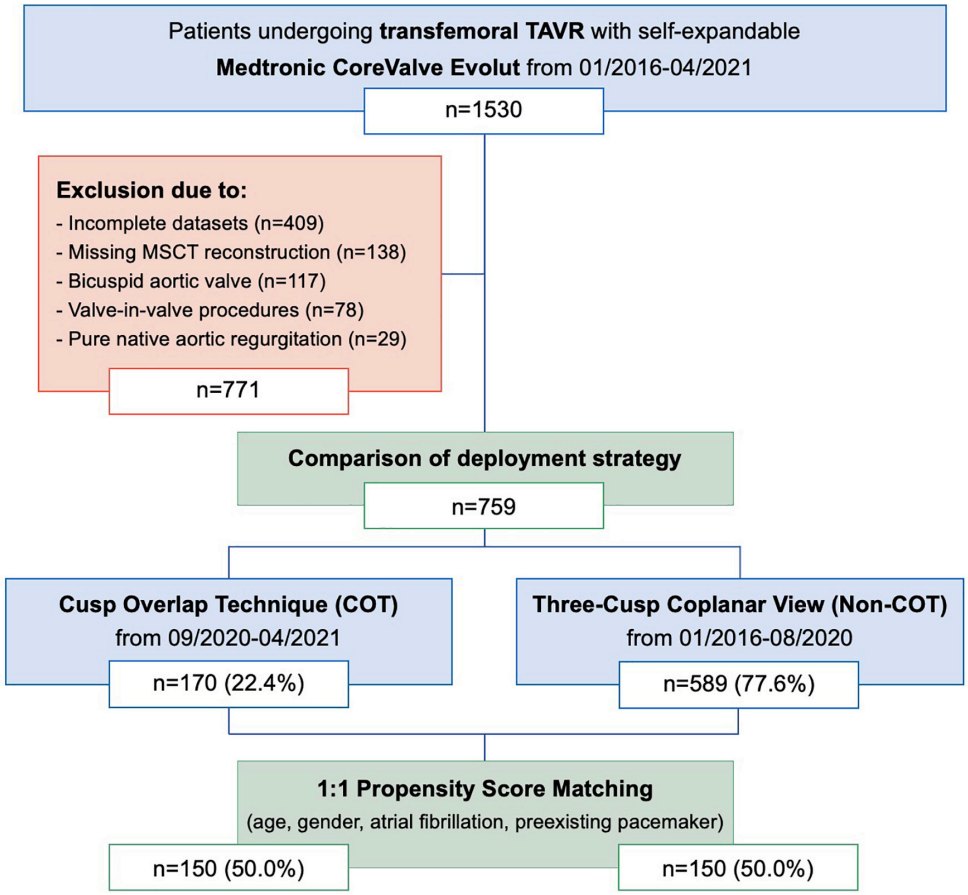


FIGURE 1
Modified CONSORT Diagram. From January 2016 to April 2021, a total of 1,530 patients underwent TAVR with the Medtronic CoreValve Evolut at the Heart Center Düsseldorf. A total of 759 patients were included in the comparison of the deployment strategy. A total of 1:1 propensity score matches analysis resulted in the final study cohort of 150 COT patients and 150 Non-COT patients. COT, cusp-overlap technique; MSCT, multislice computed tomography; TAVR, transcatheter aortic valve replacement.

The primary study endpoint was defined as the measurement of ID comparing valve deployment with and without COT during TAVR with self-expandable devices. Target ID is aspired to 3 mm for COT group, compared to target ID of 3–5 mm for Non-COT group, taking into account a measurement uncertainty of 1 mm each.

All participants in this study provided written informed consent. This study was approved by the institutional ethics committee of the Heinrich-Heine University of Düsseldorf (4080) and conducted in concordance with the Declaration of Helsinki. The study is registered at clinical trials (NCT01805739).

## 3D image analysis of multislice computed tomography

Multislice computed tomography was routinely performed as native and contrast-enhanced, electrocardiogram gated images. Pre-procedural MSCT data were transferred to a dedicated workstation for 3-dimensional volume-rendered reconstruction (3mensio Structural Heart; Pie Medical Imaging BV, Maastricht, Netherlands). Annular plane projection in the three-cusp view was routinely predicted from MSCT reconstruction and optimal angulation of the cusp-overlap view was generated by overlapping the right coronary cusp (RCC) and the left coronary cusp (LCC) on the MSCT annular plane toward right anterior oblique (RAO) and caudal angulation (6, 11).

## Procedural details

Transcatheter aortic valve replacement procedures were conducted according to current guidelines and under local anesthesia. A total of four experienced operators were involved in this trial. In 2020, Medtronic issued new best practice advice for the CoreValve Evolut system, including cusp-overlap view

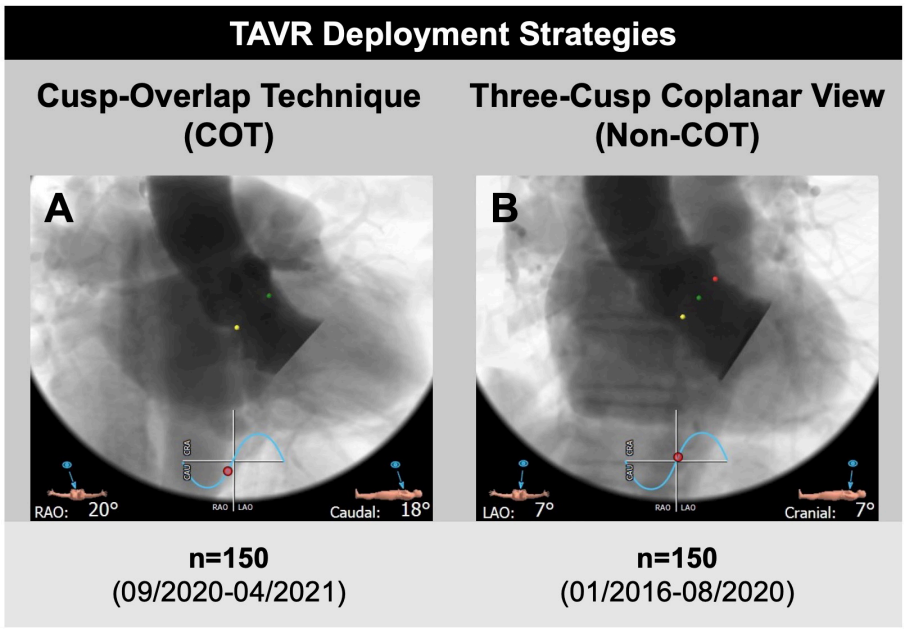


FIGURE 2
Transcatheter aortic valve replacement (TAVR) deployment strategies. **(A)** A total of 150 patients undergoing transfemoral TAVR with self-expandable Medtronic CoreValve Evolut prostheses and cusp-overlap deployment technique (COT) were compared to **(B)** 150 propensity-matched patients with application of a conventional three-cusp coplanar view only (Non-COT). The cusp-overlap view was generated by overlapping the right coronary cusp (RCC, green dot) and left coronary cusp (LCC, red dot) with isolation of non-coronary cusp (NCC, yellow dot), leading to reduction of parallax in the device and elongation of the left ventricular outflow tract.

with isolation of NCC for optimization of the ID during valve deployment. If extreme angulations of more than 30° RAO and/or 30°caudal were suggested for cusp-overlap view, a "near" cusp-overlap view with less extreme angulation was performed. Before final release, a three-cusp view was established to check for complete valve expansion and implantation depth in relation to the left coronary cusp.

The final ID of device implantation was determined angiographically in the three-cusp view after complete clearing of parallax in both COT and Non-COT groups for better visual differentiation of ID below NCC and LCC compared to the cusp overlap view (12). Distance measurements from the interventricular end of the prosthesis to the annular plane were performed afterward using the PACS system workstation (SECTRA IDS7, Linköping, Sweden). As described previously, the arithmetic means of the measured distances from the distal end of the prosthesis to the NCC and the LCC were assessed for final ID (13). Asymmetric valve deployment was defined as a more than 2 mm difference between the NCC and LCC distances. Two independent operators have performed ID measurement. The Pearson correlation coefficient was reported to assess intra- and interobserver reliability for the mean implantation depth measurements from the LCC and the NCC to the prosthesis in 50 randomly chosen cases. Results were interpreted as follows: >0.8, excellent agreement; 0.6 to 0.8, fair to good agreement; 0.4 to 0.6, moderate agreement; and <0.4, no agreement.

## Statistical analysis

Continuous data are described as mean + standard deviation (SD) for normal distribution and comparisons were performed using unpaired Student's *t*-test or Mann–Whitney *U*-test depending on the variable distribution. Categorical variables are presented as frequencies and percentages and comparisons were made using chi-square or Fisher exact test. All statistical tests were 2-tailed, and a value of $p < 0.05$ was considered statistically significant. To account for the differences in baseline characteristics of COT and Non-COT group, we performed 1:1 propensity score matched analysis using logistic regression and the nearest neighbor method with a caliper of 0.1 because of the observational nature of this study and the comparison of two non-contemporary cohorts with different group sizes. Covariates were chosen according to baseline differences between both cohorts listed in Table 1 (age, gender) as well as previous rhythm and conduction disturbances that could have a disturbing influence on the final analysis regarding new pacemaker dependency following TAVR (atrial fibrillation, preexisting pacemaker). Matching analysis resulted in a final 1:1 matched study cohort of 150 patients in both groups.

All statistical analyses were conducted using SPSS version 23.0 (IBM SPSS Inc., Chicago, IL, United States) and figures created with GraphPad Prism version 8.4 (GraphPad Software, San Diego, CA, United States).

# Results

## Baseline patient characteristics

In the unmatched cohorts ($n$ = 759), patients undergoing TAVR with COT were younger (COT 80.7 ± 6.4 years vs. Non-COT 81.9 ± 5.4 years; $p$ = 0.018), predominantly male (COT 57.1% vs. Non-COT 48.9%; $p$ = 0.061) and had a lower incidence of coronary artery disease (COT 66.5% vs. Non-COT 75.4%; $p$ = 0.021) as well as lower surgical risk (STS Score: COT 4.3 ± 3.3% vs. Non-COT 5.1 ± 4.1%; $p$ = 0.008) (Table 1). COT patients showed less frequently atrial fibrillation (AF) (COT 29.4% vs. Non-COT 41.3%; $p$ = 0.005). A total of 1:1 propensity score matching successfully eliminated any major differences between the two cohorts (Table 2).

## Procedural characteristics

After pre-procedural MSCT planning to determine the optimal cusp-overlap projection angle, we achieved a projected cusp-overlap gantry view on CT reconstruction in 121 patients (80.7%) of patients and a near cusp-overlap projection in the remaining 29 cases (19.3%).

Valve size was equally distributed with most of the procedures performed with a 29-mm CoreValve Evolut prosthesis (45.7%). COT patients had less need of contrast agent volume (COT 82.8 ± 33.4 ml vs. Non-COT 96.9 ± 33.6 ml; $p$ < 0.001) (Figure 3A) with a reduction in fluoroscopy time

TABLE 1 Patient clinical and functional characteristics in unmatched cohorts.

| | Total ($n$ = 759) | COT ($n$ = 170) | Non-COT ($n$ = 589) | $P$-value |
|---|---|---|---|---|
| Age, years | 81.6 ± 5.6 | 80.7 ± 6.4 | 81.9 ± 5.4 | *0.018* |
| Gender, male | 385 (50.7) | 97 (57.1) | 288 (48.9) | *0.061* |
| BMI, kg/m$^2$ | 26.6 ± 4.7 | 26.9 ± 5.0 | 26.6 ± 4.6 | 0.377 |
| NYHA class III/IV | 571 (75.2) | 122 (71.8) | 449 (76.2) | 0.235 |
| CAD | 557 (73.4) | 113 (66.5) | 444 (75.4) | *0.021* |
| Previous CABG | 62 (8.2) | 13 (7.7) | 49 (8.3) | 0.778 |
| Previous valve surgery | 5 (0.7) | 1 (0.6) | 4 (0.7) | 0.897 |
| Previous PPI | 102 (13.4) | 22 (12.9) | 80 (13.6) | 0.829 |
| Previous LBBB | 60 (7.9) | 11 (6.5) | 49 (8.3) | 0.787 |
| Previous RBBB | 44 (5.8) | 9 (5.3) | 35 (5.9) | 0.750 |
| Atrial fibrillation | 293 (38.6) | 50 (29.4) | 243 (41.3) | *0.005* |
| Arterial hypertension | 681 (89.7) | 147 (86.5) | 534 (90.7) | 0.113 |
| Diabetes mellitus | 176 (23.2) | 38 (22.4) | 138 (23.4) | 0.770 |
| PAD | 156 (20.6) | 35 (20.6) | 121 (20.5) | 0.990 |
| Log ES_I, % | 22.8 ± 13.7 | 20.8 ± 12.4 | 23.4 ± 14.0 | *0.020* |
| STS Score, % | 4.9 ± 3.9 | 4.3 ± 3.3 | 5.1 ± 4.1 | *0.008* |
| LVEF, % | 55.9 ± 12.1 | 54.9 ± 13.8 | 56.3 ± 11.6 | 0.290 |
| CI | 2.3 ± 0.5 | 2.3 ± 0.5 | 2.2 ± 0.5 | 0.339 |
| AVA, cm$^2$ | 0.74 ± 0.2 | 0.75 ± 0.2 | 0.74 ± 0.2 | 0.862 |
| dPmean, mmHg | 39.0 ± 16.0 | 41.2 ± 14.4 | 38.4 ± 16.3 | *0.038* |
| dPmax, mmHg | 63.5 ± 23.9 | 67.0 ± 21.9 | 62.5 ± 24.4 | 0.108 |
| Annulus perimeter, mm | 76.6 ± 7.3 | 77.6 ± 7.0 | 76.4 ± 7.3 | *0.051* |
| Annulus mean diameter, mm | 24.3 ± 2.3 | 24.6 ± 2.2 | 24.2 ± 2.3 | 0.100 |
| AVC grading mild | 222 (29.3) | 45 (26.5) | 177 (30.1) | 0.366 |
| AVC grading moderate | 170 (22.4) | 35 (20.6) | 135 (22.9) | 0.521 |
| AVC grading severe | 360 (47.4) | 89 (52.4) | 271 (46.0) | 0.145 |
| LVOT-Calcification | 384 (50.6) | 94 (55.3) | 290 (49.2) | 0.164 |

Values are mean ± SD or $n$ (%).

AVA, aortic valve area; AVC, aortic valve calcification; BMI, body mass index; CABG, coronary artery bypass graft; CAD, coronary artery disease; CCS, Canadian cardiovascular society; CI, cardiac index; COPD, chronic obstructive pulmonary disease; CVD, cerebrovascular disease; dPmean/max, mean/maximal transvalvular gradient; LBBB, left bundle branch block; Log ES_I, logistic EuroSCORE I; LVEF, left ventricular ejection fraction; LVOT, left ventricular outflow tract; MSCT, multislice computed tomography; NYHA, New York heart association; PAD, peripheral artery disease; PCI, percutaneous coronary intervention; PPI, permanent pacemaker implantation; RBBB, right bundle branch block; RRT, renal replacement therapy.

TABLE 2 Patient clinical and functional characteristics in matched cohorts.

| | Total ($n$ = 300) | COT ($n$ = 150) | Non-COT ($n$ = 150) | $P$-value |
|---|---|---|---|---|
| Age, years | 81.3 ± 4.7 | 81.3 ± 4.7 | 81.3 ± 4.7 | 0.999 |
| Gender, male | 174 (58.0) | 87 (58.0) | 87 (58.0) | 0.999 |
| BMI, kg/m$^2$ | 26.7 ± 4.7 | 26.8 ± 5.0 | 26.5 ± 4.3 | 0.826 |
| NYHA class III/IV | 214 (71.3) | 108 (72.0) | 106 (70.7) | 0.799 |
| CAD | 212 (70.7) | 104 (69.3) | 108 (72.0) | 0.612 |
| Previous CABG | 30 (10.0) | 12 (8.0) | 18 (12.0) | 0.248 |
| Previous valve surgery | 2 (0.7) | 1 (0.7) | 1 (0.7) | 0.999 |
| Previous PPI | 24 (8.0) | 12 (8.0) | 12 (8.0) | 0.999 |
| Previous LBBB | 19 (6.3) | 9 (6.0) | 10 (6.7) | 0.813 |
| Previous RBBB | 15 (5.0) | 8 (5.3) | 7 (4.7) | 0.791 |
| Atrial fibrillation | 90 (30.0) | 45 (30.0) | 45 (30.0) | 0.999 |
| Arterial hypertension | 267 (89.0) | 129 (86.0) | 138 (92.0) | 0.097 |
| Diabetes mellitus | 68 (22.7) | 32 (21.3) | 36 (24.0) | 0.581 |
| PAD | 65 (21.7) | 31 (20.7) | 34 (22.7) | 0.674 |
| Log ES_I, % | 21.8 ± 11.8 | 20.9 ± 12.3 | 22.8 ± 11.4 | 0.061 |
| STS Score, % | 4.5 ± 3.2 | 4.3 ± 3.4 | 4.8 ± 3.1 | 0.062 |
| LVEF, % | 55.3 ± 13.1 | 55.3 ± 13.4 | 54.7 ± 13.4 | 0.793 |
| CI | 2.3 ± 0.4 | 2.3 ± 0.5 | 2.2 ± 0.5 | 0.643 |
| AVA, cm$^2$ | 0.76 ± 0.2 | 0.75 ± 0.2 | 0.77 ± 0.2 | 0.527 |
| dPmean, mmHg | 39.7 ± 14.5 | 40.9 ± 14.2 | 38.6 ± 14.7 | 0.119 |
| dPmax, mmHg | 63.5 ± 21.4 | 65.4 ± 20.0 | 61.6 ± 22.0 | 0.087 |
| Annulus perimeter, mm | 77.6 ± 7.6 | 77.5 ± 6.9 | 77.4 ± 9.2 | 0.759 |
| Annulus mean diameter, mm | 24.6 ± 2.3 | 24.5 ± 2.2 | 24.7 ± 2.5 | 0.524 |
| AVC grading mild | 99 (33.0) | 47 (31.3) | 54 (36.0) | 0.392 |
| AVC grading moderate | 53 (17.7) | 28 (18.7) | 30 (20.0) | 0.770 |
| AVC grading severe | 146 (48.7) | 75 (50.0) | 66 (44.0) | 0.298 |
| LVOT-Calcification | 160 (53.3) | 80 (53.3) | 80 (53.3) | 0.999 |

Values are mean ± SD or $n$ (%).
AVA, aortic valve area; AVC, aortic valve calcification; BMI, body mass index; CABG, coronary artery bypass graft; CAD, coronary artery disease; CCS, Canadian cardiovascular society; CI, cardiac index; dPmean/max, mean/maximal transvalvular gradient; LBBB, left bundle branch block; Log ES_I, logistic EuroSCORE I; LVEF, left ventricular ejection fraction; LVOT, left ventricular outflow tract; MSCT, multislice computed tomography; NYHA, New York Heart Association; PAD, peripheral artery disease; PCI, percutaneous coronary intervention; PPI, permanent pacemaker implantation; RBBB, right bundle branch block; RRT, renal replacement therapy.

(COT 18.4 ± 7.6 min vs. Non-COT 19.8 ± 7.6 ml; $p$ = 0.023) (Figure 3B). Patients undergoing TAVR with COT had a significantly higher radiation dose area product compared to the Non-COT group (COT 4951 ± 3662 Gy × cm$^2$ vs. Non-COT 3875 ± 2775 Gy × cm$^2$; $p$ = 0.005) (Figure 3C). COT resulted in notably higher rates of device resheathing compared to the Non-COT group (COT 47.3% vs. Non-COT 28.7%; $p$ < 0.001) (Figure 3D). Additional procedural data are shown in Table 3.

## Procedural and clinical outcome

The final absolute mean ID was significantly reduced in the COT cohort (COT −4.2 ± 2.7 mm vs. Non-COT −4.9 ± 2.3 mm; $p$ = 0.007) without a significant difference in the achievement of the target ID of 3 mm in the COT group and 3–5 mm in the Non-COT group (COT 47.3% vs. Non-COT 57.3%; $p$ = 0.083) (Figures 4A,B). In COT patients valve deployment was conducted more symmetrically with a difference of less than 2 mm between NCC and LCC ID (COT 61.3% vs. Non-COT 44.0%; $p$ = 0.003) (Figure 4C). Both the intra- and the interobserver reliability showed excellent agreement ($r$ > 0.8) because we used a standardized measurement technique at our heart center for the analysis of ID after TAVR. Functional improvement was observed in both groups without significant differences concerning mean pressure gradients or paravalvular leakage assessed by TTE during 30-day follow-up (Figures 5A,B).

The rate of new PPI following TAVR was markedly reduced in the COT group (COT 8.0% vs. Non-COT 16.8%; $p$ = 0.028) (Figure 5C). The most frequent indication for pacemaker was high degree atrioventricular heart block by far (81 of 90 patients (90%) in the unmatched Non-COT group of 589 patients and 12 of 13 patients (92.3%) in the unmatched COT group of 170 patients). Other indications have been symptomatic bradycardia due to sick sinus syndrome or slowly conducted atrial fibrillation

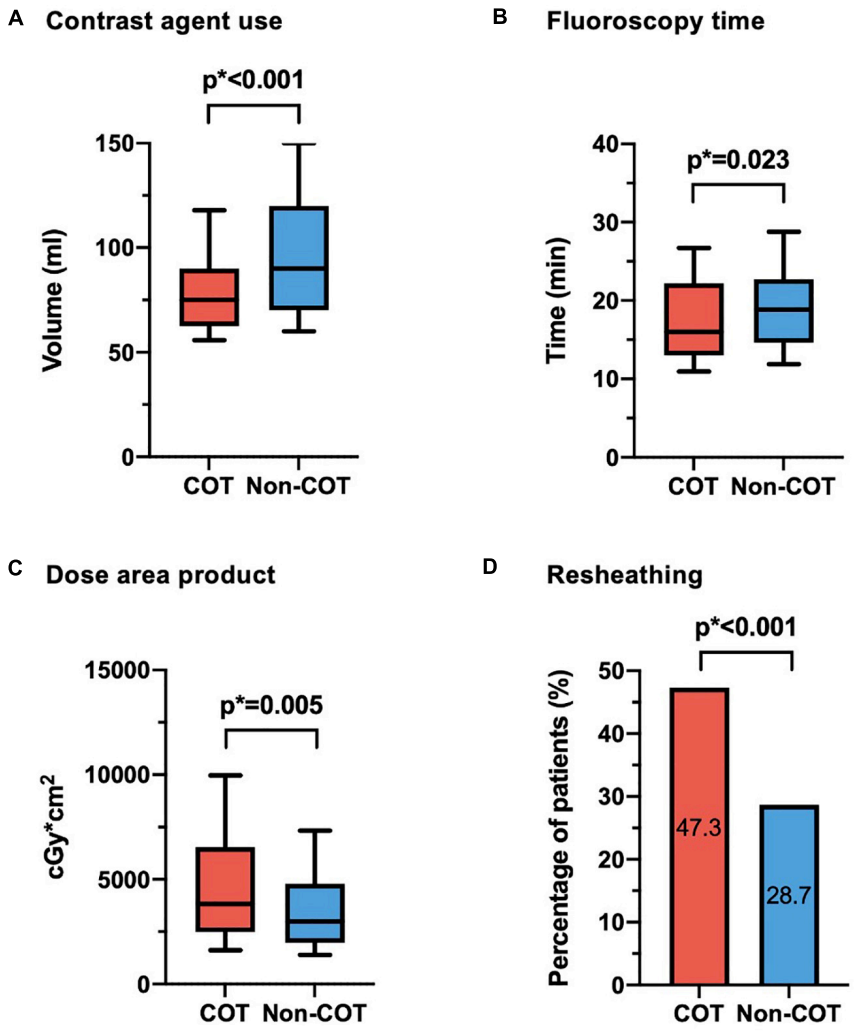


FIGURE 3
Procedural data. **(A)** Reduction of contrast agent use could be achieved in COT patients (COT 82.8 ± 33.4 ml vs. Non-COT 96.9 ± 33.6 ml; $p < 0.001$). **(B)** While fluoroscopy time was shorter (COT 18.4 ± 7.6 min vs. Non-COT 19.8 ± 7.6 ml; $p = 0.023$), **(C)** radiation dose area product was enhanced in the COT group (COT 4,951 ± 3,662 Gy × $cm^2$ vs. Non-COT 3,875 ± 2,775 Gy × $cm^2$; $p = 0.005$), probably due to more extreme angulations and **(D)** notably higher rates of device resheathing maneuvers (COT 47.3% vs. Non-COT 28.7%; $p < 0.001$) compared to the Non-COT group. COT, cusp-overlap technique.

as well as bifascicular block. Therefore, indications for new pacemaker implantation after TAVR did not significantly change over time. Furthermore, the mean time from TAVR to pacemaker implantation has been 2.34 + 0.98 days in the Non-COT group and 2.12 + 0.84 days in the COT group ($p = 0.289$).

There was also an association between COT and lower incidence of new-onset left bundle branch block (LBBB) (COT 12.8% vs. Non-COT 22.9%; $p = 0.027$). Patients implanted with COT had a shorter length of ICU stay (COT 1.6 ± 1.4 days vs. Non-COT 2.3 ± 1.8 days; $p < 0.001$) and a shorter length of total in-hospital stay compared to Non-COT patients (COT 8.4 ± 4.0 vs. Non-COT 10.3 ± 6.7 days; $p = 0.007$) (Figure 5D). All procedures were performed successfully with only one case of 30-day mortality in the Non-COT group (one septic shock during in-hospital stay after TAVR). All 30-day post-procedural outcome parameters according to VARC-2 are shown in Table 4.

The outcome results between the unmatched cohorts are in large parts similar to those between the matched cohorts and do not differ in the main results, except for new left bundle branch block following TAVR. This parameter did not reach statistical significance in unmatched cohorts (COT 13.8% vs. Non-COT 16.9%; $p = 0.364$), but finally did after 1:1 propensity score matching (COT 12.8% vs. Non-COT 22.9%; $p = 0.027$). All procedural data and 30-day procedural outcome events of the unmatched study cohorts are shown in Supplementary Tables 1, 2.

TABLE 3 Procedural characteristics in matched cohorts.

| | Total ($n$ = 300) | COT ($n$ = 150) | Non-COT ($n$ = 150) | $P$-value |
|---|---|---|---|---|
| Prosthesis size 23 mm | 4 (1.3) | 2 (1.3) | 2 (1.3) | 0.999 |
| Prosthesis size 26 mm | 73 (24.3) | 36 (24.0) | 37 (24.7) | 0.893 |
| Prosthesis size 29 mm | 137 (45.7) | 73 (48.7) | 64 (42.7) | 0.297 |
| Prosthesis size 34 mm | 85 (28.3) | 38 (25.3) | 47 (31.3) | 0.249 |
| Contrast agent, ml | 89.9 ± 34.2 | 82.8 ± 33.4 | 96.9 ± 33.6 | *< 0.001* |
| Fluoroscopy time, min | 19.1 ± 7.7 | 18.4 ± 7.6 | 19.8 ± 7.6 | *0.023* |
| Dose area product, Gy × $cm^2$ | 4413 ± 3288 | 4951 ± 3662 | 3875 ± 2775 | *0.005* |
| Pre-dilatation | 136 (45.3) | 71 (47.3) | 65 (43.3) | 0.487 |
| Post-dilatation | 42 (14.0) | 23 (15.3) | 19 (12.7) | 0.506 |
| Resheathing | 114 (38.0) | 71 (47.3) | 43 (28.7) | *< 0.001* |
| Valve dislocation | 4 (0.1) | 2 (0.1) | 2 (0.1) | 0.999 |
| Mean area oversizing,% | 7.9 ± 7.4 | 7.7 ± 6.4 | 8.1 ± 8.4 | 0.643 |
| Need for a second transcatheter valve | 2 (1.3) | 2 (1.3) | 0 (0.0) | 0.156 |
| Coronary obstruction | 0 (0.0) | 0 (0.0) | 0 (0.0) | 0.999 |
| Conversion to surgery | 0 (0.0) | 0 (0.0) | 0 (0.0) | 0.999 |

Values are mean ± SD or $n$ (%).

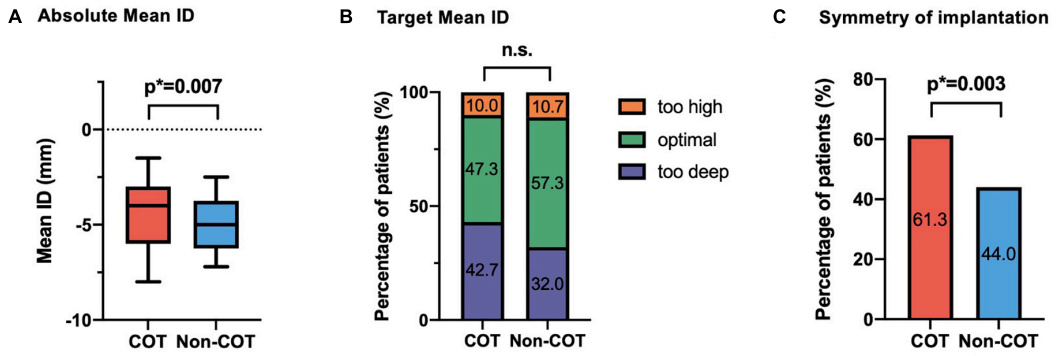


FIGURE 4
Impact of COT on implantation depth. **(A)** There was a significant reduction of final mean ID in the COT cohort (COT −4.2 ± 2.7 mm vs. Non-COT −4.9 ± 2.3 mm; $p$ = 0.007), whereas **(B)** the target ID of 3 mm in the COT group and 3–5 mm in the Non-COT group was reached similarly often. **(C)** Reduction in asymmetric valve deployment with a difference of less than 2 mm between NCC and LCC ID could be achieved more often in the COT group (COT 61.3% vs. Non-COT 44.0%; $p$ = 0.003). COT, cusp-overlap technique; ID, implantation depth.

# Discussion

Until now, the impact of the recently recommended cusp-overlap technique on the implantation depth and efficacy outcome in a real-world setting using self-expandable devices is still being evaluated with many unknowns. This study demonstrates that application of COT during transfemoral TAVR with self-expandable THV causes.

(1) Optimization of implantation depth by both reducing the mean ID and improving the symmetry of ID between NCC and LCC,

(2) Significant reduction of permanent conduction disturbances with the need for new pacemaker implantation following TAVR,

(3) Consistent quality of hemodynamic outcome regarding valve pressure gradients and paravalvular leakage, and

(4) Increase of radiation dose due to extreme angulations.

After pre-procedural MSCT planning to determine the optimal cusp-overlap projection angle, we achieved a projected cusp-overlap gantry view on CT reconstruction in 81.9% of patients and a near cusp-overlap projection in the remaining cases. Finally, no increase in adverse events during 30-day follow-up could be observed compared to TAVR procedures without the usage of COT and a three-cusp coplanar view during valve deployment instead.

## Improvement of implantation depth caused by cusp-overlap technique

To increase the accuracy of ID with Evolut CoreValve THV, we have performed COT according to the manufacturer's recommendations since September 2020. In the three-cusp coplanar view, the device is often poorly aligned and there is

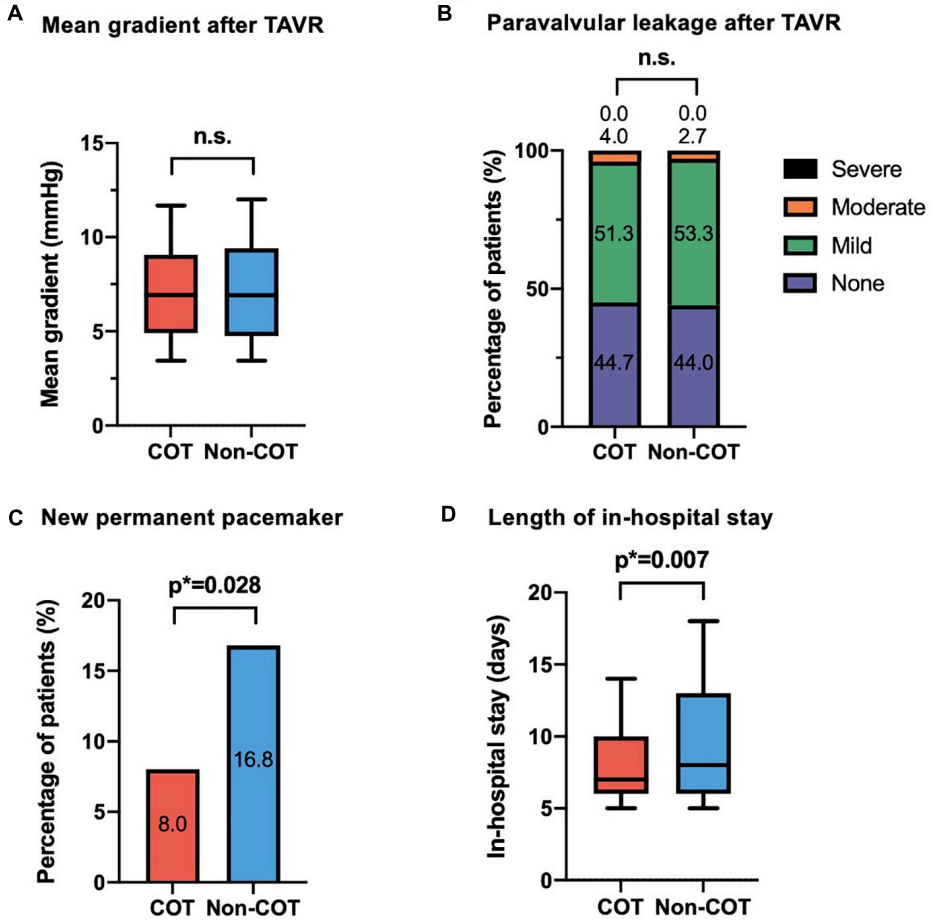


FIGURE 5
Efficacy outcome of COT. No difference could be observed in **(A)** mean aortic gradient and **(B)** paravalvular leakage following TAVR with different deployment techniques. In the COT group, fewer new permanent pacemaker implantations during 30-day follow-up were needed (COT 8.0% vs. Non-COT 16.8%; $p = 0.028$) **(C)**, and a reduced length of in-hospital stay could be achieved (COT 8.4 ± 4.0 vs. Non-COT 10.3 ± 6.7 days; $p = 0.007$) **(D)**. COT, cusp-overlap technique; TAVR, transcatheter aortic valve replacement.

no clear view of the native annulus relative to the conduction system due to the foreshortening of the LVOT (11). COT view results in an elongation of the LVOT, removement of the delivery catheter parallax, and accentuation of the NCC/RCC commissures in the center of the fluoroscopic view where the conduction system crosses the membranous septum below the atrioventricular node (6, 14). According to the new manufacturer's advice, Evolut CoreValve's target ID of 3 mm is recommended instead of a target ID of 3–5 mm as proposed before (15). Due to the wider range of former target ID of 3–5 mm in the Non-COT group (13), the present COT group with a narrow range of 3 mm target ID did not achieve higher proportions of successful target ID, but a significantly higher absolute mean ID was achieved by far. Not only the ID below a single coronary cusp but also the symmetry of valve implantation was improved. This is another benefit of COT during valve deployment because the NCC nadir is better visualized and both the device and the annulus are perpendicularly in-plane without parallax, allowing correct assessment of the true device depth below all three cusps (14).

## Reliability of cusp-overlap technique in safety and clinical outcome

Although balloon-expandable valves exert higher radial forces, rates of new PPI are higher after implantation of self-expandable THV due to differences in the design of the prosthetic frame and technique of implantation. TAVR with supra-annular, newer-generation CoreValve Evolut prostheses have been associated with the need for new PPI in 14.7 to 26.7% of patients within 30 days after the intervention (4, 5).

The proximity of the aortic valve and the cardiac conduction system is one of the reasons for the occurrence of new conduction disturbances following TAVR (16, 17). The close relationship of the left bundle branch to the aortic root

TABLE 4 A total of 30-day procedural outcome in matched cohorts.

| | Total ($n$ = 300) | COT ($n$ = 150) | Non-COT ($n$ = 150) | $P$-value |
|---|---|---|---|---|
| ID (mean NCC-LCC), mm | −4.6 ± 2.6 | −4.2 ± 2.7 | −4.9 ± 2.3 | *0.007* |
| Target ID reached | 157 (52.3) | 71 (47.3) | 86 (57.3) | 0.083 |
| Symmetric valve deployment | 154 (52.7) | 92 (61.3) | 66 (44.0) | *0.003* |
| 30-day mortality | 1 (0.3) | 0 (0.0) | 1 (0.7) | 0.317 |
| Major bleeding | 30 (10.0) | 11 (12.0) | 19 (8.0) | 0.124 |
| Major vascular complications | 32 (10.7) | 20 (13.3) | 12 (8.0) | 0.135 |
| Stroke | 10 (3.3) | 7 (4.7) | 3 (2.0) | 0.198 |
| AKI I-III | 39 (13.0) | 16 (10.7) | 23 (15.3) | 0.230 |
| New RRT | 3 (1.0) | 0 (0.0) | 3 (2.0) | 0.082 |
| New PPI | 34 (12.4) ($n$ = 276) | 11 (8.0) ($n$ = 138) | 23 (16.8) ($n$ = 138) | *0.028* |
| New LBBB | 50 (14.1) ($n$ = 281) | 18 (12.8) ($n$ = 141) | 32 (22.9) ($n$ = 140) | *0.027* |
| New-onset AF | 6 (2.9) ($n$ = 210) | 3 (2.9) ($n$ = 105) | 3 (2.9) ($n$ = 105) | 0.999 |
| Need for valve-in-valve procedure | 2 (1.3) | 2 (1.3) | 0 (0.0) | 0.156 |
| dPmean, mmHg | 7.3 ± 3.3 | 7.3 ± 3.4 | 7.3 ± 3.3 | 0.972 |
| dPmax, mmHg | 13.1 ± 6.1 | 13.2 ± 6.3 | 13.0 ± 5.8 | 0.767 |
| PVL > I° | 10 (3.3) | 6 (4.0) | 4 (2.7) | 0.520 |
| In-hospital stay, days | 9.4 ± 5.6 | 8.4 ± 4.0 | 10.3 ± 6.7 | *0.007* |
| ICU stay, days | 2.0 ± 1.7 | 1.6 ± 1.4 | 2.3 ± 1.8 | *< 0.001* |

Values are mean ± SD or $n$ (%).
AF, atrial fibrillation; AKI, acute kidney injury; dPmean/dPmax, mean/maximal transvalvular gradient; ICU, intensive care unit; ID, implantation depth; LBBB, left bundle branch block; LCC, left coronary cusp; NCC, non-coronary cusp; PPI, permanent pacemaker implantation; PVL, paravalvular leakage; RRT, renal replacement therapy.

explains why LBBB is the most common conduction disturbance following TAVR and why ID greater than the membranous septum length is an independent predictor of PPI (18–20). Interaction of the THV with the surrounding tissue induces either direct injury by radial forces or indirect injury to the conduction tissue by localized edema or hematoma. Consequently, a complete AV block–the main indication for PPI by far in our analysis–may be either the result of total interruption of AV conduction or new-onset LBBB in patients with preexisting RBBB (21, 22).

Our single-center experience using COT for valve deployment showed that only 8% of patients without preexisting pacemaker required new PPI compared to 16.8% in Non-COT group, and the incidence of new-onset LBBB could also be reduced, what is in accordance with former studies (7–9). Because confounders like age and atrial fibrillation were eliminated by propensity score matching and other known procedural predictors like post-dilatation or oversizing did not differ between both groups, the difference in deployment technique seems to be the only reasonable explanation for this improvement in outcome.

A potential limitation of the COT is the implanter's concern that a shallow THV implantation may lead to a higher rate of valve embolism with upward displacement ("pop-outs"), potentially resulting in increased procedural complexity and patient morbidity (23, 24). In our experience, we did not observe this event in COT group. Both cases with the need for a second valve in the COT group of our study were caused by moderate to severe valvular leakage after implantation of the first TAVR prosthesis due to infolding of the prosthesis and probably incorrect patient-prosthesis sizing.

The reasons for the reduction in length of in-hospital stay in the COT cohort are multifactorial, but one of them is very likely the reduced post-procedural conduction disturbances and therefore the decreased need for a temporary or permanent pacemaker. The clinical impact of new PPI following TAVR has been somehow controversial, but meta-analyses have suggested an increased risk of all-cause mortality at 1 year in patients receiving a new permanent pacemaker and a higher rate of heart failure rehospitalizations (25). Certainly, the requirement for PPI is associated with longer in-hospital stay and increased costs (26), leading to slower periprocedural recovery and increased resource utilization.

## Impact of cusp-overlap technique on procedural performance during transcatheter aortic valve replacement

Similar to our results, there are already former studies examining the effect of COT on conduction disturbances following TAVR with observation of a significant reduction in both LBBB and PPI rate after TAVR (7–9). Mendiz et al. examined primary clinical outcomes without conclusions on procedural data like the achievement of target ID or the impact of COT on procedural aspects like the volume of

contrast agent or the radiation dose used (7). Doldi et al. only reported the technical success according to the new 2021 VARC-3 criteria (27) without further procedural details (8). While Pascual et al. performed a propensity score analysis with different measurement techniques of target ID, no relevant information was published about possible procedural pitfalls of this complex implantation technique except for procedural success and fluoroscopic time without any significant difference between COT and Non-COT group (9).

At least in our hands, the price for optimized ID is a higher rate of resheathing due to a more accurate achievement of a target ID of exactly 3 mm than before with a range between 3 and 5 mm. Thus, higher rates of repositioning did not result in less device success or increased mortality of the COT group as described before during multiple resheathing (28). Thus, there is a trend toward increased stroke rates in the COT group compared to Non-COT. Although one could speculate that excessive manipulation in the aortic valve and its adjacent structures could affect stroke rates, no significant relationship has been found in former studies (28, 29). The non-randomized design of our study with different clinical and anatomical factors might have impacted this outcome, and confusion bias cannot be excluded.

Although even the length of fluoroscopy time could be reduced, the dose area product is higher in the COT group, what can be explained by more extreme angulations during cusp-overlap view with an automatic increment of radiation energy that is exposed to the patients' body surface by the X-ray tube assembly (**Figures 3B,C**).

A significant reduction of contrast medium was observed in the COT cohort. This is the consequence of the need for less contrast agent usage to visualize the NCC only (2–4 ml) during most valve positioning up to the point of no return. A larger amount of contrast agent is only necessary for the final assessment of valve position before deployment, when, as a second angulation, a three-cusp view is obtained for position control and ID measurement. In contrast, during valve positioning in three-cusp only view, more contrast agent and longer fluoroscopy time were administered to delineate all three cusps.

### Limitations

Several limitations should be considered when interpreting this study. This is a single-center observational study with a limited number of patients. Two non-contemporary groups were compared to assess differences between COT and 3-cusps coplanar view only technique with four different operators performing TAVR procedure with different levels of practical knowledge and experience. There may exist temporal, confounders and selection bias due to high rate of excluded patients with incomplete dataset that was not accounted for in our analysis. Therefore, larger multicenter randomized trials should be conducted to verify the usefulness of COT during THV deployment.

## Conclusion

Transcatheter aortic valve replacement with self-expandable valves using the cusp-overlap deployment technique is associated with an optimized implantation depth, leading to fewer permanent conduction disturbances and a shortened length of in-hospital stay. Any prevention of conduction disturbances can potentially reduce rehospitalizations and late mortality rate, whereas the procedural and functional outcome is not remarkably influenced by COT. Thus, COT should be regularly performed for TAVR with a self-expandable prosthesis to achieve optimized ID, especially as TAVR is expanded to the low-risk population with higher life expectancy.

## Data availability statement

The raw data supporting the conclusions of this article will be made available by the authors, without undue reservation.

## Ethics statement

The studies involving human participants were reviewed and approved by the Institutional Ethics Committee of the Heinrich-Heine University of Düsseldorf. The patients/participants provided their written informed consent to participate in this study.

## Author contributions

OM: conception and design, investigation, analysis and interpretation of data, drafting of the manuscript, project administration, and final approval of the manuscript. KP, SB, NB, SA, AP, RW, PH, and CJ: analysis and interpretation of data, revision of the manuscript for important intellectual content, and final approval of the manuscript. KK: analysis and interpretation of data, data curation, revision of the manuscript for important intellectual content, and final approval of the manuscript. MK: conception and design, validation, drafting of the manuscript, and final approval of the manuscript. VV and TZ: conception and design, investigation, drafting of the manuscript, project administration, and final approval of the manuscript. All authors contributed to the article and approved the submitted version.

## Funding

This study was sponsored by Medtronic (Minneapolis, MN, United States) in the context of an external research program (ERP-2020-12514).

## Acknowledgments

We thank Jenni Scharlau and Tatjana Wirachowski for their commitment to patient care and their substantial contribution to data acquisition and administration.

## Conflict of interest

VV, TZ, CJ, RW, AP, and OM had received consulting fees, travel expenses, or study honoraria from Medtronic (Minneapolis, MN, United States) and/or Edwards Lifesciences (Irvine, CA, United States).

The remaining authors declare that the research was conducted in the absence of any commercial or financial relationships that could be construed as a potential conflict of interest.

## Publisher's note

All claims expressed in this article are solely those of the authors and do not necessarily represent those of their affiliated organizations, or those of the publisher, the editors and the reviewers. Any product that may be evaluated in this article, or claim that may be made by its manufacturer, is not guaranteed or endorsed by the publisher.

## Supplementary material

The Supplementary Material for this article can be found online at: https://www.frontiersin.org/articles/10.3389/fcvm.2022.847568/full#supplementary-material

## References

1. Baumgartner H, Falk V, Bax JJ, De Bonis M, Hamm C, Holm PJ, et al. 2017 ESC/EACTS Guidelines for the management of valvular heart disease. *Eur Heart J.* (2017) 38:2739–91. doi: 10.1093/eurheartj/ehx391

2. Mack MJ, Leon MB, Thourani VH, Makkar R, Kodali SK, Russo M, et al. Transcatheter aortic-valve replacement with a balloon-expandable valve in low-risk patients. *N Engl J Med.* (2019) 380:1695–705. doi: 10.1056/NEJMoa1814052

3. Popma JJ, Michael Deeb G, Yakubov SJ, Mumtaz M, Gada H, O'Hair D, et al. Transcatheter aortic-valve replacement with a self-expanding valve in low-risk patients. *N Engl J Med.* (2019) 380:1706–15. doi: 10.1056/NEJMoa1816885

4. Sammour Y, Krishnaswamy A, Kumar A, Puri R, Tarakji KG, Bazarbashi N, et al. Incidence, predictors, and implications of permanent pacemaker requirement after transcatheter aortic valve replacement. *J Am Coll Cardiol Intv.* (2021) 14:115–34. doi: 10.1016/j.jcin.2020.09.063

5. Van Rosendael PJ, Delgado V, Bax JJ. Pacemaker implantation rate after transcatheter aortic valve implantation with early and new-generation devices: A systematic review. *Eur Heart J.* (2018) 39:2003–13. doi: 10.1093/eurheartj/ehx785

6. Tang GHL, Zaid S, Michev I, Ahmad H, Kaple R, Undemir C, et al. "Cusp-Overlap" view simplifies fluoroscopy-guided implantation of self-expanding valve in transcatheter aortic valve replacement. *J Am Coll Cardiol Intv.* (2018) 11:1663–5. doi: 10.1016/j.jcin.2018.03.018

7. Mendiz OA, Noè M, Fava CM, Guti LA, Valdivieso R, Gada H, et al. Impact of cusp-overlap view for TAVR with self-expandable valves on 30-day conduction disturbances. *J Interv Cardiol.* (2021) 2021:9991528. doi: 10.1155/2021/9991528

8. Doldi PM, Stolz L, Escher F, Steffen J, Gmeiner J, Roden D, et al. Transcatheter aortic valve replacement with the self-expandable core valve evolut prosthesis using the cusp-overlap vs. tricusp-view. *J Clin Med.* (2022) 11:1561. doi: 10.3390/jcm11061561

9. Pascual I, Hernández-Vaquero D, Alperi A, Almendarez M, Avanzas P, Kalavrouziotis D, et al. Permanent pacemaker reduction using cusp-overlapping projection in TAVR. *JACC Cardiovasc Interv.* (2022) 15:150–61. doi: 10.1016/j.jcin.2021.10.002

10. Kappetein AP, Head SJ, Généreux P, Piazza N, Van Mieghem NM, Blackstone EH, et al. Updated standardized endpoint definitions for transcatheter aortic valve implantation: The valve academic research consortium-2 consensus document (varc-2). *Eur J Cardio-Thoracic Surg.* (2012) 42:S45–60. doi: 10.1093/ejcts/ezs533

11. Piazza N, Mylotte D, Lauzier PT. Fluoroscopic "heart chamber" anatomy - The case for imaging modality-independent terminology. *EuroIntervention.* (2016) 12:Y9–15. doi: 10.4244/EIJV12SYA3

12. Hokken TW, Wolff QM, Schermers T, van Wiechen MP, Ooms JF, Adrichem R, et al. Cusp Overlap versus 3-cusps-aligned transcatheter aortic valve depth assessment with different angiography projections by multidetector computed tomography. *JACC Cardiovasc Interv.* (2022) 15:231–3. doi: 10.1016/j.jcin.2021.10.004

13. Piayda K, Hellhammer K, Veulemans V, Sievert H, Gafoor S, Afzal S, et al. Navigating the "Optimal Implantation Depth" with a self-expandable TAVR device in daily clinical practice. *J Am Coll Cardiol Intv.* (2020) 13:679–88. doi: 10.1016/j.jcin.2019.07.048

14. Ben-Shoshan J, Alosaimi H, Lauzier PT, Pighi M, Talmor-Barkan Y, Overtchouk P, et al. Double S-Curve Versus cusp-overlap technique: Defining the optimal fluoroscopic projection for TAVR with a self-expanding device. *J Am Coll Cardiol Intv.* (2021) 14:185–94. doi: 10.1016/j.jcin.2020.10.033

15. Petronio AS, Sinning JM, Van Mieghem N, Zucchelli G, Nickenig G, Bekeredjian R, et al. Optimal implantation depth and adherence to guidelines on permanent pacing to improve the results of transcatheter aortic valve replacement with the medtronic corevalve system: The CoreValve prospective, international, post-market ADVANCE-II study. *J Am Coll Cardiol Intv.* (2015) 8:837–46. doi: 10.1016/j.jcin.2015.02.005

16. Kawashima T, Sato F. Visualizing anatomical evidences on atrioventricular conduction system for TAVI. *Int J Cardiol.* (2014) 174:1–6. doi: 10.1016/j.ijcard.2014.04.003

17. Piazza N, de Jaegere P, Schultz C, Becker AE, Serruys PW, Anderson RH. Anatomy of the aortic valvar complex and its implications for transcatheter implantation of the aortic valve. *Circ Cardiovasc Interv.* (2008) 1:74–81. doi: 10.1161/CIRCINTERVENTIONS.108.780858

18. Hamdan A, Guetta V, Klempfner R, Konen E, Raanani E, Glikson M, et al. Inverse relationship between membranous septal length and the risk of atrioventricular block in patients undergoing transcatheter aortic valve implantation. *J Am Coll Cardiol Intv.* (2015) 8:1218–28. doi: 10.1016/j.jcin.2015.05.010

19. Oestreich BA, Mbai M, Gurevich S, Nijjar PS, Adabag S, Bertog S, et al. Computed tomography (CT) assessment of the membranous septal anatomy prior to

transcatheter aortic valve replacement (TAVR) with the balloon-expandable SAPIEN 3 valve. *Cardiovasc Revascularization Med.* (2018) 19:626–31.

20. Jilaihawi H, Zhao Z, Du R, Staniloae C, Saric M, Neuburger PJ, et al. Minimizing permanent pacemaker following repositionable self-expanding transcatheter aortic valve replacement. *J Am Coll Cardiol Intv.* (2019) 12:1796–807. doi: 10.1016/j.jcin.2019.05.056

21. Siontis GCM, Jüni P, Pilgrim T, Stortecky S, Büllesfeld L, Meier B, et al. Predictors of permanent pacemaker implantation in patients with severe aortic stenosis undergoing TAVR: A meta-analysis. *J Am Coll Cardiol.* (2014) 64:129–40. doi: 10.1016/j.jacc.2014.04.033

22. Siontis GCM, Praz F, Lanz J, Vollenbroich R, Roten L, Stortecky S, et al. New-onset arrhythmias following transcatheter aortic valve implantation: A systematic review and meta-analysis. *Heart.* (2018) 104:1208–15.

23. Hellhammer K, Piayda K, Afzal S, Veulemans V, Hennig I, Makosch M, et al. Micro-dislodgement during transcatheter aortic valve implantation with a contemporary self-expandable prosthesis. *PLoS One.* (2019) 14:e0224815. doi: 10.1371/journal.pone.0224815

24. Hachinohe D, Latib A, Laricchia A, Demir OM, Agricola E, Romano V, et al. Anatomic and procedural associations of transcatheter heart valve displacement following Evolut R implantation. *Catheter Cardiovasc Interv.* (2019) 93:522–9. doi: 10.1002/ccd.27827

25. Faroux L, Chen S, Muntané-Carol G, Regueiro A, Philippon F, Sondergaard L, et al. Clinical impact of conduction disturbances in transcatheter aortic valve replacement recipients: A systematic review and meta-analysis. *Eur Heart J.* (2020) 41:2771–81. doi: 10.1093/eurheartj/ehz924

26. Fadahunsi OO, Olowoyeye A, Ukaigwe A, Li Z, Vora AN, Vemulapalli S, et al. Incidence, predictors, and outcomes of permanent pacemaker implantation following transcatheter aortic valve replacement: Analysis from the U.S. Society of Thoracic Surgeons/American College of Cardiology TVT registry. *J Am Coll Cardiol Intv.* (2016) 9:2189–99. doi: 10.1016/j.jcin.2016.07.026

27. Généreux P, Piazza N, Alu MC, Nazif T, Hahn RT, Pibarot P, et al. Valve academic research consortium 3: Updated endpoint definitions for aortic valve clinical research. *Eur Heart J.* (2021) 42:1825–57. doi: 10.1093/eurheartj/ehaa799

28. Bernardi FLM, Rodés-Cabau J, Tirado-Conte G, Amat Santos IJ, Plachtzik C, Cura F, et al. Incidence, predictor, and clinical outcomes of multiple resheathing with self-expanding valves during transcatheter aortic valve replacement. *J Am Heart Assoc.* (2021) 10:e020682. doi: 10.1161/JAHA.120.020682

29. Attizzani GF, Dallan LAP, Markowitz A, Yakubow SJ, Deeb GM, Reardon MJ, et al. Impact of repositioning on outcomes following transcatheter aortic valve replacement with a self-expandable valve. *JACC Cardiovasc Interv.* (2020) 13:1816–24. doi: 10.1016/j.jcin.2020.04.028

frontiers | Frontiers in Cardiovascular Medicine

TYPE Original Research
PUBLISHED 09 August 2023
DOI 10.3389/fcvm.2023.857578



OPEN ACCESS

EDITED BY
Marko Banovic,
University of Belgrade, Serbia

REVIEWED BY
Ching-Ling (Ellen) Lien,
Children's Hospital of Los Angeles, United States
Lulin Zhou,
Nankai University, China

*CORRESPONDENCE
Xiang Wei
✉ xiangwei@tjh.tjmu.edu.cn
Lin Cheng
✉ lincheng@tjh.tjmu.edu.cn

RECEIVED 18 January 2022
ACCEPTED 26 July 2023
PUBLISHED 09 August 2023

CITATION
Yang Y, Xiao B, Feng X, Chen Y, Wang Q, Fang J, Zhou P, Wei X and Cheng L (2023) Identification of hub genes and key signaling pathways by weighted gene co-expression network analysis for human aortic stenosis and insufficiency. Front. Cardiovasc. Med. 10:857578. doi: 10.3389/fcvm.2023.857578



# Identification of hub genes and key signaling pathways by weighted gene co-expression network analysis for human aortic stenosis and insufficiency

Yang Yang[1,2,3,4,5], Bing Xiao[6], Xin Feng[1], Yue Chen[1], Qunhui Wang[1], Jing Fang[1], Ping Zhou[2,3,4,5], Xiang Wei[1]* and Lin Cheng[1]*

[1]Division of Cardiothoracic and Vascular Surgery, Tongji Hospital, Tongji Medical College, Huazhong University of Science and Technology, Wuhan, China, [2]Institute of Organ Transplantation, Tongji Hospital, Tongji Medical College, Huazhong University of Science and Technology, Wuhan, China, [3]Key Laboratory of Organ Transplantation, Ministry of Education, Wuhan, China, [4]NHC Key Laboratory of Organ Transplantation, Chinese Academy of Medical Sciences, Wuhan, China, [5]Key Laboratory of Organ Transplantation, Chinese Academy of Medical Sciences, Wuhan, China, [6]Department of Obstetrics and Gynecology, Peking University People's Hospital, Peking University, Beijing, China

**Background:** Human aortic valve stenosis (AS) and insufficiency (AI) are common diseases in aging population. Identifying the molecular regulatory networks of AS and AI is expected to offer novel perspectives for AS and AI treatment.
**Methods:** Highly correlated modules with the progression of AS and AI were identified by weighted genes co-expression network analysis (WGCNA). Gene Ontology (GO) and Kyoto Encyclopedia of Genes and Genomes (KEGG) enrichment analyses were performed by the clusterProfiler program package. Differentially expressed genes (DEGs) were identified by the DESeqDataSetFromMatrix function of the DESeq2 program package. The protein-protein interaction (PPI) network analyses were implemented using the STRING online tool and visualized with Cytoscape software. The DEGs in AS and AI groups were overlapped with the top 30 genes with highest connectivity to screen out ten hub genes. The ten hub genes were verified by analyzing the data in high throughput RNA-sequencing dataset and real-time PCR assay using AS and AI aortic valve samples.
**Results:** By WGCNA algorithm, 302 highly correlated genes with the degree of AS, degree of AI, and heart failure were identified from highly correlated modules. GO analyses showed that highly correlated genes had close relationship with collagen fibril organization, extracellular matrix organization and extracellular structure organization. KEGG analyses also manifested that protein digestion and absorption, and glutathione metabolism were probably involved in AS and AI pathological courses. Moreover, DEGs were picked out for 302 highly correlated genes in AS and AI groups relative to the normal control group. The PPI network analyses indicated the connectivity among these highly correlated genes. Finally, ten hub genes (*CD74*, *COL1A1*, *TXNRD1*, *CCND1*, *COL5A1*, *SERPINH1*, *BCL6*, *ITGA10*, *FOS*, and *JUNB*) in AS and AI were found out and verified.
**Conclusion:** Our study may provide the underlying molecular targets for the mechanism research, diagnosis, and treatment of AS and AI in the future.

KEYWORDS

aortic valve stenosis, aortic valve insufficiency, heart failure, WGCNA, co-expression modules, hub genes

# Introduction

Heart failure is a severe terminal stage of all kinds of cardiovascular diseases, which include hypertension (1), coronary heart disease (2), myocardial infarction (3), valvular heart disease (4), and cardiomyopathy (5). As the important cause of heart failure, valvular heart diseases consist of stenosis or insufficiency with specific pathophysiology among the four cardiac valves (aortic valves, mitral valves, tricuspid valves and pulmonary valves) (6). In the globe, valvular heart diseases have increasingly become the important contributor to cardiovascular morbidity and mortality according to the epidemiologic studies, which have resulted in serious social burden and economical cost on valvular heart diseases diagnosis and treatment (7). The prevalence of valvular heart diseases gradually increases with age of clinical patients (8). In terms of aortic valve lesion, aortic valve stenosis (AS) and aortic valve regurgitation (AR) are the highly popular valve lesions among various valvular heart diseases (9), the morbidities of AS and AR were 0.7% and 0.2% with the age 55–64 years, 1% and 1.3% for the age-bracket of 65–74 years, and 2% and 2.8% after 75 years old, respectively (8). Thus, due to the large aging population around the world, the aortic valvular heart diseases are still the important public health problem.

AS and AR are a kind of common aortic valve diseases, characterized by aortic valve opening area reduction or aortic valve insufficiency (AI), respectively. Currently, numerous studies have reported the pathological features and molecular mechanisms about aortic valve damage (10–13). The well-known etiologies for AS include aortic valve degeneration, rheumatic aortic stenosis, congenital valve defects, systemic inflammatory diseases, endocarditis, and many other conditions (10). Whereas, the major causes of AI are made up of various pathological changes of aortic valves, such as leaflet abnormalities, rheumatic fever, myxomatous degeneration, infective endocarditis, etc (12). Although, the current available reports have uncovered the molecular mechanisms for pathological processes of AS and AI, which include but not limit to fibro-calcific remodeling, osteogenic differentiation, lipid accumulation, inflammation, angiogenesis and hemorrhage, disorganization and remodeling of the valvular extracellular matrix (ECM) (10, 13). The vital molecules for the regulation and indication of AS and AI pathological courses still need to be further investigated. Hence, using high throughput sequencing techniques and identifying the key regulatory or indicative molecules for AS and AI may provide a feasible strategy for the diagnosis and treatment of AS and AI from the microscopic molecular viewpoints.

In this study, we analysed the expression profiles of human aortic valve samples of aortic valve stenosis (AS) and aortic insufficiency (AI) by systematic bioinformatics approaches of weighted gene co-expression network analysis (WGCNA). We constructed the gene co-expression modules by WGCNA algorithm and screened the highly correlated modules with the degree of AS, degree of AI, and heart failure, which included orange, steelblue, darkgreen, and grey60 modules. Furthermore, we selected highly correlated genes in indicated modules and performed Gene Ontology (GO) and Kyoto Encyclopedia of Genes and Genomes (KEGG) pathway enrichment analyses. The differentially expressed genes (DEGs) were identified and intersected with those 30 genes possessing high connectivity among the highly correlated genes from various modules to screen out hub genes. Finally, the mRNA expression values of ten hub genes (*CD74*, *COL1A1*, *TXNRD1*, *CCND1*, *COL5A1*, *SERPINH1*, *BCL6*, *ITGA10*, *FOS*, and *JUNB*) were validated by analyzing results of high throughput RNA sequencing from AS and AI aortic valve samples and by examining the mRNA expression levels of human AS and AI aortic valve tissues. These results may provide an avenue for the diagnosis and treatment of AS and AI in the future.

# Materials and methods

## High-throughput data acquisition and preprocessing

The high-throughput RNA-sequencing datasets were acquired from the public Gene Expression Omnibus (GEO) database with the accession number GSE153555, which contained the gene expression data from 5 human normal control (NC) aortic valves, 5 human aortic stenosis (AS) aortic valves, and 5 human aortic insufficiency (AI) aortic valves, each individual contained 2 biologically repeated aortic valve high-throughput RNA-sequencing results. The gene expression Fragments Per Kilobase of transcript per Million mapped reads (FPKM) values and count values were analysed by R software (Version 4.1.2). Clinical traits, including age, sex, body mass index (BMI), degree of AS and AI, left ventricular ejection fraction (LVEF), and disease history (diabetes, hypertension, coronary heart disease, and heart failure), for each sample were collected from the Series Matrix Files in the GEO database with GSE153555 number (14). The average gene expression FPKM values of 30 samples were calculated and ranked by size, and the top 6,000 genes with the highest average expression were screened out and used for weighted gene co-expression network analysis (WGCNA) computation. The FPKM values of the 6,000 genes from 30 samples were subjected to $\log_2(\text{FPKM} + 1)$ conversion followed by samples hierarchical clustering to eliminate 2 outlier samples (GSM4647040 and GSM4647041) using the hclust function in the R software (Version 4.1.2).

## Co-expression module construction of AS and AI by WGCNA algorithm

The WGCNA co-expression module construction was conducted as previously described (15). The soft threshold β power value for WGCNA module construction was computed by pickSoftThreshold function in the WGCNA program package. The adequate β value 16 was picked out once Scale Free Topology Model Fit, signed $R^2$ value was ≥0.8. Then, the adjacency matrix and topological overlap matrix (TOM) were constructed using the power value 16. The co-expression

modules were constructed and merged for those modules with similar expression profiles by step-by-step network construction methods. The correlation analysis among the indicated modules were performed by calculating the eigengenes, which were defined as the principal component 1 (PC1) of principal component analysis (PCA) for gene expression values in the indicated modules.

## Correlation analysis between co-expression modules and clinical traits

The correlation analyses between modules and clinical traits were performed using the eigengenes of the corresponding modules and clinical traits data to screen out the highly correlated modules with indicated clinical traits. To screen the highly correlated genes in AS and AI pathological courses, these modules relevant to degree of AS, degree of AI, and heart failure were further analysed. These modules with correlation coefficient more than 0.6 and *P* value less than 0.05 were regarded as highly correlated modules. The correlation coefficients of 6,000 genes expression values and indicated clinical traits were defined as gene significance (GS). For the associations of each module with the genes involved in the WGCNA process, module membership (MM) was defined as the correlation of module eigengenes and gene expression levels. The scatterplot of Gene Significance *vs.* Module Membership in the indicated module was plotted. These scatterplots with correlation coefficients more than 0.5 and *P* value less than 0.05 were selected. These 302 genes in indicated scatterplot with $MM > 0.8$ and $GS > 0.8$ were regarded as the highly correlated genes with corresponding module or trait, respectively, and were selected for subsequent analysis.

## Gene ontology (Go) and Kyoto encyclopedia of genes and genomes (KEGG) enrichment analyses

We performed GO and KEGG enrichment analyses for the highly correlated genes identified by the above procedures using the clusterProfiler program package. Firstly, the ENSEMBL number for each gene was transformed into the ENTREZID number using the bitr function. GO analyses including biological processes (BP), molecular functions (MF), and cellular components (CC) terms were conducted. These terms in GO and KEGG enrichment analyses with *P* value less than 0.05 were screened out and considered as significant terms in AS and AI pathological processes. The top ten terms in GO and KEGG enrichment analyses were selected for visualization and further analyses.

## Identification of differentially expressed genes (DEGs)

The DEGs analysis using the high throughput RNA-sequencing data was performed to evaluate the gene expression situation among the indicated groups using the DESeqDataSetFromMatrix function of the DESeq2 program package. Firstly, the results of DEGs analyses for total genes in high throughput RNA-sequencing data were obtained from the AS and AI group. The indicated DEGs results for the 302 highly correlated genes were screened out. These genes in AS or AI group with $|\log_2\text{FoldChange}| \geq 1$ and adjust *P* value <0.05 relative to the normal control group, were considered as the DEGs. These genes with $\log_2\text{FoldChange} \geq 1$ were defined as upregulated (UP) genes. These genes with $\log_2\text{FoldChange} \leq -1$ were defined as downregulated (DOWN) genes. These genes with $-1 < \log_2\text{FoldChange} < 1$ were defined as unchanged (NOT) genes. The volcano plots and heat maps were plotted to visualize DEGs.

## Protein-protein interaction (PPI) network analysis

PPI network analysis was performed using an online network tool STRING (https://cn.string-db.org/, version 11.5) (16). The 302 highly correlated genes were imported into STRING. The TSV file contained 302 highly correlated genes was downloaded and the PPI network was visualized by Cytoscape software (version 3.9.0) (17). The CytoHubba plug-in was used for identifying genes with high connectivity ranked by Betweenness (18). The top 30 genes with highest connectivity were picked out for further analysis. The DEGs of AS and AI group were intersected concurrently with the top 30 genes from PPI network analysis to identify these genes with significantly changed expression and high connectivity. These genes (*CD74*, *COL1A1*, *TXNRD1*, *CCND1*, *COL5A1*, *SERPINH1*, *BCL6*, *ITGA10*, *FOS*, and *JUNB*) that met the above conditions were identified as the hub genes.

## Human aortic valves sample collection and grouping

Human aortic valve samples were obtained from patients with pure AS or AI. These aortic valves samples from heart transplantation receptors or aortic dissection patients without definite lesions in aortic valves were used as normal control (NC) and mild aortic valve samples. A total of 35 aortic valve samples including 5 samples from normal control (NC) patient, 15 samples from aortic stenosis (AS) patient and 15 samples from aortic insufficiency (AI) patient were included in this study. Doppler echocardiography was used for evaluation of AR or AS severity (19, 20). The specimens were classified into 4 groups containing normal control, mild, moderate, and severe. The characteristics of aortic valves used in this study are shown in **Table 1**. All procedures involving human aortic valves samples conformed to the principles outlined in the Declaration of Helsinki. Exemption from informed consent for patients and human sampling procedures were approved by the Human

TABLE 1 Characteristics of clinical samples used in this study.

| Group | Age (years) | Sex | Body weight (kg) | Height (cm) | Degree of aortic Valve lesion | LA diameter (mm) | LV diameter (mm) | LVEF |
|---|---|---|---|---|---|---|---|---|
| NC-1 | 67 | M | 68 | 170 | Normal | 32 | 46 | 70% |
| NC-2 | 30 | F | 50 | 168 | Normal | 26 | 37 | 71% |
| NC-3 | 43 | F | 60 | 163 | Normal | 28 | 40 | 68% |
| NC-4 | 51 | M | 69 | 173 | Normal | 30 | 46 | 72% |
| NC-5 | 44 | M | 70 | 170 | Normal | 28 | 43 | 69% |
| AS-1 | 51 | M | 70 | 173 | Mild AS | 29 | 48 | 68% |
| AS-2 | 34 | F | 55 | 157 | Mild AS | 30 | 48 | 72% |
| AS-3 | 57 | F | 56 | 158 | Mild AS | 33 | 44 | 69% |
| AS-4 | 45 | F | 60 | 163 | Mild AS | 29 | 43 | 71% |
| AS-5 | 81 | M | 68 | 167 | Mild AS | 31 | 46 | 74% |
| AS-6 | 55 | M | 71 | 168 | Moderate AS | 28 | 45 | 71% |
| AS-7 | 54 | F | 65 | 163 | Moderate AS | 30 | 46 | 68% |
| AS-8 | 68 | F | 75 | 170 | Moderate AS | 35 | 48 | 68% |
| AS-9 | 58 | F | 56 | 157 | Moderate AS | 34 | 44 | 68% |
| AS-10 | 56 | M | 70 | 170 | Moderate AS | 31 | 53 | 60% |
| AS-11 | 48 | F | 46 | 156 | Severe AS | 25 | 38 | 63% |
| AS-12 | 59 | F | 76 | 163 | Severe AS | 35 | 48 | 68% |
| AS-13 | 41 | M | 75 | 171 | Severe AS | 36 | 58 | 67% |
| AS-14 | 70 | M | 80 | 168 | Severe AS | 36 | 47 | 67% |
| AS-15 | 50 | F | 46 | 151 | Severe AS | 27 | 43 | 60% |
| AI-1 | 56 | M | 70 | 173 | Mild AI | 25 | 49 | 67% |
| AI-2 | 60 | F | 56 | 156 | Mild AI | 30 | 52 | 65% |
| AI-3 | 53 | F | 46 | 153 | Mild AI | 26 | 48 | 66% |
| AI-4 | 66 | M | 68 | 168 | Mild AI | 29 | 47 | 68% |
| AI-5 | 50 | F | 55 | 160 | Mild AI | 26 | 38 | 70% |
| AI-6 | 58 | F | 60 | 160 | Moderate AI | 35 | 52 | 65% |
| AI-7 | 51 | F | 56 | 156 | Moderate AI | 36 | 51 | 68% |
| AI-8 | 59 | F | 46 | 153 | Moderate AI | 27 | 43 | 74% |
| AI-9 | 60 | F | 66 | 159 | Moderate AI | 36 | 58 | 63% |
| AI-10 | 60 | M | 68 | 170 | Moderate AI | 33 | 70 | 42% |
| AI-11 | 69 | M | 67 | 167 | Severe AI | 37 | 70 | 45% |
| AI-12 | 59 | M | 73 | 172 | Severe AI | 49 | 60 | 63% |
| AI-13 | 61 | M | 70 | 169 | Severe AI | 33 | 60 | 61% |
| AI-14 | 41 | M | 95 | 181 | Severe AI | 30 | 64 | 55% |
| AI-15 | 58 | F | 80 | 170 | Severe AI | 35 | 78 | 50% |

A total of 35 aortic valve samples were included in the study, with 5 from normal control (NC) patients, 15 from aortic stenosis (AS) patients, and 15 from aortic insufficiency (AI) patients. F, female; M, male; LA, left atrial; LV, left ventricular; LVEF, left ventricular ejection fraction.

Research Ethics Committees of Tongji Hospital of Huazhong University of Science and Technology (21).

## Real-time PCR

Real-time PCR analyses of mRNA levels in human aortic valve samples were performed as previously described (21). Briefly, the total RNA was extracted from 5 normal control aortic valve samples, 15 AS aortic valve samples, and 15 AI aortic valve samples using TRIzol reagent (15596018, Thermo Fisher Scientific) and reverse transcribed into cDNA using the Transcriptor HiScript III RT SuperMix for qPCR (+gDNA wiper) (R323-01, Vazyme). The quantitative analyses of ten hub genes mRNA expression levels were determined by real-time PCR assay using SYBR (Q311-02, Vazyme). Glyceraldehyde-3-phosphate dehydrogenase (*GAPDH*) was used for the internal reference. Primers used in this study were listed in **Table 2**.

## Statistical analysis

Statistical analysis was conducted by SPSS 23.0 software. All data are presented as the mean ± SD. Non-parametric Kruskal-Wallis H test was used for comparisons among multiple groups. $P$ value <0.05 was considered to be statistically significant.

# Results

## Construction of WGCNA co-expression modules

The data analysis process used in this study was depicted in the flow diagram (**Figure 1A**). High throughput RNA-sequencing data were preprocessed using the R software (Version 4.1.2). The average FPKM expression values for a total of 48,162 genes were calculated and ranked by size. The top 6,000 genes with the highest average

TABLE 2 Primers for the real-time PCR assays in this study.

| Gene | Species | | Sequence 5′-3′ |
|---|---|---|---|
| *CD74* | Human | F | CAGCGCGACCTTATCTCCAA |
| | | R | GGTACAGGAAGTAGGCGGTG |
| *COL1A1* | Human | F | AAGAACAGCGTGGCCTACAT |
| | | R | TTCAATCACTGTCTTGCCCCA |
| *TXNRD1* | Human | F | TGGCCATTGGAATGGACGAT |
| | | R | TGGACCCAGTACGTGAAAGC |
| *CCND1* | Human | F | GAGTGATCAAGTGTGACCCG |
| | | R | CAGATGTCCACGTCCCGC |
| *COL5A1* | Human | F | ACAACAACCCCTACATCCGC |
| | | R | TGACGCTTCACCGAAGTCAT |
| *SERPINH1* | Human | F | CCTCTCGAGCGCCTTGAAAA |
| | | R | CTGACATGCGTGACAAGTCG |
| *BCL6* | Human | F | TTTCCGGCACCTTCAGACTC |
| | | R | TGCACCTTGGTGTTGGTGAT |
| *ITGA10* | Human | F | AGACCCGGCCTATCCTCATC |
| | | R | TTTCTTATGGGCAAAGAAGCCA |
| *FOS* | Human | F | GGAGGGAGCTGACTGATACAC |
| | | R | ATCAGGGATCTTGCAGGCAG |
| *JUNB* | Human | F | GTCAAAGCCCTGGACGATCT |
| | | R | TTGGTGTAAACGGGAGGTGG |
| *GAPDH* | Human | F | CATCACCATCTTCCAGGAGCGAGA |
| | | R | TGCAGGAGGCATTGCTGATGATCT |

FPKM expression values in the datasets of the 30 samples were chosen for WGCNA computation. Sample hierarchical clustering was performed with hclust function and the height 60 was set as the threshold to screen outlier samples (Figure S1A). Two outlier samples GSM4647040 and GSM4647041 were identified and eliminated from all samples (Figure S1A). Before network construction and module detection, the clinical traits related to the sample dendrograms were visualized as the heatmap in Figure S1B. Finally, 28 samples with 6,000 genes were selected for WGCNA module construction. To screen out the suitable soft threshold power value used for WGCNA algorithm, we set an indicated range for power values and the power value 16 was picked out by pickSoftThreshold function in WGCNA package (Figure 1B). The WGCNA module construction was conducted, and those modules with similar expression profiles were merged. As depicted by the gene dendrograms, total eight modules were finally constructed, which included darkgrey (1,978 genes), lightcyan (1,158 genes), darkorange (242 genes), orange (170 genes), steelblue (35 genes), darkgreen (706 genes), grey60 (649 genes), and grey (1,062 genes) modules (Figure 1C). Those genes uncorrelated with other modules were assigned to grey module. The eigengene dendrogram and eigengene adjacency heatmap were plotted to exhibit the associations among the modules by eigengenes (Figure 1D).

## Identification of highly correlated modules connected with AS or AI

PCA for gene expression values in the indicated modules were computed. The PC1 for indicated genes was defined as eigengene. The correlation analyses for modules and clinical traits were performed by eigengenes from various modules and clinical traits data of 28 samples (Figure 2A). To find the highly correlated genes with AS and AI pathophysiologic mechanisms, these modules (correlation coefficient >0.6 and *P* value <0.05) associated with the degree of AS, degree of AI, and heart failure were subjected to further analyses (Figure 2A).

To further study the relationship between modules and clinical traits, the associations of gene expression values with degree of AS, degree of AI, and heart failure were analysed, the correlation coefficients were defined as gene significances (GS). The correlations of gene expression values with the modules (orange, steelblue, darkgreen, and grey60 modules) screened out in Figure 2A were calculated, which were marked as module memberships (MM). The scatter plots for MM and GS in the indicated modules were plotted, these plots (module membership *vs.* gene significance) with correlation coefficients more than 0.5 and *P* value less 0.05 were regarded as highly correlated for MM and GS (Figures 2B–G). These plots were used to screen highly correlated genes in AS and AI pathogenesis. These genes with GS > 0.8, MM > 0.8, and *P* value <0.05 were singled out in the plots. There were 30, 108, 133, 29, 77, and 5 genes in indicated modules screened out by the pre-set parameters (Figures 2B–G). Finally, 302 highly correlated genes were identified after removing duplicates.

## GO and KEGG enrichment analysis for highly correlated genes

In order to parse the molecular functions involved by these 302 highly correlated genes, gene function enrichment analyses of GO and KEGG were conducted using clusterProfiler program package. The results of GO enrichment analyses including BP, MF, and CC were obtained. These terms of GO and KEGG enrichment analyses were ranked by ascending *P* value and descending gene counts. We selected top 10 highly correlated terms with AS and AI as significantly enriched terms in GO and KEGG analyses.

Among these terms in BP analysis, our results showed that genes highly correlated with AS and AI were mainly enriched in collagen fibril organization (GO:0030199), extracellular matrix organization (GO:0030198), extracellular structure organization (GO:0043062), external encapsulating structure organization (GO:0045229), cell-substrate adhesion (GO:0031589), response to oxidative stress (GO:0006979), negative regulation of cellular protein localization (GO:1903828), negative regulation of interleukin-2 production (GO:0032703), pentose metabolic process (GO:0019321), and regulation of cell morphogenesis (GO:0022604) (Figure 3A). For MF analysis, the enrichment analysis results mainly included extracellular matrix structural constituent (GO:0005201), extracellular matrix structural constituent conferring tensile strength (GO:0030020), and kinds of molecular binding (GO:0005518, GO:0048407, GO:0019001, GO:0032561, GO:0005525, GO:0032550, GO:0030246, GO:0001883) (Figure 3B). In CC enrichment analysis, the significantly enriched terms mainly contained extracellular matrix

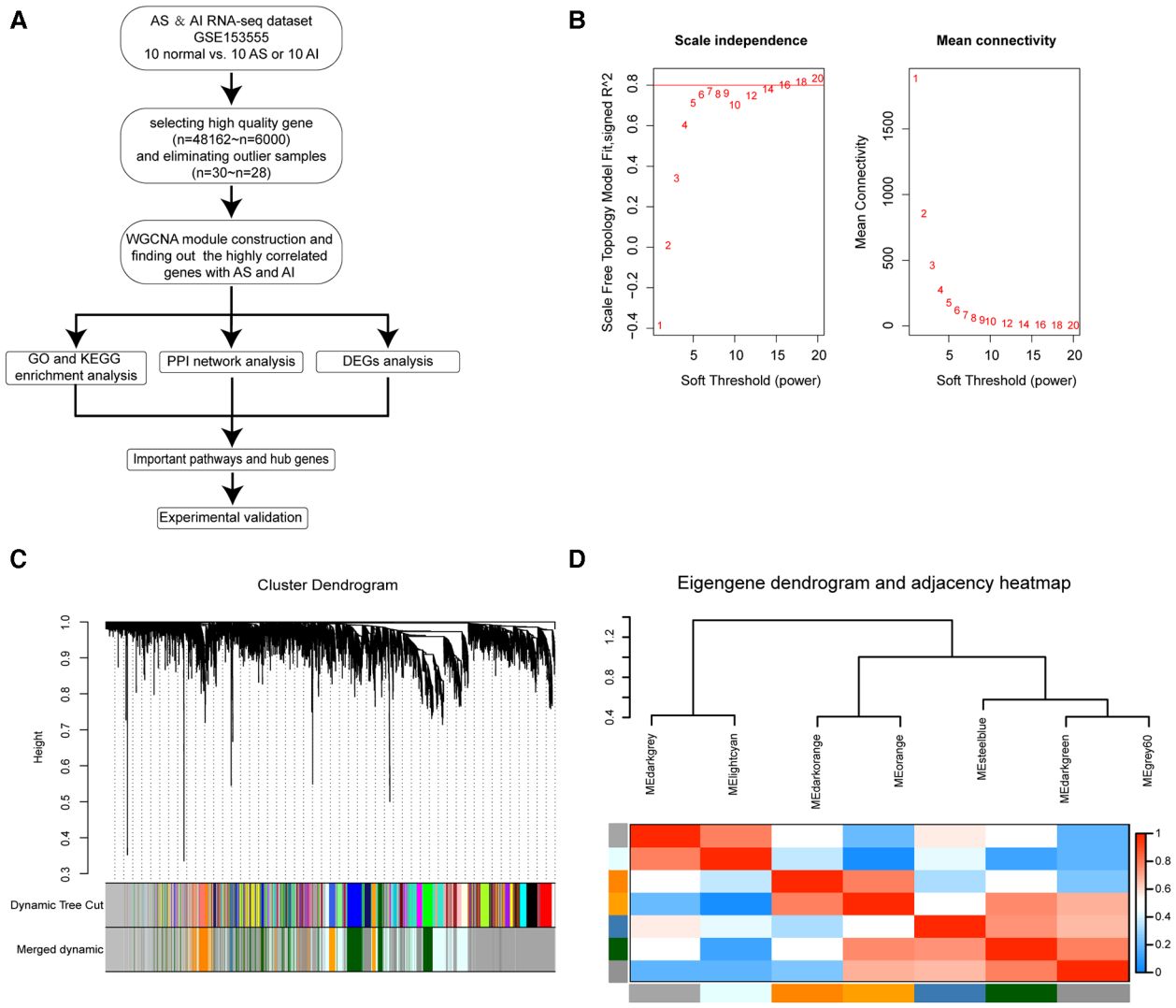


FIGURE 1
Construction of WGCNA co-expression modules. (A) The flow diagram for our WGCNA modules construction procedure in this study. (B) Analysis of scale-independence index (left panel) and mean connectivity for various soft threshold β power values, the most suitable β power value 16 was screened out. (C) Clustering dendrograms of 6,000 genes and module construction and merging according to the similar expression profiles by WGCNA algorithm. Total of eight co-expression modules were obtained including darkgrey, lightcyan, darkorange, orange, steelblue, darkgreen, grey60, and grey modules. The grey module is reserved for unassigned genes. (D) Cluster analysis for eigengenes dendrogram (Top) and correlation degree heatmap (Bottom) of eigengenes in each co-expression modules.

(GO:0062023), endoplasmic reticulum lumen (GO:0005788), collagen (GO:0005583, GO:0098643, GO:0005581, and GO:0098644), focal adhesion (GO:0005925), cell-substrate junction (GO:0030055), cell division site (GO:0032153), and actin filament bundle (GO:0032432) (Figure 3C). These results indicated that the highly correlated genes mainly functioned in these courses.

To investigate the enriched pathways of these highly correlated genes, the KEGG enrichment analyses were conducted. As shown in Figure 3D, the significantly enriched pathways included protein digestion and absorption (hsa04974), glutathione metabolism (hsa00480), Th17 cell differentiation (hsa04659), Th1 and Th2 cell differentiation (hsa04658), ferroptosis (hsa04216), phagocytosis (hsa04658), mitophagy (hsa04137), valine, leucine and isoleucine degradation (hsa00280), hippo signaling pathway (hsa04392), and pentose phosphate pathway (hsa00030). These results revealed that these pathways may be important in the development of AS and AI.

## Identification of DEGs for highly correlated genes

To understand the expression of the 302 highly correlated genes in the AS and AI groups, we performed DEGs analyses using the DESeq2 package. These genes with $|\log_2 \text{FoldChange}| \geq 1$ and adjust $P$ value <0.05 were considered as the DEGs. As depicted in Figures 4A–D, there were 31 downregulated genes, 229 unchanged genes, and 42 upregulated genes in the AI group and 35 downregulated genes, 190 unchanged genes, and 77

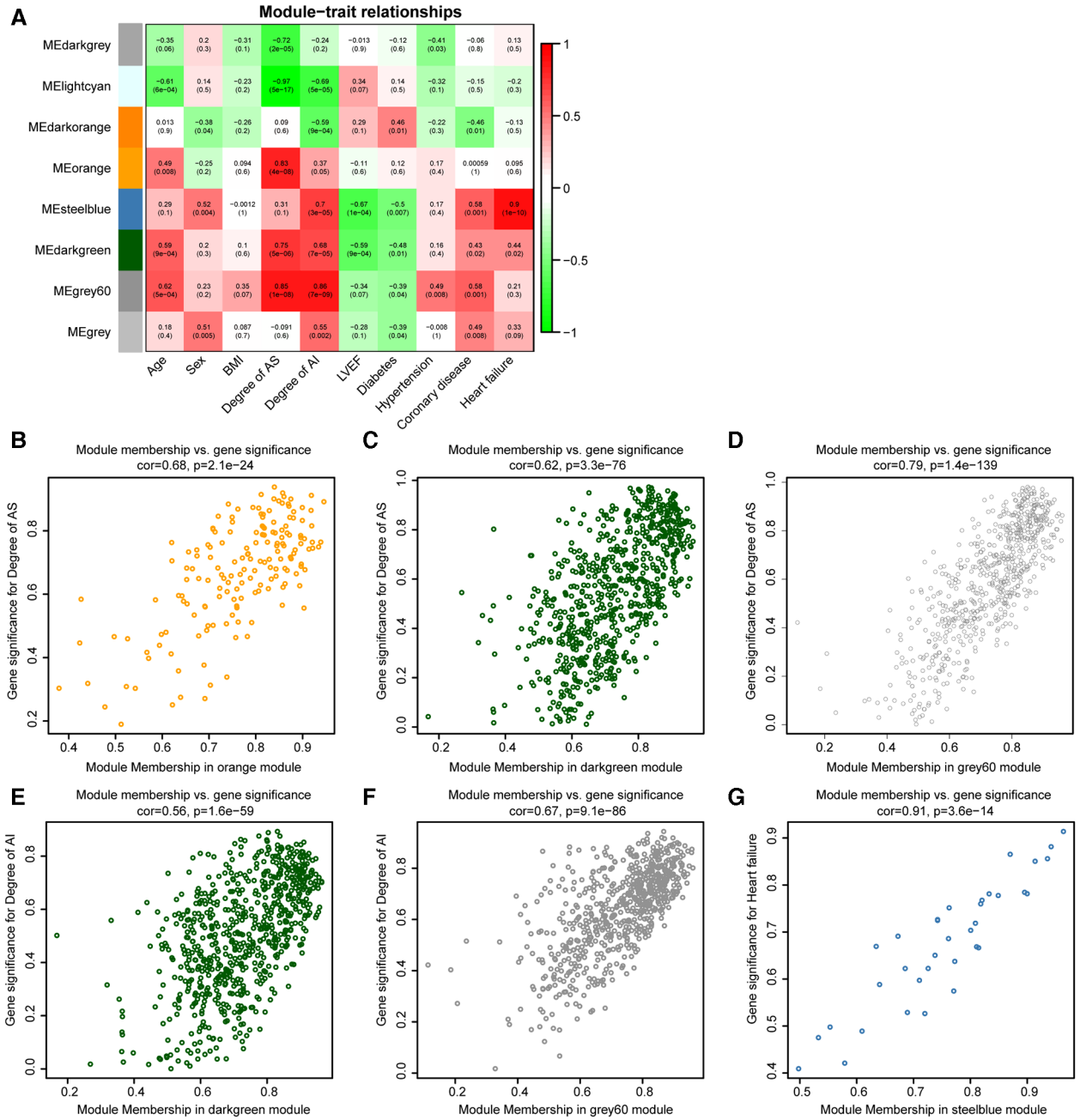


FIGURE 2
Identification of highly correlated modules connected with AS or AI. (**A**) The correlation heat map for various modules and clinical traits (age, sex, BMI, degree of AS, degree of AI, LVEF, diabetes, hypertension, coronary heart disease, and heart failure). Each cell contains the corresponding correlation coefficients and *P* value. (**B**–**G**) Scatterplot of Gene Significance (GS) for indicated clinical traits *vs.* Module Membership (MM) in the indicated modules.

upregulated genes in the AS group in comparison to the control group. These differential expression profiles among AS, AI, and control group indicated the different molecular mechanism in AS and AI pathogenesis.

## Hub genes identification by PPI analysis

Based on the above results, we next explored the important hub genes with high connectivity among these highly correlated genes. The interaction network for the 302 highly correlated genes with AS and AI pathogenesis was constructed and visualized utilizing the PPI analysis tool STRING and Cytoscape, respectively (Figure 5A). To screen out these genes with highest connectivity, the recognized plug-in Cytohubba of Cytoscape software was used to select the top 30 genes with the highest connectivity among the 302 genes by Betweenness button (Figure 5B). To identify the functionally crucial hub genes in mediating AS and AI common pathological processes, we overlapped the DEGs from AS group, AI group, and the top 30 highly connected genes

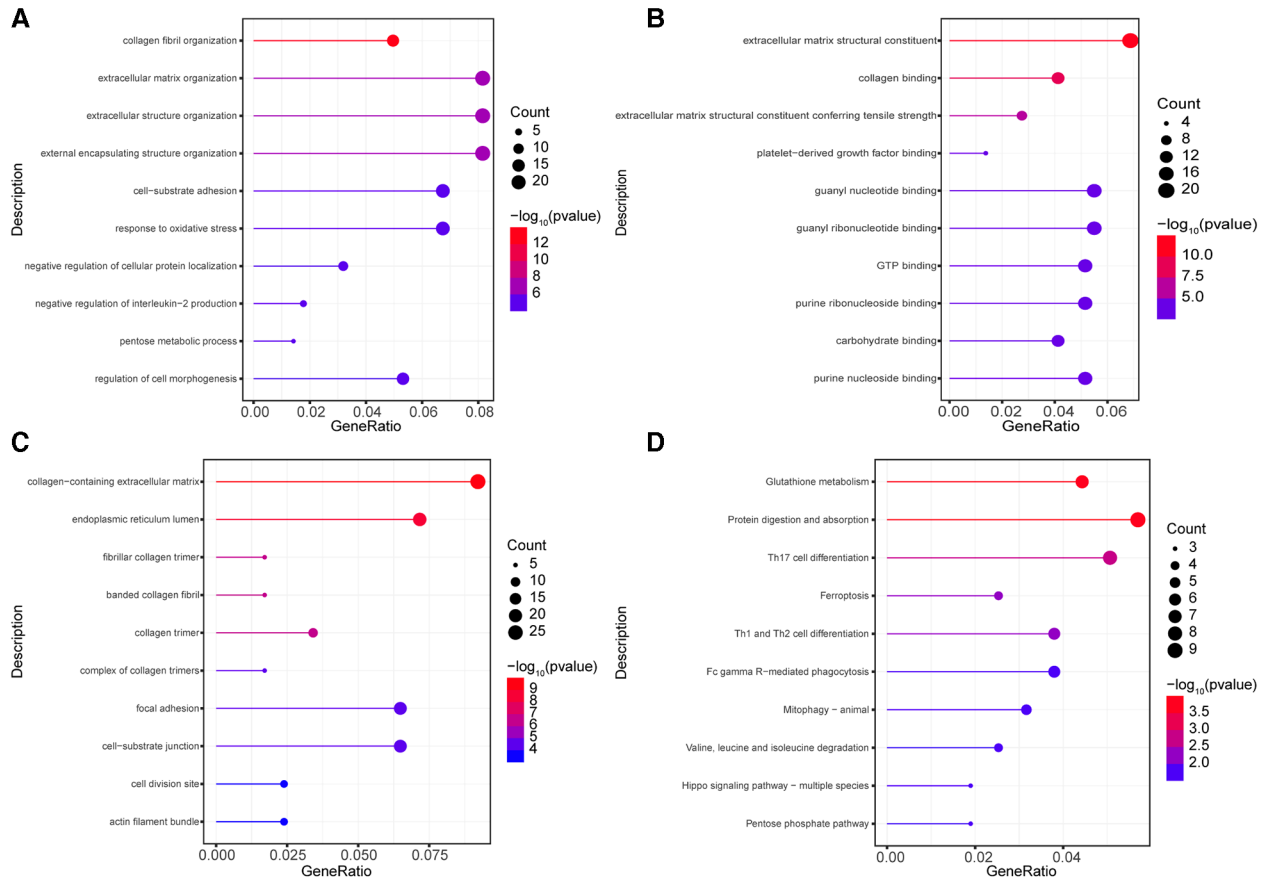


FIGURE 3
Go and KEGG enrichment analysis for highly correlated genes. (**A–C**) The GO enrichment analyses were conducted using the 302 highly correlated genes, the top 10 terms of from BP (**A**), MF (**B**), CC (**C**) were depicted. (**D**) The KEGG enrichment analyses were performed, the 10 significantly enriched pathways were identified. The circle size represents gene counts in each enriched term. The different color means significance for each enriched term.

(**Figures 5C,D**). Finally, ten hub genes including *CD74*, *COL1A1*, *TXNRD1*, *CCND1*, *COL5A1*, *SERPINH1*, *BCL6*, *ITGA10*, *FOS*, and *JUNB* were obtained according to above-mentioned analytical methods (**Figures 5C,D**). These findings indicate that AS and AI shared the common molecular regulatory network.

## Validation of hub genes expression levels

For further verifying the results acquired from above analyses, we first investigated the expression levels of the ten hub genes in AS and AI group by analyzing expression values in high throughput RNA-sequencing data. The expression levels of ten hub genes were re-analysed. The mRNA expression levels of *CD74*, *COL1A1*, *CCND1*, *COL5A1*, *SERPINH1*, *FOS*, and *JUNB* were obviously upregulated, whereas those of *TXNRD1*, *BCL6*, and *ITGA10* were evidently downregulated in AS and AI aortic valves relative to the normal controls (**Figures 6A,B**). Meanwhile, we selected 5 normal aortic valves, 15 AS aortic valves, and 15 AI aortic valves. These diseased aortic valves were divided into mild, moderate, and severe groups according to the degree of aortic valves lesion, respectively. The mRNA expression levels of *CD74*, *COL1A1*, *TXNRD1*, *CCND1*, *COL5A1*, *SERPINH1*, *BCL6*, *ITGA10*, *FOS*, and *JUNB* were detected. As shown in **Figures 6C, D**, although there was not evident degree of lesion-dependent trend, the mRNA expression levels of the ten hub genes were consistent with the results in **Figures 6A,B** from high-throughput sequencing. These highly consistent data suggest that the vital function of the ten hub genes in regulating and indicating the disease course for AS and AI.

# Discussion

Herein, using the published high throughput RNA-sequencing data (GSE153555) for AS and AI aortic valves, we conducted WGCNA to identify the key co-expression modules and hub genes involved in AS and AI pathogenesis. Total of eight modules including darkgrey, lightcyan, darkorange, orange, steelblue, darkgreen, grey60, and grey modules were constructed. The associations of modules and clinical traits were computed, and these modules associated with the development and outcome of AS and AI were further analysed to screened out the highly

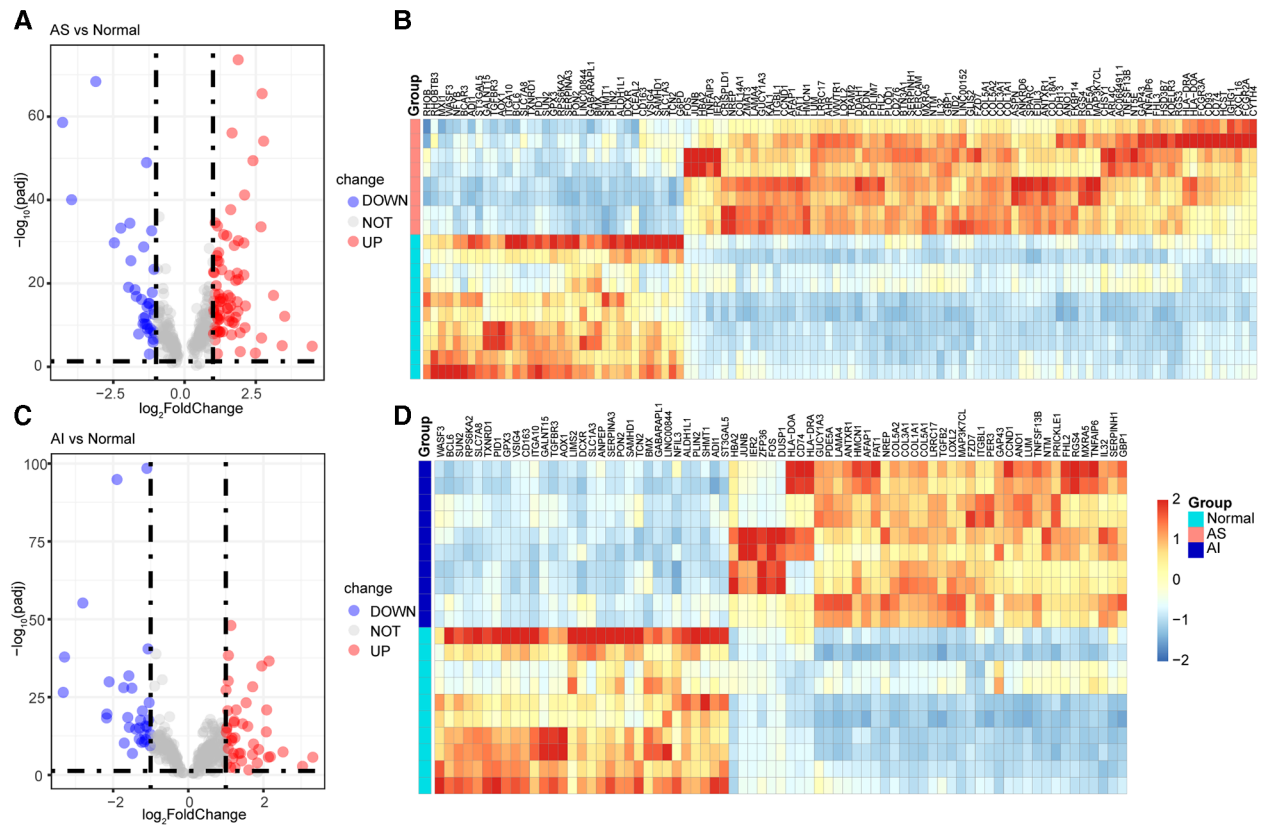


FIGURE 4
Identification of DEGs for highly correlated genes. (**A**–**D**) The 302 highly correlated genes with AS and AI were used for DEGs expression analyses. These genes with $|\log_2 FoldChange| \geq 1$ and adjust *P* value <0.05 were regarded as the DEGs in AS and AI group in comparison to the normal control group. The volcano plots and heatmaps were used for visualization of the DEGs for indicated group. The blue dots of volcano plots represent the downregulated genes (DOWN) in AS (**A**) and AI (**C**) group. The gray dots of volcano plots represent the unchanged genes (NOT) in AS (**A**) and AI (**C**) group. The red dots of volcano plots represent the upregulated genes (UP) in AS (**A**) and AI (**C**) group. The heatmaps of DEGs from (**A**,**C**) of AS (**B**) and AI (**D**) group were depicted, the color scale bar of heatmap represents the scale (from −2 to 2) for the expression levels of genes presented in the heatmaps with a breakpoint of zero represented by white.

correlated genes with AS and AI pathogenesis. The 302 highly correlated genes were obtained from the indicated modules, and GO and KEGG functional enrichment analyses were performed to explore the potential biological processes and signaling pathways involved in these genes. Furthermore, the expression profiles of the 302 highly correlated genes were used for DEGs analyses. There were 31 downregulated genes, 229 unchanged genes, and 42 upregulated genes in AI group and 35 downregulated genes, 190 unchanged genes, and 77 upregulated genes in AS group, respectively. The PPI network analyses were performed and visualized by STRING online tool and Cytoscape software. The top 30 genes with highest connectivity were singled out and intersected with the DEGs in AS and AI group to find out the common functional hub molecules in AS and AI pathogenesis. Ultimately, ten hub genes (*CD74*, *COL1A1*, *TXNRD1*, *CCND1*, *COL5A1*, *SERPINH1*, *BCL6*, *ITGA10*, *FOS*, and *JUNB*) were obtained and the validation of expression levels was performed to elucidate the molecular mechanism of AS and AI pathological processes.

By exploiting WGCNA module construction, we screened seven significant gene modules associated with AS and AI. We selected highly correlated modules with AS and AI for further analysis, and the 302 highly correlated genes were picked out. Our study found that these highly correlated genes were mainly implicated in the regulation of collagen fibril and extracellular matrix (ECM) by GO analyses, which was consistent with the previous studies (22, 23). These results indicate that the disorders of collagen fibril and ECM may largely impact the normal function of aortic valves. According to the results of KEGG analyses, we enriched top 10 pathways for AS and AI affected mechanism, which included nutrient metabolism, T cell differentiation, ferroptosis, phagocytosis, mitophagy, and Hippo signaling pathway. Glutathione metabolism is the pivotal pathophysiological course for anti-oxidative stress and anti-aging (24). We identified that glutathione metabolism pathway was the significantly enriched term, this hinted that oxidative stress response could be the vital molecular mechanism in regulating the development of AS and AI. Our analysis results were similar with those of David R. A. Reyes et al. (25) and Michael Mahmoudi et al. (26), which manifested the highly reliability of our study. Besides, our study uncovered Th17 cell differentiation and Th1 and Th2 cell differentiation pathway were associated

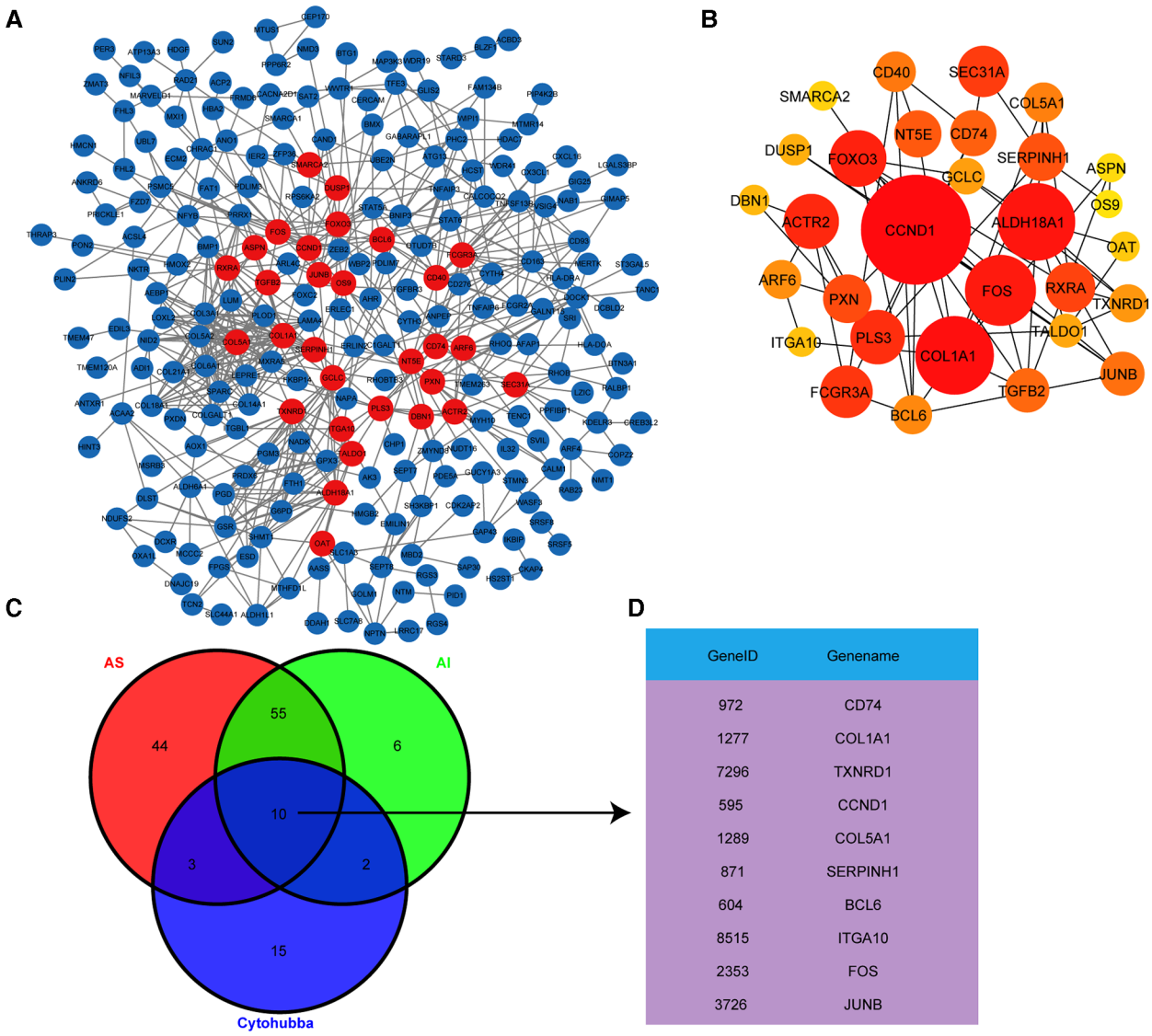


FIGURE 5
Hub genes identification by PPI analysis. (A) The PPI network analysis for the 302 highly correlated genes was conducted using the STRING online tool and visualized by Cytoscape software. Each node represents the gene, the different quantity of connecting line among these nodes represents connectivity. (B) The PPI network shown the top 30 genes with highest connectivity from (A) screened out with Cytohubba plug-in by Betweenness button, the node size represents different connectivity. (C) Venn diagram exhibited the overlapping of the DEGs from group and the top 30 genes with highest connectivity from (B) to screen out the hub genes. (D) These hub genes were exhibited in the gene list.

with AS and AI pathogenesis. As the distinctly important contributors for orchestrating adaptive immune responses, Th1, Th2, and Th17 cells are responsible to various intracellular or extracellular pathogens as well as organ-specific autoimmunity, which were activated by a series of cytokines (27, 28). Further, Immune Cell Abundance Identifier (ImmuCellAI) (29) is introduced for precisely estimating the abundance of immune cell types from the high throughput RNA-sequencing data (GSE153555). As shown in Supplementary **Figure S2**, the box plots demonstrated that AS and AI patients had a higher level of cytotoxic T cells, gamma delta T cells (γδ T), iTreg, Th2 and Tr1 and a lower level of macrophages, neutrophils, and Th17. Our findings indicated that tackling immune responses may become a possibility for harnessing the pathogenesis of AS and AI. Another, we identified the other significantly enriched pathways as the AS and AI underlying mechanisms, such as ferroptosis, phagocytosis, mitophagy, and Hippo signaling pathway. However, the detailed and direct functions in AS and AI for these identified pathways still needed for investigation deeply in the future.

To find out the important regulatory and indicative molecules for AS and AI, we focused on the 302 genes for further analysis. By DEGs analysis and screening these genes with high connectivity, we found out ten hub genes including *CD74*, *COL1A1*, *TXNRD1*, *CCND1*, *COL5A1*, *SERPINH1*, *BCL6*, *ITGA10*, *FOS*, and *JUNB*. In terms of the expression levels for the ten hub genes, our results manifested that *CD74*, *COL1A1*, *CCND1*, *COL5A1*, *SERPINH1*, *FOS*, and *JUNB* were significantly up-regulated.

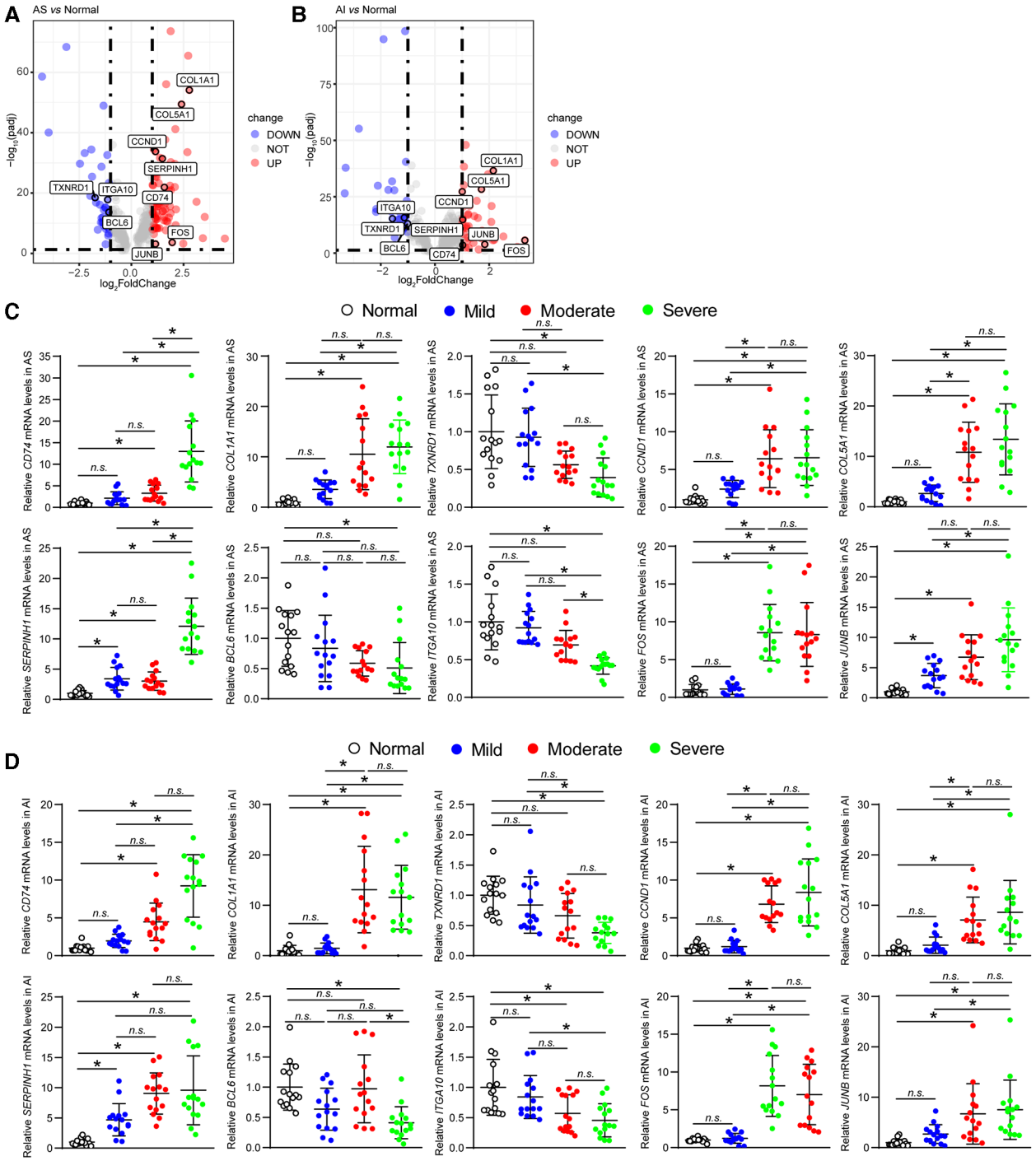


FIGURE 6
Validation of hub genes expression levels. (**A**,**B**) The mRNA expression levels of the ten hub genes (*CD74*, *COL1A1*, *TXNRD1*, *CCND1*, *COL5A1*, *SERPINH1*, *BCL6*, *ITGA10*, *FOS*, and *JUNB*) of AS and AI group were analysed using the expression values from the high throughput RNA-sequencing data. These genes were marked in the indicated volcano plot. (**C**,**D**) The mRNA expression levels of the ten hub genes (*CD74*, *COL1A1*, *TXNRD1*, *CCND1*, *COL5A1*, *SERPINH1*, *BCL6*, *ITGA10*, *FOS*, and *JUNB*) of AS and AI group were detected by real-time PCR assay using the human aortic valve samples of AS and AI. The mRNA levels were normalized to those of glyceraldehyde-3-phosphate dehydrogenase (*GAPDH*) ($n = 5$). *$P < 0.05$ *vs.* the normal control group, *n.s.*, no significance.

Whereas those of *TXNRD1*, *BCL6*, and *ITGA10* were obviously down-regulated. Although, transcriptional profiles of AS and AI pathological processes have been well parsed by Christina L. Greene et al. (14), the identification of highly correlated genes with the progression of AS and AI by systematic computerized algorithm remains unimplemented. Greene et al. used DEGs analysis only to screen for genes of interest, our analysis strategy may be more comprehensive and diverse. Our study may provide the relatively reliable molecular markers for mechanism researches, diagnosis, and treatment of AS and AI.

CD74 (MHC class II invariant chain, Ii), is a kind of type II transmembrane glycoprotein (30). CD74 functions in multiple biological processes and disease types, including lung adenocarcinoma (31), kidney disease (32), spondyloarthritis (33), colitis (34), etc. Collagen type I alpha 1 chain (COL1A1) and collagen type V alpha 1 chain (COL5A1) are the members of collagen family (35), mainly involved in various courses of tumor development, such as hepatocellular carcinogenesis and metastasis (36), immune infiltration in mesothelioma (37), metastasis of lung adenocarcinoma (38), tumor progression in ovarian cancer (39). Thioredoxin reductase 1 (TXNRD1) is a member of the thioredoxin system, regulating hepatocellular carcinoma (40), epilepsy (41), osteosarcoma (42). Cyclin D1 (CCND1) functions as a regulator of CDK kinases and regulates the cell-cycle during G1/S transition (43). Serpin family H member 1 (SERPINH1) is a member of the serpin superfamily of serine proteinase inhibitors and binds specifically to collagen, has been identified acting in gastric cancer metastasis (44) and proliferation and migration of retinal endothelial cells (45). B cell lymphoma 6 (BCL6) is a recognized sequence-specific transcriptional repressor and critical for regulating germinal centers homeostasis (46). Integrin subunit alpha 10 (ITGA10) is a receptor for collagen, has been supposed to be the prognostic biomarker for skin cutaneous melanoma and ovarian cancer (47, 48). Fos proto-oncogene, AP-1 transcription factor subunit (FOS) has been uncovered adjusting cell proliferation, differentiation, and transformation (49). JunB proto-oncogene, AP-1 transcription factor subunit (JUNB) is a member for AP-1 complex, has been identified as the cell proliferation inhibitor and senescence inducer (50), which involves in the regulation of oral squamous cell carcinoma (51) and osteoarthritis (52), etc. However, the molecular functions for these ten hub genes identified by our study in aortic valve were still unclear. Our study provided the feasible molecular bases for the mechanism research or clinical diagnosis and treatment targeting AS and AI, whereas the specific role for these molecules in AS and AI should be further confirmed using *in vitro* or *in vivo* experimental models of AS and AI. Collectively, we identified the key signaling pathways and hub genes (*CD74*, *COL1A1*, *TXNRD1*, *CCND1*, *COL5A1*, *SERPINH1*, *BCL6*, *ITGA10*, *FOS*, and *JUNB*) in AS and AI pathological processes, which may become the potential indicative biomarkers or important regulatory targets in AS and AI pathogenesis. Our findings probably provided the vital theoretical foundation for AS and AI study in the future.

## Data availability statement

The datasets presented in this study can be found in online repositories. The names of the repository/repositories and accession number(s) can be found in the article/**Supplementary Material**.

## Ethics statement

The studies involving humans were approved by Human Research Ethics Committees of Tongji Hospital of Huazhong University of Science and Technology. The studies were conducted in accordance with the local legislation and institutional requirements. The participants provided their written informed consent to participate in this study.

## Author contributions

LC, YY, JF, and XW conceived the study and designed the experiments; YY, ZP, XF, BX, YC, and QW analyzed the data; LC drafted the manuscript; YY, BX, PZ, and XF prepared the human aortic valve samples. LC and YY performed the experiments; LC, YY, PZ, XF, BX, YC, QW, JF, and XW reviewed and revised the manuscript. All authors contributed to the article and approved the submitted version.

## Funding

This work was supported by the National Natural Science Foundation of China (NO. 82070488, NO. 81873458, NO. 81800256).

## Conflict of interest

The authors declare that the research was conducted in the absence of any commercial or financial relationships that could be construed as a potential conflict of interest.

## Publisher's note



## Supplementary material

The Supplementary Material for this article can be found online at: https://www.frontiersin.org/articles/10.3389/fcvm.2023.857578/full#supplementary-material

# References


1. Messerli FH, Rimoldi SF, Bangalore S. The transition from hypertension to heart failure: contemporary update. *JACC Heart Fail*. (2017) 5(8):543–51. doi: 10.1016/j.jchf.2017.04.012

2. Flaherty JD, Bax JJ, De Luca L, Rossi JS, Davidson CJ, Filippatos G, et al. Acute heart failure syndromes in patients with coronary artery disease. *J Am Coll Cardiol*. (2009) 53(3):254–63. doi: 10.1016/j.jacc.2008.08.072

3. Bahit MC, Kochar A, Granger CB. Post-Myocardial infarction heart failure. *JACC Heart Fail*. (2018) 6(3):179–86. doi: 10.1016/j.jchf.2017.09.015

4. Gill H, Chehab O, Allen C, Patterson T, Redwood S, Rajani R, et al. The advantages, pitfalls and limitations of guideline-directed medical therapy in patients with valvular heart disease. *Eur J Heart Fail*. (2021) 23(8):1325–33. doi: 10.1002/ejhf.2097

5. Seferović PM, Polovina M, Bauersachs J, Arad M, Gal TB, Lund LH, et al. Heart failure in cardiomyopathies: a position paper from the heart failure association of the European society of cardiology. *Eur J Heart Fail*. (2019) 21(5):553–76. doi: 10.1002/ejhf.1461

6. Fleury MA, Clavel MA. Sex and race differences in the pathophysiology, diagnosis, treatment, and outcomes of valvular heart diseases. *Can J Cardiol*. (2021) 37(7):980–91. doi: 10.1016/j.cjca.2021.02.003

7. Benjamin EJ, Muntner P, Alonso A, Bittencourt MS, Callaway CW, Carson AP, et al. Heart disease and stroke statistics—2019 update: a report from the American heart association. *Circulation*. (2019) 139:10. doi: 10.1161/CIR.0000000000000659

8. Nkomo VT, Gardin JM, Skelton TN, Gottdiener JS, Scott CG, Enriquez-Sarano M. Burden of valvular heart diseases: a population-based study. *Lancet*. (2006) 368 (9540):1005–11. doi: 10.1016/S0140-6736(06)69208-8

9. Iung B, Vahanian A. Epidemiology of valvular heart disease in the adult. *Nat Rev Cardiol*. (2011) 8(3):162–72. doi: 10.1038/nrcardio.2010.202

10. Akahori H, Tsujino T, Masuyama T, Ishihara M. Mechanisms of aortic stenosis. *J Cardiol*. (2018) 71(3):215–20. doi: 10.1016/j.jjcc.2017.11.007

11. Bing R, Cavalcante JL, Everett RJ, Clavel M, Newby DE, Dweck MR. Imaging and impact of myocardial fibrosis in aortic stenosis. *JACC Cardiovasc Imaging*. (2019) 12(2):283–96. doi: 10.1016/j.jcmg.2018.11.026

12. Akinseye OA, Pathak A, Ibebuogu UN. Aortic valve regurgitation: a comprehensive review. *Curr Prob Cardiol*. (2018) 43(8):315–34. doi: 10.1016/j.cpcardiol.2017.10.004

13. Ravalli F, Kossar AP, Takayama H, Grau JB, Ferrari G. Aortic valve regurgitation: pathophysiology and implications for surgical intervention in the era of TAVR. *Struct Heart*. (2020) 4(2):87–98. doi: 10.1080/24748706.2020.1719446

14. Greene CL, Jaatinen KJ, Wang H, Koyano TK, Bilbao MS, Woo YJ. Transcriptional profiling of normal, stenotic, and regurgitant human aortic valves. *Genes (Basel)*. (2020) 11(7):789. doi: 10.3390/genes11070789

15. Langfelder P, Horvath S. WGCNA: an R package for weighted correlation network analysis. *BMC Bioinform*. (2008) 9:559. doi: 10.1186/1471-2105-9-559

16. Szklarczyk D, Gable AL, Nastou KC, Lyon D, Kirsch R, Pyysalo S, et al. The STRING database in 2021: customizable protein–protein networks, and functional characterization of user-uploaded gene/measurement sets. *Nucleic Acids Res*. (2021) 49(D1):D605–12. doi: 10.1093/nar/gkaa1074

17. Shannon P, Markiel A, Ozier O, Baliga NS, Wang JT, Ramage D, et al. Cytoscape: a software environment for integrated models of biomolecular interaction networks. *Genome Res*. (2003) 13(11):2498–504. doi: 10.1101/gr.1239303

18. Chin CH, Chen SH, Wu HH, Ho CW, Ko MT, Lin CY. Cytohubba: identifying hub objects and sub-networks from complex interactome. *BMC Syst Biol*. (2014) 8 (Suppl 4):S11. doi: 10.1186/1752-0509-8-S4-S11

19. Zoghbi WA, Adams D, Bonow RO, Enriquez-Sarano M, Foster E, Grayburn PA, et al. Recommendations for noninvasive evaluation of native valvular regurgitation: a report from the American society of echocardiography developed in collaboration with the society for cardiovascular magnetic resonance. *J Am Soc Echocardiog*. (2017) 30:303–71. doi: 10.1016/j.echo.2017.01.007

20. Zakkar M, Bryan AJ, Angelini GD. Aortic stenosis: diagnosis and management. *BMJ-Brit Med J*. (2016) 355:i5425. doi: 10.1136/bmj.i5425

21. Fang J, Li T, Zhu X, Deng K, Ji Y, Fang C, et al. Control of pathological cardiac hypertrophy by transcriptional corepressor IRF2BP2 (interferon regulatory factor-2 binding protein 2) novelty and significance. *Hypertension*. (2017) 70(3):515–23. doi: 10.1161/HYPERTENSIONAHA.116.08728

22. Di Vito A, Donato A, Presta I, Mancuso T, Brunetti FS, Mastroroberto P, et al. Extracellular matrix in calcific aortic valve disease: architecture, dynamic and perspectives. *Int J Mol Sci*. (2021) 22(2):913. doi: 10.3390/ijms22020913

23. Urban P, Rabajdova M, Spakova I, Sabol F, Mickova H, Lakatosova K, et al. Molecular recognition of aortic valve stenosis and regurgitation. *Eur Rev Med Pharmacol Sci*. (2019) 23(24):10996–1003. doi: 10.26355/eurrev_201912_19805

24. Homma T, Fujii J. Application of glutathione as anti-oxidative and anti-aging drugs. *Curr Drug Metab*. (2015) 16(7):560–71. doi: 10.2174/1389200216666151015114515

25. Reyes DRA, Gomes MJ, Rosa CM, Pagan LU, Zanati SG, Damatto RL, et al. Exercise during transition from compensated left ventricular hypertrophy to heart failure in aortic stenosis rats. *J Cell Mol Med*. (2019) 23(2):1235–45. doi: 10.1111/jcmm.14025

26. Mahmoudi M, Gormaz JG, Erazo M, Howard M, Baeza C, Feelisch M, et al. Early oxidative stress response in patients with severe aortic stenosis undergoing transcatheter and surgical aortic valve replacement: a transatlantic study. *Oxid Med Cell Longev*. (2019) 2019:1–8. doi: 10.1155/2019/6217837

27. Luckheeram RV, Zhou R, Verma AD, Xia B. CD4+T cells: differentiation and functions. *Clin Dev Immunol*. (2012) 2012:1–12. doi: 10.1155/2012/925135

28. Park H, Park H, Lee J, Bothwell A, Choi J. Sex-based selectivity of PPARγ regulation in th1, th2, and th17 differentiation. *Int J Mol Sci*. (2016) 17(8):1347. doi: 10.3390/ijms17081347

29. Miao YR, Zhang Q, Lei Q, Luo M, Xie GY, Wang H, et al. ImmuCellAI: a unique method for comprehensive T-cell subsets abundance prediction and its application in cancer immunotherapy. *Adv Sci (Weinh)*. (2020) 7(7):1902880. doi: 10.1002/advs.201902880

30. Su H, Na N, Zhang X, Zhao Y. The biological function and significance of CD74 in immune diseases. *Inflamm Res*. (2017) 66(3):209–16. doi: 10.1007/s00011-016-0995-1

31. Fernandez-Cuesta L, Plenker D, Osada H, Sun R, Menon R, Leenders F, et al. CD74–NRG1 fusions in lung adenocarcinoma. *Cancer Discov*. (2014) 4(4):415–22. doi: 10.1158/2159-8290.CD-13-0633

32. Valiño-Rivas L, Baeza-Bermejillo C, Gonzalez-Lafuente L, Sanz AB, Ortiz A, Sanchez-Niño MD. CD74 in kidney disease. *Front Immunol*. (2015) 6:483. doi: 10.3389/fimmu.2015.00483

33. Sogkas G, Klose K, Baerlecken N, Schweikhard E, Matthias T, Kniesch K, et al. CD74 is a T cell antigen in spondyloarthritis. *Clin Exp Rheumatol*. (2020) 38 (2):195–202. doi: 10.55563/clinexprheumatol/lezc69

34. Hoffman JM, Rankin CR, Pothoulakis C. Here to heal: mucosal CD74 signaling in colitis. *Cell Mol Gastroenterol Hepatol*. (2020) 10(1):197–8. doi: 10.1016/j.jcmgh.2020.03.002

35. Ricard-Blum S. The collagen family. *Cold Spring Harb. Perspect Biol*. (2011) 3(1):a4978. doi: 10.1101/cshperspect.a004978

36. Ma H, Chang H, Bamodu OA, Yadav VK, Huang T, Wu ATH, et al. Collagen 1A1 (COL1A1) is a reliable biomarker and putative therapeutic target for hepatocellular carcinogenesis and metastasis. *Cancers (Basel)*. (2019) 11(6):786. doi: 10.3390/cancers11060786

37. Zhang C, Liu S, Wang X, Liu H, Zhou X, Liu H. COL1A1 is a potential prognostic biomarker and correlated with immune infiltration in mesothelioma. *Biomed Res Int*. (2021) 2021:1–13. doi: 10.1155/2021/5320941

38. Liu W, Wei H, Gao Z, Chen G, Liu Y, Gao X, et al. COL5A1 may contribute the metastasis of lung adenocarcinoma. *Gene*. (2018) 665:57–66. doi: 10.1016/j.gene.2018.04.066

39. Zhang J, Zhang J, Wang F, Xu X, Li X, Guan W, et al. Overexpressed COL5A1 is correlated with tumor progression, paclitaxel resistance, and tumor-infiltrating immune cells in ovarian cancer. *J Cell Physiol*. (2021) 236(10):6907–19. doi: 10.1002/jcp.30350

40. Fu B, Meng W, Zeng X, Zhao H, Liu W, Zhang T. TXNRD1 is an unfavorable prognostic factor for patients with hepatocellular carcinoma. *Biomed Res Int*. (2017) 2017:1–8. doi: 10.1155/2017/4698167

41. Kudin AP, Baron G, Zsurka G, Hampel KG, Elger CE, Grote A, et al. Homozygous mutation in TXNRD1 is associated with genetic generalized epilepsy. *Free Radical Bio Med*. (2017) 106:270–7. doi: 10.1016/j.freeradbiomed.2017.02.040

42. Huang S, Zhu X, Ke Y, Xiao D, Liang C, Chen J, et al. LncRNA FTX inhibition restrains osteosarcoma proliferation and migration via modulating miR-320a/TXNRD1. *Cancer Biol Ther*. (2020) 21(4):379–87. doi: 10.1080/15384047.2019.1702405

43. González-Ruiz L, González-Moles MÁ, González-Ruiz I, Ruiz-Ávila I, Ramos-García P. Prognostic and clinicopathological significance of CCND1/cyclin d1 upregulation in melanomas: a systematic review and comprehensive meta-analysis. *Cancers (Basel)*. (2021) 13(6):1314. doi: 10.3390/cancers13061314

44. Tian S, Peng P, Li J, Deng H, Zhan N, Zeng Z, et al. SERPINH1 regulates EMT and gastric cancer metastasis via the Wnt/beta-catenin signaling pathway. *Aging (Albany NY)*. (2020) 12(4):3574–93. doi: 10.18632/aging.102831

45. Hu L, Liu Y, Wei C, Jin H, Mei L, Wu C. SERPINH1, targeted by miR-29b, modulated proliferation and migration of human retinal endothelial cells under high glucose conditions. *Diabetes Metab Syndr Obes*. (2021) 14:3471–83. doi: 10.2147/DMSO.S307771

46. Leeman-Neill RJ, Bhagat G. BCL6 as a therapeutic target for lymphoma. *Expert Opin Ther Targets*. (2018) 22(2):143–52. doi: 10.1080/14728222.2018.1420782

47. Nurzat Y, Su W, Min P, Li K, Xu H, Zhang Y. Identification of therapeutic targets and prognostic biomarkers among integrin subunits in the skin

cutaneous melanoma microenvironment. *Front Oncol.* (2021) 11:751875. doi: 10.3389/fonc.2021.751875

48. Zhu T, Chen R, Wang J, Yue H, Lu X, Li J. The prognostic value of ITGA and ITGB superfamily members in patients with high grade serous ovarian cancer. *Cancer Cell Int.* (2020) 20:1. doi: 10.1186/s12935-020-01344-2

49. Acquaviva C, Bossis G, Ferrara P, Brockly F, Jariel-Encontre I, Piechaczyk M. Multiple degradation pathways for fos family proteins. *Ann N Y Acad Sci.* (2002) 973:426–34. doi: 10.1111/j.1749-6632.2002.tb04677.x

50. Piechaczyk M, Farràs R. Regulation and function of JunB in cell proliferation. *Biochem Soc T.* (2008) 36(5):864–7. doi: 10.1042/BST0360864

51. Tsunoda M, Fukasawa M, Nishihara A, Takada L, Asano M. Junb can enhance the transcription of IL-8 in oral squamous cell carcinoma. *J Cell Physiol.* (2021) 236 (1):309–17. doi: 10.1002/jcp.29843

52. Lin Z, Miao J, Zhang T, He M, Wang Z, Feng X, et al. JUNB-FBXO21-ERK axis promotes cartilage degeneration in osteoarthritis by inhibiting autophagy. *Aging Cell.* (2021) 20(2):e13306. doi: 10.1111/acel.13306

# Frontiers in
# Cardiovascular Medicine

**Innovations and improvements in cardiovascular treatment and practice**

Focuses on research that challenges the status quo of cardiovascular care, or facilitates the translation of advances into new therapies and diagnostic tools.

---

## Discover the latest Research Topics

See more →

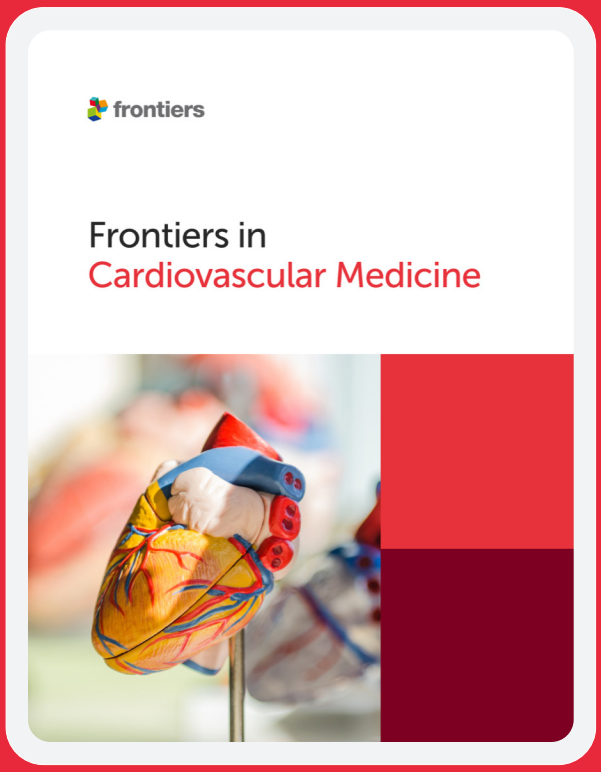


**Frontiers**

Avenue du Tribunal-Fédéral 34
1005 Lausanne, Switzerland
frontiersin.org

**Contact us**

+41 (0)21 510 17 00
frontiersin.org/about/contact